Synthesis of asymmetric glycoclusters to investigate the nature of carbohydrate recognition

Dissertation

in fulfillment of the requirements for
the doctoral degree “Dr. rer. nat.”
at the Faculty of Mathematics and Natural Sciences
at Kiel University

submitted by

Jasna Löw, née Brekalo

Otto Diels Institute of Organic Chemistry

Kiel, 14. 05. 2020

First Examiner: Prof. Dr. Thisbe K. Lindhorst

Second Examiner: Prof. Dr. Ulrich Lüning

Date of the oral examination: 13. 07. 2020

Prof. Dr. Frank Kempken
Dean of the Faculty of Mathematics and Natural Sciences
at Kiel University

This research work was performed under the supervision of Prof. Dr. Thisbe K. Lindhorst and co-supervision of Dr. Guillaume Despras in the period time from January 2016 till May 2020 at Otto Diels Institute of Organic Chemistry of Christiana Albertina University of Kiel.

I hereby confirm that apart from the supervisor`s guidance the contest and design of the thesis is all my own work. It has not been submitted either partially or wholly as part of a doctoral degree to another examining body. Parts of the thesis have been published. This thesis has been prepared according to the Rules of Good Scientific Practice of the German Research Foundation. This is my first doctoral attempt.

X

Jasna Löw, née Brekalo

”*Life´s meaning derives from the challenges we face*.”

Kwame Anthony Akroma-Ampim Kusi Appiah

Acknowledgment

First and foremost I would like to thank Prof. Dr. Thisbe K. Lindhorst for the given opportunity to do my PhD in her group. I appreciate her time spent to supervise me what additionally motivated me to investigate my projects in a deeper concern. I am particularly pleased that we wrote our full paper together when I learned the most and gained valuable experience and understanding of research at the highest level. I am sincerely grateful for her support to present our work and attend various international conferences. Thank you for teaching me and thank you for supporting women in science.

Special thanks to Dr. Guillaume Despras for all our discussions and puzzling through problems together. Thank you for being my co-supervisor and giving valuable advice on improving my practical skills. Thank you for your French touch in the group. Merci.

Many thank Prof. Dr. Ulrich Lüning for a given time to prove my thesis. Thank you for your advice on how important it is to speak German at Kiel University. Besten Dank.

I am very grateful for all the assistance from the analytical and technical staff at the Otto Diels Institute of Organic Chemistry. Many thanks to Prof. Frank D. Sönnichsen for always having extra time and interest for new analytical methods that relate to my doctoral thesis.

I would like to thank to SFB and the GDCh organizations for financial support.

Many thanks to the AK Lindhorst Group for all our team trips: Summer trips, Christmas /Easter celebrations and our weekly Friday brunch. These are one of the many wonderful memories of all of you. Special thanks to the group members in room 109, I have always enjoyed playing music for you. Thank you for a nice working atmosphere. Many thanks to Elwira Klima, Dr. Vivek Pooenthiyil, Dr. Anne Heitmann, Dr. Claudia Fessele and Dr. Christian Müller for sharing their gained experience with me. Dankeschön.

I am deeply grateful to my family for always being the loudest support in the room. Thank you for encouraging and supporting me to do my best. Many thanks to my very international friends (Bosnian, Croatian, French, German, Italian, English and Spanish) who made my doctoral thesis funnier and happier. Hvala. My special thanks to Roland Löw for positive and unconditional support. На марс и назад.

All figures and schemes, respectively, depicted in this thesis were designed and drawn by me if not otherwise stated. **Figures 1.2** and **Figure 1.3** are modifications of published graphical work as cited.

Throughout my PhD study period, the following papers were published:

- J. Brekalo, G. Despras and T. K. Lindhorst, Pseudoenantiomeric glycoclusters: Synthesis and testing of heterobivalency in carbohydrate-protein interactions, *Org. Biomol. Chem.,* **2019**, *17*, 5929-5942.
- G. Cutolo, F. Reise, M. Schuler, R. Nehmé, G. Despras, J. Brekalo, P. Morin, P.-Y. Renard, Th. K. Lindhorst, A. Tatibouët, Bifunctional mannoside-glucosinolate glycoconjugates as enzymatically triggered isothiocyanates and FimH ligand, *Org. Biomol. Chem.,* **2018**, *16*, 4900-4913.

Abstract

A modern aspect in the investigation of carbohydrate-protein interactions is the study of the influence of relative carbohydrate orientation on carbohydrate recognition. Apparently, carbohydrate-specific proteins, in particular the lectins, distinguish between different spatial and relative arrangements of specific carbohydrate ligands. Here, tailor-made glycomimetics were prepared to investigate such phenomena. Hence, the focus of this thesis is based on the synthesis of enantiomeric scaffold molecules for the asymmetric assembly of homo- and heterovalent glycoclusters. Two main synthetic approaches were used; asymmetric synthesis and chiral pool synthesis to stereoselectively prepare tri- and tetrafunctional scaffold molecules. The synthesis of a pair of diasteromeric glycoclusters with altered configuration at the central scaffold stereocenter allows the variation of the orientation of the ligated carbohydrate in space. In the first project, SHARPLESS epoxidation of a primary allylic alcohol was employed to access enantiomeric tetrafunctional scaffold molecules. Different analytical validation methods were applied to determine the enantioselectivity of this reaction. However, only one of three potential glycosylation steps was accomplished so far as further optimizations of the glycosylation reactions are still needed. However, with the described synthetic route, a promising entry into the stereoselective synthesis of heterotrivalent diastereomeric glycoclusters has been introduced. The second project of this thesis refers to the synthesis of trifunctional enantiomeric scaffolds from the chiral pool to achieve a focused library of "pseudoenantiomeric" heterobivalent glycoclusters. The enantiomeric amino acids L- and D-serine were used as chiral pool starting materials. Carbohydrate recognition was then investigated in an adhesion-inhibition study with type 1-fimbriated *E. coli* bacteria and additionally, with the plant lectin concanavalin A. The inhibitory potencies of pseudoenantiomeric glucose-mannose glycoclusters revealed striking differences in FimH-mediated bacterial adhesion. Building on this striking result, glycoarrays were fabricated with spacer-functionalized variations of the same diastereomeric glycoclusters, which were mounted onto *N*-hydroxysuccinimide-prefunctionalized surfaces. The prepared glycoarrays were then tested in adhesion assays with *E. coli* bacteria under static and dynamic flow conditions. Here, the results supported the previous finding but especially the testings under flow have to be further validated. In conclusion, the biological tests revealed the importance of carbohydrate orientation on ligand recognition as well as a heterocluster effect. In a final subproject, the chiral pool synthetic approach was applied for the synthesis of isomeric homotrivalent glycoclusters. Trifunctional enantiomeric scaffolds were successfully synthesized in analogy to previous work, however, the following glycosylation steps to achieve homotrivalent mannosides were hampered by anomerization and orthoester formation. In conclusion, pseudoenantiomeric glycoclusters were achieved, thereby introducing a novel type of multivalent glycoarchitecture for the investigation of ligand orientation in carbohydrate orientation. Some of these new molecular tools clearly showed the importance of relative scaffolding on carbohydrate recognition. This opens a door into a new regime of glycobiological studies.

Kurzzusammenfassung

Ein moderner Aspekt bei der Untersuchung von Kohlenhydrat-Protein-Wechselwirkungen ist die Untersuchung des Einflusses der relativen Kohlenhydratorientierung auf die Kohlenhydraterkennung. Offensichtlich unterscheiden kohlenhydratspezifische Proteine, wie Lektine, zwischen unterschiedlichen räumlichen und relativen Anordnungen spezifischer Kohlenhydratliganden. Hierbei wurden maßgeschneiderte Glycocluster hergestellt, um solche Phänomene zu untersuchen. Der Schwerpunkt dieser Arbeit liegt auf der Synthese enantiomerer Scaffoldmoleküle für die asymmetrische Bildung von homo- und heterovalenten Glycoclustern. Mit der asymmetrischen Synthese und der chiralen Poolsynthese wurden zwei Hauptsyntheseansätze verwendet, um tri- und tetra-funktionelle Scaffoldmoleküle stereoselektiv herzustellen. Die Synthese eines Paares diastereomere Glycocluster mit veränderter Konfiguration am zentralen Scaffoldstereozentrum ermöglicht die Variation der Orientierung des ligierten Kohlenhydrats im Raum. Im ersten Projekt wurde die SHARPLESS -Epoxidierung eines primären Allylalkohols eingesetzt, um Zugang zu enantiomeren tetrafunktionellen Scaffoldmolekülen zu erhalten. Zu diesem Zeitpunkt konnte nur eine von drei Glykankomponenten eingebaut werden und eine weitere Glykolisierungsoptimierung ist erforderlich. Mit dem beschriebenen Syntheseweg wurde jedoch ein vielversprechender Einstieg in die stereoselektive Synthese heterotrivalenter diastereomerer Glycocluster eingeführt. Das zweite Projekt dieser Arbeit bezieht sich auf die Synthese trifunktioneller enantiomerer Scaffolds aus dem chiralen Pool von L- und D-Serin Aminosäuren, um eine eine fokussierte Bibliothek von "pseudoenantiomeren" heterobivalenten Glycoclustern zu erhalten. Die Kohlenhydraterkennung wurde durch eine Adhäsionshemmungsstudie mit Typ 1-fimbrierten *E. coli* Bakterien und zusätzlich mit dem Pflanzenlektin Concanavalin A untersucht. Die Hemmpotenzen des pseudoenantiomeren Glucose-Mannose-Glycocluster-Paares zeigten bemerkenswerte Unterschiede bei FimH-vermittelter Bakterienadhäsion. Aufbauend auf diesem Ergebnis wurden Glycoarrays mit Spacer-funktionalisierten Variationen desselben diastereomeren Paares von Glycoclustern hergestellt, die auf mit *N*-Hydroxysuccinimid vorfunktionalisierten Oberflächen montierten wurden. Die hergestellten Glycoarrays wurden folgend unter statischen und flussdynamischen Bedingungen mittels Adhäsionstests mit *E. coli* Bakterien untersucht. Hier stützten die Ergebnisse den vorherigen Befund, wobei die Tests unter Durchflussbedingungen weiter validiert werden müssen. Die biologischen Tests zeigen die Wichtigkeit der Kohlenhydratorientierung sowie einen Heteroclustereffekt für die Ligandenerkennung. Im letzten Teilprojekt wurde der Syntheseansatz aus chiralen Pools für die Synthese trifunktionaler enantiomerer Scaffolds angewendet. Die folgenden Glykosylierungsschritte zur Erzielung homotrivalenter Mannoside wurden jedoch durch Anomerisierung und Orthoesterbildung verhindert. Zusammenfassend wurden pseudoenantiomere Glycocluster erzielt, wodurch ein neuartiger Typ einer multivalenten Glycoarchitektur zur Untersuchung der Ligandenorientierung in der Kohlenhydratorientierung eingeführt wurde. Diese neuen molekularen Werkzeuge zeigen deutlich die Bedeutung der relativen Orientirung für die Erkennung von Kohlenhydraten. Dies öffnet neue Regime glykobiologischer Studien.

Table of contents

A guide to this thesis

This thesis comprises nine chapters.

The first chapter provides an introduction with basic information about carbohydrate-protein interactions. This chapter especially refers to the modification of carbohydrate recognition through variation of asymmetric centers from the scientific reported studies which are complied with our study.

Chapter 2 explains the objectives of this thesis.

Chapters 3-6 present the individual subprojects. Each chapter starts with a paragraph introducing individual objectives with the following section about results and discussion. Molecule numbering is specific for each chapter. Figures, schemes and tables follow the sequenced order numbering of individual chapters.

Chapter 7 provides a comprehensive conclusion.

The experimental procedures and the NMR spectra related to all projects are collected in chapter 8. The experimental procedures of performed biological adhesion assays are also given in chapter 8 with reference to chapter 5.

All Scientific references are given in chapter 9.

1 General Introduction

From the scientific point of view it is difficult to provide a definition to life, but it is sensible to note that life is a process. Every organism has a life cycle, can grow and adapt to the environment, undergo metabolism, reproduce and evolve. A cell, often called the building block of life, is the structural and organizational unit of life. At a molecular level, a cell consists of biomolecules such as proteins, lipids, nucleic acids and carbohydrates. Human origin arises from these essential molecules. WATSON and CRICK suggested the DNA helical structure in 1953[1] showing the clear structural basis of a gene, influencing the particular characteristics of an individual organism. The historical discovery of the human A, B and O blood groups back in 1900 play a crucial role for the understanding of the structural basis of individual erythrocytes.[2] The structure of the lipid bilayer was discovered by GORTER and GRENDEL in the 20th century. Up to then the importance of the cell membrane with its function was disregarded.[3] The cell membrane except separating interior and extracellular space of the cell was found to control substance exchange between cells and their environment. This discovery laid the foundation of the significance of the cell membrane as an essential factor that contributes to the cell function.[4]

Each component of an organism in a variety of ways is involved in the life-sustaining chemical pathways. Also ligands and receptors are important players. Ligands[5] were first regarded as informational messengers while receptors (lectin and proteins, respectively)[6] activate the primary effect which is then often linked with second messengers and coordinate secondary effects and so forth. Therefore, multicellular organisms through multiple molecular interactions are able to specifically control complex functions. The interactions of carbohydrates with lipids and proteins play a key role in many biological functions and are involved in one of the most important life processes.[7] Carbohydrates covering the cell surface are regarded as cell surface recognition code ("sugar code"). This code is "decoded" by lectins. Hence they were termed as cell surface recognition code. Our understanding of lectin-carbohydrate interactions goes back to jack bean hemagglutinin which was found to precipitate not only red blood cells but also fat emulsions and yeast cells.[8] Glycosylated proteins, peptides and lipids play a variety of functions in the immune system and are indicators of the healthy or diseased state of a human body.[9] For instance, adhesion of *Helicobacter*

pylori bacteria on epithelial cells causes inflammations and tissue damage.[10] Moreover, the well-known human fertilization process between the sperm plasma membrane and egg's zona pellucida is potentiated by Sialyl-LewisX (sLeX) tetrasaccharide.[11] Additionally, it is also reported that carbohydrate-carbohydrate or protein-protein interactions also play an important role in cell-cell interaction processes.[12] To date, many naturally occurring glycans and a variety of synthetic glycomimetics are known as bioactive substrates in different biological applications. Despite of all these and many other findings the function of glycans in biology is still not well understood. Hence, the glycosciences are a field of research that seeks to understand carbohydrate recognition in more detail and in a conclusive way.

1.1 Carbohydrate-protein interactions

Among many possible cell-cell interactions, carbohydrate-protein interactions were found as one of the most fundamental processes in cell biology. Carbohydrates and proteins are found on every cell surface. The discovery of erythrocyte agglutination with the toxin lectin ricin[13] recalls that there are two possible approaches to study carbohydrate-protein interactions. Back in the 19th century seminal work of LEE *and* LEE demonstrated that one way is of a protein side and the other way is from a carbohydrate side.[14] In general, a protein that binds to a carbohydrate is named a lectin. The name is derived from Latin "*lectus"* to choose or to select. Lectins are found to bind carbohydrates with high specificity. LANDSTEINER illustrated the specificity concept in his book chapter "*The Specificity of Serological reactions*" by the end of 1936.[15] The majority of lectins contain more than one carbohydrate recognition domain (CRD).[16] A lectin may bind to a free complex carbohydrate in solution or to the carbohydrate moiety found as a part of glycolipids or glycoproteins (glycans) on cell surfaces.[17] The interactions of glycans with lectins in a solution refer to the process known as protein precipitation. Moreover, when a lectin interacts with carbohydrates on a cell surface (*e.g.* red blood cells) the multiple interactions cause the cross-linking of the cells resulting in agglutination. Agglutination became the oldest method used to study carbohydrate-protein interactions.[18] To date, there are several methods developed for their investigation. Kinetics and near-equilibrium method include titration calorimetric studies and surface plasmon resonance where non-equilibrium methods include glycan microarray screening. Nevertheless, investigation of carbohydrate-proteins interaction is mostly based on lectin-specific

recognition and binding. The ability of carbohydrates to code information raised an interest in the design of various glycan structures. Thus it is important to investigate the characteristics of both lectins and glycans.

1.1.1 The lectins and their ligands

Glycan binding proteins (GBPs) are found in all kinds of living organisms and they play an important role in many biological processes. In general, GBPs can be divided into two major classifications: lectins and glycosaminoglycan-binding proteins.[6] Glycosaminoglycan (GAG) proteins bind to highly negatively charged glycosaminoglycan polysaccharides. Antithrombin specifically recognizes heparin and its activity were discovered back in 1939 for regulating normal blood coagulation.[19] On the other hand, lectins neither have enzymatic activity neither they act as antibodies.[20] They are found ubiquitously in nature and there are several ways of lectin classification.

Back to the very beginning, the lectin from Venomous snake[21] might have been the first lectin to be found to cause erythrocytes agglutination. This recalls that animal lectin was probably the first lectin to show binding activity to carbohydrates without even being reported. However, MARCHALONIS and EDELMAN reported a natural hemagglutinin from the hemolymph of the horseshoe crab *Limulus polyphemus* in 1968.[22] At the beginning of 19th century, the plant lectin Concanavalin A (ConA) was isolated from Jack Beans *(Canavalia ensiformis)* and it was the first lectin isolated in pure form (**Figure 1.1**).[23] SUMNER and HOWELL reported that ConA agglutinates erythrocyte cells and yeast but also precipitates glycogen from solution. At this point, it was first assumed that ConA binds to carbohydrates on the cell surfaces as well as to carbohydrates in a solution.[24] In the following, the concept of non-covalent lectin-carbohydrate interactions was extended to other lectins and different mono- and oligosaccharide ligands.[25] These findings led to a lectin classification according to their CRD domain: (i) mannose-specific, (ii) galactose and *N*-acetylgalactosamine specific, (iii) *N*-acetylglucosamine specific, (iv) L-fucose specific and (v) *N*-acetylneuraminic acid (sialic acid) specific.[26] ConA recognizes α-mannosides, α-glucosides and the mannotrioside Man-α-1,3-(Man-α-1,6)-Man and it is first used for X-ray crystallographic studies to elucidate the structural details of carbohydrate-lectins interactions.[23a] In the meantime, lectins were also found in bacteria and viruses, where they serve as either hemagglutinins or adhesins and

toxins.[27] Lectins can also be toxic and targeted by the pathogens for the human immune system causing some of the most lethal infections.[28] For instance, FimH lectin (**Figure 1.1**) is known to mediate the adhesion of uropathogenic *E. coli* bacteria (UPEC) to adhere to the α-D-mannoside of urothelial epithelial cells. One of the most pathological conditions is caused by *E. coli* urinary tract infections (UTi).[29]

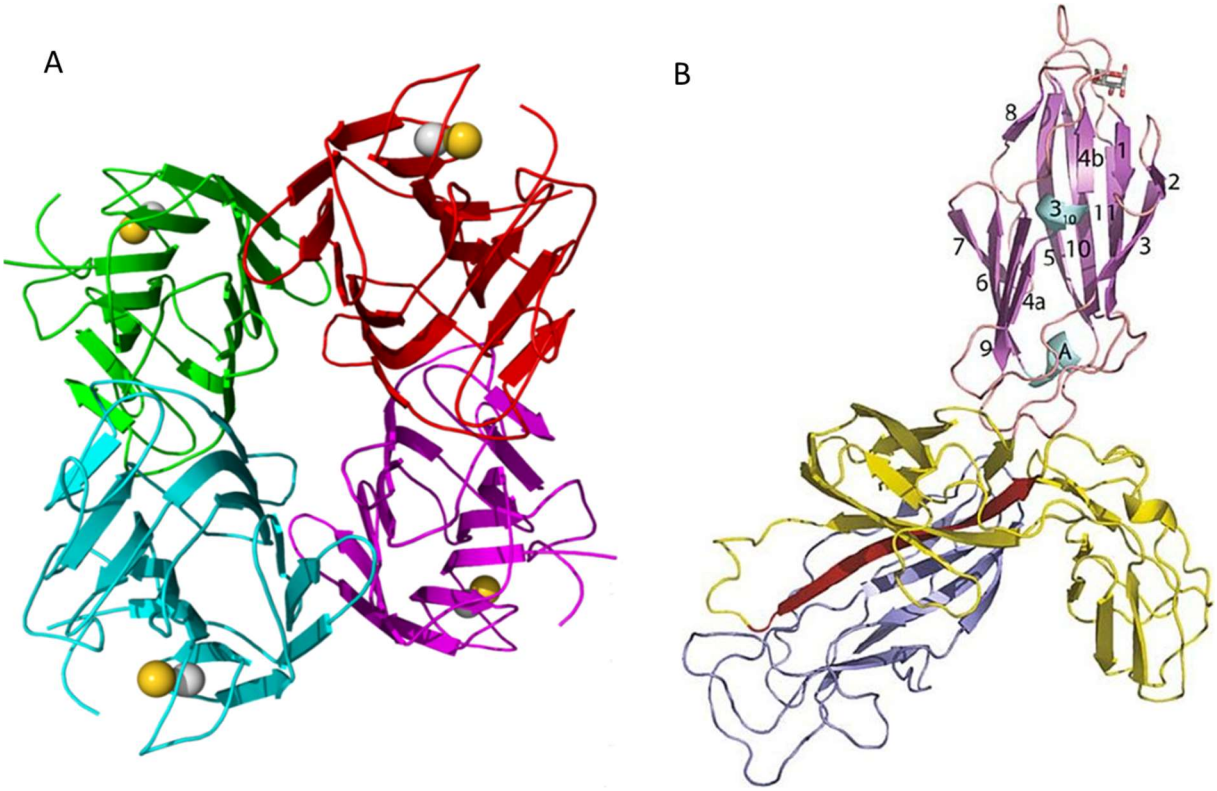

Figure 1.1: (**A**) ConA crystal structure in homotetramer form (monomers colored in violet, red, green, magenta) bound to calcium (gold) and manganese (grey) metallic cations[30]; (**B**) Crystal structure of FimH binding domain (violet) to α-D-mannose (binding pocket of FimH) in complexation with chaperone FimC (yellow) and pili domain of FimH (purple). FimH lectin is adhesin of type 1 fimbriated *E. coli* bacteria.[31]

Based on lectins evolutionary relatedness they can be classified into (i) plant lectins, (ii) animal lectins and (iii) microbial lectins. Even when lectins are of the same biological relationship the primary structure and molecular organization of lectins are highly specific. The human influenza virus binds to α2-6 linked sialic acid whereas the bird influenza virus binds to α2-3 linked sialic acid.[32] Furthermore, the biggest group of animal lectins so-called C-type lectins coordinate with metal ions like Ca^{2+} or Mg^{2+} which are essential for binding to carbohydrate.[33] Here the presence of metal ions is involved in the complex formation where for legume lectins (plant lectins) those metal ions are not necessarily essentials but are im-

portant for CRD coordination in recognition processes.[34] To date, many C-type lectins were found as large transmembrane glycoproteins. On the other hand, galectins are small soluble lectins specific for β-galactosides with biological relationships from *Dictyostelium discoideum* to mammalian tissues.[35] The most investigated C-type lectins can be grouped into selectins, collectins and endocytic lectins. Interestingly, selectins are C-type lectins, including P-, L- and E-selectins, which bind to carbohydrates that come along with proteins such as cell surface mucins.[36] More commonly many lectins are divided into (i) simple lectins, (ii) mosaic or multidomain and (iii) macromolecular assembly.[26] Lectins and their interplay with carbohydrates is of the most importance in the glycoscience and structural composition, ligand density, multivalency, spatial and regional control are factors that are studied in particular.[37]

1.1.2 Naturally occurring carbohydrates

Carbohydrate functions were thought to be limited up to the discovery of their roles as recognition agents.[38] Classically carbohydrates are known to serve in energy storage in the human body. However, at the beginning of 19th century carbohydrates were termed as "*lettres de noblesse*"- extremely important molecules.[39] They are, in fact, biological regulatory molecules. Moreover, carbohydrates found in nature impregnate a variety of complex structures conjugated to other biological molecules. The glycocalyx, found on the external surface of every eukaryotic cell, is a thick sugar coat consisting of diverse carbohydrate moieties named glycans. Thus, carbohydrates play an important role in many biological processes *e*.*g*. cell-cell recognition and cell adhesion.[40] Moreover, glycans found on the cell surfaces are conjugated on their aglycone part in form of glycolipids or glycoproteins (**Figure 1.2**).[41] Glycolipids are a form of bilayer consisting of the non-polar fatty acid tails connected to the inner part of a cell membrane and polar head groups on the outer membrane surface. Divers glycan moieties are linked glycosidically to the lipid polar head group. There are two main subgroups of glycolipids divided on the glycerol- and the sphingo-glycolipid backbone, respectively.[42] The majority of animal glycosphingolipids (GSLs) contain glucose or galactose O-glycosidically linked on the terminal C-1 primary hydroxyl group of the lipid moiety (*e*.*g*. ceramide). Glucosylceramide is one example of GSL found both in plants and animals.[43] Furthermore, glycoglycerolipids are minor constituents of GSL where glycans are linked to the C-3 hydroxyl group of glycerol moiety.[44]

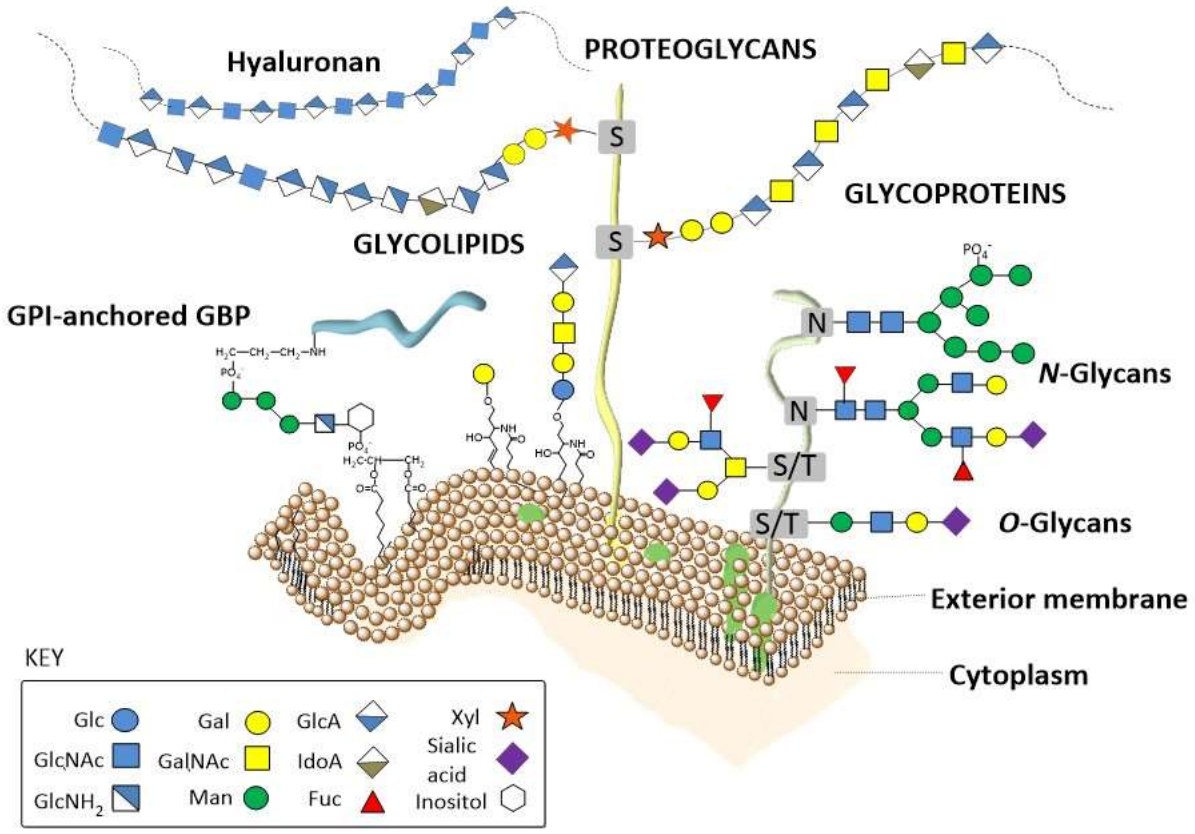

Figure 1.2: Illustration of the eukaryotic cell membrane focused on presentation and diversity of glycan classes found in nature. Glycans are linked to their aglyconic part *e.g.* lipids or proteins in form of glycoproteins, glycolipids, proteoglycans and GPI-anchoring glycan-binding proteins (GBP) or are found free and not linked to the cell surface *e.g.* Hyaluronan.[41]

A term glycoprotein, on the other hand, comes from a conjugated system where the glycan part is mostly N- or O-covalently linked to the amino acid side chains of a protein. N-glycans are typically carbohydrate units β-glycosylated on the amine side chain of asparagine (Asn) or arginine (Arg) commonly involving *N*-acetylglucosamine (GlcNAc) residues.[45] O-glycans are O-linked saccharides (*e.g*. *N*-acetylgalactosamine, glucose and mannose) mostly found on the hydroxyl side chain of serine or threonine amino acid of a protein.[46] The majority of glycoproteins have been discovered through the animal kingdom and some of the common glycoproteins found in nature are represented in **Figure 1.3**.[41] Other types of glycoproteins are called proteoglycans with long sulfated glycosaminoglycan chains. They are usually found with a reducing xylose residue linked on the serine primary hydroxyl group of a "core protein".[47] Microbes, on the other hand, show the variety of glycans that are very unique and not found in plants or animals.[48]

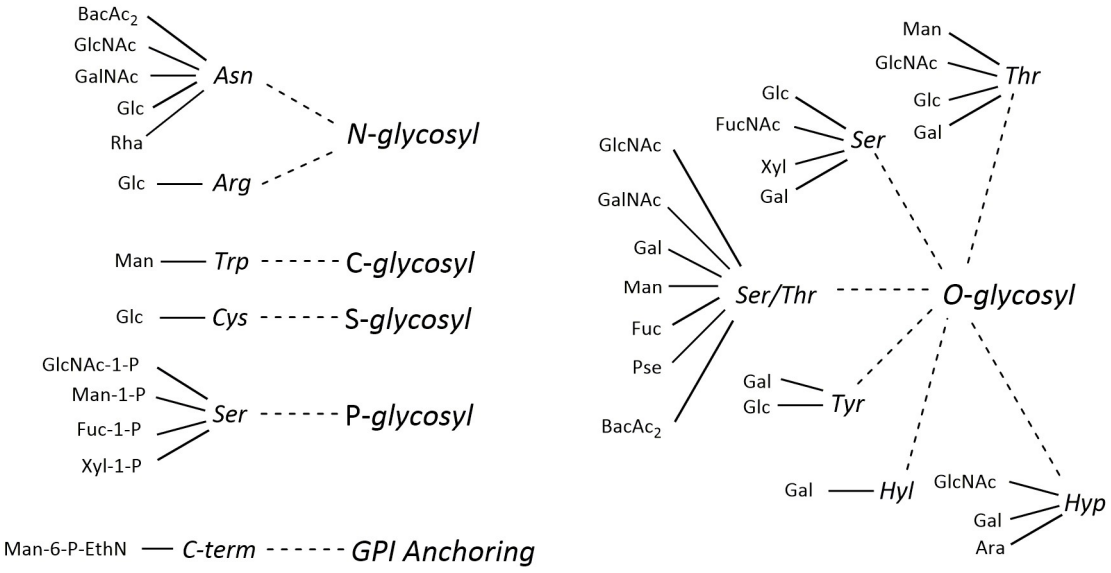

Figure 1.3: The most common glycan-protein linkages isolated from the animal kingdom.[48]

Lipopolysaccharides (LPs), capsular polysaccharides (CPs) and exopolysaccharides (EPs) are parts of bacterial cell membranes rich in glycan diversity. S-glycans have been currently characterized only in bacteria where a glycan moiety is linked to the sulfur of cysteine residue.[49] This type of glycans was first reported in some eukaryotes but not characterized. On the other hand, widespread C-mannosyl glycans found in mammalians appears to be absent in bacteria and yeast.[50] This unique type of glycans incorporates mannose residues through the carbon-carbon bond to the tryptophan amino acid residue of proteins.[50b] Common for all types of glycans is that their free hydroxyl group of each monomeric unit can be sulfated or phosphorylated. Heparan sulfate occurs as proteoglycan where the GlcNAc subunit is sulfated both on 6-*O* sulfate and 2-*N* sulfate position.[51] On the other hand, hyaluronan glycosaminoglycan (GAG) found in some bacteria as capsular polysaccharide appears to exist primarily as a free glycan in some animal cells (unattached to any aglycone).[52] Nevertheless, common to numerous glycans conjugated to aglycone fraction (amino acids) are oligosaccharidic structures constitute the most internal part of glycans, namely, the core of glycans or invariant fraction of glycans. **Figure 1.4** represents the core of glycans found on most of the *O*-glycosyl proteins (**A**), saccharide linear core that exist in most of the proteoglycans (**B**) and branched core common to all *N*-glycosyl proteins (**C**).[53] The glycan structures are created by invariant core and divers glycosidic structures that confer specificity on the glycans and thus constitute the variable fraction of glycans.

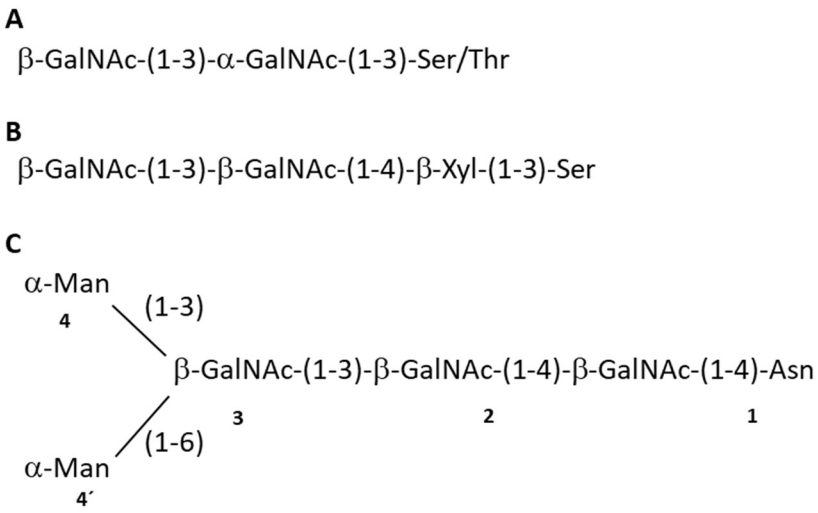

Figure 1.4: Schematic illustration of common oligosaccharides internal cores of glycoproteins.[53]

For instance, mucins, -highly glycosylated proteins-, contain hundreds of heterogenous O-GalNAc glycans with various functions. The carbohydrates found on the variable fraction of O-GalNAc glycans include GalNAc, Gal, GlcNAc, Fuc and Sia. GalNAc O-linked to Ser/Thr is the initiating sugar of O-GalNAc glycans and is sometimes extended to form one of four common core structures giving linear or branched O-GalNAc glycans (**Figure 1.5**).

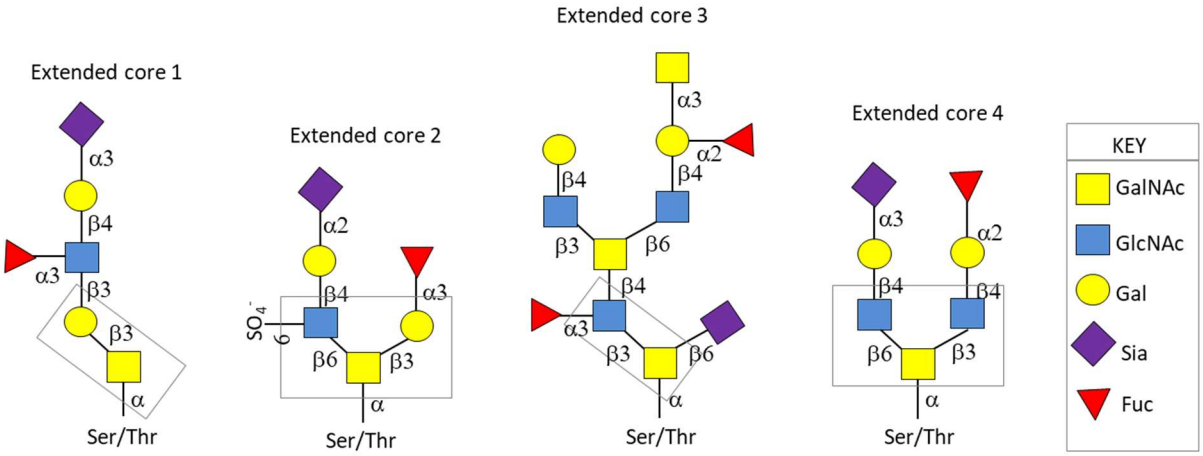

Figure 1.5: Schematic illustration of complex O-GalNAc glycans attached to the mucin with different cores identified by gray boxes. Extended core 1, 2, 3 and 4 O-GalNAc glycans are from human respiratory mucins and the extended core 3 is from human colonic mucins. All four core structures can be extended, branched and terminated with Fuc, Sia or blood group determinants.[41]

The length of O-GalNAc glycans may vary from a single to more than 20 carbohydrate residues on mucins. This complexity often makes it very difficult to assign functions of individual O-GalNAc glycans. Moreover, on the structural basis, the spatial conformations of many gly-

cosidic structures extending the core remain less well explored hence can be termed as "antennae". The importance of the determination of the structural nature of glycosidic linkage and the order in which the residue of monosaccharides of the branching point are conjugated was essential to establish the relationships between glycan structure and their specific biological activity. For instance, in the carbohydrate metabolism, it is known that each sialyltransferase is specific for a particular sugar substrate and depends on the nature of glycosidic linkage formed between sialic acid and the carbohydrate acceptor. PAULSON and coworkers who isolated β-D-galactoside-α-(2-6)-sialyltransferase from bovine colostrum, demonstrated that the enzyme forms only the α-(2-6)-sialyl linkage incorporating Sia onto the specific sequence β-Gal-(1-4)-GlcNAc.[54] On the other hand, isomers β-Gal-(1-3)-GlcNAc and β-Gal-(1-6)-GlcNAc are poor sequence acceptors for the incorporation.[55] Sialic acids (Sias) are typically found to be terminating branches of N-glycans, O-glycans and gangliosphinoglypids with remarkable potential for biologically significant diversity. On the other hand, Sias attached to a glycoconjugate must eventually be removed at some point in the life cycle of the molecule. It was found that deficiency in α-neuraminidase (sialidase) enzyme brings to sialidosis disease and causes abnormal accumulation of complex carbohydrates in patient tissues and urine, generally fatal. Some of the isolated heterogenous oligosaccharidic structures from siallidosis urine are given in **Figure 1.6**.[53, 56]

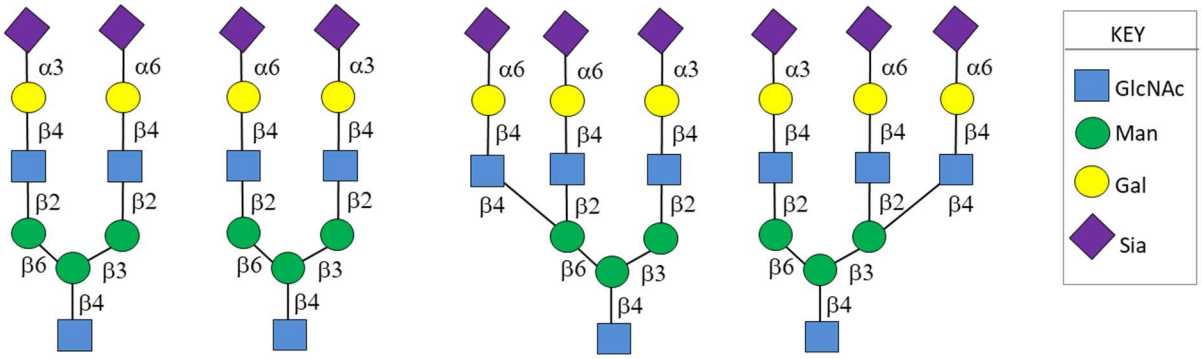

Figure 1.6: Schematic illustration of some of the major oligosaccharides isolated from Sialidosis Urine with internal cores of N-glycans.[53]

Knowledge of the structure of the isolated oligosaccharides allowed the definition of the nature of enzyme deficiency and also important information on glycoprotein biology. Here, the nature of the glycosidic linkage between monosaccharides and the proper glycan conformation could be determined by NMR studies concerning the glycosidic order of Sia residue.[53] Despite the diversity of glycoproteins in nature their carbohydrate components have

many common structural features. First branched N-glycans of plant origin were isolated from soybean agglutinin containing the same internal core as those from many animal glycoproteins, fungi and yeast (**Figure 1.7**).[57] Here, the triantennary highly mannosylated N-glycan was found identical to oligomannoside isolated from the Chinese hamster ovary cell membrane or bovine lactotransferrin protein.[58] The same triantennary oligosaccharide was isolated from major glycoprotein of mouse, cattle and human urinary bladder epithelium that can serve as the receptor for the FimH lectin adhesin of type 1-fimbriated *E. coli*, the organism that causes a great majority of urinary tract infections.[59] Due to this and many other pathogenic infections caused by host-pathogen interaction various synthetic glycomimetics were developed as potential inhibitors of pathogens from a different origin.[60] By the beginning of 20th interesting finding was reported from FIRON and coworkers showing that synthetic conformational isomer of the previously mentioned natural triantennary oligosaccharide isolate exhibited more than a 20 fold higher inhibitory activity for preventing *E.coli* adhesion.[61] Nevertheless, the function and biological activity of carbohydrates refer to their large prospective in glycobiological studies.[62] Glycobiology studies the structure, biosynthesis and biology of glycans which are widely distributed in nature. Some of these phenomenons are discussed in the following chapters of this thesis.

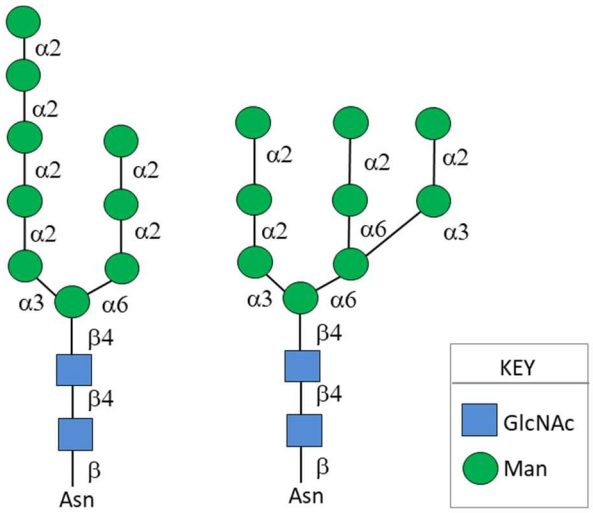

Figure 1.7: Schematic illustration of some of the major N-glycans found on internal cores of glycoproteins from different biological origins.

1.2 Multivalency in carbohydrate-protein interactions

Despite the isolation and characterization of many proteins and their carbohydrate ligands, the mechanistic details of the interaction between those fundamental molecules are still not fully understood. Many factors can potentially contribute to a complex carbohydrate-protein interaction. In the study of the agglutination process, it is hypothesized that the interaction between carbohydrates and proteins occurs in a multivalent manner, respectively through cross-linking interactions.[14] Here, plenty of carbohydrate copies on a cell surface interact with lectins, which are also found to interact in multiple modes (**Figure 1.8**). As suggested, the interactions between a single carbohydrate and a protein are rather weak and the binding affinity increases through complex binding mechanisms.[63] This phenomenon was first demonstrated by Y. C. LEE when investigating the ASHWELL receptor, contained out of a various number of terminal galactoside residues, that was exposed in binding to lectin with multiple numbers of CRD and elucidated the difference in 10,000-fold higher binding affinity for the ligand with an increased number of galactose residues.[64] This effect was termed as "cluster effect" by Y. C. LEE and coworkers employing low molecualr weight glycoclusters or bovine serum albumin (BSA)-conjugated neoglycoproteins, respectively.[14] This brought to the finding that many carbohydrate-protein interactions occur through a multivalent fashion.[65] Moreover, LEE and LEE also demonstrated that the binding affinity of multiple monovalent interactions add to an overall binding strength which is called aviditiy.

However, various investigations led to various postulations about the mechanisms of carbohydrate-protein recognition. Overall, multivalent interactions of ligands with receptors normally occur through intra- or intermolecular binding assuming a proper orientation of ligands. A proper pre-orientation of ligands is closely related to the well-known chelate effect.[66] One of the possible explanations for the high affinity of multivalent glycoligands is based on thermodynamics. In case of the chelate effect, entropy is significantly altered in every stage of the formation of a multivament carbohydrate-prtien complex, whereas enthalpy stays unchanged (**Figure 1.8**).

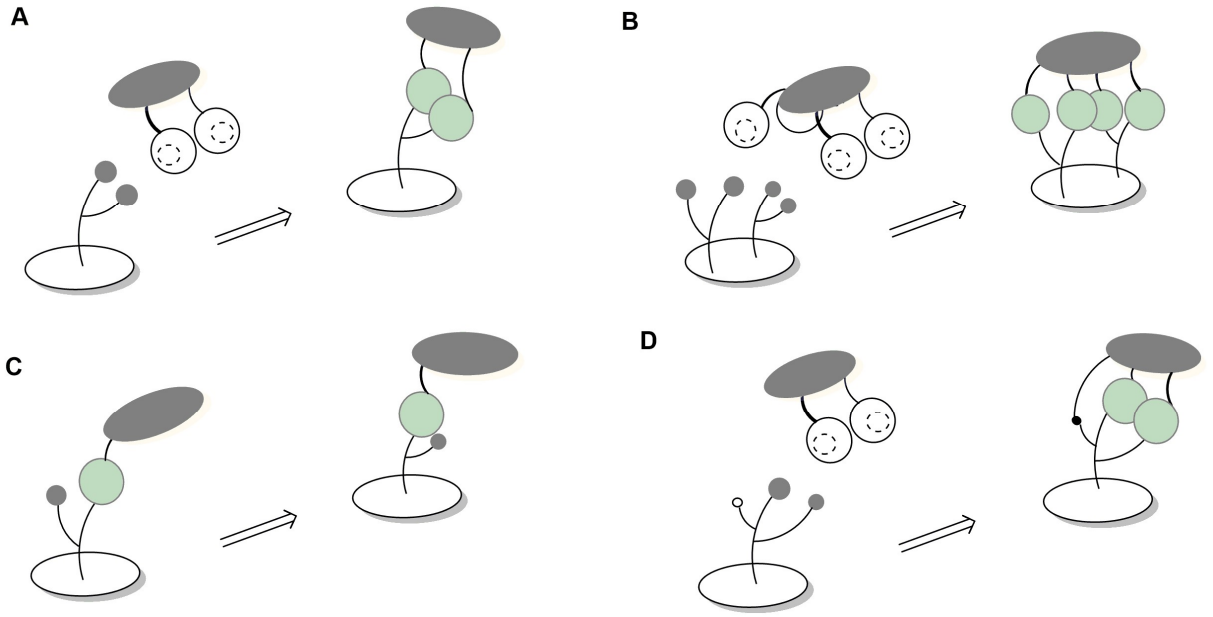

Figure 1.8: Mechanisms illustrations of possible ligand-receptor binding: (**A**) Chelation effect achieved by the perfect fit of divalent ligand to the divalent receptor;[67] (**B**) Illustration of multivalent binding what could bring to a receptor clustering;[68] (**C**) Statistical rebinding illustration of divalent ligand and monomeric receptor binding;[69] (**D**) Ligand subside unit binding with a secondary binding site of a receptor.[70]

One of many examples, where carbohydrate recognition is operated through the chelate effect is definitively the inhibition of Shiga like toxin (SLT) by the STARFISH ligand introduced by BUNDLE and coworkers.[71] The determined avidity in the inhibition of SLT and the importance of a multivalent effect seen in comparison of a pentavalent STARFISH ligand with a known monovalent trisaccharide ranges in the subnanomolar range. Namely, the translational, rotational, conformational and solvation-associated entropies were found as idealized factors for observation of carbohydrate-protein interactions. An interesting finding to demonstrate entropy importance for carbohydrate-lectin binding was illustrated through the rebinding mechanism. BREWER and coworkers reported this finding in the study of soybean agglutinin interactions (SBA), a tetrameric GalNAc specific lectin, with modified linear glycoprotein (mucin). Favorable binding entropy measured by isothermal titration calorimetry (ITC) was explained as binding and jumping of the lectin from GalNAc to GalNAc residue of the mucin.[69] This way we can also better understand the mechanism behind lectin binding to multivalent glycoconjugates. However, calorimetric studies are challenging and often lectin structural modifications are the main consideration to obtain high binding avidity. Interesting modifications were shown with designed model molecules for inhibition of norovirus-

es. A multivalent inhibitor with α-L-fucoside residue on polyacrylamide scaffold showed increased binding avidity to the virus once when a competitive ligand is attached, compared with the prototype ligand without a competitive ligand.[70] These types of ligands are found to interact with a secondary binding site of the receptor. A deeper and more conclusive understanding of multivalency effects in carbohydrate recognition may lead to potential inhibitors that would prevent microbial entry in host cells. Strikingly, it is assumed that human milk protects infants against noroviruses mostly due to the presence of multiple glycan chains attached to the viruses and thus preventing the infections. This again suggests that the designs of further multivalent ligand architectures are of major interest in developing the theory behind carbohydrate-protein interactions.

1.2.1 Mutlivalency in ligand design

Since it is known that lectin CRDs can be of homogeneous or heterogeneous nature, many glycoligands are synthesized according to this theory. Synthetic glycoligands with well-defined structures possess a considerable potential for the elucidation of the mechanism of carbohydrate binding. Different types of core molecules were employed to display synthetic oligo- and polysaccharides (**Figure 1.9**). One example is polyamidoamine core (PAMAM) made of the repetitively branched subunit of amide and amine functional group.[72] Spherical carbohydrate display of glycomimetics is in overall in close connection to the dendrimeric architecture of saccharides found in nature. Back to 1985 such an architectural model was integrated by NEWKOME and ever since was used for the synthesis of many glycodendrons.[73] Mostly small molecules are used as a core molecule for the preparation of branched and antennary oligosaccharides.

The well-known core molecules are tris(hydroxymethyl)methylamine (TRIS) or pentaerythritol (PE).[74] When carbohydrate ligands are ligated to small core molecules like TRIS or PE, the resulting molecules are called glycoclusters where in contrast to polysaccharides the polymer-based multivalent architectures are called glycopolymers. Different synthetic approaches facilitate the synthesis of homomultivalent glycoclusters and glycodendrimers, respectively. The ability to expand the focal point to a dendrimeric core provided some of the largest multivalent glycoconjugates.[75] A series of glycodendrimers were built while branching up the same parent dendrimeric core. This brought to the understanding of car-

bohydrate valency and the investigation of carbohydrates affinity for lectin binding. Furthermore, these are the main factors used in the study of multivalency effect. Furthermore, these are the main structural factors used in the study of multivalency effects. Overall, different types of multivalent glycoconjugates can be divided into linear, branched and cyclic architectures (**Figure 1.10**). Alternatively, an orthogonal functional group at the scaffold focal point allows further immobilization with different marker molecules (*e.g*. biotin linkers, porphyrins, peptides, or rhodamine fluorophores) or immobilization to various surfaces (*e.g*. gold, glass), respectively.

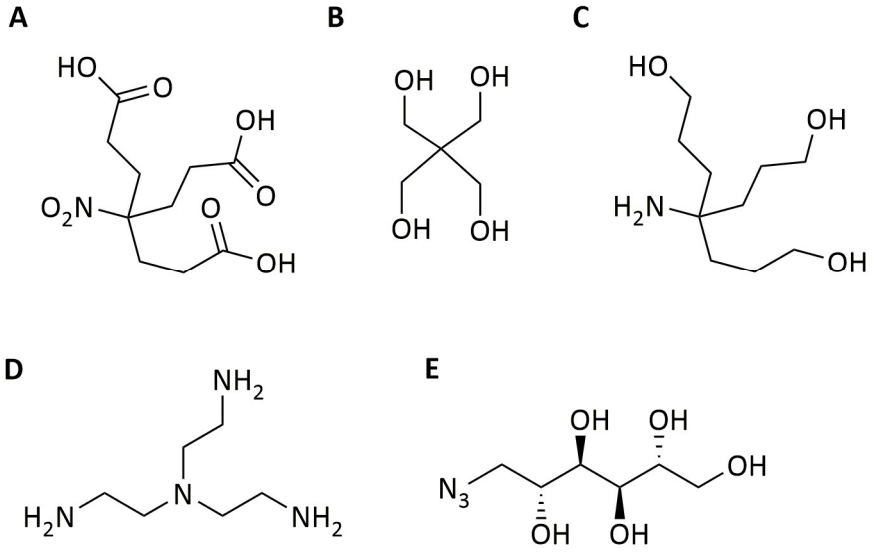

Figure 1.9: Different structures of core molecules employed in the synthesis of glycoclusters: (**A**) NEWKOME type scaffold, (**B**) Pentaerythritol, (**C**) TRIS (tris (hydroxymethyl) aminomethane), (**D**) Tris(2-aminoethyl) amine), (**E**) Mannitol scaffold.

To test more complex glycoligands that are structurally closer to the heterogeneous display of cell surfaces, first heteroglycoclusters were reported from the DANISHEFSKY group.[76] Glycopeptides connected to three different carbohydrate-based antitumor antigens were used for total synthetic vaccine development. Furthermore, LINDHORST and coworkers [77] reported an orthogonal protection strategy for mixed type glycodendrons employing glycerol and glycerol-glycol polyether scaffold. These were the first model molecules with distinct carbohydrate moieties conjugated with a scaffold molecule with an additional functional group at the focal point of the glycocluster. This way KATAJISTO and LÖNNBERG combined the benefits of orthogonal protection to obtain a small library of triantennary peptide glycoclusters.[78] Furthermore, GARCÍA FERNÁNDEZ and coworkers pointed out the importance of the "heterocluster effect" in their work with homo- and heteroglycoclusters based on β-cyclodextrins (βCD) and

tested with different lectins (ConA, PNA).[79] The term heterocluster effect refers to an increased binding affinity of a lectin to a glycocluster carrying various carbohydrate ligands.[79c] It was observed that the binding affinity of protein receptors for mixed type heteroglycoclusters exhibited higher affinity than those of homomultivalent clusters. The same group investigated the binding affinity of homomultivalent and heteromultivalent derivatives in high- and low-cluster density.[79b] Thus, ligand valency and density are both main parameters in carbohydrate recognition.

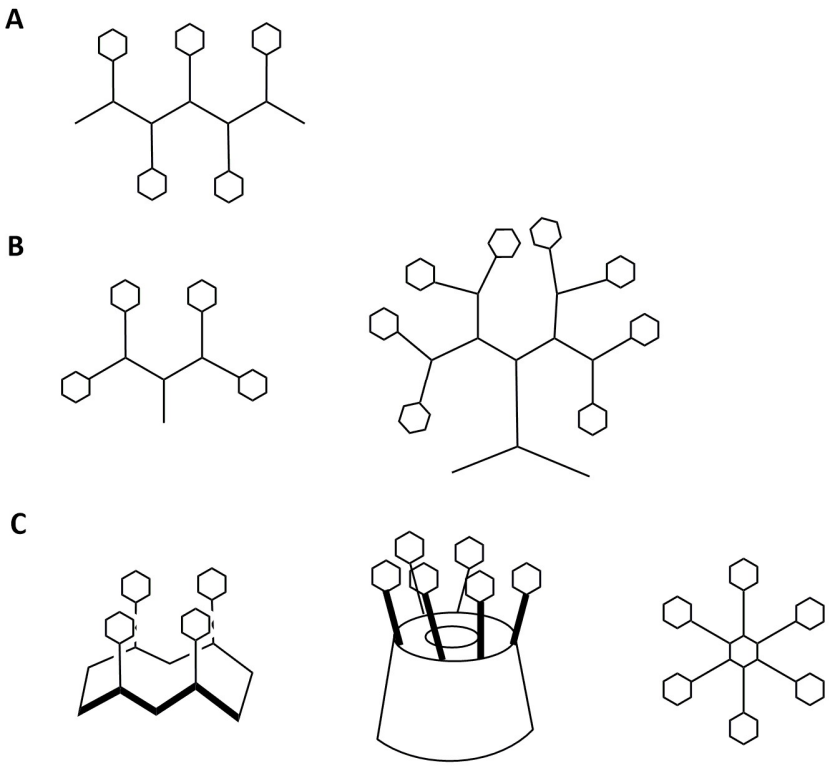

Figure 1.10: Schematic overview on some of the common core designs for glycan representation: (**A**) linear core for polymers and peptide assembly, (**B**) branched cores for dendron and dendrimer assembly, (**C**) cyclic cores for cyclopeptide, cyclodextrin and macrocycle assembly.

A series of glycoligands differing in homo/heterogeneity, in valency, nature of scaffolding, length of the linkers and in the nature of carbohydrate ligands were evaluated in recent years.[74, 80] The investigation of a variety of hetero- and homomultivalent ligands on surfaces allowed scientists to draw conclusions about multivalent natural ligand epitopes found on cell surfaces. Multivalency and the spatial orientation of carbohydrates contribute to overall binding avidity.[81] Mannopyranosyl assembly on the peptide backbone demonstrated in particular that scaffolding and epitope spatial orientation is one of the primary structural pa-

rameters for effective ligand recognition.[82] Furthermore, spatial and temporal orientation study with photoswitchable ligands, linked to the surfaces[83] provided more information on proper lectin recognition.[84] On the other hand, homovalent glycoconjugates for specific lectin recognition were used.[84b] The nature of lectin recognition in carbohydrate-protein interactions is often very difficult to define. For example, FimH adhesive lectin of *E. coli* bacterium, known to possess only one carbohydrate recognition domain, recognizes multivalent glycoligands.[85] Additionally, it is reported that especially many trivalent and tetravalent ligands exhibit higher binding affinity than monovalent ones. However, the attempt to investigate lectin binding affinity, the LINDHORST group referred to the concentration-dependent fabrication of glycoclusters in valency dependent adhesives on glycoarrays.[86] The cell surface presents a more heterogeneous and complex system than synthetically fabricated glycoarrays. A variety of multivalent synthetic ligands exhibited strong binding avidity but mostly the specificity of individual lectins and their unique characteristics are of higher interest to investigate carbohydrate-protein interactions in a deeper concern. Hence, the primary structural modifications of carbohydrate ligands are great tools to investigate the theory behind.

1.3 Modification of carbohydrate recognition through variation of asymmetric centers

More than 80 carbohydrate-binding lectins are identified up to date and many of them demonstrated high stereoselective binding specificity. The plant lectin ConA exhibits a higher binding affinity for α-D-mannosides than for β-D-mannosides.[87] Owing to their complex structural nature, proteins have the ability to discriminate between chiral substrates (**Figure 1.11**).

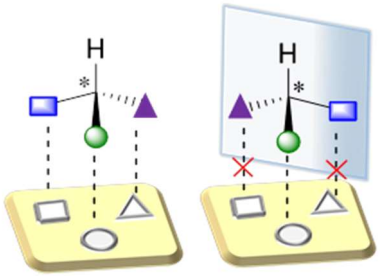

Figure 1.11: Illustration of stereoselective receptor recognition of chiral substrates in the binding mechanism.

Hence, the high enantiomeric purity and dedicated stereochemistry are one of the principal properties of chiral substrates involved in biochemical reactions.[88] To mimic the structural cell coat, different amino acids or carbohydrates were used as scaffold molecules in the epitope presentation of many glycoligands and their biological evaluation, respectively.[81b, 82, 89] Back in 1979, the amino acid lysine was used as scaffold molecule in seminal work of DENKWALTER reporting a first chiral dendrimer.[90] However, it was evaluated that mannopyranoside scaffolding on a peptide backbone exhibits a significant difference in inhibitory potency for lectin binding due to distinct carbohydrates spatial orientation.[82] Conformational flexibility of the peptide backbone allowed the formation of stereochemically controlled scaffolding for spatial carbohydrate orientation. Stereochemical communication between peptide and carbohydrate domains was previously studied showing that there are distinct and measurable differences in binding to stereochemically defined ligands.[91]

Apart from previous studies probably the first example referring on lectin selective binding to the stereospecific controlled configuration of carbohydrate ligands was reported by the REYMOND group.[92] A pair of stereoisomeric glycodendrimers was derived either from a D- or a L-configured peptide core. The formed pair of dendrimers exhibited distinct differences in the inhibition of LecB binding for *Pseudomonas aeruginosa* biofilms formation. For the sake of clarity, the glycopeptide dendrimer containing D-amino acid was designed to enhance dendrimer stability towards proteolysis. However, it was reported that the glycodendrimer based on an L-amino acid peptide core exhibited a 38-fold higher binding affinity to LecB than its stereoisomer, built on the respective D-peptide core. The bacterial C-type lectin LecB binds to L-fucose and D-mannose and conjugates of these two monosaccharides. Because D-mannose establishes hydrogen bonds via 6-OH group with the amino acid serine of LecB lectin the group of TITZ and coworkers hypothesized that the chirality at the C6 position and the orientation of 6-OH group, as well as neighboring aglyconic substituents of the C7 position at mannoheptose derivatives would influence on the lectin binding. A series of novel diastereomeric mannoheptoses were designed for the stereoisomeric examination of the binding affinity to LecB.[56c] The hypothesis that the configuration on the C6 position might influence on binding affinity was found promising. All mannoheptose derivatives with *S*-configuration on the C6 position exhibited higher binding affinity with a selectivity of a factor of three than their *R* configured isomers (**Figure 1.11**, molecules in section **A**). Moreover, the ability to modify the C6 position of D-mannose demonstrated the potentially in-

creased lectin specificity. In contrast to LecB, the other bacterial lectin of *Pseudomonas aeruginosa* LecA specifically recognizes D-galactose derivatives even in the µM range.[93]

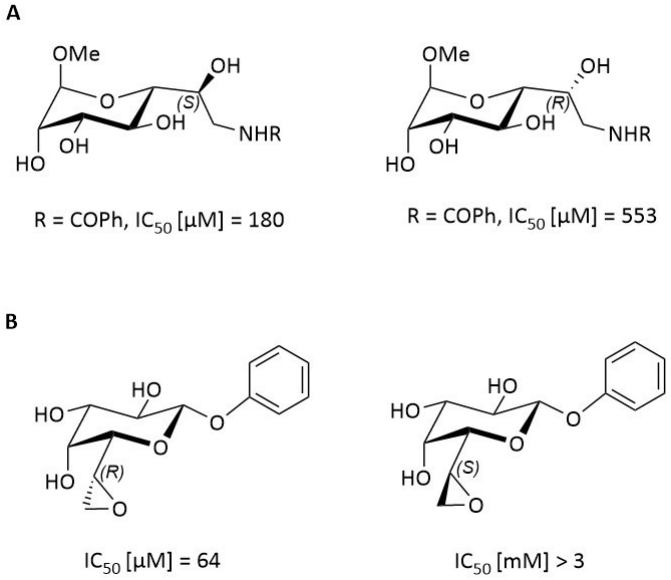

Figure 1.11: Inhibitory potency of isomeric pair of carbohydrate ligands for the inhibition of LecB (**A**)[93] and LecA (**B**)[94]

In order to determine whether the carbohydrate recognition domain of LecA lectin would display stereospecific properties similar to LecB, a pair of chiral epoxygalactoheptoses were designed.[94] Here, the stereochemistry of the examinated epoxides was used mainly for targeting cysteine residue (Cys69) in covalent binding to lectin active side and avoid dissociation from the lectin. The biological evaluation of prepared diastereomeric ligands indicated a distinct difference in stereoselectivity of LecA binding to prepared D- and L-glycoisomers (**Figure 1.11**, molecules in section **B**). The obtained data revealed that configuration of the asymmetric center of both ligands is a relevant parameter for further investigation of carbohydrate-protein interactions. In recent reports of antivirulence drugs, similar findings based on carbohydrate recognition revealed that the variation of the asymmetric center is relevant for inhibition of UTI biofilm formation.[95] The group of JANETKA and coworkers reported a series of isomeric hydroxymethyl C-mannoside ligands with improved pharmacokinetic properties for UPEC inhibition. The binding of FimH adhesive lectin of UPEC was evaluated with stereoisomeric C-mannosides. Additionally, the *C*-glycosidic bond of the same compounds was exchanged with the *O*-glycosidic bond to evaluate the ligand's metabolic stability. However, it was found that stereoselectivity of bacterial adhesive lectin FimH exhibits a 50-fold higher affinity in binding to *R*-isomeric ligand when compared to its *S*-configured

ligand. The structures of tested isomers with significant pharmacokinetic properties are shown in **Figure 1.12**. Here again it was shown that the stereochemistry of asymmetric centre siginificantly effected lectin binding. Thus, the study of ligand orientation through variation of the chirality of an aglyconic scaffold part might lead to a step forward for the more comprehensible understanding of carbohydrate-protein interactions.

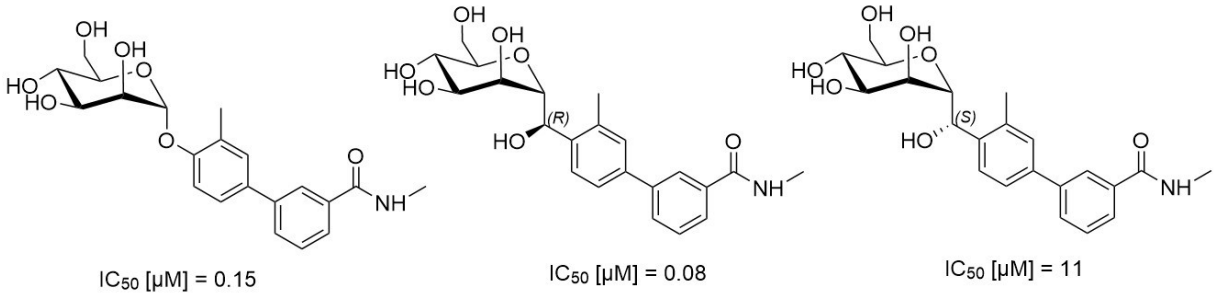

Figure 1.12: Inhibitory potency of stereochemically addressed *C*-glycosides for the inhibition of UTI biofilm formation.[95]

2 Objectives

Many of the life biological processes are regulated through carbohydrate-protein interactions. The importance of understanding these processes raised scientific interest in the formation of different glycomimetic architectures. Structural diversity, carbohydrate density, valency, and spatial orientation are some of the parameters varied in glycomimetics construction. Moreover, a variety of synthetic glycans were used to study the mechanism of the rather complex carbohydrate-protein interactions. Nature already demonstrated that rather specific and stereoselective events occur in biological systems. Many receptors are known as chiral and are therefore highly stereospecific in recognition processes. In this thesis, we aimed to investigate whether the variation of the configuration at the focal point of a glycocluster would affect lectin binding in different way. Variation of the focal point configuration allows the specific alteration of the relative carbohydrate orientation, such as in diastereomeric pairs of glycoclusters. Two main synthetic pathways were used in the synthesis of multifunctional enantiomeric scaffolds for the preparation of hetero- and homomultivalent glycoclusters (**Figure 2.1**). Asymmetric synthesis was employed to access enantiomeric tetrafunctional scaffolds while chiral pool synthesis was employed to stereoselective prepare trifunctional scaffold molecules.

In the third chapter, an asymmetric stereoselective synthesis combined with an orthogonal protection strategy is discused towards the synthesis of asymmetric heterotrivalent glycoclusters. Moreover, SHARPLESS epoxidation of primary alcohols allows the formation of asymmetric center and formation of desired compounds in high enantiomeric excess. Hence was used in the preparation of target tetrafunctional enantiomeric scaffolds. Tetrafunctional enantiomeric scaffold molecules carry three orthogonally protecting groups that were adjustable for the following glycosylation reactions. Once prepared, heterotrivalent glycoclusters can be used to investigate the nature of carbohydrate recognition. Enantiopure L- and D-serine amino acids were used in the derivatization of trifunctional enantiomeric scaffolds for homo- and heteromultivalent glycoclusters assembly. In chapter four the preparation of various divalent glycoclusters and their biological evaluation is discussed. Standard adhesion assays were used to test FimH-mediated bacterial adhesion and Concanavalin A binding to mannosylated surfaces. Adhesion assay is one of the methods used to test lectin binding

affinity under different environmental conditions.[96] Glycoarray assembly of pseudodiastereomeric glycoclusters are themed in chapter five, which focuses on the adhesion of type 1 fimbriated *E. coli* bacteria under static as well as under flow conditions.

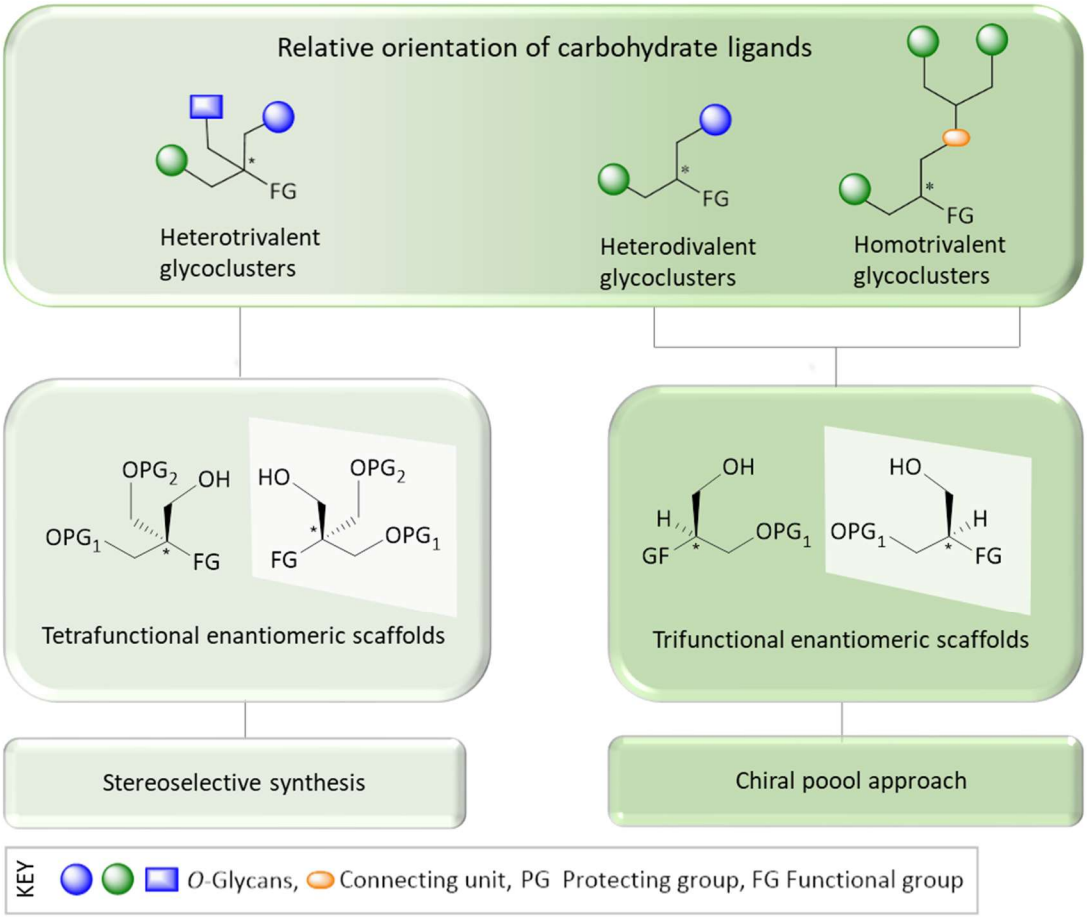

Figure 2.1: Schematic representation with the thesis thematics focused on the relative orientation of carbohydrate ligands on various enantiomeric scaffolds. Employed stereoselective synthesis and chiral pool approach are two main approaches used towards the synthesis of hetero- and homomultivalent glycoclusters.

The chiral pool approach was also used in the synthesis of trifunctional enantiomeric scaffolds for the formation of homomutivalent glycoclusters. Chapter six refers to the architecture of the formed scaffold that allows for the attachment of three identical carbohydrate motifs without racemization at the focal stereocenter. Additionally, the scaffold can be used for glycocluster mounting on various surfaces. In overall, carbohydrate relative orientation assembled on chiral scaffolding is a new promising scope for a better understanding of carbohydrate-protein interactions.

3 Asymmetric synthesis of enantiomeric tetrafunctional molecules for glycocluster assembly

It was LOUIS PASTEUR who first demonstrated molecular chirality and explained stereoisomerism.[97] Enantiomerically pure molecules that are mirror images of each other often exhibit a marked difference in biological activity because they interact with asymmetric receptors. Amino acids and carbohydrates are molecules from the chiral pool occurring as L- and D-stereoisomers and can be used as building blocks to provide a defined molecular morphology. Another way to control stereochemistry is the application of asymmetric catalysis. The demanding task of asymmetric catalysis is reaction enantioselectivity that favors the formation of one enantiomer or diastereoisomer over another. Our aim to control the configuration of the focal carbon center of tetrafunctional scaffolds relies on enantioselectivity achieved thanks to an appropriate catalyst. SHARPLESS asymmetric epoxidation of allyl alcohol derivatives is one method of choice to achieve high enantioselectivity, generally more than 90 % enantiomeric excess.[98] The catalysts involved in this reaction are asymmetric metal-coordinated complexes (titanium center) formed using enantiopure chiral ligands (tartaric acid derivatives) and thus providing chiral 2,3-epoxy alcohols from primary and secondary allylic alcohols (**Figure 3.1**).

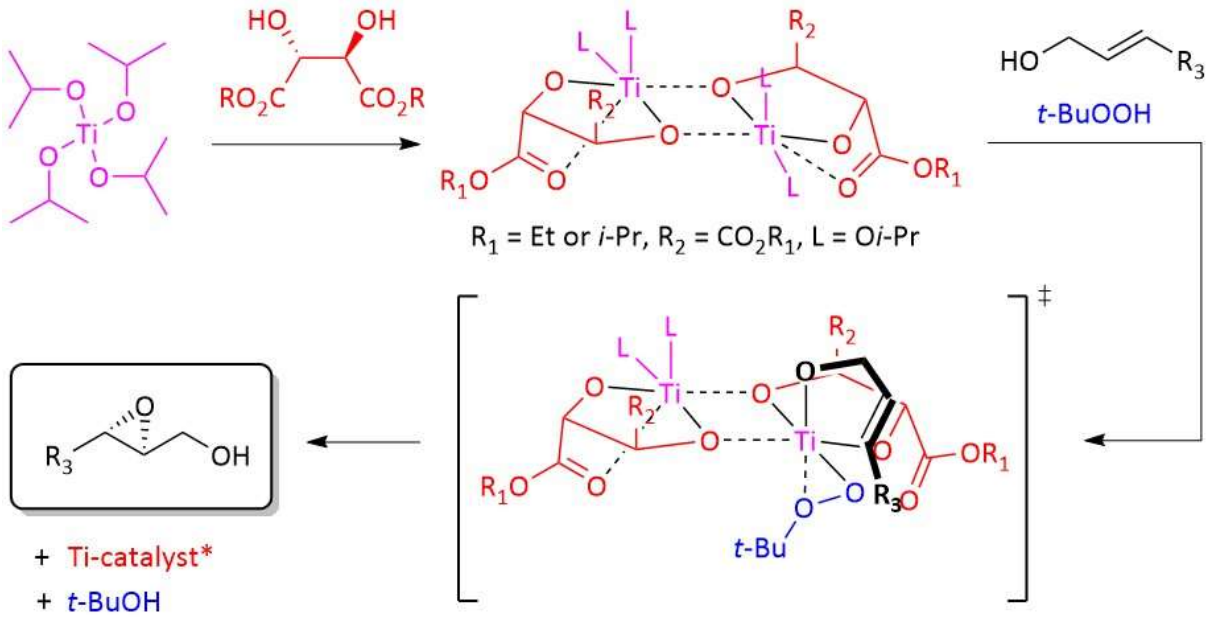

Figure 3.1: SHARPLESS enantioselective epoxidation of allylic alcohol is catalyzed by an asymmetric dinuclear titanium-tartrate complex. The allylic alcohol motif is essential for the formation of the reactive complex species.

After the formation of a dinuclear asymmetric titanium-tartrate complex, the oxidizing agent, generally a hydroperoxide, binds as a ligand to the titanium center. Then, the allylic alcohol substrate also complexes the same metal center than the hydroperoxide but at the opposite side and the enantioselective epoxidation takes place. One great advantage of this method is the predictability: according to a model defined by SHARPLESS, epoxidation catalyzed with (-)-tartaric esters occurs at the top face of the olefin while with the complex comprising (+)-tartrate ligands, the oxidation takes place at the bottom face (**Figure 3.2**).[98]

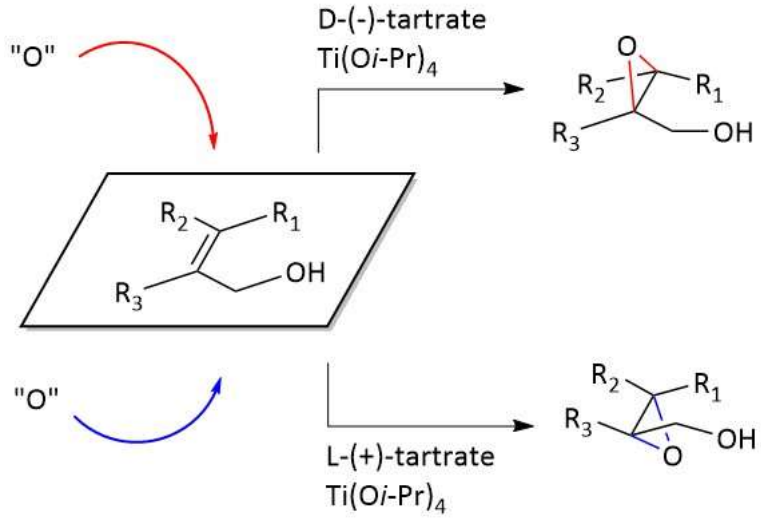

Figure 3.2. SHARPLESS' prediction rule for the stereochemistry of the resulting epoxy alcohol; "O" symbolizes the oxidant (generally a hydroperoxide).

In this chapter, is described the synthesis of tetrafunctional enantiomeric scaffolds **1a** and **1b** (**Figure 3.3**) using SHARPLESS enantioselective epoxidation as the key reaction.

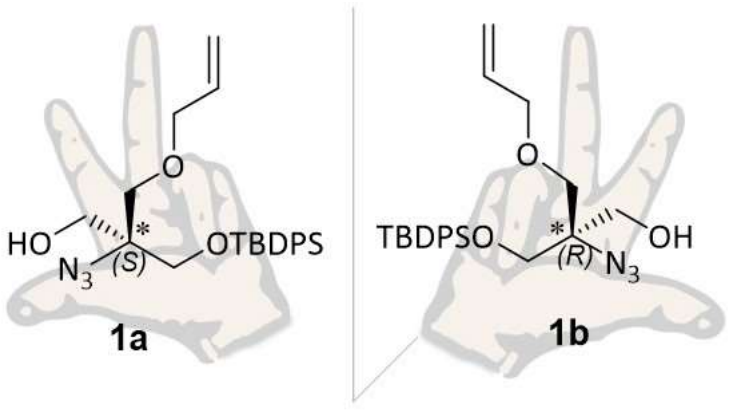

Figure 3.3: Tetrafunctional enantiomeric scaffolds **1a** and **1b** designed for the posiblle-formation of heterotrivalent glycoclusters.

Once prepared, the scaffolds can be used in the formation of different heterotrivalent glycoclusters. Variation in the scaffold glycosylation pattern with distinct carbohydrate motifs would bring to the formation of asymmetric glycocluster pairs. The defined stereochemistry at the scaffold's focal point would then be used to alter the relative carbohydrate ligand orientation in order to finally study putative asymmetric ligand recognition by a lectin. Furthermore, the prepared scaffold also allows a further preparation of glycoarrays through the immobilization of the glycoclusters on different surfaces.

3.1 Introduction of the focal stereocentre via SHARPLESS epoxidation and characterization of the chiral epoxy alcohols

The symmetrical allylic alcohol 2-methylene-1,3-propanediol **2** was used as the starting material in this synthesis (**Scheme 3.1**). First, it was selectively monoprotected introducing a *tert*-butyldiphenyl silyl (TBDPS) protecting group under basic conditions to give **3** in 76 % yield. SHARPLESS epoxidation using chiral tartrate diesters D-(-)-diethyl tartrate or L-(+)-diethyl tartrate (DET) allows the formation of two distinct epoxides with the opposite configuration on the quaternary asymmetric center. In general, the metalo-complex between tartrate and titanium (IV) isopropoxide, in the presence of *tert*-butyl hydroperoxide (TBHP) as the oxidizing agent, allows asymmetric epoxidation of allylic alcohol to be carried out only with 5 to 10 mol % of catalyst.[98] The configuration of resulting epoxides depends on the stereochemistry of chiral tartrate diester employed in the reaction. On the other hand, compound **3** displays the required alcohol directing group for epoxidation reactions. Epoxidation of the rather slowly reacting allylic alcohol **3** was successfully carried out by using a molar ratio (according to **1**) Ti/DETof 10:13, therefore furnishing **4a** and **4b** up to 83 % yield respectively.

The reaction was carried out in three distinct stages: Ti-DET complex formation, coordination of the hydroperoxide to the chiral complex, epoxidation upon addition of the allylic alcohol substrate. Each stage required a different temperature to achieve good conversion and high enantioselectivity (**Table 3.1**). Besides, the reaction time in each step was modulated for optimizing the process and the epoxidation was performed at different scales (100 mg to gram scale). It was observed that the epoxidation of allyl alcohol **3** on larger reaction scales (1-2 g) using (+)-DET showed higher enantioselectivity than the enantioselectivity achieved using (-)-DET catalyst. Also, high enantioselectivity of up to 91 % *ee* was achieved

using (+)-DET catalyst on a 1 g reaction scale under the described reaction conditions (cf. chapter 8, **Figure 8.11**).

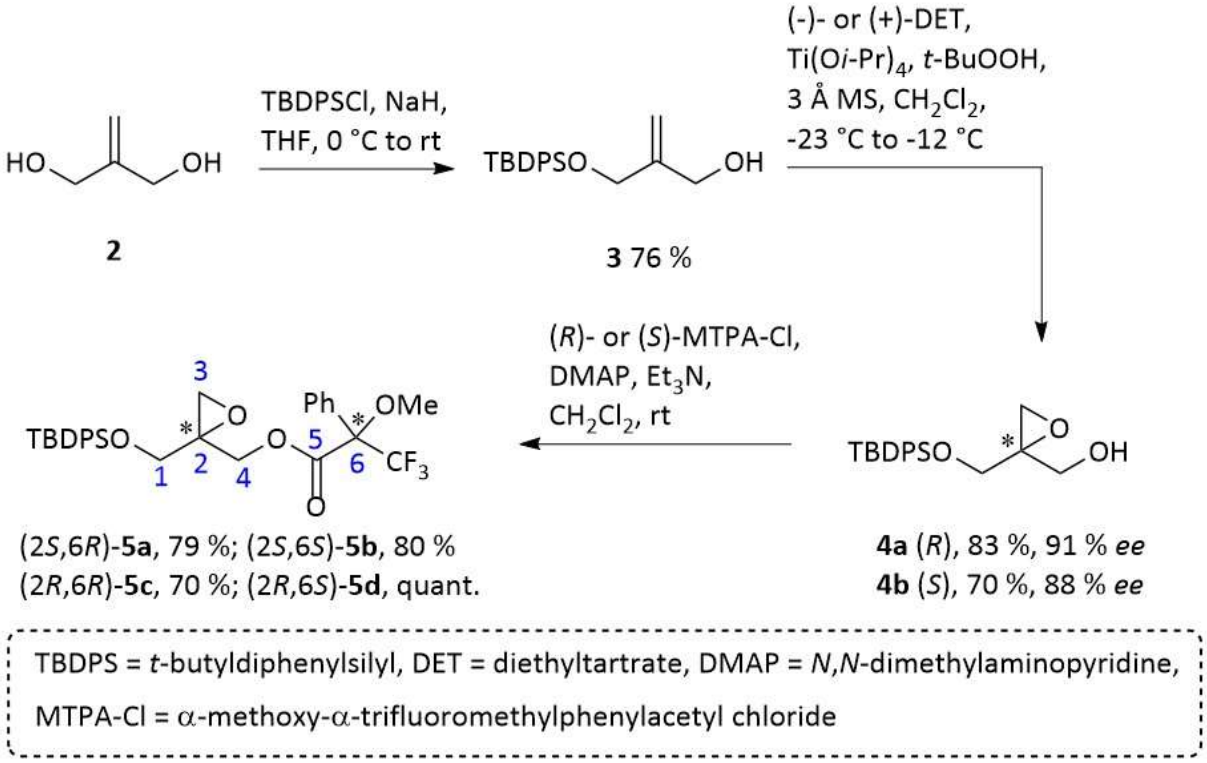

Scheme 3.1. Synthesis of enantiomeric epoxides **4a**/**4b** and installation of a focal stereocentre via SHARPLESS asymmetric epoxidation. The resulting epoxy alcohol enantiomers were respectively derivatized into diastereomeric compounds **5a** - **5d** using the acyl chloride of MOSHER acid.

Table 3.1: Reaction optimization for SHARPLESS epoxidation of primary allylic alcohol **3.**

Entry	Scale	Catalyst	Time A	Time B	Time C	Yield	*ee*
1	1.0 g	(+) DET	15 min	45 min	150 min	83 %	91 %
2	1.5 g	(-) DET	20 min	60 min	150 min	83 %	82 %
3	1.7 g	(+) DET	20 min	60 min	150 min	70 %	88 %
4	2 g	(+) DET	20 min	60 min	180 min	72 %	88 %
5	2 g	(-) DET	20 min	60 min	180 min	70 %	80 %

Step A: DET/Ti(O*i*-Pr)$_4$ complex formation at 0 °C.
Step B: Coordination of oxidizing agent t-BuOOH at -20 °C.
Step C: Epoxide formation at -23 °C.

To determine both the enantiomeric excess and the absolute configuration of the resulting stereocenter, the MOSHER ester method was used.[99] To this end, **4a** and **4b** were quantitatively reacted with *S*-(+)- or *R*-(-)-α-methoxy-α-(trifluoromethyl)phenylacetyl chloride (S-(+)- or R-(-)-MTPA-Cl) to provide a set of four diastereomeric ester products **5a** - **5d** (**Scheme 3.1**). Each respective pair of diastereoisomers (**5a**/**5b** and **5c**/**5d**) can there-

fore be investigated by NMR spectroscopy, showing distinct characteristic signals both in ^{1}H and ^{13}C spectra. In contrast to deuterated chloroform, ^{1}H NMR spectra measured in deuterated benzene showed sufficient signal splitting and were used for the determination of enantiomeric excess (*ee*) only. Hence, the *ee* values can be determined by measuring the integral ratio of the protons at position 3 (CH_2 position of the epoxide ring) in each respective pair of diastereoisomers (**Figure 3.4, A - B**). Consequently, the comparison of the pair **5a**/**5b** provides an enantiomeric excess of 82 % for the formation of epoxy alcohol **4a** while the comparison of **5c**/**5d** shows that **4b** was formed also in 88 % *ee*. Here depicted enantiomeric excess relates to the epoxidation of **3** which was carried out with both catalysts on a c.a. reaction scale of 1.5 g (**Table 3.1**, Entry 2 and 3).

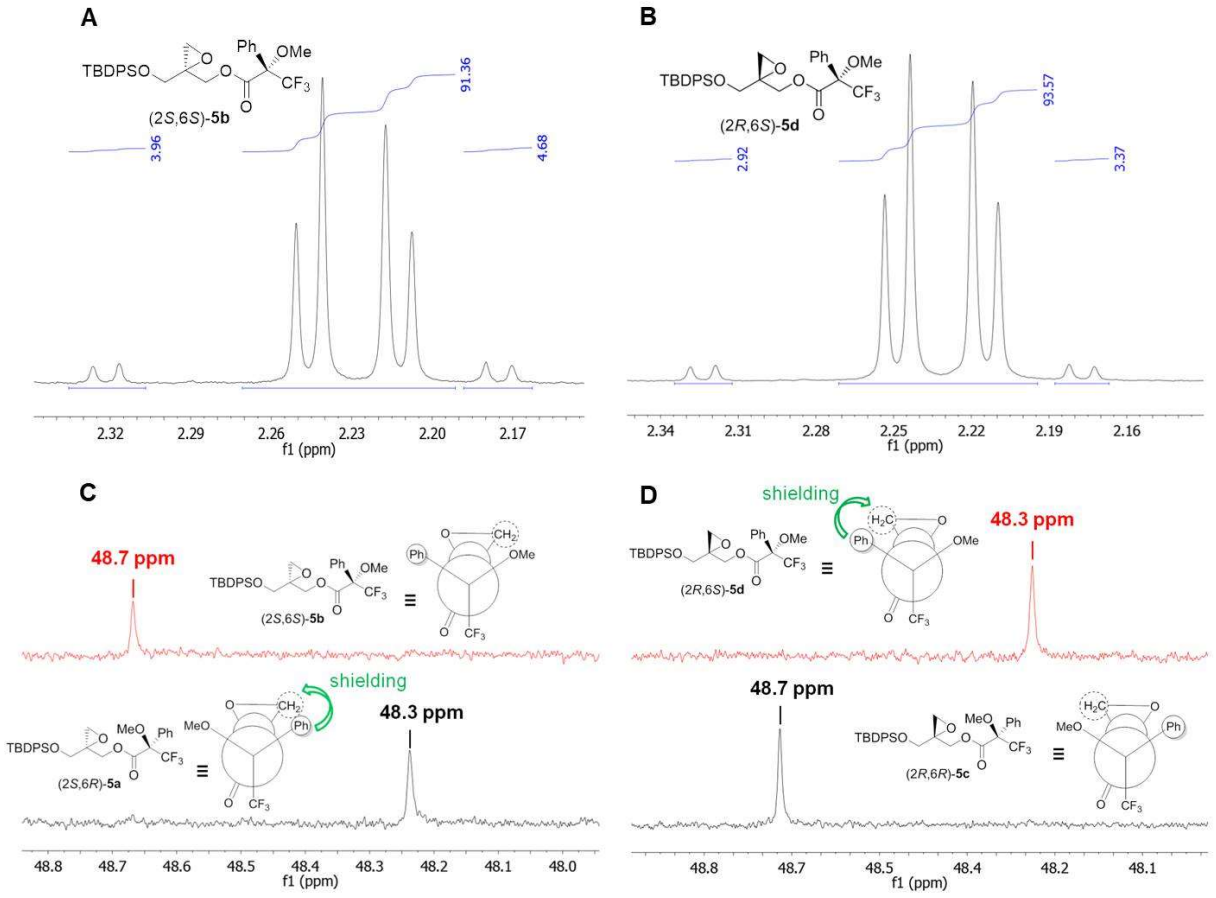

Figure 3.4. Analysis of the stereochemical outcome of the Sharpless epoxidation reaction. The enantiomeric excess was determined by comparing diastereomeric ratios obtained after derivatization of the epoxy alcohols **4a** and **4b** with (*R*)-(-)-MTPCl to give diastereoisomeric esters **5b** and **5d** (**A**, **B**); the stereochemistry of the epoxide was determined by comparing the respective chemical shifts of the C-3 position (CH_2 epoxide): a shielding effect should be observed when the phenyl group of the MOSHER ester is *syn* to the C-3 position (**C**, **D**).

The determination of the absolute configuration of the stereogenic center formed upon epoxidation was a more complex task. Based on literature reports, an empirical model described for chiral secondary alcohols was used (**Figure 3.4, C-D**). According to this model, the preferred conformer of the MOSHER ester should exhibit s-*trans* conformation for the ester O-C(O) bond while the CF_3 group and the C=O bond are coplanar. Although the conformational bias for compounds **5a** - **5d** may be different than those for esters derived from secondary alcohols, such a model was used for solving the stereochemistry of **4a** and **4b**. Therefore, it is expected to observe a magnetic shielding effect when the CH_2 group of the epoxide is *syn* to the phenyl ring of the MOSHER ester group (**Figure 3.4, C - D**). Based on the MOSHER method, ^{13}C NMR chemical shift of a certain carbon in the (*S*)-MTPA ester and the chemical shift of the same carbon in the (*R*)-MTPA ester are expressed using $\Delta\delta^{SR}$ parameter ($\Delta\delta^{SR} = \delta - \delta^{R}$). With the respect to the phenyl group of the MTPA moiety, the use of $\Delta\delta^{SR}$ expresses that the carbons that are shielded in the (*R*)-MTPA derivative give positive $\Delta\delta^{SR}$, while those that are shielded in the (*S*)-MTPA derivative give a negative $\Delta\delta^{SR}$ value.[99] All ^{13}C NMR chemical shifts of **5a** - **5d** were methodologically arranged and deduced $\Delta\delta^{SR}$ values were used to assign the absolute configuration of **4a** and **4b** (**Table 3.2**).

Table 3.2: Deduced $\Delta\delta^{SR}$ values from ^{13}C NMR (500 MHz C_6D_6) of **4a** (*R*) and **4b** (*S*) with (*S*)-MTPCl and (*R*)-MTPCl for the assignment of the absolute configuration. (*S*)-MTPCl results in (R)-MTPA ester where (*R*)-MTPCl results in (S)-MTPA ester of **5a** - **5d**. The values for ^{13}C NMR chemical shifts (δ) are measured in ppm.

	4a (*R*)			**4b** (*S*)		
Atom	δ (2*S*, 6*R*)-**5a**	δ (2*S*,6*S*)-**5b**	$\Delta\delta^{SR}$	δ (2*R*,6*R*)-**5c**	δ (2*R*,6*S*)-**5d**	$\Delta\delta^{SR}$
C-$1_{a,b}$	64.3	63.9	-0.4	63.9	64.3	+0.4
C-2	57.3	57.2	-0.1	57.2	57.3	+0.1
C-$3_{a,b}$	48.3	48.7	+0.4	48.7	48.3	-0.4
C-$4_{a,b}$	64.7	65.3	+0.6	65.3	64.7	-0.6

$\Delta\delta^{SR} = \delta^{S} - \delta^{R}$

As shown in **Figure 3.4**, the comparison of the chemical shifts of the peak corresponding to the C3 position in each pair **5a**/**5b** and **5c**/**5d** indicates that **5a**/**5b** are respectively (2*S*,6*R*)- and (2*S*,6*S*)-configured while **5c**/**5d** are respectively (2*R*,6*R*)- and (2*R*,6*S*)-configured. From these data, the configuration at the focal point could be assigned as *R* for **4a** and *S* for **4b**, respectively obtained in the presence of (-)- and (+)-diethyl tartrate. This is under the prediction according to the SHARPLESS rule for epoxy alcohol stereochemistry (see **Figure 3.2**). Moreover, this is also consistent with the comparison of the measured opti-

cal rotation values, which are given in the literature for similar structures (**cf. chapter 8, page 82-83**).[100]

3.2 Synthesis of the tetrafunctional chiral scaffold 1b

The key epoxy alcohol intermediates **4a** and **4b** were next reacted with trichloracetonitrile in the presence of the non-nucleophilic base diazabicycloundecene (DBU), providing 2,3-epoxy-1-trichloroacetimidates **6a** and **6b** in moderate yields (**Scheme 3.2**).[101] Upon treatment of **6a**/**6b** with a catalytic amount of diethyl aluminium chloride (Et_2AlCl) and the required presence of molecular sieves, an intramolecular cyclization reaction at the C-2 quaternary center resulted in the formation of oxazolines **7a** and **7b** by regioselective epoxide opening[102], respectively in 72 and 70 % yields. After this stage, only one of the two enantiomeric scaffolds was used for completion of the synthesis. Indeed, it was not possible to achieve the other enantiomer because of a lack of time.

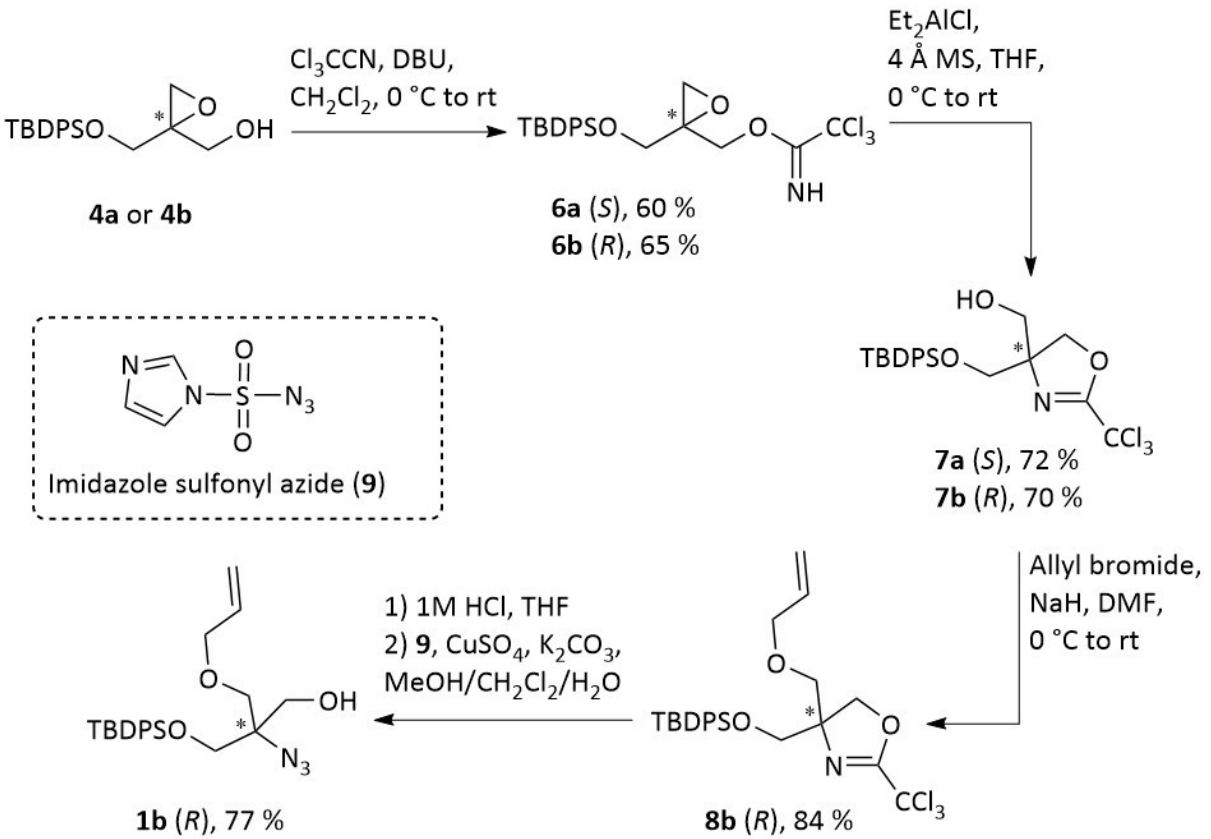

Scheme 3.2. Synthesis of tetrafunctionalized chiral scaffolds **1b** via formation of an oxazoline ring.

The newly generated primary hydroxyl group of **7b** was then protected under strongly basic conditions with an allyl ether group, furnishing **8b** in very good yield (84 %). With two primary alcohol groups orthogonally protected, a third primary hydroxyl function had to be installed on the chiral scaffold. For this purpose, the substrate **8b** was treated under mild acidic hydrolysis conditions to open the oxazoline ring, thereby forming an intermediate with a free amine at the focal point and free primary alcohol. A subsequent diazo-transfer reaction with imidazole sulfonyl azide hydrochloride **9**[103] under basic condition led to the formation of the target scaffold molecule **1b** in 77 % yield over two steps. The chiral scaffold molecule **1b** (**Scheme 3.2**) carries a free primary hydroxyl group and can be therefore used as a glycosyl acceptor in a further glycosylation reaction.

3.3 Mannosylation of the chiral scaffold

The azido group on molecule **1b** can be used for further ligand immobilization on surfaces. Also, this functional group is inert under a wide scope of reaction conditions, including acidic/strong acidic conditions, which is crucial for glycosylation reactions.

Glycosylation reactions of the chiral scaffold **1b** were carried out with perbenzoylated glycosyl donors since benzoyl protecting groups are known to be stable against migration under acidic conditions.[104] In a first glycosylation attempt, the thiomannoside donor **10**[105] was used, employing *N*-iodosuccinimide (NIS) and trifluoromethanesulfonic acid (TfOH) as promotor system (**Scheme 3.3**).[106] However, under these conditions, the expected glycosylation reaction did not take place probably due to a competition between the allyl group of the acceptor and the sulfide of the donor for the iodonium transfer. The donor could be recovered and no glycosylation activation occurred at this stage. The second attempt involved the trichloroacetimidate donor **11** under activation with boron trifluoride diethyl etherate. However, the reaction, in this case, didn't take place due to the donor hydrolysis. In a third try, donor **11** was used again, changing the promotor to trimethylsilyl trifluoromethanesulfonate (TMSOTf).[107] Also in this case, the reaction failed due to donor hydrolysis and the formation of a polar by-product that could not be isolated by column chromatography. Further optimization conditions for glycosylation of **1b** were not performed but the synthetic pathway was found suitable for the formation of tetrafunctional enantiomeric scaffolds toward the preparation of heterotrivalent isomeric glycoclusters.

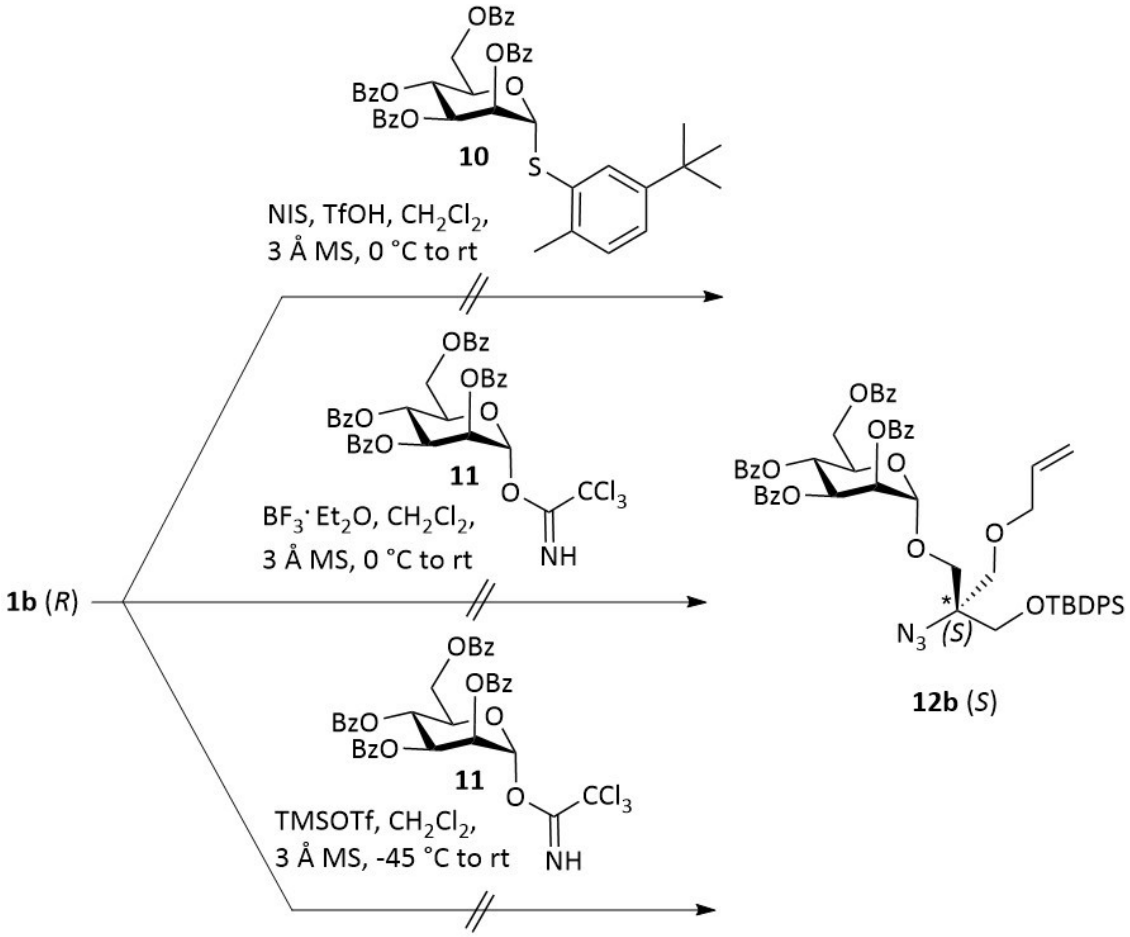

Scheme 3.3: Synthesis of **12b** in mannosylation attempts of **1b** with benzoylated thioglycoside and imidate donors.

On the other hand, a new synthetic pathway using the oxazoline derivative **7a** as glycosyl acceptor was implemented. The great advantage to use **7a** as a precursor molecule is that only one orthogonally protection group would be then used in the preparation of heterotrivalent isomeric glycoclusters (**Scheme 3.4**). This then results in 2 steps shorter synthetic pathways when compared to the previously presented pathway.

The glycosylation of **7a** was performed following KOENIGS-KNORR conditions[108], therefore using mannosyl bromide **13** as the donor, silver triflate as the promotor and the bulky non-nucleophilic base *sym*-collidine (2,4,6-trimethylpyridine) as a proton scavenger. Indeed, to prevent the acid-mediated opening of the oxazoline ring, and resulting racemization at the focal carbon, it was critical to buffer the glycosylation medium. The KOENIGS-KNORR glycosylation led to the formation of two main products: the target glycoside **14a** and the orthoester **15**, respectively isolated in 19 % and 51 % yield. For both products, the focal stereocenter remained intact, thanks to the neutral conditions, as proven by ^{1}H-NMR analysis (cf.

chapter 8, **Figure 8.27** and **Figure 8.29**). Each product was isolated as a mixture of two isomers, approximately in a 9:1 ratio; this is not surprising given that the batch of acceptor **7a** used in this glycosylation was obtained from an epoxidation reaction with an *ee* of c.a. 80 % and therefore an enantiomeric ratio of 9:1. Moreover, only the *exo* isomer of the orthoester **14** may have been formed during the glycosylation reaction, since no other isomer could be detected on the NMR spectra.

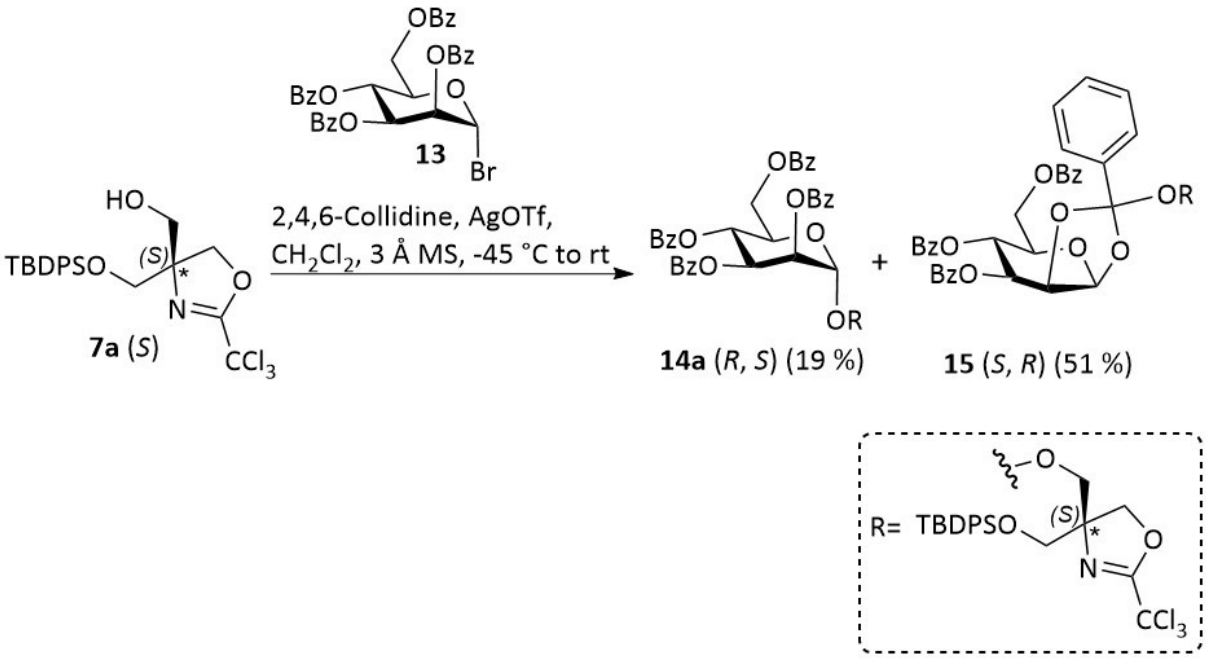

Scheme 3.4: Synthesis of **14a** in the second glycosylation approach involving the use of glycosyl acceptor **7a** under KOENIGS-KNORR conditions.

The predominance of orthoester **15** might be explained by the use of the base, which probably impaired the glycosylation pathway. In fact, the nucleophilic attack of the alcohol acceptor on the intermediate arising from the anchimeric assistance of the 2-*O*-benzoyl group can occur either at the anomeric carbon or the carbon atom of dioxolane ring, respectively giving the glycoside and the 1,2-orthoester products (**Scheme 3.5**). It is known that the second pathway is favored when the medium is neutral or even basic.[109] Also, the glycosylation reaction of **7a** by bromide **13** was further attempted using insoluble silver carbonate salt (Ag_2CO_3)[110] but this again led to an unsuccessful outcome with the orthoester formation. Alternatively, the 1,2-orthoester rearrangement using the Lewis acid trimethylsilyl trifluoromethanesulfonate (TMSOTf) as a catalyst could lead to the expected glycoside **14a**.[61a, 111] However, as written above, such reaction conditions could be detrimental for the oxazoline ring and may lead to the epimerization of the focal stereocenter. The experiments for the

scaffold glycosylation were not further pursued because even slightly acidic conditions would bring to non-selective glycosylation activation with the concomitant ring-opening of oxazoline on **7a**/**7b**. Based on these experimental facts, the study to obtain asymmetric heteroglycocluster pairs was later continued through the chiral pool approach for the preparation of divalent heteroglycoclusters as discussed in Chapter 4.

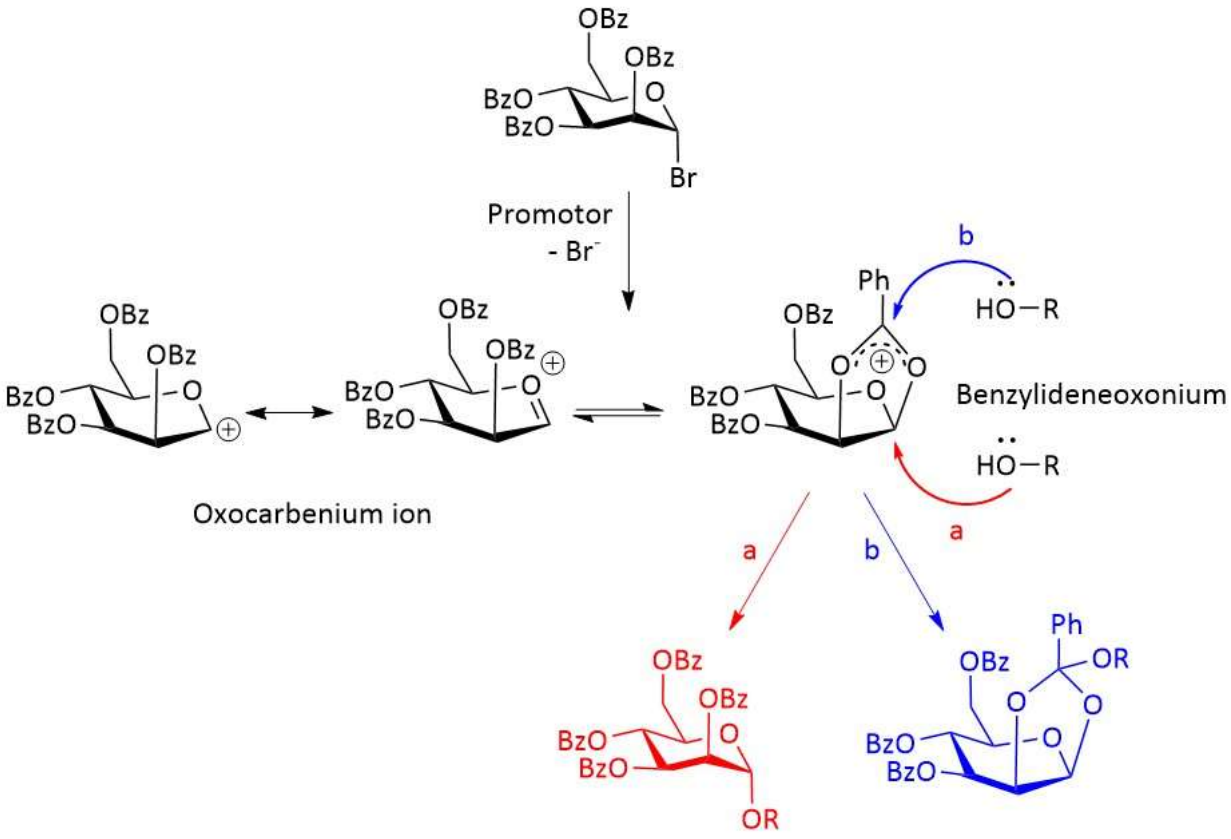

Scheme 3.5: Schematic pathways for a) glycosylation with the 2-*O*-benzoyl participating group (red pathway) and b) 1,2-orthoester formation resulting from the nucleophilic attack of the glycosyl acceptor on the carbon of the dioxolane ring (blue pathway).

3.4 Conclusion

In conclusion, the stereoselective synthetic approach using the well-known selective SHARPLESS epoxidation method allowed the formation of two distinct enantiomeric substrates for tetrafunctional scaffolds assembly. The highest obtained enantiomeric excess of 91 % with the described reaction conditions is strictly reaction scale-dependent. Often was found that high selectivity occurs on the larger reaction scale comparing to the smaller scale. Moreover, when the same reaction conditions for the epoxidation were carried out, the same reaction selectivity could not be observed for both catalysts. Thus was necessary to optimize reaction conditions at each stage. MOSHER ester analysis was applied after each performed epoxidation step to deduce enantiomeric selectivity. The absolute configuration of the formed enantiomeric epoxides could be deduced from their diastereomeric MTPA esters. Each enantiomer was reacted either with *S*-(+)- or *R*-(-)-α-methoxy-α-(trifluoromethyl)phenylacetyl chloride (S-(+)- or R-(-)-MTPA-Cl) to provide a set of four diastereomeric esters. Due to the magnetic shielding effect from the phenyl group of the MTPA moiety conformational skeleton of the formed esters could be determined. Thus, the epoxidation with (-)- and (+)-diethyl tartrate led to the formation of **4a** (*R*) and **4b** (*S*) epoxides with expected stereoselectivity. In the following synthetic pathway, the targeted tetrafunctional enantiomeric scaffold **1b** could be obtained in a relatively good yield. On the other hand, the glycosylation of the formed scaffold could not be carried out in a successful outcome and requires further reaction optimization. Here, we rather proceeded with a two-step shorter synthetic pathway for the formation of heterotrivalent glycoclusters and used oxazoline precursor molecule **7b** in the following glycosylation step. The advantage of such a synthetic pathway lies in the presence of only one protection group in the synthetic pathway towards the heterotrivalent glycocluster assembly. Glycosylation of **7a** applying the KOEGNIS-KNORR reaction conditions under neutral conditions was significantly altered by the 1,2-orthoester formation. However, the glycosylation of the enantiomeric scaffold **7a** was successful, and the first glycan moiety α-D-mannoside, could be addressed at this stage. For the proof of concept, it was found that the enantiomeric scaffolds formed in the synthetic route represent a potential for the glycosylation of various alcohols and the promising *en route* towards heterotrivalent glycoclusters assembly should be carried out in the future.

4 Chiral pool synthesis of enantiomeric trifunctional scaffold molecules for glycocluster assembly

4.1. Overview

Carbohydrate-protein interactions are intensively investigated in the context of cell-cell and host-cell interactions. The synthetic preparation of carbohydrate ligands and their biological evaluation are one of the principal approaches towards the investigation of carbohydrate-protein interactions. Synthesis of carbohydrate ligands is often a challenge. Structurally, glycans found on the cell a surface often consist of multiply branched epitopes and organized scaffolding. Moreover, they are found in the form of glycolipids or glycoproteins conjugated to chiral amino acids or lipids. The investigation of multiply displayed ligands with the variation of various other structural parameters should lead to a better insight into carbohydrate-protein interactions. Interestingly, lectins are highly specific for their carbohydrate ligands and minor differences in ligand orientation, for example, can influence lectin binding. The LINDHORST group has already demonstrated by the use of photoswitchable units that ligand orientation is of importance for proper lectin recognition.

Here a new strategy to vary carbohydrate orientation based on a chiral pool approach using D- and L-amino acids as starting materials was presented. In comparison to the stereoselective synthesis, the use of the chiral pool starting materials was of the advantage to provide a trifunctional enantiomeric scaffold with defined stereochemistry at the focal point. D- and L-serine gave access to the trifunctional enantiomeric scaffolds **10a** and **10b** for the putative variation of carbohydrate ligand orientation. The successful synthetic pathways applied in this approach allowed us to prepare a small library of heterodivalent diastereomeric pairs of glycoclusters.

Furthermore, we were able to perform binding studies with two different lectins, the plant lectin Concavalanin A (ConA) and *E. coli* bacteria, where carbohydrate recognition is mediated by the bacterial lectin FimH.[i] The two pseudoenantiomeric glucose-containing glycoclusters as inhibitors of FimH-mediated bacterial adhesion demonstrated striking differences in the inhibitory potencies. The pseduoenantiomeric ligand that is based on the L-serine-derived scaffold exhibited 20 times stronger inhibitory potency than D-serine derived

analog (**Figure 4.1**). This work was published as a full paper and all overcome synthetic barriers are part of the following paper.

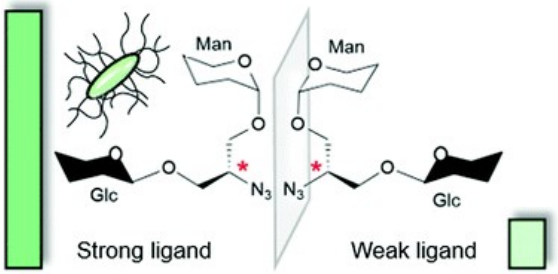

Figure 4.1: Difference in inhibitory potency between diastereomeric glucose-mannose glycocluster pairs for type 1 fimbriated *E. coli* bacterial adhesion.[104]

[i] For the interpretation of the binding assays (cf. **Fig.2** in publication tables S1-S10 in supporting information) valency-corrected (vc) relative inhibition potencies (RIP) for the divalent cluster mannoside **6** were obtained by dividing the respective RIP by two. Alternatives to this calculation of RIP_{vc} values can be considered in the future, such as valency correction based on measured IC_{50} values.

4.2 Published paper: "Pseudoenantiomeric glycoclusters: synthesis and testing of heterobivalency in carbohydrate-protein interactions"

Reproduced from:

Jasna Brekalo, Guillaume Despras and Thisbe K. Lindhorst

Org. Biomol. Chem., 2019, **17**, 5929-5942.

DOI: 10.1039/C9OB00124G

with permission from The Royal Society of Chemistry.

Own contribution: The synthesis of all molecules, their analytical and biological studies were performed by Jasna Brekalo under the supervision of Dr. Guillaume Despras and Prof. Dr. Thisbe. K. Lindhorst. Molecular modeling was done by Dr. Guillaume Despras. The manuscript was written by all three authors. The final manuscript was submitted by Prof. Dr. Thisbe. K. Lindhorst. The cover image was drawn by Julia Hain.

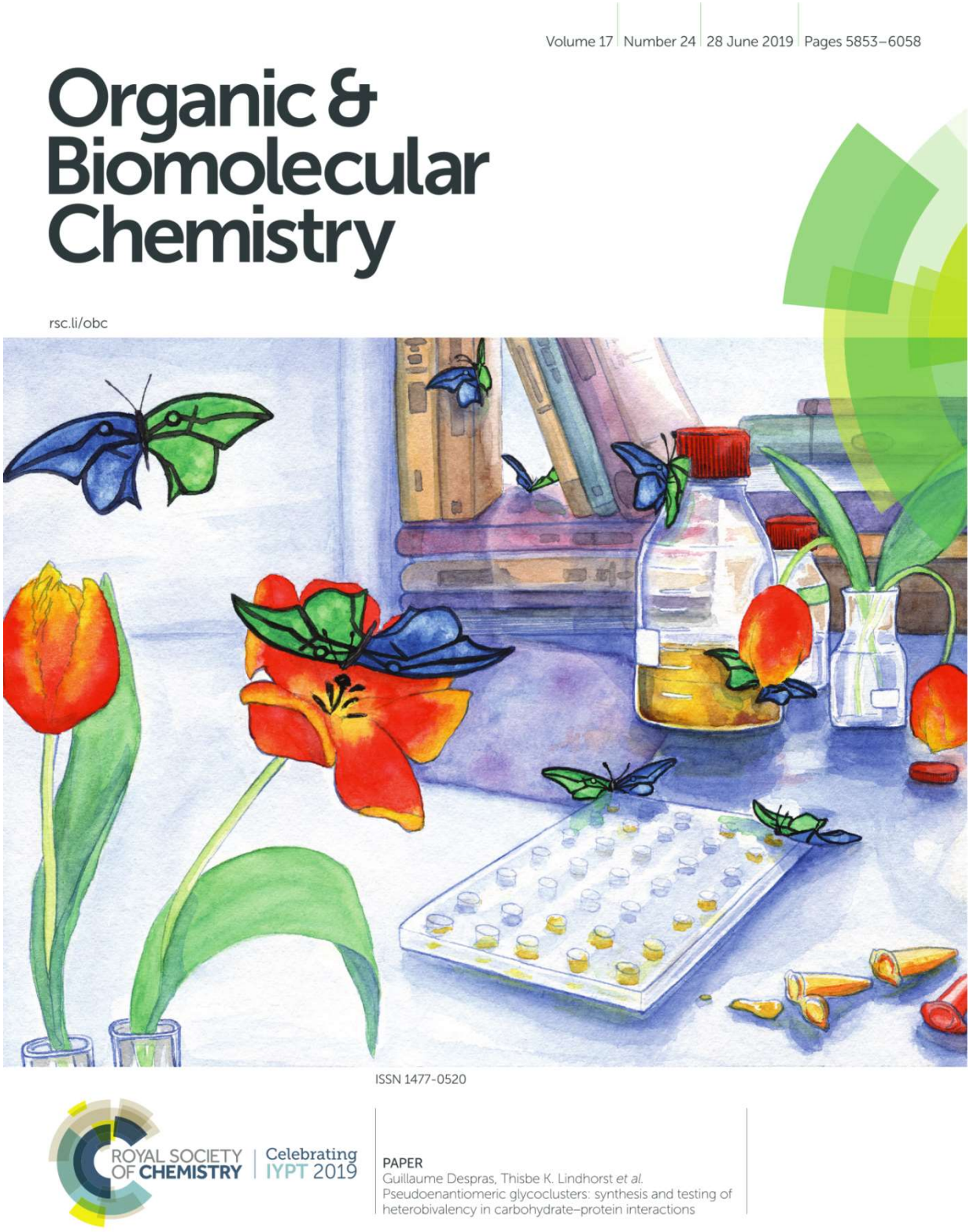

The cover image was drawn by Julia Hain.

Organic & Biomolecular Chemistry

PAPER

View Article Online
View Journal | View Issue

Cite this: *Org. Biomol. Chem.*, 2019, **17**, 5929

Pseudoenantiomeric glycoclusters: synthesis and testing of heterobivalency in carbohydrate–protein interactions†

Jasna Brekalo, Guillaume Despras * and Thisbe K. Lindhorst *

Multivalent carbohydrate–protein interactions are key events in cell recognition processes and have been extensively studied by means of synthetic glycomimetics. To date, frequently the valency, *i.e.* the multiplicity of the ligand attached to a polyvalent scaffold, has been considered in the design of multivalent structures but these studies have not led to a conclusive understanding of glycan recognition at the molecular level. In this work, we add a new aspect to carbohydrate–lectin recognition studies by designing the first heterobivalent diastereomeric glycoclusters in order to investigate the influence of both heteromultivalency and relative ligand orientation. Two enantiomeric scaffolds, derived from D- and L-serine, respectively, were glycosylated with two distinct carbohydrate ligands to obtain a library of pseudoenantiomeric glycoclusters. They all have an α-D-mannosyl residue in common as a specific ligand for lectins FimH and ConA, while they differ in the second carbohydrate portion, consisting of a β-D-glucosyl, a β-D-galactosyl or a β-D-glucosaminyl residue as unspecific ligands. The synthesised heteroclusters were tested in standard binding-inhibition assays investigating FimH-mediated bacterial adhesion and ConA binding to mannosylated surfaces. A striking difference was observed between the potencies of the two pseudoenantiomeric glucose-containing glycoclusters as inhibitors of FimH-mediated bacterial adhesion. For the other diastereomeric glycocluster pairs smaller inhibitory potency differences were detected in the bacterial adhesion assay. In contrast, the assays with ConA showed no significant variation for all tested cluster pairs. The results obtained with the diastereomeric glucose–mannose glycocluster pair were rationalised by molecular docking. Binding energies for the FimH carbohydrate recognition domain were calculated for both diastereomers and are in agreement with experimental data obtained in the bacterial adhesion assays.

Received 16th January 2019,
Accepted 3rd April 2019

DOI: 10.1039/c9ob00124g

rsc.li/obc

Introduction

Cell surface carbohydrates play an essential role in key cellular communication processes, which are, *i.a.*, mediated by carbohydrate–lectin interactions. These include signalling, cell trafficking and cell adhesion.[1] In particular, the adhesion of pathogens to tissues, an initial step in infection, is often mediated by the specific recognition of host cell glycoconjugates by pathogen adhesins (lectins).[2] For instance, the adhesion of uropathogenic *E. coli* bacteria (UPEC) to the endothelial cells of the host organism occurs through binding of α-mannosyl residues by the bacterial lectin FimH, which is located at the tips of the so-called type 1 fimbriae.[3] Fimbriae are adhesive organelles, projected multiple times from the bacterial cell surface.[4] Hence, carbohydrate-specific bacterial adhesion clearly relies on multivalent interactions between cell surfaces.

As manifold copies of a variety of carbohydrate epitopes are expressed on cell surfaces, multivalent interactions with lectins, which often possess several recognition domains, lead to strong binding as a result of a proper combination of single low-affinity interactions in a cooperative fashion. This cluster effect has long been known[5] and has been exploited extensively, in particular employing synthetic polyvalent glycomimetics. These studies have advanced our understanding of carbohydrate–protein interactions and have also opened the door to the application of carbohydrates as antiadhesives to treat infectious diseases.[6]

However, multivalency effects in carbohydrate recognition are not conclusively understood as yet. While some of the synthetic multivalent glycomimetics were able to bind lectins with high avidity (up to the picomolar range),[7] others unexpectedly

Christiana Albertina University of Kiel, Otto Diels Institute of Organic Chemistry, Otto-Hahn-Platz 3-4, D-24118 Kiel, Germany. E-mail: gdespras@oc.uni-kiel.de, tklind@oc.uni-kiel.de

†Electronic supplementary information (ESI) available: Synthetic procedures, NMR spectra, biological testing with inhibition curves, and molecular modelling data. See DOI: 10.1039/c9ob00124g

View Article Online
Paper Organic & Biomolecular Chemistry

exhibited poor binding ability despite of a large number of displayed ligands.[3b,6d] In light of these contrasting results, it was important to investigate multivalency effects in an extended and advanced way than taking into account only the multiplicity of the sugar epitope.[8] For instance, appropriate distances between ligands, their spatial arrangement and the flexibility of the linker moieties are important factors and have been investigated in several studies.[9] In order to test more complex glycoconjugates which are structurally closer to the heterogeneous sugar coat of eukaryotic cells (glycocalyx), García-Fernández and coworkers prepared heteroglycoclusters and evaluated their glycobiology. Strikingly, these compounds showed a remarkable "heterocluster effect" towards binding to lectins such as concanavalin A (ConA) and peanut agglutinin (PNA), in comparison with their counterparts displaying only the specific lectin ligand.[10] With these findings, a new thinking about multivalency effects in carbohydrate recognition has begun.[11]

Furthermore, some reports showed that the presentation mode of carbohydrate ligands on a surface is also critical for proper recognition by lectins.[12] Among others, our group showed that the specific recognition of α-D-mannosyl residues by the lectin FimH is clearly impacted by the orientation of the sugar epitopes. This was demonstrated by using photoswitchable azobenzene mannosides attached onto gold surfaces (glycoSAMs) or the surface of human cells to systematically reorient sugar ligands.[12b,c]

Based on the reported findings, we believe that multivalency effects in carbohydrate recognition strongly depend on the three-dimensional organization of carbohydrate ligands and glycoepitopes, respectively.[13] In order to further investigate how the relative positioning of ligands governs sugar recognition, we approached a new design of heterobivalency in which two different sugars are arranged on enantiomeric scaffold molecules. This leads to a pair of diastereomeric glycoclusters, which can be regarded as pseudoenantiomers with respect to the configuration at the focal point of the scaffold moiety (Fig. 1A). Hence, the sugar ligands conjugated in a particular bivalent heterocluster are displayed in different relative orientations. We targeted three principal heterobivalent pseudoenantiomeric glycocluster pairs, combining β-D-glucopyranosyl (Glc), β-D-galactopyranosyl (Gal) and β-D-glucosaminyl (GlcNHR) moieties, respectively, with an α-D-mannopyranoside (Fig. 1B).

The diastereomeric pairs of heterobivalent glycoclusters are based on scaffold molecules derived from D- and L-serine, respectively. These enantiomeric α-amino acids were converted into the respective mono-protected 2-azido-propanediol derivatives (Fig. 1C) and subjected to two sequential glycosylation reactions, employing suitable glycosyl donors to achieve the target glycoclusters βGlc-αMan, βGal-αMan, and βGlcNAc-αMan. In order to have a bivalent reference compound in hand, we also prepared the respective homobivalent mannose glycocluster $(\alpha Man)_2$ from the symmetrical diol 2-azido-propanediol (Scheme 1). As our synthetic approach is based on enantiomeric bivalent scaffold molecules from the chiral pool, it is highly flexible and allows for the rapid preparation of

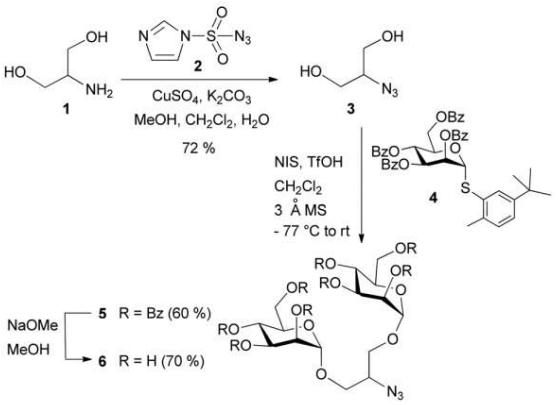

Scheme 1 Synthesis of the homobivalent cluster mannoside **6**.

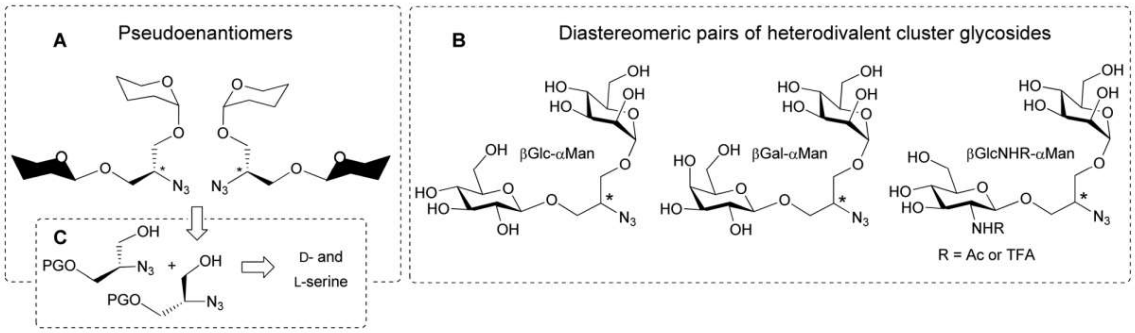

Fig. 1 Pseudoenantiomeric cluster glycosides (A) were targeted, comprising two different carbohydrate moieties (black and white chairs), and differing in the configuration at the focal point stereocenter (*) of the scaffold moiety. Four diastereomeric pairs of heterobivalent glycoclusters were synthesised (B), βGlc-αMan, βGal-αMan, βGlcNHR-αMan, together with the analogous homobivalent mannoside cluster $(\alpha Man)_2$ for comparison (not shown, *cf.* Scheme 1). The diastereomeric glycoclusters were built on mono-protected 2-azido-propanediol enantiomers (C), which were derived from D- and L-serine as enantiopure chiral pool scaffold molecules. TFA = trifluoroacetyl; PG = protecting group.

View Article Online
Organic & Biomolecular Chemistry Paper

libraries of "mirror image" glycoclusters, without the need for separation of diastereomers during the synthesis. The employed carbohydrates – mannose, glucose, galactose, and GlcNAc – were selected for their biological relevance as lectin ligands. All cluster glycosides prepared herein were thus tested in binding studies, on the one hand with the plant lectin ConA[14] and on the other hand in bacterial adhesion studies with live type 1-fimbriated *E. coli* bacteria, where carbohydrate binding is mediated by the adhesin FimH.[3]

Results and discussion

Synthesis

At first, we required the homobivalent mannoside cluster **6** (Scheme 1) as a reference compound for later testing of heterobivalency effects. The synthesis of **6** was accomplished in three steps starting from serinol (**1**), which was converted into the respective azido-functionalised diol **3**[15] with imidazole sulfonyl azide (**2**)[16] in 72% yield. The bivalent scaffold **3** was then glycosylated using the known thiomannoside **4** as a glycosyl donor.[17] The mannosyl donor **4** was activated at −77 °C with *N*-iodosuccinimide (NIS) and a catalytic amount of triflic acid.[18] Then, the reaction mixture was allowed to warm to room temperature over three hours to provide the benzoyl-protected bivalent cluster mannoside **5** in 60% yield after work up and purification. Deprotection of **5** with sodium methoxide in methanol gave the pure target molecule **6**.

The synthesis of the targeted diastereomeric pairs of heterobivalent cluster glycosides (Fig. 1B) was based on D- and L-serine, **7a** and **7b**, respectively, as enantiopure chiral pool compounds (Scheme 2). First of all, the α-amino function of each enantiomeric amino acid was Boc-protected under standard conditions,[19] and the resulting crude material was directly converted into the respective methyl ester in the presence of iodomethane and potassium carbonate. The enantiomeric serine derivatives **8a** and **8b** were thus received in 79 and 82% yields, respectively, over two steps.[20] In order to block the primary alcohol of the serine scaffold, the *tert*-butyldiphenylsilyl (TBDPS) ether was used and introduced with *tert*-butyldiphenylsilyl chloride and imidazole.[21] The resulting crude silyl ethers were used in the next reduction step with lithium borohydride and after purification, the alcohols **9a** and **9b** were both obtained in 90% yield over two steps. We also tried to reduce the methyl esters with lithium aluminium hydride, but remarkably, this gave only poor yields. The primary alcohols **9a** and **9b** were further used as acceptor molecules in the first glycosylation step. However, we found that the *N*-Boc protecting group was labile under the acidic conditions required for the glycosylation reaction, whereas under the same conditions the TBDPS group was stable. Therefore, compounds **9a** and **9b** were first treated with trifluoroacetic acid in order to cleave the *N*-Boc group and the resulting free amines were converted into the respective azides in a diazo transfer reaction employing **2** under similar conditions as described above.[16] The two enantiomeric scaffold molecules **10a** and **10b** were isolated in 80% and 79% yields, respectively, over two steps. Notably, no racemization was observed in any of the described steps.

With the enantiomeric building blocks **10a** and **10b** in hand, the first glycosylation reaction was carried out to obtain the pivotal mono-mannosylated acceptor molecules as precursors for the synthesis of all bivalent heteroclusters. As expected, the glycosylation of **10a** and **10b** proceeded much better compared to when the carbamates **9a** and **9b** were employed. In the first mannosylation attempts, the well-known tetraacetylated α-D-mannosyl trichloroacetimidate[22] was used as the glycosyl donor. However, the resulting glycosides were isolated in only unsatisfactory yields (36 to 56%) which we could not further optimise. This was due to acetyl migration resulting in the acetylation of the acceptor alcohol.[23] Thus, we used the benzoylated thiophenyl mannoside **4**,[17] as benzoyl groups are less prone to acyl migration under acidic conditions.[24] The thioglycoside **4** was again activated under standard conditions employing NIS and triflic acid to provide the mannosides **11a** and **11b** in very satisfactory yields of around 80%. Then, the subsequent desilylation with TBAF (*n*-tetrabutylammonium fluoride) afforded compounds **12a** and **12b**

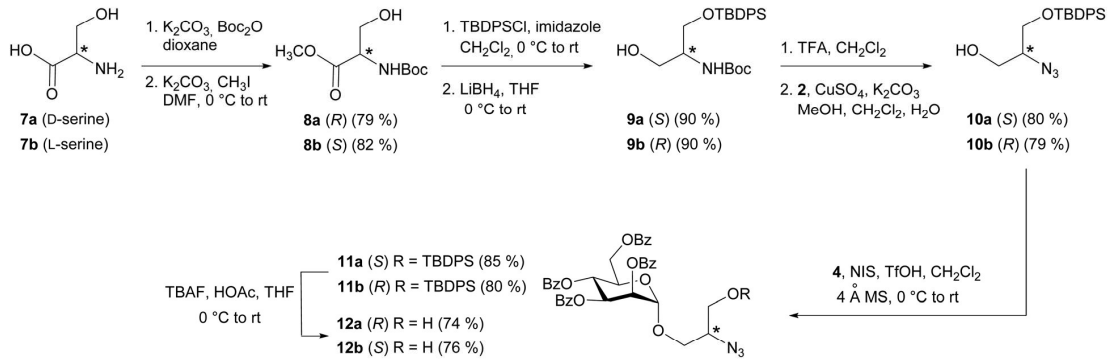

Scheme 2 Synthesis of a diastereomeric pair of mannosides, derived from D- and L-serine as enantiopure scaffold molecules from the chiral pool. The obtained mannosides **12a** and **12b** were needed as acceptor alcohols for all following glycosylation reactions (*cf.* Scheme 3).

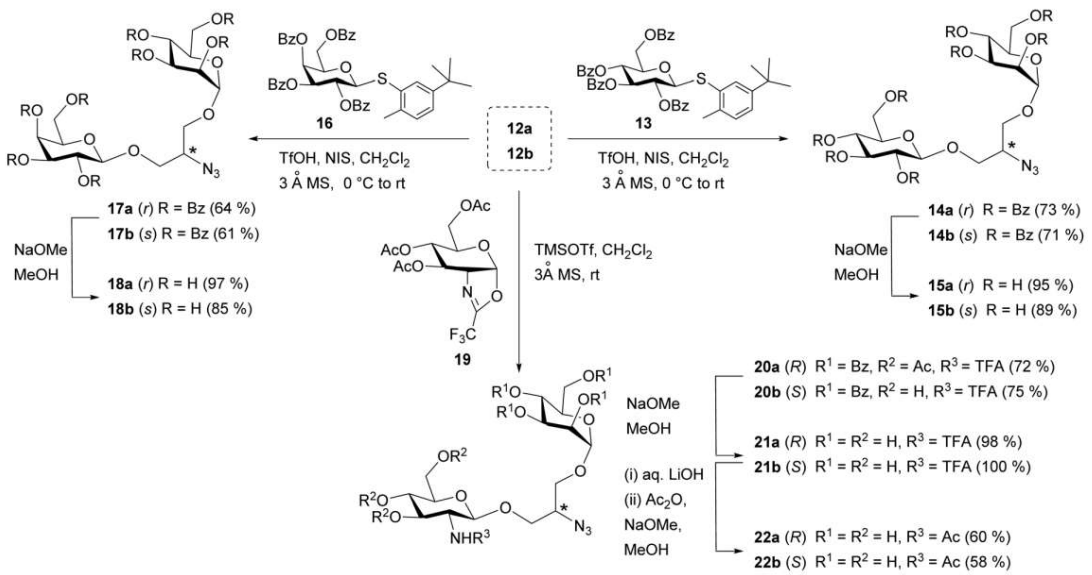

Scheme 3 Synthesis of four diastereomeric pairs of heterobivalent glycoclusters. In the diastereomeric pairs βGlc-αMan and βGal-αMan, the focal point represents a pseudoasymmetric centre as the two attached sugar moieties only differ in their configuration (Glc, Man, and Gal have the same constitution). Thus, the configuration at the focal point is assigned by using small letters, *r* and *s*. Otherwise, the two diastereomeric pairs βGlcNHAc-αMan and βGlcNHTFA-αMan comprise sugars of different masses and hence capitalised descriptors *R* and *S* are used to assign the configuration at the focal point. (Note that according to IUPAC, the diastereomeric pairs comprising mannosyl and glucosaminyl residues cannot be called "pseudoenantiomeric".) Please note further that for assigning the CIP priorities of the sugar moieties, their anomeric configuration is decisive, with a sugar with anomeric (*R*)-configuration having a higher priority than its isomer with anomeric (*S*)-configuration. CIP = Cahn–Ingold–Prelog.

in good yields, hence setting a further alcohol group available for the second glycosylation step.

We targeted three principal diastereomeric pairs of heterobivalent cluster glycosides (Fig. 1B). For this, we used glucose, galactose and GlcNAc donors for the glycosylation of the mannosides **12a** and **12b**. The protected diastereomeric pairs βGlc-αMan and βGal-αMan were obtained employing the benzoyl-protected thioglucoside (**13**)[17] and the respective thiogalactoside donor (**16**) (Scheme 3). The glycosylation reactions proceeded efficiently, furnishing **14a/b** and **17a/b** in yields from 61 to 71%. Deprotection under Zemplén conditions[25] provided the final diastereomeric cluster pairs **15a/b** and **18a/b**, respectively, in very good to excellent yields after purification by size exclusion chromatography.

For the synthesis of the βGlcNAc-αMan glycocluster, the acetylated trifluoromethyl oxazoline **19**,[26] derived from D-glucosamine, was used as the donor in a glycosylation reaction promoted by a catalytic amount of trimethylsilyl trifluoromethanesulfonate at room temperature.[27] The β-configured glycosides **20a** and **20b** were isolated in good yields and no α-anomer was obtained. The following standard Zemplén deprotection delivered the diastereomeric βGlcNTFA-αMan pair **21a**/**21b**. In order to achieve the respective βGlcNAc-αMan pair, the *N*-trifluoroacetyl (TFA) derivatives were cleaved with aqueous lithium hydroxide[28] and subsequent *N*-acetylation in methanol under basic conditions afforded compounds **22a** and **22b** (Scheme 3). Both heterobivalent diastereomeric pairs involving glucosamine, **21a**/**21b** (βGlcNTFA-αMan) and **22a**/**22b** (βGlcNAc-αMan), were used in lectin binding studies (see below).

Biological testing

The synthesised bivalent glycoclusters were tested in solution as inhibitors of the adhesion of type 1 fimbriae-mediated *E. coli* bacteria and of the binding of ConA, respectively, to a mannan-coated microtiter plate surface. The type 1-fimbrial lectin is FimH, exhibiting a pronounced specificity for α-D-mannosyl residues.[3] ConA on the other hand recognises α-D-mannosides as well as α-D-glucosides.[29] Depending on the pH, ConA exists in two forms, as a dimer (at pH ≤ 5.6) or as a tetramer (at pH 5.8 to 7).[14] Accordingly, in the assay performed here, ConA is tested as a tetramer.

In the employed assays, a soluble inhibitor has to compete with the bacterial lectin FimH or ConA, respectively, for binding to a mannosylated (mannan-coated) surface. Using 96-well plates, serial dilutions of each tested inhibitor were applied in order to measure dose–response inhibition curves (*cf.* ESI†) from which IC_{50} values can be determined. The IC_{50} value of a specific compound reflects the concentration at which bacterial or ConA binding is reduced by 50% and thus correlates with its inhibitory potency. Bacterial binding (adhesion) and ConA binding to the surface were measured by fluorescence read-out. For this, we used the *E. coli* strain PKL1162, expressing the green fluorescent protein (GFP)[30] and

fluorescein-labelled ConA. In all assays, methyl α-D-mannopyranoside (MeMan) was tested as a reference inhibitor on the same plate in order to allow the quantitative comparison of all tested cluster glycosides, even when tested in different experiments. Hence, we report relative inhibitory potency (RIP) values which are all related to the inhibitory potency of MeMan, tested in the same experiment. We also compared the various heteroclusters with the homobivalent mannoside **6**, tested on the same microplate, to observe whether a heteromultivalency effect occurs.[10] In this respect, we also report valency-corrected RIP values (RIP_{vc}), where the determined RIP value is divided by the number of clustered mannose ligands (two in the case of **6**).

The so-determined IC_{50} values are summarised in Table 1 for the inhibition of both adhesion of type 1-fimbriated *E. coli* and ConA binding. The corresponding RIP values are compared in Fig. 2. Overall, the homobivalent cluster mannoside **6** and every tested heterobivalent glycocluster show more or less pronounced multivalency effects with RIP values higher than 1, with the exception of the *N*-GlcNAc-containing glycoclusters **22a**/**b** as inhibitors of ConA binding (Fig. 2, top chart). As inhibitors of FimH-mediated bacterial adhesion (Fig. 2, bottom chart), some of the heterobivalent glycoclusters, **15b**, **18b**, **21a** and **21b**, also exhibit a heterocluster effect with RIP values 2- to 6-fold higher than RIP_{vc} of **6** (always tested in parallel). On the other hand, in the ConA assay, no significant heterocluster effects were observed. This is not surprising according to the results reported by García Fernández *et al.* with ConA, which evidenced the heteromultivalency effect occurring only at a high density of ligands on the scaffold.[10]

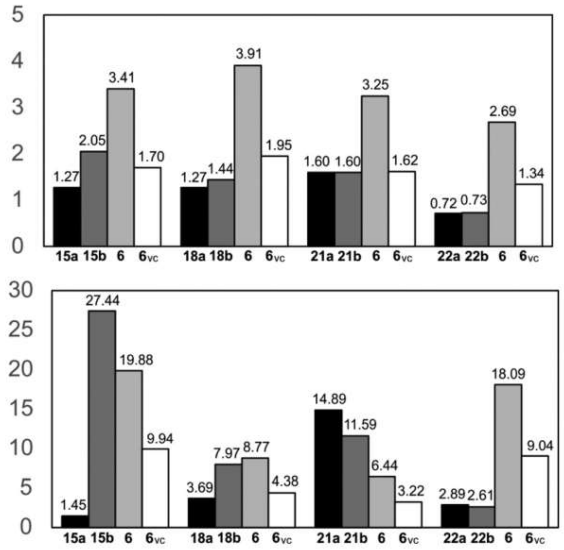

Fig. 2 Relative inhibitory potencies (RIP values) of the tested compounds deduced from the measured IC_{50} values as listed in Table 1. Top chart: Inhibition of ConA (FITC-labelled) binding to mannan; bottom chart: Inhibition of *E. coli* (GFP-PKL1162) adhesion to mannan. RIP values are based on the inhibitory potency of methyl α-D-mannopyranoside (MeMan) tested on the same microplate (MeMan, IP ≡ 1); RIP = IC_{50}(MeMan)/IC_{50} (tested compound). For the homobivalent cluster mannoside $(\alpha Man)_2$ (**6**) also the valency-corrected value RIP_{vc} (**6**$_{vc}$) is depicted for comparison.

Table 1 IC_{50} values of synthetic inhibitors of type 1 fimbriae-mediated adhesion of *E. coli* cells and of ConA binding, respectively, both to mannan-coated microtiter plates, employing the *E. coli* strain GFP-PKL1162 and FITC-labelled ConA

	FITC-ConA	GFP-PKL1162
Inhibitor	IC_{50} (SD)[a] [mmol]	IC_{50} (SD)[a] [mmol]
MeMan	5.55 (±0.48)	11.87 (±0.96)
βGlc-αMan **15a**	4.37 (±0.33)	8.17 (±0.9)
βGlc-αMan **15b**	2.71 (±0.76)	0.43 (±0.06)
$(\alpha Man)_2$ **6**	1.62 (±0.12)	0.60 (±0.10)
MeMan	4.95 (±1.29)	13.31 (±4.00)
βGal-αMan **18a**	3.43 (±0.97)	3.63 (±0.10)
βGal-αMan **18b**	3.88 (±0.92)	1.68 (±0.19)
$(\alpha Man)_2$ **6**	1.27 (±0.33)	1.54 (±0.33)
MeMan	5.78 (±1.06)	6.47 (±1.13)
βGlcTFA-αMan **21a**	3.60 (±0.21)	0.44 (±0.24)
βGlcTFA-αMan **21b**	3.60 (±0.18)	0.57 (±0.19)
$(\alpha Man)_2$ **6**	1.78 (±0.17)	1.00 (±0.09)
MeMan	4.76 (±0.36)	6.67 (±0.67)
βGlcNAc-αMan **22a**	6.48 (±0.15)	2.31 (±0.88)
βGlcNAc-αMan **22b**	6.56 (±0.41)	2.66 (±0.29)
$(\alpha Man)_2$ **6**	1.77 (±0.10)	0.37 (±0.04)

[a] IC_{50} values are averaged from the mean values obtained in at least two independent adhesion experiments (*cf.* ESI). Note that the IC_{50} values can vary significantly in independent experiments as live bacteria are investigated. SD: standard deviation; GFP: green fluorescent protein; FITC: fluorescein isothiocyanate.

We were especially excited to test, if the pseudoenantiomeric pairs of heterobivalent glycoclusters would show any significant difference in their inhibitory potencies. In the ConA-based assay, the pseudoenantiomeric glycoclusters performed very similar or equal. Only some RIP difference was observed with the βGlc-αMan pair (1.27 and 2.05, respectively, for **15a** and **15b**). However, a striking difference was indeed observed for the same βGlc-αMan pair **15a** and **15b** when tested as inhibitors of bacterial adhesion. Hence, **15b**, based on the L-serine-derived scaffold, is nearly 20-fold more potent (RIP = 27.44) than its isomer **15a** (RIP = 1.45). We confirmed this exciting result in several independent assays (*cf.* ESI†).[31] A similar trend was observed for the galactose-containing clusters **18a** and **18b**, although their RIP values differ only by a factor of approx. 2 in favour of **18b** (RIP = 7.97). The *N*-TFA-β-GlcNAc-containing glycoclusters **21a** and **21b** exhibited a small RIP difference, in this case in favour of the D-serine-derived cluster **21a** (RIP = 14.89). The GlcNAc-containing clusters **22a**/**b** only displayed weak inhibitory potencies with almost no difference between the diastereomers. It might be concluded at this point that the *N*-trifluoroacetyl group seems to have a beneficial effect on the inhibition of bacterial adhesion.

To rationalise the remarkable difference in inhibitory power, which was seen in the bacterial adhesion assay with the pseudoenantiomeric heterobivalent glycoclusters **15a** and **15b**, we studied their interactions with the bacterial adhesin FimH by molecular modelling. At this point we concentrated on **15a**/**b** and did not consider the molecular interactions of the other pseudoenantiomeric pairs which showed less pronounced effects.

Molecular modelling

We figured that the spatial orientation of the glucosyl residue in **15a** *versus* **15b** might have a significant influence on the recognition of the bivalent structure by the bacterial adhesin FimH. To support this assumption, we examined the interaction of both cluster glycosides with the lectin by molecular modelling based on force-field methods. We first performed a molecular docking study involving **15a** and **15b** and the homobivalent cluster mannoside **6** for comparison. For docking, Glide was used, a specific software implemented in the Schrödinger suite.[32] FimH has been crystallised in two conformations, a "closed" form[33] and an "open" one,[34] depending on the orientation of two tyrosine residues (Tyr 48 and Tyr 137) which flank the carbohydrate recognition domain (CRD) and form the so-called "tyrosine gate". Thus, we used both the closed and the open crystal structures of the lectin (pdb codes 1UWF and 1KLF, respectively) for docking. Because docking scores do not generally reflect the affinity of ligands, each docking output was next subjected to a MM-GBSA calculation (molecular mechanics energies combined with the generalised Born and surface area continuum solvation)[35] to provide binding energies.[36] These values are more reliable than docking scores to estimate and compare protein–ligand interactions.[37]

Table 2 depicts the docking score for the clusters **6**, **15a** and **15b** along with the corresponding lowest binding energy for both the open and the closed gate conformation of the lectin FimH. The obtained ranking of the glycoclusters is consistent with the RIP values deduced from the adhesion inhibition assays, with **15b** forming a more stable complex with FimH compared to **6** and **15a**.

As the difference in energy between **15b** and **15a** is more important in the closed gate conformation (about 9.5 kJ mol^{-1}), we selected the corresponding docking conformations for comparing the position of the different ligands bound to FimH (Fig. 3). While the α-D-mannosyl residue of each cluster equally fits into the binding pocket (Fig. 3A), there is a clear difference in the orientation of the glucoside moiety. In case of **15b**, a stacking of the glucosyl residue with a polar domain

Table 2 Docking scores[a] and binding energies[b] of the clusters **6**, **15a**, and **15b** in complex with the open and closed gate conformation of FimH

	Docking score[c]	Docking score[c]	Binding energy (kJ mol^{-1})	Binding energy (kJ mol^{-1})
Ligand	Open gate	Closed gate	Open gate	Closed gate
6	−9.911	−8.231	−74.892	−68.407
15a	−9.561	−8.552	−72.526	−60.940
15b	−9.340	−8.858	−78.104	−70.465

[a] Calculated with Glide. [b] Calculated using the MM-GBSA method based on the docking output. [c] The lower the docking score, the better the predicted binding.

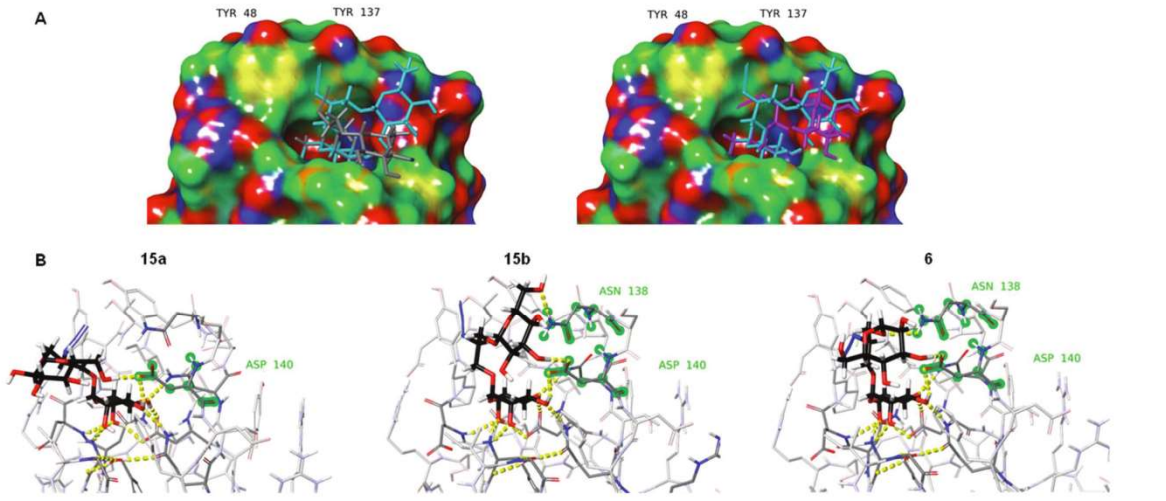

Fig. 3 Interaction of FimH (closed gate conformation, pdb code 1UWF) with clusters **15a**, **15b** (diastereomeric βGlc-αMan pair) and **6** $(\alpha Man)_2$. A: Partial charge coloured Connolly description[38] (negative charges in red, positive in blue); left image: overlay of **15a** (grey) and **15b** (blue) in the carbohydrate recognition domain (CRD) of FimH; right image: overlay of **6** (purple) and **15b** (blue) in the FimH CRD. B: H-Bond network between **15a** (left), **15b** (middle) and **6** (right) and the CRD of FimH: the amino acid residues interacting with the cluster outside of the binding pocket are highlighted in green, suggesting that **15b** and **6** are better FimH ligands than **15a**.

View Article Online
Organic & Biomolecular Chemistry Paper

of the CRD is visible and the nonpolar azido group points towards the tyrosine gate. In case of **15a** on the other hand, the azido function is further away from the tyrosine gate while the glucoside portion is shifted closer to a hydrophobic domain of the CRD.

The hydrogen bond network was also examined (Fig. 3B). Hence, the mannoside ligand in both diastereomers, **15a** and **15b**, forms exactly the same H-bond pattern with the amino acids of the FimH binding pocket. The difference between **15a** and **15b** resides in the non-covalent interactions of the glucoside portion. In **15b**, two hydrogen bonds are provided by the two protein residues forming the aforementioned polar domain (Asn 138 and Asp 140). In contrast, only a single H-bond with the same asparagine residue Asn 138 is observed for **15a**. Hence, the results of our modelling study provide a good basis for a possible explanation of the differences between the heterobivalent diastereomeric glycoclusters **15a** and **15b** (the pseudoenantiomeric βGlc-αMan pair) which was observed in the bacterial adhesion–inhibition assay. It might also give hints for the interpretation of data obtained earlier and likewise for the future design of inhibitors and the understanding of carbohydrate recognition in a complex environment.

Conclusions

In conclusion, we introduced the first pseudoenantiomeric cluster glycosides as a new tool for investigating the influence of the relative epitope orientation on lectin binding. A small library of heterobivalent glycoclusters was readily prepared from two enantiomeric scaffolds derived from L- and D-serine, leading to pairs of diastereomers according to the configuration at the focal point of the molecules. All synthesised heterobivalent glycoclusters contain one α-mannosyl residue and vary in the nature of the second sugar epitope. They were tested as inhibitors of bacterial adhesion, mediated by the lectin FimH, and as ligands of the lectin ConA. Both lectins, FimH and ConA, specifically recognise α-mannosyl epitopes. The results reveal a sharp difference in the inhibitor potency of the diastereomeric βGlc-αMan pair **15a**/**b** when tested in bacterial adhesion. Much smaller potency gaps were detected with the other pseudoenantiomeric glycocluster pairs. In the ConA-based assays on the other hand, almost no significant variations were seen. In addition to the effect of the focal point stereochemistry, a marked heterocluster effect was observed with several derivatives, but again only in the context of inhibition of bacterial adhesion.

Molecular docking with FimH provided means for rationalizing the experimental data found with the βGlc-αMan clusters. In fact, the models of the cluster-lectin complexes showed a clear difference in the orientation of the glucosyl residue and the resulting stabilization of the sugar-FimH complex by H-bonds in the periphery of the CRD depending on sugar scaffolding. We believe that our study opens new prospects in the design of multivalent glycomimetics and the understanding of carbohydrate recognition. Further analytical methods, more complex glycoconjugates and other lectins shall be employed to deepen the approach we have introduced herein.

Experimental section

General information

Air- or moisture-sensitive reactions were carried out under nitrogen in dry glassware unless otherwise stated. All reactions were monitored by thin layer chromatography (TLC) on silica gel plates (F 254, Merck). Detection of spots was effected by UV light and/or subsequent charring with 10% sulphuric acid in ethanol, vanillin, or ninhydrin followed by heat treatment at ~150 °C. Flash chromatography was performed on silica gel 60 (0.040–0.063 mm) using distilled solvents. Optical rotations were measured with a PerkinElmer 241 polarimeter (sodium D-line: 589 nm) in the solvents indicated. ^{1}H and ^{13}C NMR spectra were recorded on a Bruker DRX-500 spectrometer at 300 K. Chemical shifts (in ppm) are relative to residual non-deuterated solvent as an internal reference. Full assignment of the peaks was achieved with the aid of 2D NMR techniques (^{1}H–^{1}H COSY, ^{1}H–^{13}C HSQC, ^{1}H–^{13}C HMBC and ^{1}H–^{1}H NOESY). ESI mass spectra were recorded on a Mariner 5280 instrument (Applied Biosystems).

For diastereomeric compounds, the one based on D-serine is specified as "a", while the other one, based on L-serine, is called "b". Molecule names are according to the IUPAC nomenclature. To facilitate the assignment of NMR peaks, the glycocluster skeleton was numbered as shown in Fig. 4. The nature of the carbohydrate portion is indicated by "Gal" (D-galactose), "Glc" (D-glucose), "GlcNAc" (*N*-acetyl-D-glucosamine), "GlcNTFA" (*N*-trifluoroacetyl-D-glucosamine), and "Man" (D-mannose) subscripts, respectively.

General procedure for glycosylation (general procedure A)

To a round bottom flask containing the acceptor, the donor and 3 Å molecular sieves, dry dichloromethane (c = 0.1 M) was added. After stirring at room temperature for 15 min, the mixture was cooled to 0 °C and then *N*-iodosuccinimide (1.5 eq.) and trifluoromethanesulfonic acid (0.15 eq.) were sequentially added. After stirring at 0 °C for 30 min, the mixture was allowed to warm to room temperature and stirred until completion and then diluted with dichloromethane and filtered over Celite. After washing with satd aq. sodium

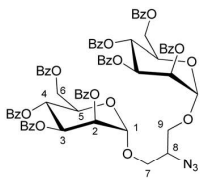

Fig. 4 Numbering of the synthesized molecules for assignment of NMR data.

View Article Online
Paper Organic & Biomolecular Chemistry

bicarbonate and satd aq. sodium thiosulfate, the aqueous layer was extracted with dichloromethane and then the combined organic layers were dried over magnesium sulfate, filtered and concentrated. The crude residue was purified by flash chromatography to afford the expected compound.

General procedure for glycosylation (general procedure B)

To a round bottom flask containing the acceptor, the donor and 3 Å molecular sieves, dry dichloromethane (c = 0.1 M) was added. After stirring at room temperature for 15 min, trimethylsilyl trifluoromethanesulfonate (0.1 eq.) was added and the mixture was stirred until completion. The reaction mixture was neutralised with triethylamine and then diluted with dichloromethane, filtered over Celite and concentrated. The crude residue was purified by flash chromatography to afford the expected compound.

General procedure for ester cleavage (general procedure C)

To a solution of the ester-protected glycocluster in dry methanol (c = 0.03 M), sodium methoxide (c = 5.4 M in methanol, two drops) was added and the mixture was stirred at room temperature until completion and then neutralised with Amberlite IR120-H^+, diluted with methanol, filtered and concentrated. The residue was taken up into a 1 : 1 mixture of water and methanol and then washed with diethyl ether and the aqueous layer was concentrated to dryness. The residue was purified by size exclusion chromatography on Sephadex G10 gel and eluted with deionised water.

General procedure for silyl cleavage (general procedure D)

The silylated starting material was dissolved in anhydrous tetrahydrofuran (c = 0.1 M) and then the mixture was buffered with acetic acid (6 eq.) before dropwise adding 1 M *n*-tetrabutylammonium fluoride in tetrahydrofuran (3 eq.). The mixture was stirred until completion and then diluted with ethyl acetate. After washing with satd aq. sodium bicarbonate and then 1 N hydrochloric acid, the aqueous phases were extracted with ethyl acetate and then the combined organic layers were dried over magnesium sulfate, filtered and concentrated. The crude residue was purified by flash chromatography to afford the expected compound.

General procedure for cleavage of the *N*-trifluoroacetyl group and subsequent *N*-acetylation (general procedure E)

To a solution of the *N*-trifluoroacetyl derivative in methanol (c = 0.03 M), 2 M aq. lithium hydroxide (40 eq.) was added at room temperature. The solution was sonicated at 40 °C until completion and then neutralised with Amberlite IR120-H^+, diluted with methanol, filtered and concentrated to dryness. The residue was dissolved in dry methanol (c = 0.03 M) and then sodium methoxide (c = 5.4 M in methanol, two drops) and acetic anhydride (5 eq.) were sequentially added under nitrogen. After stirring overnight at room temperature, sodium methoxide (c = 5.4 M in methanol, two drops) was added and the mixture was stirred for further 30 min and then neutralised with Amberlite IR120-H^+, diluted with methanol, filtered and concentrated.

2-Azido-1,3-di-*O*-(2,3,4,6-tetra-*O*-benzoyl-α-D-mannopyranosyl)-1,3-propanediol (5). General procedure A was applied to acceptor **3** (27.0 mg, 227 μmol) and donor **4** (207 mg, 273 μmol, 1.2 eq.). Reagents and conditions: *N*-Iodosuccinimide (76.8 mg, 340 μmol, 1.5 eq.), trifluoromethanesulfonic acid (2.3 μl, 20.0 μmol, 0.15 eq.), dichloromethane (c = 0.1 M, 2.8 mL), T = −77 °C to room temperature after three hours. Flash chromatography with ethyl acetate/cyclohexane (2.5/7.5) afforded compound **5** as a white foam (174 mg, 60%); R_f = 0.3 (ethyl acetate/cyclohexane 3/7); $[\alpha]_{20}^{D}$ = −46.1 (c 0.7, dichloromethane); ^{1}H NMR (500 MHz, $CDCl_3$) δ 8.13–8.10 (m, 4H, 4 H–Ar), 8.06–8.04 (m, 4H, 4 H–Ar), 7.98–7.96 (m, 4H, 4 H–Ar), 7.84–7.82 (m, 4H, 4 H–Ar),7.61–7.55 (m, 4H, 4 H–Ar), 7.50–7.45 (m, 3H, 3 H–Ar), 7.44–7.37 (m, 10H, 10 H–Ar), 7.35–7.31 (m, 4H, 4 H–Ar) 7.28–7.26 (m, 1H, H–Ar), 7.25–7.23 (m, 2H, 2 H–Ar), 6.20–6.14 (m, 2H, 2 H-4), 5.97–5.92 (m, 2H, 2 H-3), 5.77 (dd, $^3J_{2,3}$ = 3.3 Hz, $^3J_{1,2}$ = 1.8 Hz, 2H, 2 H-2), 5.21 (d, $^3J_{1,2}$ = 1.8 Hz, 1H, H-1), 5.19 (d, $^3J_{1,\ 2}$ = 1.7 Hz, 1H, H-1), 4.79–4.75 (m, 2H, 2 H-6a), 4.58–4.47 (m, 4H, 2 H-6b, 2 H-5), 4.07–4.03 (m, 3H, H-8, H-7a, H-9a), 3.84–3.74 (m, 2H, H-7b, H-9b) ppm; ^{13}C NMR (126 MHz, $CDCl_3$) δ 166.1, 165.5, 165.4, 165.3 (8C, 8 PhC=O), 133.5, 133.4, 133.1, 129.9, 129.8, 129.2, 129.0, 128.9, 128.6, 128.5, 128.4, 128.3 (48C, 48 C–Ar), 98.2, 97.8 (2C, 2 C-1), 70.2 (2C, 2 C-2), 69.9, 69.8 (2C, 2 C-3), 69.4, 69.4 (2C, 2 C-5), 67.6, 67.5 (2C, C-7, C-9), 66.7, 66.6 (2C, 2 C-4), 62.7 (2C, 2 C-6), 59.9 (C-8) ppm; IR (ATR) ν_{max}/cm^{-1} 2097, 1721, 1258, 1092, 705; ESI-HRMS: m/z calcd for $C_{71}H_{59}N_3O_{20}$ + Na^+: 1296.35590 $[M + Na]^+$; found 1296.35841.

2-Azido-1,3-di-*O*-(α-D-mannopyranosyl)-1,3-propanediol (6). General procedure C was applied to compound **5** (500 mg, 392 μmol). Reagents and conditions: Sodium methoxide (c = 5.4 M in methanol, two drops), methanol (c = 0.03 M, 7.84 mL). Compound **6** (100 mg, 70%) was obtained as a white foam after lyophilisation; $[\alpha]_{20}^{D}$ = +53.5 (c 0.7, water); ^{1}H NMR (500 MHz, D_2O) δ 4.89–4.86 (m, 2H, 2 H-1), 3.98–3.87 (m, 6H, 2 H-2, 2 H-4, 2 H-6a), 3.85–3.80 (m, 3H, 2 H-3, H-8), 3.76–3.70 (m, 3H, H-9a, H-9b, H-6b), 3.66–3.59 (m, 5H, H-7a, H-7b, 2 H-5, H-6b) ppm; ^{13}C NMR (126 MHz, D_2O) δ 100.3, 99.8 (2C, 2 C-1), 73.1, 73.1 (2C, 2 C-4), 70.5 (2C, 2 C-3), 69.9 (2C, 2 C-2), 67.2 (C-6), 66.7 (2C, 2 C-5), 66.7 (C-6), 61.0 (2C, C-7, C-9), 60.1 (C-8) ppm; IR (ATR) ν_{max}/cm^{-1} 3332, 2927, 2097, 1048; ESI-HRMS: m/z calcd for $C_{15}H_{27}N_3O_{12}$ + Na^+: 464.14869; $[M + Na]^+$; found 464.14822.

(*S*)-2-Azido-1-*O*-(*tert*-butyldiphenylsilyl)-3-*O*-(2,3,4,6-tetra-*O*-benzoyl-α-D-mannopyranosyl)-1,3-propanediol (11a). General procedure A was applied to acceptor **10a** (169 mg, 476 μmol) and donor **4** (434 mg, 572 μmol, 1.2 eq.). Reagents and conditions: *N*-Iodosuccinimide (160.7 mg, 715 μmol, 1.5 eq.), trifluoromethane sulfonic acid (4.8 μl, 47.0 μmol, 0.1 eq.), dichloromethane (c = 0.1 M, 4.76 mL). Flash chromatography with ethyl acetate/cyclohexane (1/9) yielded compound **11a** (374 mg, 85%) as a white foam; R_f = 0.3 (ethyl acetate/cyclohexane 1/9); $[\alpha]_{20}^{D}$ = −26.9 (c 0.4, dichloromethane); ^{1}H NMR (500 MHz, $CDCl_3$) δ 8.11–8.09 (m, 2H, 2 H–Ar), 8.06–8.04

(m, 2H, 2 H–Ar), 7.96–7.94 (m, 2H, 2 H–Ar), 7.85–7.84 (m, 2H, 2 H–Ar), 7.70–7.67 (m, 4H, 4 H–Ar), 7.62–7.48 (m, 3H, 3 H–Ar), 7.46–7.33 (m, 15H, 15 H–Ar), 6.14 (dd, $^3J_{3,4} = {}^3J_{4,5} = 9.9$ Hz, 1H, H-4), 5.91 (dd, $^3J_{3,4} = 10.1$ Hz, $^3J_{2,3} = 3.3$ Hz, 1H, H-3), 5.71 (dd, $^3J_{2,3} = 3.3$ Hz, $^3J_{1,2} = 1.8$ Hz, 1H, H-2), 5.10 (d, $^3J_{1,2} = 1.8$ Hz, 1H, H-1), 4.70 (dd, $^2J_{6a,6b} = 13.4$ Hz, $^3J_{5,6a} = 3.6$ Hz, 1H, H-6a), 4.50–4.43 (m, 2H, H-5, H-6b), 3.93 (dd, $^2J_{7a,7b} = 9.9$ Hz, $^3J_{7a,8} = 7.0$ Hz, 1H, H-7a), 3.84–3.73 (m, 4H, H-8, H-9a, H-9b, H-7b), 1.08 (s, 9H, Si–C(C$\underline{H}_3$)$_3$) ppm; ^{13}C NMR (126 MHz, $CDCl_3$) δ 166.1, 165.4, 165.3 (4C, 4 PhC$\underline{}$=O), 135.54, 133.4, 133.2, 133.0, 132.7, 130.0, 129.9, 129.8, 129.7, 129.2, 129.0, 128.9, 128.6, 128.4, 128.3, 127.9 (36C, 36 C–Ar), 97.7 (C-1), 70.1 (C-2), 69.9 (C-3), 69.2 (C-5), 67.7 (C-7), 66.6 (C-4), 63.5 (C-9), 62.7 (C-6), 62.0 (C-8), 26.6 (Si–C(C$\underline{H}_3$)$_3$), 19.2 (Si–C$\underline{}$(CH$_3$)$_3$) ppm; IR (ATR) ν_{max}/cm^{-1} 2103, 1724, 1451, 1260, 1093, 705, 503; ESI-HRMS: *m*/*z* calcd for $C_{53}H_{51}N_3O_{11}Si + Na^+$: 956.31851 $[M + Na]^+$; found 956.31719.

(*R*)-2-Azido-1-*O*-(*tert*-butyldiphenylsilyl)-3-*O*-(2,3,4,6-tetra-*O*-benzoyl-α-D-mannopyranosyl)-1,3-propanediol (11b). General procedure A was applied to acceptor **10b** (300 mg, 843 μmol) and donor **4** (768 mg, 1.01 mmol, 1.2 eq.). Reagents and conditions: *N*-Iodosuccinimide (284 mg, 1.26 mmol, 1.5 eq.), trifluoromethane sulfonic acid (8.4 μl, 50.0 μmol, 0.1 eq.), dichloromethane (*c* = 0.1 M, 8.4 mL). Flash chromatography with ethyl acetate/cyclohexane (1/9) afforded compound **11b** (665 mg, 85%) as a white foam; R_f = 0.3 (ethyl acetate/cyclohexane 1/9); $[\alpha]_{20}^{D}$ = −33.8 (*c* 0.6, dichloromethane); ^{1}H NMR (500 MHz, $CDCl_3$) δ 8.12–8.02 (m, 4H, 4 H–Ar), 7.91–7.89 (m, 2H, 2 H–Ar), 7.85–7.83 (m, 2H, 2 H–Ar), 7.65 (m, 4H, 4 H–Ar), 7.64–7.47 (m, 4H, 4 H–Ar), 7.47–7.33 (m, 14H, 14 H–Ar), 6.18–6.06 (dd, $^3J_{3,4} = {}^3J_{4,5} = 10.0$ Hz, 1H, H-4), 5.89 (dd, $^3J_{3,4} = 10.1$ Hz, $^3J_{2,3} = 3.3$ Hz, 1H, H-3), 5.71 (dd, $^3J_{2,3} = 3.3$ Hz, $^3J_{1,2} = 1.8$ Hz, 1H, H-2), 5.12 (d, $^3J_{1,2} = 1.7$ Hz, 1H, H-1), 4.71–4.61 (dd, $^2J_{6a,6b} = 11.8$ Hz, $^3J_{5,6a} = 2.1$ Hz, 1H, H-6a), 4.43 (m, 2H, H-5, H-6b), 3.99 (dd, $^2J_{7a,7b} = 8.4$ Hz, $^3J_{7a,8} = 2.4$ Hz, 1H, H-7a), 3.87–3.82 (m, 2H, H-9a, H-9b), 3.77–3.70 (m, 2H, H-8, H-7b), 1.09 (s, 9H, Si–C(C$\underline{H}_3$)$_3$) ppm; ^{13}C NMR (126 MHz, $CDCl_3$) δ 166.2, 165.5, 165.4, 165.3 (4C, 4 PhC$\underline{}$=O), 135.6, 133.5, 133.2, 133.1, 132.8, 132.7, 130.0, 129.8, 129.9, 129.8, 129.7, 129.8, 129.7, 129.2, 129.0, 128.9, 128.6, 128.5, 128.3, 127.9, (36C, 36 C–Ar), 98.2 (C-1), 70.2 (C-2), 69.8 (C-3), 69.2 (C-5), 67.7 (C-7), 66.7 (C-4), 63.5 (C-9), 62.6 (C-6), 62.0 (C-8), 26.9 (Si–C(C$\underline{H}_3$)$_3$), 19.2 (Si–C$\underline{}$(CH$_3$)$_3$); IR (ATR) ν_{max}/cm^{-1} 2101, 1724, 1451, 1259, 1067, 704, 504; ESI-HRMS: *m*/*z* calcd for $C_{19}H_{25}N_3O_2Si + Na^+$: 956.31851 $[M + Na]^+$; found 956.31800.

(*R*)-2-Azido-1-*O*-(2,3,4,6-tetra-*O*-benzoyl-α-D-mannopyranosyl)-1,3-propanediol (12a). General procedure D was applied to compound **11a** (593 mg, 634 μmol). Reagents and conditions: Tetrabutylammonium fluoride (*c* = 1 M, 1.91 mL, 1.91 mmol, 3 eq.), acetic acid (0.22 mL, 3.81 mmol, 6 eq.), and tetrahydrofuran (*c* = 0.1 M, 6.35 mL). Flash chromatography with ethyl acetate/cyclohexane (1/9 to 2/8) afforded compound **12a** (348 mg, 78%) as a white foam; R_f = 0.3 (ethyl acetate/cyclohexane 2/3); $[\alpha]_{20}^{D}$ = −57.8 (*c* 0.5, dichloromethane); ^{1}H NMR (500 MHz, $CDCl_3$) δ 8.09–8.07 (m, 2H, 2 H–Ar), 8.05–8.03 (m, 2H, 2 H–Ar), 7.96–7.94 (m, 2H, 2 H–Ar), 7.84–7.82 (m, 2H, 2 H–Ar), 7.63–7.48 (m, 3H, 3 H–Ar), 7.45–7.34 (m, 8H, 8 H–Ar), 7.29–7.26 (m, 1H, H–Ar), 6.12 (dd, $^3J_{3,4} = {}^3J_{4,5} = 10.0$ Hz, 1H, H-4), 5.92 (dd, $^3J_{3,4} = 10.1$ Hz, $^3J_{3,2} = 3.4$ Hz, 1H, H-3), 5.73 (dd, $^3J_{2,3} = 3.3$ Hz, $^3J_{1,2} = 1.8$ Hz, 1H, H-2), 5.15 (d, $^3J_{1,2} = 1.8$ Hz, 1H, H-1), 4.74–4.69 (dd, $^2J_{6a,6b} = 11.9$ Hz, $^3J_{5,6a} = 2.3$ Hz, 1H, H-6a), 4.54–4.45 (m, 2H, H-5, 6b), 4.02 (dd, $^2J_{7a,7b} = 10.0$ Hz, $^3J_{7a,8} = 7.5$ Hz, 1H, H-7a), 3.94–3.88 (m, 1H, H-8), 3.83 (dd, $^2J_{9a,9b} = 11.5$ Hz, $^3J_{8,9a} = 4.4$ Hz, 1H, H-9a), 3.78 (dd, $^2J_{7a,7b} = 10.0$ Hz, $^3J_{7b,8} = 4.3$ Hz, 1H, H-7b), 3.71 (dd, $^2J_{9a,9b} = 11.5$ Hz, $^3J_{8,9b} = 5.9$ Hz, 1H, H-9b) ppm; ^{13}C NMR (126 MHz, $CDCl_3$) δ 166.2 165.5, 165.4, (4C, 4 PhC=O), 129.9, 129.8, 129.7, 128.6, 128.5, 128.3 (24C, 24 C–Ar), 97.7 (C-1), 70.2 (C-2), 69.8 (C-3), 69.3 (C-5), 67.9 (C-7), 66.7 (C-4), 62.4 (C-6), 62.1 (C-8), 62.0 (C-9) ppm; IR (ATR) ν_{max}/cm^{-1} 2933, 2095, 1723, 1451, 1259, 1093, 705, 503; ESI-HRMS: *m*/*z* calcd for $C_{37}H_{33}N_3O_{11} + Na^+$: 718.20073 $[M + Na]^+$; found 718.19969.

(*S*)-2-Azido-1-*O*-(2,3,4,6-tetra-*O*-benzoyl-α-D-mannopyranosyl)-1,3-propanediol (12b). General procedure D was applied to compound **11b** (393 mg, 427 μmol). Reagents and conditions: Tetrabutylammonium fluoride (*c* = 1 M, 1.28 mL, 3 eq.), acetic acid (150 μl, 2.56 mmol, 6 eq.), and tetrahydrofuran (*c* = 0.1 M, 4.3 mL). Flash chromatography with ethyl acetate/cyclohexane (1/9 to 2/8) afforded compound **12b** (586 mg, 76%) as a white foam; R_f = 0.3 (ethyl acetate/cyclohexane 2/3); $[\alpha]_{20}^{D}$ = −45.6 (*c* 0.42, dichloromethane); ^{1}H NMR (500 MHz, $CDCl_3$) δ 8.10–8.08 (m, 2H, 2 H–Ar), 8.06–8.04 (m, 2H, 2 H–Ar), 7.98–7.96 (m, 2H, 2 H–Ar), 7.85–7.83 (m, 2H, 2 H–Ar), 7.64–7.34 (m, 10H, 10 H–Ar), 7.29–7.27 (m, 2H, 2 H–Ar), 6.13 (dd, $^3J_{4,5} = {}^3J_{3,4} = 10.0$ Hz, 1H, H-4), 5.90 (dd, $^3J_{3,4} = 10.1$ Hz, $^3J_{2,3} = 3.3$ Hz, 1H, H-3), 5.73 (dd, $^3J_{2,3} = 3.3$ Hz, $^3J_{1,2} = 1.8$ Hz, 1H, H-2), 5.16 (d, $^3J_{1,2} = 1.8$ Hz, 1H, H-1), 4.74–4.69 (dd, $^2J_{6a,6b} = 11.9$ Hz, $^3J_{5,6a} = 2.3$ Hz, 1H, H-6a), 4.53–4.45 (m, 2H, H-5, H-6b), 4.07 (dd, $^2J_{7a,7b} = 10.1$ Hz, $^3J_{7a,8} = 4.1$ Hz, 1H, H-7a), 3.89–3.72 (m, 4H, H-8, H-9a, H-9b, H-7b), 1.88 (br s, 1H, OH) ppm; ^{13}C NMR (126 MHz, $CDCl_3$) δ 166.2, 165.5, 165.4 (4C, 4 PhC$\underline{}$=O), 133.6, 133.5, 133.3, 133.2, 129.9, 129.8, 129.2, 129.0, 128.9, 128.6, 128.5, 128.4 (24C, 24 C–Ar), 98.0 (C-1), 70.2 (C-2), 69.8 (C-3), 69.2 (C-5), 67.8 (C-7), 66.7 (C-4), 62.8 (C-6), 62.1 (2C, C-8, C-9) ppm; IR (ATR) ν_{max}/cm^{-1} 2932, 2094, 1722, 1451, 1258, 1093, 705, 504; ESI-HRMS: *m*/*z* calcd for $C_{37}H_{33}N_3O_{11} + Na^+$: 718.20073 $[M + Na]^+$; found 718.19968.

(*r*)-2-Azido-1-*O*-(2,3,4,6-tetra-*O*-benzoyl-α-D-mannopyranosyl)-3-*O*-(2,3,4,6-tetra-*O*-benzoyl-β-D-glucopyranosyl)-1,3-propanediol (14a). General procedure A was applied to acceptor **12a** (325 mg, 468 μmol) and donor **13** (426 mg, 561 μmol, 1.5 eq.). Reagents and conditions: *N*-Iodosuccinimide (157 mg, 702 μmol, 1.5 eq.), trifluoromethane sulfonic acid (4.7 μl, 50.0 μmol, 0.1 eq.), and dichloromethane (*c* = 0.1 M, 4.68 mL). Flash chromatography with ethyl acetate/cyclohexane (1/4) yielded compound **14a** (434 mg, 73%) as a white foam; R_f = 0.3 (ethyl acetate/cyclohexane 3/7); $[\alpha]_{20}^{D}$ = −15.8 (*c* 1.0, dichloromethane); ^{1}H NMR (600 MHz, $CDCl_3$) δ 8.11–8.07 (m, 2H, 2 H–Ar), 8.06–8.01 (m, 4H, 4 H–Ar), 7.98–7.96 (m, 4H, 4 H–Ar), 7.92–7.90 (m, 2H, 2 H–Ar), 7.86–7.81 (m, 4H, 4 H–Ar), 7.60–7.58 (m, 2H, 2 H–Ar), 7.53–7.44 (m, 4H, 4 H–Ar), 7.45–7.33 (m, 15H, 15 H–Ar), 7.29–7.27 (m, 3H, 3 H–Ar),

6.10 (dd, $^3J_{4,5}$ = $^3J_{3,4}$ = 10.1 Hz, 1H, H-4$_{Man}$), 5.94 (dd, $^3J_{3,4}$ = $^3J_{3,2}$ = 9.7 Hz, 1H, H-3$_{Glc}$), 5.85 (dd, $^3J_{3,4}$ = 10.1 Hz, $^3J_{3,2}$ = 3.3 Hz, 1H, H-3$_{Man}$), 5.72 (dd, $^3J_{3,4}$ = $^3J_{4,5}$ = 9.9 Hz, 1H, H-4$_{Glc}$), 5.70–5.68 (dd, $^3J_{2,3}$ = 3.3 Hz, $^3J_{1,2}$ = 1.8 Hz, 1H, H-2$_{Man}$), 5.57 (dd, $^3J_{2,3}$ = 9.8 Hz, $^3J_{1,2}$ = 7.8 Hz, 1H, H-2$_{Glc}$), 5.00 (d, $^3J_{1,2}$ = 1.6 Hz, 1H, H-1$_{Man}$), 4.98 (d, $^3J_{1,2}$ = 7.9 Hz, 1H, H-1$_{Glc}$), 4.70 (dd, $^2J_{6a,6b}$ = 12.2 Hz, $^3J_{5,6a}$ = 3.1 Hz, 1H, H-6a$_{Glc}$), 4.65 (dd, $^2J_{6a,6b}$ = 12.2 Hz, $^3J_{5,6a}$ = 2.5 Hz, 1H, H-6a$_{Man}$), 4.54 (dd, $^2J_{6a,6b}$ = 12.2 Hz, $^3J_{5,6a}$ = 4.9 Hz, 1H, H-6b$_{Glc}$), 4.46 (dd, $^2J_{6a,6b}$ = 12.2 Hz, $^3J_{5,6a}$ = 4.2 Hz, 1H, H-6b$_{Man}$), 4.43–4.38 (m, 1H, H-5$_{Man}$), 4.25–4.20 (m, 1H, H-5$_{Glc}$), 4.11 (dd, $^2J_{9a,9b}$ = 10.1 Hz, $^3J_{8,9a}$ = 3.9 Hz, 1H, H-9a), 3.90 (dd, $^2J_{7a,7b}$ = 10.4 Hz, $^3J_{7a,8}$ = 3.6 Hz, 1H, H-7a), 3.88–3.80 (m, 2H, H-8, H-9b), 3.59–3.57 (dd, $^2J_{7a,7b}$ = 10.5 Hz, $^3J_{7a,8}$ = 5.6 Hz, 1H, H-7b) ppm; ^{13}C NMR (151 MHz, $CDCl_3$) δ 166.1, 165.8, 165.5, 165.3, 165.2, 165.1 (8C, 8 PhC=O), 133.5, 133.3, 133.2, 133.1, 130.0, 129.9, 129.8, 129.8, 129.7, 129.5, 129.2, 129.0, 128.9, 128.8, 128.6, 128.5, 128.4, 128.3, (48C, 48 C–Ar) 101.5 (C-1$_{Glc}$), 97.9 (C-1$_{Man}$), 72.8 (C-3$_{Glc}$), 72.4 (C-5$_{Glc}$), 71.7 (C-2$_{Glc}$), 70.1 (C-2$_{Man}$), 69.9 (C-3$_{Man}$), 69.5 (C-4$_{Glc}$), 69.4 (C-9), 69.2 (C-5$_{Man}$), 67.9 (C-7), 66.6 (C-4$_{Man}$), 62.8 (C-6$_{Glc}$), 62.7 (C-6$_{Man}$), 60.2 (C-8) ppm; IR (ATR) ν_{max}/cm^{-1} 2933, 2095, 1722, 1451, 1258, 1093, 704; ESI-HRMS; *m*/*z* calcd for $C_{71}H_{59}N_3O_{20}$ + H^+: 1274.37647 [M + H]$^+$; found 1274.37451.

(*s*)-2-Azido-1-*O*-(2,3,4,6-tetra-*O*-benzoyl-α-D-mannopyranosyl)-3-*O*-(2,3,4,6-tetra-*O*-benzoyl-β-D-glucopyranosyl)-1,3-propanediol (14b). General procedure A was applied to acceptor **12b** (102 mg, 147 μmol) and donor **13** (134 mg, 176 μmol, 1.5 eq.). Reagents and conditions: *N*-Iodosuccinimide (49.6 mg, 220 μmol, 1.5 cq.), trifluoromethanc sulfonic acid (1.5 μl, 15.0 μmol, 0.1 eq.), and dichloromethane (*c* = 0.1 M, 1.47 mL). Flash chromatography with ethyl acetate/cyclohexane 2.5/7.5 afforded compound **14b** (210 mg, 71%) as a white foam; R_f = 0.3 (ethyl acetate/cyclohexane 3/7); $[\alpha]_{20}^{D}$ = −11.9 (*c* 1.0, dichloromethane); ^{1}H NMR (500 MHz, $CDCl_3$) δ 8.13–8.11 (m, 2H, 2 H–Ar), 8.07–8.01 (m, 4H, 4 H–Ar), 7.99–7.89 (m, 6H, 6 H–Ar), 7.86–7.78 (m, 4H, 4 H–Ar), 7.59 (m, 2H, 2 H–Ar), 7.54–7.47 (m, 3H, 3 H–Ar), 7.46–7.22 (m, 19H, 19 H–Ar), 6.11 (dd, $^3J_{4,5}$ = $^3J_{3,4}$ = 10.1 Hz, 1H, H-4$_{Man}$), 5.93 (dd, $^3J_{2,3}$ = $^3J_{3,4}$ = 9.7 Hz, 1H, H-3$_{Glc}$), 5.87 (dd, $^2J_{3,4}$ = 10.1 Hz, $^3J_{2,3}$ = 3.3 Hz, 1H, H-3$_{Man}$), 5.73–5.66 (m, 2H, H-2$_{Man}$, H-4$_{Glc}$), 5.54 (dd, $^2J_{2,3}$ = 9.8 Hz, $^3J_{1,2}$ = 7.8 Hz, 1H, H-2$_{Glc}$), 4.96–4.90 (m, 2H, H-1$_{Man}$, H-1$_{Glc}$), 4.69 (dd, $^2J_{6a,6b}$ = 12.2 Hz, $^3J_{5,6a}$ = 3.1 Hz, 1H, H-6a$_{Glc}$), 4.63 (dd, $^2J_{6a,6b}$ = 12.2 Hz, $^3J_{5,6a}$ = 2.5 Hz, 1H, H-6a$_{Man}$), 4.53 (dd, $^2J_{6a,6b}$ = 12.2 Hz, $^3J_{5,6b}$ = 5.1 Hz, 1H, H-6b$_{Glc}$), 4.44 (dd, $^2J_{6a,6b}$ = 12.3 Hz, $^3J_{5,6b}$ = 4.0 Hz, 1H, H-6b$_{Man}$), 4.37–4.31 (m, 1H, H-5$_{Man}$), 4.21 (m, 1H, H-5$_{Glc}$), 4.04 (dd, $^2J_{9a,9b}$ = 10.6 Hz, $^3J_{8,9a}$ = 5.0 Hz, 1H, H-9a), 3.96–3.89 (m, 1H, H-8), 3.86 (dd, $^2J_{7a,7b}$ = 10.1 Hz, $^3J_{7a,8}$ = 7.7 Hz, 1H, H-7a), 3.75–3.65 (m, 2H, H-9b, H-7b) ppm; ^{13}C NMR (126 MHz, $CDCl_3$) δ 166.1, 165.8, 165.4, 165.2, 165.0 (8C, 8 PhC=O), 133.5, 133.4, 133.3, 133.2, 133.1, 130.0, 129.9, 129.8, 129.7, 129.5, 129.3, 129.1, 129.0, 128.8, 128.60, 128.5, 128.4, 128.3, (48C, 48 C–Ar) 101.5 (C-1$_{Glc}$), 97.7 (C-1$_{Man}$), 72.7 (C-3$_{Glc}$), 72.5 (C-5$_{Glc}$), 71.7 (C-2$_{Glc}$), 70.1, 69.8, 69.6 (3C, C-4$_{Glc}$, C-2$_{Man}$, C-3$_{Man}$), 69.2 (C-5$_{Man}$), 68.6 (C-9), 67.9 (C-7), 66.6 (C-4$_{Man}$), 62.9 (C-6$_{Glc}$), 62.6 (C-6$_{Man}$), 60.4 (C-8); IR (ATR) ν_{max}/cm^{-1} 2933, 2095, 1722, 1451, 1258, 1092, 705; *m*/*z* calcd for $C_{71}H_{59}N_3O_{20}$ + H^+: 1274.37647 [M + H]$^+$; found 1274.37450.

(*r*)-2-Azido-1-*O*-(α-D-mannopyranosyl)-3-*O*-(β-D-glucopyranosyl)-1,3-propanediol (15a). General procedure C was applied to compound **14a** (410 mg, 322 μmol). Reagents and conditions: Sodium methoxide (*c* = 5.4 M in methanol, two drops), methanol (*c* = 0.03 M, 10.7 mL). Compound **15a** (135 mg, 96%) was obtained as a white foam after lyophilisation; $[\alpha]_{20}^{D}$ = +27.0 (*c* 0.8, water); ^{1}H NMR (600 MHz, D_2O) δ 4.87 (d, $^3J_{1,2}$ = 1.6 Hz, 1H, H-1$_{Man}$), 4.47 (d, $^3J_{1,2}$ = 8.0 Hz, 1H, H-1$_{Glc}$), 4.05 (dd, $^2J_{9a,9b}$ = 11.1 Hz, $^3J_{8,9a}$ = 4.0 Hz, 1H, H-9a), 4.00–3.85 (m, 5H, H-2$_{Man}$, H-5$_{Man}$, H-6a$_{Man}$, H-6a$_{Glc}$, H-7a), 3.82 (dd, $^3J_{2,3}$ = 9.1 Hz, $^3J_{3,4}$ = 3.4 Hz, 1H, H-3$_{Man}$), 3.79–3.58 (m, 6H, H-8, H-4$_{Man}$, H-6b$_{Glc}$, H-9b, H-7b, H-6b$_{Man}$), 3.52–3.41 (m, 2H, H-3$_{Glc}$, H-5$_{Glc}$), 3.40–3.34 (m, 1H, H-4$_{Glc}$), 3.28 (dd, $^3J_{2,3}$ = 9.4 Hz, $^3J_{2,1}$ = 8.0 Hz, 1H, H-2$_{Glc}$) ppm; ^{13}C NMR (151 MHz, D_2O) δ 102.8 (C-1$_{Glc}$), 100.3 (C-1$_{Man}$), 75.9 (C-5$_{Glc}$), 75.7 (C-3$_{Glc}$), 73.1 (C-2$_{Glc}$), 73.0 (C-4$_{Man}$), 70.4 (C-3$_{Man}$), 69.9 (C-5$_{Man}$), 69.6 (C-4$_{Glc}$), 69.0, 67.2 (C-6$_{Man}$ or C-6$_{Glc}$), 66.7 (C-7), 61.0 (C-6$_{Glc}$ or C-6$_{Man}$), 60.7 (C-9), 60.7 (C-8) ppm; IR (ATR) ν_{max}/cm^{-1} 3325, 2932, 2127, 1672, 1021; ESI-HRMS: *m*/*z* calcd for $C_{15}H_{27}N_3O_{12}$ + Na^+ = 464.14869 [M + Na]$^+$; found 464.14853.

(*s*)-2-Azido-1-*O*-(α-D-mannopyranosyl)-3-*O*-(β-D-glucopyranosyl)-1,3-propanediol (15b). General procedure C was applied to compound **14b** (123 mg, 96.0 μmol). Reagents and conditions: Sodium methoxide (*c* = 5.4 M in methanol, two drops), methanol (*c* = 0.03 M, 3.2 mL). Compound **15b** (37.2 mg, 89%) was obtained as a white foam after lyophilisation; $[\alpha]_{20}^{D}$ = +51.9 (*c* 0.8, watcr); ^{1}H NMR (600 MHz, D_2O) δ 4.89 (d, $^3J_{1,2}$ = 1.5 Hz, 1H, H-1$_{Man}$), 4.47 (d, $^3J_{1,2}$ = 8.0 Hz, 1H, H-1$_{Glc}$), 4.00–3.95 (m, 3H, H-2$_{Man}$, H-3$_{Man}$, H-9a), 3.92–3.79 (m, 5H, H-4$_{Man}$, H-9b, H-6a$_{Man}$, H-6a$_{Glc}$, H-7a), 3.77–3.68 (m, 3H, H-7b, H-6b$_{Man}$, H-6b$_{Glc}$), 3.66–3.62 (m, 2H, H-5$_{Man}$, H-8), 3.47 (dd, $^3J_{2,3}$ = $^3J_{3,4}$ = 9.2 Hz, 1H, H-3$_{Glc}$)3.45–3.41 (m, 1H, H-5$_{Glc}$), 3.39–3.34 (dd, $^3J_{3,4}$ = $^3J_{4,5}$ = 9.4 Hz, 1H, H-4$_{Glc}$), 3.28 (dd, $^3J_{2,3}$ = 9.3 Hz, $^3J_{1,2}$ = 8.0 Hz, 1H, H-2$_{Glc}$) ppm; ^{13}C NMR (151 MHz, D_2O) δ 102.4 (C-1$_{Glc}$), 99.7 (C-1$_{Man}$), 76.0 (C-3$_{Glc}$), 75.7 (C-5$_{Glc}$), 73.1 (C-4$_{Man}$), 73.0 (C-2$_{Glc}$), 70.4 (C-2$_{Man}$), 69.9 (C-3$_{Man}$), 69.72 (C-4$_{Glc}$), 69.6 (C-5$_{Man}$), 68.7 (C-6$_{Man}$ or C-6$_{Glc}$), 66.9 (C-6$_{Man}$ or C-6$_{Glc}$), 61.0 (C-7), 60.7 (C-9), 60.2 (C-8) ppm; IR (ATR) ν_{max}/cm^{-1} 3338, 2932, 2115, 1259, 1033; ESI-HRMS: *m*/*z* [M + Na]$^+$ calcd for $C_{15}H_{27}N_3O_{12}$ + Na^+ = 464.14869 [M + Na]$^+$; found 464.14847.

(*r*)-2-Azido-1-*O*-(2,3,4,6-tetra-*O*-benzoyl-α-D-mannopyranosyl)-3-*O*-(2,3,4,6-tetra-*O*-benzoyl-β-D-galactopyranosyl)-1,3-propanediol (17a). General procedure A was applied to acceptor **12a** (167 mg, 241 μmol) and donor **16** (274 mg, 361 μmol, 1.5 eq.). Reagents and conditions: *N*-Iodosuccinimide (109 mg, 482 μmol, 2 eq.), trifluoromethane sulfonic acid (4.8 μl, 48.0 μmol, 0.1 eq.), and dichloromethane (*c* = 0.1 M, 2.05 mL). Flash chromatography with ethyl acetate/cyclohexane (2.5/7.5) afforded compound **17a** (196 mg, 64%) as a white foam; R_f = 0.3 (ethyl acetate/cyclohexane 3/7); $[\alpha]_{20}^{D}$ = −16.3 (*c* 1, dichloromethane); ^{1}H NMR (600 MHz, $CDCl_3$) δ 8.13–8.07 (m, 4H, 4 H–Ar), 8.03–8.01 (m, 4H, 4 H–Ar), 7.98–7.92 (m, 4H, 4 H–Ar), 7.83–7.77 (m, 4H, 4 H–Ar), 7.62–7.28 (m, 22H, 22 H–Ar), 7.24–7.22 (m, 2H, 2 H–Ar) 6.11 (dd, $^3J_{4,5}$ = $^3J_{3,4}$ = 10.1 Hz, 1H,

H-4$_{Man}$), 6.01 (dd, $^3J_{3,4}$ = 3.4 Hz, $J_{4,5}$ = 1.0 Hz, 1H, H-4$_{Gal}$), 5.86 (dd, $^3J_{3,4}$ = 10.1 Hz, $^3J_{2,3}$ = 3.3 Hz, 1H, H-3$_{Man}$), 5.80 (dd, $^3J_{2,3}$ = 10.4 Hz, $^3J_{1,2}$ = 7.9 Hz, 1H, H-2$_{Gal}$), 5.67 (dd, $^3J_{2,3}$ = 3.3 Hz, $^3J_{2,1}$ = 1.8 Hz, 1H, H-2$_{Man}$), 5.63 (dd, $^3J_{2,3}$ = 10.4 Hz, $^3J_{3,4}$ = 3.5 Hz, 1H, H-3$_{Gal}$), 4.90–4.87 (m, 2H, H-1$_{Man}$, H-1$_{Gal}$), 4.71 (dd, $^2J_{6a,6b}$ = 11.4 Hz, $^3J_{5,6a}$ = 6.5 Hz, 1H, H-6a$_{Man}$), 4.63 (dd, $^2J_{6a,6b}$ = 12.2 Hz, $^3J_{5.6a}$ = 2.5 Hz, 1H, H-6a$_{Gal}$), 4.48–4.41 (m, 2H, H-6b$_{Man}$, H-6b$_{Gal}$), 4.40–4.35 (1H, H-5$_{Gal}$), 4.35–4.30 (m, 1H, H-5$_{Man}$), 4.11 (dd, $J_{9a,9b}$ = 10.6 Hz, $J_{8,9a}$ = 5.1 Hz, 1H, H-9a), 3.99–3.91 (m, 1H, H-8), 3.85 (dd, $J_{7a,7b}$ = 10.2 Hz, $J_{7a,8}$ = 7.9 Hz, 1H, H-7a), 3.74–3.67 (m, 2H, H-7b, H-9b) ppm; ^{13}C NMR (151 MHz, $CDCl_3$) δ 166.1, 166.0, 165.6, 165.54, 165.4, 165.4, 165.3, 165.2 (8C, 8 PhC=O), 133.6, 133.5, 133.5, 133.4, 133.3, 133.2, 133.1, 130.0, 129.9, 129.8, 129.8, 129.8, 129.8, 129.7, 129.7, 129.4, 129.2, 129.2, 129.0, 128.9, 128.7, 128.6, 128.5, 128.3, 128.2 (48C, 48 C–Ar), 101.9 (C-1$_{Gal}$), 97.6 (C-1$_{Man}$), 71.6 (C-3$_{Gal}$ or C-5$_{Gal}$), 71.5 (C-3$_{Gal}$ or C-5$_{Gal}$), 70.0 (C-2$_{Man}$), 69.8 (C-3$_{Man}$), 69.6 (C-2$_{Gal}$), 69.2 (C-5$_{Man}$), 68.7 (C-9), 68.1 (C-4$_{Gal}$ or C-7), 68.0 (C-4$_{Gal}$ or C-7), 66.5 (C-4$_{Man}$), 62.5 (C-6$_{Gal}$), 61.9 (C-6$_{Man}$), 59.9 (C-8) ppm; IR (ATR) ν_{max}/cm^{-1} 2096, 1722, 1451, 1257, 1091, 705; ESI-HRMS: *m*/*z* calcd for $C_{71}H_{59}N_3O_{20}$ + Na^+: 1296.35841 $[M + Na]^+$; found 1296.35802.

(*s*)-2-Azido-1-*O*-(2,3,4,6-tetra-*O*-benzoyl-α-D-mannopyranosyl)-3-*O*-(2,3,4,6-tetra-*O*-benzoyl-β-D-galactopyranosyl)-1,3-propanediol (17b). General procedure A was applied to acceptor **12b** (226 mg, 324 μmol) and donor **16** (369 mg, 486 μmol, 1.5 eq.). Reagents and conditions: *N*-Iodosuccinimide (195 mg, 648 μmol, 2 eq.), trifluoromethane sulfonic acid (6.5 μl, 64.0 μmol, 0.1 eq.) and dichloromethane (*c* = 0.1 M, 3.24 mL). Flash chromatography with ethyl acetate/cyclohexane (2.5/7.5) afforded compound **17b** (251 mg, 61%) as a white foam; R_f = 0.3 (ethyl acetate/cyclohexane 3/7); $[\alpha]_{20}^{D}$ = −21.1 (*c* 1, dichloromethane); ^{1}H NMR (600 MHz, $CDCl_3$) δ 8.11–8.08 (m, 4H, 4 H–Ar), 8.03–8.01 (m, 6H, 6 H–Ar), 7.96–7.95 (m, 2H, 2 H–Ar), 7.84–7.78 (m, 4H, 4 H–Ar), 7.63–7.33 (m, 22H, 22 H–Ar), 7.27–7.23 (m, 2H, 2 H–Ar), 6.11 (dd, $^3J_{4,5}$ = $^3J_{3,4}$ = 10.1 Hz, 1H, H-4$_{Man}$), 6.02 (dd, $J_{3,4}$ = 3.4 Hz, $J_{4,5}$ = 0.7 Hz, 1H, H-4$_{Gal}$), 5.87–5.82 (m, 2H, H-3$_{Man}$, H-2$_{Gal}$), 5.68 (dd, $^3J_{2,3}$ = 3.3 Hz, $^3J_{1,2}$ = 1.8 Hz, 1H, H-2$_{Man}$), 5.64 (dd, $^3J_{3,4}$ = 10.4 Hz, $^3J_{2,3}$ = 3.5 Hz, 1H, H-3$_{Gal}$), 4.99 (d, $^3J_{1,2}$ = 1.6 Hz, 1H, H-1$_{Man}$), 4.96 (d, $^3J_{1,2}$ = 7.9 Hz, 1H, H-1$_{Gal}$), 4.73 (dd, $^2J_{6a,6b}$ = 11.2 Hz, $^3J_{5,6a}$ = 6.3 Hz, 1H, H-6a$_{Man}$), 4.65 (dd, $J_{6a,6b}$ = 12.2 Hz, $J_{5.6a}$ = 2.5 Hz, 1H, H-6a$_{Gal}$), 4.48–4.43 (m, 2H, H-6b$_{Gal}$, H-6b$_{Man}$), 4.42–4.38 (m, 2H, H-5$_{Man}$, H-5$_{Gal}$), 4.17 (dd, $^2J_{9a,9b}$ = 10.4 Hz, $J_{8,9a}$ = 3.8 Hz, 1H, H-9a), 3.92–3.87 (m, 2H, H-8, H-7a), 3.85 (dd, $^2J_{9a,9b}$ = 10.3 Hz, $^3J_{8,9b}$ = 7.7 Hz, 1H, H-9b), 3.61 (dd, $^2J_{7a,7b}$ = 11.6 Hz, $^3J_{7b,8}$ = 6.7 Hz, 1H, H-7b) ppm; ^{13}C NMR (151 MHz, $CDCl_3$) δ 166.1, 166.0, 165.6, 165.5, 165.3, (8C, 8 PhC=O), 133.6, 133.5, 133.3, 133.2, 133.1, 132.9, 130.1, 129.9, 129.8, 129.8, 129.6, 129.5, 129.3, 129.2, 129.0, 129.0, 128.9, 128.7, 128.7, 128.6, 128.5, 128.5, 128.4, 128.3, (48C, 48 C–Ar), 102.0 (C-1$_{Gal}$), 97.9 (C-1$_{Man}$), 71.6 (C-3$_{Gal}$ or C-5$_{Gal}$), 71.5 (C-3$_{Gal}$ or C-5$_{Gal}$), 70.1 (C-2$_{Man}$), 69.8 (C-3$_{Man}$ or C-2$_{Gal}$), 69.7 (C-9), 69.6 (C-3$_{Man}$ or C-2$_{Gal}$), 69.2 (C-5$_{Man}$), 68.0 (C-7), 67.9 (C-4$_{Gal}$), 62.6 (C-6$_{Gal}$), 61.9 (C-6$_{Man}$), 60.3 (C-8) ppm; IR (ATR) ν_{max}/cm^{-1} 2933, 2094, 1721, 1451, 1258, 1066, 705; ESI-HRMS: *m*/*z* calcd for $C_{71}H_{59}N_3O_{20}$ + Na^+: 1296.35841 $[M + Na]^+$; found 1296.35793.

(*r*)-2-Azido-1-*O*-(α-D-mannopyranosyl)-3-*O*-(β-D-galactopyranosyl)-1,3-propanediol (18a). General procedure C was applied to compound **17a** (196 mg, 153 μmol). Reagents and conditions: Sodium methoxide (*c* = 5.4 M in methanol, two drops) and methanol (*c* = 0.03 M, 4.02 mL). Compound **18a** (71.3 mg, 98%) was obtained as a white foam after lyophilisation; $[\alpha]_{20}^{D}$ = +37.1 (*c* 0.8, water); ^{1}H NMR (600 MHz, D_2O) δ 4.89 (d, $^3J_{1,2}$ = 1.6 Hz, 1H, H-1$_{Man}$), 4.40 (d, $^3J_{1,2}$ = 7.9 Hz, 1H, H-1$_{Gal}$), 4.01–3.95 (m, 3H, H-2$_{Man}$, H-3$_{Man}$, H-9a), 3.92–3.70 (m, 9H, H-4$_{Man}$, H-5$_{Man}$, H-6$_{Man}$, H-6$_{Gal}$, H-9b, H-7), 3.67 (dd, $^3J_{3,4}$ = 8.0 Hz, $^3J_{4,5}$ = 4.1 Hz, 1H, H-4$_{Gal}$), 3.65–3.61 (m, 3H, H-3$_{Gal}$, H-8, H-5$_{Gal}$), 3.51 (dd, $^3J_{2,3}$ = 9.9 Hz, $^3J_{2,1}$ = 7.9 Hz, 1H, H-2$_{Gal}$) ppm; ^{13}C NMR (151 MHz, D_2O) δ 102.9 (C-1$_{Gal}$), 99.7 (C-1$_{Man}$), 75.2 (C-4$_{Gal}$), 73.0 (C-3$_{Gal}$ or C-5$_{Gal}$), 72.7 (C-3$_{Gal}$ or C-5$_{Gal}$), 70.7 (C-2$_{Gal}$), 70.4 (C-4$_{Man}$ or C-5$_{Man}$), 69.9 (C-3$_{Man}$), 68.6 (C-4$_{Man}$ or C-5$_{Man}$), 68.6 (C-9), 66.9 (2C, C-7, C-8), 61.0 (2C, C-6$_{Man}$, C-6$_{Gal}$), 60.2 (C-2$_{Man}$) ppm; IR (ATR) ν_{max}/cm^{-1} 3338, 2933, 2124, 1640, 1032; ESI-HRMS: *m*/*z* calcd for $C_{15}H_{27}N_3O_{12}$ + Na^+ = 464.14869 $[M + Na]^+$; found 464.14847.

(*s*)-2-Azido-1-*O*-(α-D-mannopyranosyl)-3-*O*-(β-D-galactopyranosyl)-1,3-propanediol (18b). General procedure C was applied to compound **17b** (210 mg, 165 μmol). Reagents and conditions: Sodium methoxide (*c* = 5.4 M in methanol, two drops), methanol (*c* = 0.03 M, 5.5 mL). Compound **18b** (61.8 mg, 85%) was obtained as a white foam after lyophilisation; $[\alpha]_{20}^{D}$ = +22.9 (*c* 0.8, water); ^{1}H NMR (600 MHz, D_2O) δ 4.88 (d, $^3J_{1,2}$ = 1.6 Hz, 1H, H-1$_{Man}$), 4.40 (d, $^3J_{1,2}$ = 7.9 Hz, 1H, H-1$_{Gal}$), 4.06 (dd, $^2J_{9a,9b}$ = 11.0 Hz, $^3J_{8,9a}$ = 4.0 Hz, 1H, H-9a), 3.99–3.86 (m, 5H, H-2$_{Man}$, H-5$_{Gal}$, H-6a$_{Man}$, H-3$_{Man}$, H-7a), 3.82 (dd, $^3J_{3,4}$ = 9.0 Hz, $^3J_{4,5}$ = 3.4 Hz, 1H, H-4$_{Gal}$), 3.79–3.71 (m, 4H, H-6a$_{Gal}$, H-7b, H-9b, H-6b$_{Man}$), 3.70–3.61 (m, 5H, H-8, H-3$_{Gal}$, H-5$_{Man}$, H-4$_{Man}$, H-6b$_{Gal}$), 3.52 (dd, $^3J_{2,3}$ = 9.9 Hz, $^3J_{1,2}$ = 7.9 Hz, 1H, H-2$_{Gal}$) ppm; ^{13}C NMR (151 MHz, D_2O) δ 103.4 (C-1$_{Gal}$), 100.4 (C-1$_{Man}$), 75.2 (C-5$_{Man}$), 73.0 (C-4$_{Man}$ or C-3$_{Gal}$), 72.7 (C-4$_{Man}$ or C-3$_{Gal}$), 70.7 (C-2$_{Gal}$), 70.4 (C-4$_{Gal}$), 69.9 (C-5$_{Gal}$), 69.0 (C-7), 68.7 (C-3$_{Man}$), 67.2 (C-9), 66.7 (C-2$_{Man}$), 61.0 (2C, C-6$_{Gal}$, C-6$_{Man}$), 60.7 (C-8) ppm; IR (ATR) ν_{max}/cm^{-1} 3337, 2933, 2103, 1639, 1038; ESI-HRMS: *m*/*z* calcd for $C_{15}H_{27}N_3O_{12}$ + Na^+ = 464.14869 $[M + Na]^+$; found 464.14846.

(*R*)-2-Azido-1-*O*-(2-deoxy-2-trifluoroacetamido-3,4,6-tri-*O*-acetyl-β-D-glucopyranosyl)-3-*O*-(2,3,4,6-tetra-*O*-benzoyl-α-D-mannopyranosyl)-1,3-propanediol (20a). General procedure B was applied to acceptor **12a** (188 mg, 271 μmol) and donor **19** (125 mg, 325 μmol, 1.2 eq.). Reagents and conditions: Trimethylsilyl trifluoromethanesulfonate (5.0 μl, 27.0 μmol, 0.1 eq.) and dichloromethane (*c* = 0.1 M, 2.7 mL). Flash chromatography with ethyl acetate/cyclohexane (2/3) afforded compound **20a** (215 mg, 73%) as a white foam; R_f = 0.3 (ethyl acetate/cyclohexane 2/3); $[\alpha]_{20}^{D}$ = −37.10 (*c* 0.8, dichloromethane); ^{1}H NMR (500 MHz, $CDCl_3$) δ 8.09–8.07 (m, 2H, 2 H–Ar), 8.03–8.01 (m, 2H, 2 H–Ar), 7.97–7.95 (m, 2H, 2 H–Ar), 7.84–7.81 (m, 2H, 2 H–Ar), 7.61–7.56 (m, 2H, 2 H–Ar), 7.53–7.49 (m, 1H, H–Ar), 7.47–7.35 (m, 7H, 7 H–Ar), 7.32–7.27 (m, 3H, 2 H–Ar, NHCOCF$_3$), 6.17 (dd, $^3J_{4,5}$ = $J_{3,4}$ = 10.1 Hz, 1H,

View Article Online
Paper Organic & Biomolecular Chemistry

H-4$_{Man}$), 5.89 (dd, $^3J_{3,4}$ = 10.2 Hz, $^3J_{2,3}$ = 3.3 Hz, 1H, H-3$_{Man}$), 5.72 (dd, $^3J_{2,3}$ = 3.2 Hz, $^3J_{1,2}$ = 1.9 Hz, 1H, H-2$_{Man}$), 5.43 (dd, $^3J_{3,4}$ = 10.7 Hz, $^3J_{2,3}$ = 9.3 Hz, 1H, H-3$_{GlcNTFA}$), 5.16–5.10 (m, 2H, H-1$_{Man}$, H-4$_{GlcNTFA}$), 4.84 (d, $^3J_{1,2}$ = 8.3 Hz, 1H, H-1$_{GlcNTFA}$), 4.79 (dd, $^2J_{6a,6b}$ = 12.2 Hz, $^3J_{5,6a}$ = 2.9 Hz, 1H, H-6a$_{Man}$), 4.54–4.41 (m, 2H, H-5$_{Man}$, H-6b$_{Man}$), 4.31 (dd, $^2J_{6a,6b}$ = 12.4 Hz, $^3J_{5,6a}$ = 4.7 Hz, 1H, H-6a$_{GlcNTFA}$), 4.19 (dd, $^2J_{6a,6b}$ = 12.4 Hz, $J_{5,6b}$ = 2.3 Hz, 1H, H-6b$_{GlcNTFA}$), 4.15–3.98 (m, 3H, H-2$_{GlcNTFA}$, H-7a, H-9a), 3.87–3.78 (m, 3H, H-8, H-5$_{GlcNTFA}$, H-7b), 3.75 (dd, $^2J_{9a,9b}$ = 10.4 Hz, $^3J_{8.9a}$ = 5.7 Hz, 1H, H-9b), 2.08, 2.05, 2.03 (each s, each 3H, 3 C$\underline{H}_3$C=O) ppm; ^{13}C NMR (126 MHz, $CDCl_3$) δ 170.8, 170.7, 169.3, 166.4, 165.8, 165.5, 165.4 (7C, 4 Ph$\underline{C}$=O, 3 CH$_3\underline{C}$=O), 157.6, (q, J = 37.4 Hz, $CF_3\underline{C}$=O) 133.6, 133.5, 133.4, 133.2, 129.8, 129.8, 129.7, 129.1, 128.9, 128.6, 128.5, 128.4 (24C, 24 C–Ar), 100.7 (C-1$_{GlcTFA}$), 98.0 (C-1$_{Man}$), 72.2 (C-5$_{GlcNTFA}$), 71.5 (C-3$_{GlcNTFA}$), 70.1 (C-2$_{Man}$), 70.0 (C-3$_{Man}$), 69.2 (C-5$_{Man}$), 68.8 (C-9), 68.2 (C-4$_{GlcNTFA}$), 67.7 (C-7), 66.6 (C-4$_{Man}$), 62.7 (C-6$_{Man}$), 61.7 (C-6$_{GlcNTFA}$), 59.8 (C-8), 55.0 (C-2$_{GlcNTFA}$), 20.7, 21.0, 20.4 (3C, 3 C$\underline{H}_3$C=O) ppm; IR (ATR) ν_{max}/cm^{-1} 3327, 2933, 2308, 2103, 1723, 1219, 1027, 708; ESI-HRMS: m/z calcd for $C_{51}H_{49}F_3N_4O_{19}$ + H^+: 1079.30159 $[M + H]^+$; found 1079.29950.

(*S*)-2-Azido-1-*O*-(2-deoxy-2-trifluoroacetamido-3,4,6-tri-*O*-acetyl-β-D-glucopyranosyl)-3-*O*-(2,3,4,6-tetra-*O*-benzoyl-α-D-mannopyranosyl)-1,3-propanediol (20b). General procedure B was applied to acceptor **12b** (150 mg, 216 μmol) and donor **19** (99.2 mg, 258 μmol, 1.2 eq.). Reagents and conditions: Trimethylsilyl trifluoromethanesulfonate (3.7 μl, 22.0 μmol, 0.1 eq.) and dichloromethane (c = 0.1 M, 2.87 mL). Flash chromatography with ethyl acetate/cyclohexane (2/3) afforded compound **20b** (175 mg, 75%) as a white foam; R_f = 0.3 (ethyl acetate/cyclohexane 2/3); $[\alpha]_{20}^{D}$ = −14.4 (c 0.8, dichloromethane); ^{1}H NMR (600 MHz, $CDCl_3$) δ 8.11–8.09 (m, 2H, 2 H–Ar), 8.03–8.01 (m, 2H, 2 H–Ar), 7.98–7.96 (m, 2H, 2 H–Ar), 7.85–7.83 (m, 2H, 2 H–Ar), 7.61–7.56 (m, 2H, 2 H–Ar), 7.53–7.51 (m, 1H, H–Ar), 7.47–7.36 (m, 7H, 7 H–Ar), 7.29–7.27 (m, 2H, 2 H–Ar), 6.94 (d, J = 8.9 Hz, 1H, N$\underline{H}$COCF$_3$), 6.14 (dd, $J_{4,5}$ = $J_{3,4}$ = 10.0 Hz, 1H, H-4$_{Man}$), 5.86 (dd, $^3J_{3,4}$ = 10.2 Hz, $^3J_{2,3}$ = 3.3 Hz, 1H, H-3$_{Man}$), 5.70 (dd, $^3J_{2,3}$ = 3.2 Hz, $^3J_{2,\ 1}$ = 1.8 Hz, 1H, H-2$_{Man}$), 5.38–5.32 (m, 1H, H-3$_{GlcNTFA}$), 5.16 (dd, $J_{4,5}$ = $J_{3,4}$ = 9.6 Hz, 1H, H-4$_{GlcNTFA}$), 5.09 (d, $^3J_{1,2}$ = 1.6 Hz, 1H, H-1$_{Man}$), 4.83 (d, $^3J_{1,2}$ = 8.3 Hz, 1H, H-1$_{GlcNTFA}$), 4.75 (dd, $^2J_{6a,6b}$ = 11.8 Hz, $J_{5,6a}$ = 2.3 Hz, 1H, H-6a$_{Man}$), 4.48 (m, 2H, H-5$_{Man}$, H-6b$_{Man}$), 4.32 (dd, $^2J_{6a,6b}$ = 12.4 Hz, $^3J_{5,6a}$ = 4.5 Hz, 1H, H-6a$_{GlcNTFA}$), 4.22 (dd, $^2J_{6a,6b}$ = 12.4 Hz, $^3J_{5,6b}$ = 2.3 Hz, 1H, H-6b$_{GlcNTFA}$), 4.15 (dd, $^2J_{9a,9b}$ = 10.0 Hz, $^3J_{8,9a}$ = 3.9 Hz, 1H, H-9a), 4.12–4.06 (m, 1H, H-2$_{GlcNTFA}$), 3.98 (dd, $^2J_{7a,7b}$ = 10.5 Hz, $^3J_{7a,8}$ = 4.2 Hz, 1H, H-7a), 3.86–3.78 (m, 3H, H-5$_{GlcNTFA}$, H-8, H-9b), 3.70 (dd, $^2J_{7a,7b}$ = 10.5 Hz, $^3J_{7b,8}$ = 4.8 Hz, 1H, H-7b), 2.09, 2.06, 2.05 (each s, each 3H, 3 C$\underline{H}_3$C=O) ppm; ^{13}C NMR (151 MHz, $CDCl_3$) δ 170.9, 170.7, 169.3, 166.3, 165.8, 165.5, 165.4 (7C, 4 Ph$\underline{C}$=O, 3 CH$_3\underline{C}$=O), 133.6, 133.4, 133.2, 129.9, 129.8, 129.8, 129.7, 129.1, 128.9, 128.6, 128.5, 128.4 (24C, 24 C–Ar), 100.5 (C-1$_{GlcNTFA}$), 97.8 (C-1$_{Man}$), 72.3 (C-5$_{GlcNTFA}$), 71.6 (C-3$_{GlcNTFA}$), 70.0 (2C, C-2$_{Man}$, C-3$_{Man}$), 69.5 (C-9), 69.3 (C-5$_{Man}$), 68.0 (C-4$_{GlcNTFA}$), 67.7 (C-7), 66.6 (C-4$_{Man}$), 62.7 (C-6$_{Man}$), 61.7 (C-6$_{GlcNTFA}$), 59.7 (C-8), 55.0 (C-2$_{GlcNTFA}$), 21.8, 20.6, 20.4 (3 CH$_3$C=O) ppm; IR (ATR) ν_{max}/cm^{-1} 2933, 2308, 2105, 1724, 1260, 1067, 708; ESI-HRMS: m/z calcd for $C_{51}H_{49}F_3N_4O_{19}$ + H^+: 1079.30159 $[M + H]^+$; found 1079.29953.

(*R*)-2-Azido-1-*O*-(2-deoxy-2-trifluoroacetamido-β-D-glucopyranosyl)-3-*O*-(α-D-mannopyranosyl)-1,3-propanediol (21a). General procedure C was applied to compound **20a** (169 mg, 157 μmol). Reagents and conditions: Sodium methoxide (c = 5.4 M in methanol, two drops), methanol (c = 0.03 M, 5.23 mL). Compound **21a** (74.2 mg, 98%) was obtained as a white foam after lyophilisation; $[\alpha]_{20}^{D}$ = +14.6 (c 0.8, water); ^{1}H NMR (600 MHz, D_2O) δ 4.86 (d, $^3J_{1,2}$ = 1.5 Hz, 1H, H-1$_{Man}$), 4.65 (d, $^3J_{1,2}$ = 8.5 Hz, 1H, H-1$_{GlcNTFA}$), 4.00–3.84 (m, 5H, H-2$_{Man}$, H-5$_{GlcNTFA}$, H-9a, H-6a$_{GlcNTFA}$, H-6a$_{Man}$), 3.82–3.73 (m, 6H, H-6b$_{Man}$, H-6b$_{GlcNTFA}$, H-9b, H-7a, H-2$_{GlcNTFA}$, H-3$_{Man}$), 3.69–3.58 (m, 4H, H-7b, H-4$_{Man}$, H-3$_{GlcNTFA}$, H-4$_{GlcNTFA}$), 3.48–3.45 (m, 2H, H-8, H-5$_{Man}$) ppm; ^{13}C NMR (151 MHz, D_2O) δ 100.6 (C-1$_{GlcNTFA}$), 99.9 (C-1$_{Man}$), 76.1 (C-8), 73.0 (2C, C-3$_{GlcNTFA}$, C-4$_{GlcNTFA}$), 70.4 (C-3$_{Man}$), 69.9 (C-2$_{Man}$ or C-5$_{GlcNTFA}$), 69.8 (C-2$_{Man}$ or C-5$_{GlcNTFA}$), 68.9 (C-9), 66.8 (C-7), 66.6 (C-4$_{Man}$), 60.8 (C-6$_{GlcNTFA}$), 60.6 (C-6$_{Man}$), 59.9 (C-5$_{Man}$), 56.0 (C-2$_{GlcNTFA}$) ppm; IR (ATR) ν_{max}/cm^{-1} 3306, 2933, 2102, 1707, 1023; ESI-HRMS: m/z calcd for $C_{17}H_{27}F_3N_4O_{12}$ + Na^+: 559.14776 $[M + Na]^+$; found 559.14681.

(*S*)-2-Azido-1-*O*-(2-deoxy-2-trifluoroacetamido-β-D-glucopyranosyl)-3-*O*-(α-D-mannopyranosyl)-1,3-propanediol (21b). General procedure C was applied to compound **20b** (159 mg, 147 μmol). Reagents and conditions: Sodium methoxide (c = 5.4 M in methanol, two drops), methanol (c = 0.03 M, 5.0 mL). Compound **21b** (74.3 mg, quantitative) was obtained as a white foam after lyophilisation; $[\alpha]_{20}^{D}$ = +11.8 (c 0.8, water); ^{1}H NMR (600 MHz, D_2O) δ 4.83 (d, $^3J_{1,2}$ = 1.7 Hz, 1H, H-1$_{Man}$), 4.64 (d, $^3J_{1,2}$ = 8.5 Hz, 1H, H-1$_{GlcNTFA}$), 4.10 (dd, $^2J_{9a,9b}$ = 10.9 Hz, $^3J_{8,9a}$ = 3.5 Hz, 1H, H-9a), 3.95 (dd, $^3J_{2,3}$ = 3.3 Hz, $^3J_{1,2}$ = 1.6 Hz, 1H, H-2$_{GlcNTFA}$), 3.94–3.91 (m, 1H, H-6a$_{Man}$), 3.90–3.85 (m, 3H, H-7a, H-4$_{GlcNTFA}$, H-6a$_{GlcNTFA}$), 3.82–3.72 (m, 4H, H-3$_{Man}$, H-2$_{GlcNTFA}$, H-5$_{GlcNTFA}$, H6b$_{Man}$), 3.69–3.60 (m, 4H, H-6b$_{GlcNTFA}$, H-9b, H-4$_{Man}$, H-3$_{GlcNTFA}$), 3.57–3.52 (m, 1H, H-7b), 3.50–3.45 (m, 2H, H-5$_{Man}$, H-8) ppm; ^{13}C NMR (151 MHz, D_2O) δ 100.9 (C-1$_{GlcTFA}$), 100.3 (C-1$_{Man}$), 76.0 (C-8), 73.0 (C-3$_{GlcNTFA}$ or C-4$_{Man}$), 70.4 (C-3$_{Man}$), 69.9 (C-2$_{Man}$), 69.4 (C-9), 67.0 (C-7), 66.7 (C-3$_{GlcNTFA}$ or C-4$_{Man}$), 60.6 (C-6$_{GlcNTFA}$), 60.5 (2C, C-5$_{Man}$, C-6$_{Man}$), 56.1 (C-2$_{GlcNTFA}$) ppm; IR (ATR) ν_{max}/cm^{-1} 3288, 2933, 2108, 1707, 1022; ESI-HRMS: m/z calcd for $C_{17}H_{27}F_3N_4O_{12}$ + Na^+: 559.14776 $[M + Na]^+$; found 559.14623.

(*R*)-2-Azido-1-*O*-(2-deoxy-2-acetamido-β-D-glucopyranosyl)-3-*O*-(α-D-mannopyranosyl)-1,3-propanediol (22a). General procedure E was applied to compound **21a** (76.8 mg, 141 μmol). Reagents and conditions: (i) aq. lithium hydroxide (c = 2 M, 2.80 mL, 5.66 mmol, 40 eq.) and methanol (c = 0.03 M, 4.70 mL); (ii) sodium methoxide (c = 5.4 M in methanol, two drops), acetic anhydride (44 μl, 465 μmol, 5 eq.), and methanol (c = 0.03 M, 3.1 mL). Compound **22a** (28.0 mg, 60%) was obtained as a white foam after lyophilisation; $[\alpha]_{20}^{D}$ = +3.1 (c 0.8, water); ^{1}H NMR (500 MHz, D_2O) δ 4.84 (d, $^3J_{1,2}$ = 1.7 Hz,

1H, H-1$_{Man}$), 4.53 (d, $^{3}J_{1,2}$ = 8.5 Hz, 1H, H-1$_{GlcNAc}$), 4.09 (dd, $^{2}J_{9a,9b}$ = 10.9 Hz, $^{3}J_{8,9a}$ = 3.5 Hz, 1H, H-9a), 3.96 (dd, $^{3}J_{2,3}$ = 3.4 Hz, $^{3}J_{2,1}$ = 1.8 Hz, 1H, H-2$_{Man}$), 3.93–3.83 (m, 4H, H-6a$_{GlcNAc}$, H-7a, H-5$_{GlcNAc}$, H-6a$_{Man}$), 3.81 (dd, $^{3}J_{3,4}$ = 9.4 Hz, $^{3}J_{2,3}$ = 3.4 Hz, 1H, H-3$_{Man}$), 3.78–3.62 (m, 6H, H-6b$_{GlcNAc}$, H-4$_{Man}$, H-8, H-3$_{GlcNAc}$, H-7b, H-9b), 3.58–3.50 (m, 2H, H-5$_{Man}$, H-6b$_{Man}$), 3.44 (m,2H, H-4$_{GlcNAc}$, H-2$_{GlcNAc}$), 2.04 (s, 3H, C$\underline{H}_3$C═O) ppm; ^{13}C NMR (126 MHz, D_2O) δ 177.4 (CH$_3\underline{C}$═O), 104.4 (C-1$_{GlcNAc}$), 103.1 (C-1$_{Man}$), 78.7 (C-4$_{GlcNAc}$ or C-2$_{GlcNAc}$), 76.5 (C-5$_{GlcNAc}$), 75.7 (C-4$_{Man}$), 73.2 (C-3$_{Man}$), 72.7 (C-2$_{Man}$), 72.6 (C-4$_{GlcNAc}$ or C-2$_{GlcNAc}$), 72.3 (C-9), 69.8 (C-6$_{Man}$), 69.4 (C-3$_{GlcNAc}$), 63.7 (C-7 or C-6$_{GlcNAc}$), 63.5 (C-7 or C-6$_{GlcNAc}$), 63.4 (C-5$_{Man}$), 58.3 (C-8), 25.0 ($\underline{C}H_3C$═O) ppm IR (ATR) ν_{max}/cm^{-1} 3279, 2103, 1557, 1410, 1054; ESI-HRMS: *m*/*z* calcd for $C_{17}H_{30}N_4O_{12}$ + Na$^+$: 505.17524 [M + Na]$^+$; found 505.17514.

(*S*)-2-Azido-1-*O*-(2-deoxy-2-acetamido-β-D-glucopyranosyl)-3-*O*-(-α-D-mannopyranosyl)-1,3-propanediol (22b). General procedure E was applied to compound **21b** (74.0 mg, 137 μmol). Reagents and conditions: (i) aq. lithium hydroxide (*c* = 2 M, 2.8 mL, 5.51 mmol, 40 eq.) and methanol (*c* = 0.03 M, 4.59 mL); (ii) sodium methoxide (*c* = 5.4 M in methanol, two drops), acetic anhydride (34 μl, 363 μmol, 5 eq.), methanol (*c* = 0.03 M, 2.4 mL). Compound **22b** (23.0 mg, 58%) was obtained as a white foam after lyophilisation; $[\alpha]_{20}^{D}$ = +3.4 (*c* 0.8, water); ^{1}H NMR (500 MHz, D_2O) δ 4.88 (d, $^{3}J_{1,2}$ = 1.7 Hz, 1H, H-1$_{Man}$), 4.56 (d, $^{3}J_{1,2}$ = 8.4 Hz, 1H, H-1$_{GlcNAc}$), 3.99–3.95 (m, 2H, H-2$_{Man}$, H-6a$_{Man}$), 3.94–3.85 (m, 3H, H-5$_{Man}$, H-5$_{GlcNAc}$, H-6b$_{Man}$), 3.83–3.60 (m, 9H, H-3$_{Man}$, H-2$_{GlcNAc}$, H-7a, H-7b, H-9a, H-9b, H-4$_{Man}$, H-6$_{GlcNAc}$), 3.57–3.50 (m, 1H, H-3$_{GlcNAc}$), 3.46–3.40 (m, 2H, H-4$_{GlcNAc}$, H-8), 2.04 (s, 3H, C$\underline{H}_3$C═O) δ ppm; ^{13}C NMR (151 MHz, D_2O) δ 174.7 (CH$_3\underline{C}$═O), 101.2 (C-1$_{GlcNAc}$), 99.8 (C-1$_{Man}$), 76.0 (C-4$_{GlcNAc}$), 73.8 (C-3$_{GlcNAc}$), 73.0 (C-4$_{Man}$), 70.4 (C-3$_{Man}$ or C-5$_{Man}$), 68.5 (C-8), 69.9 (C-5$_{GlcNAc}$), 68.7 (C-3$_{Man}$ or C-5$_{Man}$), 66.7 (C-2$_{Man}$), 60.9 (C-6$_{Man}$ or C-6$_{GlcNAc}$), 60.7 (C-6$_{Man}$ or C-6$_{GlcNAc}$), 59.9 (C-2$_{GlcNAc}$), 55.5 (C-7 or C-9), 48.9 (C-7 or C-9), 22.3 ($\underline{C}H_3C$═O) ppm; IR (ATR) ν_{max}/cm^{-1} 3266, 2114, 1557, 1410, 1054; ESI-HRMS: *m*/*z* calcd for $C_{17}H_{30}N_4O_{12}$ + Na$^+$: 505.17524 [M + Na]$^+$; found 505.17505.

Conflicts of interest

There are no conflicts to declare.

Acknowledgements

The authors are grateful for funding by the DFG (SFB 677) and by the Fonds of the Chemical Industry (FCI). We are also very thankful to Dr Claudia Fessele for teaching J. B. the biological assays.

Notes and references

1 (*a*) B. Alberts, A. Johnson, J. Lewis, D. Morgan, M. Raff, K. Roberts and P. Walter, in *Molecular Biology of the Cell*, ed. B. Alberts, Garland Science, New York, 6th edn, 2014, ch. 15, pp. 813–888; (*b*) B. E. Collins and J. C. Paulson, *Curr. Opin. Chem. Biol.*, 2004, **8**, 617–625; (*c*) L. L. Kiessling and R. A. Splain, *Annu. Rev. Biochem.*, 2010, **79**, 619–653; (*d*) P. R. Crocker, *Curr. Opin. Struct. Biol.*, 2002, **12**, 609–615.

2 (*a*) I. Ofek, D. Mirelman and N. Sharon, *Nature*, 1977, **265**, 623–625; (*b*) N. Sharon and H. Lis, *Glycobiology*, 2004, **14**, 53R–62R; (*c*) K. Ohlsen, T. A. Oelschlaeger, J. Hacker and A. S. Khan, *Top. Curr. Chem.*, 2009, **288**, 17–65.

3 (*a*) S. D. Knight and J. Bouckaert, *Top. Curr. Chem.*, 2009, **288**, 67–107; (*b*) M. Hartmann and T. K. Lindhorst, *Eur. J. Org. Chem.*, 2011, 3583–3609.

4 J. Lillington, S. Geibel and G. Waksman, *Biochim. Biophys. Acta*, 2014, **1840**, 2783–2793.

5 J. J. Lundquist and E. J. Toone, *Chem. Rev.*, 2002, **102**, 555–578.

6 (*a*) Y. C. Lee and R. T. Lee, *Acc. Chem. Res.*, 1995, **28**, 321–327; (*b*) T. K. Lindhorst, C. Kieburg and U. Krallmann-Wenzel, *Glycoconjugate J.*, 1998, **15**, 605–613; (*c*) A. Imberty, J. M. Chabre and R. Roy, *Chem. – Eur. J.*, 2008, **14**, 7490–7499; (*d*) A. Bernardi, *et al.*, *Chem. Soc. Rev.*, 2013, **42**, 4709–4727.

7 (*a*) P. I. Kitov, J. M. Sadowska, G. Mulvey, G. D. Armstrong, H. Ling, N. S. Pannu, R. J. Read and D. R. Bundle, *Nature*, 2000, **403**, 669–672; (*b*) M. Touaibia, A. Wellens, T. C. Shiao, Q. Wang, S. Sirois, J. Bouckaert and R. Roy, *ChemMedChem*, 2007, **2**, 1190–1201; (*c*) H. M. Branderhorst, R. Kooij, A. Salmincn, L. H. Jongcncel, C. J. Arnusch, R. M. Liskamp, J. Finn and R. J. Pieters, *Org. Biomol. Chem.*, 2008, **6**, 1425–1434.

8 C. Müller, G. Despras and T. K. Lindhorst, *Chem. Soc. Rev.*, 2016, **45**, 3275–3302.

9 (*a*) K. L. Prime and G. M. Whitesides, *J. Am. Chem. Soc.*, 1993, **115**, 10714–10721; (*b*) F. Pertici and R. J. Pieters, *Chem. Commun.*, 2008, **48**, 4008–4010; (*c*) H. M. Branderhorst, R. M. J. Liskamp, G. M. Visser and R. J. Pieters, *Chem. Commun.*, 2007, 5043–5045; (*d*) D. Schwefel, C. Maierhofer, J. G. Beck, S. Seeberger, K. Diederichs, H. M. Möller, W. Welte and V. Wittmann, *J. Am. Chem. Soc.*, 2010, **132**, 8704–8719; (*e*) S. Igde, S. Röblitz, A. Müller, K. Kolbe, S. Boden, C. Fessele, T. K. Lindhorst, M. Weber and L. Hartmann, *Macromol. Biosci.*, 2017, **17**, 1700198.

10 (*a*) M. Gómez-García, J. M. Benito, D. Rodríguez-Lucena, J.-X. Yu, K. Chmurski, C. Ortiz Mellet, R. Gutiérrez Gallego, A. Maestre, J. Defaye and J. M. García Fernández, *J. Am. Chem. Soc.*, 2005, **127**, 7970–7971; (*b*) M. Gómez-García, J. M. Benito, R. Gutiérrez-Gallego, A. Maestre, C. Ortiz Mellet, J. M. García Fernández and J. L. Jimenez-Blanco, *Org. Biomol. Chem.*, 2010, **8**, 1849–1860; (*c*) M. Gómez-García, J. M. Benito, A. P. Butera, C. Ortiz Mellet, J. M. García Fernández and J. L. Jimenez-Blanco, *J. Org. Chem.*, 2012, **77**, 1273–1288.

11 (*a*) J. L. Jiménez Blanco, C. Ortiz Mellet and J. M. García Fernández, *Chem. Soc. Rev.*, 2013, **42**, 4518–4531;

(*b*) M. I. García-Moreno, F. Ortega-Caballero, R. Rísquez-Cuadro, C. Ortiz Mellet and J. M. García Fernández, *Chem. – Eur. J.*, 2017, **23**, 6295–6304; (*c*) E. T. Sletten, R. S. Loka, F. Yu and H. M. Nguyen, *Biomacromolecules*, 2017, **18**, 3387–3399; (*d*) C. Pifferi, B. Thomas, D. Goyard, N. Berthet and O. Renaudet, *Chem. – Eur. J.*, 2017, **23**, 16283–16296.

12 (*a*) N. Strömberg, P.-G. Nyholm, I. Pascher and S. Normark, *Proc. Natl. Acad. Sci. U. S. A.*, 1991, **88**, 9340–9344; (*b*) T. Weber, V. Chandrasekaran, I. Stamer, M. B. Thygesen, A. Tefort and T. K. Lindhorst, *Angew. Chem., Int. Ed.*, 2014, **53**, 14583–14586; (*c*) L. Möckl, A. Müller, C. Bräuchle and T. K. Lindhorst, *Chem. Commun.*, 2016, **52**, 1254–1257.

13 (*a*) R. Haag, *Beilstein J. Org. Chem.*, 2015, **11**, 848–849; (*b*) A. K. Ciuk and T. K. Lindhorst, *Beilstein J. Org. Chem.*, 2015, **11**, 668–674.

14 T. K. Lindhorst, in *Handbook of Carbohydrate-Modifying Biocatalysts*, ed. P. Grunwald, Pan Stanford Series on Biocatalysis 2, Pan Stanford Publishing, Singapore, 2016, pp. 147–215.

15 M. Zieringer, M. Wyszogrodzka, K. Biskup and R. Haag, *New J. Chem.*, 2012, **36**, 402–406.

16 E. D. Goddard-Borger and T. V. Stick, *Org. Lett.*, 2007, **9**, 3797–3800.

17 M. Collot, J. Savreux and J. M. Mallet, *Tetrahedron*, 2008, **64**, 1523–1535.

18 G. H. Veeneman, S. H. van Leeuwen and J. H. van Boom, *Tetrahedron Lett.*, 1990, **31**, 1331–1334.

19 M. Cortes-Clerget, O. Gager, M. Montcil, J. L. Pirat, E. Migianu-Griffoni, J. Deschamp and M. Lecouvey, *Adv. Synth. Catal.*, 2016, **358**, 34–40.

20 D. Bélanger, X. Tong, S. Soumaré, Y. L. Dory and Y. Zhao, *Chem. – Eur. J.*, 2009, **15**, 4428–4436.

21 (*a*) A. Avenoza, C. Cativiela, F. Corzana, J. M. Peregrina and M. M. Zurbano, *Synthesis*, 1997, 1146–1150; (*b*) A. Ollivier, M. Goubert, A. Tursun, I. Canet and M. E. Sinibaldi, *ARKIVOC*, 2010, (ix), 108–126.

22 R. R. Schmidt, *Angew. Chem., Int. Ed. Engl.*, 1986, **25**, 212–235.

23 T. Ziegler, P. Kováč and C. P. J. Glaudemans, *Liebigs Ann. Chem.*, 1990, 613–615.

24 D. Sail and P. Kováč, *Carbohydr. Res.*, 2012, **357**, 47–53.

25 G. Zemplén and E. Pascu, *Ber. Dtsch. Chem. Ges. B*, 1929, **62**, 1613–1614.

26 (*a*) P. Busca and O. R. Martin, *Tetrahedron Lett.*, 1998, **39**, 8101–8104; (*b*) V. W.-F. Tai and B. Imperiali, *J. Org. Chem.*, 2001, **66**, 6217–6228.

27 G. Despras, A. Alix, D. Urban, B. Vauzeilles and J.-M. Beau, *Angew. Chem., Int. Ed.*, 2014, **53**, 11912–11916.

28 Y. Nagai, N. Ito, I. Sultana and T. Sugai, *Tetrahedron*, 2008, **64**, 9599–9606.

29 K. D. Hardman and C. F. Ainsworth, *Biochemistry*, 1972, **11**, 4910–4919.

30 M. Hartmann, A. K. Horst, P. Klemm and T. K. Lindhorst, *Chem. Commun.*, 2010, **46**, 330332.

31 It is known that adhesion–inhibition assays with live bacteria lead to varying IC_{50} values in individual experiments. However, RIP values, based on the potency of a reference inhibitor like MeMan, which is tested on the same plate, are highly reproducible. Hence, when we repeated the inhibition assay with different batches of bacteria, other IC_{50} values as given in Table 1 (entry 1) were measured but the corresponding RIP values were found to be very similar (*cf.* ESI†).

32 *Schrödinger Release 2017-4: Glide, version 7.0*, Schrödinger, LLC, New York, NY, 2017.

33 J. Bouckaert, J. Berglund, M. Schembri, E. De Genst, L. Cools, M. Wuhrer, C.-S. Hung, J. Pinkner, R. Slättegård, A. Zavialov, D. Choudhury, S. Langermann, S. J. Hultgren, L. Wyns, P. Klemm, S. Oscarson, S. D. Knight and H. De Greve, *Mol. Microbiol.*, 2005, **55**, 441–455.

34 C. S. Hung, J. Bouckaert, D. Hung, J. Pinkner, C. Widberg, A. DeFusco, C. G. Auguste, R. Strouse, S. Langermann, G. Waksman and S. J. Hultgren, *Mol. Microbiol.*, 2002, **44**, 903–915.

35 *Schrödinger Release 2017-4, Prime*, Schrödinger, LLC, New York, NY, 2017.

36 G. Cutolo, F. Reise, M. Schuler, R. Nehmé, G. Despras, J. Brekalo, P. Morin, P.-Y. Renard, T. K. Lindhorst and A. Tatibouët, *Org. Biomol. Chem.*, 2018, **16**, 4900–4913.

37 (*a*) F. Adasme-Carreño, C. Muñoz-Gutierrez, J. Caballero and J. H. Alzate-Morales, *Phys. Chem. Chem. Phys.*, 2014, **16**, 14047–14058; (*b*) F. Chen, H. Liu, H. Sun, P. Pan, Y. Li, D. Li and T. Hou, *Phys. Chem. Chem. Phys.*, 2016, **18**, 22129–22139.

38 (*a*) M. L. Connolly, *Science*, 1983, **221**, 709–713; (*b*) M. L. Connolly, *J. Appl. Crystallogr.*, 1983, **16**, 548–558.

5 Bacterial adhesion to synthetic glycoarrays

ln the LINDHORST group, carbohydrate-specific adhesion of type 1-fimbriated *E. coli* bacteria has been frequently used to test carbohydrate recognition in cell-cell interactions that are ruled by carbohydrate-lectin interactions. *E. coli* are commensal bacteria in humans, but they can also be pathogenic. For instance, urinary tract infections (UTIs) caused by adhesion of uropathogenic *Escherichia coli* bacteria (UPEC) are one of the most common infections worldwide.[29] Bacteria use adhesive organelles so-called fimbriae with a lectin unit at their very end to adhere to glycans of the cell surface glycocalyx. Adhesion to host cell surfaces and bacterial colonization can sometimes lead to fatal infections. There are several reported methods [112] for the treatment and prevention of UTIs but a molecular understanding of the involved processes is crucial for the treatment of diseases arising from microbial adhesion.

Understanding the complete mechanism behind bacterial adhesion is a challenging task. Inhibition of bacterial adhesion to host cell surface or glycoarrays, respectively, is one of the methods that are frequently used to study carbohydrate-protein interactions. Lectins bind to glycoproteins and other sugar-containing entities on the surface of various cells. Thus, synthetic saccharides might be used to prevent bacterial adhesion in the frame of an anti-adhesion therapy.[60c, 113]

Microarrays are a means to study carbohydrate-protein interactions, including bacterial adhesion. Multiple strategies to fabricate microarrays have been reported including covalent and non-covalent (passive) carbohydrate immobilization on various solid supports. Among others, -glass, gold, quartz and polystyrene surfaces are commonly used for the preparation of glycoarrays.[114] Non-covalent immobilization mostly depends on hydrophobic interactions.[115] For the relatively small and hydrophilic oligosaccharides, various conjugation methods have been established. One common approach is oligosaccharide biotinylation and their immobilization on streptavidin-coated surfaces.[116] On the other hand, covalent carbohydrate immobilization has been used in the form of self-assembled monolayers on the gold surfaces, so-called SAMs.[117] SHIN's group reported the use of glass slides with thiol groups as solid support for covalent saccharide immobilization.[118] A relatively well-known method for covalent carbohydrate immobilization includes succinimide active ester groups for amide ligation. In addition, different methods were developed in a similar manner and are all based on the pre-functionalization of a glass surface. Epoxy-silane, amino, azide, al-

dehyde and active ester substrates are among the functional groups used as glass coating with the capacity to form covalent bonds with amino-, thio- and hydroxy-functionalized carbohydrates (**Figure 5.1**). Bacterial adhesion and its inhibition can be tested using one of such established glycoarrays.

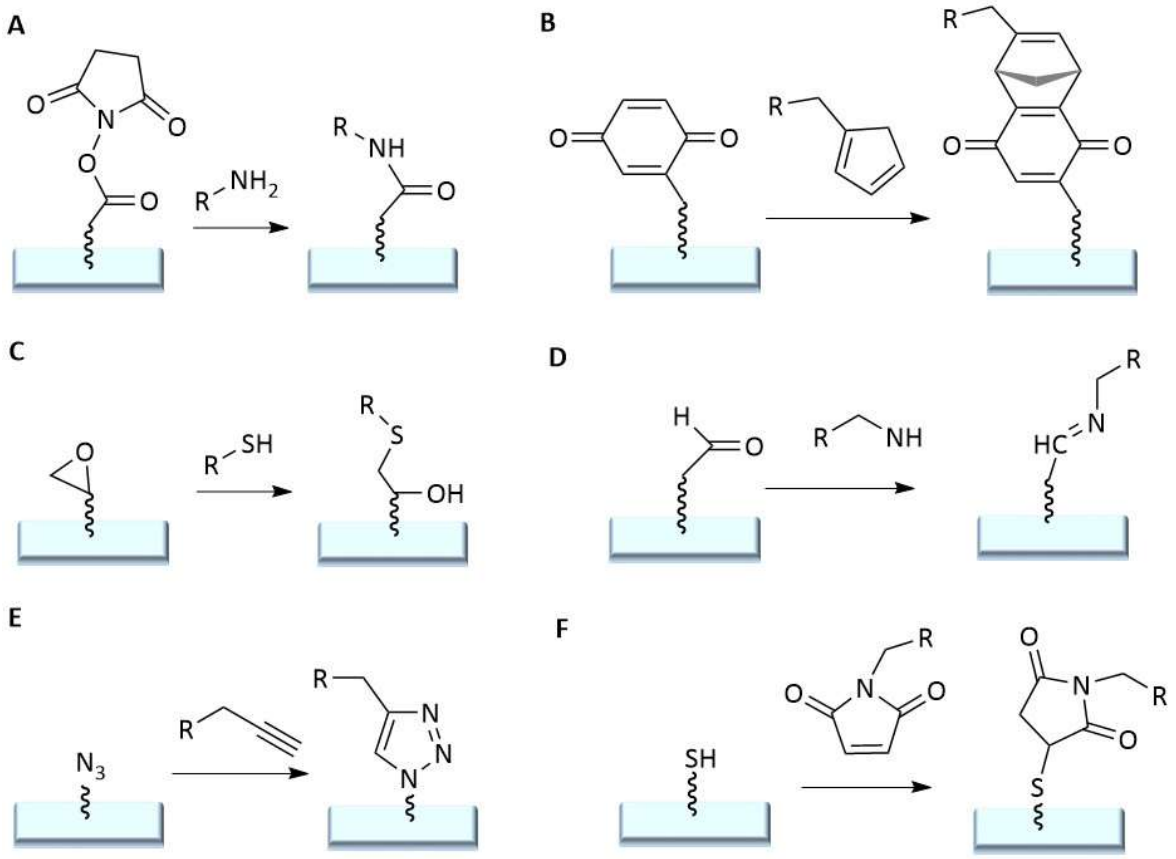

Figure 5.1: Schematic representation of the glycoarrays fabrication: (**A**) Succinimide ester activation for the amide bond formation; (**B**) DIELS-ALDER ligation; (**C**) Epoxy nucleophilic activation; (**D**) Schiff´s base aldehyde-amine ligation; (**E**) 1,3-dipolar cycloaddition between azide and alkynes; (**F**) thiol-maleimide ligation; R-carbohydrate residue.

In order to test bacterial adhesion on such fabricated glycoarrays, two main factors have to be considered. One is important from a chemical point of view and the other is more relevant from the point of view of the environmental or dynamic nature of performed assays. Depending on the type of functional group on the surface it is of importance to test nonspecific bacterial adhesion on the surfaces. Thus, suitable blocking reagents are used for blocking unspecific adhesion. Furthermore, because it is known that the length of a linker used for carbohydrate immobilization influences the affinity of bacterial adhesion, its nature for non-

specific binding was also investigated.[74] Oligoethylene glycol linkers were found favorable for the prevention of nonspecific binding.[119] The density concept studied by FERNANDEZ and coworkers with their cyclodextrin model was proved efficient also for glycoarrays assembly.[79b, 79c] Moreover, the LINDHORST group pointed out the importance of ligands concentration in their study with different ligand valencies used to vary carbohydrate density on polyester surfaces.[115b] Furthermore, different methods were used to establish glycoarrays with more experimental flexibility which would imitate the form of glycoconjugates in the natural state.[120] With respect to the naturally occurring adhesive environment, different dynamic conditions were considered in assays in order to provide more realistic conditions in the study of bacterial adhesion. Hence, bacterial adhesion can be investigated under different flow conditions with respect to the physiological natural flow or the flow of interest *e*.*g*. vein flow or capillary flow. Especially the regulation of shear stress under flow conditions was found to be relevant in lectin binding activity as demonstrated in different studies.[121] The bacterial adhesin (lectin) FimH of *E. coli* bacteria exerts so-called catch-bonds under flow conditions.[122]

Here, we have prepared glycoarrays with the novel pseudoenantiomeric heterodivalent glycoclusters using pre-functionalized polystyrene surfaces. With these glycoarrays, bacterial adhesion was tested under static conditions, as commonly performed in our group. The sharp difference in bacterial adhesion-inhibition assay demonstrated with βGlc-αMan diastereomeric pair discussed in chapter 4 evoked our interest to test bacterial adhesion to glycoarrays with pseudoenantiomeric pair of ligands. Bacterial adhesion to formed glycoarrays was additionally tested under different dynamic environmental conditions. Hence, the same glycoconjugates were immobilized on a glass surface *via* succinimide ester activation for the testing of bacterial adhesion under shear stress.

5.1. Synthesis of pseudoenantiomeric glycoarrays

For the immobilization of the divalent pseudoenantiomeric glycoclusters, a heterobifunctional polyethylene glycol linker (PEG), terminated with a propargyl and an amine group, respectively, were found suitable. The propargyl group was used for Cu(I)-catalyzed 1,3-dipolar cycloaddition with the azido functional group present in synthesized glycoclusters. The amino-functional group of the heterobifunctional linker, on the other hand, can be used for the immobilization on surfaces. Both homobifunctional and heterobifunctional linkers can be varied in length and are readily commercially available.

The regioselective covalent modification of only one terminal functional group of the linker often presents a challenge. The modified synthetic methodology used herein for the synthesis of the heterobifunctional linker molecule **5** comprises four steps (**Scheme 5.1**). The use of the inexpensive starting material **1** (OEG_4) allowed the formation of the required terminal propargyl group under basic conditions, providing compound **2** in a modest 55 % yield. Then, the replacement of the primary halide in **2** using sodium azide gave alkyl azide **3**. This functionality was used for the preparation of primary amine **4** under STAUDINGER reaction conditions. Then, the formed amino group was *N*H-Boc protected to obtain compound **5** prior to the use in Cu(I)-catalyzed 1,3-dipolar cycloaddition reaction with azide-functionalized glycocluster (**Scheme 5.1**).

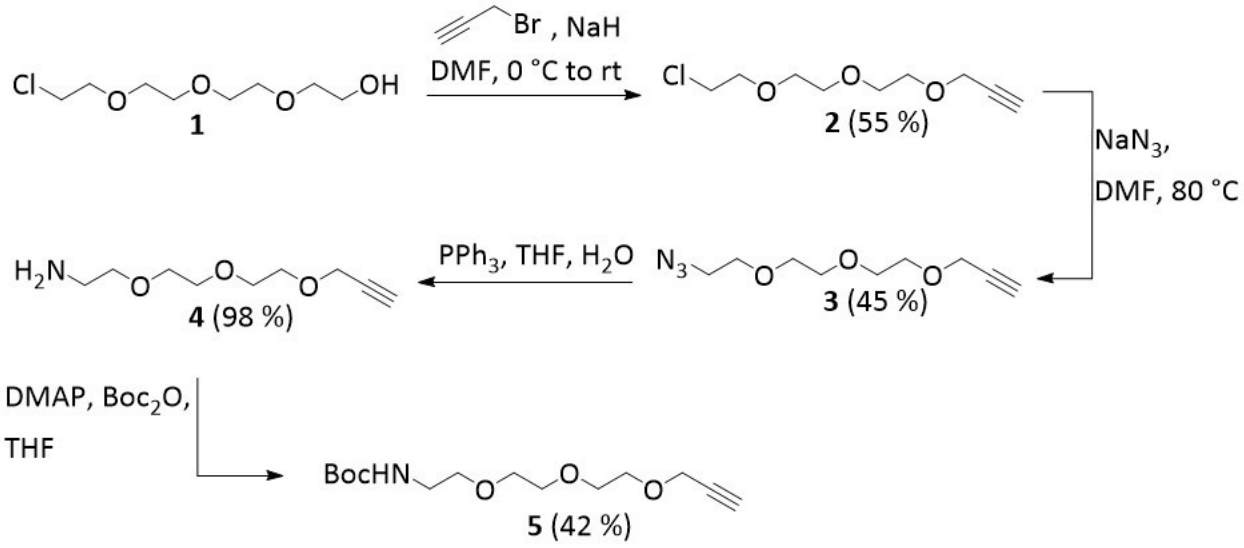

Scheme 5.1: Synthesis of heterobifunctional linker **5** used for the fabrication of glycoarrays.

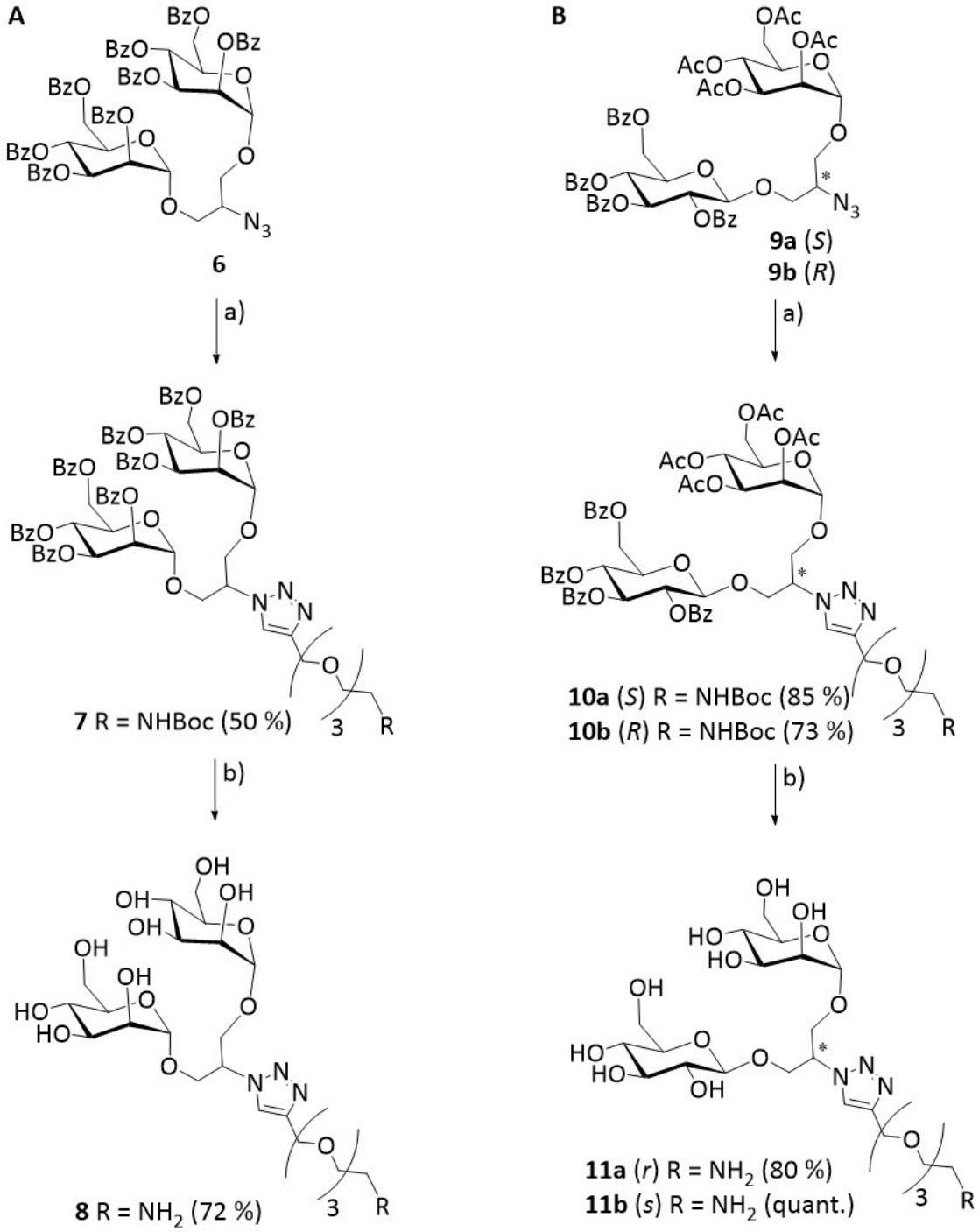

Scheme 5.2: Synthesis of (**A**) Dimannoside cluster **8** ligated to the polyethylene glycol linker **5** with available primary amino group for the immobilization on surfaces; (**B**) pseudoenantiomeric glycoclusters **11a** and **11b** ligated to the polyethylene glycol linker **5** for the immobilization on surfaces; Reagents and conditions: a) linker **5**, sodium ascorbate, copper(II) sulfate, water, *N*,*N*-dimethylformamide; b) first step: sodium methoxide solution, methanol; second step: trifluoroacetic acid, water.

The synthetic linker **5** was then used in a click reaction with the dimannoside **6** for the preparation of compound **7** as a reference compound for the heterocluster effect study. Dimannoside **6** was prepared as previously reported in our published paper.[104] Standard deprotection according to ZEMPLÉN followed by treatment with trifluoroacetic acid for the cleavage of the *N*H-Boc protection group allowed the formation of **8** in 72 % yield (**Scheme 5.2**). Synthesis of the pseudoenantiomeric glycoclusters **9a** and **9b** was based on the same synthetic strategy as previously published[104] but with the minor change in the protection group strategy. The here reported molecules contained acetyl protection groups, whereas in the published paper the use of benzoyl groups was reported. They were found more favored since they are less prone to acetyl migration under acidic conditions. Here, the glycoclusters **9a** and **9b** were obtained from *O*-acetylated precursors. Next, the synthesized glycocluster pairs **9a** and **9b** derived from reported trifunctional enantiomeric scaffolds were further used in Cu(I)-catalyzed 1,3-dipolar cycloaddition reaction with **5** where **10a** and **10b** isomers were isolated up to 85 % yield. Deprotection according to ZEMPLÉN and the *N*H-Boc deprotection furnished **11a** and **11b**. Thus, the formation of the primary amino group allowed further fabrication of **8**, **11a** and **11b** on different pre-functionalized surfaces under favorable reaction conditions.

5.2. Tests under static conditions

The previous studies of βGlc-αMan pseudoenantiomeric glycocluster pairs revealed a striking 20 fold difference in inhibitory potency for type 1 fimbriae-mediated *E. coli* bacteria adhesion. Hence we were interested to investigate the bacterial adhesion on glycoarrays of the same ligand pairs under different adhesive dynamic conditions. Thus, in our first attempt, the formed carbohydrate derivatives **8**, **11a** and **11b** were used for the fabrication of carbohydrates to the pre-functionalized polystyrene surfaces. The formed glycoarrays were used for the testing adhesion of type 1 fimbriae-mediated *E. coli* bacteria under static conditions. The immobilization of formed ligand derivatives was carried out under pH = 9 in carbonate buffer on the pre-activated 96-well microtiter plate to yield **12**, **13a** and **13b** glycoarrays (**Figure 5.2**). A serial dilution of amino-functionalized carbohydrate derivatives led to a concentration-dependent series of inhibition conditions, starting from 8 mM up to 7.8 µM con-

centration range. The concentration range was in close relation to the IC_{50} depicted concentration values reported from the previous adhesion-inhibition assays.[104]

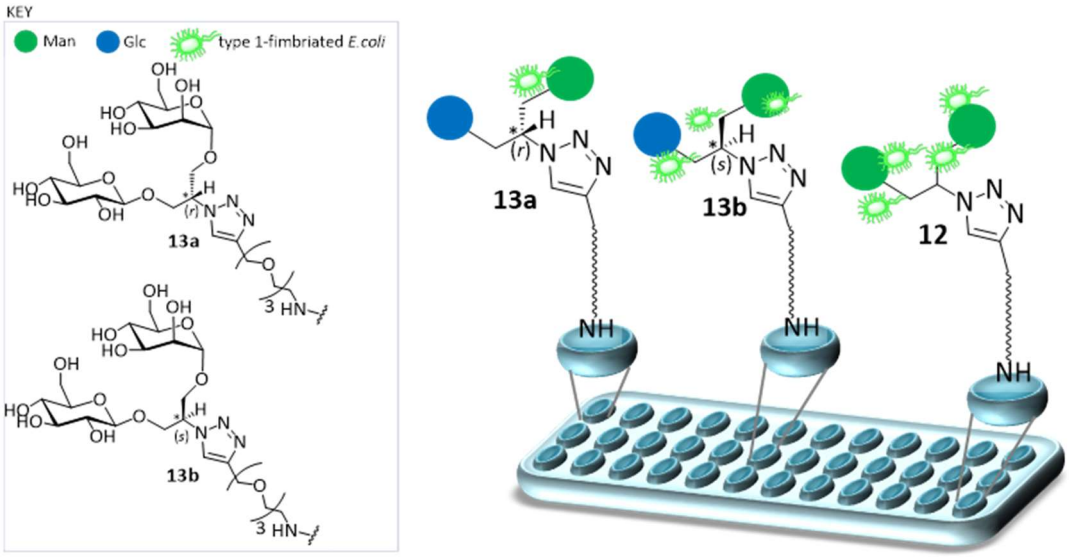

Figure 5.2: Schematic illustration of amino-functionalized carbohydrate derivatives for **12**, **13a** and **13b** glycoarrays formation on the pre-functionalized microtiter plate.

Each inhibitory concentration of **13a** and **13b** were tested in triplicates on the same plate, whereas dimannoside **12** were tested in duplicates on the same plate. After the immobilization of carbohydrate derivatives, the nonbound carbohydrate derivatives are washed with phosphate buffer saline-tween (PBST) multiple times. Remained unreacted surface groups were blocked with 2-aminoethanol. The same fabrication was used for the preparation of three individual microtiter plates for the testing of bacterial adhesion under static conditions. Adhesion to the glycoarrays was deduced from the fluorescence readout employed PKL1162 *E. coli* strain expressing the green fluorescence protein (GFP).[96] On each plate, a negative control was employed with the set of wells containing only 2-aminoethanol reagent fabricated on the surfaces of wells. Thus we were able to determine the ratio between bacteria adhered to the glycoarrays and those bound to the negative control and deduce the relative adhesion. In the employed assays with type 1-fimbriated *E. coli*, the bacterial lectin FimH mediates binding to α-D-mannosyl residues.[31, 85]

Hence we were able to study heterocluster effect in bacterial adhesion to the two distinct heterobivalent stereoisomers **13a** and **13b** compared to the adhesion on homobiva-

lent ligand **12**.[79c] The results are presented in **Figure 5.3** where adequate interpretation valency-corrected values are also depicted. From the shown results, a slight decrease of adhesiveness to fabricated glycoarrays can be observed looking from higher (8 mM) to lower (7.8 µM) concentration dilution range. Concentration-dependent fabrication of glycoarrays highly depends on the cluster valency as previously reported by LINDHORST group.[86] Hence, it was expected that when approached micromolar concentration range a gradual decreased bacterial adhesion can be observed due to the decreased ligands presentation for lectins to adhere. However, the high error bars represented at the micromolar range indicates uncertainty in the interpretation of bacterial adhesion in this region.

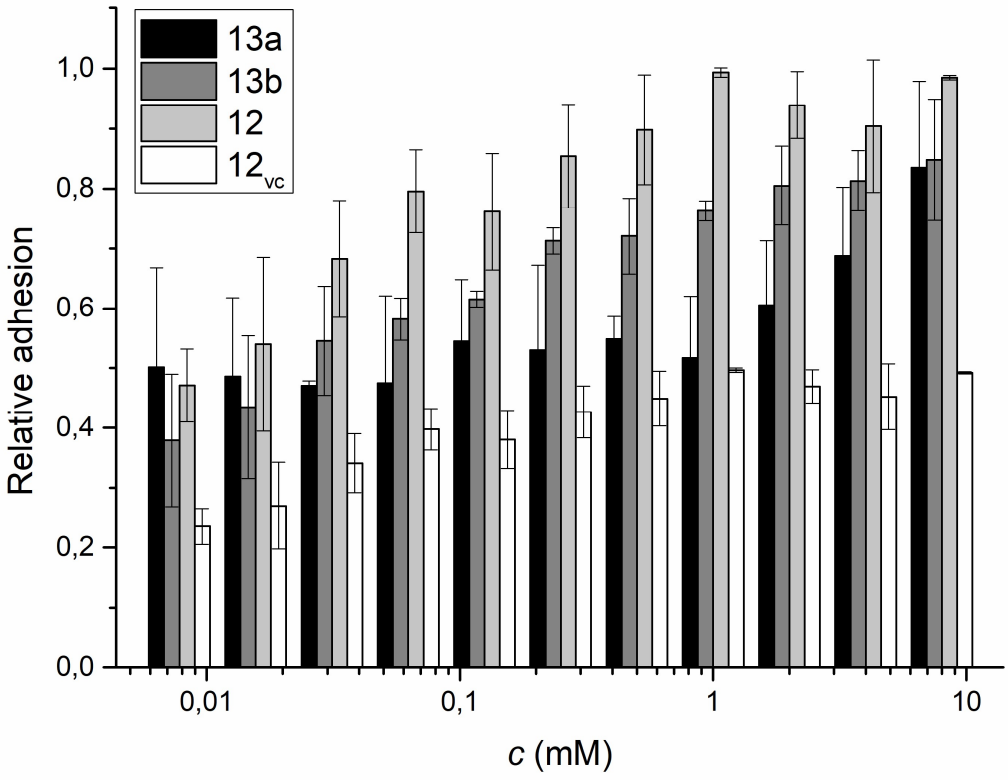

Figure 5.3: Relative adhesion of *E. coli* to glycoarrays under static conditions at graded concentrations. The relative adhesion values are the means values from three independent measurements. Error bars are given as standard error of the mean (SEM) of experiments with three independent sets.[i]

Table 5.1. Depicted relative adhesion values for E*. coli* bacteria to glycoarrays under static conditions.

Relative adhesion	Inhibitor concentration										
	8 (mM)	4 (mM)	2 (mM)	1 (mM)	500 (µM)	250 (µM)	125 (µM)	62.5 (µM)	31.3 (µM)	15.6 (µM)	7.8 (µM)
13a	0.84	0.69	0.61	0.52	0.55	0.53	0.54	0.48	0.47	0.49	0.50
13b	0.85	0.81	0.80	0.76	0.72	0.71	0.62	0.58	0.55	0.43	0.38
12	0.98	0.90	0.94	1.00	0.90	0.85	0.76	0.80	0.68	0.54	0.47
12_{vc}	0.50	0.45	0.47	0.50	0.45	0.43	0.38	0.40	0.34	0.27	0.24

Presented values in **Table 5.1** demonstrate minor changes in graduated relative bacterial adhesion to clusters in the two last points of the micromolar range. In overall, glycoarray **12** fabricated with homobivalent ligand exhibited the highest bacterial adhesion at each concentration stage in comparison to the heterobivalent ligands. At a higher concentration range of glycoarray **12**, the adhesion of type 1-fimbriated *E. coli* nearly reached fully relative adherence.

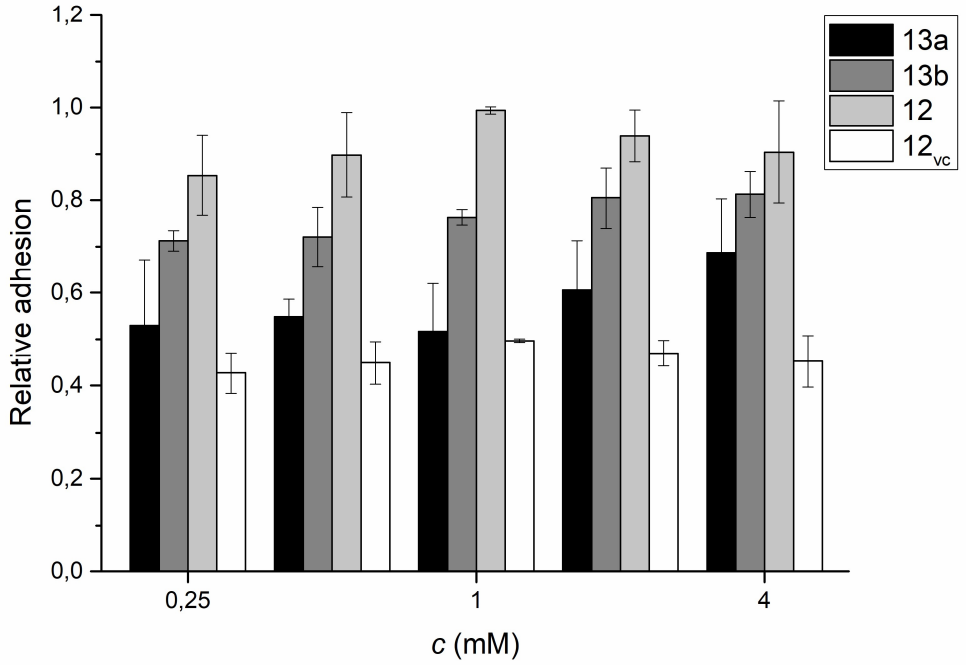

Figure 5.4: Relative adhesion of *E. coli* to glycoarrays under static conditions at high-density glycoarrays. The diagram presents the zoomed version of the concentration range of interest previously shown in **Figure 5.3**.[i]

Furthermore, a comparison of the valency-corrected values of **12_{vc}** demonstrated a pronounced heterocluster effect for both **13a** and **13b** isomers at each of the depicted concentrations. The same was previously found in the reported adhesion inhibition assay for iso-

meric βGlc-αMan asymmetric glycocluster pairs.[104] Hence, the carbohydrate nature of the second nonspecifically recognized motif by type 1-fimbriated *E. coli* bacteria supports the theory of heterocluster effect for increased affinity towards binding.[79c] From another point of view, a more significant finding is the difference in bacterial adhesion to the two heterobivalent stereoisomers at fabricated **13a** and **13b** glycoarrays. Here, glycoarray **13b** exhibited a more than 20 fold higher bacterial adherence when compared to its diastereomeric pair displayed at **13a** glycoarray. The results presented in **Table 5.1** for isomeric ligands **13a** and **13b** show the pronounced difference in relative bacterial adhesion at high glyocoarray density. The distinct adhesive difference occurs at a ligand concentration of 1 mM or more (**Figure 5.4**), whereas in the micromolar region the difference in bacterial adhesion is remarkably reduced. The same difference was previously demonstrated in solution, testing the inhibitory potency of isomeric βGlc-αMan glycocluster in bacterial adhesion.[104] Here again, the assays gave evidence that besides heterogeneity, FimH-mediated binding of *E. coli* cells depends on the three-dimensional organization glycoligands architecture.

[i] For the interpretation of the binding assays (cf**. Fig. 5.3** and **5.4**) valency-corrected (vc) adhesion for the divalent cluster mannoside **12** were obtained by dividing the respective adhesion by two. As an alternative to this approach, half concentrations should be applied in the binding assays to obtain valency corrected adhesion to glycoarray **12**.

5.3. Tests under flow conditions

In a published paper of ISBERG and BARNES flow-dependent bacterial adhesion to host cells was described as a complex dance in which two partners encourage and discourage each other approaches.[123] Bacteria use adhesive organelles to mediate "the dance" with the glycosylated cell surface of their host cells. These organelles are called fimbriae and the comprised lectin subunits that are frequently found at the fimbriae tips. Type 1 fimbriae are particular fimbriae found in *E. coli* bacteria, mediating mannose-specific adhesion to host cells promoted by the adhesin FimH. FimH is comprised by a lectin domain and in addition by a pilin domain that integrates the protein within the fimbrial shaft (cf. chapter 1, **Figure 1.2**). The flexible linker region between these two domains can alter the FimH structure under different dynamic conditions. For example, shear stress or a mechanical force leads to the extension of the flexible interdomain linker chain and hence to the enhancement of FimH-receptor interactions.

Changing the conditions under which adhesion is measured was consequently used to study the molecular mechanism of lectin function in the interplay between a glycosylated surface and soluble ligands.[124] BROOKS AND TRUST suggested appropriate adhesion-stimulating conditions already 30 years ago.[125] Red blood cell hemagglutination by *Aeromonas salmonicida* was enhanced under shear stress allowing maximal agglutination. Another example, where dynamic conditions are of functional importance is leukocyte rolling over endothelium is also promoted by lectins, in this case, selectins.[126] For selectins, shear stress is physiologically important in order to prevent leukocyte aggregation and a proper interaction within the blood vessel wall. Also, the interaction of guinea pig red blood cells with FimH was found to be stimulated under flow-induced shear stress, where lower flow rates prevented adhesion of erythrocytes. SOKURENKO e*t al*. used a FimH variant identical to the one expressed by uropathogenic *E. coli* strain to demonstrate a 10-fold increase of bacterial attachment to erythrocytes under shear stress.[124] In addition, the study of *Pseudomonas aeruginosa* bacterial adhesion to different antibiotics revealed a linear colleration as the flow rate increased.[127] Consequently, it appears important to study bacterial adhesion under different dynamic conditions in order to reflect conditions that occur naturally in pathogen interactions with hosts.

In our approach to study bacterial adhesion under flow conditions, carbohydrate derivatives **11a** and **11b** were fabricated on succinimide ester NHS pre-activated glass slides. A 5 mM carbonate buffer was used for the fabrication of glycoarrays with ligands **11a** and **11b** to provide high-density glycoarrays **13a** and **13b** (**Figure 5.5**). On the one glass slide, two of six wells chamber were treated with ligand **11a**, two with **11b** and the remaining two wells chamber were used as the negative control. After multiple washing with PBST and PBS buffer, the remained unfunctionalized surface was blocked with 2-aminoethanol blocking reagent and then again washed with PBS.

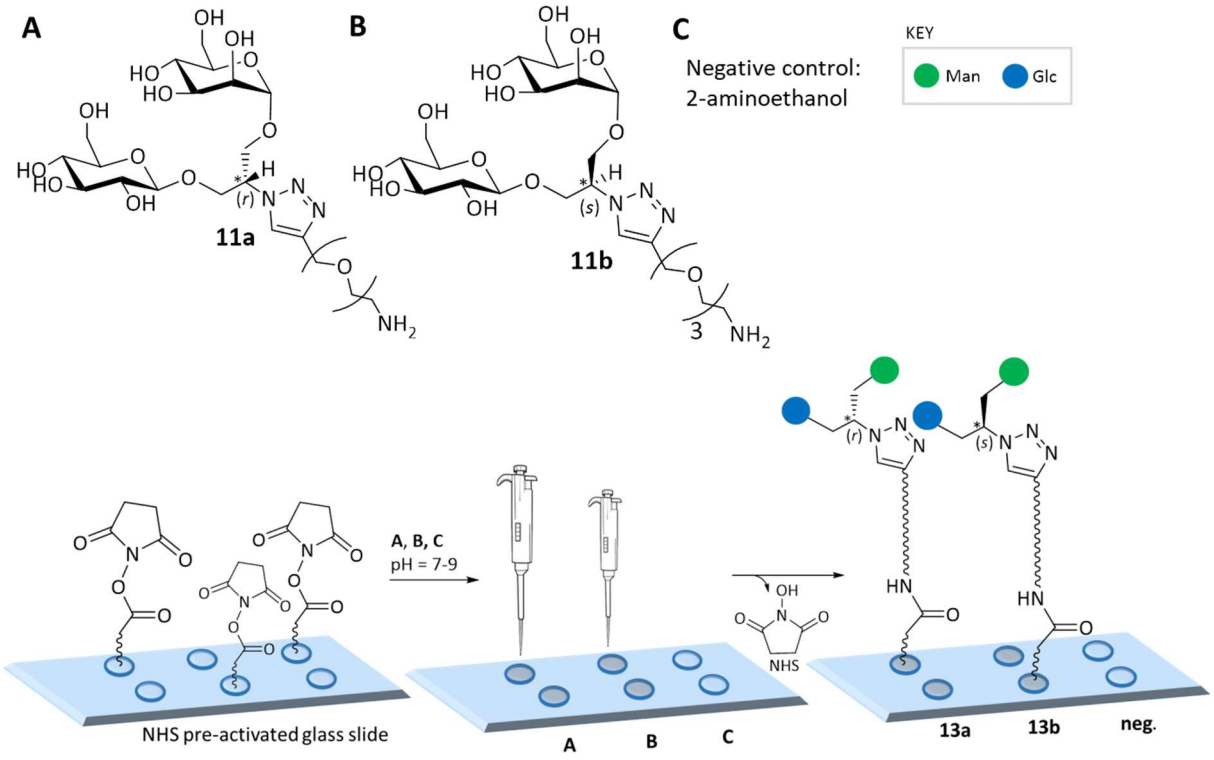

Figure 5.5: Amino conjugation of carbohydrate ligands **11a** and **11b** on the NHS pre-functionalized surfaces in carbonate buffer, pH = 9, for the formation of **13a** and **13b** glycoarrays.

On to the dried NHS-glass glycoarrays, the sticky channel slides IBIDI VI$^{0.4}$ with a self-adhesive underside were mounted. These parallel microfluidic channels provide a method for the investigation of bacterial adhesion under flow, where various dynamic conditions can be applied. The experimental set up can be used for different shear stress range depending on the channel height. Physiological shear stress can vary between almost 0 and 120 dyn/cm^2 depending on the vessel type and the size of the organism (*e.g.*, mice, human).

In our preliminary experiments, the shear stress of 0.18 dyne/cm^2 was applied in the flow rate of 0.10 mL/min in a time period of half an hour. The flow rate in human urethra covers a wide range since it specifically depends on individuals characteristics.[128] Mechanical forces induced by the friction of adhesion medium against the glycoarray are of a great impact on the physiological behavior and adhesion properties (**Figure 5.6**). In this regard, the two domain part between FimH, adhesin domain and FimH pilin domain, can be altered under shear stress. Ligand-receptors interactions are reinforced by mechanical stress so-called called catch-bond mechanism.

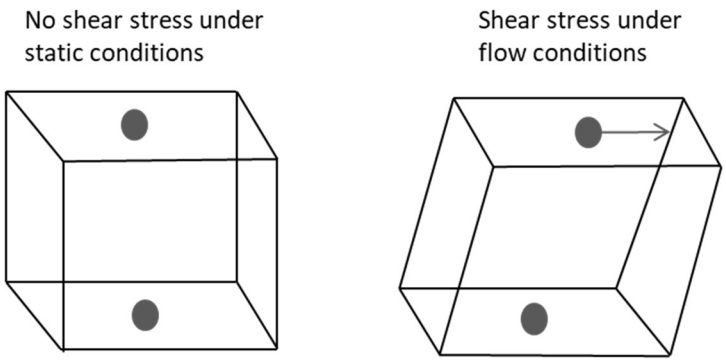

Figure 5.6: Shear stress in biofluidic system induced by the friction of liquid to surfaces.

In here tested *E. coli* bacterial adhesion study the unidirectional laminar flow was applied for 30 minutes. Under the continuous force through microfluidic channels, both the flow direction and viscosity can be assumed as constant over some time. These conditions are required for the experimental conditions of homogenous laminar flow. Additionally, the shear stress in a channel is dependent on the obtained viscosity at the performed temperature. However, we applied rather a small shear stress for bacterial adhesion testing and the optimal flow rate for activating catch bond mechanism still needs to be simulated. Bacterial adhesion was measured by the fluorescence readout of the used *E. coli* strain PKL1162 expressing the green fluorescence protein (GFP) as in the tests under static conditions. Additionally, bacterial adhesion was studied using fluorescence microscopy for visual observation of adhered bacteria on individual glycoarrays. The relative adhesion was defined as the ratio between bacteria adhered to the glycoarrays **13a** and **13b**, respectively, and negative control. The first preliminary results could be obtained for bacterial adhesion under flow conditions to **13a** and **13b** glycoarrays from three independent experiments (**Figure 5.7**). The distinct difference in the bacterial adhesion could be observed after an applied laminar flow of

0.18 dyn/cm^2. Nearly a complete bacterial adhesion to glycoarray **13b** could be obtained. Hence, more than a 20 fold higher bacterial adhesion to the glycoarray **13b** was observed in comparison to its isomer **13a**. This finding was not unexpected since our previous studies under static conditions indicated a similar difference in bacterial adhesion to the same pair of isomers. On the other hand, more dense glycoarrays are required for a significant amount of *E. coli* bacteria to adhere.[129]

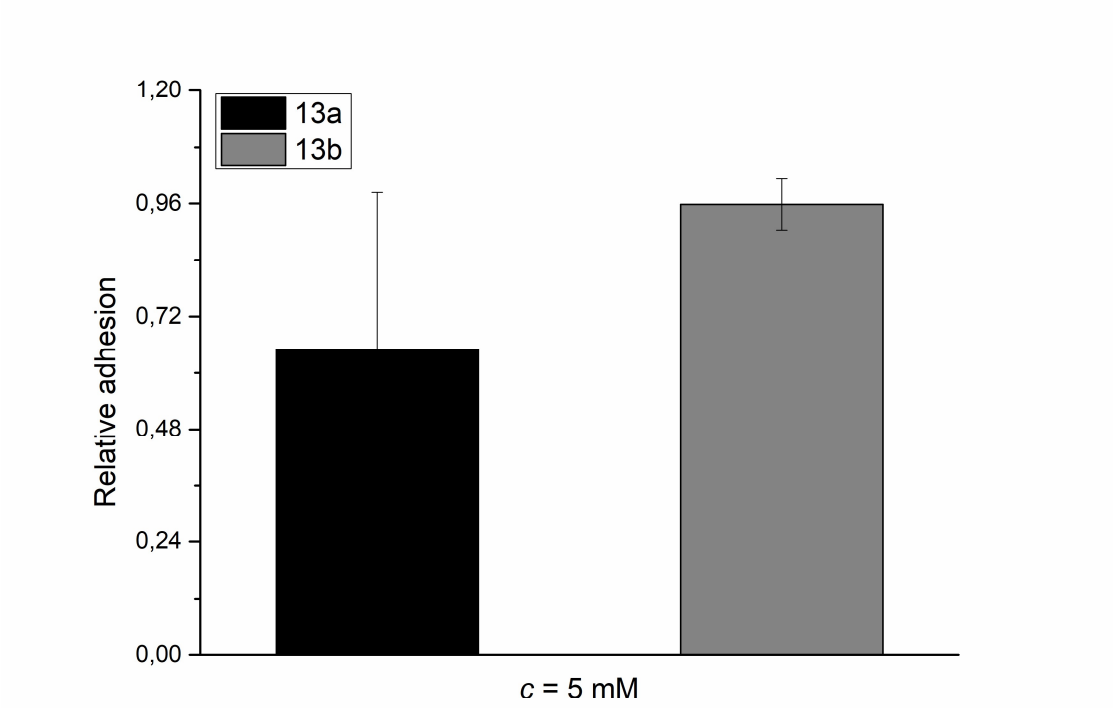

Figure 5.7: Relative adhesion of *E. coli* to glycoarrays under dynamic conditions and flow rate of 0.10 mL/min at 5 mM concentrations. The relative adhesion values are the mean values from three independent measurements. Error bars are given as standard error of the mean (SEM) of experiments with three independent sets.

However, in the obtained relative adhesion values shown in **Figure 5.7**, the standard deviations are rather high for the performed experiments under flow conditions. Regarding the relative adhesion values from independent experiments due to uncertainties in the performed experiments no definite conclusion can be drawn from these results (**Figure 5.8**). Since we are working with live *E. coli* bacteria, the applied mechanic forces implemented from the flow rate has a great impact on the physiological behavior and adhesive properties of the bacteria.

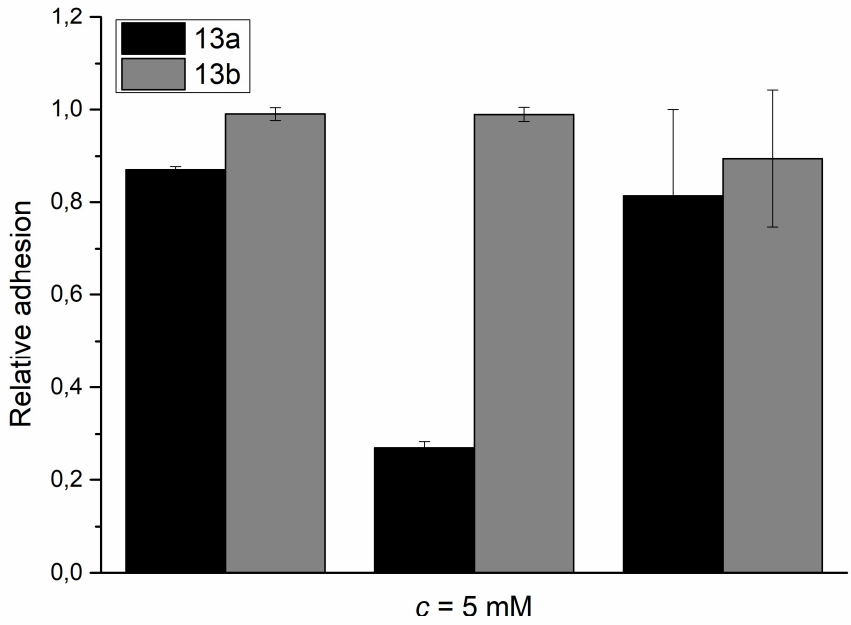

Figure 5.8: Relative adhesion of *E. coli* to glycoarrays under dynamic conditions and flow rate of 0.10 mL/min at 5 mM concentrations performed on three individual plates. The relative adhesion values are the mean values from duplicates on the same plate. Error bars are given as standard error of the mean (SEM).

However, we were interested to investigate if unspecific bacterial adhesion to the surface might be the reason for the high deviations found in our experiments. As sometimes the data obtained from the negative control can be an offset to the fabricated glycoarrays we used fluorescence microscopy for visual observation of adhered bacteria (**Figure 5.9**).

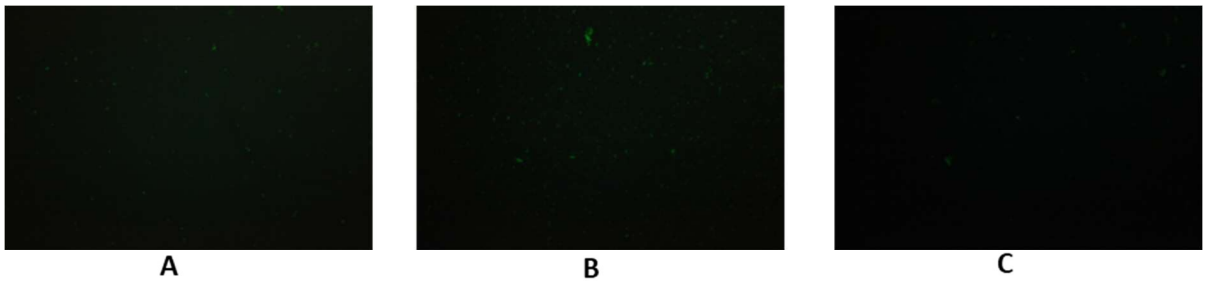

Figure 5.9: Relative adhesion of *E. coli* to glycoarrays under dynamic conditions and flow rate of 0.10 mL/min at 5 mM concentrations performed on one individual plate. (**A**) shows bacteria adhered to glycoarray **13a**, (**B**) shows bacteria adhesion to glycoarray **13b** and (**C**) shows negative control- blocking reagent 2-amino ethanol.

As expected, adhered bacterial cells were found in the maximal amount on the glycoarray **13b**. On the other hand, the amount of adhered bacteria found on the negative control and glycoarray **13a** was in the same ratio, with rather decreased number of adhered cells than to **13b**. It could be observed that on both wells of negative control in our experimental setup a significant amount of bacterial adhered in the comparison to the number of bacteria adhered to glycoarrays **13a** and **13b**. Nevertheless, it was expected that none or bare amount of bacteria should adhere on negative control and especially not in the number observed. Hence it is hypothesized that the non-specific binding of bacterial adhesion could be the main source found for the uncertainty in the performed assays. There are two possible reasons to consider when giving this hypothesis. One reason is the insufficient concentration of blocking reagent to block remained functional groups on the glass slides and avoid unspecific binding and the other more technical reason is the loss of pressure in the applied flow rate due to not properly mounted sticky chambers on glass slides what can significantly alter the flow rate. Often it was found that an increased flow rate strongly decreases unspecific bacterial binding to the surfaces.

Summarizing the results from numerous performed assays for evaluation of the isomeric glycocluster pairs towards bacterial adhesion, no conclusive results could be obtained. Based on this, further technical improvement should be made in order to resolve our questions and establish an experimental set up for testing bacterial adhesion under flow conditions.

6 *En route* to pseudoenantiomeric homotrivalent glycoclusters

Many reports have shown that multivalency is a crucial factor to effect stronger binding of lectins to their ligands, hence increasing the avidity of lectin ligands. However, in addition to multivalency effects, ligand binding is also strongly dependant on the overall ligand presentation. Here, such effects were tested with appropriate oligosaccharide mimetics and the α-D-mannoside-specific adhesion of type 1-fimbriated bacterial cells, mediated by FimH. Although the bacterial lectin FimH is a monovalent lectin with only one CRD, many tri- and tetra-mannosides were found as potent inhibitors of type 1 fimbriae-mediated adhesion of *E. coli*.[85] It is apparent, that the enhanced affinity of α-D-mannosides with aromatic aglycon for FimH is due to their interaction with the so-called tyrosine gate of the lectin, formed by Tyr48 and Tyr137 and flanking the binding pocket. On the other hand, it is a bit odd that an increased number of carbohydrate ligands leads to improved binding in this testing system.[14] Possibly, an increased ligand concentration contributes to the effect observed in these carbohydrate-protein interactions.[86] Interestingly, ligand density studies together with heteromultivalency effects and demonstrate that the binding affinity clearly depends on the relative orientation of carbohydrate ligands.[79a] Also in our group, the effects of carbohydrate valency, the spatial arrangement and the conformational flexibility of carbohydrate ligands on their interactions with the specific receptors were demonstrated.[82, 84b] Recently JANETKA and RATH pointed out that lectins affinity differs depending on the stereospecific modulation of carbohydrate ligands.[95] Today, the interest in the binding effects of various small carbohydrate ligands has grown enormously. Different structural parameters that might potentially influence a lectin affinity of ligands increase our understanding of the binding phenomena we observe.

In this subproject, a chiral pool approach was used to achieve trifunctional enantiomeric scaffolds for the synthesis of homotrivalent cluster glycosides in which the three-dimensional assembly of sugar ligands is varied in a specific way as shown in **Figure 6.1** (glycocluster assembly). We were interested to see if the configuration at the focal stereocenter of the scaffold molecule contributes to different affinity of the resulting trivalent cluster-mannosides for FimH, or in other words, if the variation of the focal point configuration leads to different results in adhesion-inhibition assays with type a-fimbriated *E*. *coli* cells.

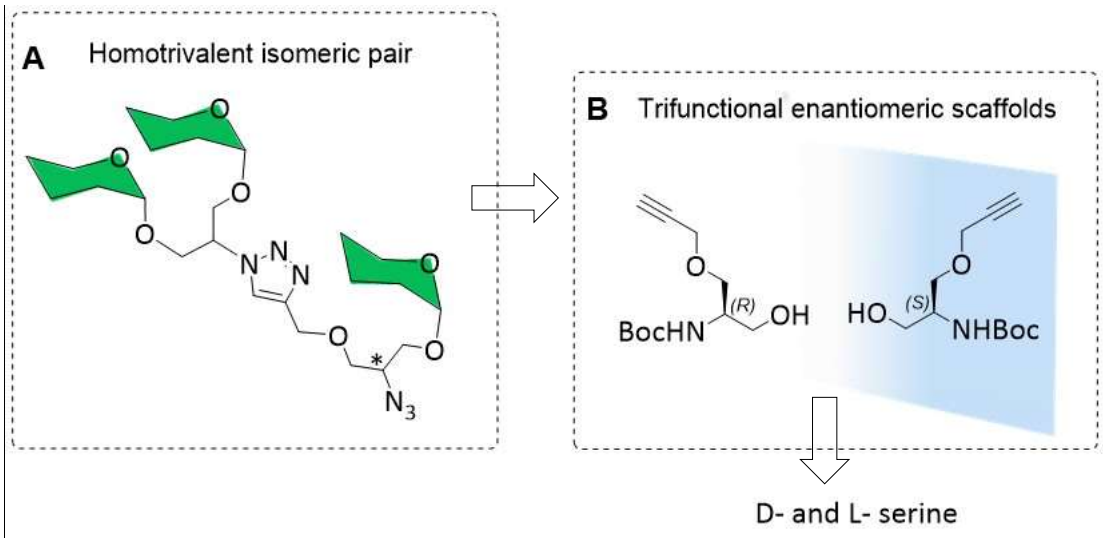

Figure 6.1: Schematic illustration of the two targeted diastereomeric homotrivalent glycocluster assembly (**A**) based on trifunctional enantiomeric scaffolds (**B**) that are derived from chiral D- and L-serine starting materials.

It was planned, to functionalize trifunctional enantiomeric scaffolds by Cu(I)-catalyzed 1,3-dipolar cycloaddition using the azido-functionalized divalent mannoside cluster, followed by a final α-D-mannosylation step. Hence, a propargyl group was required and introduced into the enantiomerically pure *N*H-Boc protected amino acid, D- or L-serine, respectively, by WILLIAMSON etherification (**Scheme 6.1**). Then, the esterification of the carboxyl group was performed in the same pot using potassium carbonate and iodomethane to yield *O*-propargylated esters **2a** and **2b** in relatively good yield. The synthesized intermediates were enantiomerically pure and in the agreement with the literature reports. In the next reaction step, lithium boron hydride was employed and the following acidic workup gave the primary alcohols **3a** and **3b** in yields around 60 %. This synthetic pathway was not further optimized.

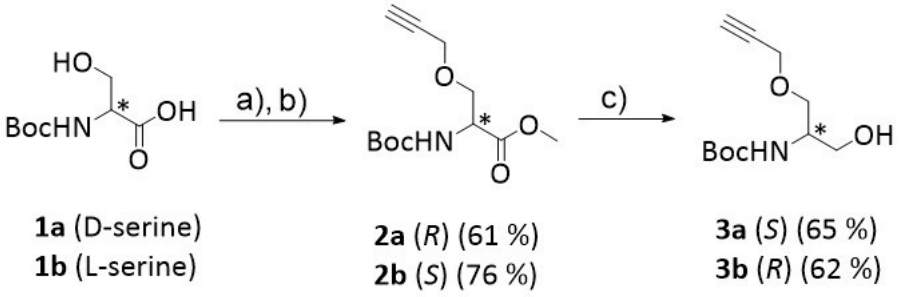

Scheme 6.1: Synthesis of the enantiomeric scaffold molecules **3a** and **3b**: a) propargyl bromide, sodium hydride, *N*,*N*-dimethylformamide, 0 °C to rt; b) iodomethane, potassium carbonate, *N*,*N*-dimethylformamide, 0 °C to rt; c) lithium boron hydride, tetrahydrofuran, 0 °C to rt.

The obtained pair of enantiomeric scaffold alcohols was further used for the assembly of the desired diastereomeric trivalent glycoclusters. First the known divalent glycoside **4** was employed, which was prepared according to the literature.[104] Cu(I)-catalyzed 1,3-dipolar cycloaddition ligated the azide-modified cluster **4** with the enantiomeric scaffold molecules **3a** and **3b**, yielding the respective **5a** and **5b** in less than two hours under microwave heating (**Scheme 6.2**). This synthetic approach facilitated the recovery of starting materials. Finally, the *N*H-Boc group was deprotected under acidic conditions in order to furnish the respective free amine for a subsequent diazo-transfer reaction with imidazole sulfonyl azide. Indeed, the desired azide-functionalized-derivatives **6a** and **6b** were obtained in more than 70 % yield. An advantage of this approach is to avoid possible polymerization in the click reaction step and also it is known that the formed azide functional group is more favorable in glycosylation reactions than a *N*H-Boc carbamate group. Additionally, the azide group can be used for further immobilization on surfaces with heterobifunctional linker molecules.

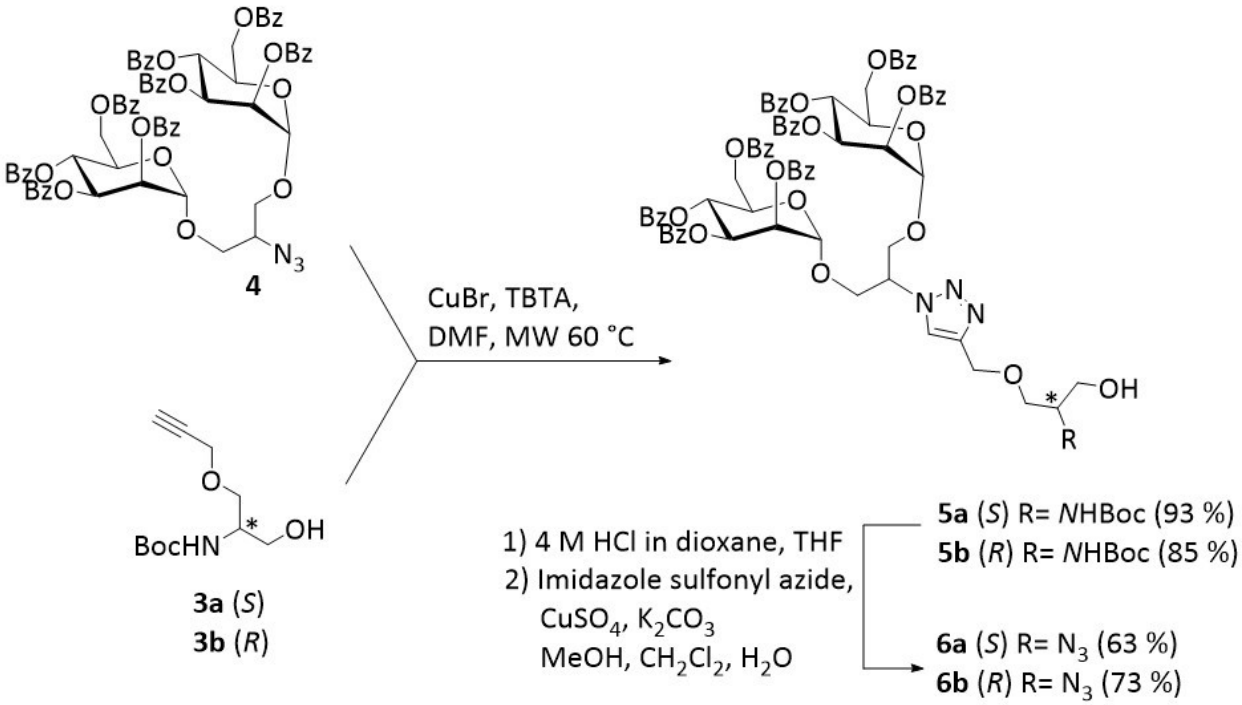

Scheme 6.2: Synthesis of **5a** and **5b** *via* CuAAc click reaction between alkyne-functionalized scaffold molecules and the azide-modified cluster glycoside **4**. The same was further used in the diazo transfer reaction for the formation of **6a** and **6b**.

In the next step, varieties of glycosylation conditions were applied for the mannosylation of **6a** and **6b**, respectively (**Figure 6.2**). Three different mannosyl donors **7a**, **7b** and **7c** were applied for the mannosylation of **6a** and **6b**, respectively, but, unfortunately, the expected 2-

trans glycosides were not formed. As the starting material was recovered in most of the cases, it is assumed that the primary hydroxyl group of the glycosyl acceptor is probably to sterically hindered to allow a proper reaction.

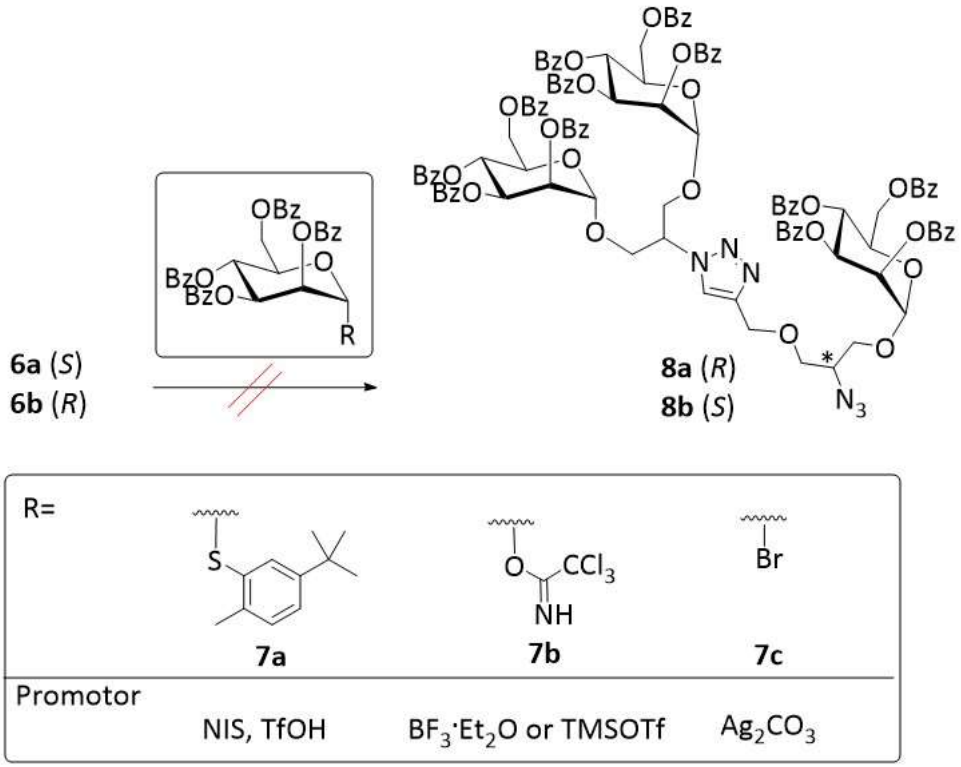

Figure 6.2: Attempts to achieve **8a** and **8b** by mannosylation of **6a** and **6b**. The mannosyl donors **7a**, **7b** and **7c** were employed under appropriate conditions. All reactions were performed in anhydrous dichloromethane, and with 3 Å molecular sieves. Special reaction conditions for **7a** and **7c**: 0° C to rt; using **7b**: 0 °C to rt with $BF_3{\cdot}Et_2O$ or -45 °C to rt with TMSOTf.

However, when **7d** was used as a mannosyl donor for the glycosylation of **6a** under a promotion with triflic anhydride (Tf_2O) and buffering with 2,6-di-*tert*-butyl-4-methylpyridine (DTBMP) the formation of **9a** as α,β-isomeric mixture occurred in poor 14 % yield (**Scheme 6.3**). This glycosylation method is particularly used for the glycosylation of unreactive nucleophiles. On the other hand, this type of glycosyl donor is known to often lead to the formation of α,β-isomeric mixtures.[130] Also here, even in the presence of participating benzoyl groups, the reaction led to the α,β-isomeric mixture of **9a**. The gated decoupled ^{13}C NMR spectrum shows the heterocoupling constant $J_{C\text{-}1,\,H\text{-}1}$ of 173.88 Hz for all three C-1 mannosyl carbon atoms, a value indicating the formation of α-conformation of all three glycosidic linkages[111, 131] (cf. chapter 8, **Figure 8.66**). Based on the chemical shift of both hydrogen and carbon atoms on the HSQC NMR spectra (cf. chapter 8, **Figure 8.65**) it can be hypothesized

that the α- and β-anomeric mixture was formed. On the other hand, the ratio of the obtained stereoisomers could not be determined at this point since chemical peaks of both α- and β-anomeric atoms are overlapping with other hydrogen atoms of molecule **9a**.

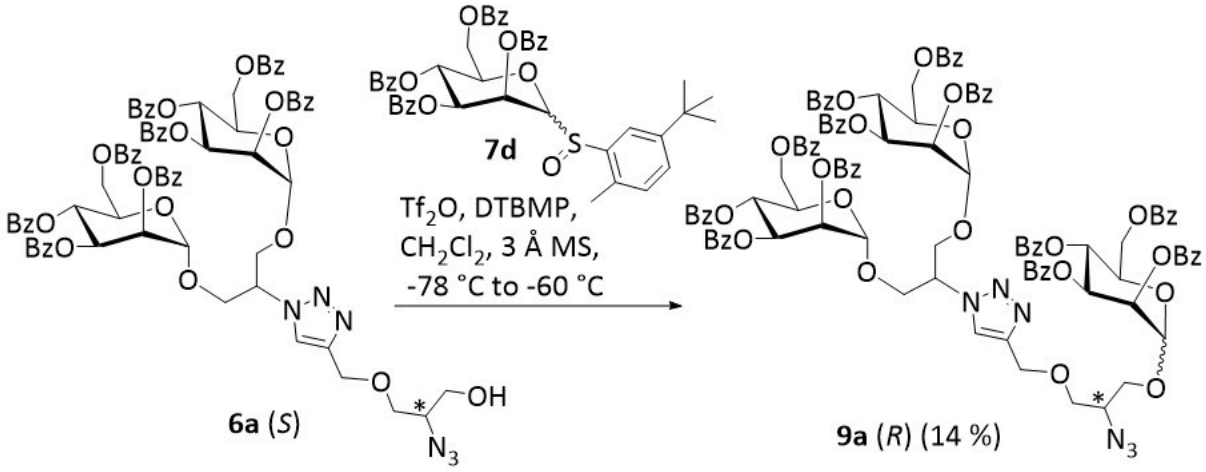

Scheme 6.3: Synthesis of the undesired α,β-isomeric mixture of **9a** in glycosylation attempt of **6a** when **7d** mannosyl donor was used.

Because of the undesired and unexpected results in the mannosylation of the azide **6** a new synthetic pathway was seeked, employing the enantiomeric scaffold molecules **3a** and **3b** in a glycosylation reaction with the known mannosyl bromide **7c** under mild reaction conditions using silver triflate and buffering with acid scavenger 2,4,6-collidine (**Scheme 6.4**).

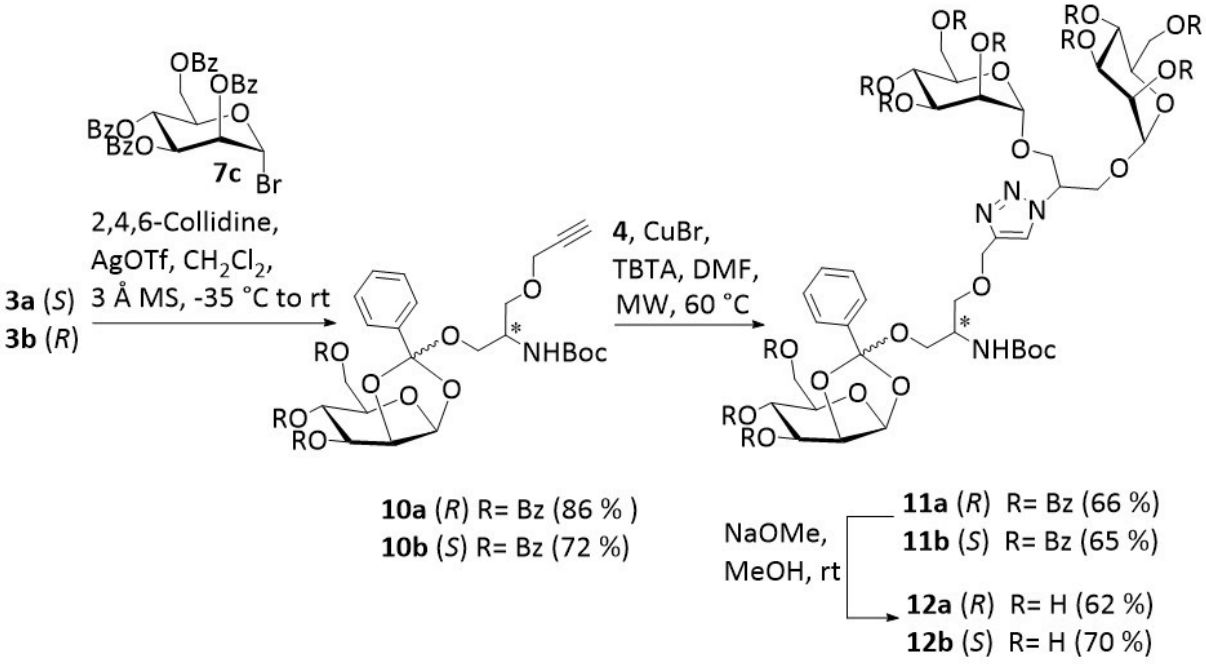

Scheme 6.4: Synthesis of undesired 1,2-orthoesters **12a** and **12b**. The mannosylation of the enantiomeric scaffold molecules **3a** and **3b** with glycosyl donor **7c** yielded *endo*/*exo* isomeric mixture of 1,2-orthoesters **10a** and **10b**.

However, this reaction led to a diastereomeric mixture of glycosyl orthoesters, **10** and **10b**. The orthoester formation occurs when the acceptor attacks the electrophilic carbon of the dioxolane ring of the bicyclic intermediate instead of on the anomeric carbon. Here, β-1,2-orthoester *endo*/*exo* isomeric mixture was formed (**Figure 6.3**). This was revealed after a final deprotection step, when the NMR analysis of **12a** and **12b** revealed the alkoxy group at the dioxolan ring of *endo*/*exo* isomers.[132] The full determination of individual compounds is represented in the supplementary information (cf. chapter 8, page 175-183).

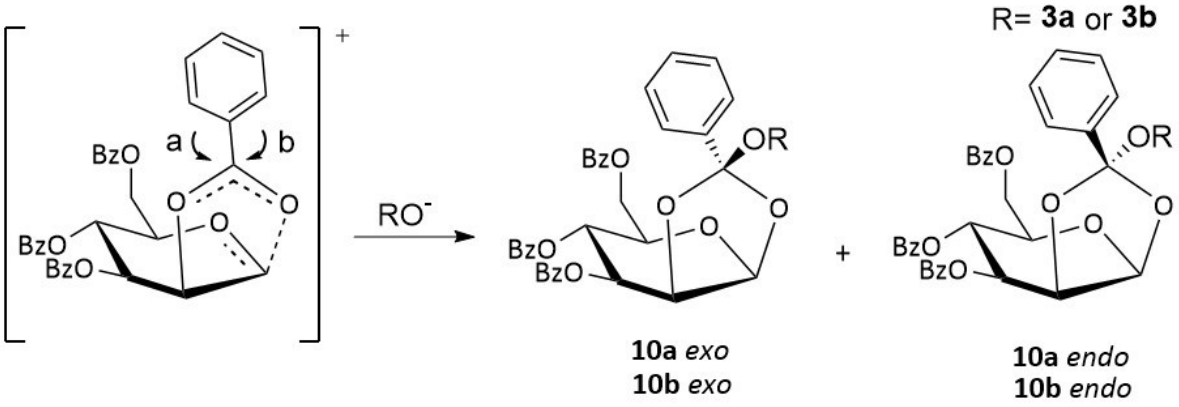

Figure 6.3: Schematic illustration of *exo*/*endo* 1,2-orthoester formation. Synthetic pathways a) and b) show possible ways for the formation of *exo* and *endo* isomers configured dioxolane rings from benzylidene derivative.

At first sight, the formation of the 1,2-orthoester could not be identified clearly. The chemical shift for H-1 mannosyl proton of the respective mannosyl 1,2-orthoester was found downfield-shifted in the ^{1}H NMR spectra and in this case overlapped with the H-4 mannosyl proton. Hence, the coupling constant for anomeric proton could not be measured. However, the formation of 1,2-orthoesters could be confirmed with the HMBC NMR spectrum with 152 MHz what indicated multiple bond correlations between the quaternary carbon of the formed orthoester, the neighboring *ortho*-protons of the phenyl ring and H-1 mannosyl proton (cf. chapter 8, **Figure 8.81** and **Figure 8.85**). The clear identification of the formed orthoesters was observed in the final step after the ZEMPLÉN deprotection of **11a** and **11b** in the synthesis of **12a** and **12b**. The gated decoupled ^{13}C NMR spectrum shows the characteristic heterocoupling constant $J_{C\text{-}1,\,H\text{-}1}$ of 171.6 Hz for C-1 mannosyl carbons of dimannoside residue[133] where coupling constant $J_{C\text{-}1,\,H\text{-}1}$ of 177.9 Hz was found characteristic for β-mannosyl 1,2-orthoesters[134] (cf. chapter 8, **Figure 8.82** and **Figure 8.86**). Additionally, all formed 1,2-

orthoesters in the synthetic pathway were characterized by HMBC NMR spectra measured under 152 MHz.

The performed three-step synthetic route provided the undesired 1,2-orthoester intermediates in a rather high yield. Hence, we aimed to isomerize the orthoesters into the respective glycosides and the unprotected intermediates **12a** and **12b** were treated with TMSOTf as a catalyst for orthoesters rearrangement.[61a, 111, 135] The catalytic role of TMSOTf is to provide reaction conditions for the formation of 1,2-benzylidene oxonium which then can be attacked by the masked silyl ether Me_3SiOR and form the expected 1,2-trans-glycosides. However, the use of TMSOTf catalyst in the presence of deuterated water as a solvent reaction led to α,β-isomeric mixture of **A** and substrate **B** (**Figure 6.4**). Orthoester rearrangement should be performed with **10a** and **10b** substrates in an organic solvent. Alternatively, the glycosylation conditions of **3a** and **3b** should be further optimized.

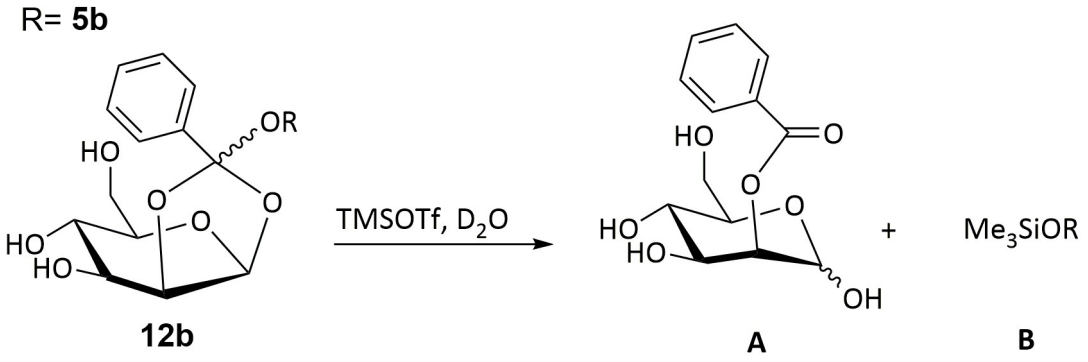

Figure 6.4: Schematic illustration of 1,2-orthoester rearrangement of **12b**. Under the described reaction conditions, hydrolyzed compound **A** and silylated compound **B** were obtained.

7 Summary

The work of this thesis was focused around the question if the relative orientation of carbohydrates in space is a critical factor that directs carbohydrate-protein interactions. In order to probe this hypothesis, for which some evidence has been provided recently, various approaches were followed to achieve novel glycoclusters of different architecture. They all had in common that through the variation of the configuration at a central stereocentre within the scaffold moiety, the three-dimensional carbohydrate presentation was varied. In the first section of this thesis, stereoisomeric heterotrivalent glycoclusters were targeted and for this, stereoselective synthesis was used for the preparation of tetrafunctional enantiomeric scaffold molecules. Here, SHARPLESS epoxidation of an allylic alcohol formed the key step of the synthetic pathway. Enantiomeric epoxides were achieved with up to 91 % *ee* (enantiomeric excess) and their configuration was assigned using the MOSHER reagent and analysis by NMR spectroscopy. In the second part of the synthetic pathway, the obtained enantiomeric scaffold molecules were submitted to regioselective orthogonal protection-deprotection steps in order to form tetrafunctional enantiomeric scaffold molecules for the further glycosylation. Two different attempts were undertaken to achieve the targeted heterotrivalent glycoclusters. In the first glycosylation pathway, the enantiomeric tetrafunctional scaffolds were used as glycosyl acceptors. But along this route, an allyl protecting group was found to be not suitable for glycosylation step due to its electron-withdrawing properties. Thus, a silyl ether (TBDPS)-protected oxazoline intermediate was used as the glycosyl acceptor in the second glycosylation pathway. However, in this case, the formation of undesired 1,2-orthoester side products was observed under KOENIGS-KNORR glycosylation conditions, and unfortunately, attempts to rearrange the formed orthoester were not successful. To eventually arrive at the target glycocluster stereoisomers, the essential enantiomeric scaffolds were provided with the herein described work (**Figure 7.1**).

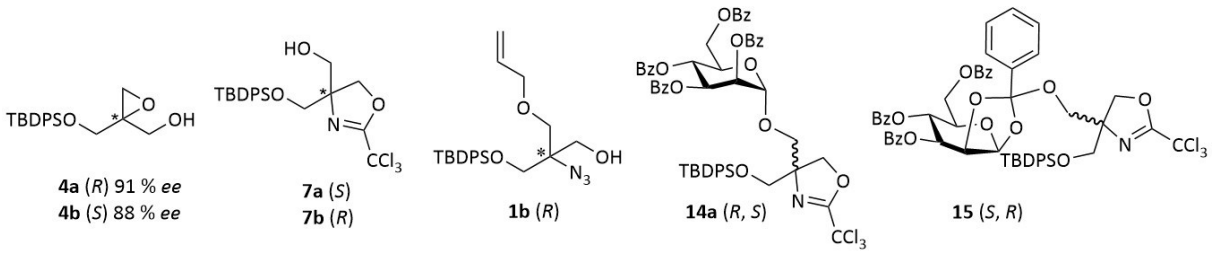

Figure 7.1: Summary of the prepared tetrafunctional scaffolds and isomeric glycosides.

In the second part of this thesis, a chiral pool approach was followed to provide a focused library of heterodivalent glycoclusters diastereomers, which can be considered "pseudoenantiomers". Readily available D- and L-serine, respectively, were used as enantiopure starting materials and converted into enantiomeric trifunctional scaffold molecules carrying an azido functional group and two hydroxyl groups which could be subsequently addressed in glycosylation steps with various glycosyl donors.

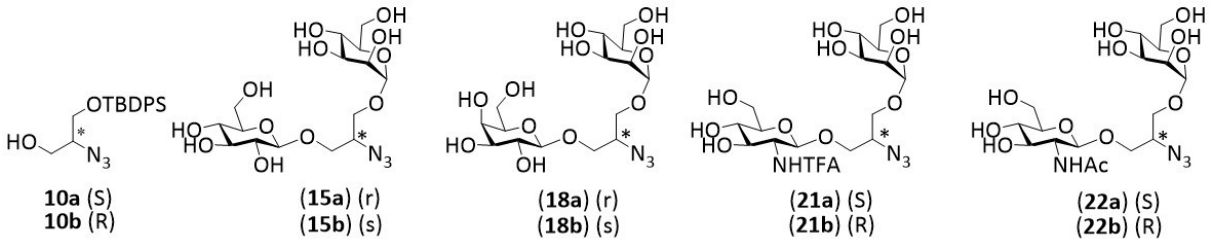

Figure 7.2: Summary of the prepared trifunctional scaffolds and from them heterodivalent glycoclusters derivatives.

All synthesized glycoclusters contain α-D-mannoside moiety, which is known as the ligand of the bacterial lectin FimH, which is found on the tips of type 1 fimbriae, expressed by *E. coli* bacteria (**Figure 7.2**). Four pairs of diastereomeric heterodivalent glycoclusters were obtained and tested as inhibitors of type 1 fimbriae-mediated bacterial adhesion and in addition as ligands of the Jack Bean lectin Concanavalin A.

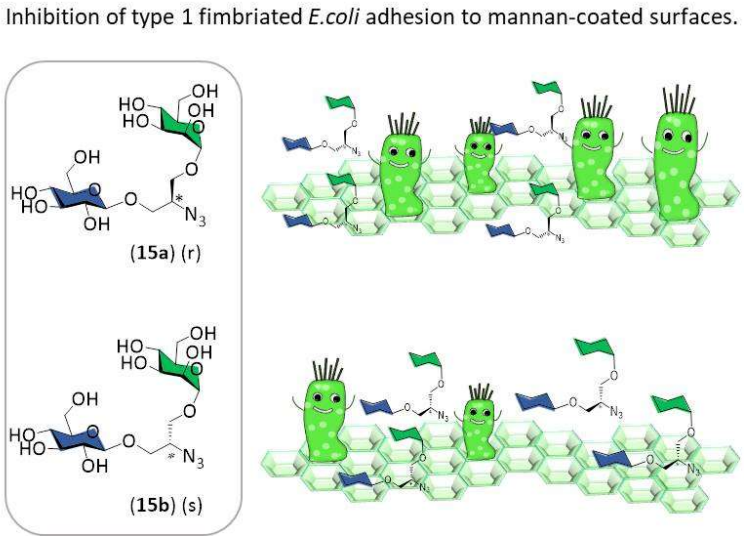

Figure 7.3: Biological evaluation of diastereomeric αManβGlc glycocluster pair in the standard adhesion-inhibition assay. All illustrations shown on the upper side of this figure are referring to αManβGlc glycocluster pair derived from D-serine amino acid whereas on the bottom side the effect of the αManβGlc glycocluster derived from L-serine is depicted.

Strikingly, the diastereomeric pair of the β-D-glucoside-α-D-mannose glycocluster, exhibited very different potency as inhibitors of type 1 fimbriae-mediated bacterial adhesion. The glycocluster based on the L-serine-derived scaffold exhibited a 20-fold higher inhibitory potency than its D-serine derived analog (**Figure 7.3**). On the other hand, no significant binding difference was seen with the plant ConA lectin. These exciting findings were partly rationalized by molecular modeling (performed by Dr. G. DESPRAS) but in the future, the thermodynamic parameters of the observed carbohydrate-protein interaction with diastereomeric heterobivalent glycoclusters should be further investigated, involving isothermal titration calorimetry and other analytical methods.

In the end, numerous assays were performed to test the influence of carbohydrate orientation on fabricated glycoarrays. For these tests, the most relevant diastereomeric heterodivalent glycoclusters were derivatized and ligated to glass slides. Type 1 fimbriae-mediated adhesion of *E. coli* to the fabricated glycoarrays was tested under static conditions as well as under flow (**Figure 7.4**). Again it was demonstrated, that the relative stereochemistry of carbohydrate presentation on a surface is a regulating factor in carbohydrate-protein interactions. However, the results obtained in the biological testing under flow remain preliminary at this point due to methodological inadequacies.

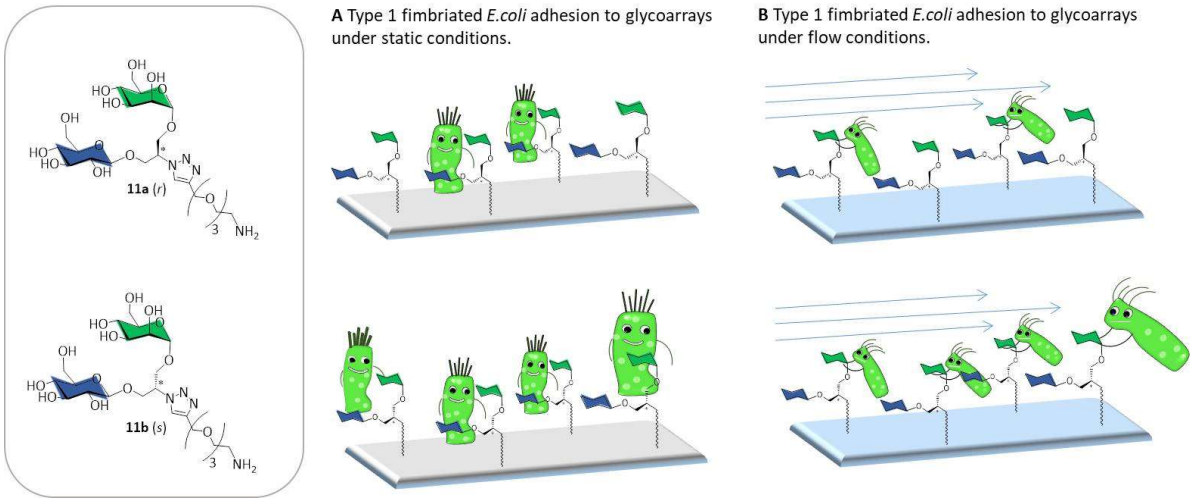

Figure 7.4: Biological evaluation of diastereomeric αManβGlc glycocluster pair in different biological assays (**A** and **B**). All illustrations shown on the upper side of this figure are referring to αManβGlc glycocluster pair derived from D-serine amino acid whereas on the bottom the effect of αManβGlc glycocluster pair derived from L-serine is depicted.

In the third part of this thesis, diastereomeric pairs of homotrivalent cluster mannosides were targeted, building on intermediates that were made available by preceding work (**Figure 7.5**). The synthesis of homotrivalent glycoclusters was undertaken from two different synthetic pathways. In the first synthetic pathway employing CuAAC ligation a divalent mannose cluster was first provided, but the final mannosylation caused unexpected problems. It turned out that in the last mannosylation step the undesired α,β mixture of anomers was formed. Therefore, a different synthetic pathway was used, where the primary hydroxyl group of the trifunctional enantiomeric scaffold was first used as a glycosyl acceptor for a mannosylation attempt. Here again, the mannosylation step led to the undesired 1,2-orthoester formation as a mixture of endo and exo isomers. Again, orthoesters rearrangement was not successful.

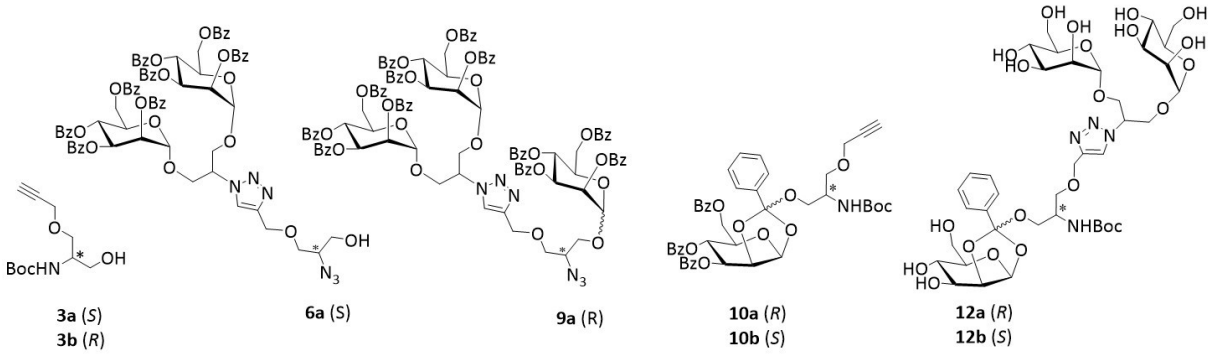

Figure 7.5: Summary of the prepared trifunctional scaffolds and from them homovalent glycoclusters derivatives.

In conclusion, novel homo- and heterovalent glycoclusters were achieved, in which the configuration at a central stereocenter of the scaffold moiety is varied (inverted). Two classical approached were successfully followed, stereoselective synthesis and a chiral pool approach. Most importantly, the obtained molecular tool indeed allowed us to show, that carbohydrate presentation makes a difference in carbohydrate-protein interactions. In spite of the fact that some data collected in this thesis remain preliminary, a new door into a better understanding of how carbohydrate recognition is regulated in nature has been opened: Relative orientation of carbohydrate ligands is a regulating structural parameter in carbohydrate-protein interactions as shown with some of the herein presented new glycoclusters. It will be interesting to further investigate whether and how the variation of asymmetric centers and overall carbohydrate orientation influences lectin binding.

8 Experimental section

8.1 General methods

Reaction and reaction monitoring

Air- or moisture-sensitive reactions were carried out under nitrogen in dry glassware unless otherwise stated. Solvents were purchased as technical grade solvents and purified by distillation before use. All reactions were monitored by thin-layer chromatography (TLC) on silica gel plates (GF 254, Merck). Detection of spots was effected by UV light and/or subsequent charring with 10 % sulphuric acid in ethanol, vanillin, or ninhydrin followed by heat treatment at ∼150 °C. Flash chromatography was performed on silica gel 60 (0.040–0.063 mm) using distilled solvents or with column machine "Interchim PuriFlash 450". Optical rotations were measured with a PerkinElmer 241 polarimeter (sodium D-line: 589 nm) in the solvents indicated. Cryostat FP40 machine was used to maintain constant temperatures at low temperatures from -20 to -25 ° C.

Spectroscopic methods

Nuclear magnetic resonance-NMR

^{1}H and ^{13}C NMR spectra were recorded on a Bruker Avance 200, Bruker ARX300, Bruker AvanceNeo 500 and Bruker Avance 600 spectrometer at 298 K. Chemical shifts (in ppm) are relative to residual non-deuterated solvent as an internal reference if not differently stated. Full assignment of the peaks was achieved with the aid of 2D NMR techniques (^{1}H-^{1}H COSY, ^{1}H-^{13}C HSQC, ^{1}H-^{13}C HMBC and ^{1}H-^{1}H NOESY). Data are presented as follows: chemical shift, multiplicity (s = singlet, d = doublet, t = triplet, q = quartet, m = multiplet, and br = broad signal), coupling constant in Hertz (Hz) and, integration.

Infrared spectroscopy-IR

Infrared spectra were measured with a Perkin Elmer FT-IR Paragon 1000 (ATR) spectrometer and were reported in cm^{-1}.

Mass spectroscopy-MS

ESI mass spectra were recorded on an Applied Biosystems (Applera) Mariner 5280 instrument ESI-TOF and HR (high resolution) MS ESI spectra on a ThermoFisher Orbitrap (Q Exactive Plus from Thermo Scientific).

8.2 Synthetic procedures for Chapter 3

For the characterization of enantiomeric scaffolds, carbon atoms of the core moiety are numbered as described in **Figure 8.1**. Compounds derived after SHARPLESS epoxidation with (-) DET catalyst are specified by an "a", and their enantiomeric counterparts, derived from (+) DET catalyst, by "b". Compounds are named according to IUPAC nomenclature.

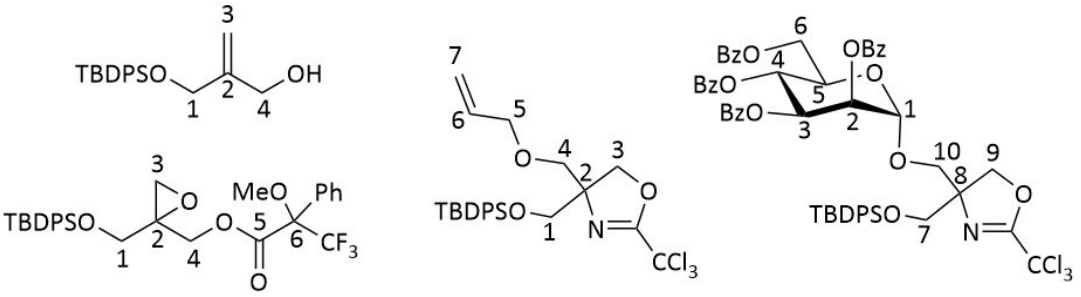

Figure 8.1. Atom numbering for NMR data description of the synthesized compounds.

General procedure for catalytic asymmetric SHARPLESS epoxidation (procedure A).[100a, 136] To a round bottom flask with activated 3 Å molecular sieves (35 % of the mass of allyl alcohol), anhydrous dichloromethane (c = 0.6 M) was added. To the flask was added either (-) or (+) diethyl tartrate (0.13 eq.) and titanium(IV) isopropoxide (0.1 eq.) at 0 °C (ice bath). The reaction mixture was stirred for 20 min at 0 °C then it was cooled down to -20 °C, using a cryostat machine and *tert*-butyl hydroperoxide (2.4 eq., c = 5.5 M in decane, over 4 Å molecular sieves) was added dropwise in a period of 15 minutes at 500 rpm at -20 °C. The reaction mixture was stirred for 45 min at -20 °C. The monoprotected allylic alcohol was dissolved in anhydrous dichloromethane (c = 1.0 M) in the presence of 3 Å molecular sieves (6.7 % of the mass of allyl alcohol) and the resutlting solution with molecular sieves was added dropwise to the reaction mixture at an initial temperature at -23 °C in a period of 15 minutes at 500 rpm. The mixture was stirred at 500 rpm for 2.5 hours at -23 °C in a cryostat then stirred at the same speed at -12 °C until completion. Afterwards, the solution was warmed to 0 °C, quenched with water and stirred additionally for 45 min at 0 °C. To the reaction mixture were added 5 to 6 drops of 30 % sodium hydroxide in satd. sodium chloride solution and stirred vigorously to clear out the formed white emulsion what allowed the phase separa-

tion. The aqueous phases were extracted with dichloromethane and the combined organic layers were washed with brine, dried over magnesium sulfate, filtered and concentrated. The residue was purified by flash chromatography to afford the expected compound as translucent syrup.

General procedure and analysis for MOSHER ester formation of epoxy alcohols (procedure B).[99, 137] This method was used for the determination of enantiomeric excess (*ee*) and for the assignment of the absolute configuration of formed epoxy alcohols after asymmetric SHARPLESS epoxidation. The epoxy alcohol was dissolved with anhydrous dichloromethane (c = 0.3 M) then 4-(dimethylamino)pyridine (1 eq.), triethylamine (4.7 eq.) and either *S*-(+) or *R*-(-)-α-methoxy-α-(trifluoromethyl)phenylacetyl chloride (MTPA chloride, 1.4 eq.) were added sequentially at room temperature. The solution warmed up and turned orange. Reactions were generally completed in 30 min to 60 min. It is important to ensure full completion of reaction since kinetic resolution in an incomplete reaction might significantly alter *ee* determination. The reaction was quenched by the addition of 3-(dimethylamino)propylamine (1-3 drops) and concentrated. The residue was passed through a short plug of silica gel in order to remove polar impurities.

General procedure for trichloroacetimidate formation from epoxy primary alcohol (procedure C). The starting material was dissolved in anhydrous dichloromethane (c = 0.2 M) and 1,8-diazabicycloundec-7-ene (0.1 eq.) and trichloroacetonitrile (1.1 eq.) were added at 0 °C (ice bath). The mixture was allowed to warm to room temperature then stirred until completion. Aq. satd. solution of sodium bicarbonate was added to the mixture at 0 °C. The aqueous phases were extracted with dichloromethane then the combined organic layers were washed with brine, dried over magnesium sulfate, filtered and concentrated. The residue was purified by flash chromatography to afford the expected compound.

General procedure for Et_2AlCl-catalyzed cyclization of epoxy trichloroacetimidates (procedure D). The epoxy trichloroacetimidate was dissolved in anhydrous tetrahydrofuran (c = 0.15 M) and activated 4 Å molecular sieves were added (30 % of the mass of starting material). To the mixture, diethyl aluminum chloride (0.5 eq., c = 1.0 M in hexane) was added dropwise at 0 °C. The mixture was allowed to warm to room temperature then stirred until reaction completion and aq. satd. sodium bicarbonate was added at 0 °C. The aqueous phas-

es were extracted with dichloromethane then the combined organic layers were washed with brine, dried over magnesium sulfate, filtered and concentrated. The residue was purified by flash chromatography to afford the expected compound.

2-(*tert*-Butyldiphenylsilanyloxymethyl)prop-2-en-1-ol (3). Sodium hydride (60 % dispersion in mineral oil, 90.0 mg, 22.7 mmol, 1 eq.) was added to a solution of 2-methylene-1,3-propanediol (2.0 g, 22.7 mmol) in anhydrous tetrahydrofuran (*c* = 0.4 M, 56 mL) at 0 °C (ice bath). After stirring for 1 h *tert*-butyl(chloro)diphenylsilane (5.90 mL, 22.7 mmol, 1 eq.) was added and the mixture was stirred for 18 h at room temperature. The solution was then cooled to 0 °C, quenched with ice/water (60 mL) and aqueous phases were extracted with ethyl acetate. Then the combined organic layers were washed with brine, dried over magnesium sulfate, filtered and concentrated. The residue was purified by flash chromatography to afford the expected compound **3** as colorless oil (5.60 g, 76 %). Analytical and spectroscopic data were found to be in agreement with the reported literature[138]; ^{1}H NMR (500 MHz, $CDCl_3$, TMS) δ 7.73–7.60 (m, 4H, 4 H-Ar), 7.48-7.32 (m, 6H, 6 H-Ar), 5.16-5.14 (m, 1H, H-3a), 5.12-5.11 (m, 1H, H-3b), 4.26 (s, 2H, H-1), 4.17 (s, 2H, H-4), 1.09-1.03 (m, 9H, Si-C(C$\underline{H}_3$)$_3$) ppm; ^{13}C NMR (126 MHz, $CDCl_3$, TMS) δ 147.1 (C-2), 135.5, 133.2, 129.8, 127.7 (4 C, 4 C-Ar), 111.2 (C-3), 65.6 (C-1), 64.5 (C-4), 26.8 (Si-C($\underline{C}H_3$)$_3$), 19.2 (Si-$\underline{C}$(CH$_3$)$_3$) ppm.

(*R*)-2-((*tert*-Butyldiphenylsilanyloxymethyl)-oxiran-2-yl)-propane-1-ol (4a). General procedure A for SHARPLESS epoxidation was applied to **3** (1.50 g, 4.60 mmol). Reagents and conditions: (-)-diethyl tartrate (102 µL, 598 µmol, 0.13 eq.), titanium(IV) isopropoxide (136 µL, 460 µmol, 0.1 eq.), *tert*-butyl hydroperoxide (2.0 mL, 2.4 eq., *c* = 5.5 M in decane, over 4 Å molecular sieves), anhydrous dichloromethane (*c* = 0.4 M, 11.5 mL). Flash chromatography with ethyl acetate/cyclohexane 15/85 yielded compound **4a** (1.30 g, 83 %, 83 % *ee*) as a translucent syrup; R_f = 0.3 (ethyl acetate/cyclohexane 1.5/8.5); $[\alpha]_{20}^{D}$ = + 6.0 (*c* 1 , chloroform); ^{1}H NMR (600 MHz, $CDCl_3$) δ 7.72-7.61 (m, 4H, 4 H-Ar), 7.48-7.35 (m, 6H, 6 H-Ar), 3.94 (dd, $^{2}J_{4a,4b}$ = 12.3 Hz, $^{3}J_{4a,OH}$ = 4.8 Hz, 1H, H-4a), 3.88-3.74 (m, 3H, H-4b, H-1), 2.85 (d, $^{2}J_{3a,3b}$ = 4.8 Hz, 1H, H-3a), 2.66 (d, $^{2}J_{3a,3b}$ = 4.8 Hz, 1H, H-3b), 1.81 (dd, $^{3}J_{4b,OH}$ = 8.2 Hz, $^{3}J_{4a,OH}$ = 4.8 Hz, 1H, OH), 1.06 (s, 9H, Si-(C$\underline{H}_3$)$_3$) ppm; ^{13}C NMR (151 MHz, $CDCl_3$) δ 135.6, 132.9, 132.8, 129.9, 127.8 (12 C, 10 C-Ar), 64.8 (C-1), 61.8 (C-4), 59.6 (C-2), 48.9 (C-3), 26.8 (Si-C($\underline{C}H_3$)$_3$), 19.2 (Si-$\underline{C}$(CH$_3$)$_3$) ppm; IR (ATR) ν_{max}/cm^{-1} 3433, 3071, 2930, 2857, 1427, 1110, 700; ESI-HRMS: m/z calcd. for $C_{20}H_{26}O_3Si$ + Na^+ = 365.15434 $[M+Na]^+$; found 365.15414.

(*S*)-2-((*tert*-Butyldiphenylsilanyloxymethyl)-oxiran-2-yl)-propane-1-ol (4b). General procedure A for SHARPLESS epoxidation was applied to **3** (1.70 g, 5.1 mmol). Reagents and conditions: (+)-diethyl tartrate (113 µL, 662 µmol, 0.13 eq.), titanium(IV) isopropoxide (151 µL, 510 µmol, 0.1 eq.), *tert*-butyl hydroperoxide (2.30 mL, 2.4 eq., *c* = 5.5 M in decane, over 4 Å molecular sieves), anhydrous dichloromethane (*c* = 0.4 M, 12.8 mL). Flash chromatography with ethyl acetate/cyclohexane 1/4 yielded compound **4b** (1.20 g, 70 %, 88 % *ee*) as a translucent syrup; R_f = 0.3 (ethyl acetate/cyclohexane 1/4); $[\alpha]_{20}^{D}$ = - 6.1 (*c* 1, chloroform); ^{1}H NMR (500 MHz, $CDCl_3$) δ 7.70-7.63 (m, 4H, 4 H-Ar), 7.49-7.35 (m, 6H, 6 H-Ar), 3.95 (dd, $^2J_{4a,4b}$ = 12.3 Hz, $^3J_{4a,OH}$ = 4.8 Hz, 1H, H-4a), 3.88-3.76 (m, 3H, H-4b, H-1), 2.87 (d, $^2J_{3a,3b}$ = 4.8 Hz, 1H, H-3a), 2.67 (d, $^2J_{3a,3b}$ = 4.8 Hz, 1H, H-3b), 1.81 (dd, $^3J_{4b,OH}$ = 8.2 Hz, $^3J_{4a,OH}$ = 4.8 Hz, 1H, OH), 1.09 (s, 9H, Si-(C$\underline{H}_3$)$_3$) ppm; ^{13}C NMR (126 MHz, $CDCl_3$) δ 135.6, 132.9, 132.8, 129.9, 127.8 (12 C, 12 C-Ar), 64.9 (C-1), 61.9 (C-4), 59.5 (C-2), 48.9 (C-3), 26.8 (Si-C(C$\underline{H}_3$)$_3$), 19.2 (Si-C$\underline{(CH_3)_3}$) ppm; IR (ATR) ν_{max}/cm^{-1} 3443, 3071, 2930, 2857, 1427, 1109, 700; ESI-HRMS: m/z calcd. for $C_{20}H_{27}O_3Si$ + Na^+ + H^+ = 343.17240 $[M+Na+H]^+$; found 343.17226.

(*S*)-2-((*tert*-Butyldiphenylsilanyloxymethyl)-oxirane)-propyl-(*R*)-α-methoxy-α-trifluoromethyl-phenylacetate (2*S*, 6*R*)-5a. General procedure B for MOSHER ester analysis was applied to starting material **4a** (*R*) (11.0 mg, 32.0 µmol). Reagents and conditions: (*S*)-(+)-α-methoxy-α-trifluoromethylphenylacetyl chloride (8.0 µL, 42.0 mmol, 1.3 eq.), 4-(dimethylamino)pyridine (4.0 mg, 32.0 µmol, 1 eq.), triethylamine (21.0 µL, 150 µmol, 4.7 eq.), 3-(dimethylamino)propylamine (1-3 drops), anhydrous dichloromethane (*c* = 0.3 M, 106 µL). The residue was passed through short plug of silica gel in order to remove polar impurities with ethyl acetate/cyclohexane 1/20 providing MOSHER ester **(2*S*, 6*R*)-5a** (14.0 mg, 79 %) as yellow syrup. The product was obtained along with the minor diastereoisomer **(2*R*, 6*R*)-5c**; R_f = 0.3 (ethyl acetate/cyclohexane 1/20); $[\alpha]_{20}^{D}$= + 18.0 (*c* 0.8 , chloroform); ^{1}H NMR (500 MHz, C_6D_6, TMS) δ 7.74-7.63 (m, 6H, 6 H-Ar), 7.23-7.17 (m, 6H, 6 H-Ar), 7.10-6.97 (m, 3H, 3 H-Ar), 4.53 (d, $^2J_{4a,4b}$ = 11.9 Hz, 1H, H-4a), 4.25 (d, $^2J_{4a,4b}$ = 11.9 Hz, 1H, H-4b), 3.59 (ABq, $\Delta\delta_{1a,1b}$ = 0.05 ppm, $^2J_{1a,1b}$ = 11.5 Hz, 2H, H-1), 3.57 (br s, 3H, O-CH_3), 2.24 (ABq, $\Delta\delta_{3a,3b}$ = 0.14 ppm, $^2J_{3a,3b}$ = 4.9 Hz, 2H, H-3), 1.10 (s, 9H, Si-(C$\underline{H}_3$)$_3$) ppm; ^{13}C NMR (126 MHz, C_6D_6, TMS) δ 166.3 (R-$\underline{C}O_2R'$), 136.0, 135.9, 133.3, 133.2, 130.2, 129.8, 128.7, 128.3, 128.2, 128.0 (18 C, 18 C-Ar), 85.4 ($\underline{C}F_3$), 64.7 (C-4), 64.3 (C-1), 57.3 (C-2), 55.4 (O-$\underline{C}H_3$), 48.3 (C-3), 27.2, 26.9 (Si-

C($\underline{C}H_3)_3$), 19.4 (Si-$\underline{C}(CH_3)_3$) ppm; IR (ATR) ν_{max}/cm^{-1} 2931, 2857, 1754, 1472, 1168, 1107, 700; ESI-HRMS: m/z calcd. for $C_{30}H_{34}O_5F_3Si + H^+$ = 559.21221 $[M+H]^+$; found 559.21183.

(*S*)-2-((*tert*-Butyldiphenylsilanyloxymethyl)-oxirane)-propyl-(*S*)-α-methoxy-α-trifluoromethyl-phenylacetate (2*S*, 6*S*)-5b. General procedure B for MOSHER ester analysis was applied to starting material **4a** (*R*) (10.0 mg, 30.0 µmol). Reagents and conditions: (*R*)-(-)-α-methoxy-α-trifluoromethylphenylacetyl chloride (7.0 µL, 37.0 µmol, 1.3 eq.), 4-(dimethylamino)pyridine (4.0 mg, 30.0 µmol, 1 eq.), triethylamine (19.0 µL, 136 µmol, 4.7 eq.), 3-(dimethylamino)propylamine (1-3 drops), anhydrous dichloromethane (*c* = 0.3 M, 100 µL). The residue was passed through short plug of silica gel in order to remove polar impurities with ethyl acetate/cyclohexane 1/20 providing MOSHER ester **(2*S*, 6*S*)-5b** (13.0 mg, 80 %) as a yellow syrup. The product was obtained along with the minor diastereoisomer **(2*R*, 6*S*)-5d**. Enantiomeric excess was determined by ^{1}H NMR analysis in C_6D_6 at 500 MHz focusing on the terminal methylene protons between δ 2.40-2.10 ppm; R_f = 0.3 (ethyl acetate/cyclohexane 1/20); $[\alpha]_{20}^{D}$ = - 17 (*c* 0.8 , chloroform); ^{1}H NMR (500 MHz, C_6D_6, TMS) δ 7.71-7.65 (m, 6H, 6 H-Ar), 7.22-7.17 (m, 6H, 6 H-Ar), 7.08-7.00 (m, 3H, 3 H-Ar), 4.35 (ABq, $\Delta\delta_{4a,4b}$ = 0.17 ppm, $^2J_{4a,4b}$ = 11.8 Hz, 2H, H-4), 3.61 (br s, 2H, H-1), 3.38 (br s, 3H, O-CH_3), 2.23 (ABq, $\Delta\delta_{3a,3b}$ = 0.04 ppm, $^2J_{3a,3b}$ = 4.23 Hz, 2H, H-3), 1.09 (s, 9H, Si-($C\underline{H}_3)_3$) ppm; ^{13}C NMR (126 MHz, C_6D_6, TMS) δ 166.3 (R-$\underline{C}O_2R'$), 136.0, 135.9, 133.46, 133.2, 130.2, 129.8, 128.6, 128.3, 128.2, 127.9 (18 C, 18 C-Ar), 85.4 ($\underline{C}F_3$), 65.3 (C-4), 63.9 (C-1), 57.2 (C-2), 55.4 (O-$\underline{C}H_3$), 48.7 (C-3), 26.9 (Si-C($\underline{C}H_3)_3$), 19.4 (Si-$\underline{C}(CH_3)_3$) ppm; IR (ATR) ν_{max}/cm^{-1} 2931, 2857, 1754, 1472, 1168, 1107, 700; ESI-HRMS: m/z calcd. for $C_{30}H_{34}O_5F_3Si + H^+$ = 559.21221 $[M+H]^+$; found 559.21190.

(*R*)-2-((*tert*-Butyldiphenylsilanyloxymethyl)-oxiran-2-yl)-propyl-(*R*)-α-methoxy-α-trifluoromethyl-phenylacetate (2*R*, 6*R*)-5c. General procedure B for MOSHER ester analysis was applied to **4b** (*S*) (13.0 mg, 39.0 µmol). Reagents and conditions: (*S*)-(+)-α-methoxy-α-trifluoromethylphenylacetyl chloride (10.0 µL, 51.0 mmol, 1.3 eq.), 4-(dimethylamino)pyridine (5.0 mg, 39.0 µmol, 1 eq.), triethylamine (26.0 µL, 183 µmol, 4.7 eq.), 3-(dimethylamino)propylamine (1-3 drops), anhydrous dichloromethane (*c* = 0.3 M, 130 µL). The residue was passed through short plug of silica gel in order to remove polar impurities with ethyl acetate/cyclohexane 1/20 providing MOSHER ester **(2*R*, 6*R*)-5c** (15.0 mg,

70 %) as a yellow syrup. The product was obtained along with the minor diastereoisomer **(2*S*, 6*R*)-5a**. Enantiomeric excess was determined by ^{1}H NMR analysis in C_6D_6 at 500 MHz focusing on the terminal methylene between δ 2.40-2.10 ppm; R_f = 0.3 (ethyl acetate/cyclohexane 1/20); $[\alpha]_{20}^{D}$ = + 16 (*c* 1 , chloroform); ^{1}H NMR (500 MHz, C_6D_6) δ 7.73-7.62 (m, 6H, 6 H-Ar), 7.23-7.17 (m, 6H, 6 H-Ar), 7.10-6.98 (m, 3H, 3 H-Ar), 4.35 (ABq, $\Delta\delta_{4a,4b}$ = 0.17 ppm, $^{2}J_{4a,4b}$ = 11.8 Hz, 2H, H-4), 3.61 (br s, 2H, H-1), 3.38 (br s, 3H, O-CH_3), 2.23 (ABq, $\Delta\delta_{3a,3b}$ = 0.04 ppm, $^{2}J_{3a,3b}$ = 4.86 Hz, 2H, H-3), 1.09 (s, 9H, Si-(C$\underline{H}_3$)$_3$) ppm; ^{13}C NMR (126 MHz, C_6D_6, TMS) δ 166.3 (R-$\underline{C}O_2R'$), 136.0, 135.9, 133.46, 133.2, 130.2, 129.8, 128.6, 128.2, 127.9 (18 C, 18 C-Ar), 85.0 ($\underline{C}F_3$), 65.3 (C-4), 63.9 (C-1), 57.2 (C-2), 55.4 (O-$\underline{C}H_3$), 48.7 (C-3), 26.9 (Si-C($\underline{C}H_3$)$_3$), 19.4 (Si-$\underline{C}$(CH$_3$)$_3$) ppm; IR (ATR) ν_{max}/cm^{-1} 2931, 2857, 1754, 1472, 1168, 1107, 700; ESI-HRMS: m/z calcd. for $C_{30}H_{34}O_5F_3Si$ + H^+ = 559.21221 $[M+H]^+$; found 559.21162.

(*R*)-2-((*tert*-Butyldiphenylsilanyloxymethyl)-oxiran-2-yl)-propyl-(*S*)-α-methoxy-α-trifluoromethyl-phenylacetate (2*R*, 6*S*)-5d. General procedure B for MOSHER ester analysis was applied to starting material **4b** (*S*) (10.0 mg, 28.0 µmol). Reagents and conditions: (*R*)-(-)-α-methoxy-α-trifluoromethylphenylacetyl chloride (7.0 µL, 36.0 µmol, 1.3 eq.), 4-(dimethylamino)pyridine (3.40 mg, 28.0 µmol, 1 eq.), triethylamine (18 µL, 132 µmol, 4.7 eq.), 3-(dimethylamino)propylamine (1-3 drops), anhydrous dichloromethane (*c* = 0.3 M, 100 µL). The residue was passed through a short plug of silica gel in order to remove polar impurities with ethyl acetate/cyclohexane 1/20 providing MOSHER ester **(2*R*, 6*S*)-5d** (16.0 mg, quantitative) as a yellow syrup. The product was obtained along with the minor diastereoisomer **(2*S*, 6*S*)-5b**; R_f = 0.3 (ethyl acetate/cyclohexane 1/20); $[\alpha]_{20}^{D}$ = - 19 (*c* 1, chloroform); ^{1}H NMR (500 MHz, C_6D_6, TMS) δ 7.73-7.65 (m, 6H, 6 H-Ar), 7.24-7.18 (m, 6H, 6 H-Ar), 7.10-6.99 (m, 3H, 3 H-Ar), 4.53 (d, $^{2}J_{4a,4b}$ = 11.9 Hz, 1H, H-4a), 4.26 (d, $^{2}J_{4a,4b}$ = 11.9 Hz, 1H, H-4b), 3.59 (ABq, $\Delta\delta_{1a,1b}$ = 0.05 ppm, $^{2}J_{1a,1b}$ = 11.6 Hz, 2H, H-1), 3.36 (br s, 3H, O-CH_3), 2.32 (d, $^{2}J_{3a,3b}$ = 4.8 Hz, 1H, H-3a), 2.18 (d, $^{2}J_{3a,3b}$ = 4.8 Hz, 1H, H-3b), 1.10 (s, 9H, Si-(C$\underline{H}_3$)$_3$) ppm; ^{13}C NMR (126 MHz, C_6D_6, TMS) δ 166.3 (R-$\underline{C}O_2R'$), 136.0, 135.9, 133.3, 133.2, 132.8, 130.2, 129.8, 128.7, 128.3, 128.2 (18 C, 18 C-Ar), 85.0 ($\underline{C}F_3$), 64.7 (C-4), 64.3 (C-1), 57.3 (C-2), 55.3 (O-$\underline{C}H_3$), 48.3 (C-3), 26.9 (Si-C($\underline{C}H_3$)$_3$), 19.4 (Si-$\underline{C}$(CH$_3$)) ppm; IR (ATR) ν_{max}/cm^{-1} 2931, 2857, 1754, 1472, 1168, 1107, 700; ESI-HRMS: m/z calcd. for $C_{30}H_{34}O_5F_3Si$ + H^+ = 559.21221 $[M+H]^+$; found 559.21194.

(*S*)-2-((*tert*-Butyldiphenylsilanyloxymethyl)-oxiran-2-yl)-propane-1-trichloroacetimidate (6a). General procedure C for trichloroacetimidate formation was applied to **4a** (*R*) (1.0 g, 3.10 mmol). Reagents and conditions: 1,8-diazabicycloundec-7-ene (46.0 µL, 306 µmol, 0.1 eq.), trichloroacetonitrile (340 µL, 3.40 mmol, 1.1 eq.), anhydrous dichloromethane (*c* = 0.2 M, 15.4 mL). Flash chromatography with ethyl acetate/cyclohexane 1/20 yielded compound **6a** (*S*) (900 mg, 60 %) as a yellow viscous gel; R_f = 0.3 (ethyl acetate/cyclohexane 1/20); $[\alpha]_{20}^{D}$ = + 3 (*c* 1 , chloroform); ^{1}H NMR (500 MHz, $CDCl_3$) δ 8.38 (s, 1H, NH), 7.78-7.60 (m, 4H, 4 H-Ar), 7.51-7.35 (m, 6H, 6 H-Ar), 4.54 (ABq, $\Delta\delta_{4a,4b}$ = 0.07 ppm, $^2J_{4a,4b}$ = 11.4 Hz, 2H, H-4), 3.86 (ABq, $\Delta\delta_{1a,1b}$ = 0.08 ppm, $^2J_{1a,\,1b}$ = 11.4 Hz, 2H, H-1), 2.87 (d, $^2J_{3a,3b}$ = 4.9 Hz, 1H, H-3a), 2.77 (d, $^2J_{3a,3b}$ = 4.9 Hz, 1H, H-3b), 1.06 (s, 9H, Si-(C$\underline{H}_3$)$_3$) ppm; ^{13}C NMR (126 MHz, $CDCl_3$) δ 162.5 (NH=$\underline{C}$-CCl_3), 135.6, 132.9, 129.8, 127.8 (12C, 12 C-Ar), 91.1 (NH=C-$\underline{C}Cl_3$), 68.5 (C-4), 63.7 (C-1), 57.7 (C-2), 49.2 (C-3), 26.7 (Si-C($\underline{C}H_3$)$_3$) 19.3 (Si-$\underline{C}$(CH_3)$_3$) ppm; IR (ATR) ν_{max}/cm^{-1} 3343, 3071, 2930, 2857, 1666, 1111, 1085, 795; ESI-HRMS: m/z calcd. for $C_{22}H_{27}NO_3Cl_3Si$ = 486.08203 $[M+H]^+$; found 486.08203.

(*R*)-2-((*tert*-Butyldiphenylsilanyloxymethyl)-oxiran-2-yl)-propane-1-trichloroacetimidate (6b). General procedure C for trichloroacetimidate formation was applied to **4b** (*S*) (1.20 g, 3.50 mmol). Reagents and conditions: 1,8-diazabicycloundec-7-ene (53.0 µL, 350 µmol, 0.1 eq.), trichloroacetonitrile (386 µL, 3.90 mmol, 1.1 eq.), anhydrous dichloromethane (*c* = 0.2 M, 17.5 mL). Flash chromatography with ethyl acetate/cyclohexane 1/20 yielded compound **6b** (*R*) (1.10 g, 65 %) as a yellow viscous gel; R_f = 0.3 (ethyl acetate/cyclohexane 1/20); $[\alpha]_{20}^{D}$ = - 3 (*c* 1 , chloroform); ^{1}H NMR (500 MHz, $CDCl_3$, TMS) δ 8.37 (s, 1H, NH), 7.72-7.60 (m, 4H, 4 H-Ar), 7.50-7.34 (m, 6H, 6 H-Ar), 4.54 (ABq, $\Delta\delta_{4a,4b}$ = 0.07 ppm, $^2J_{4a,4b}$ = 11.7 Hz, 2H, H-4), 3.85 (ABq, $\Delta\delta_{1a,1b}$ = 0.07 ppm, $^2J_{1a,1b}$ = 11.4 Hz, 2H, H-1), 2.88 (d, $^2J_{3a,3b}$ = 4.9 Hz, 1H, H-3a), 2.77 (d, $^2J_{3a,3b}$ = 4.9 Hz, 1H, H-3b), 1.06 (s, 9H, Si-(C$\underline{H}_3$)$_3$) ppm; ^{13}C NMR (126 MHz, $CDCl_3$, TMS) δ 162.5 (NH=$\underline{C}$-CCl_3), 135.6, 132.9, 129.9, 129.8, 127.8, 127.7 (12C, 12 C-Ar), 91.0 (NH=C-$\underline{C}Cl_3$), 68.5 (C-4), 63.7 (C-1), 57.9 (C-2), 49.2 (C-3), 26.7 (Si-C($\underline{C}H_3$)$_3$), 19.3 (Si-$\underline{C}$(CH_3)$_3$) ppm; IR (ATR) ν_{max}/cm^{-1} 3343, 3071, 2930, 2857, 1666, 1111, 1085, 795; ESI-HRMS: m/z calcd. for $C_{22}H_{27}NO_3Cl_3Si + Na^+$ = 508.06397 $[M+Na]^+$; found 508.06382.

(*S*)-4-((*tert*-Butyldiphenylsilanyloxymethyl)-hydroxymethyl)-2-(trichloromethyl)-2-oxazoline (7a). General procedure D for oxazoline formation was applied to **6a** (*S*) (600 mg, 1.23 mmol). Reagents and conditions: diethylaluminium chloride (616 µL, 0.5 eq., *c* = 1.0 M in hexane), anhydrous tetrahydrofuran (*c* = 0.15 M, 8.20 mL). Flash chromatography with ethyl acetate/cyclohexane 15/85 yielded compound **7a** (*S*) (430 mg, 72 %) as a white viscous gel; R_f = 0.3 (ethyl acetate/cyclohexane 15/85); $[\alpha]_{20}^{D}$ = - 14 (*c* 1 , chloroform); ^{1}H NMR (600 MHz, $CDCl_3$, TMS) δ 7.72-7.55 (m, 4H, 4 H-Ar), 7.55-7.33 (m, 6H, 6 H-Ar), 4.77 (d, $^{2}J_{4a,4b}$ = 8.3 Hz, 1H, H-4a), 4.62 (d, $^{2}J_{4a,4b}$ = 8.3 Hz, 1H, H-4b), 3.85-3.58 (m, 4H, H-3, H-1), 1.9 (br s, 1H, OH), 1.06 (s, 9H, Si-(C$\underline{H}_3$)$_3$) ppm; ^{13}C NMR (151 MHz, $CDCl_3$, TMS) δ 164.2 (N=$\underline{C}$-CCl_3), 135.6, 135.5, 132.7, 132.6, 131.9, 130.3, 129.9, 128.1, 127.8 (12C, 12 C-Ar), 86.4 (N=C-$\underline{C}Cl_3$), 77.5 (C-2), 74.9 (C-4), 65.8 (C-3 or C-1), 65.0 (C-3 or C-1), 26.8 (Si-C($\underline{C}H_3$)$_3$), 19.3 (Si-$\underline{C}$(CH_3)$_3$) ppm; IR (ATR) ν_{max}/cm^{-1} 3398, 3071, 2930, 2857, 1660, 1427, 1106, 795, 700; ESI-HRMS: m/z calcd. for $C_{22}H_{27}NO_3Cl_3Si$ + H^+ = 486.08212 $[M+H]^+$; found 486.08203.

(*R*)-4-((*tert*-Butyldiphenylsilanyloxymethyl)-hydroxymethyl)-2-(trichloromethyl)-2-oxazoline (7b). General procedure D for oxazoline formation was applied to **6b** (*R*) (1.0 g, 2.10 mmol). Reagents and conditions: diethylaluminium chloride (1.0 mL, 0.5 eq., *c* = 1.0 M in hexane), anhydrous tetrahydrofuran (*c* = 0.15 M, 13.7 mL). Flash chromatography with ethyl acetate/cyclohexane 1/9 yielded compound **7b** (*R*) (1.40 g, 70 %) as a white viscous gel; R_f = 0.3 (ethyl acetate/cyclohexane 1/9); $[\alpha]_{20}^{D}$ = + 14 (*c* 1 , chloroform); ^{1}H NMR (500 MHz, $CDCl_3$, TMS) δ 7.68-7.63 (m, 4H, 4 H-Ar), 7.50-7.35 (m, 6H, 6 H-Ar), 4.77 (d, $^{2}J_{4a,4b}$ = 8.3 Hz, 1H, H-4a), 4.62 (d, $^{2}J_{4a,4b}$ = 8.3 Hz, 1H, H-4b), 3.85-3.61 (m, 4H, H-3, H-1), 1.79 (br s, 1H, OH), 1.06 (s, 9H, Si-(C$\underline{H}_3$)$_3$) ppm; ^{13}C NMR (126 MHz, $CDCl_3$, TMS) δ 164.2 (N=$\underline{C}$-Cl_3), 135.7, 135.6, 132.7, 132.6, 129.9, 127.9, 127.8 (12C, 12 C-Ar), 86.4 (N=C-$\underline{C}Cl_3$), 77.5 (C-2), 74.9 (C-4), 65.8 (C-1) , 65.0 (C-3), 26.8 (Si-C($\underline{C}H_3$)$_3$), 19.3 (Si-$\underline{C}$(CH_3)$_3$) ppm; IR (ATR) ν_{max}/cm^{-1} 3398, 3071, 2930, 2857, 1660, 1427, 1106, 795, 700; ESI-HRMS: m/z calcd. for $C_{22}H_{27}NO_3Cl_3Si$ + H^+ = 486.08212 $[M+H]^+$; found 486.08203.

(*R*)-4-((*tert*-Butyldiphenylsilanyloxymethyl)-allyloxymethyl)-2-(trichloromethyl)-2-oxazoline (8b). The oxazoline derivative **7b** (*R*) (428 mg, 812 µmol) was dissolved in anhydrous *N*,*N*-dimethylformamide (*c* = 0.5 M, 300 µL) then sodium hydride (60 % dispersion in mineral oil, 7.0 mg, 182 µmol, 1.2 eq.), allyl bromide (39.4 µL, 456 µmol, 3.0 eq.) were added

sequentially at 0 °C (ice bath). The mixture was stirred until completion at 0 °C and ethyl acetate and water were added. The organic phases were washed with brine, dried with magnesium sulfate, filtered and concentrated. Flash chromatography with ethyl acetate/cyclohexane 1/20 yielded compound **7b** (*R*) (68.0 mg, 84 %) as a translucent viscous gel; R_f = 0.3 (ethyl acetate/cyclohexane 1/20); $[\alpha]_{20}^{D}$ = + 21 (*c* 0.7 , chloroform); ^{1}H NMR (500 MHz, $CDCl_3$, TMS) δ 7.69-7.65 (m, 4H, 4 H-Ar), 7.45-7.34 (m, 6H, 6 H-Ar), 5.86-5.76 (m, 1H, H-6), 5.21 (dq, *J* = 17.3 Hz, *J* = 1.6 Hz, 1H, H-7a), 5.14 (dq, *J* = 10.4, *J* = 1.5 Hz, 1H, H-7b), 4.67 (ABq, $\Delta\delta_{4a,4b}$ = 0.12 ppm, $^{2}J_{4a,4b}$ = 8.2 Hz, 2H, H-4), 4.03-3.19 (m, 2H, H-5), 3.78 (ABq, $\Delta\delta_{1a,1b}$ = 0.07 ppm, $^{2}J_{1a,1b}$ = 10.4 Hz, 2H, H-1), 3.52 (ABq, $\Delta\delta_{3a,3b}$ = 0.1 ppm, $^{2}J_{3a,3b}$ = 9.7 Hz, 2H, H-3), 1.05 (s, 9H, Si-($C\underline{H}_3$)$_3$) ppm; ^{13}C NMR (126 MHz, $CDCl_3$, TMS) δ 163.2 (N=$\underline{C}$-Cl_3), 135.7 (2C, 2 C-Ar), 134.2 (C-6), 133.0, 132.8, 129.9, 129.8, 127.8 (10C, 10 C-Ar), 117.1 (C-7), 86.7 (N=C-$\underline{C}Cl_3$), 76.7 (C-2), 75.1 (C-4), 72.5 (C-5), 71.9 (C-1), 65.8 (C-3), 26.82 (Si-C($\underline{C}H_3$)$_3$), 19.3 (Si-$\underline{C}(CH_3)_3$) ppm.

(*R*)-2-Azido-((*tert*-butyldiphenylsilanyloxymethyl)-allyloxymethyl)-propane-1-ol (1b). The starting material **8b** (*R*) (240 mg, 455 µmol) was dissolved in anhydrous tetrahydrofuran (*c* = 0.15 M, 3.0 mL) and 1.0 N hydrochloric acid (455 µL, 1 eq.) was added. The reaction was stirred for 18 h then diluted with ethyl acetate and concentrated to dryness. The residue was dissolved in a mixture of 2/1/1 methanol/dichloromethane/water mixture (*c* = 0.1 M, 5.0 mL). Than potassium carbonate (126 mg, 910 µmol, 2 eq.), copper(II) sulfate pentahydrate (1.0 mg, 0.45 µmol, 0.01 eq.) and imidazole-1-sulfonyl azide hydrochloride (152 mg, 729 µmol, 1.6 eq.) were added sequentially. The blue mixture turned brown after reaction duration of 16 h and then concentrated to dryness. Then ethyl acetate and water were pured in and the aqueous phase was extracted with ethyl acetate and the combined organic phases were washed with brine, dried over magnesium sulfate then concentrated. Flash chromatography with ethyl acetate/cyclohexane 1/9 yielded compound **1b** (*R*) (150 mg, 77 %) as a translucent viscous gel; R_f = 0.3 (ethyl acetate/cyclohexane 1/9); $[\alpha]_{20}^{D}$ = - 65 (*c* 0.8, chloroform); ^{1}H NMR (500 MHz, $CDCl_3$, TMS) δ 7.67–7.62 (m, 4H, 4 H-Ar), 7.46-7.34 (m, 6H, 6 H-Ar), 5.90-5.83 (m, 1H, H-6), 5.24 (dq, *J* = 17.3 Hz, *J* = 1.6 Hz, 1H, H-7a), 5.17 (dq, *J* = 17.3 Hz, *J* = 1.5 Hz1H, H-7a), 3.96 (dt, $^{2}J_{5a,5b}$ = 5.5 Hz, $^{3}J_{5,6}$ = 1.5 Hz, 2H, H-5), 3.60 (ABq, $\Delta\delta_{a,b}$ = 0.05 ppm,$^{2}J_{a,b}$ = 9.9 Hz, 2H, H-1 or H-4), 3.53 (ABq, $\Delta\delta_{a,b}$ = 0.03 ppm,$^{2}J_{a,b}$ = 10.8 Hz, 2H, H-1 or H-4), 3.43 (ABq, $\Delta\delta_{3a,3b}$ = 0.02 ppm,$^{2}J_{3a,3b}$ = 9.0 Hz, 2H, H-3), 1.05 (s, 9H, Si-($C\underline{H}_3$)$_3$) ppm; ^{13}C

NMR (126 MHz, $CDCl_3$, TMS) δ 135.6 (2C, 2 C-Ar), 134.5 (C-6), 133.1, 129.8, 127.8 (10C, 10 C-Ar), 116.9 (C-7), 72.9 (C-3), 72.4 (C-5), 66.5, 65.8 (2C, C-1, C-4), 56.8 (C-2), 26.9 (Si-C($\underline{C}H_3)_3$), 19.3 (Si-$\underline{C}(CH_3)_3$) ppm.

(*R*)-4-*O*-(*tert*-Butyldiphenylsilanyloxymethyl)-4-*O*-(2,3,4,6-tetra-*O*-benzoyl-α-D-mannopyranosyl)methyl)-2-(trichloromethyl)-2-oxazoline (14a). To a round bottom flask with glycosyl acceptor **7a** (116.3 mg, 238 µmol) and activated 3 Å molecular sieves anhydrous dichloromethane (*c* = 0.1 M, 2.40 mL) was added. The solution was stirred at room temperature for 15 min. Then the mixture was cooled to -41 °C (dry ice/acetonitrile) and treated with 2,4,6-collidine (34.7 µL, 286 µmol**,** 1.2 eq.) and silver trifluoromethanesulfonate (74.3 mg, 286 µmol, 1.2 eq.). Then glycosyl donor **12** (189 mg, 286 µmol, 1.2 eq.) was added at an initial temperature of -41 °C. The mixture was stirred at -41 °C for three hours and then was allowed to warm to room temperature and stirred until completion. The resulting mixture was then diluted with ethyl acetate and filtrated over celite bed. The filtrate is subsequently washed with ice-cold 1 N hydrochloride acid, dried over magnesium sulfate, filtered and concentrated. Flash chromatography with ethyl acetate/cyclohexane 1.5/8.5 afforded compound **14a** (*R*, *S*) as white foam (47.0 mg, 19 %) and orthoester **15** (*S*, *R*) as a white amorphous solid (130 mg, 51 %) with intensive hazelnut smell. Compound **14a** (*R*, *S*): R_f = 0.3 (ethyl acetate/cyclohexane 1.5/8.5); ^{1}H NMR (500 MHz, $CDCl_3$, TMS) δ 8.09-8.05 (m, 2H, 2 H-Ar), 8.04-8.01 (m, 2H, 2 H-Ar), 7.92-7.89 (m, 2H, 2 H-Ar), 7.84-7.80 (m, 2H, 2 H-Ar), 7.73-7.68 (m, 4H, 4 H-Ar), 7.60-7.47 (m, 4H, 4 H-Ar), 7.42-7.31 (m, 12H, 12 H-Ar), 7.28- 7.22 (m, 2H, 2 H-Ar), 6.10 (t, $^3J_{3,4}$ = $^3J_{4,5}$ = 10.0 Hz, 1H, H-4_{Man}), 5.83 (dd, $^3J_{3,4}$ = 10.1 Hz, $^3J_{2,3}$ = 3.4 Hz, 1H, H-3_{Man}), 5.70 (dd, $^3J_{2,3}$ = 3.3 Hz, $^3J_{1,2}$ = 1.8 Hz, 1H, H-2_{Man}), 5.12 (d, $^3J_{1,2}$ = 1.7 Hz, 1H, H-1_{Man}), 4.74 (ABq, $\Delta\delta_{7a,7b}$ = 0.1 ppm, $^2J_{7a,7b}$ = 8.6 Hz, 2H, H-7), 4.64 (dd, $^2J_{6a,6b}$ = 11.9 Hz, $^3J_{5,6a}$ = 2.3 Hz, 1H, H-$6a_{Man}$), 4.46-4.35 (m, 2H, H-5_{Man}, H-$6b_{Man}$), 3.98 (d, $^2J_{10a,10b}$ = 10.4 Hz, 1H, H-10a), 3.86 (ABq, $\Delta\delta_{9a,9b}$ = 0.08 ppm, $^2J_{9a,9b}$ = 10.4 Hz, 2H, H-9), 3.76 (d, $^2J_{10a,10b}$ = 10.4 Hz, 1H, H-10b), 1.09 (s, 9H, Si-($C\underline{H}_3)_3$) ppm; ^{13}C NMR (126 MHz, $CDCl_3$, TMS) δ 171.1 (N=$\underline{C}$-CCl_3), 166.1, 165.4, 165.2, 163.8 (5C, 5 PhC=O), 135.7, 135.6, 133.5, 133.2, 133.1, 132.7, 132.6, 130.1, 130.0, 129.9, 129.8, 129.7, 129.3, 129.1, 128.9, 128.6, 128.5, 128.4, 128.3, 127.9 (36 C, 36 C-Ar), 98.2 (C-1_{Man}), 86.4 ($\underline{C}Cl_3$), 76.4 (C-8), 75.2 (C-7), 70.0 (C-2_{Man}), 69.9 (C-3_{Man}), 69.8 (C-10), 69.2 (C-5_{Man}), 66.7 (C-4_{Man}), 65.5 (C-9), 62.6 (C-6_{Man}), 26.9 (Si-C($\underline{C}H_3)_3$), 19.3 (Si-$\underline{C}(CH_3)_3$) ppm.

Orthoester **15** (*S*, *R*)-exo: R_f = 0.3 (ethyl acetate/cyclohexane 2/8); ^{1}H NMR (500 MHz, $CDCl_3$, TMS) δ 8.00-7.97 (m, 2H, 2 H-Ar), 7.90-7.86 (m, 4H, 4 H-Ar), 7.63-7.58 (m, 6H, 6 H-Ar), 7.54-7.46 (m, 3H, 3 H-Ar), 7.43-7.30 (m, 13H, 13 H-Ar), 7.29-7.23 (m, 2H, 2 H-Ar), 5.83-5.78 (m, 1H, H-4_{Man}), 5.67-5.62 (m, 2H, H-3_{Man}, H-1_{Man}), 4.93-4.90 (m, 1H, H-2_{Man}), 4.61 (ABq, $\Delta\delta_{7a,7b}$ = 0.13 ppm, $^2J_{7a,7b}$ = 8.6 Hz, 2H, H-7), 4.48 (dd, $^2J_{6a,6b}$ = 12.1 Hz, $^3J_{5,6a}$ = 3.6 Hz, 1H, H-6a$_{Man}$), 4.33 (dd, $^2J_{6a,6b}$ = 12.0 Hz, $^3J_{5,6a}$ = 5.0 Hz, 1H, H-6b$_{Man}$), 4.12-4.06 (m, 1H, H-5_{Mans}), 3.67 (ABq, $\Delta\delta_{9a,9b}$ = 0.09 ppm, $^2J_{9a,9b}$ = 10.5 Hz, 2H, H-9), 3.46 (ABq, $\Delta\delta_{10a,10b}$ = 0.06 ppm, $^2J_{10a,10b}$ = 9.7 Hz, 2H, H-10), 0.99 (s, 9H, Si-($C\underline{H}_3$)$_3$) ppm; ^{13}C NMR (126 MHz, $CDCl_3$) δ 171.2 (N=$\underline{C}$-CCl_3), 166.0, 165.9, 165.2, 163.3 (4C, 4 PhC=O), 135.7, 135.6, 133.5, 133.4, 133.0, 132.8, 132.6, 130.1, 129.9, 129.8, 129.7, 129.5, 128.9, 128.4, 128.3, 128.2, 127.8, 127.7 (36 C-Ar), 126.4 (2C, 2 C-Ph$_{ortho}$), 122.5 (orthoester C_q), 98.0 (H-1_{Man}), 86.5 ($\underline{C}Cl_3$), 76.1 (2C, C-8, C-2_{Man}), 75.1 (C-7), 72.4 (C-5_{Man}), 70.6 (C-3_{Man}), 66.5 (C-4_{Man}), 65.8, 65.7 (2C, C-9, C-10), 63.2 (C-6_{Man}), 26.9 (Si-C($\underline{C}H_3$)$_3$), 19.2 (Si-$\underline{C}$(CH_3)$_3$) ppm.

8.2.1 NMR spectra of new molecules for Chapter 3

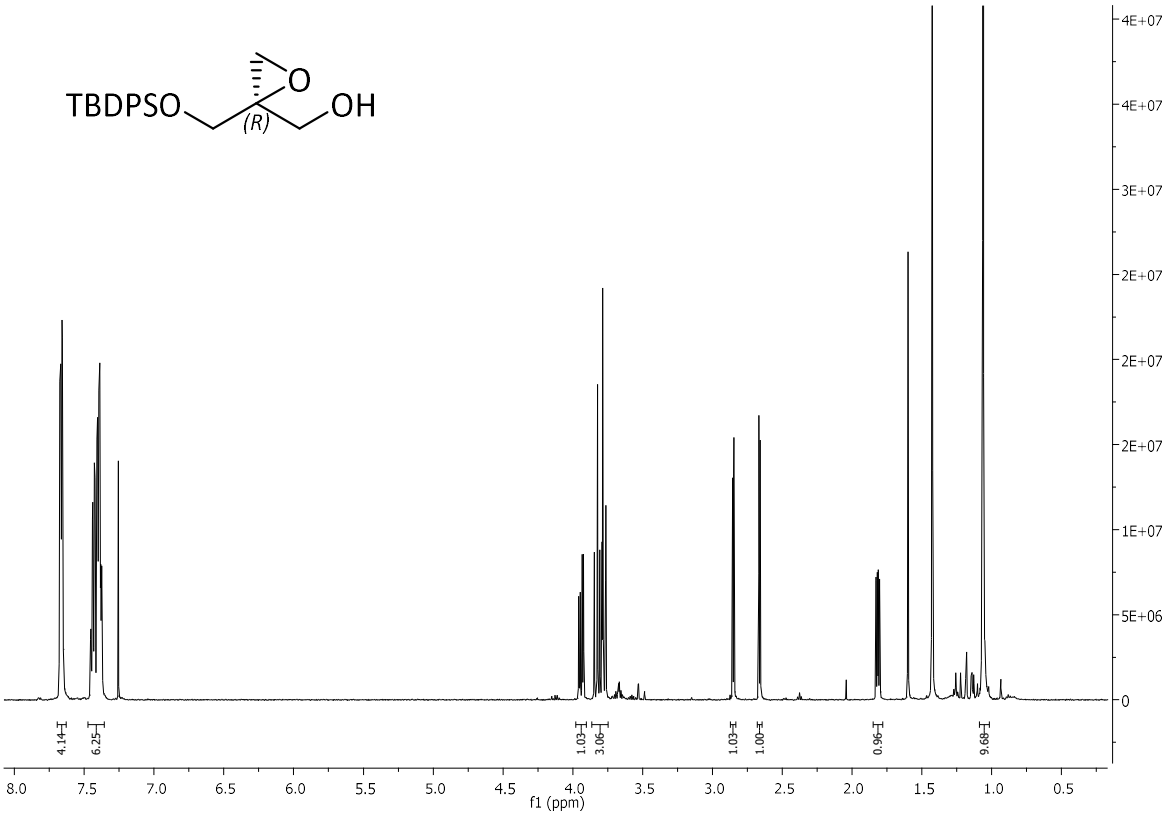

Figure 8.2: ^{1}H NMR (600 MHz, $CDCl_3$) spectrum of compound **4a**.

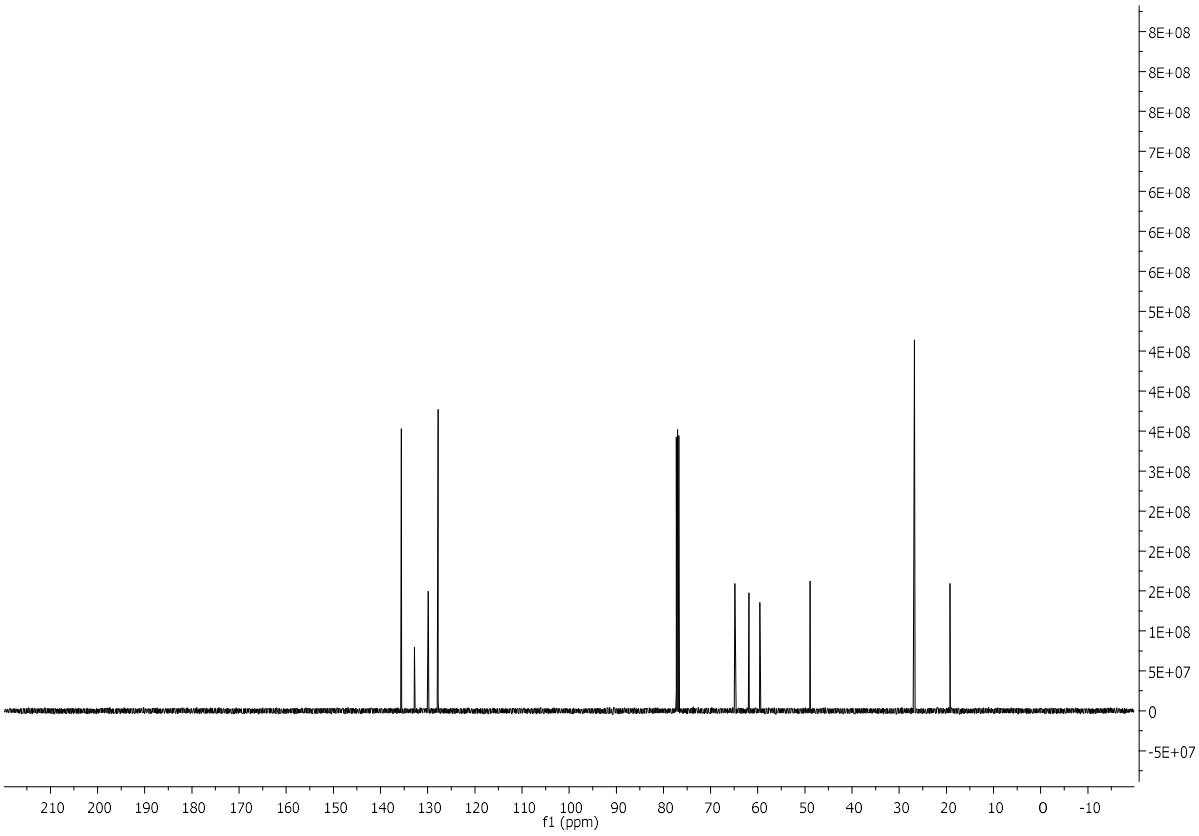

Figure 8.3: ^{13}C NMR (151 MHz, $CDCl_3$) spectrum of compound **4a**.

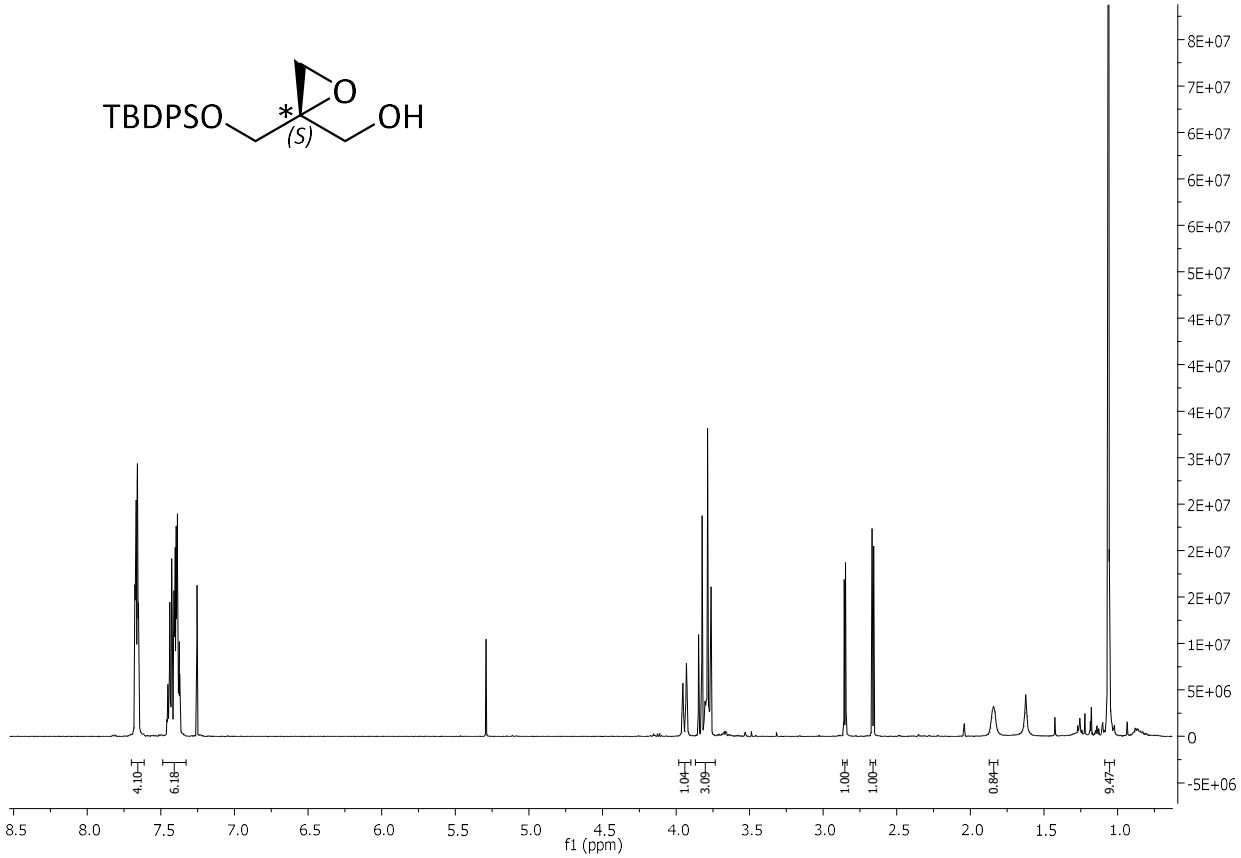

Figure 8.4: ^{1}H NMR (500 MHz, $CDCl_3$) spectrum of compound **4b**.

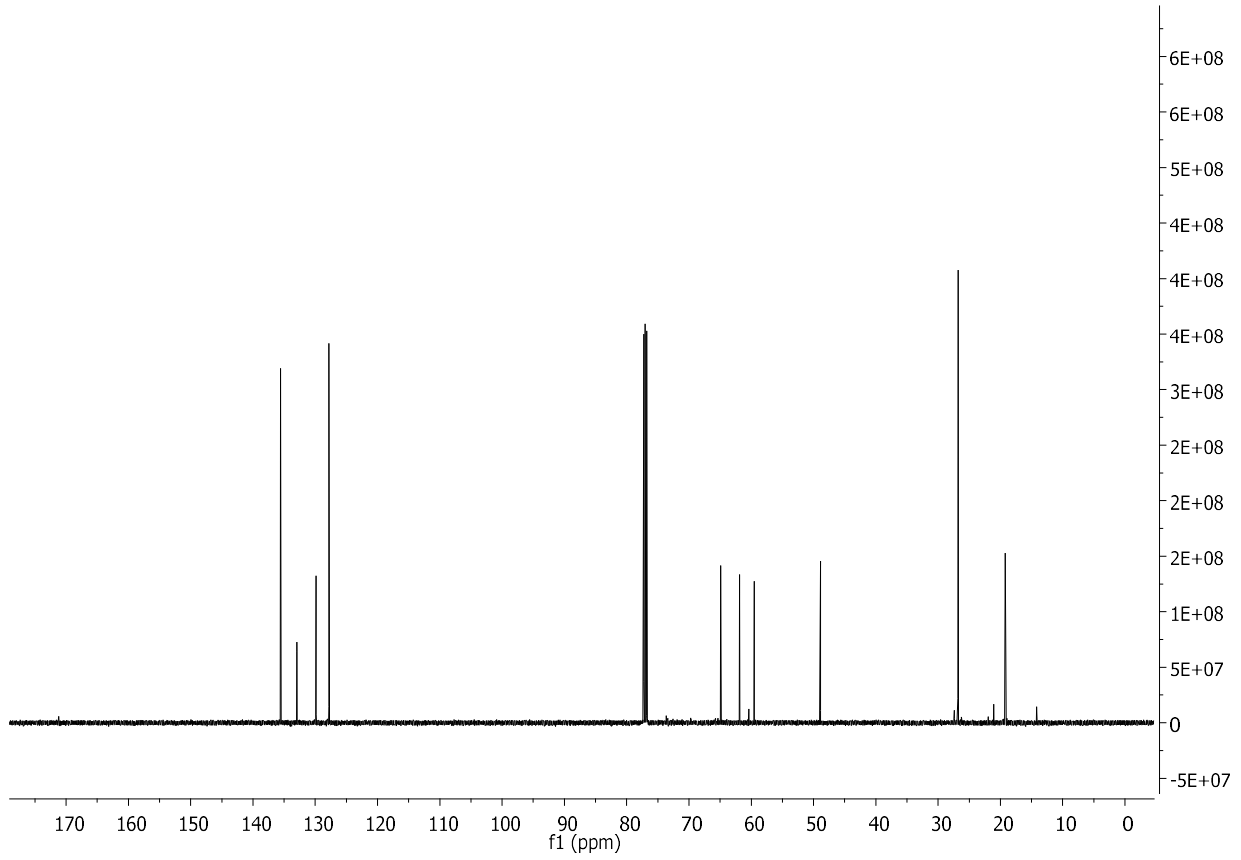

Figure 8.5: ^{13}C NMR (126 MHz, $CDCl_3$) spectrum of compound **4b**.

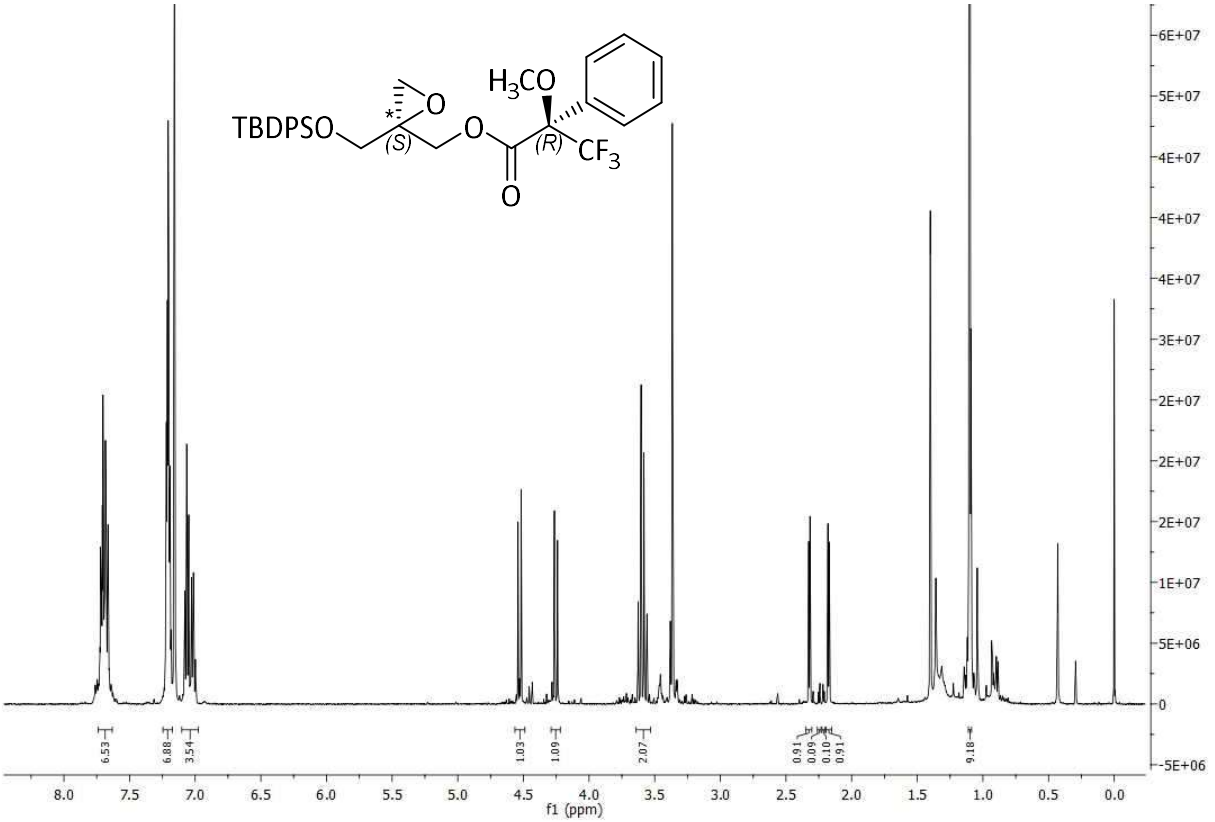

Figure 8.6: ^{1}H NMR (600 MHz, $CDCl_3$) spectrum of compound (2*S*,6*R*)-**5a** MOSHER ester.

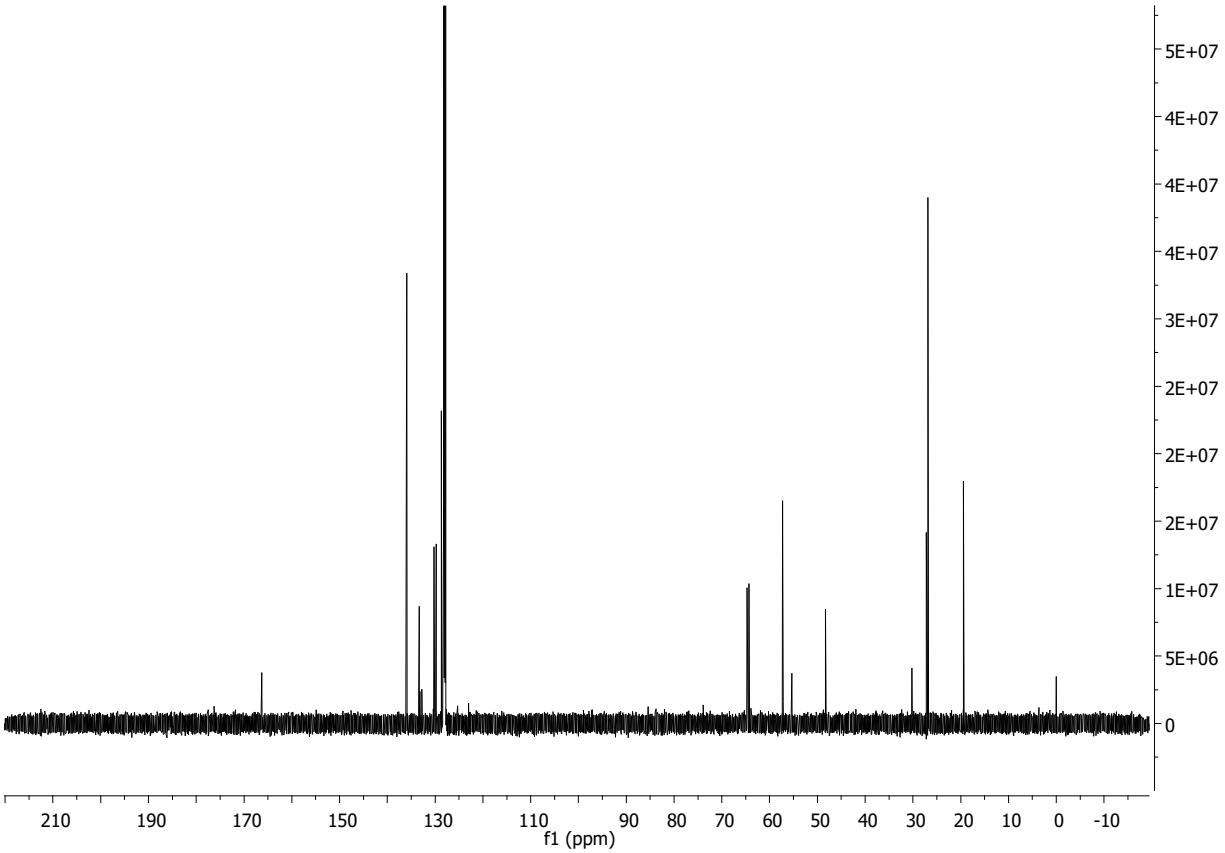

Figure 8.7: ^{13}C NMR (126 MHz, C_6D_6) spectrum of compound (2*S*,6*R*)-**5a** MOSHER ester.

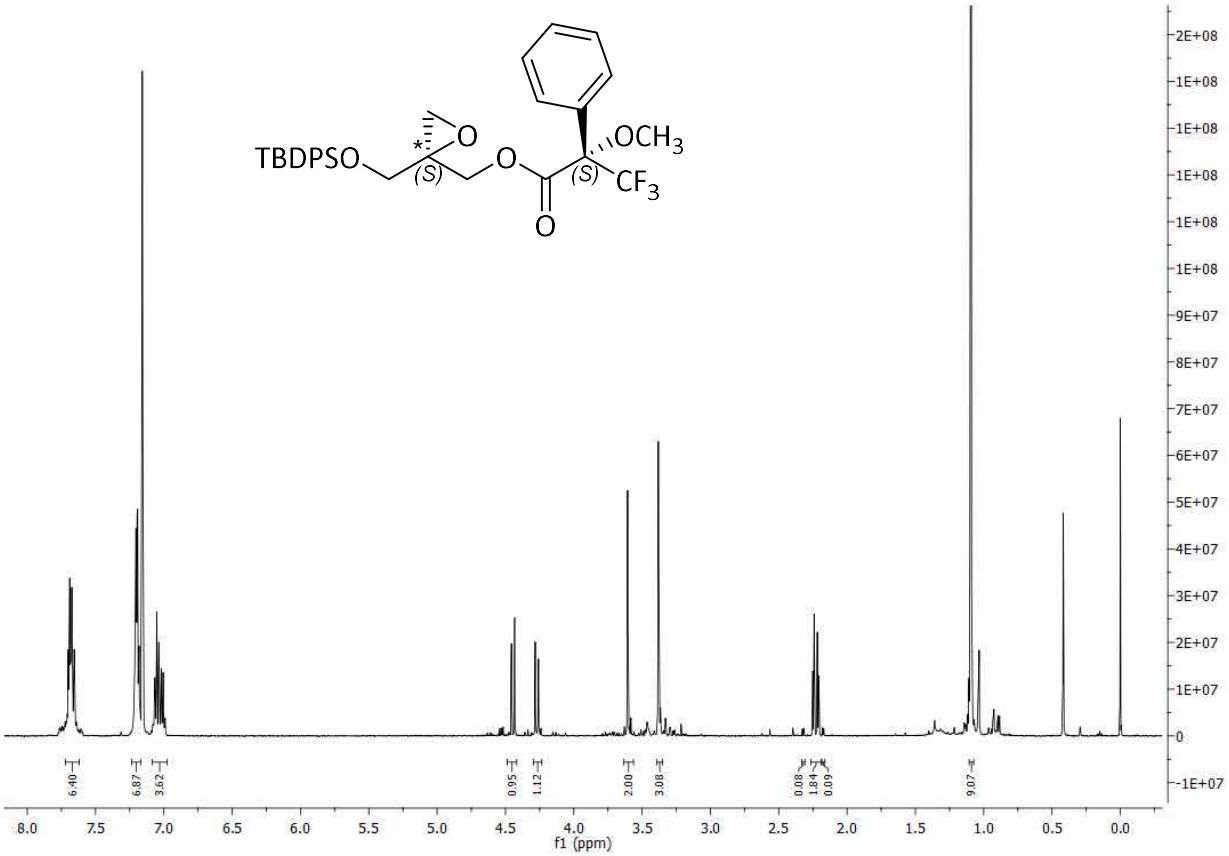

Figure 8.8: ^{1}H NMR (500 MHz, C_6D_6) spectrum of compound (2*S*,6*S*)-**5b** MOSHER ester.

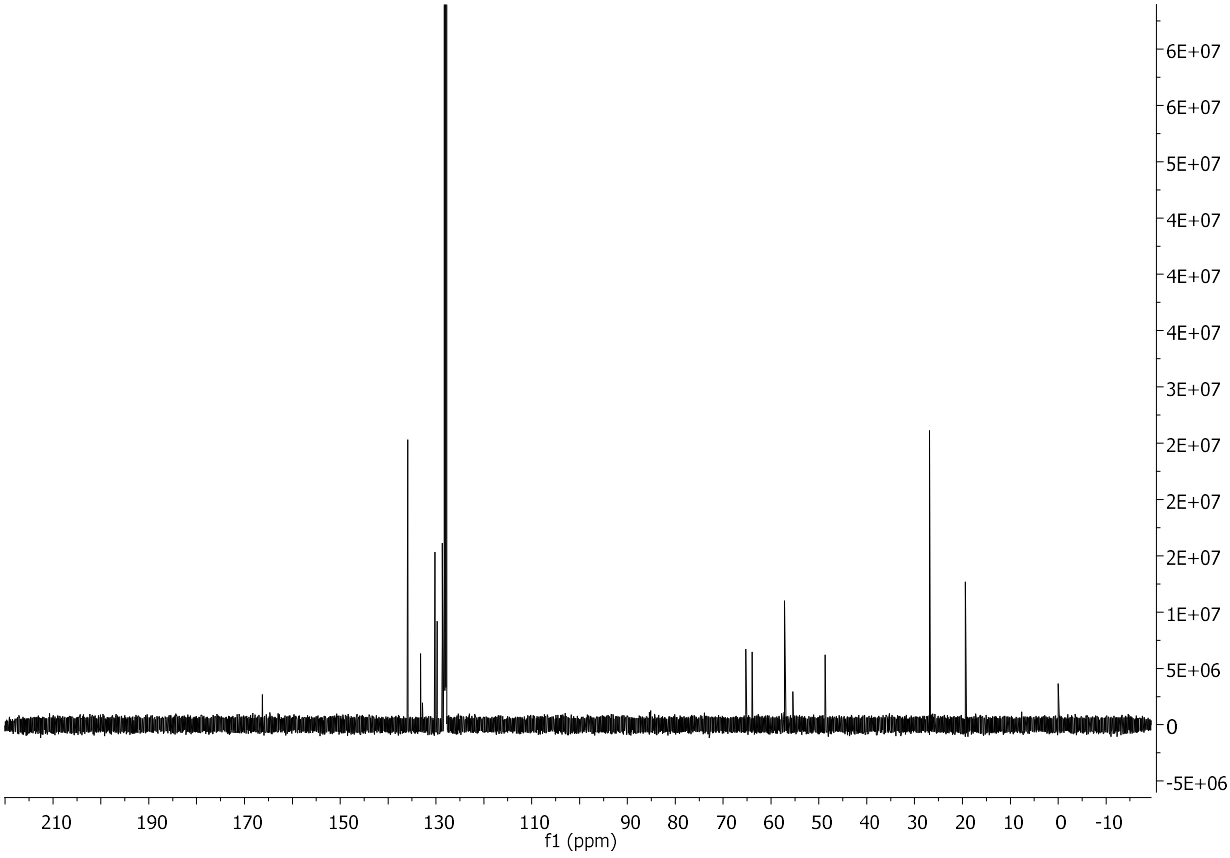

Figure 8.9: ^{13}C NMR (126 MHz, C_6D_6) spectrum of compound (2*S*,6*S*)-**5b** MOSHER ester.

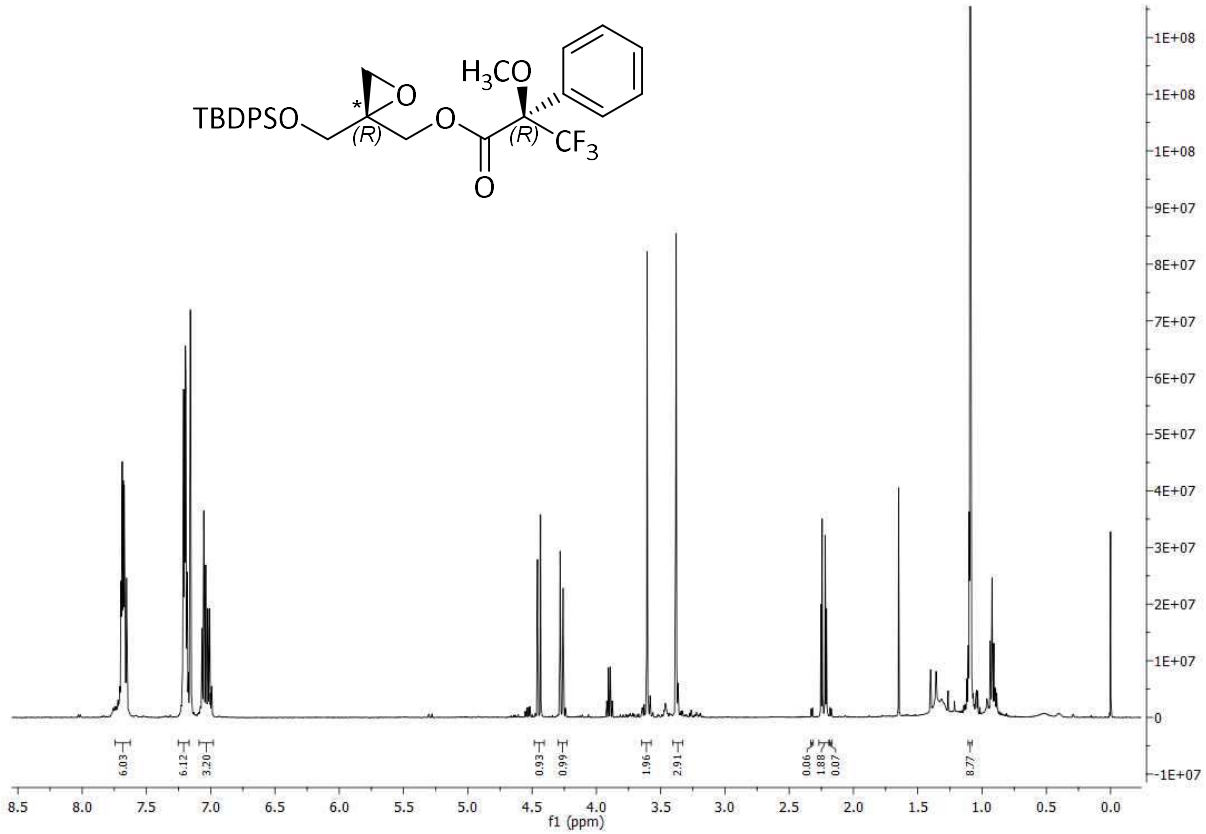

Figure 8.10: ^{1}H NMR (500 MHz, C_6D_6) spectrum of compound (2*R*,6*R*)-**5c** MOSHER ester with obtained 88 % *ee*.

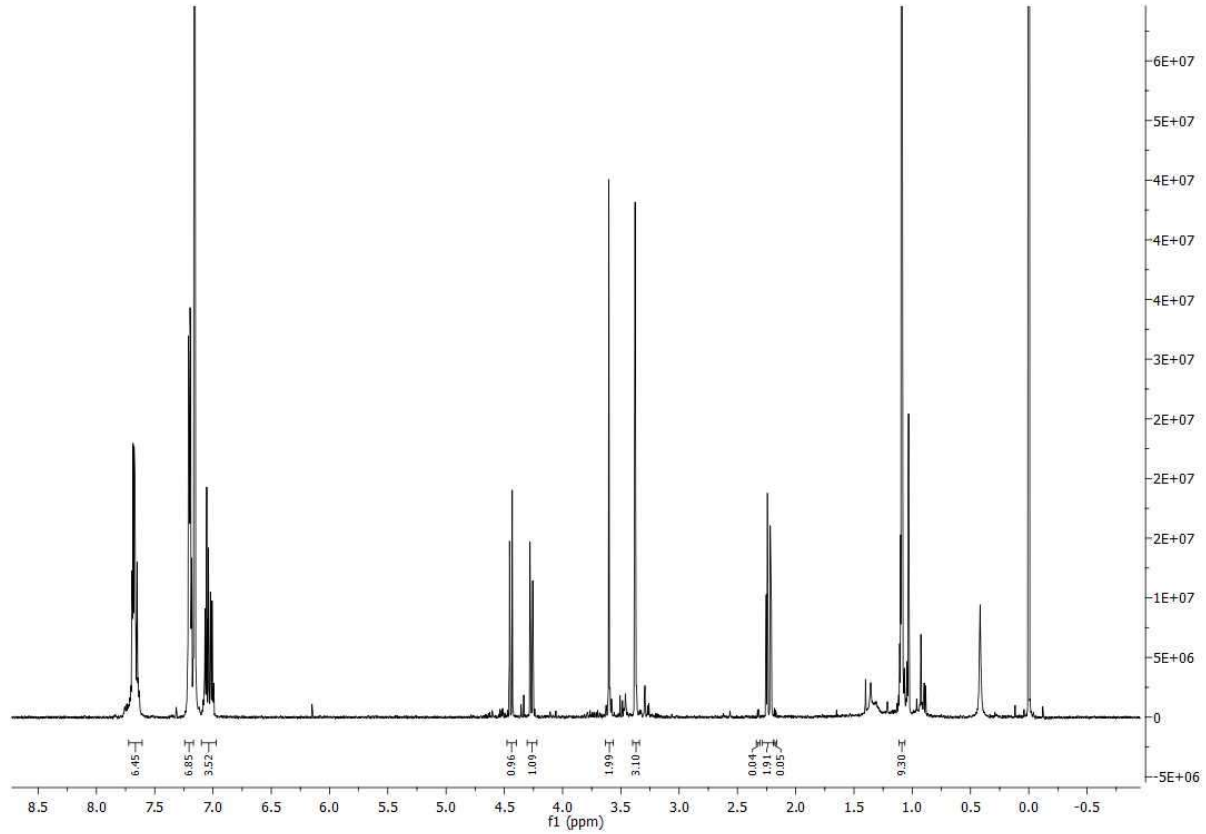

Figure 8.11: ^{1}H NMR (500 MHz, C_6D_6) spectrum of compound (2*R*,6*R*)-**5c** MOSHER ester with obtained 91 % *ee*.

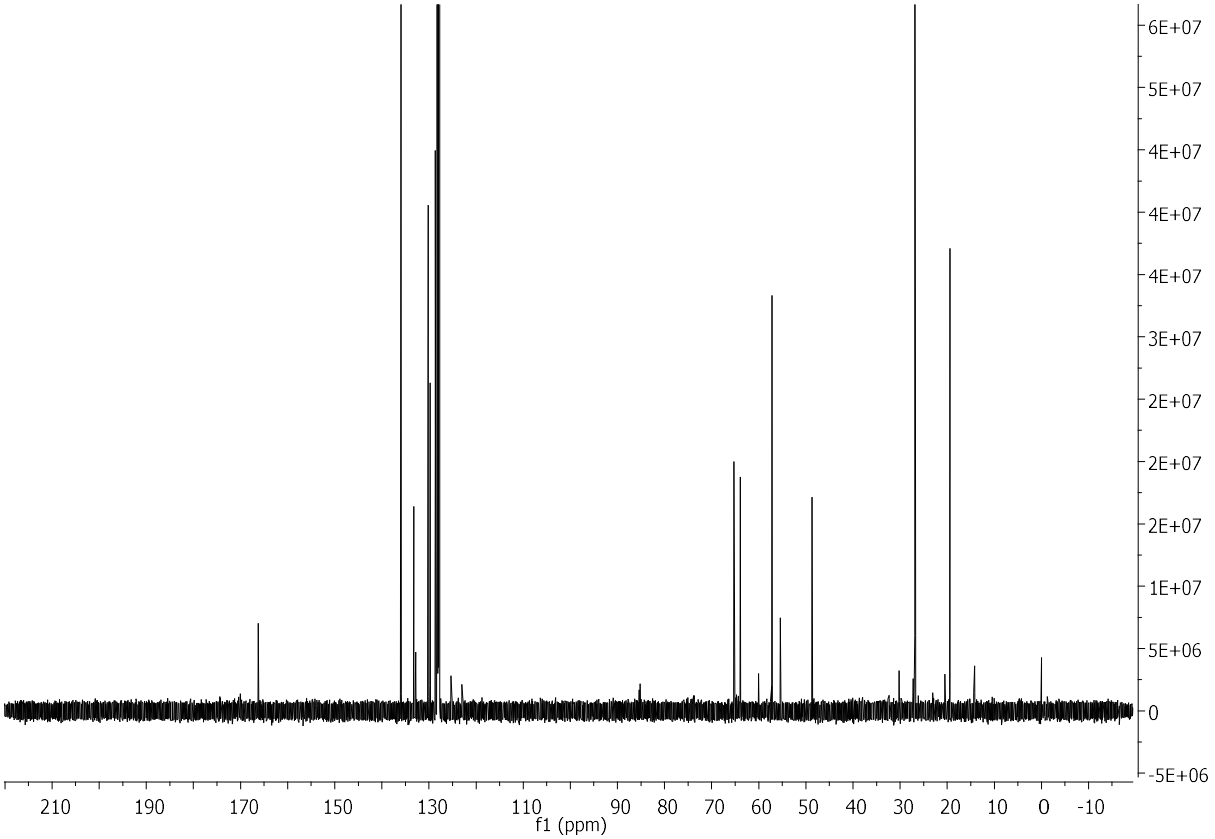

Figure 8.12: ^{13}C NMR (126 MHz, C_6D_6) spectrum of compound (2*R*,6*R*)-**5c** MOSHER ester.

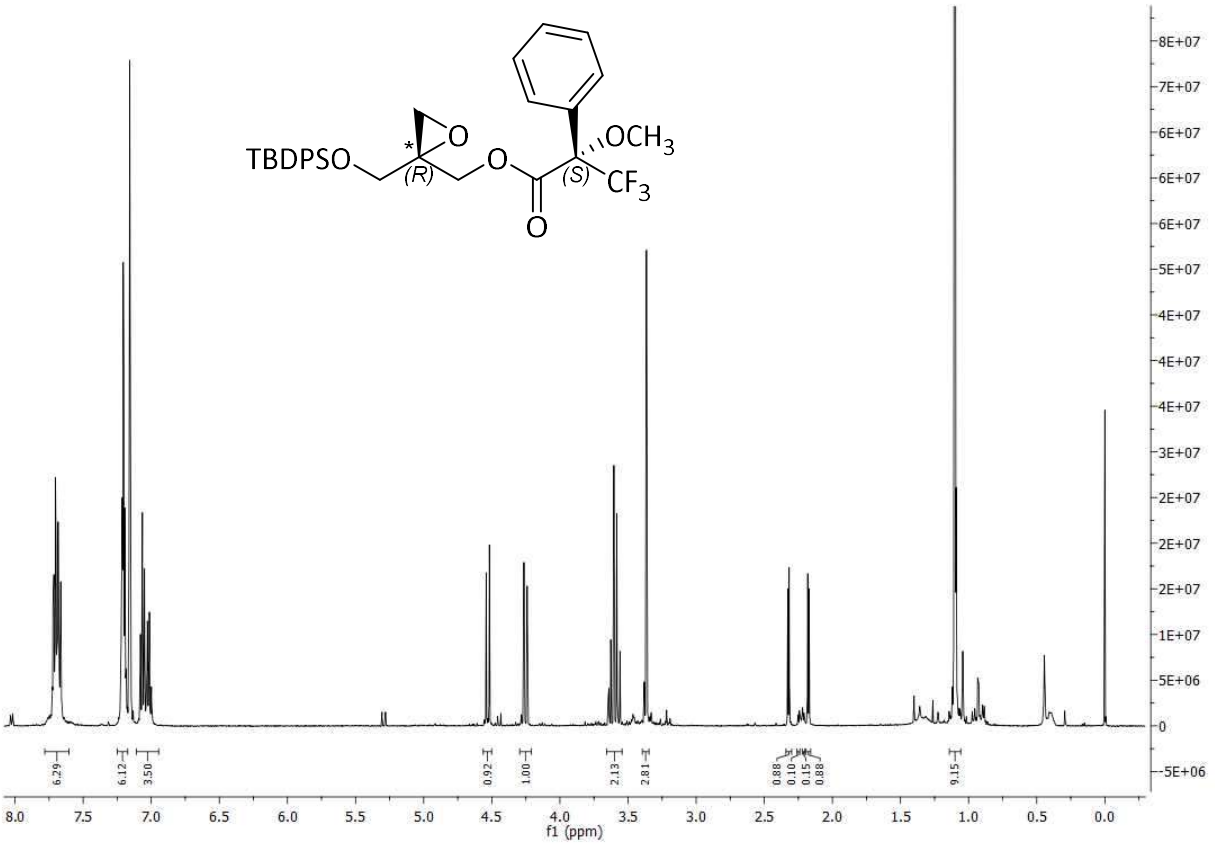

Figure 8.13: ^{1}H NMR (500 MHz, C_6D_6) spectrum of compound (2*R*,6*S*)-**5d** MOSHER ester.

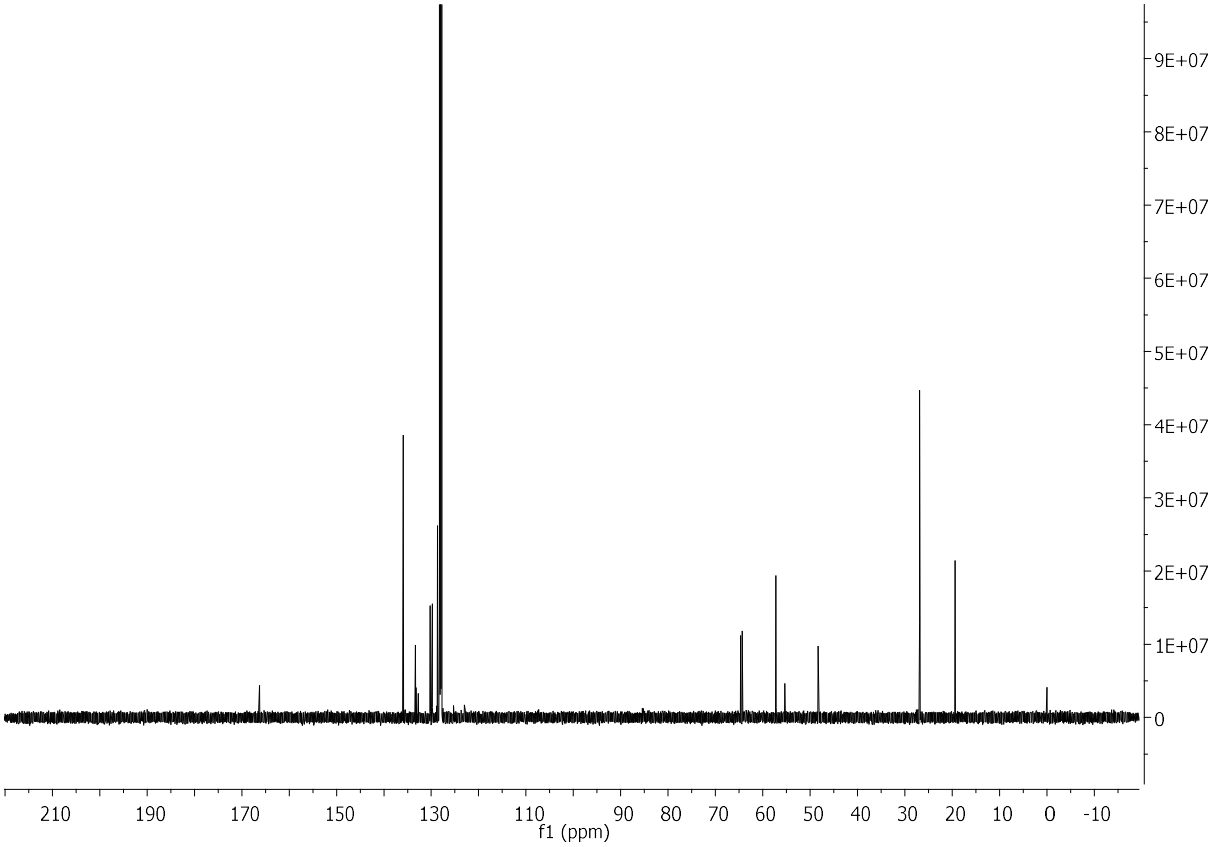

Figure 8.14: ^{13}C NMR (126 MHz, C_6D_6) spectrum of compound (2*R*,6*S*)-**5d** MOSHER ester.

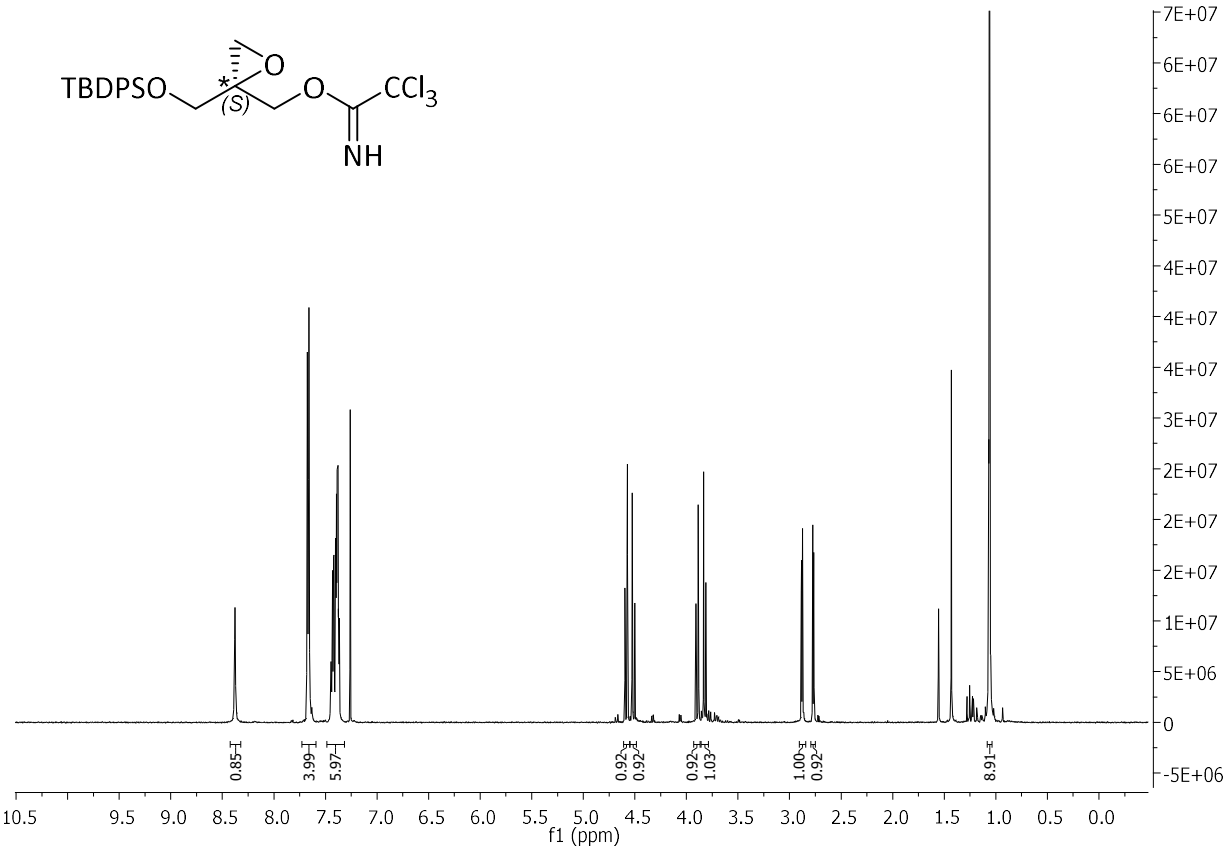

Figure 8.15: ^{1}H NMR (500 MHz, $CDCl_3$) spectrum of compound **6a**.

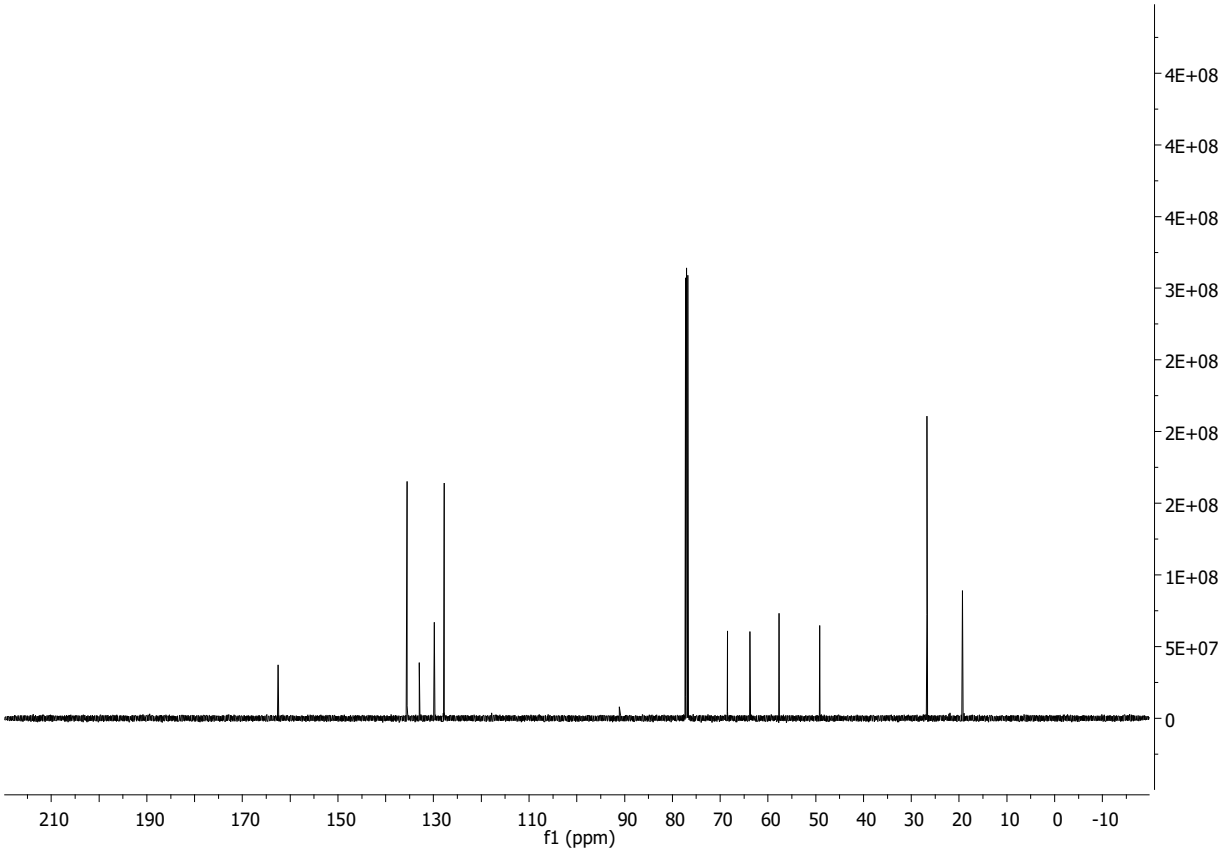

Figure 8.16: ^{13}C NMR (126 MHz, $CDCl_3$) spectrum of compound **6a**.

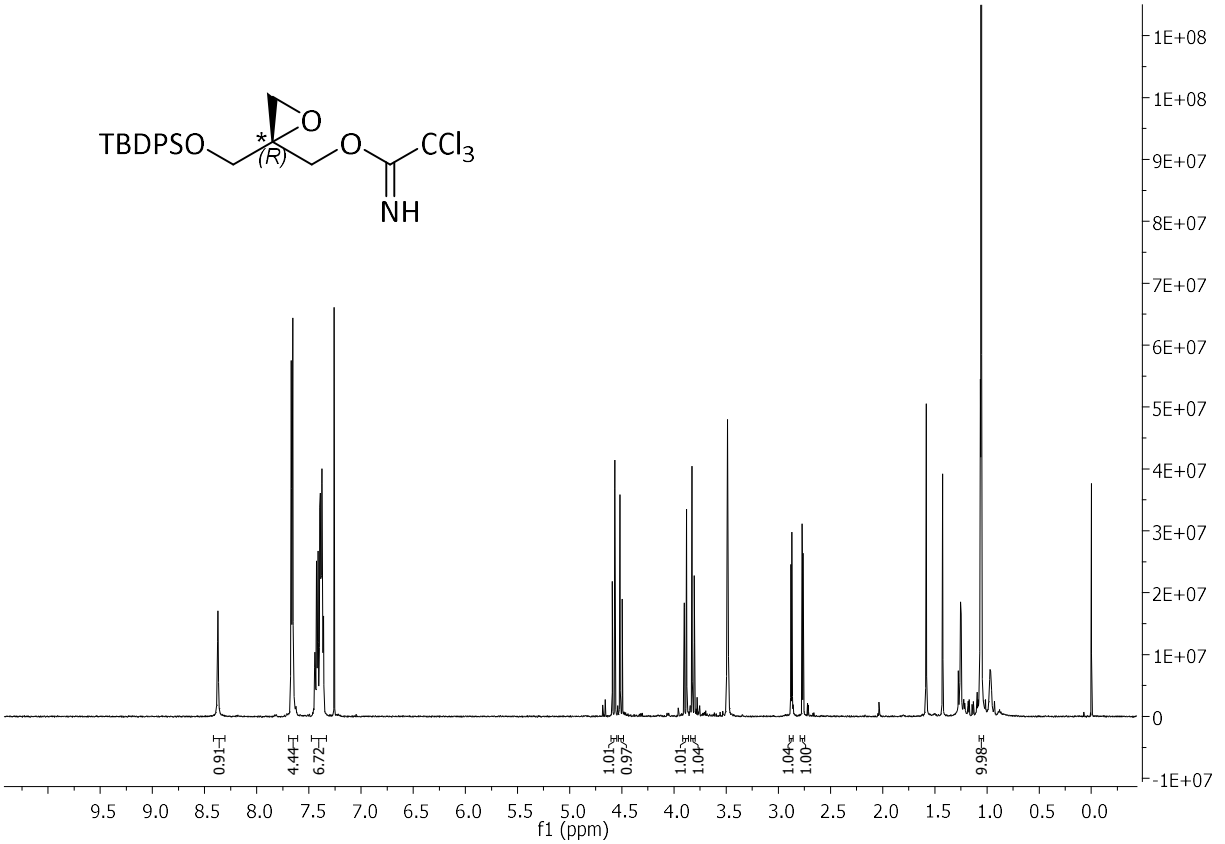

Figure 8.17: ^{1}H NMR (500 MHz, $CDCl_3$) spectrum of compound **6b**.

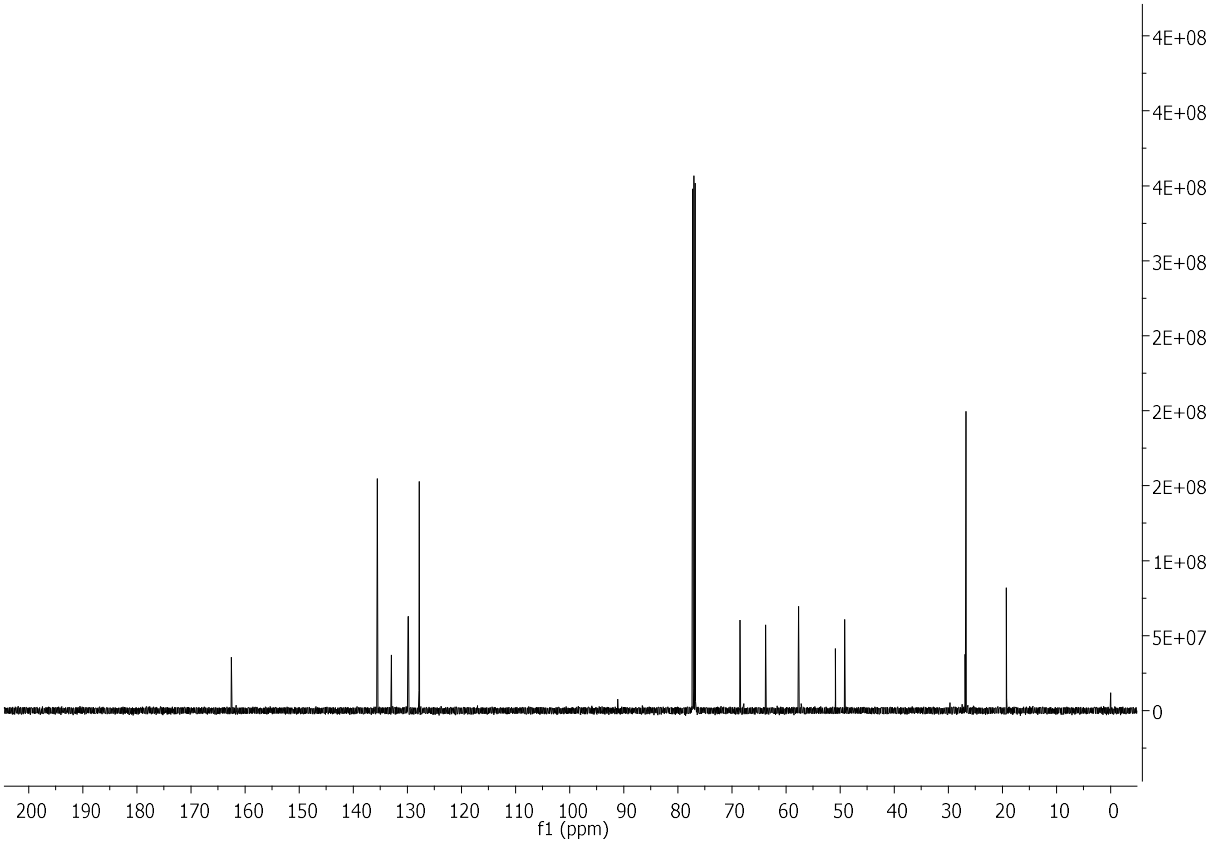

Figure 8.18: ^{13}C NMR (126 MHz, $CDCl_3$) spectrum of compound **6b**.

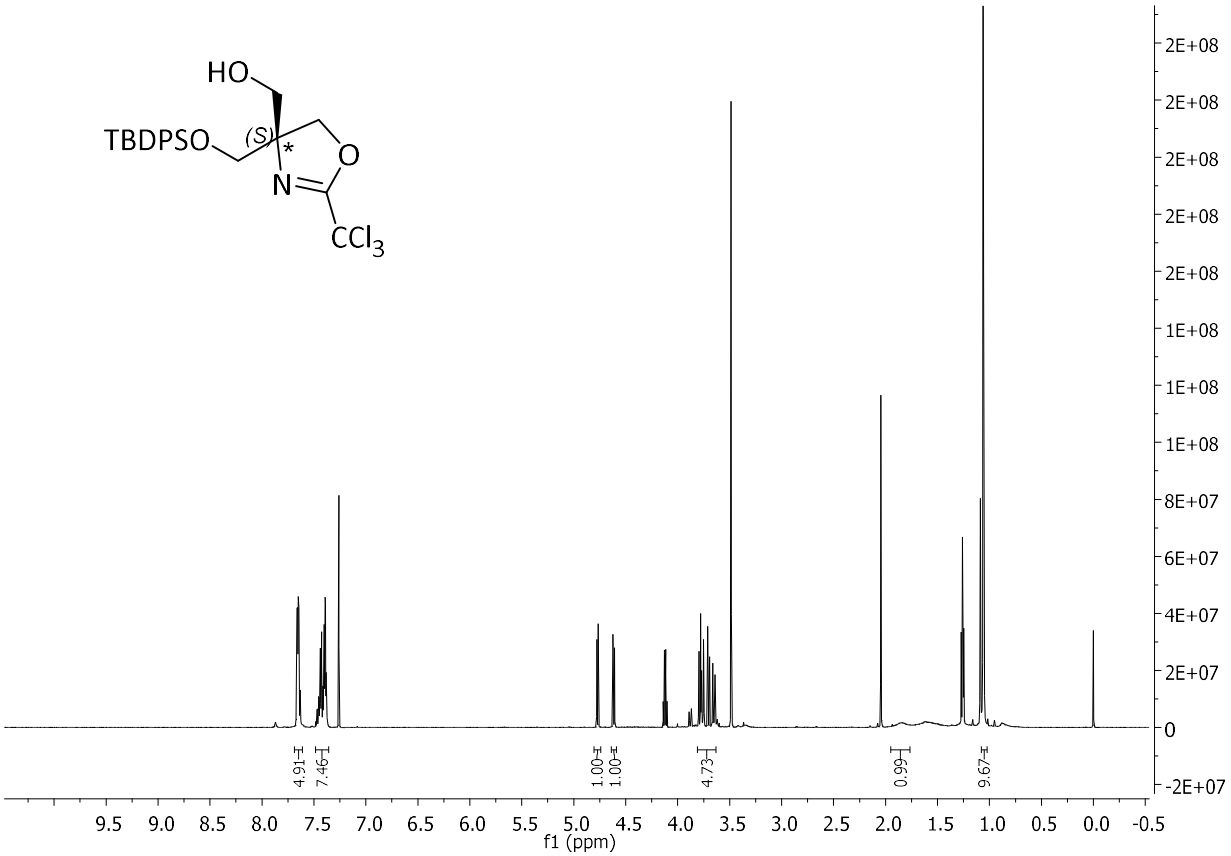

Figure 8.19: ^{1}H NMR (600 MHz, $CDCl_3$) spectrum of compound **7a**.

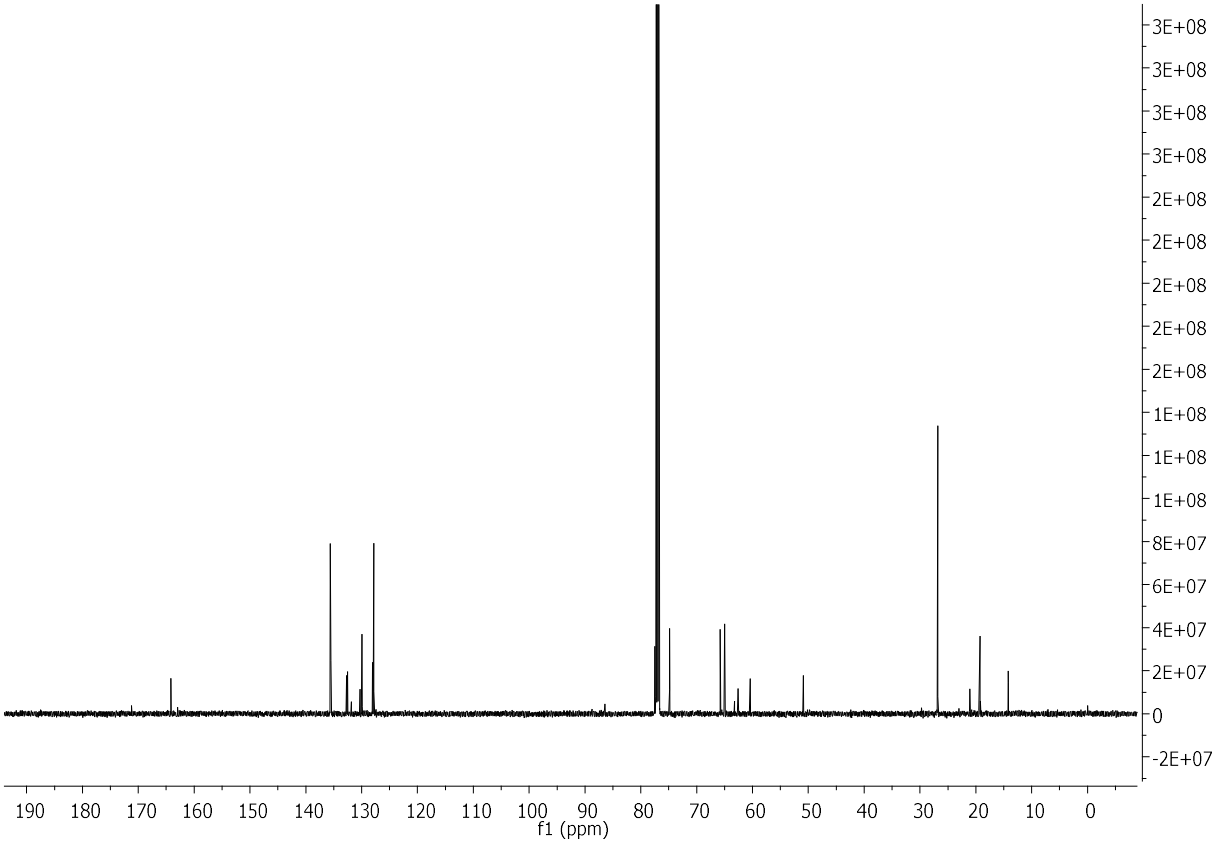

Figure 8.20: ^{13}C NMR (151 MHz, $CDCl_3$) spectrum of compound **7a**.

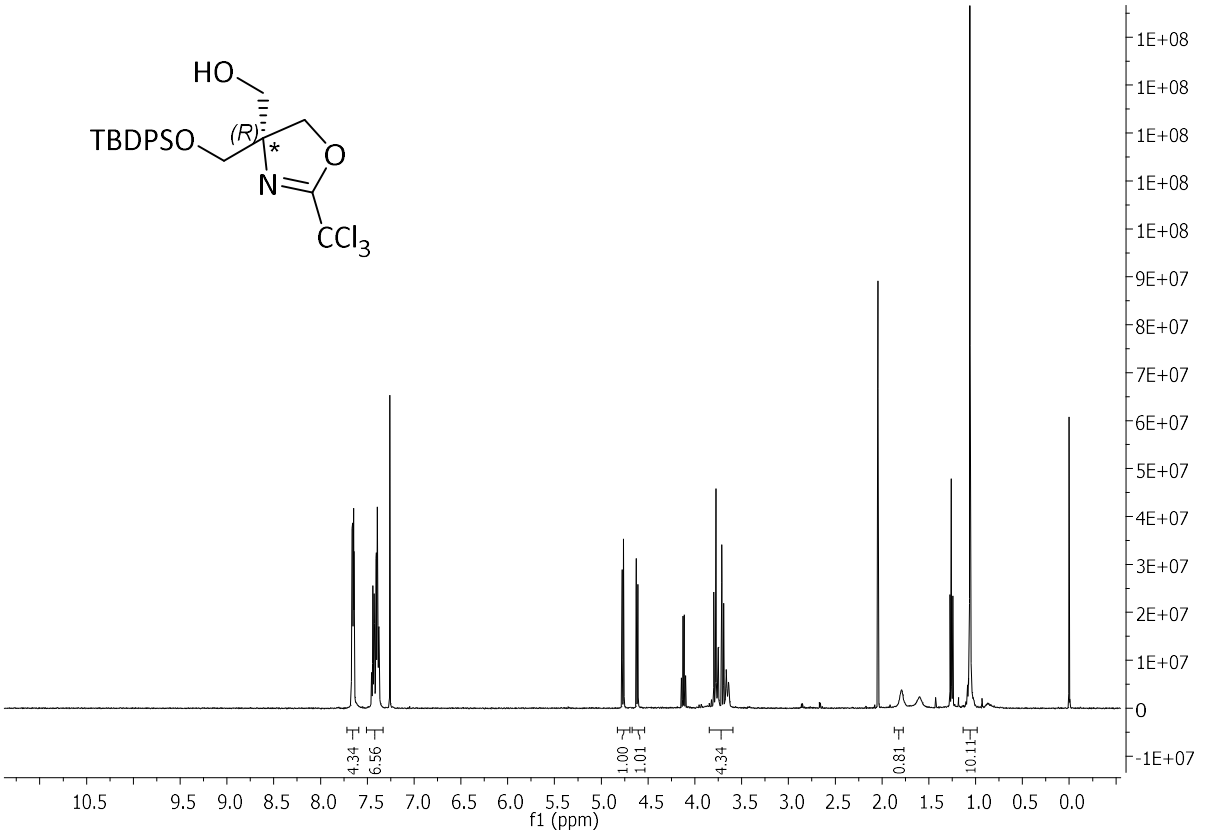

Figure 8.21: ^{1}H NMR (500 MHz, $CDCl_3$) spectrum of compound **7b**.

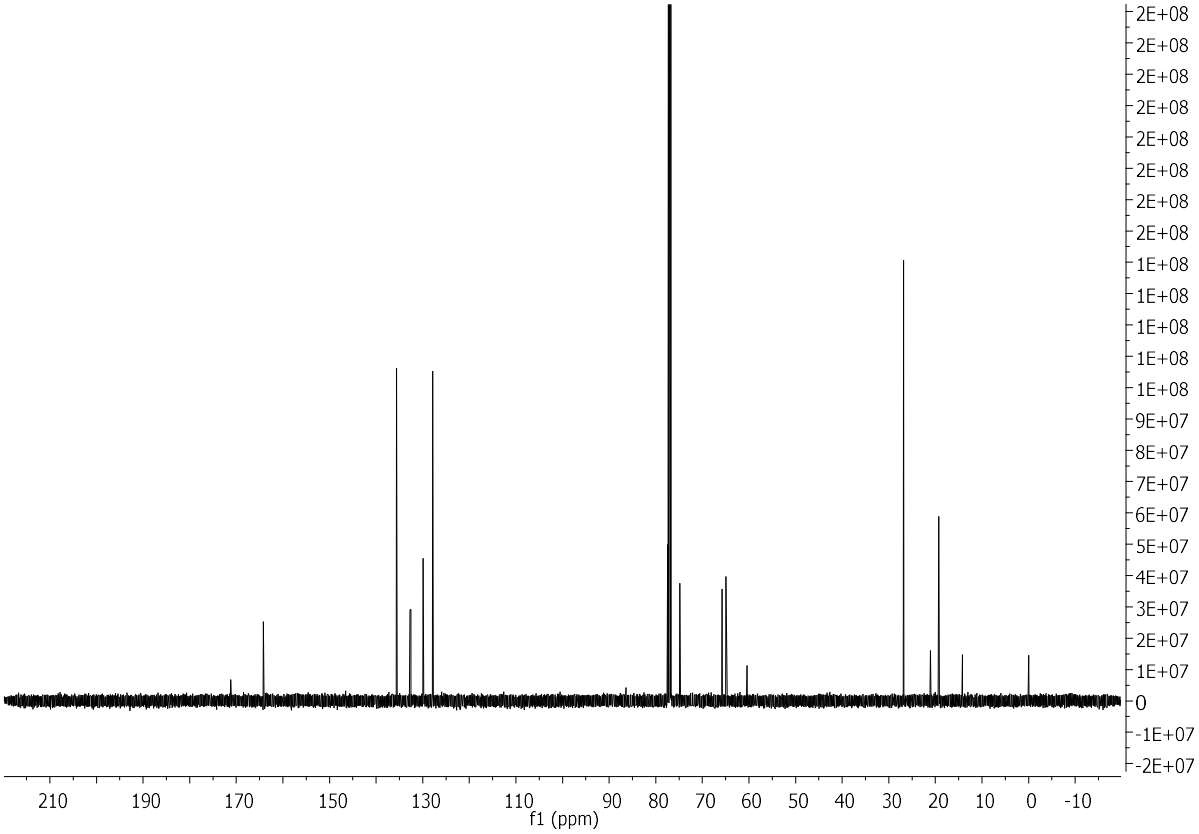

Figure 8.22: ^{13}C NMR (126 MHz, $CDCl_3$) spectrum of compound **7b**.

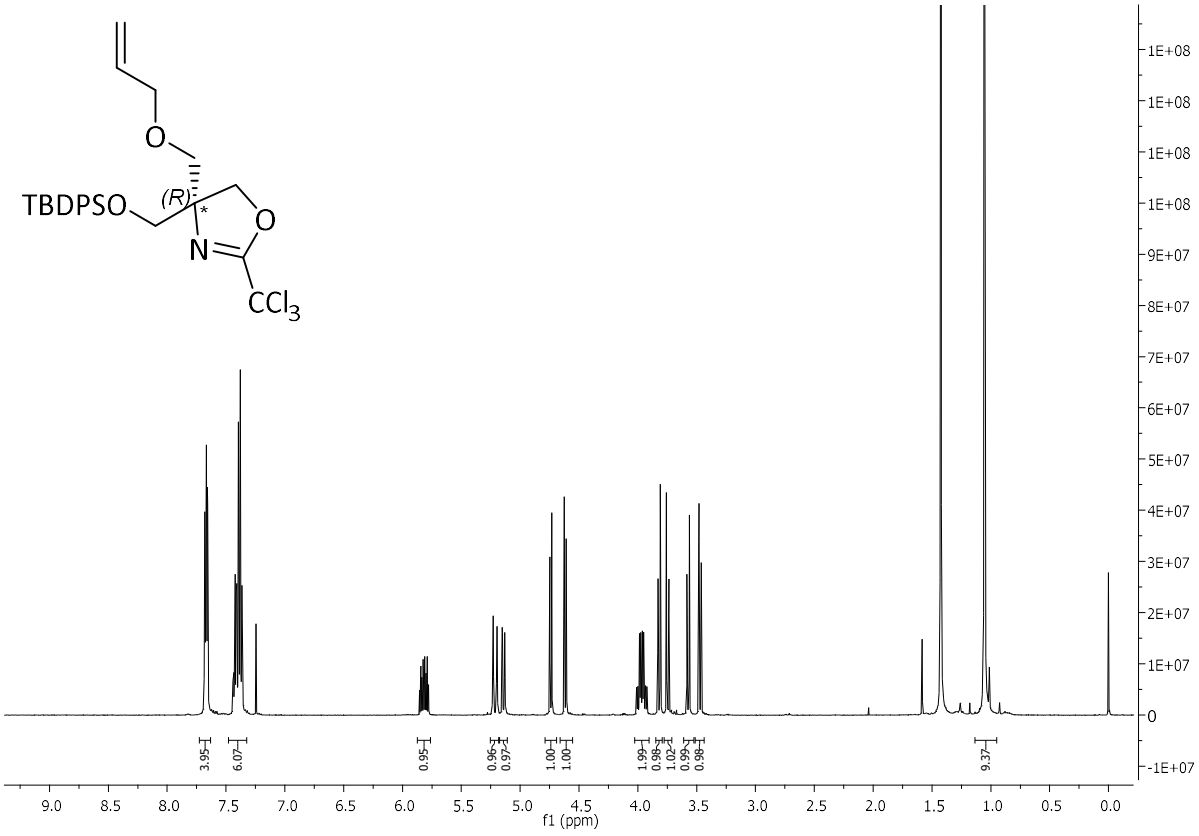

Figure 8.23: ^{1}H NMR (500 MHz, $CDCl_3$) spectrum of compound **8b**.

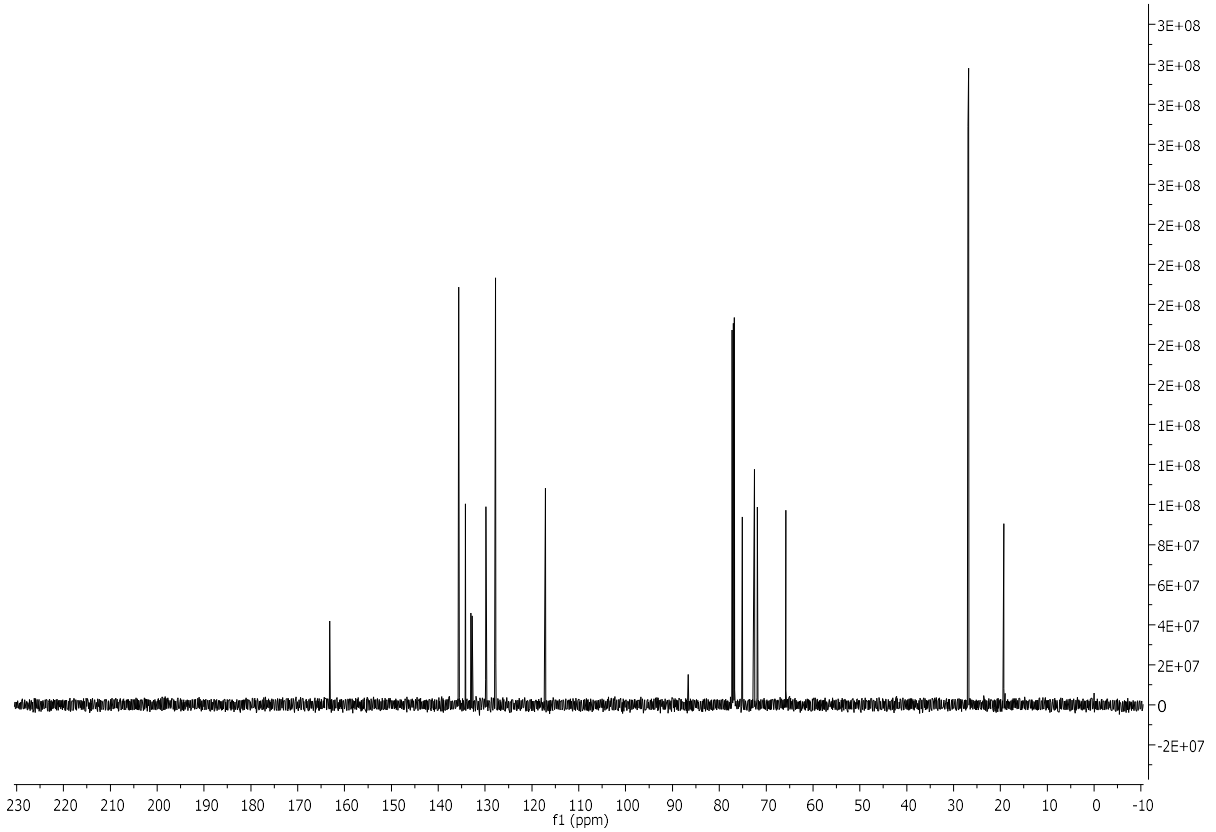

Figure 8.24: ^{13}C NMR (126 MHz, $CDCl_3$) spectrum of compound **8b**.

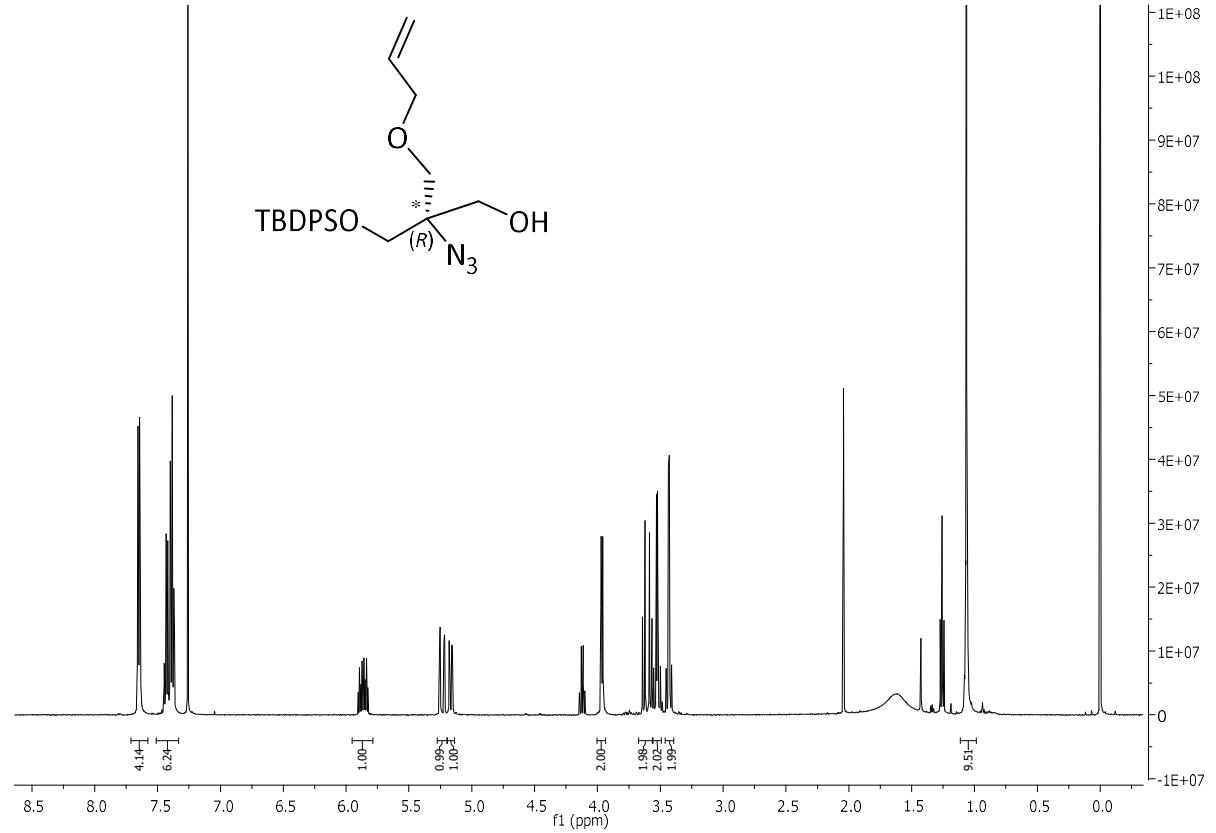

Figure 8.25: ^{1}H NMR (500 MHz, $CDCl_3$) spectrum of compound **1b**.

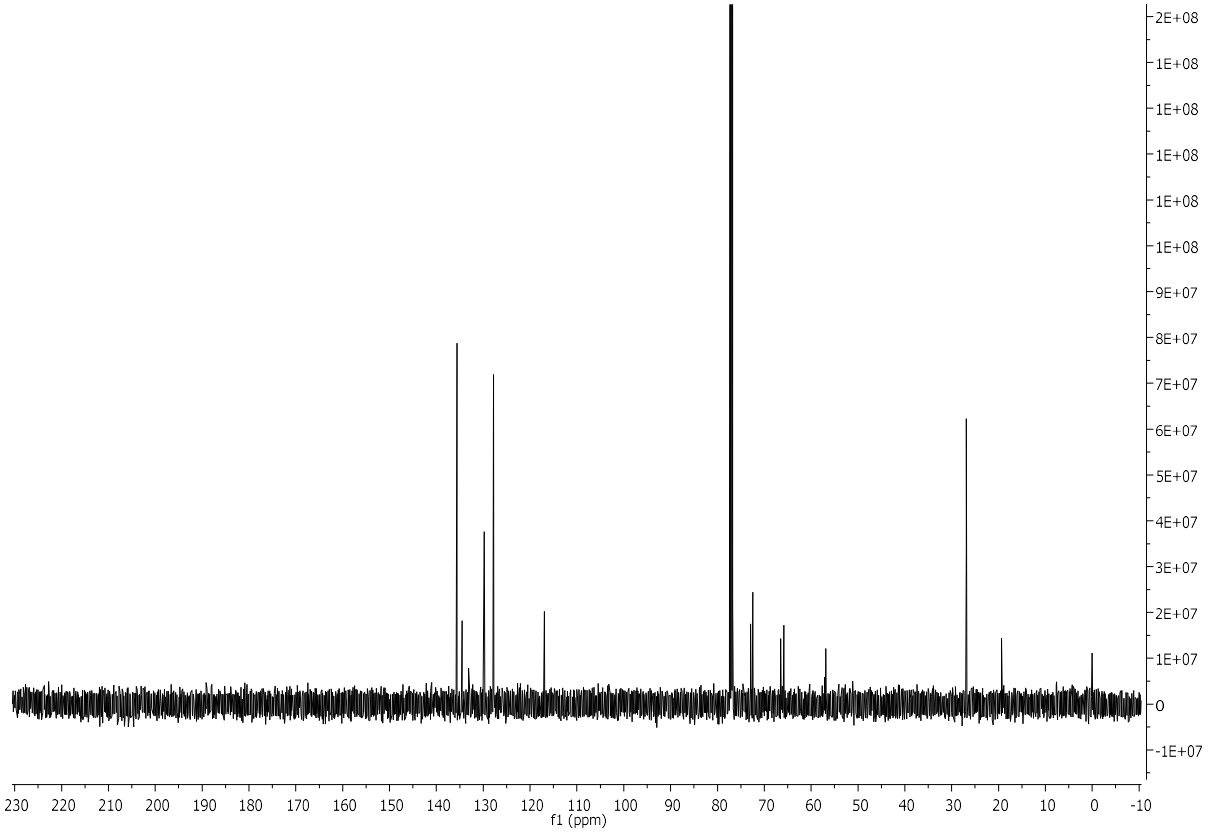

Figure 8.26: ^{13}C NMR (126 MHz, $CDCl_3$) spectrum of compound **1b**.

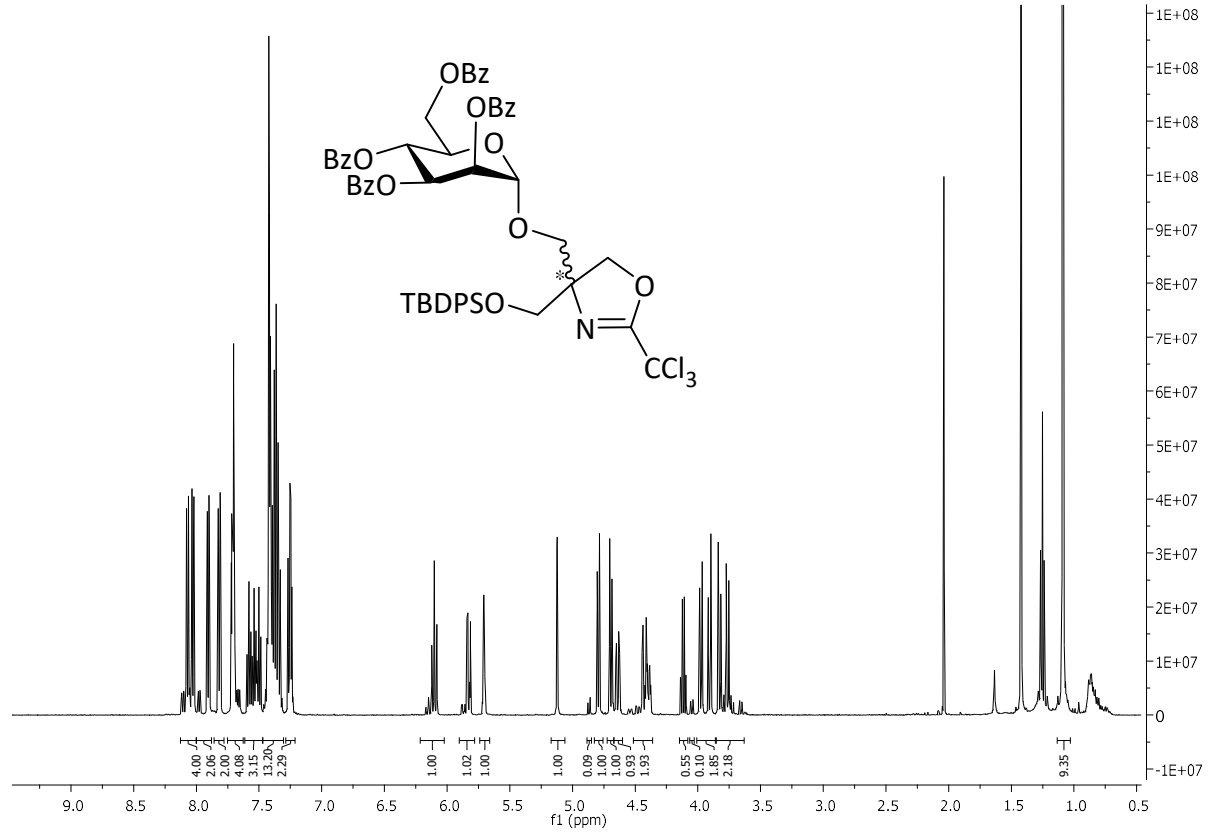

Figure 8.27: ^{1}H NMR (500 MHz, $CDCl_3$) spectrum of compound **14a**.

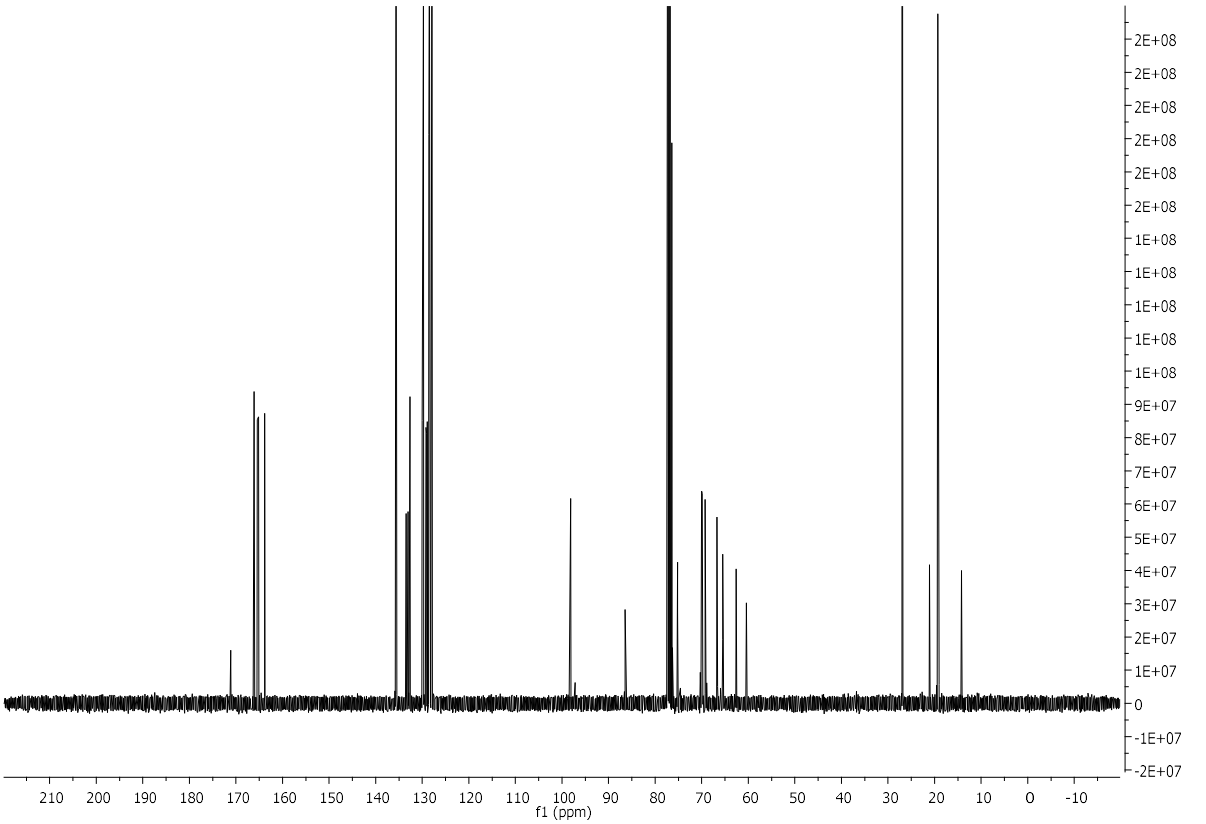

Figure 8.28: ^{13}C NMR (126 MHz, $CDCl_3$) spectrum of compound **14a**.

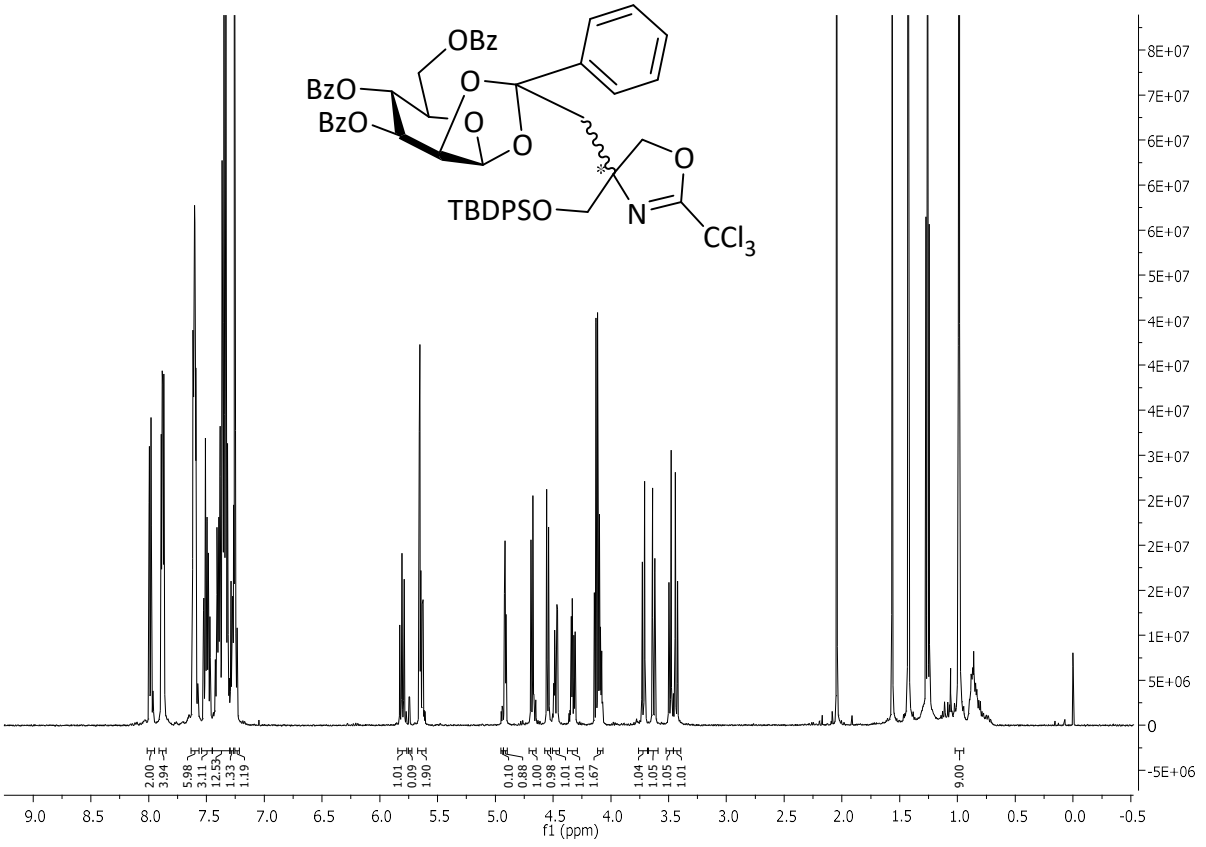

Figure 8.29: ^{1}H NMR (500 MHz, $CDCl_3$) spectrum of **15** orthoester.

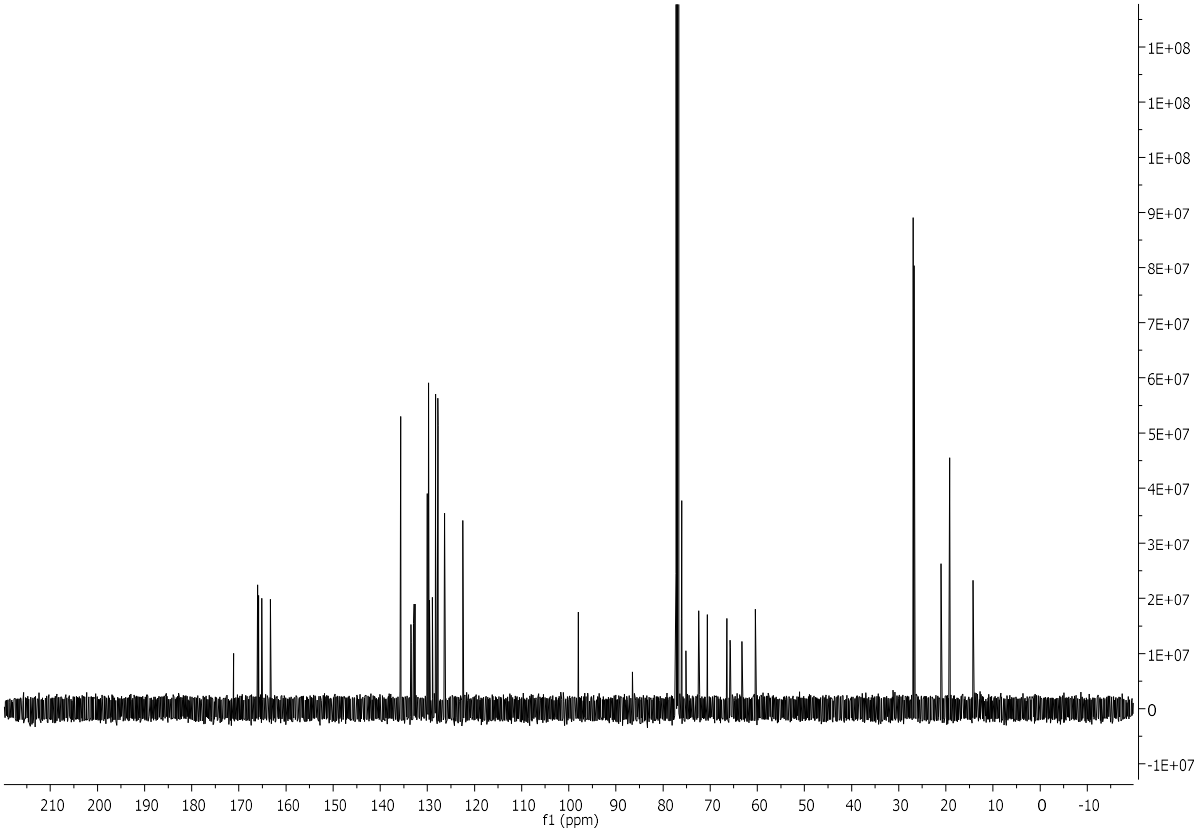

Figure 8.30: ^{13}C NMR (126 MHz, $CDCl_3$) spectrum of **15** orthoester.

8.3 Supporting information for published paper in Chapter 4 "*Pseudoenantiomeric glycoclusters: synthesis and testing of heterobivalency in carbohydrate-protein interactions*"

Electronic Supplementary Information (ESI)

for

Pseudoenantiomeric glycoclusters: Synthesis and testing of heterobivalency in carbohydrate-protein interactions

Jasna Brekalo,[a] Guillaume Despras*[a] and Thisbe K. Lindhorst*[a]

[a] Christiana Albertina University of Kiel, Otto Diels Institute of Organic Chemistry, Otto-Hahn-Platz 3-4, D-24118, Kiel, Germany

jbrekalo@oc.uni-kiel.de, gdespras@oc.uni-kiel.de and tklind@oc.uni-kiel.de

Table of contents

1. Synthesis of the serine-derived scaffold molecules and of the glycosyl donors

General information

For the characterization of serine-derived enantiomeric scaffolds, the carbon atoms of the core moiety are numbered as described on Figure S1. Compounds derived from D-serine are specified by an "a", and their enantiomeric counterparts, based on L-serine, by a "b". Compounds are named according to IUPAC nomenclature.

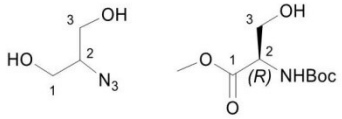

Figure S1. Molecule numbering used for assignment of NMR signals.

General procedure for the preparation of thioglycoside donors (general procedure A).

The perbenzoylated starting material was dissolved in dry dichloromethane (*c* = 0.3 M) in a round-bottom flask and 2-methyl-5-*tert*-butylphenylthiol (1.2 eq.) was added at room temperature. Then the mixture was cooled to 0 ˚C and boron trifluoride diethyl etherate (1.5 eq.) was added dropwise. The mixture was allowed to warm to room temperature then stirred until completion of the reaction, and stopped by diluting with dichloromethane and neutralizing with aq. satd. sodium bicarbonate at 0 ˚C. The aqueous phases were extracted with dichloromethane then the combined organic layers were washed with brine, dried over magnesium sulfate, filtered and concentrated. The residue was purified by flash chromatography to afford the expected compound.

General procedure for *N*-Boc protection and subsequent methyl ester formation (general procedure B).

D- or L-serine and sodium carbonate (1 eq.) were added into a 50 % satd. aq. sodium bicarbonate solution. Di-*tert*-butyl dicarbonate (1.2 eq.) in dioxane (*c* = 4.8 M) was added dropwise at 0 ˚C. The reaction was stirred for 48 h at room temperature then concentrated. The residue was taken up in water and citric acid was added until pH = 2-4 was reached. The aqueous phases were extracted with ethyl acetate and the combined organic layers were dried over magnesium sulfate, filtered and concentrated. The resulting yellow syrup was dissolved in DMF (*c* = 1.2 M) and potassium carbonate (1.1 eq.) was added. Afterwards, methyl iodide (2.0 eq.) was added dropwise at 0 ˚C. The mixture was stirred at room temperature until completion then diluted with water and the aqueous phases were extracted with ethyl acetate. The combined organic layers were dried over magnesium sulfate, filtered and concentrated and the residue was purified by flash chromatography to afford the expected compound.

General procedure for silylation of primary alcohols and subsequent ester reduction (general procedure C).

The starting material was dissolved in anhydrous dichloromethane (*c* = 0.35 M) and *tert*-butyldiphenylsilyl chloride (2 eq.) was added. The solution was cooled to 0 ˚C and imidazole (2 eq.) was added portionwise within 15 min. The mixture was stirred for 18 h at room temperature then diluted with water. The organic phase was sequentially washed with water, satd. aq. sodium carbonate and brine then dried over magnesium sulfate, filtered and concentrated. The resulting residue was dissolved in anhydrous tetrahydrofuran (*c* = 0.4 M) and 2 M lithium borohydride in tetrahydrofuran (1.5 eq.) was added dropwise at 0 ˚C. The reaction was stirred for 12 h at room temperature then treated at 0 ˚C with satd. aq. ammonium chloride. The aqueous phases were extracted with ethyl acetate and the combined organic layers were dried over magnesium sulfate, filtered and concentrated then the residue was purified by flash chromatography to afford the expected compound.

General procedure for *N*-Boc cleavage and subsequent diazo transfer reaction (general procedure D). The *N*-Boc-protected starting material was dissolved in anhydrous dichloromethane (*c* = 0.2 M) and trifluoroacetic acid (13 eq.) was added slowly at 0 °C. The reaction was stirred for 3 h at 0 °C and diluted with ethyl acetate then concentrated to dryness. The residue was dissolved in a 2:1:1 methanol/dichloromethane/water mixture (*c* = 0.1 M) then potassium carbonate (2 eq.), copper (II) sulfate pentahydrate (0.01 eq.) and imidazole1-sulfonyl azide hydrochloride (1.6 eq.) were added sequentially. The blue mixture turned brown after stirring for 16 h then it was concentrated to dryness. The residue was diluted with ethyl acetate and water. The aqueous phase was extracted with ethyl acetate and the combined organic phases were washed with brine, dried over magnesium sulfate then concentrated. The residue was purified by flash chromatography to afford the expected compound.

(2–Methyl-5-*tert*-butylphenyl) α–D–(2,3,4,6–tetra–*O*–benzoyl)–thiomannopyranoside (4). General procedure A was applied to 1,2,3,4,6-penta-*O*-benzoyl-α,β-D-mannopyranoside (7.00 g, 10.0 mmol) . Reagents and conditions: 2-methyl-5-*tert*-butylphenyl thiol (3.7 mL, 7.62 mmol, 1.2 eq.), boron trifluoride diethyl etherate (6.2 mL, 15.0 mmol, 1.5 eq.), dichloromethane (*c* = 0.3 M, 33.0 mL). Flash chromatography with ethyl acetate/ cyclohexane 1/20 yielded compound **4** (4.24 g, 56 %) as a white foam. Analytical and spectroscopic data were found to be in agreement with reported literature.[1]

***N*–(*tert*–Butoxycarbonyl)–D–serine methyl ester (8a).** General procedure B was applied to D-serine (15.0 g, 14.3 mmol). Reagents and conditions: (i) sodium carbonate (18.2 g, 17.1 mmol, 1 eq.), di-*tert*-butyl dicarbonate (37.4 g, 17.1 mmol, 1.2 eq.), 50 % satd. sodium bicarbonate solution (*c* = 0.7 M, 204 mL), dioxane (*c* = 4.8 M, 35.7 mL), water (500 mL); (ii) potassium carbonate (21.7 g, 157 mmol, 1.1 eq.), methyl iodide (40.5 g, 141 mmol, 2.0 eq.), DMF (*c* = 1.2 M, 120 mL). Flash chromatography with ethyl acetate/cyclohexane 2/8 to 4/6 afforded compound **8a** (24.7 g, 79 %) as a yellow oil. Analytical and spectroscopic data were found to be in agreement with reported literature;[2] R_f= 0.3 (ethyl acetate/cyclohexane 2/3); $[\alpha]_{20}^{D}$ = -9.3 (*c* 0.8, dichloromethane); ^{1}H NMR (500 MHz, $CDCl_3$) δ 5.47 (br s, 1H, NH), 4.38 (br s, 1H, H-2), 3.92 (m, 2H, H-3a, H-3b), 3.78 (s, 3H, $CO_2C\underline{H}_3$), 2.30 (br s, 1H, OH), 1.45 (s, 9H, $NHCO_2C(C\underline{H}_3)_3$) ppm; ^{13}C NMR (126 MHz, $CDCl_3$) δ 171.3 ($\underline{C}O_2CH_3$), 155.7 ($NH\underline{C}O_2(CH_3)_3$), 80.3 ($NHCO_2\underline{C}(CH_3)_3$), 63.6 (C-3), 55.7 (C-2), 52.6 ($CO_2\underline{C}H_3$), 28.3 ($NHCO_2C(\underline{C}H_3)_3$) ppm.

***N*–(*tert*–Butoxycarbonyl)–L–serine methyl ester (8b).** General procedure B was applied to L-serine amino acid (15.0 g, 14.3 mmol). Reagents and conditions: (i) sodium carbonate (18.2 g, 17.1 mmol, 1 eq.), di-*tert*-butyl dicarbonate (37.4 g, 17.1 mmol, 1.2 eq.), 50 % satd. sodium bicarbonate solution (*c* = 0.7 M, 204 mL), dioxane (*c* = 4.8 M, 35.7 mL), water (500 mL); (ii) potassium carbonate (21.7 g, 157 mmol, 1.1 eq.), methyl iodide (40.5 g, 141 mmol, 2.0 eq.), DMF (*c* = 1.2 M, 120 mL). Flash chromatography with ethyl acetate/cyclohexane 2/8 to 4/6 afforded compound **8b** (25.7 g, 82 %) as a yellow oil. Analytical and spectroscopic data were found to be in agreement with reported literature;[2] R_f= 0.3 (ethyl acetate/cyclohexane 3/7); $[\alpha]_{20}^{D}$ = +9.2 (*c* 0.7, dichloromethane); ^{1}H NMR (500 MHz, $CDCl_3$) δ 5.48 (br s, 1H, NH), 4.37 (br, 1H, H-2), 3.92 (m, 2H, H-3a, H-3b), 3.77 (s, 3H, $CO_2C\underline{H}_3$), 2.58-2.13 (m, 1H, OH), 1.44 (s, 9H, NH-$CO_2C(C\underline{H}_3)_3$) ppm; ^{13}C NMR (126 MHz, $CDCl_3$) δ 171.3 ($\underline{C}O_2CH_3$), 155.8 ($NH\underline{C}O_2C(CH_3)_3$), 80.3 ($NHCO_2\underline{C}(CH_3)_3$), 63.5 (C-3), 55.7 (C-2), 52.6 ($CO_2\underline{C}H_3$), 28.3 ($NHCO_2C(\underline{C}H_3)_3$) ppm.

(*S*)–2–*N*–(*tert*–Butoxycarbonyl)–1–*O*–(*tert*–butyldiphenylsilyl)–1,3–propanediol (9a). General procedure C was applied to compound **8a** (14.0 g, 63.8 mmol). Reagents and conditions: (i) *tert*-butyldiphenylsilyl chloride (35.1 g, 127 mmol, 2 eq.), imidazole (8.60 g, 127 mmol, 2 eq.), dichloromethane (*c* = 0.35 M, 182 mL); (ii) lithium borohydride (48.0 mL, 95.7 mmol, 1.5 eq.), tetrahydrofuran (*c* = 0.4 M, 160 mL). Flash chromatography with cyclohexane/ethyl acetate 20/1 to 4/1 afforded compound **9a** (24.6 g, 90 %) as a white solid. Analytical and spectroscopic data were found to be in agreement with reported literature;[3] R_f= 0.3 (ethyl acetate/ cyclohexane 4/1); $[\alpha]_{20}^{D}$ = +8.9 (*c* 0.6, dichloromethane);^{1}H

NMR (500 MHz, $CDCl_3$) δ 7.84-7.59 (m, 4H, 4H-Ar), 7.49-7.34 (m, 6H, 6 H-Ar), 5.07 (br s, 1H, NH), 3.91-3.60 (m, 4H, H-1a, H-3a, H-3b, H-2), 3.49 (s,1H, H-1b), 2.42 (br s, 1H, OH), 1.45 (s, 9H, $NHCO_2C(C\underline{H}_3)_3$), 1.08 (s, 9H, $Si(C\underline{H}_3)_3$) ppm; ^{13}C NMR (126 MHz, $CDCl_3$) δ 156.1 ($NH\underline{C}O_2C(CH_3)_3$), 135.5, 134.9 132.8, 129.9, 127.8, 127.6 (12C, 12 C-Ar), 79.6 ($NHCO_2\underline{C}(CH_3)_3$), 64.2 (C-1 or C-3), 63.7 (C-1 or C-3), 53.0 (C-2), 28.4 ($NHCO_2C(\underline{C}H_3)_3$), 26.9 ($SiC(\underline{C}H_3)_3$), 19.2 ($Si\underline{C}(CH_3)_3$) ppm.

(*R*)–2–*N*–(*tert*–Butoxycarbonyl)–1–*O*–(*tert*–butyldiphenylsilyl)–1,3–propanediol (9b). General procedure C was applied to compound **8b** (16.0 g, 73.3 mmol). Reagents and conditions: (i) *tert*-butyldiphenylsilyl chloride (40.3 g, 146 mmol, 2 eq.), imidazole (9.90 g, 146 mmol, 2 eq.) dichloromethane (*c* = 0.35 M, 210 mL); (ii) of lithium borohydride (55.0 mL, 110 mmol, 1.5 eq.), tetrahydrofuran (*c* = 0.4 M, 183 mL). Flash chromatography with cyclohexane/ethyl acetate 20/1 to 4/1 afforded compound **9b** (28.3 g, 90 %) as a white solid. Analytical and spectroscopic data were found to be in agreement with reported literature;[3] R_f= 0.3 (ethyl acetate/ cyclohexane 1/4); $[\alpha]_{20}^{D}$ = -5.8 (*c* 0.5, dichloromethane); ^1H NMR (500 MHz, $CDCl_3$) δ 7.72-7.55 (m, 4H, 4 H-Ar), 7.49-7.34 (m, 6H, 6 H-Ar), 5.08 (br s, 1H, NH), 3.77 (m, 4H, H-1a, H-2, H-3a, H-3b), 3.50 (s, 1H, H-1b), 2.37 (br, 1H, OH), 1.45 (s, 9H, $NHCO_2C(C\underline{H}_3)_3$), 1.08 (s, 9H, $Si(C\underline{H}_3)_3$) ppm; ^{13}C NMR (126 MHz, $CDCl_3$) δ 155.8 ($NH\underline{C}O_2C(CH_3)_3$), 135.5, 135.2, 134.8 132.8, 129.9, 129.6, 127.9, 127.7 (12C, 12 C-Ar), 79.6 ($NHCO_2\underline{C}(CH_3)_3$), 64.2 (C-1 or C-3), 63.7 (C-1 or C-3), 53.0 (C-2), 28.4 ($NHCO_2C(\underline{C}H_3)_3$), 26.9 ($SiC(\underline{C}H_3)_3$), 19.2 ($Si\underline{C}(CH_3)_3$).

(*S*)–2–Azido–1–*O*–(*tert*–butyldiphenylsilyl)–1,3–propanediol (10a). General procedure D was applied to compound **9a** (20.4 g, 47.0 mmol). Reagents and conditions: (i) trifluoroacetic acid (47.6 mL, 617 mmol, 13 eq.), dichloromethane (*c* = 0.2 M, 235 mL); (ii) potassium carbonate (13.0 g, 97.0 mmol, 2 eq.), copper(II) sulfate pentahydrate (122 mg, 470 µmol, 0.01 eq.), imidazole-1-sulfonyl chloride (**2**[4]) (15.8 g, 75.0 mmol, 1.6 eq.), methanol/dichloromethane/water mixture 2:1:1 (*c* = 0.14 M, 335 mL). Flash chromatography with ethyl acetate/ cyclohexane 1/20 yielded **10a** (17.5 g, 80 %) as a colorless syrup; R_f= 0.3 (ethyl acetate/ cyclohexane 1/20); $[\alpha]_{20}^{D}$ = +21.5 (*c* 0.5, dichloromethane); ^1H NMR (500 MHz, $CDCl_3$) δ 7.77-7.65 (m, 4H, 4 H-Ar), 7.53-7.36 (m, 6H, 6 H-Ar), 3.82 (d, ^3J= 5.7 Hz, 2H, H-1a, H-1b), 3.74 (dd, $^2J_{3a,3b}$= 10.4 Hz, $^3J_{2,3a}$ = 3.3 Hz, 1H, H-3a), 3.68-3.60 (m, 2H, H-2, H-3b), 2.09 (br s, 1H, OH), 1.12 (s, 9H, $SiC(C\underline{H}_3)_3$) ppm; ^{13}C NMR (126 MHz, $CDCl_3$) δ 135.6, 135.5, 132.8, 132.7, 130.0, 127.9 (12C, 12 C-Ar), 64.5 (C-2), 64.2 (C-1), 62.7 (C-3), 26.8 ($SiC(\underline{C}H_3)_3$), 19.2 ($Si\underline{C}(CH_3)_3$) ppm; IR (ATR) ν_{max}/cm^{-1} 3399, 2932, 2112, 1428, 1113, 631, 538; ESI-HRMS: m/z calcd. for $C_{19}H_{25}N_3O_2Si + Na^+$ = 378.16082 $[M+Na]^+$; found 378.16066.

(*R*)–2–Azido–1–*O*–(*tert*–butyldiphenylsilyl)–1,3–propanediol (10b). General procedure D was applied to compound **9b** (26.4 g, 61.5 mmol). Reagents and conditions: (i) dichloromethane (*c* = 0.2 M, 308 mL), trifluoroacetic acid (61.6 mL, 800 mmol, 13 eq.); (ii) potassium carbonate (17.0 g, 123 mmol, 2 eq.), copper(II) sulfate pentahydrate (160 mg, 620 µmol, 0.01 eq.), imidazole-1-sulfonyl chloride (**2**[4]) (20.6 g, 98.4 mmol, 1.6 eq.), methanol/dichloromethane/water 2:1:1 (*c* = 0.14 M, 440 mL). Flash chromatography with ethyl acetate/ cyclohexane 1/20 afforded compound **10b** (17.3 g, 79 %) as a colorless syrup; R_f= 0.3 (ethyl acetate/ cyclohexane 1/20); $[\alpha]_{20}^{D}$ = -19.8 (*c* 0.5, dichloromethane); ^1H NMR (500 MHz, $CDCl_3$) δ 7.68-7.66 (m, 4H, 4H-Ar), 7.48-7.36 (m, 6H, 6 H-Ar), 3.78 (d, ^3J= 5.4 Hz, 2H, H-1a, H-1b), 3.73 (dd, $^2J_{3a,\,3b}$= 11.0 Hz, $^3J_{2,3a}$ = 4.0 Hz, 1H, H-3a), 3.66-3.57 (m, 2H, H-2, H-3b), 1.80 (br s, 1H, OH), 1.08 (s, 9H, $SiC(C\underline{H}_3)_3$) ppm; ^{13}C NMR (126 MHz, $CDCl_3$) δ 135.6, 135.5, 132.7, 130.0, 127.9 (12C, 12C-Ar), 64.4 (C-2), 64.2 (C-1), 62.4 (C-3), 26.7 ($SiC(\underline{C}H_3)_3$), 19.1 ($Si\underline{C}(CH_3)_3$) ppm; IR (ATR) ν_{max}/cm^{-1}.3404, 2931, 2130, 1428, 1113, 631, 538; ESI-HRMS: m/z calcd. for $C_{19}H_{25}N_3O_2Si + Na^+$: 378.16082 $[M+Na]^+$; found 378.16046.

(2–Methyl-5-*tert*-butylphenyl) α–D–(2,3,4,6–tetra–*O*–benzoyl) thioglucopyranoside (13). General procedure A was applied to 1,2,3,4,6-penta-*O*-benzoyl-α–D-glucopyranoside (6.0 g, 8.56 mmol). Reagents and conditions: 2-methyl-5-*tert*-butylphenyl thiol (1.9 mL, 10.3 mmol, 1.2 eq.), boron trifluoride diethyl etherate (1.6 mL, 12.84 mmol, 1.5 eq.), dichloromethane (*c* = 0.3 M, 12.7 mL). Flash chromatography with

Published supporting information correction: in the preparation of **10a** and **10b** imidazole-1-sulfonyl azide was used instead of imidazole-1-sulfonyl chloride.

ethyl acetate/ cyclohexane 1/9 afforded compound **13** (3.34 g, 51 %) as a white foam. Analytical and spectroscopic data were found to be in agreement with reported literature.[1]

(2–Methyl-5-*tert*-butylphenyl) α–D–(2,3,4,6–tetra–*O*–benzoyl) thiogalactopyranoside (16). General procedure A was applied to 1,2,3,4,6-penta-*O*-benzoyl-α-D-galactopyranoside (4.40 g, 6.4 mmol). Reagents and conditions: 2-methyl-5-tertbutylphenylthiol (3.7 mL, 7.62 mmol, 1.2 eq.), boron trifluoride diethyl etherate (1.2 mL, 9.52 mmol, 1.5 eq.), dichloromethane (*c* = 0.5 M, 12.7 mL). Flash chromatography with ethyl acetate/ cyclohexane 1/9 afforded compound **16** (2.71 g, 56 %) as a white foam; R_f= 0.3 (ethyl acetate/ cyclohexane 1/9); $[\alpha]_{20}^{D}$ = +96.6 (*c* 0.1, dichloromethane); ^{1}H NMR (500 MHz, $CDCl_3$) δ 8.06-7.97 (m, 6H, 6 H-Ar), 7.79 (dd, ^3J = 8.4 Hz, ^4J =1.3 Hz, 2H, 2 H-Ar), 7.66-7.36 (m, 11H, 11 H-Ar), 7.29 (dd, $^3J_{para,\ meta}$ = 8.0 Hz, $^4J_{para,ortho}$ = 2.1 Hz, 1H, H-*para*-thioaryl), 7.27 – 7.23 (m, 2H, 2 H-Ar), 7.15 (d, $^3J_{meta,para}$ = 8.1 Hz, 1H, H-*meta*-thioaryl), 6.04 (dd, $^3J_{3,4}$ = 3.4 Hz, $^3J_{4,5}$ = 0.8 Hz, 1H, H-4), 5.88 (dd,$^3J_{1,2}$ = $^3J_{2,3}$ = 10.0 Hz, 1H, H-2), 5.64 (dd, $^3J_{2,\ 3}$ = 9.9 Hz, $^3J_{3,4}$ = 3.4 Hz, 1H, H-3), 5.01 (d, $^3J_{1,2}$ = 10.1 Hz, 1H, H-1), 4.67 (dd, $^2J_{6a,\ 6b}$ = 11.3 Hz, $^3J_{5,6a}$ = 6.4 Hz, 1H, H-6a), 4.43 (dd, $^2J_{6a,\ 6b}$ = 11.3 Hz, $^3J_{5,6b}$= 6.6 Hz, 1H, H-6b), 4.36-4.34 (m, 1H, H-5), 2.35 (s, 3H, $C\underline{H}_3$ thioaryl), 1.25 (s, 9H, $C(C\underline{H}_3)_3$ thioaryl) ppm; ^{13}C NMR (126 MHz, $CDCl_3$) δ 166.2, 165.6, 165.4 (4C, 4 PhC=O), 149.8, 138.6, 133.7, 133.4, 132.2, 131.2, 130.2, 129.9, 129.5, 129.2, 128.9, 128.8, 128.6, 128.4, 126.2 (23C, 23 C-Ar), 88.2 (C-1), 75.1 (C-5), 73.1 (C-3), 68.6 (C-2), 68.4 (C-4), 62.3 (C-6), 34.5 ($\underline{C}(CH_3)_3$ thioaryl), 31.3 ($C(\underline{C}H_3)_3$ thioaryl), 20.8 ($\underline{C}H_3$ thioaryl) ppm; HRMS (ESI): m/z: calcd for $C_{45}H_{42}O_9S + H^+$: 759.26223 [M+H$^+$]; found: 759.26177.

2–Trifluoromethyl–(3,4,6–tri–*O*–acetyl–1,2–dideoxy–α–D–glucopyranose)–[1,2,*d*]–2–oxazoline (19). (D)-glucosamine hydrochloride (5.00 g, 23.0 mmol) was dissolved in methanol (*c* = 0.3 M, 76.6 mL) and triethylamine (32.0 mL, 230 mmol, 10 eq.) was added. After stirring for 15 min, trifluoracetic anhydride (9.81 mL, 690 mmol, 3 eq.) was added slowly at 0 °C. After stirring for 30 min, the mixture was allowed to warm to room temperature and stirred until completion then concentrated to dryness. The residue was dissolved in pyridine (*c* = 0.5 M, 46 mL) and acetic anhydride (10.9 mL, 115 mmol, 5 eq.) was added. After completion of the reaction, the mixture was diluted with methanol and concentrated. The residue was dissolved in ethyl acetate and washed with aq. 2 N hydrochloric acid, dried over magnesium sulfate and concentrated. Purification with ethyl acetate/cyclohexane 1/9 afforded 2-deoxy-2-trifluoroacetamido-1,3,4,6-tetra-*O*-acetyl-α,β-D-glucopyranoside (3.19 g, 31 %) as a white solid. Analytical and spectroscopic data were found to be in agreement with reported literature.[5b] The residue was dissolved in DMF (*c* = 0.25 M, 28.8 mL) and hydrazine acetate (729 mg, 7.92 mmol, 1.1 eq.) was added. The reaction was heated at 55-60 °C until completion and diluted with water. The aqueous layer was extracted with ethyl acetate then the combined organic layers were dried over magnesium sulfate and concentrated. Purification with ethyl acetate/ cyclohexane 4/6 afforded the title compound (1.23 g, 43 %). The residue was dissolved in anhydrous acetonitrile (*c* = 0.06 M, 51.5 mL) and methanesulfonic anhydride (1.61 g, 9.26 mmol) was added. The mixture was stirred for 45 min at room temperature then triethylamine (8.60 mL, 61.7 mmol, 20 eq.) was added and the mixture was stirred at room temperature until completion. The mixture was diluted with dichloromethane and sodium hydrogen carbonate. The aqueous phases were extracted with dichloromethane then the combined organic layers were dried over magnesium sulfate and concentrated. Purification with ethyl acetate/ cyclohexane 3/7 afforded compound **19** (700 mg, 60 %) as a yellow syrup. Analytical and spectroscopic data were found to be in agreement with reported literature.[5]

2. NMR spectra of new compounds

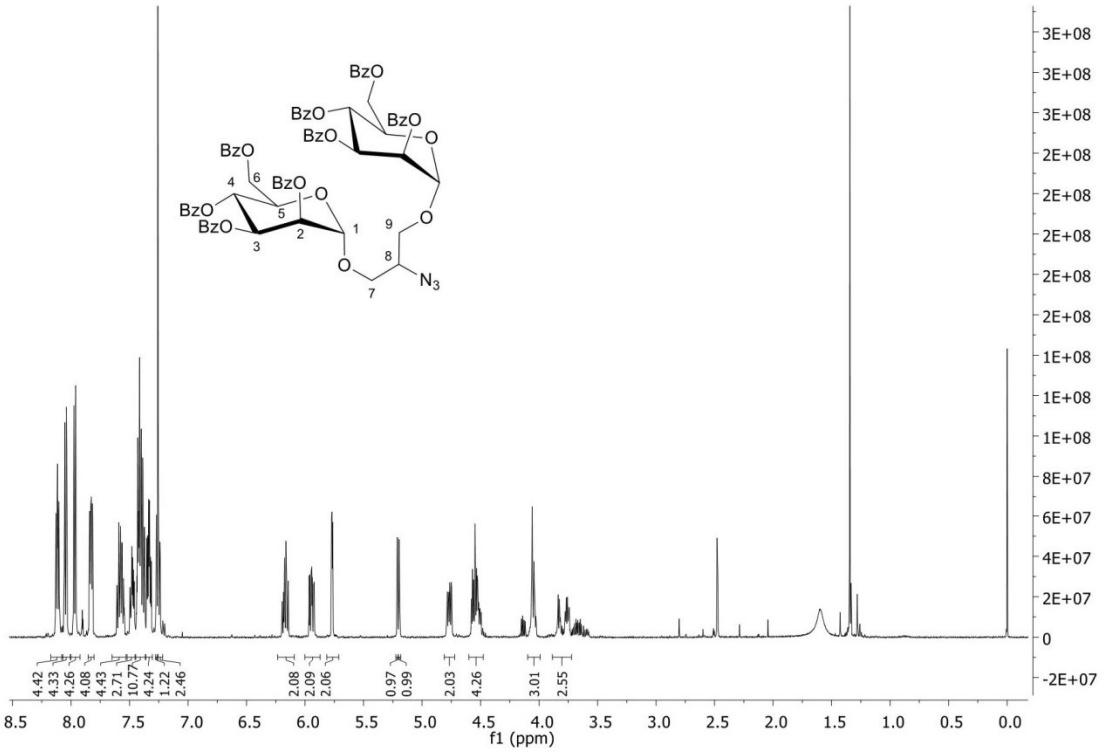

Figure S2. ^{1}H NMR (500 MHz, $CDCl_3$) spectrum of compound **5**.

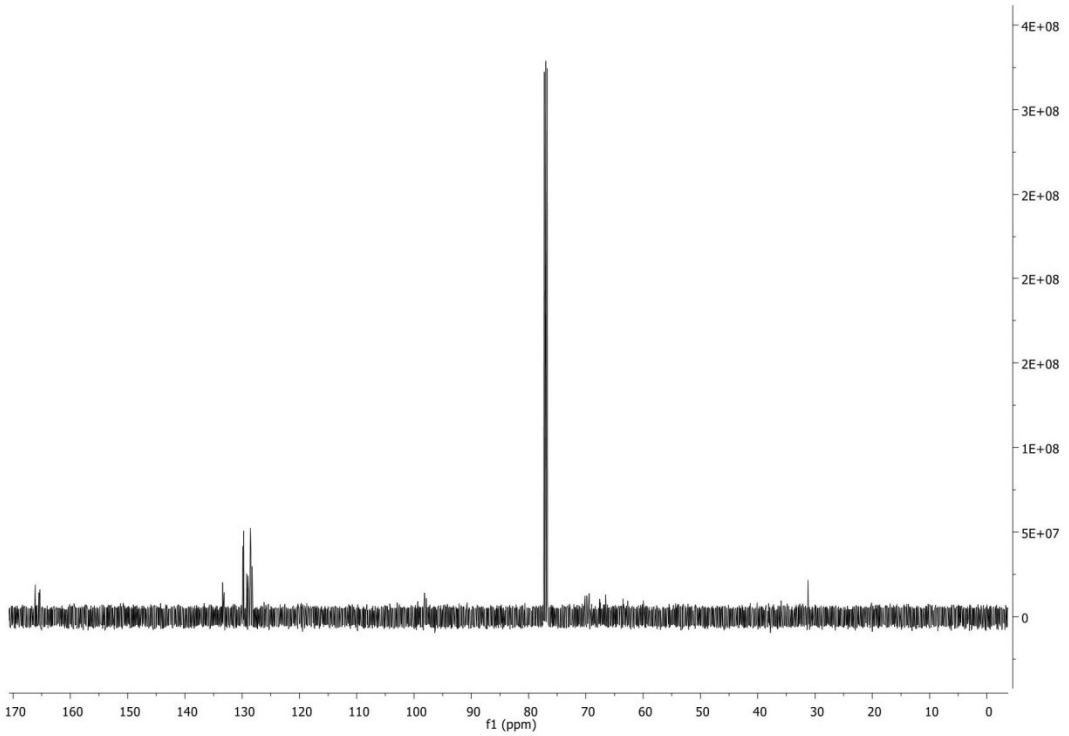

Figure S3.^{13}C NMR (126 MHz, $CDCl_3$) spectrum of compound **5**.

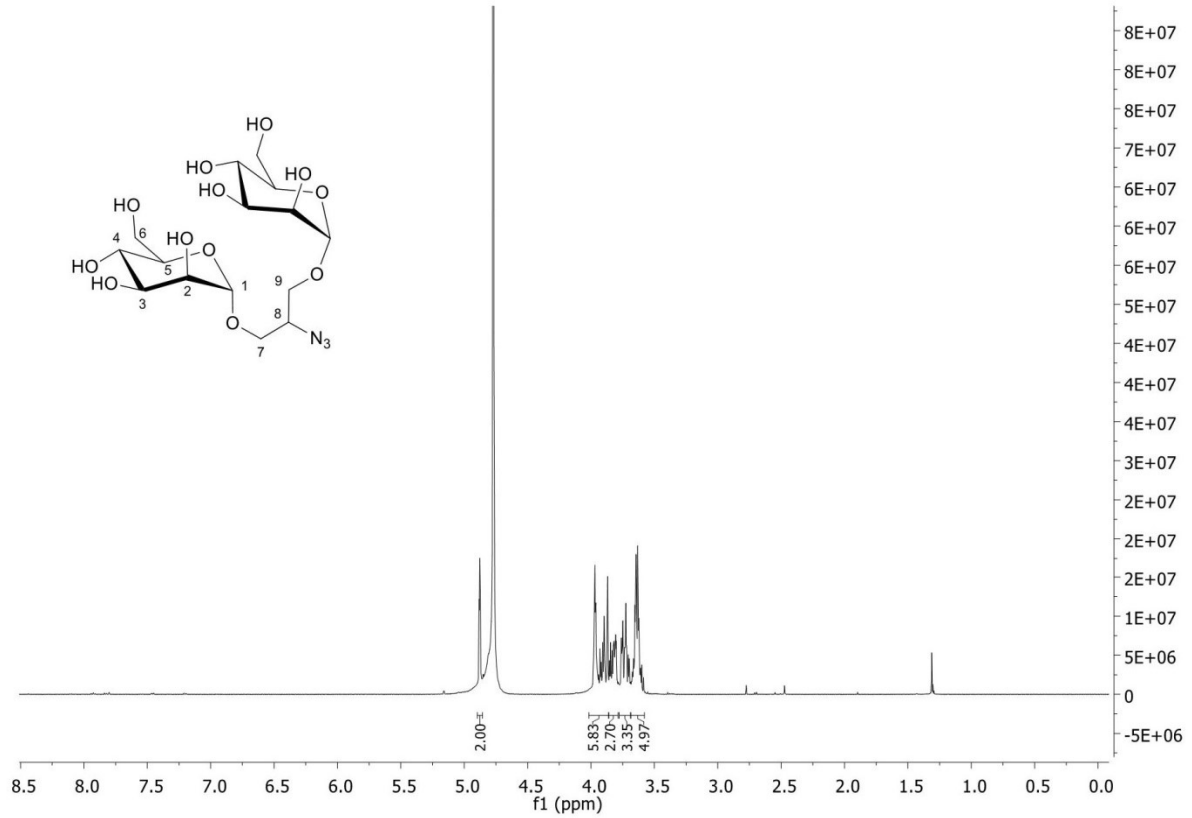

Figure S4. ^{1}H NMR (500 MHz, D_2O) spectrum of compound **6**.

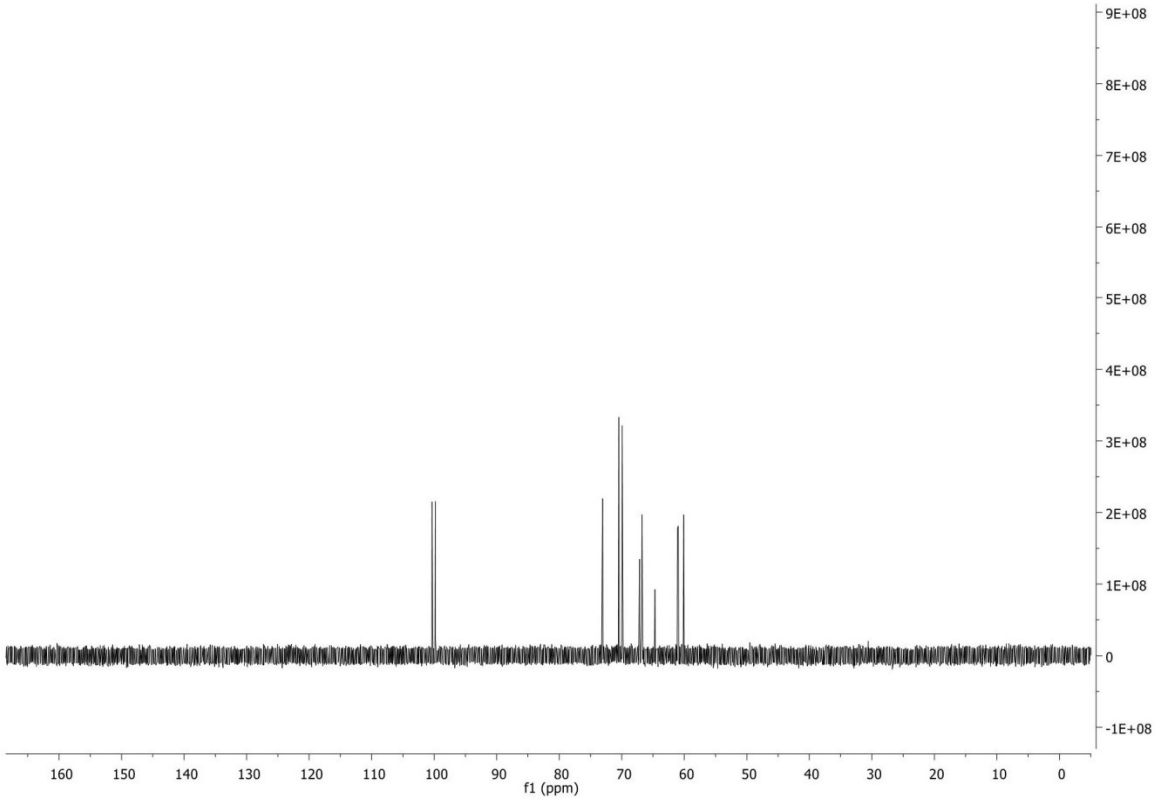

Figure S5.^{13}C NMR (126 MHz, D_2O) spectrum of compound **6**.

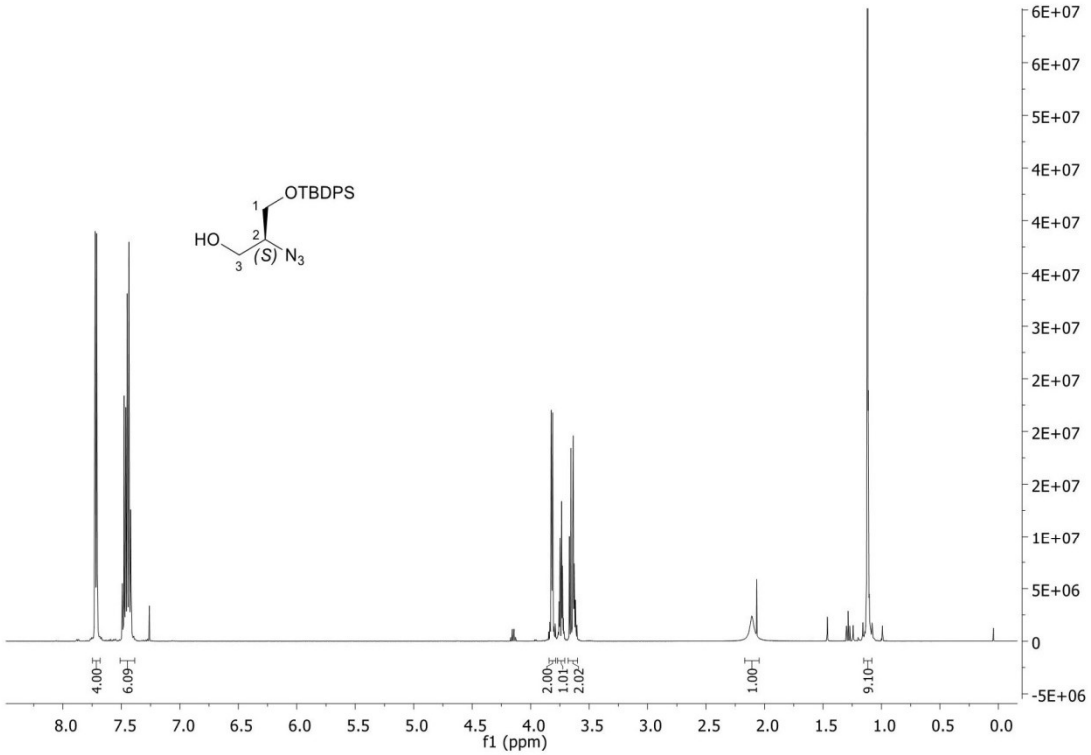

Figure S6. ^{1}H NMR (500 MHz, $CDCl_3$) spectrum of compound **10a**.

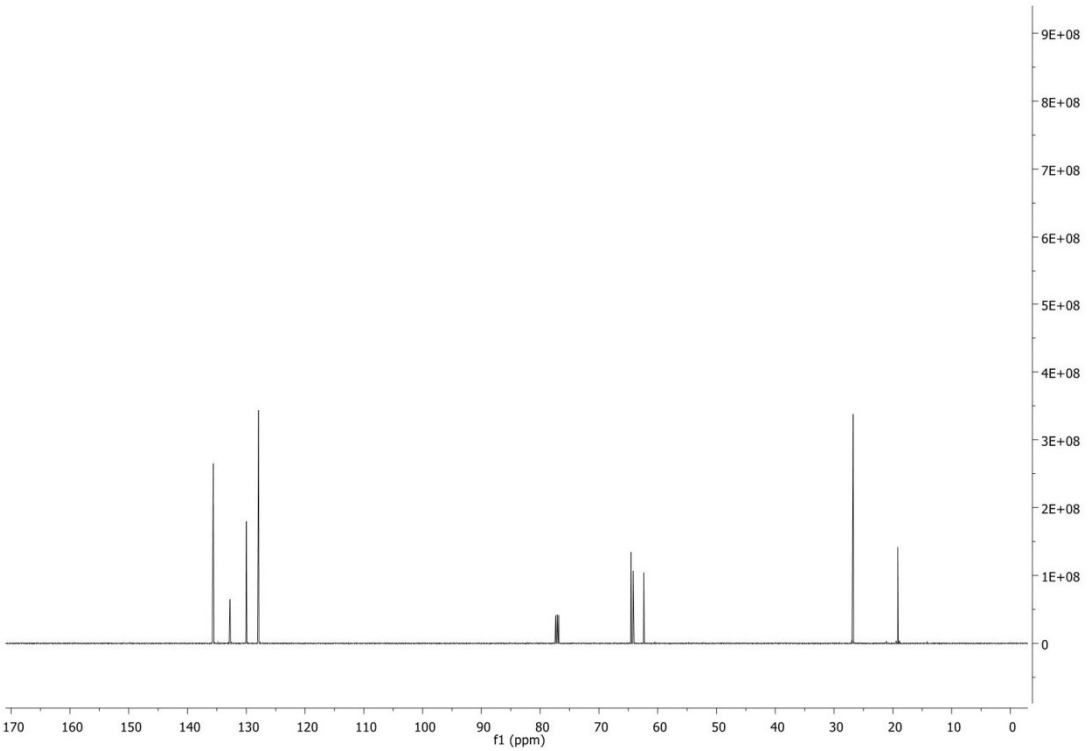

Figure S7. ^{13}C NMR (126 MHz, $CDCl_3$) spectrum of compound **10a**.

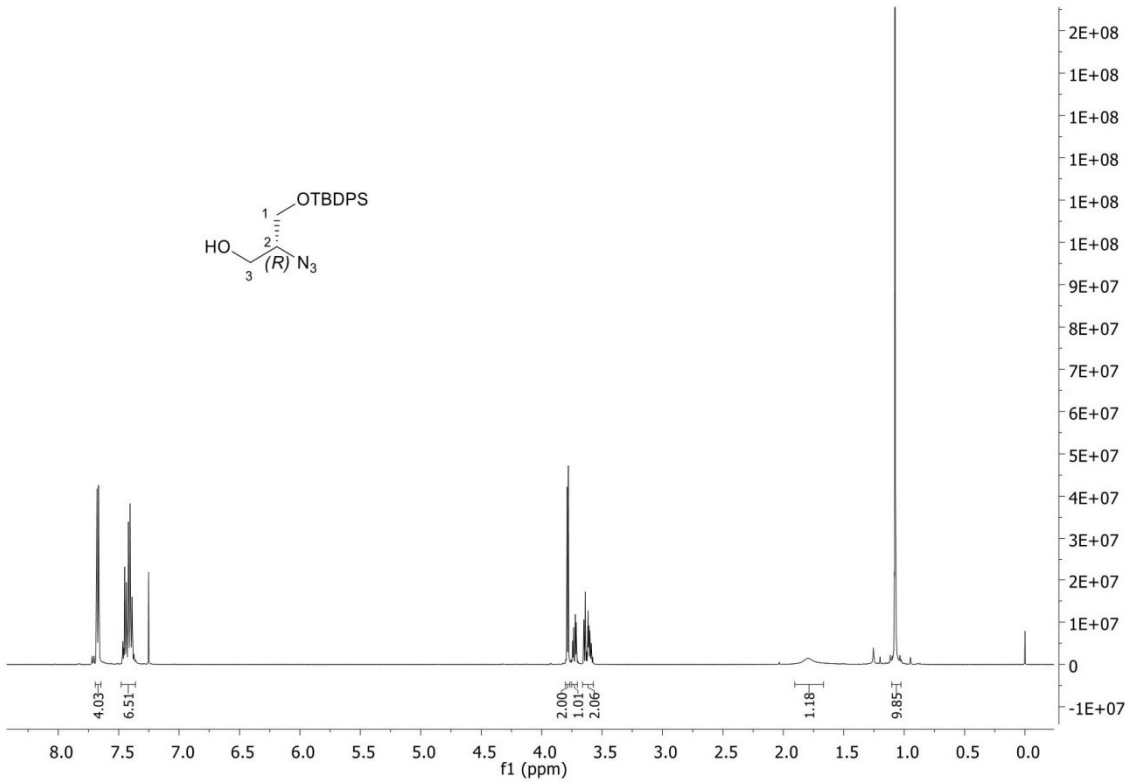

Figure S8. ^{1}H NMR (500 MHz, $CDCl_3$) spectrum of compound **10b**.

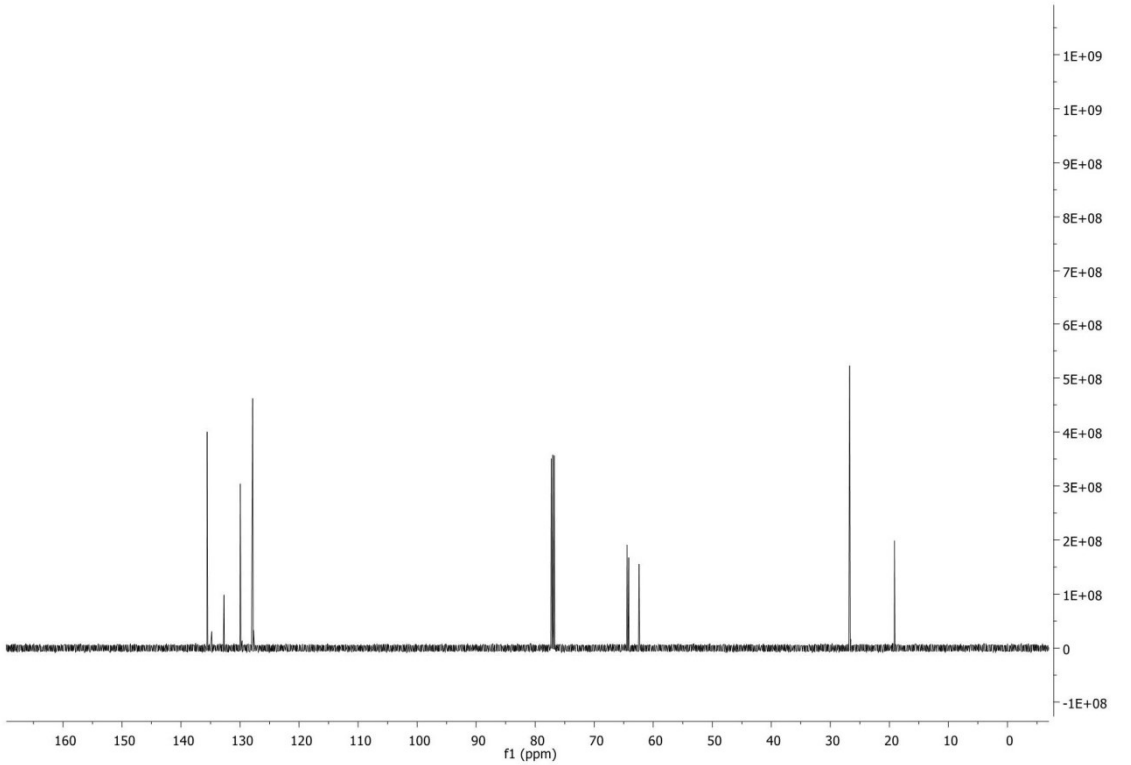

Figure S9. ^{13}C NMR (126 MHz, $CDCl_3$) spectrum of compound **10b**.

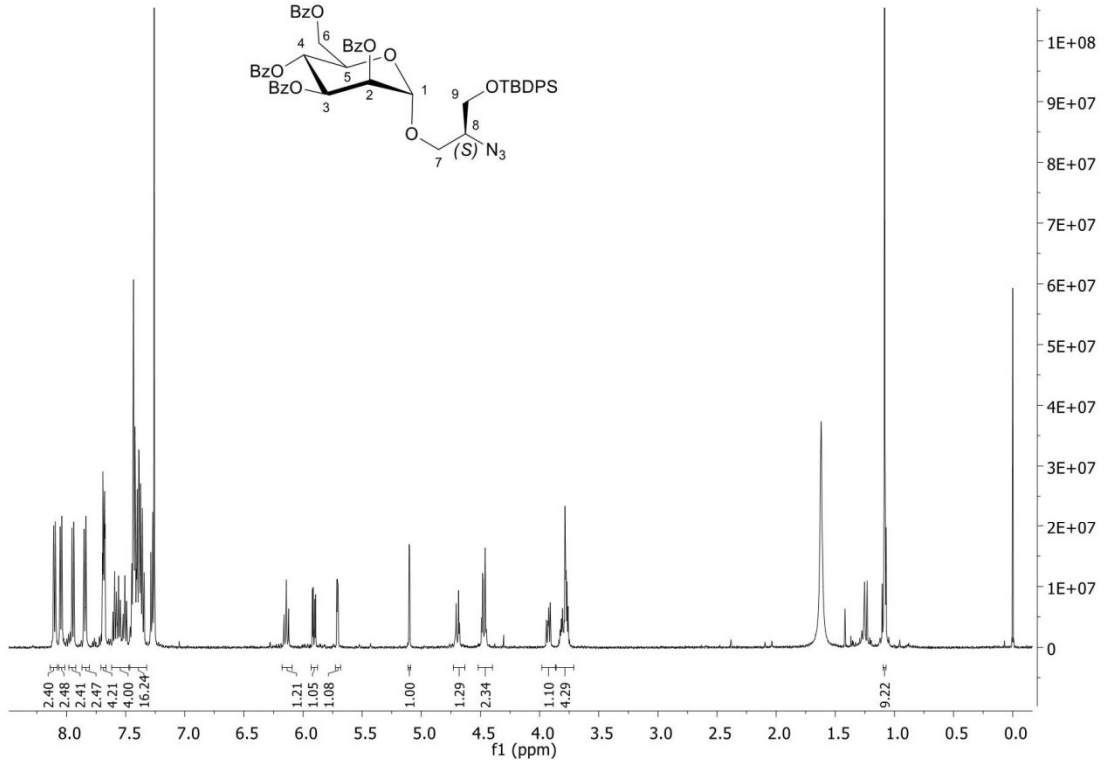

Figure S10. ^{1}H NMR (500 MHz, $CDCl_3$) spectrum of compound **11a**.

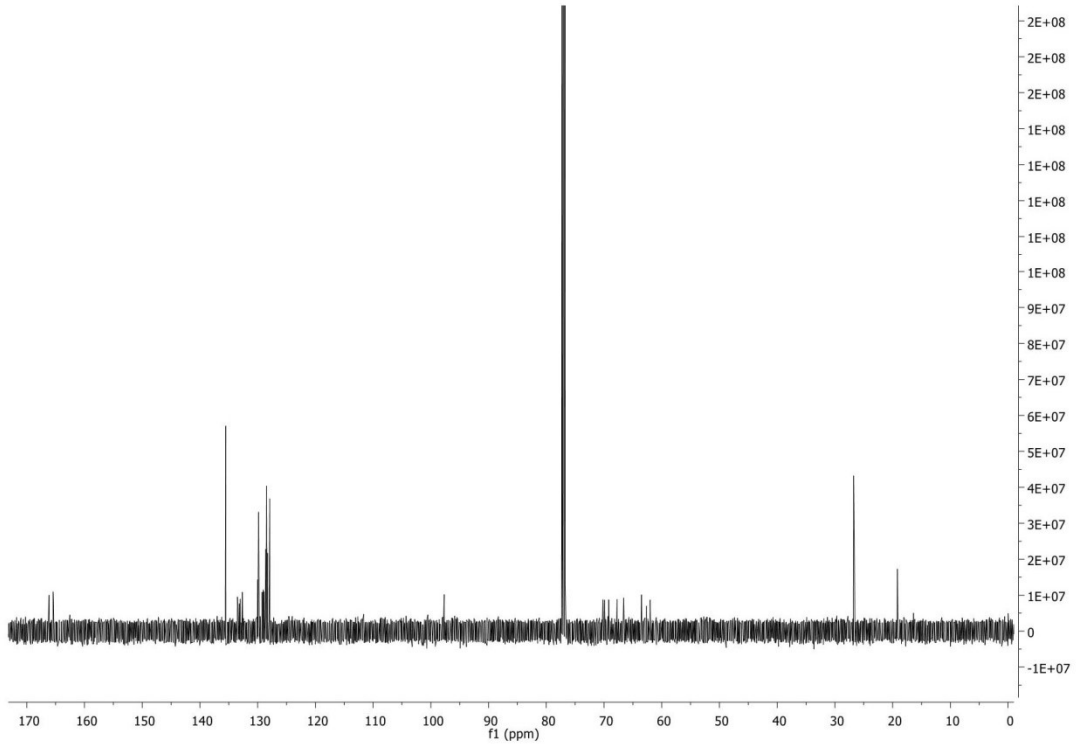

Figure S11. ^{13}C NMR (126 MHz, $CDCl_3$) spectrum of compound **11a**.

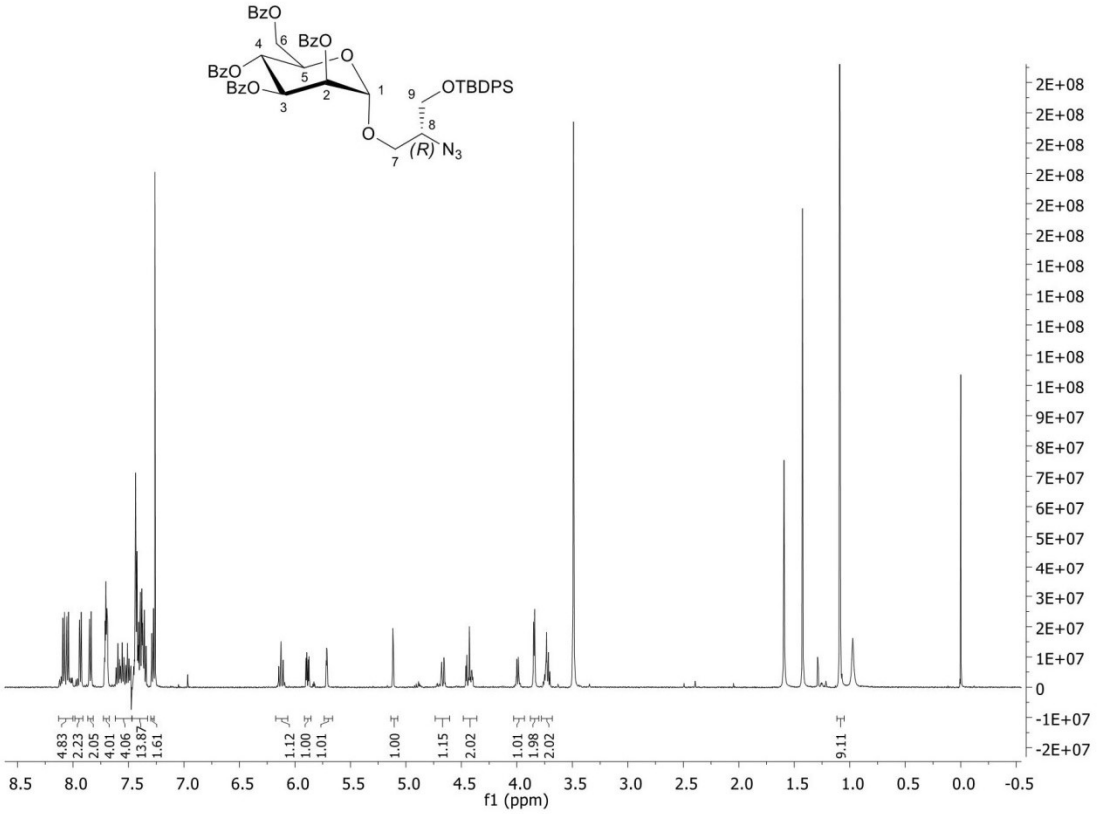

Figure S12. ^{1}H NMR (500 MHz, $CDCl_3$) spectrum of compound **11b**.

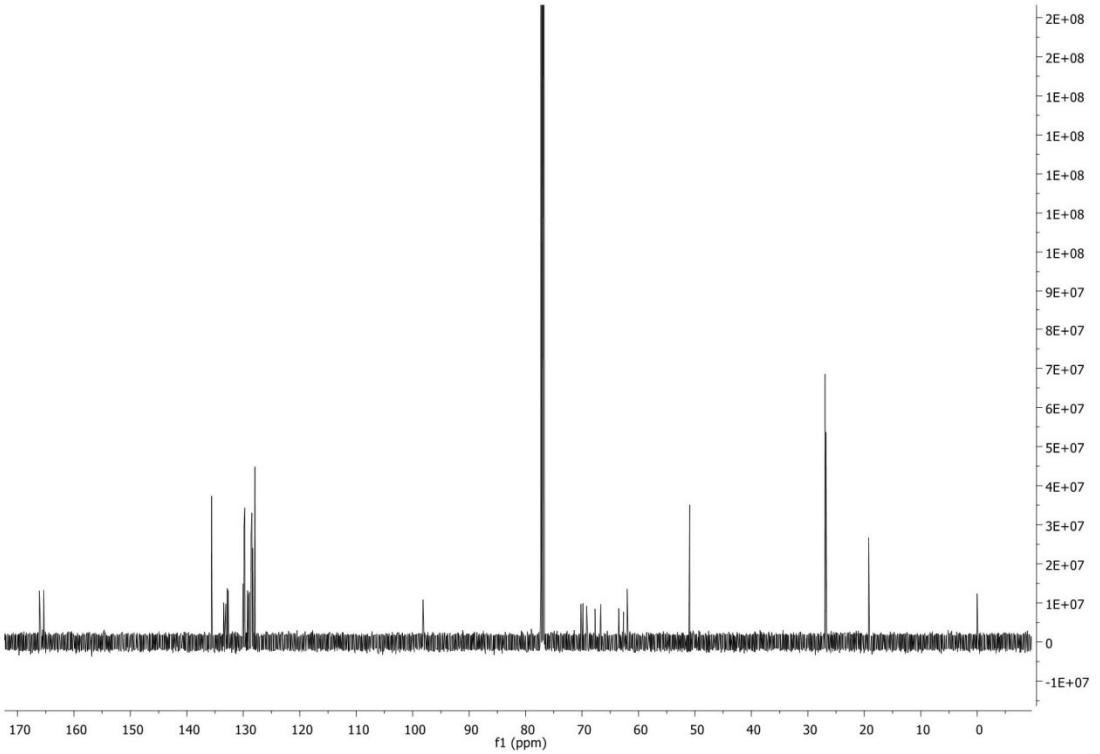

Figure S13. ^{13}C NMR (126 MHz, $CDCl_3$) spectrum of compound **11b**.

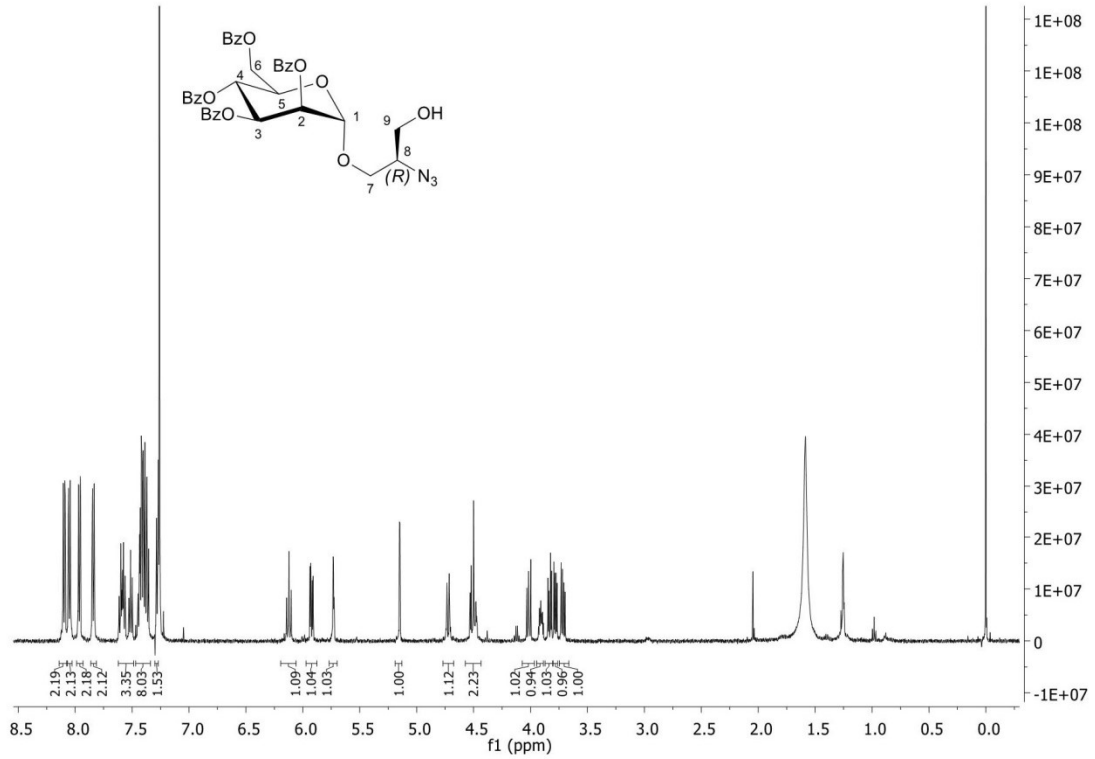

Figure S14. ^{1}H NMR (500 MHz, $CDCl_3$) spectrum of compound **12a**.

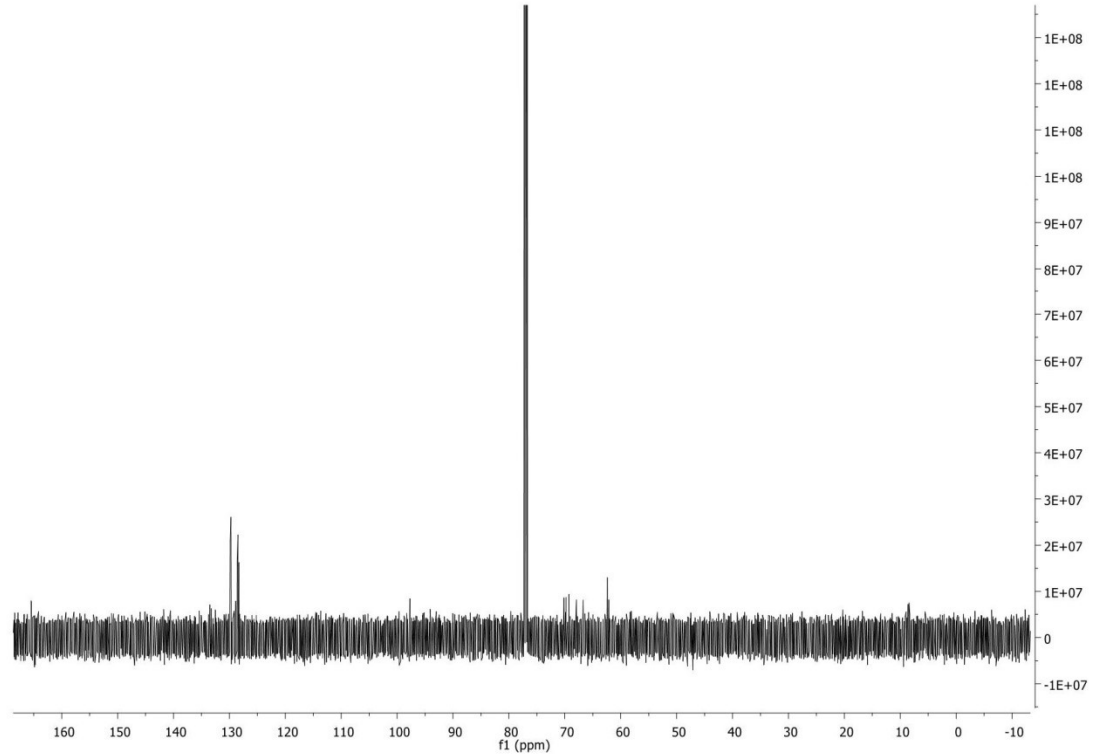

Figure S15. ^{13}C NMR (126 MHz, $CDCl_3$) spectrum of compound **12a**.

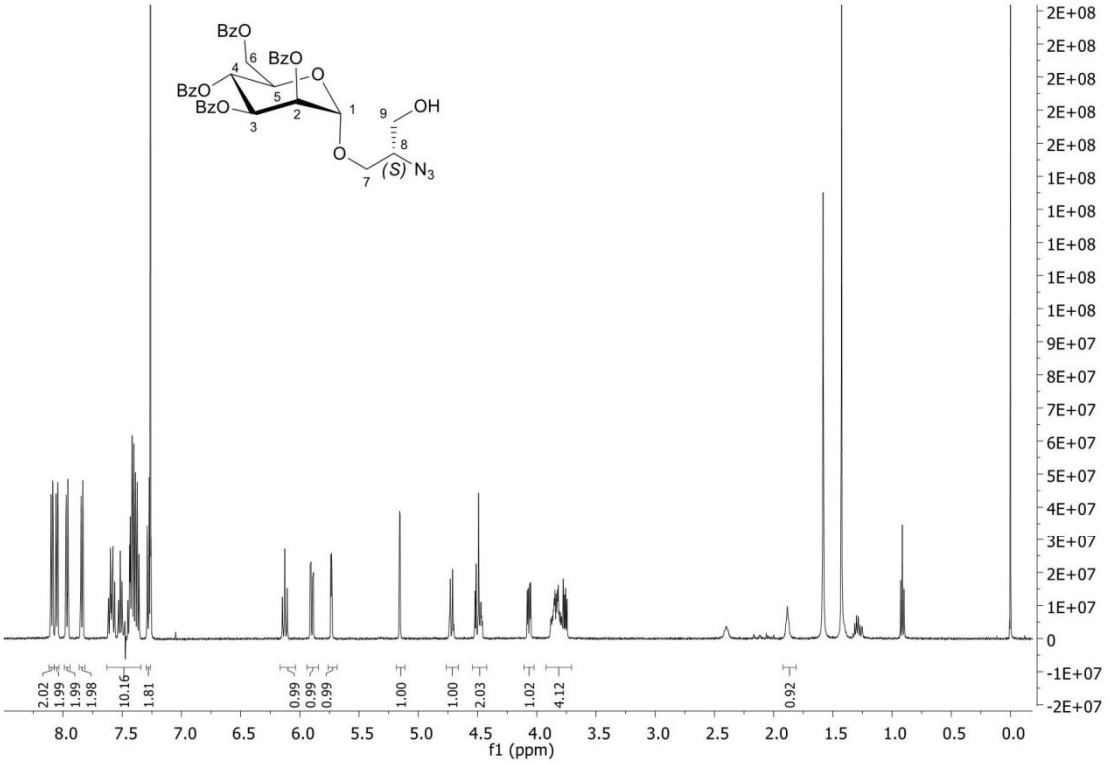

Figure S16. ^{1}H NMR (500 MHz, $CDCl_3$) spectrum of compound **12b**.

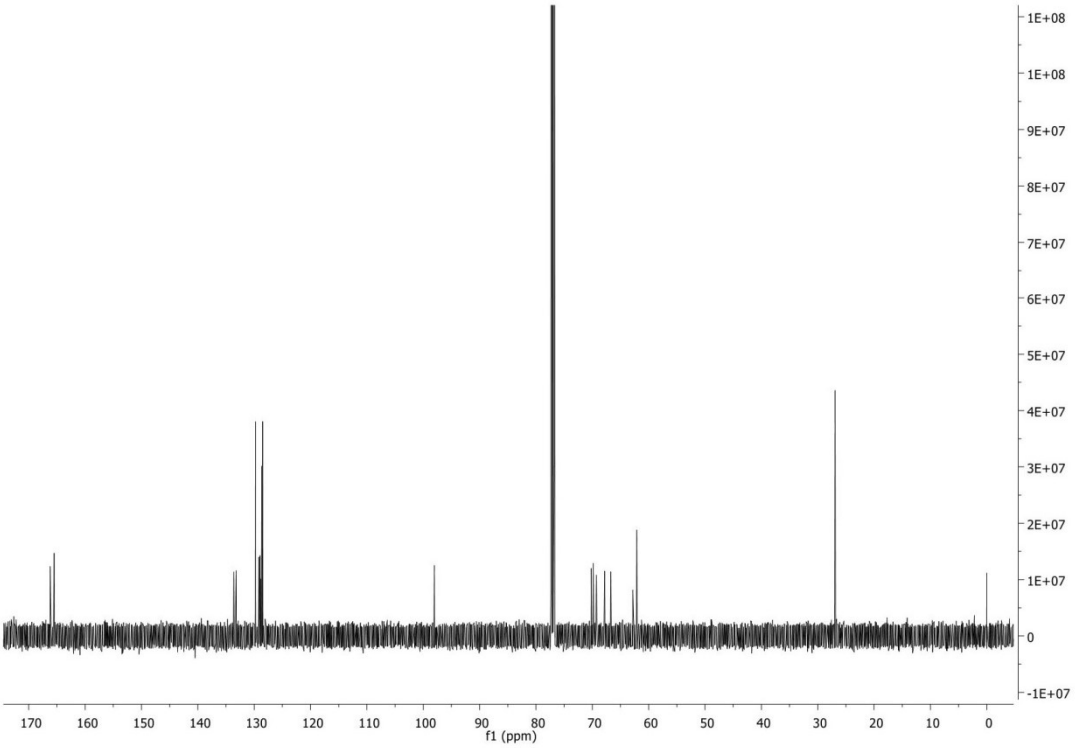

Figure S17. ^{13}C NMR (126 MHz, $CDCl_3$) spectrum of compound **12b**.

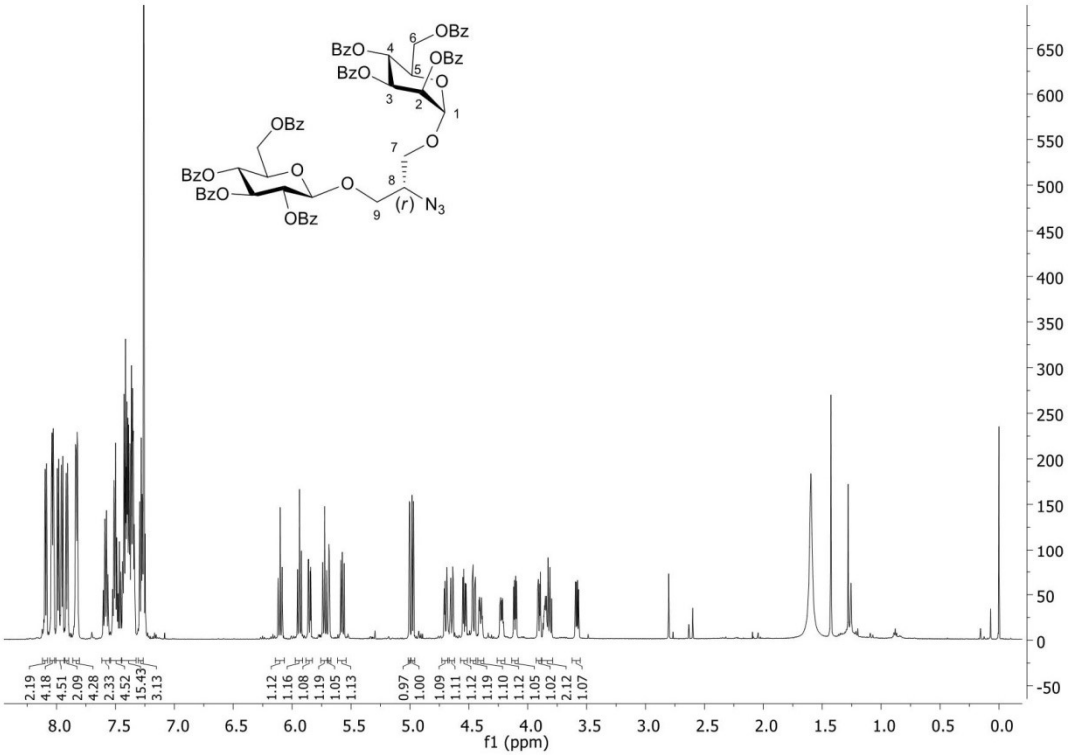

Figure S18. ^{1}H NMR (500 MHz, $CDCl_3$) spectrum of compound **14a**.

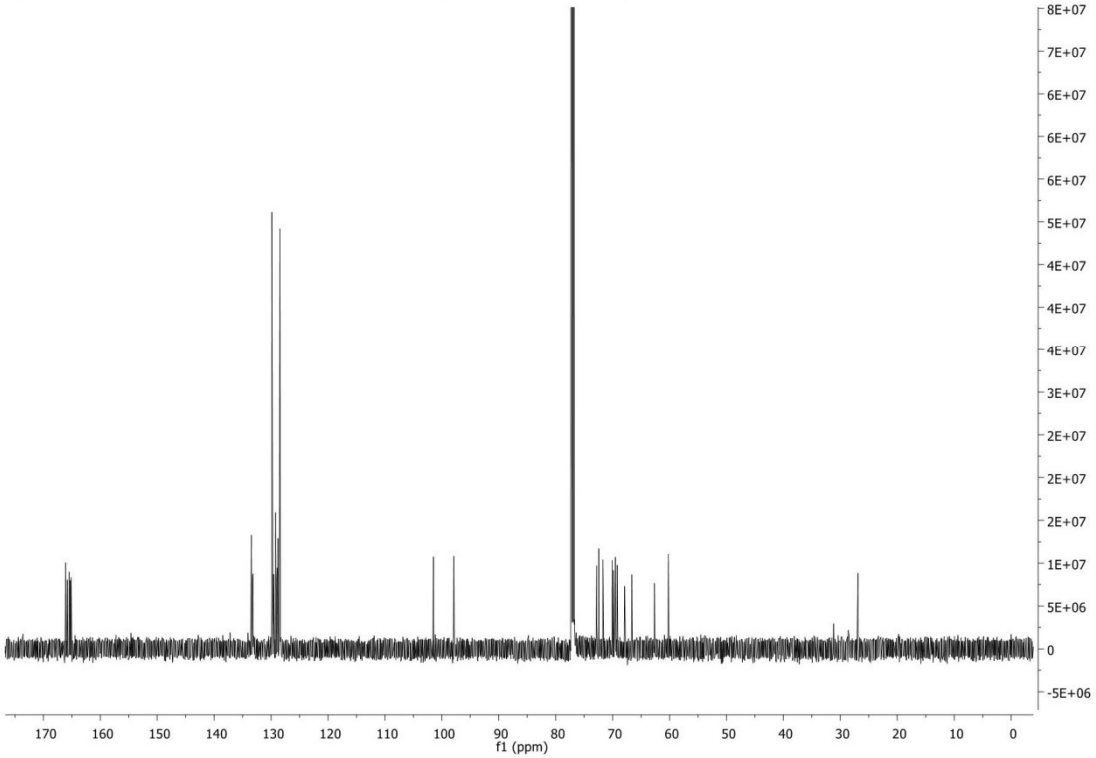

Figure S19. ^{13}C NMR (126 MHz, $CDCl_3$) spectrum of compound **14a**.

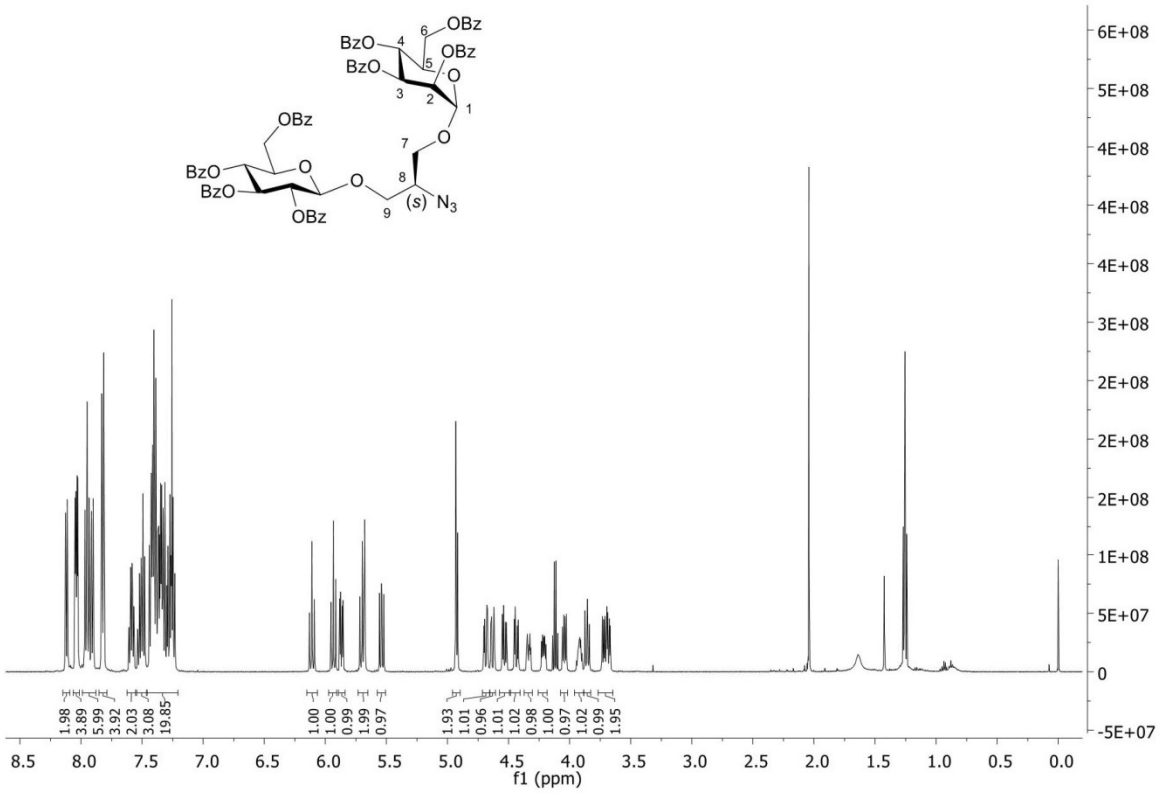

Figure S20. ^{13}C NMR (126 MHz, $CDCl_3$) spectrum of compound **14b**.

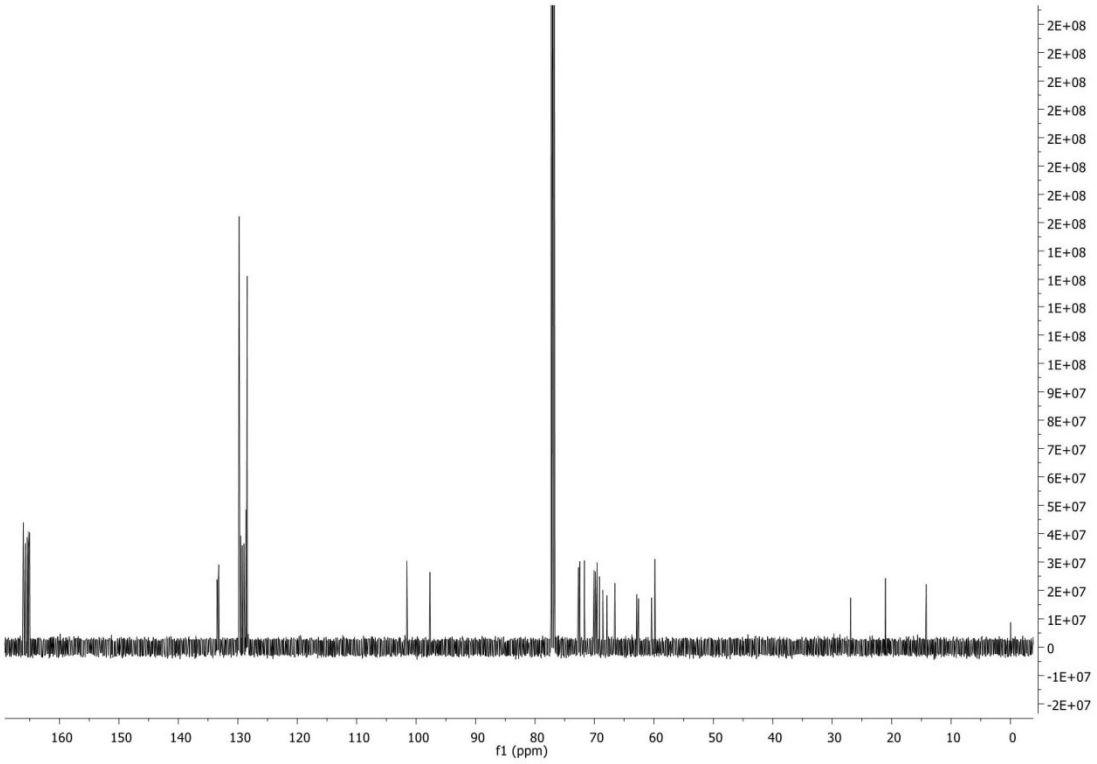

Figure S21. ^{1}H NMR (500 MHz, $CDCl_3$) spectrum of compound **14b**.

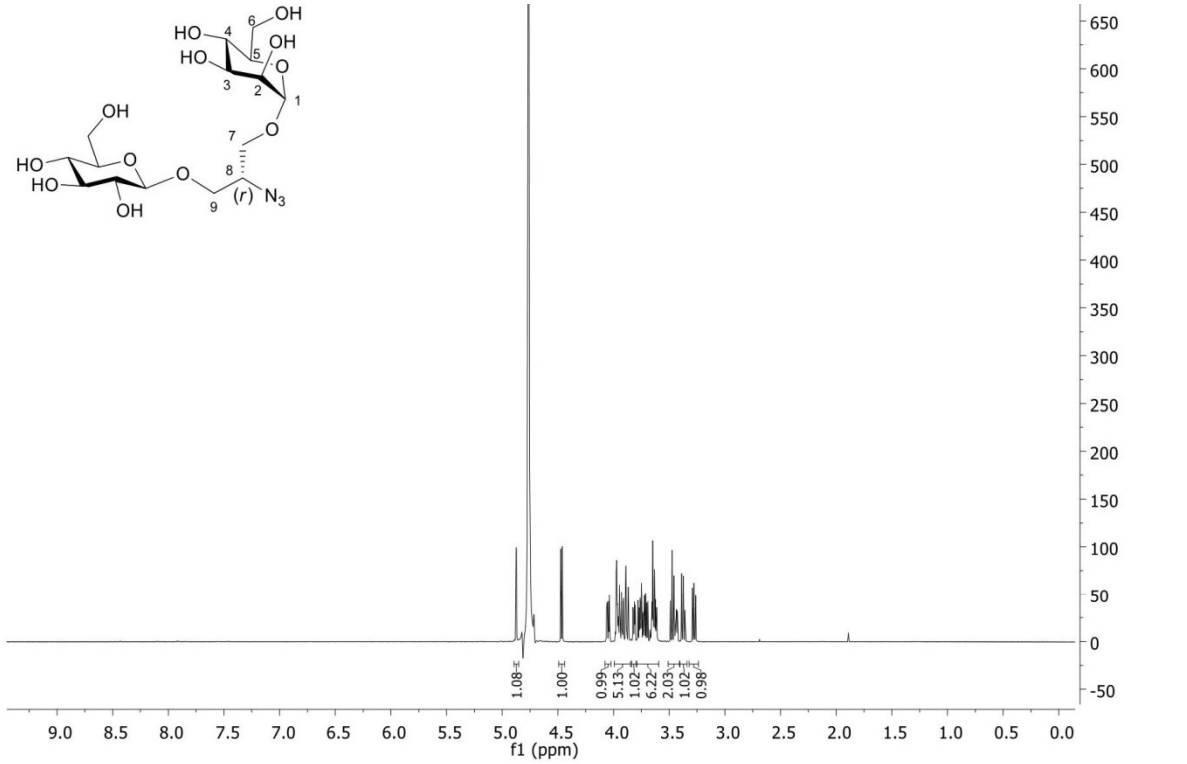

Figure S22. ^{1}H NMR (500 MHz, D_2O) spectrum of compound **15a**.

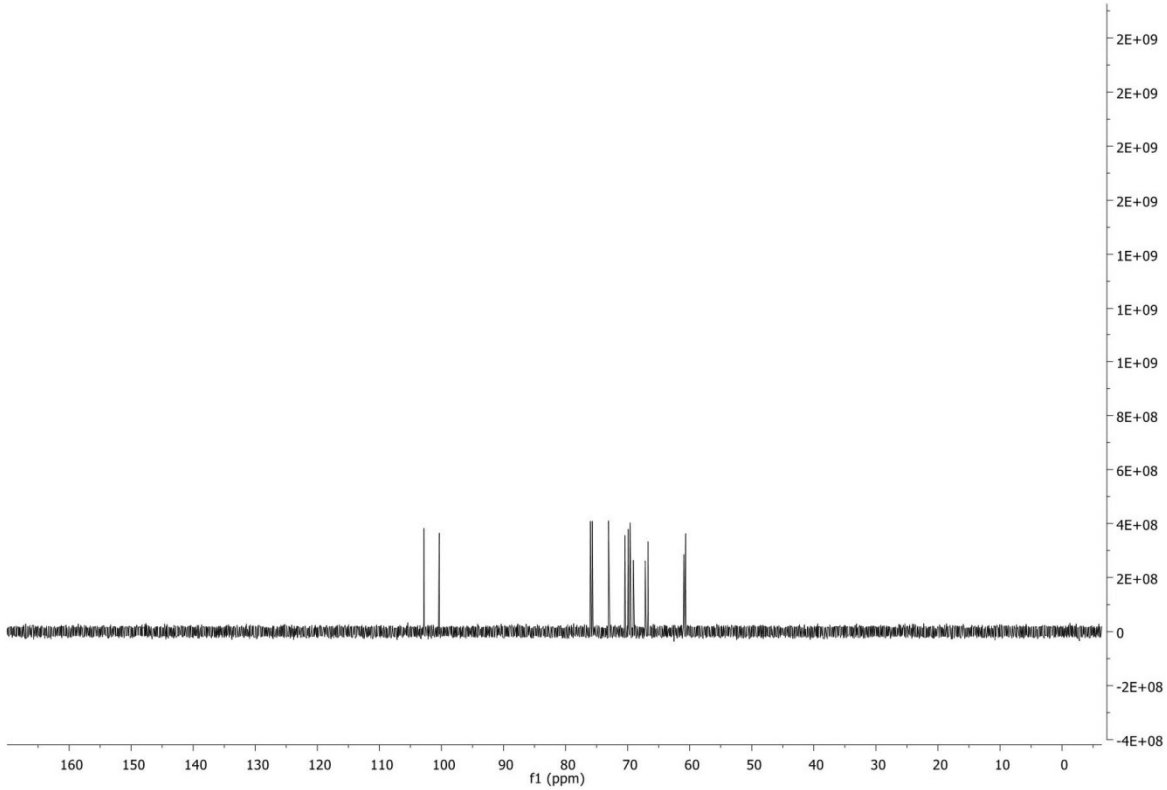

Figure S23. ^{13}C NMR (126 MHz, D_2O) spectrum of compound **15a**.

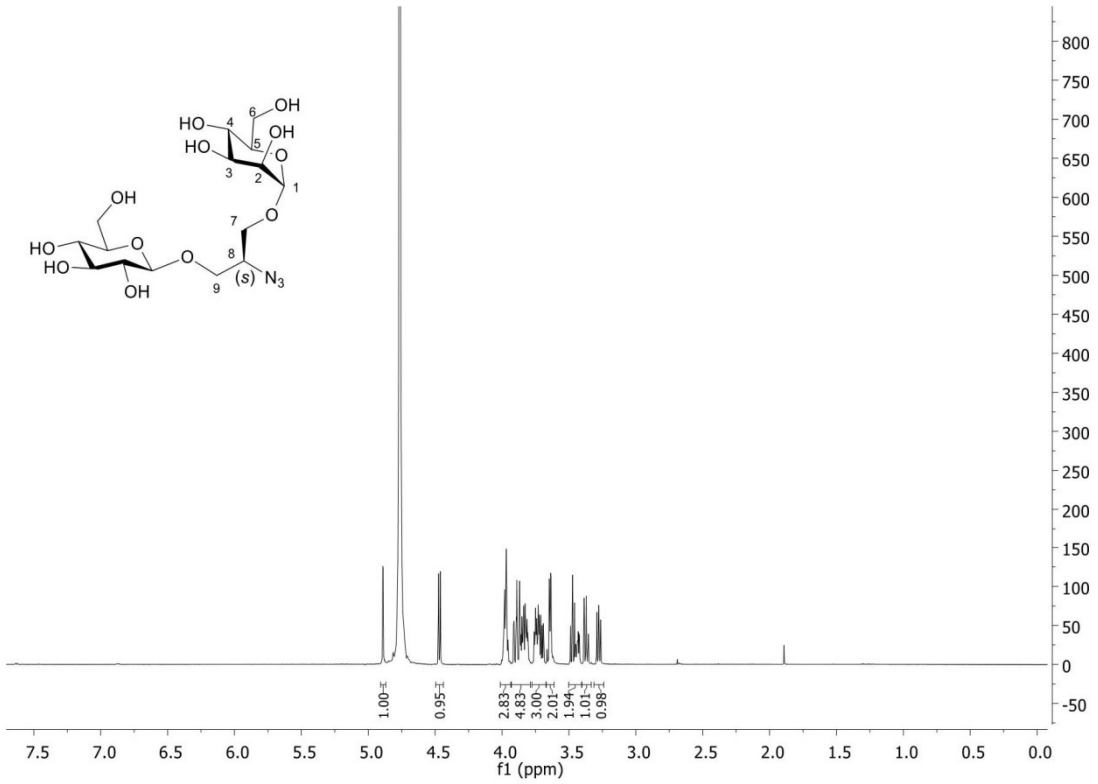

Figure S24. ^{1}H NMR (500 MHz, D_2O) spectrum of compound **15b**.

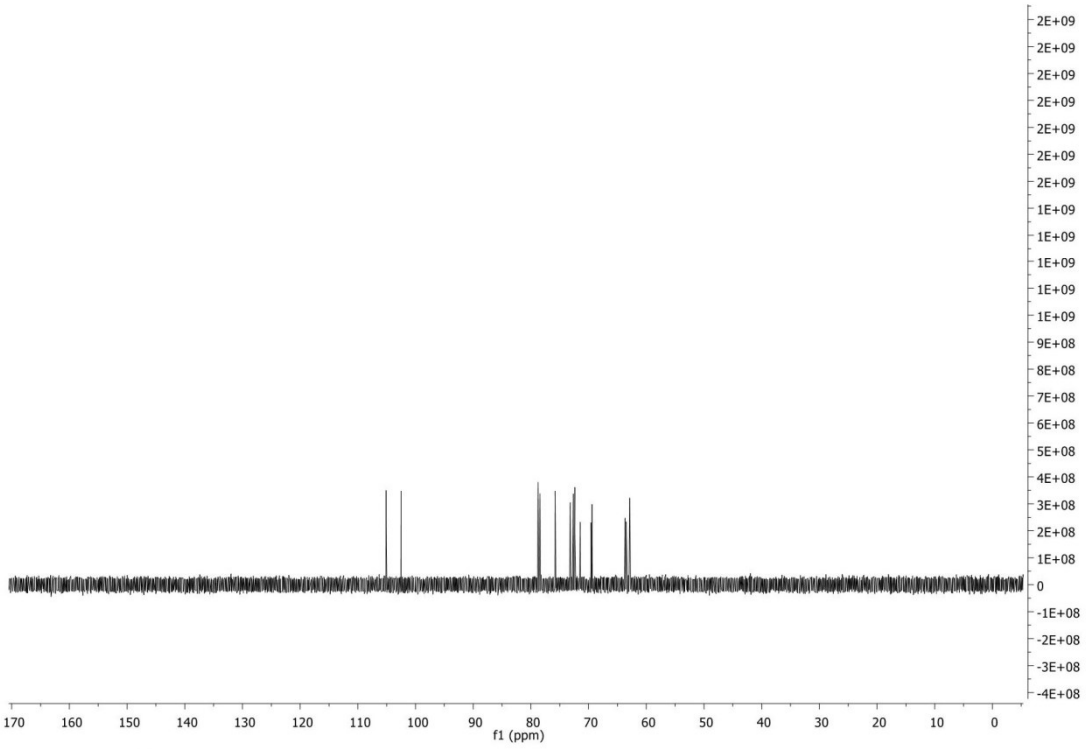

Figure S25. ^{13}C NMR (126 MHz, D_2O) spectrum of compound **15b**.

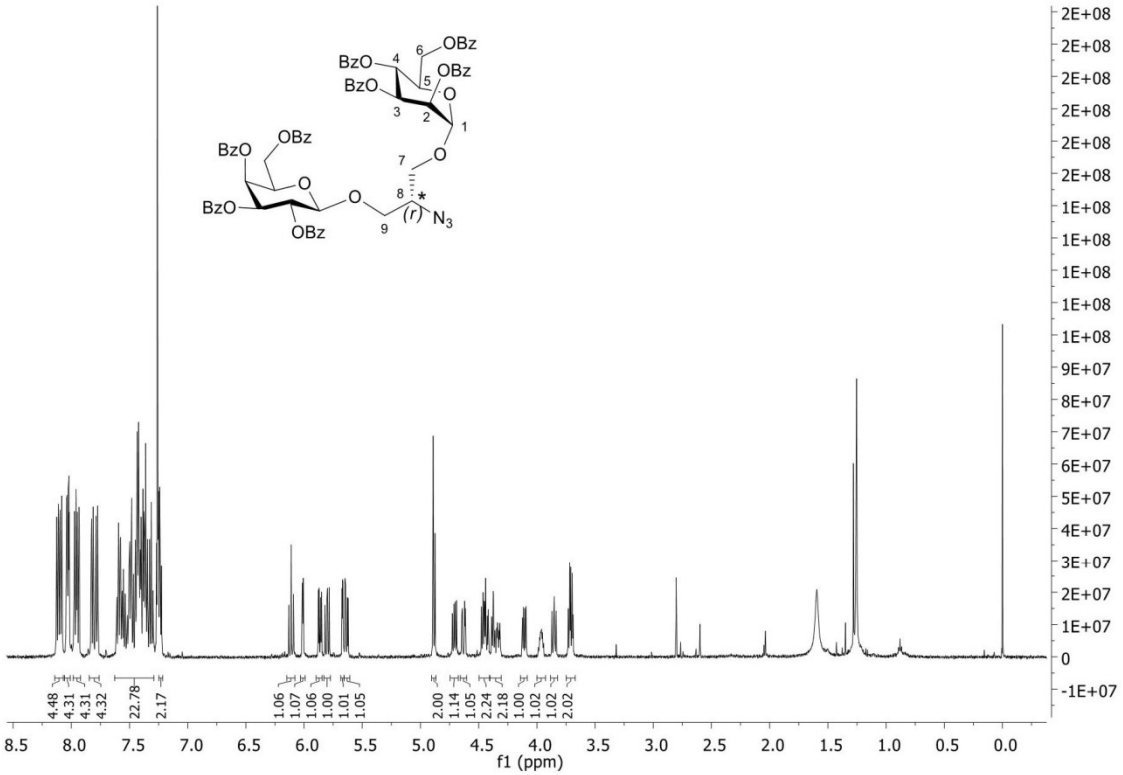

Figure S26. ^{1}H NMR (500 MHz, $CDCl_3$) spectrum of compound **17a**.

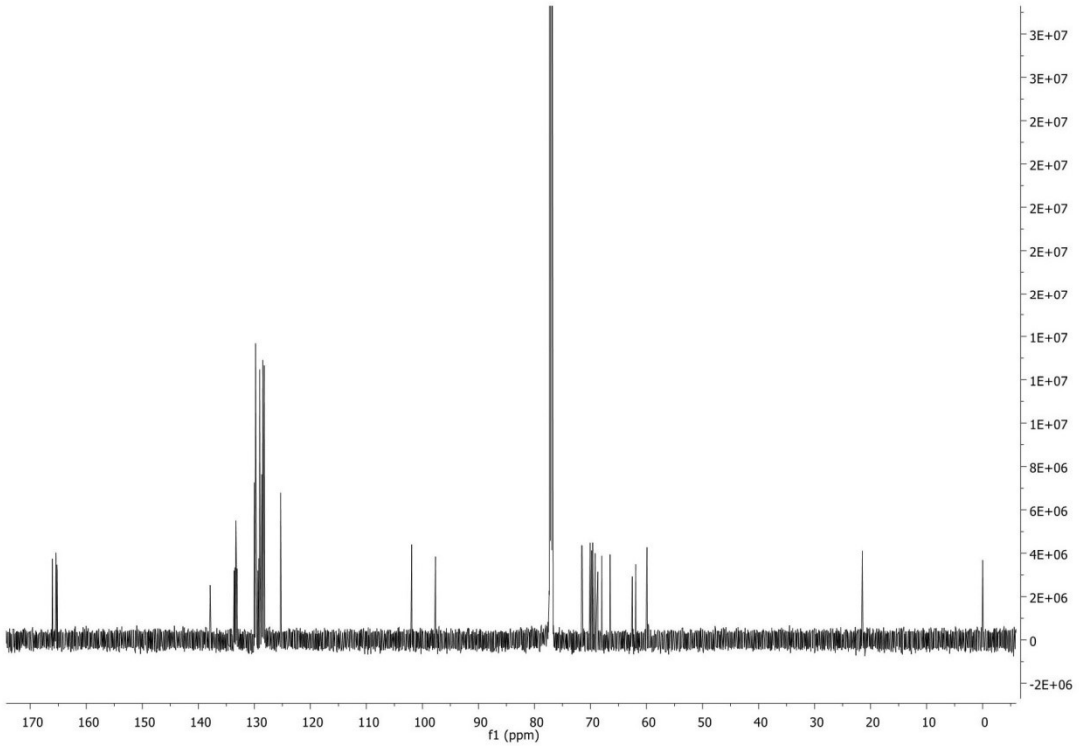

Figure S27. ^{13}C NMR (126 MHz, $CDCl_3$) spectrum of compound **17a**.

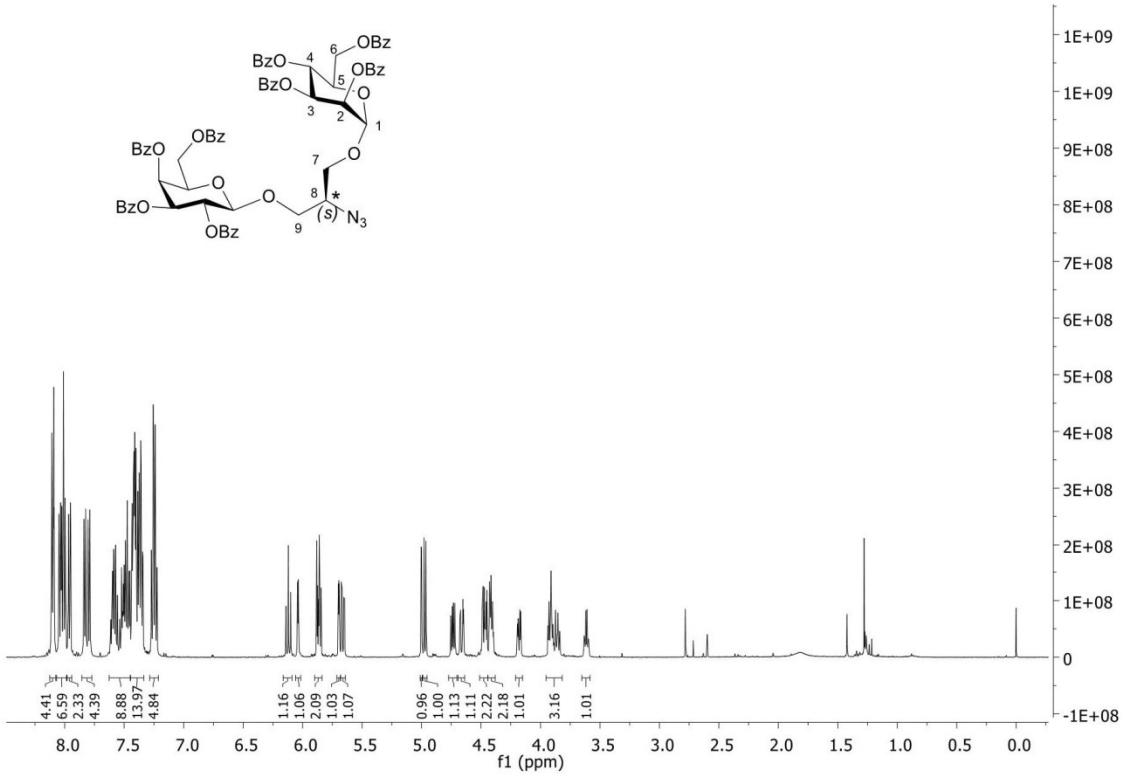

Figure S28. ^{1}H NMR (500 MHz, $CDCl_3$) spectrum of compound **17b**.

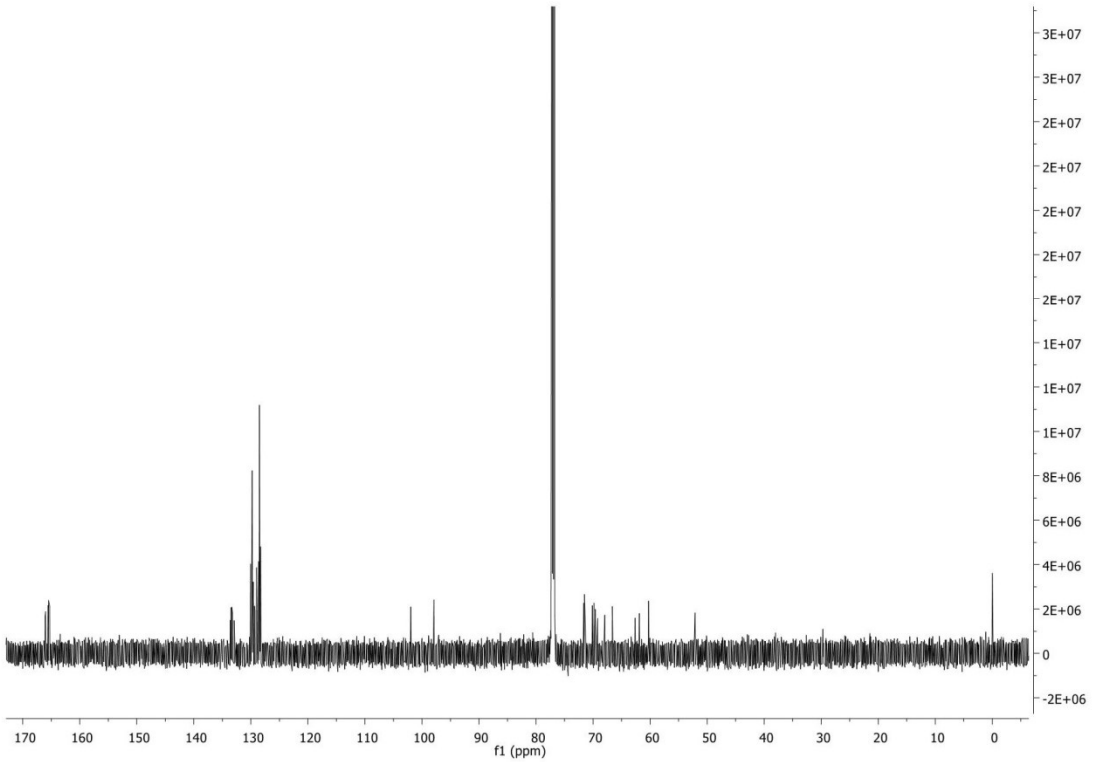

Figure S29. ^{13}C NMR (126 MHz, $CDCl_3$) spectrum of compound **17b**.

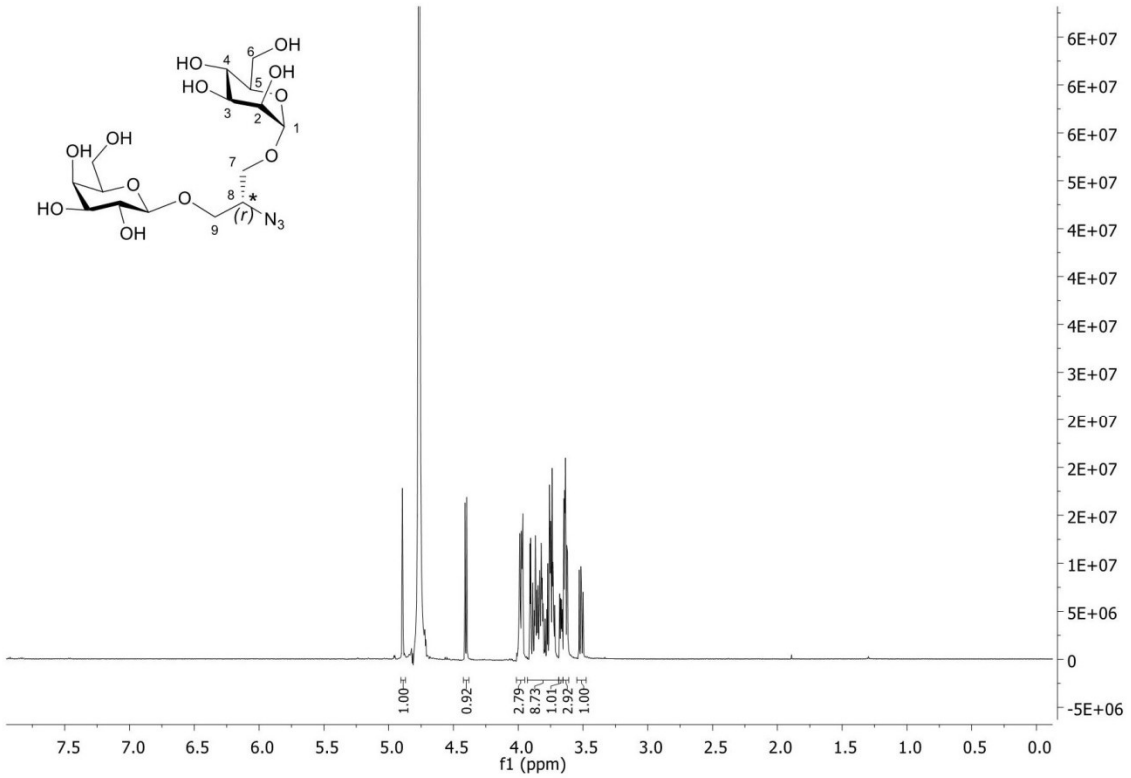

Figure S30. ^{1}H NMR (500 MHz, D_2O) spectrum of compound **18a**.

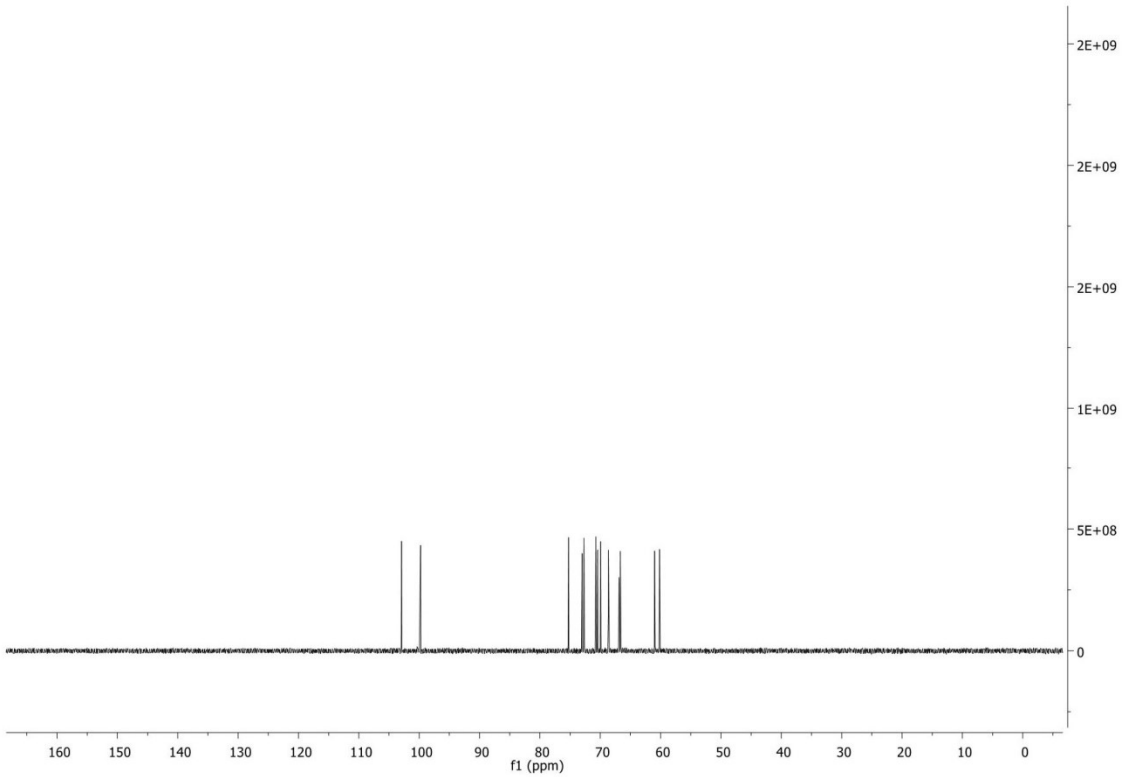

Figure S31. ^{13}C NMR (126 MHz, D_2O) spectrum of compound **18a**.

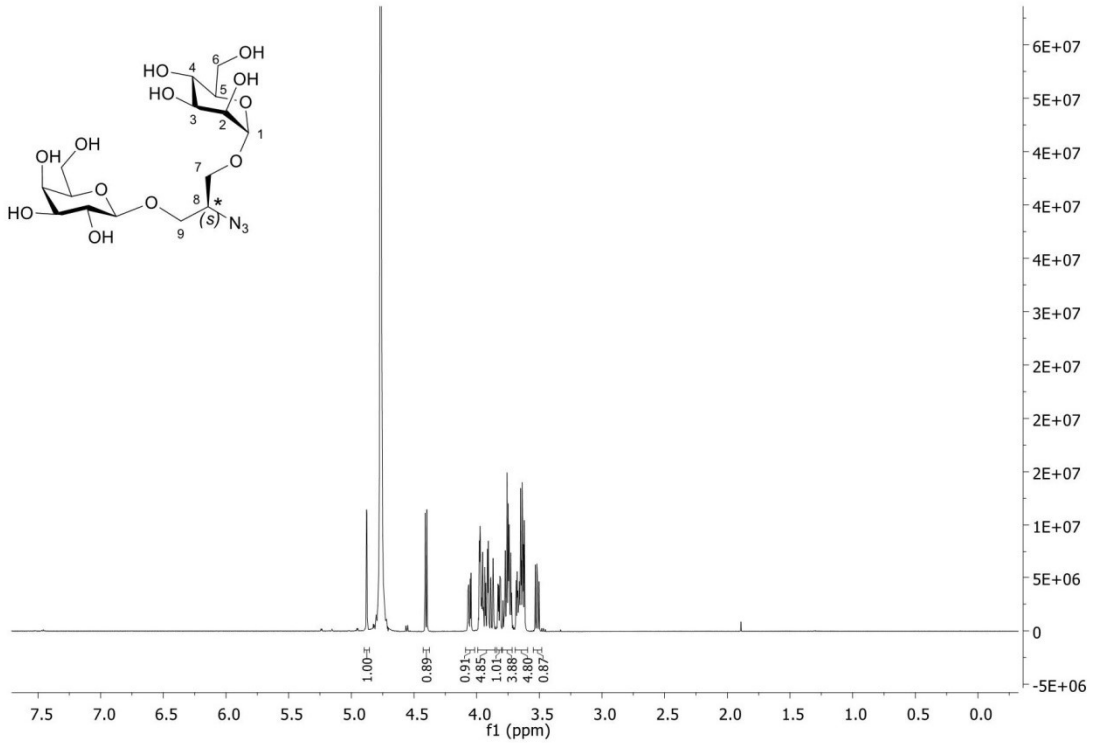

Figure S32. ^{1}H NMR (500 MHz, D_2O) spectrum of compound **18b**.

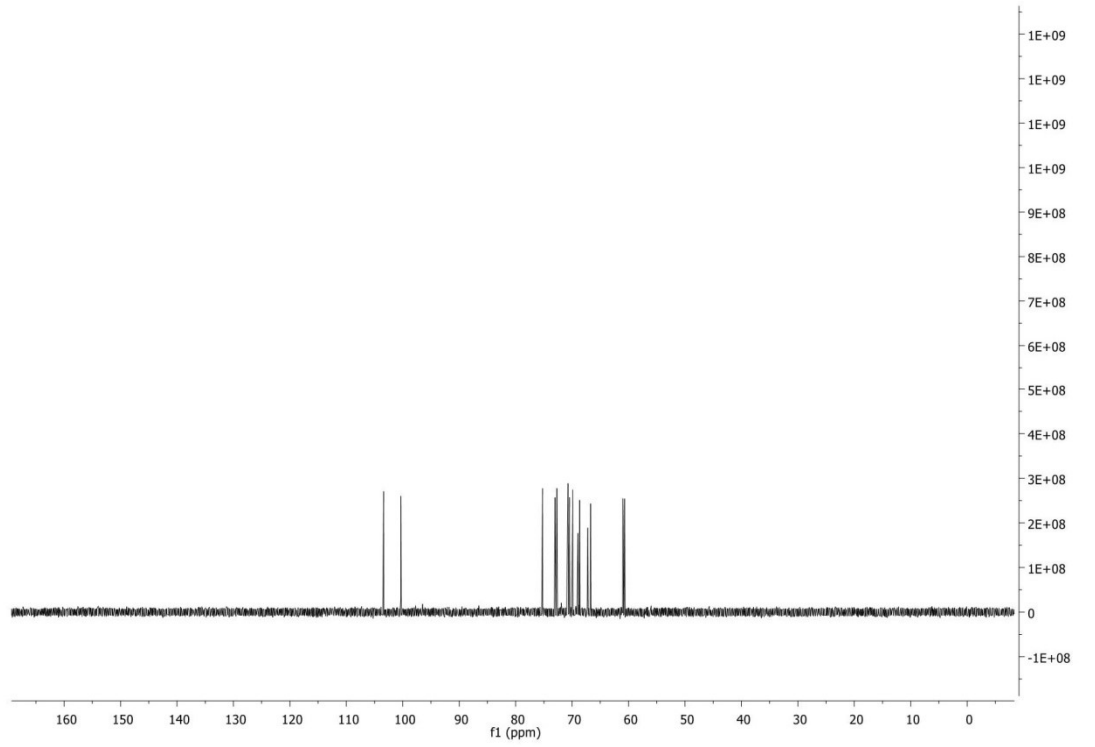

Figure S33. ^{13}C NMR (126 MHz, D_2O) spectrum of compound **18b**.

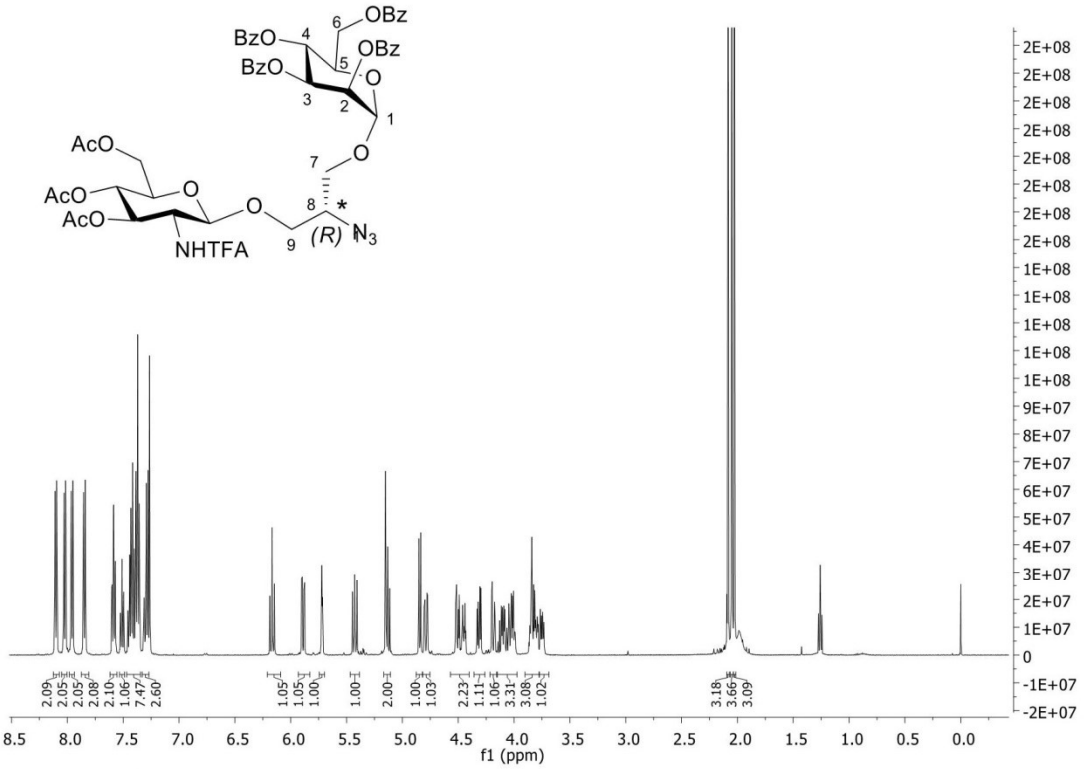

Figure S34. ^{1}H NMR (500 MHz, $CDCl_3$) spectrum of compound **20a**.

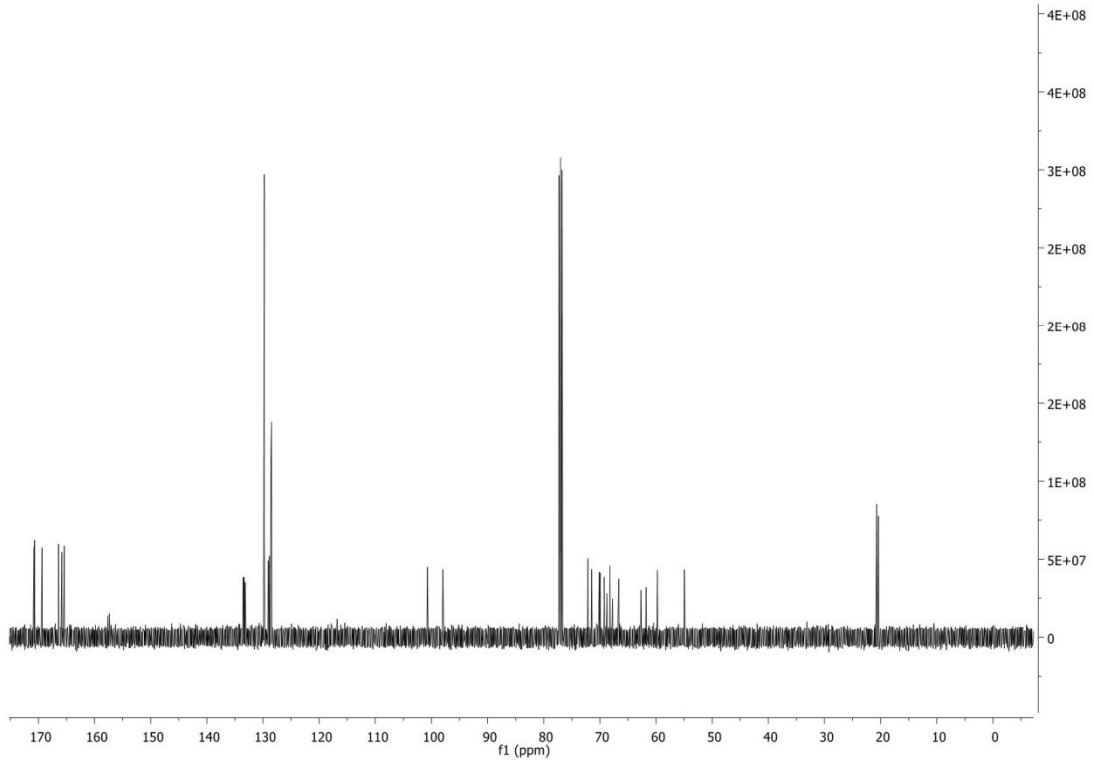

Figure S35. ^{13}C NMR (126 MHz, $CDCl_3$) spectrum of compound **20a**.

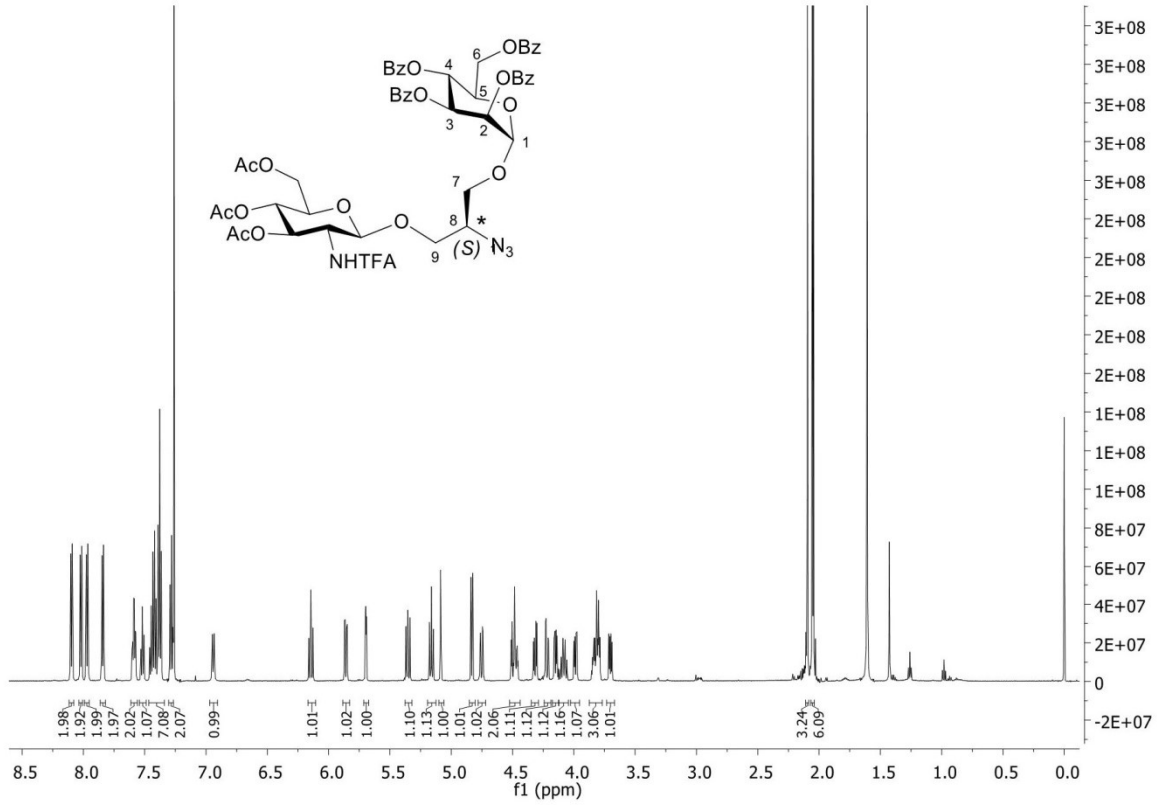

Figure S36. ^{1}H NMR (500 MHz, $CDCl_3$) spectrum of compound **20b**.

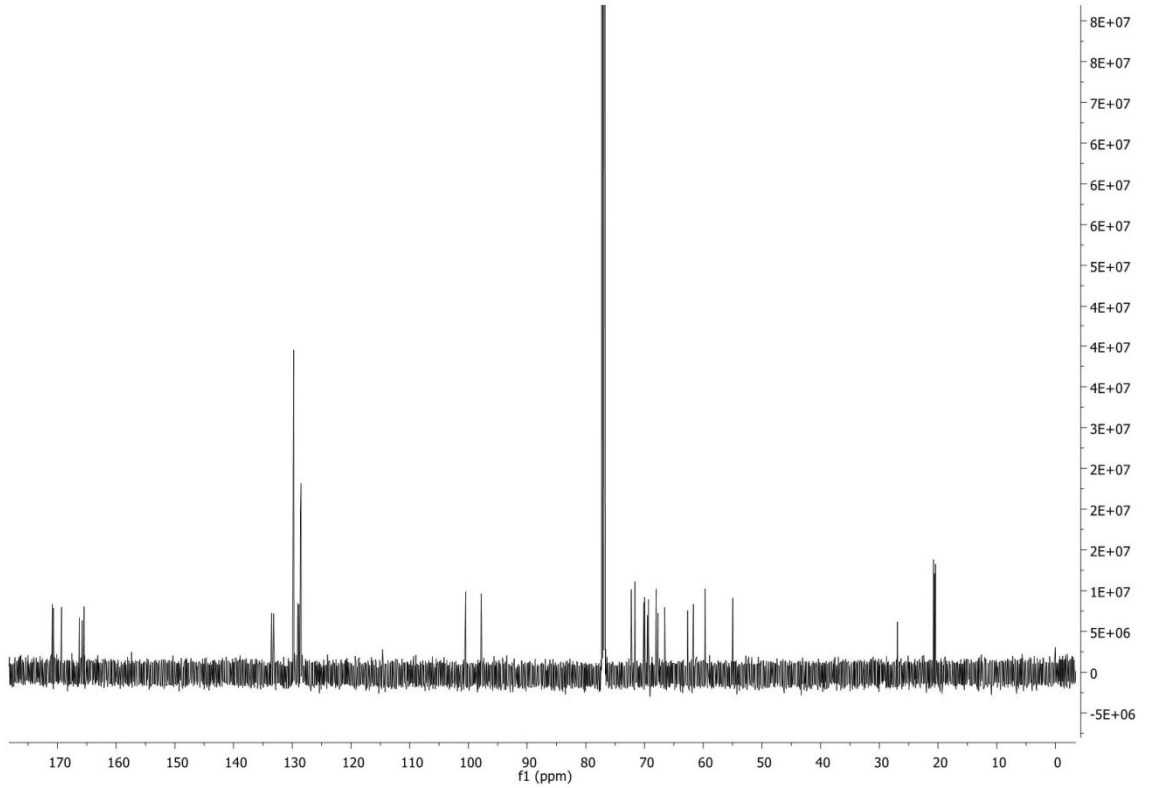

Figure S37. ^{13}C NMR (126 MHz, $CDCl_3$) spectrum of compound **20b**.

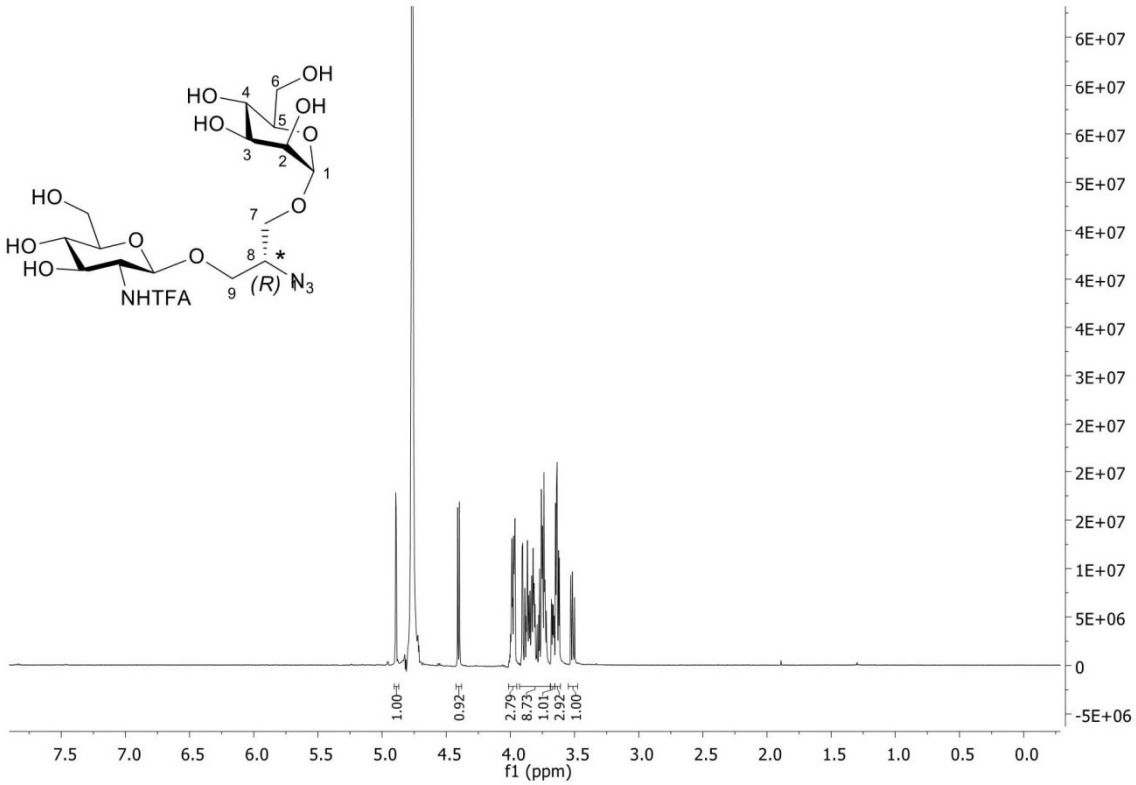

Figure S38. ^{1}H NMR (500 MHz, D_2O) spectrum of compound **21a**.

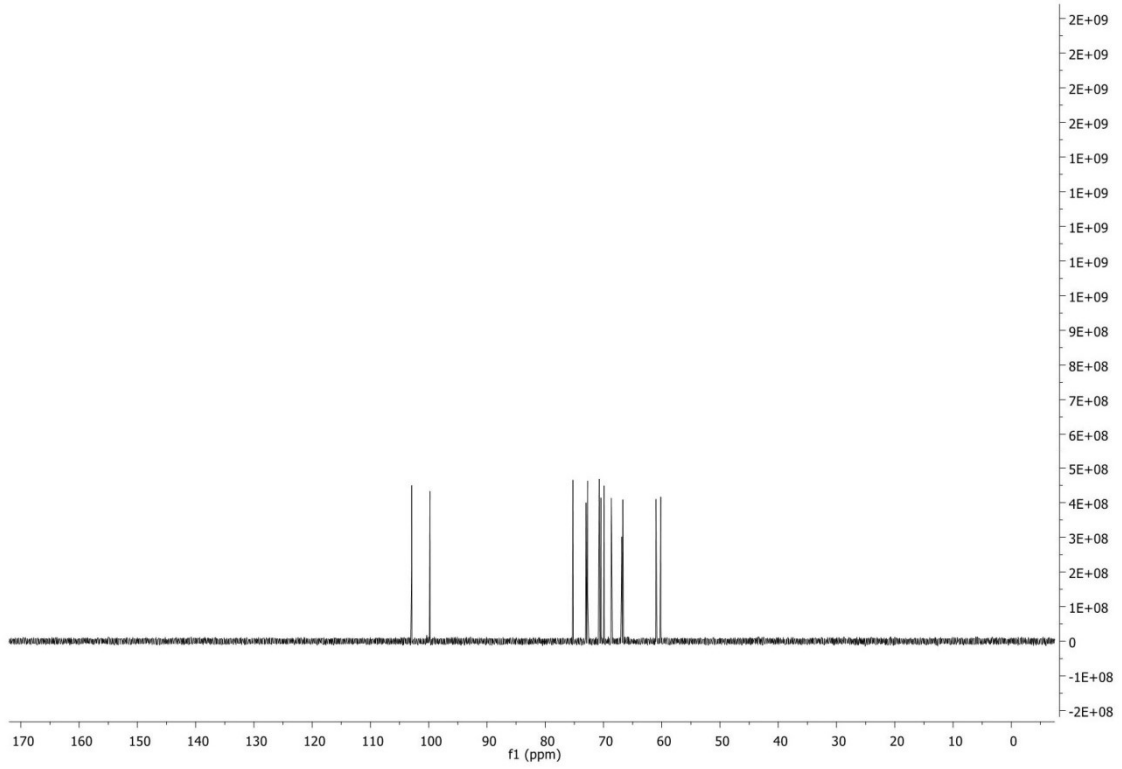

Figure S39. ^{13}C NMR (126 MHz, D_2O) spectrum of compound **21a**.

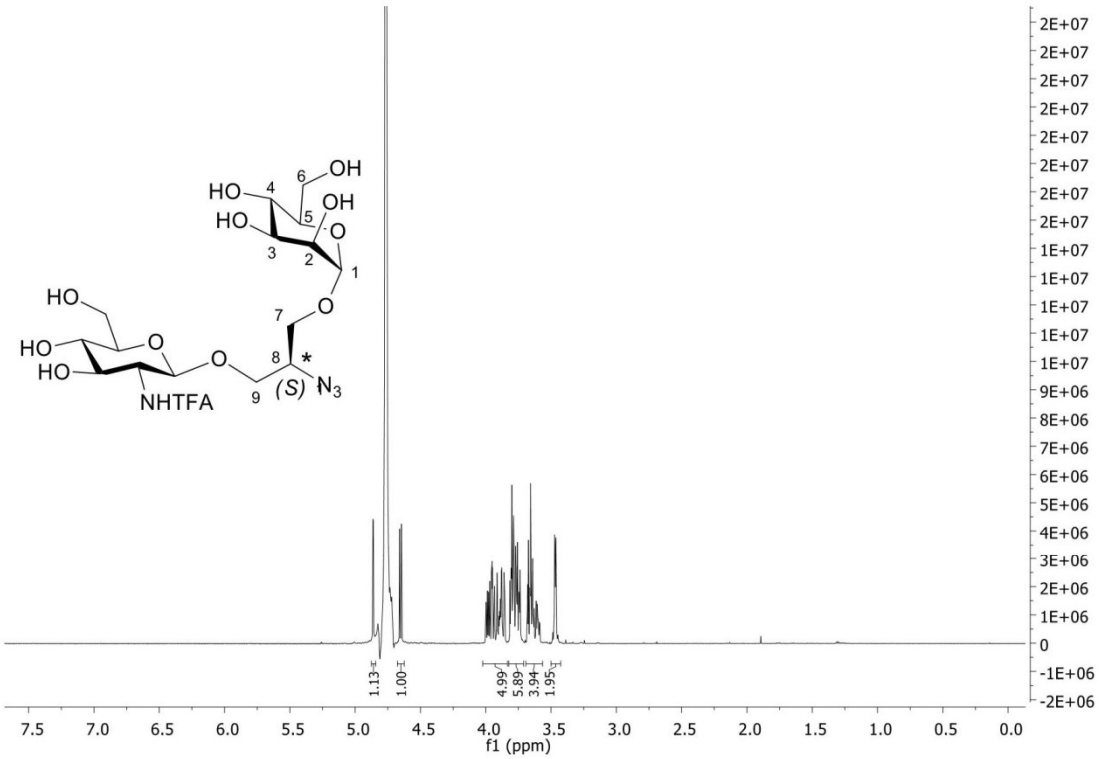

Figure S40. ^{1}H NMR (500 MHz, D_2O) spectrum of compound **21b**.

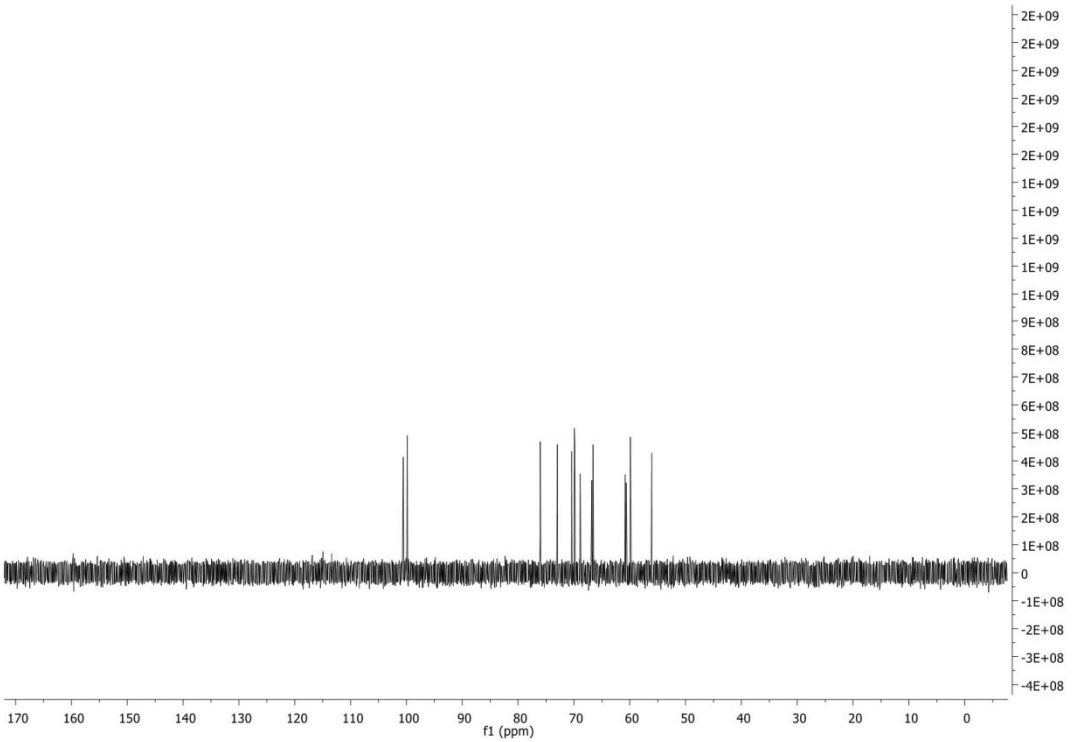

Figure S41. ^{13}C NMR (126 MHz, D_2O) spectrum of compound **21b**.

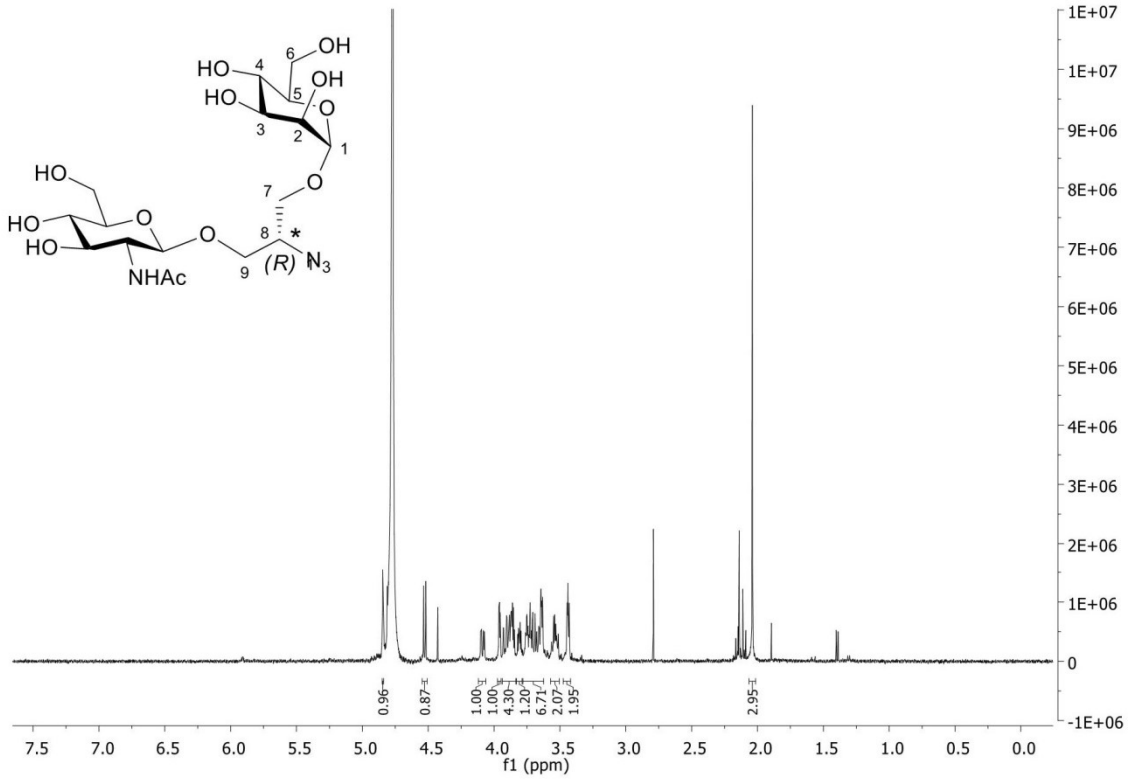

Figure S42. ^{1}H NMR (500 MHz, D_2O) spectrum of compound **22a**.

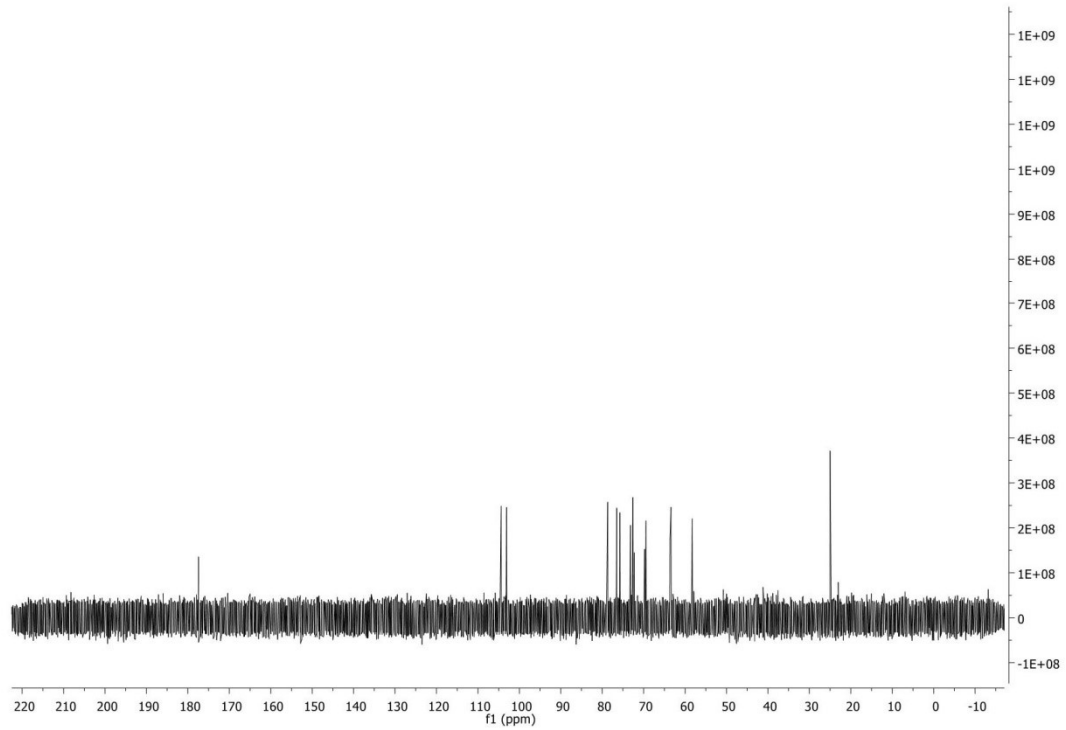

Figure S43. ^{13}C NMR (126 MHz, D_2O) spectrum of compound **22a**.

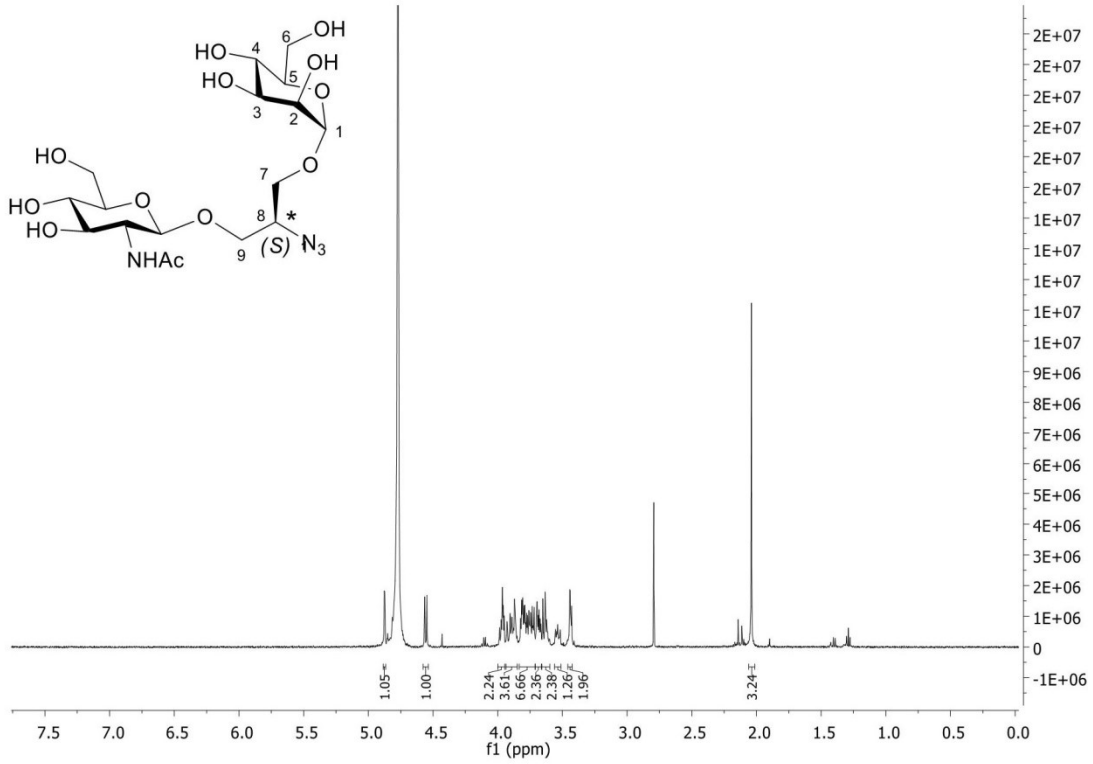

Figure S44. ^{1}H NMR (500 MHz, D_2O) spectrum of compound **22b**.

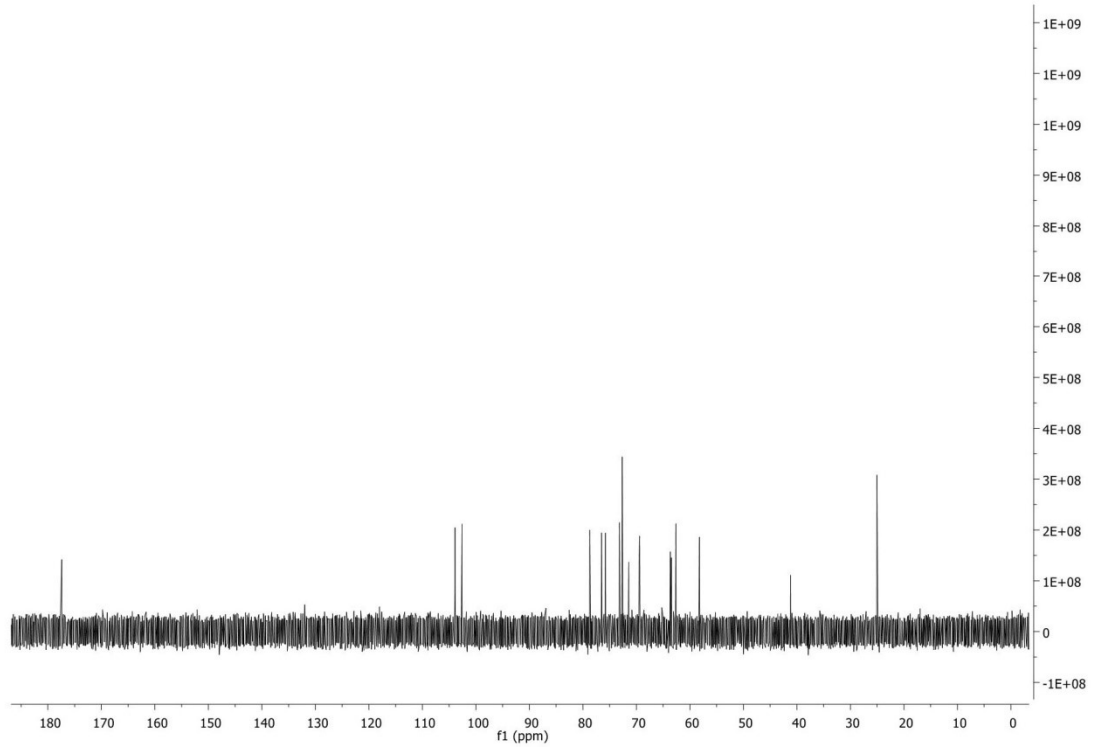

Figure S45. ^{13}C NMR (126 MHz, D_2O) spectrum of compound **22b**.

3. Biological experiments

3.1. General methods

Buffer solutions and media

Carbonate buffer: sodium carbonate (10.6 g) and sodium hydrogen carbonate (8.40 g) dissolved in bi-distilled water (1 L), pH = 9.6; PBS buffer: PBS tablets obtained from Gibco containing phosphates as 10 mM sodium phosphate, 2.68 mM potassium chloride and 140 mM sodium chloride dissolved in bi-distilled water (1 L), pH = 7.45; PBS buffer containing calcium chloride dihydrate (0.1 mM) and manganese(II) chloride tetrahydrate (0.1 mM) was used for FITC-ConA assays; PBST buffer (PBS buffer + 0.05 % v/v Tween®20); pH values were adjusted by using 0.1 M aq. hydrochloric acid or 0.1 M aq. sodium hydroxide; Lysogeny broth medium-LB medium (sterilized): tryptone (10 g L^{-1}), yeast extract (5 g L^{-1}), sodium chloride (10 g L^{-1}) in bi-distilled water (1 L), pH = 7.0, ampicillin (100 mg L^{-1}) and chloramphenicol (50 mg L^{-1}) antibiotics.

Preparation of bacterial suspension and concentration adjustment of FITC-ConA suspension

The synthesized compounds were tested as potential inhibitors of two adherents: type 1 fimbriae GFP-PKL1162 *E.coli* and type IV FITC-ConA conjugate.[6] The bacterial *E. coli* strain PKL1162 was cultured from frozen stock in LB media overnight at 37 °C. The bacterial pellet obtained after centrifugation and decantation of the medium was washed twice with PBS (2 mL) then suspended in PBS buffer. The bacterial suspension was adjusted to OD_{600} = 0.4 with PBS. For the assays with ConA, the concentration of the suspension of FITC-ConA conjugate was adjusted by measuring the fluorescence intensity (λ_{exc} = 485 nm, λ_{em} = 535 nm) of bound ConA conjugate onto mannan surface at different lectin concentrations. Therefore, all the adhesion inhibition assays were performed with a suspension of FITC-ConA conjugate in PBS buffer at *c* = 0.8 mg mL^{-1} (Figure S53).

Inhibition assays with GFP-PKL1162 E. coli bacteria and the FITC-ConA conjugate

According to literature,[6,7] 96-well black microtiter plates (Nunc, MaxiSorp) were incubated overnight with mannan from *Saccharomyces cerevisiae* (1.2 mg mL^{-1}) in carbonate buffer (120 µL per well) at 37 °C, shaking at 175 rpm. After washing three times with PBST, the microtiter plates were blocked with polyvinyl alcohol (PVA) by adding a 1 % PVA in PBS solution (120 µL per well) and incubated at 37 °C, shaking at 175 rpm for three hours. The plates were washed with PBST twice and PBS once. Finally, a serial dilution of the tested diastereomeric pair was performed starting with *c* = 50 mM (if not mentioned differently) in PBS buffer (50 µL per well) and the tested adherent was added (50 µL per well). After incubation for one hour at 37 °C and shaking at 100 rpm, the microtiter plates were washed three times with PBS and filled with PBS (120 µL per well) for relative fluorescence intensity readout (λ_{exc} = 485, λ_{em}= 535 nm).

Inhibitor concentration

The synthesized compounds were tested in duplicates or triplicates on the same microplate with methyl-α-D-mannopyranoside (MeMan) and the glycocluster $(\alpha Man)_2$ (**6**) as reference compounds. The potential concentration of the tested divalent heteroglycoclusters was selected according to preliminary assays carried out with $(\alpha Man)_2$ (**6**), starting from *c* = 50 mM. This concentration was chosen for all assays except with βGlcNAc-αMan (**22a**) and βGlcNAc-αMan (**22b**) (*c* = 20 mM) in case of inhibition assay with FITC-ConA. Compounds were tested in at least two independent experiments. The obtained IC_{50} values were referenced to the one corresponding to MeMan in order to obtain relative inhibitory potencies (RIP). For valency-corrected RIP values of $(\alpha Man)_2$ (**6**) the RIP value was divided by the number of clustered mannosyl ligands.

3.2. List of tested compounds

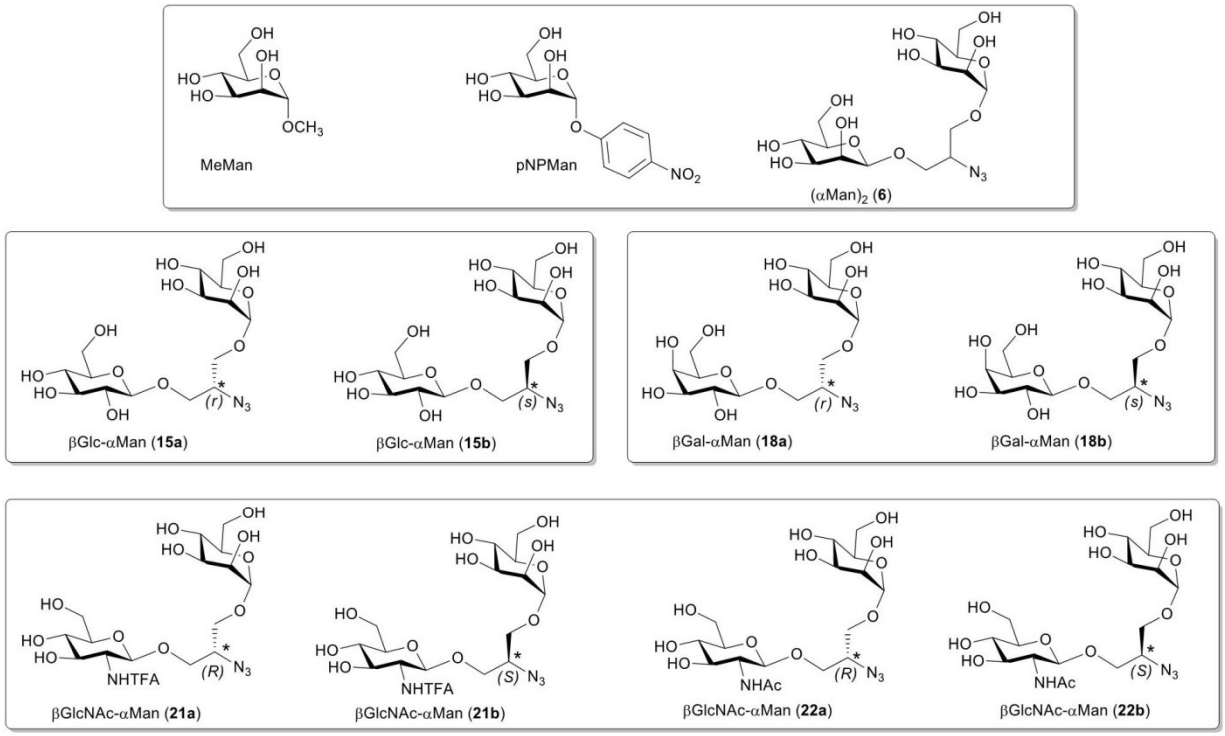

Figure S46. Structures of tested compounds.

3.3. Bacterial adhesion-inhibition assays

In preliminary experiments, the $(\alpha Man)_2$ cluster **6**, MeMan and the known inhibitor *p*-nitrophenyl α-mannopyranoside (*p*NPMan) were employed as 50 mM stock solutions and serially diluted. It is known that the inhibitory activity of pNPMan is roughly 2 orders of magnitude higher than that of MeMan is.[8] The inhibitory potency of cluster **6** was found to be in the range of *p*NPMan.

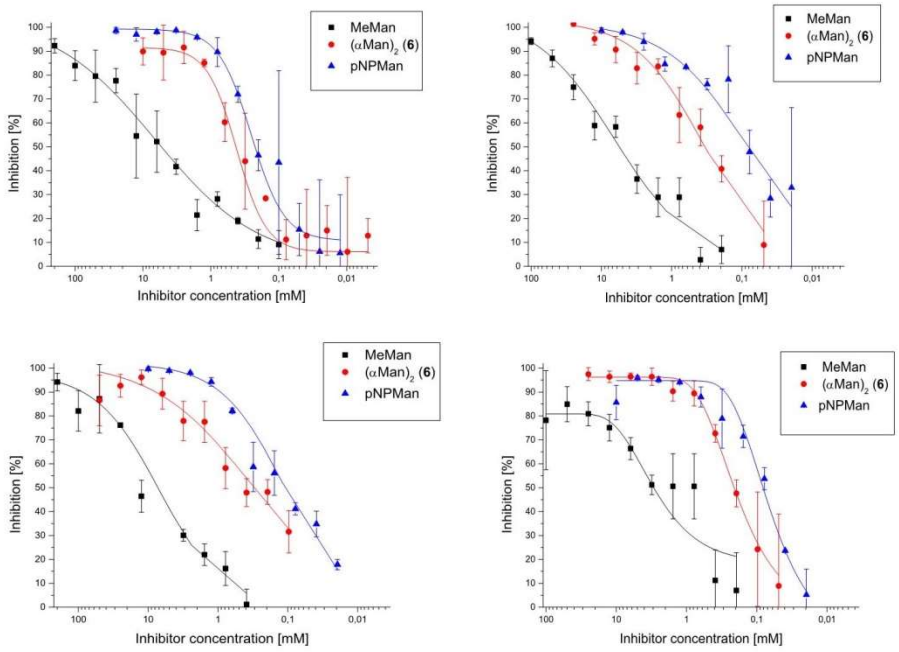

Figure S47. Inhibition curves obtained with MeMan, $(\alpha Man)_2$ (**6**) and pNPMan in adhesion-inhibition assays wit GFP-PKL1162 *E. coli* bacteria.

Table S1. IC_{50} values as deduced from the inhibition curves obtained with MeMan, $(\alpha Man)_2$ (**6**), pNPMan and corresponding RIP values; RIP_{vc} = valency-corrected relative inhibitory potency.

ENTRY	MeMan	$(\alpha Man)_2$ (**6**)	pNPMan
IC_{50}* [mM]	5.342	0.430	0.223
IC_{50}* [mM]	5.591	0.339	0.081
IC_{50}* [mM]	2.925	0.211	0.081
IC_{50}* [mM]	7.271	0.300	0.107
IC_{50}* [mM] (SD)#	5.282 (±1.79)	0.320 (±0.09)	0.123 (±0.07)
RIP	defined as 1	16.507	42.94
RIP_{vc}		8.253	

* IC_{50} value determined from triplicates for MeMan and$(\alpha Man)_2$ (**6**) and duplicates for pNPMan on the same plate.
# Standard deviation of the mean of IC_{50} values from four independent measurements.

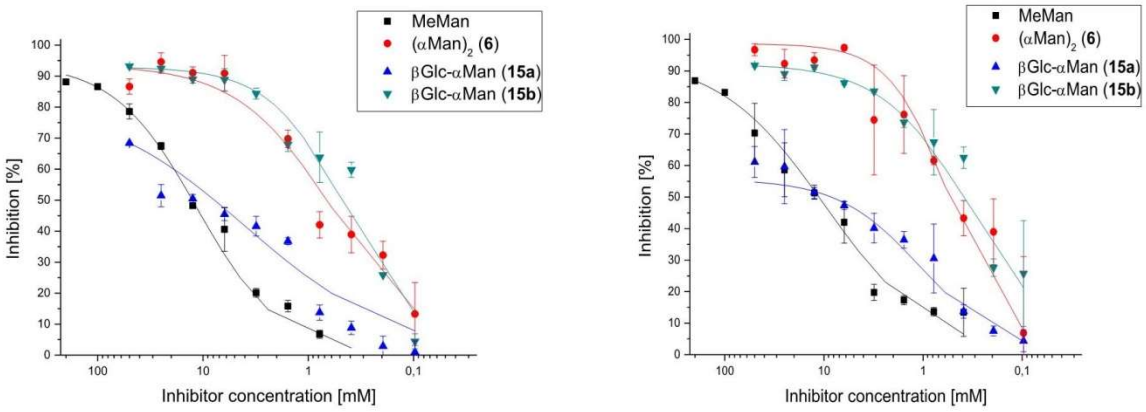

Figure S48. Inhibition curves obtained with MeMan, βGlc-αMan (**15a**), βGlc-αMan (**15b**), $(\alpha Man)_2$ (**6**) in adhesion-inhibition assays wit GFP-PKL1162 *E. coli* bacteria.

Table S2. IC_{50} values as deduced from the inhibition curves obtained with MeMan, βGlc-αMan (**15a**), βGlc-αMan (**15b**), $(\alpha Man)_2$ (**6**) and corresponding RIP values; RIP_{vc} = valency-corrected relative inhibitory potency.

ENTRY	MeMan	βGlc-αMan (**15a**)	βGlc-αMan (**15b**)	$(\alpha Man)_2$ (**6**)
IC_{50}* [mM]	12.55	7.82	0.48	0.67
IC_{50}* [mM]	11.19	8.52	0.39	0.53
IC_{50}* [mM] (SD)#	11.87 (±0.96)	8.17 (±0.49)	0.43 (±0.06)	0.60 (±0.10)
RIP		1.45	27.44	19.88
RIP_{vc}				9.94

* IC_{50} value determined from duplicates on the same plate.
# Standard deviation of the mean of IC_{50} values from two independent measurements.

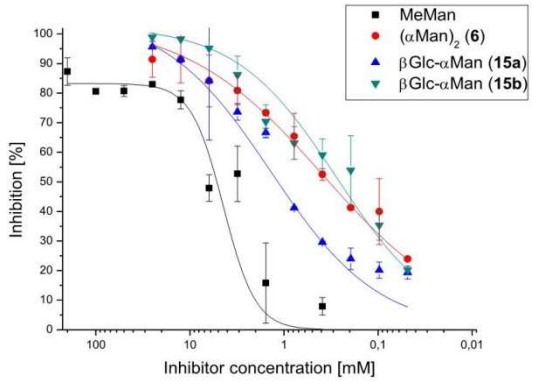

Figure S49. Inhibition curves obtained with MeMan, βGlc-αMan (**15a**), βGlc-αMan (**15b**), $(\alpha Man)_2$ (**6**) for inhibition of GFP-PKL1162 *E. coli* with a different culture of bacteria.

Table S3. IC_{50} values as deduced from the inhibition curves obtained with MeMan, βGlc-αMan (**15a**), βGlc-αMan (**15b**), $(\alpha Man)_2$ (**6**) and corresponding RIP values; RIP_{vc} = valency-corrected relative inhibitory potency.

ENTRY	MeMan	βGlc-αMan (**15a**)	βGlc-αMan (**15b**)	$(\alpha Man)_2$ (**6**)
IC_{50}* [mM]	5.20	1.17	0.25	0.33
RIP		4.45	20.72	15.67
RIP_{vc}				7.83

* IC_{50} value determined from duplicates on the same plate.

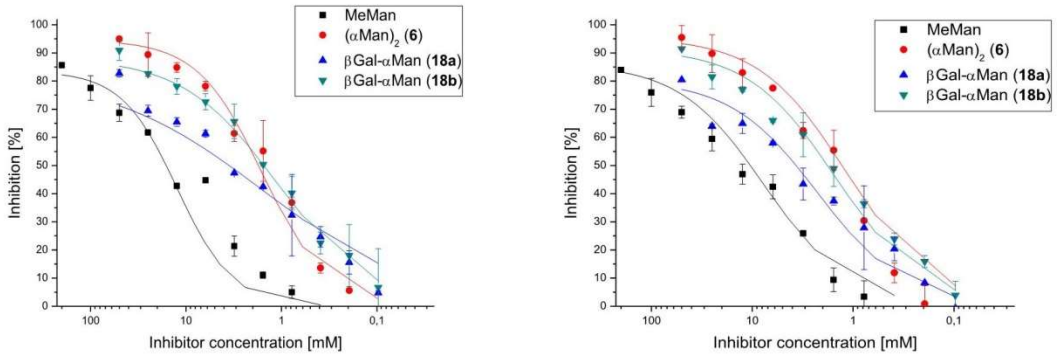

Figure S50. Inhibition curves obtained with MeMan, βGal-αMan (**18a**), βGal-αMan (**18b**), $(\alpha Man)_2$ (**6**) for inhibition of GFP-PKL1162 *E. coli*.

Table S4. IC_{50} values as deduced from the inhibition curves obtained with MeMan, βGal-αMan (**18a**), βGal-αMan (**18b**), $(\alpha Man)_2$ (**6**) and corresponding RIP values; RIP_{vc} = valency-corrected relative inhibitory potency.

ENTRY	MeMan	βGal-αMan (**18a**)	βGal-αMan (**18b**)	$(\alpha Man)_2$ (**6**)
IC_{50}* [mM]	16.14	3.53	1.54	1.75
IC_{50}* [mM]	10.49	3.68	1.80	1.29
IC_{50}* [mM] (SD)#	13.31 (±3.99)	3.61 (±0.11)	1.67 (±0.19)	1.52 (±0.32)
RIP		4.05	8.75	9.63
RIP_{vc}				4.81

* IC_{50} value determined from duplicates on the same plate.
# Standard deviation of the mean of IC_{50} values from two independent measurements.

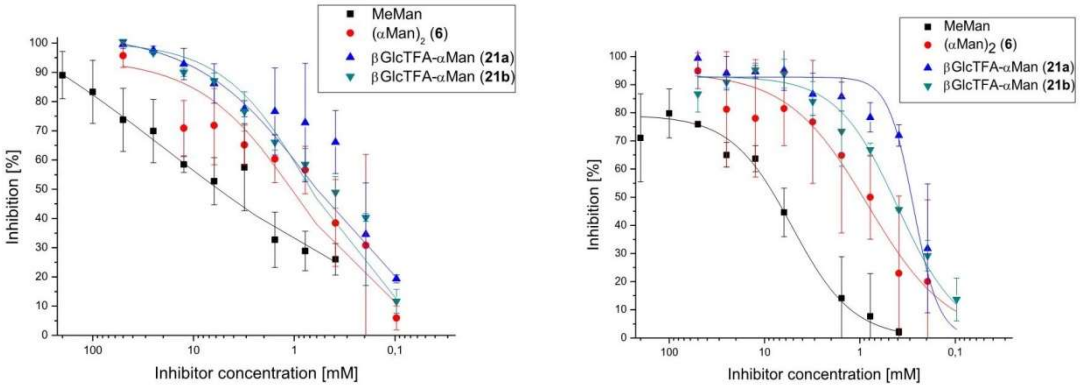

Figure S51. Inhibition curves obtained with MeMan, βGlcNTFA-αMan (**21a**), βGlcNTFA-αMan (**21b**), $(\alpha Man)_2$ (**6**) for inhibition of GFP-PKL1162 *E. coli*.

Table S5. IC_{50} values as deduced from the inhibition curves obtained with MeMan, βGlcNTFA-αMan (**21a**), βGlcNTFA-αMan (**21b**), $(\alpha Man)_2$ (**6**) and corresponding RIP values; RIP_{vc} = valency-corrected relative inhibitory potency.

ENTRY	MeMan	βGlcNTFA-αMan (**21a**)	βGlcNTFA-αMan (**21b**)	$(\alpha Man)_2$ (**6**)
IC_{50}* [mM]	6.11	0.60	0.69	1.07
IC_{50}* [mM]	7.27	0.27	0.43	0.93
IC_{50}* [mM] (SD)#	6.98 (±1.24)	0.43 (±0.23)	0.56 (±0.18)	1.00 (±0.09)
RIP		16.08	12.52	6.96
RIP_{vc}				3.48

* IC_{50} value determined from duplicates on the same plate.
# Standard deviation from the mean of IC_{50} values from two independent measurements.

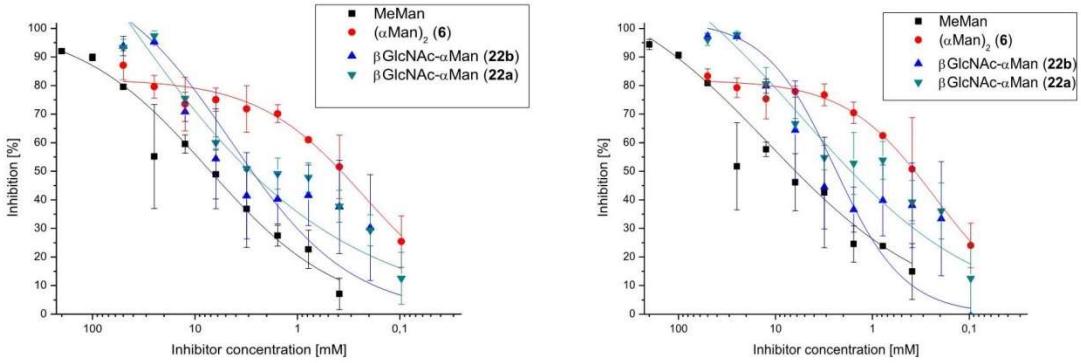

Figure S52. Inhibition curves obtained with MeMan, βGlcNAc-αMan (**22a**), βGlcNAc-αMan (**22b**), $(\alpha Man)_2$ (**6**) for inhibition of GFP-PKL1162 *E.coli*.

Table S6. IC_{50} values as deduced from the inhibition curves obtained with MeMan, βGlcNAc-αMan (**22a**), βGlcNAc-αMan (**22b**), $(\alpha Man)_2$ (**6**) and corresponding RIP values; RIP_{vc} = valency-corrected relative inhibitory potency.

ENTRY	MeMan	βGlcNAc-αMan (**22a**)	βGlcNAc-αMan (**22b**)	$(\alpha Man)_2$ (**6**)
IC_{50}* [mM]	7.15	2.93	2.77	0.37
IC_{50}* [mM]	6.19	1.68	2.37	0.38
IC_{50}* [mM] (SD)#	6.67 (±0.67)	2.31 (±0.88)	2.57 (±0.29)	0.37 (±0.01)
RIP		2.89	2.60	18.09
RIP_{vc}				9.04

* IC_{50} value determined from duplicates on the same plate.
# Standard deviation from the mean of IC_{50} values from two independent measurements.

3.4. FITC-ConA binding inhibition assays

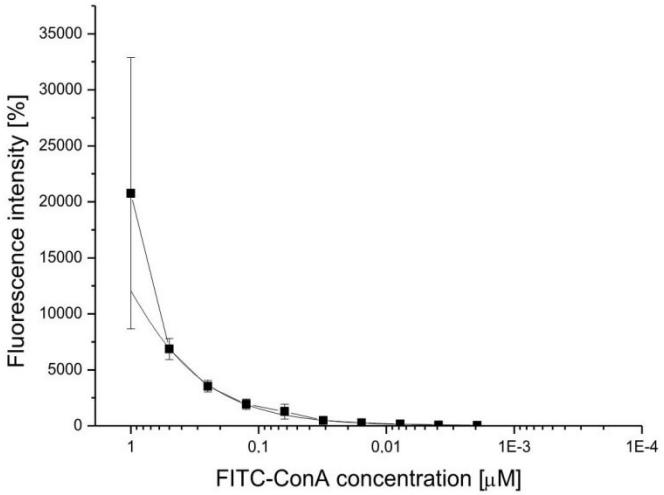

Figure S53. Fluorescence intensity of bound ConA onto a mannan-coated microplate surface at different lectin concentrations.

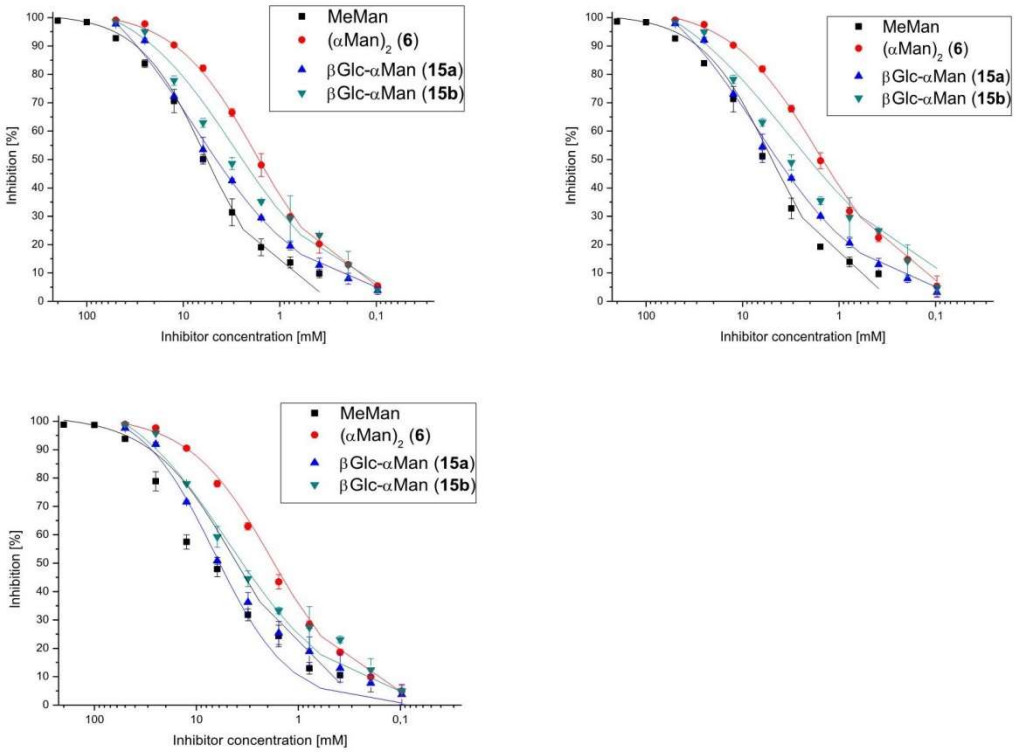

Figure S54. Inhibition curves obtained with MeMan, βGlc-αMan (**15a**), βGlc-αMan (**15b**), $(\alpha Man)_2$ (**6**) for inhibition of ConA binding.

Table S7. IC_{50} values as deduced from the inhibition curves obtained with MeMan, βGlc-αMan (**15a**), βGlc-αMan (**15b**), $(\alpha Man)_2$ (**6**) and corresponding RIP values; RIP_{vc} = valency-corrected relative inhibitory potency.

ENTRY	MeMan	βGlc-αMan (**15a**)	βGlc-αMan (**15b**)	$(\alpha Man)_2$ (**6**)
IC_{50}* [mM]	5.67	4.66	2.51	1.65
IC_{50}* [mM]	5.02	4.44	2.06	1.50
IC_{50}* [mM]	5.96	4.01	3.55	1.73
IC_{50}* [mM] (SD)#	5.55 (±0.48)	4.37 (±0.33)	2.71 (±0.76)	1.62 (±0.12)
RIP		1.27	2.05	3.41
RIP_{vc}				1.70

* IC_{50} value determined from duplicates on the same plate.
# Standard deviation of the mean of IC_{50} values from three independent measurements.

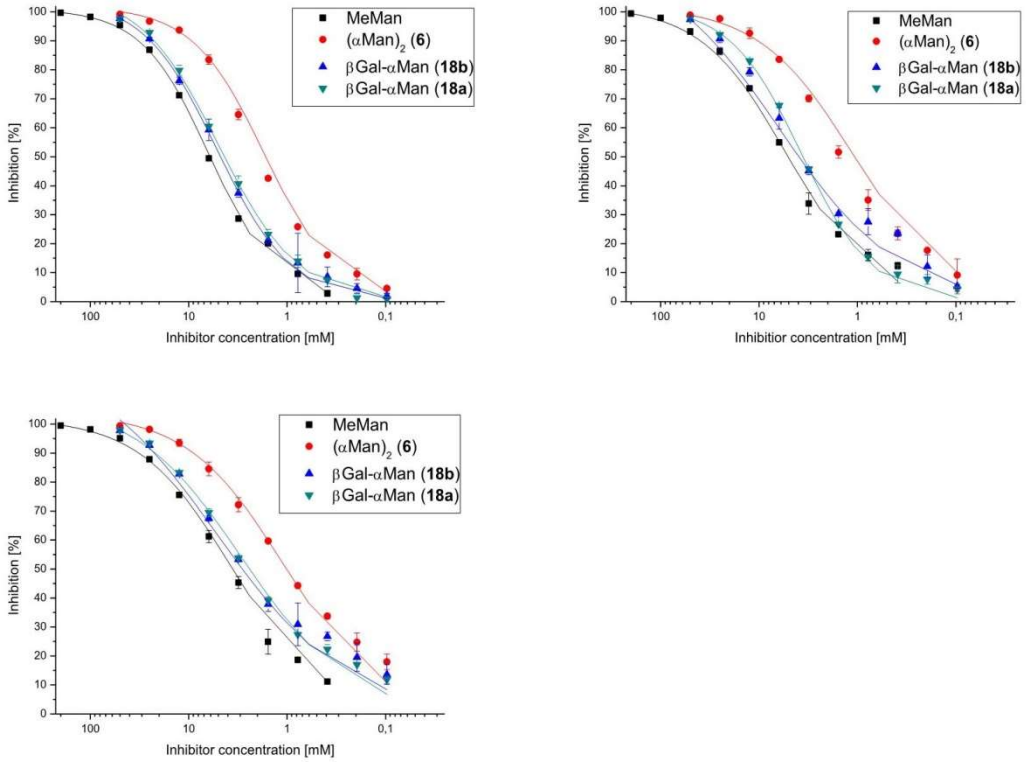

Figure S55. Inhibition curves obtained with MeMan, βGal-αMan (**18a**), βGal-αMan (**18b**), $(\alpha Man)_2$ (**6**) for inhibition of GFP-ConA conjugate.

Table S8. IC_{50} values as deduced from the inhibition curves obtained with MeMan, βGal-αMan (**18a**), βGal-αMan (**18b**), $(\alpha Man)_2$ (**6**) and calculated RIP values; RIP_{vc} = valency-corrected relative inhibitory potency.

ENTRY	MeMan	βGal-αMan (**18a**)	βGal-αMan (**18b**)	$(\alpha Man)_2$ (**6**)
IC_{50}* [mM]	6.10	4.31	4.76	1.64
IC_{50}* [mM]	5.19	3.58	3.95	1.07
IC_{50}* [mM]	3.56	2.40	2.92	1.09
IC_{50}* [mM] (SD)#	4.95 (±1.29)	3.43 (±0.97)	3.88 (±0.92)	1.27 (±0.33)
RIP		1.28	1.44	3.91
RIP_{vc}				1.95

* IC_{50} value determined from duplicates on the same plate.
# Standard deviation of the mean of IC_{50} values from three independent measurements.

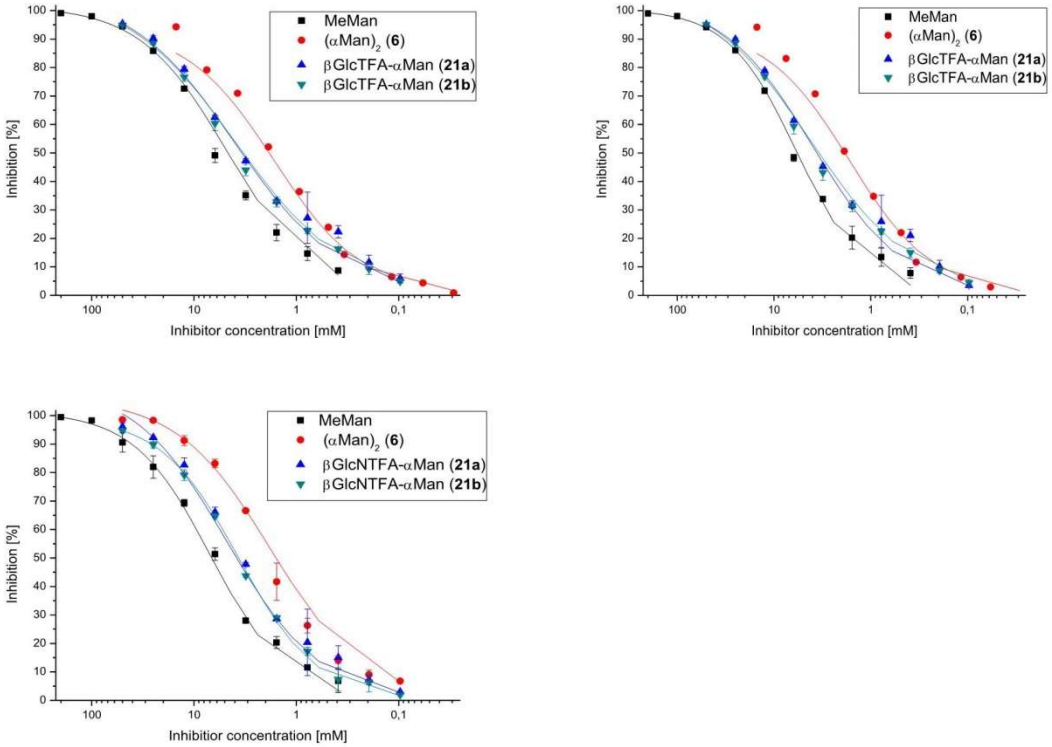

Figure S56. Inhibition curves obtained with MeMan, βGlcNTFA-αMan (**21a**), βGlcNTFA-αMan (**21b**), $(\alpha Man)_2$ (**6**) for inhibition of GFP-ConA conjugate.

Table S9. IC_{50} values as deduced from the inhibition curves obtained with MeMan, βGlcNTFA-αMan (**21a**), βGlcNTFA-αMan (**21b**), $(\alpha Man)_2$ (**6**) and calculated RIP values; RIP_{vc} = valency-corrected relative inhibitory potency.

ENTRY	MeMan	βGlcNTFA-αMan (**21a**)	βGlcNTFA-αMan (**21b**)	$(\alpha Man)_2$ (**6**)
IC_{50}* [mM]	5.85	3.48	3.75	1.885
IC_{50}* [mM]	4.69	3.49	3.40	1.88
IC_{50}* [mM]	6.80	3.85	3.66	1.58
IC_{50}* [mM] (SD)#	5.78 (±1.06)	3.60 (±0.21)	3.60 (±0.18)	1.78 (±0.17)
RIP		1.60	1.60	3.25
RIP_{vc}				1.62

* IC_{50} value determined from duplicates on the same plate.
# Standard deviation of the mean of IC_{50} values from three independent measurements.

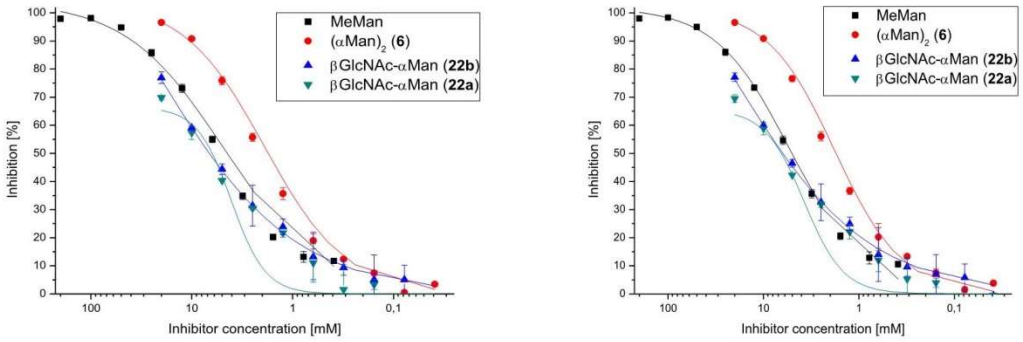

Figure S57. Inhibition curves obtained with MeMan, βGlcNAc-αMan (**22a**), βGlcNAc-αMan (**22b**), $(\alpha Man)_2$ (**6**) for inhibition of ConA binding.

Table S10. IC_{50} values as deduced from the inhibition curves obtained with MeMan, βGlcNAc-αMan (**22a**), βGlcNAc-αMan (**22b**), $(\alpha Man)_2$ (**6**) and calculated RIP values; RIP_{vc} = valency-corrected relative inhibitory potency.

ENTRY	MeMan	βGlcNAc-αMan (**22a**)	βGlcNAc-αMan (**22b**)	$(\alpha Man)_2$ (**6**)
IC_{50}* [mM]	4.509	6.38	6.85	1.76
IC_{50}* [mM]	5.01	6.58	6.27	1.77
IC_{50}* [mM] (SD)#	4.76 (±0.36)	6.48 (±0.15)	6.56 (±0.41)	1.77 (±0.01)
RIP		0.72	0.73	2.69
RIP_{vc}				1.34

* IC_{50} value determined from duplicates on the same plate.
# Standard deviation of the mean of IC_{50} values from two independent measurements.

4. Molecular modelling

Molecular modelling was performed using the Schrödinger software package implementing the Maestro interface.[9] The ligands were built using Maestro then minimized using MacroModel,[10] with the OPLS3 force field in implicit water (GB/SA continuum solvation model). The minimized structures were prepared for docking using LigPrep.[11] The docking studies were performed on the open gate (PDB code: 1klf),[12] or on the closed gate (PDB code: 1uwf) crystal structure of FimH.[13] Receptor grids suitable for docking were built with the Glide docking software,[14] by defining an outer box of 35 Å centered on the ligand from the crystal structure. Each grid was generated using the OPLS3 force field and including aromatic protons as H-bond donors. Extra precision (XP) docking was carried out with Glide, setting the ligand flexible and including aromatic protons as H-bond donors. At most ten poses per ligand were written out, discarding poses as duplicate if both RMS deviation was less than 0.5 Å and the maximum atomic displacement was less than 1.3 Å. For re-scoring, the docking outputs were processed in a MM-GBSA (molecular mechanics-generalized born surface area) calculation,[15] giving the free energy of binding in kJ mol^{-1}. The MM-GBSA calculation was performed using the VGSB solvation model and the OPLS3 force field. The extensive docking and MM-GBSA results are listed in Tables S11–S14.

Table S11. Scoring values for docking of (αMan)$_2$ (**6**), βGlc-αMan (**15a**) and βGlc-αMan (**15b**) into the open gate crystal structure of FimH.

Compound	docking score	XP GScore	glide gscore	glide evdw	glide ecoul	glide energy	glide einternal	glide emodel	XP HBond
6	-9.911	-9.911	-9.911	-23.302	-33.633	-56.935	10.285	-89.279	-5.232
6	-9.128	-9.128	-9.128	-21.57	-35.451	-57.02	9.566	-90.431	-5.232
6	-9.276	-9.276	-9.276	-20.792	-35.924	-56.716	9.047	-91.543	-5.232
6	-9.350	-9.35	-9.35	-23.475	-34.443	-57.917	9.229	-90.907	-5.232
6	-9.662	-9.662	-9.662	-23.038	-34.558	-57.596	9.317	-89.201	-5.232
6	-9.715	-9.715	-9.715	-23.399	-32.978	-56.377	0	-90.555	-5.232
6	-9.891	-9.891	-9.891	-23.38	-34.401	-57.781	10.238	-89.697	-5.232
6	-10.381	-10.381	-10.381	-22.147	-34.498	-56.644	9.189	-89.524	-5.232
15a	-9.561	-9.561	-9.561	-25.376	-32.333	-57.709	6.882	-90.972	-5.551
15a	-9.385	-9.385	-9.385	-22.8	-33.531	-56.33	0	-89.324	-5.551
15a	-10.011	-10.011	-10.011	-22.778	-36.129	-58.907	7.781	-87.294	-5.551
15a	-9.886	-9.886	-9.886	-25.168	-33.997	-59.165	14.666	-87.07	-5.551
15a	-7.792	-7.792	-7.792	-18.093	-48.505	-66.598	0	-92.914	-5.551
15a	-8.333	-8.333	-8.333	-15.145	-40.694	-55.839	4.271	-86.953	-5.551
15b	-9.340	-9.34	-9.34	-19.091	-40.007	-59.099	11.012	-90.405	-5.55
15b	-9.308	-9.308	-9.308	-24.917	-34.928	-59.846	11.312	-90.68	-5.55
15b	-8.027	-8.027	-8.027	-19.167	-46.419	-65.586	13.659	-94.252	-5.55
15b	-9.957	-9.957	-9.957	-25.245	-32.239	-57.484	7.241	-92.672	-5.55
15b	-8.263	-8.263	-8.263	-14.498	-39.951	-54.449	6.181	-91.282	-5.55
15b	-9.826	-9.826	-9.826	-20.608	-36.088	-56.695	8.681	-92.095	-5.55
15b	-8.975	-8.975	-8.975	-22.724	-38.829	-61.553	7.689	-95.696	-5.55
15b	-9.553	-9.553	-9.553	-21.923	-34.504	-56.427	8.045	-93.394	-5.55

Table S12. Scoring values for docking of (αMan)$_2$ (**6**), βGlc-αMan (**15a**) and βGlc-αMan (**15b**) into the closed gate crystal structure of FimH.

Compound	docking score	XP GScore	glide gscore	glide evdw	glide ecoul	glide energy	glide einternal	glide emodel	XP HBond
6	-8.231	-8.231	-8.231	-18.781	-41.71	-60.491	8.582	-87.755	-5.951
6	-9.825	-9.825	-9.825	-20.487	-37.603	-58.09	11.524	-93.689	-5.951
6	-8.382	-8.382	-8.382	-20.399	-39.392	-59.791	6.346	-89.738	-5.951
6	-8.216	-8.216	-8.216	-20.662	-39.353	-60.015	8.826	-87.709	-5.951
6	-8.970	-8.97	-8.97	-20.106	-36.612	-56.718	6.151	-88.568	-5.951
6	-7.520	-7.52	-7.52	-20.672	-36.596	-57.268	2.885	-87.879	-5.951
6	-7.537	-7.537	-7.537	-20.408	-36.768	-57.175	2.479	-88.307	-5.951
15a	-8.552	-8.552	-8.552	-21.329	-41.609	-62.937	5.074	-90.161	-6.075
15a	-8.544	-8.544	-8.544	-23.821	-36.981	-60.802	4.901	-87.005	-6.075
15a	-8.469	-8.469	-8.469	-20.248	-42.848	-63.096	0	-91.468	-6.075
15a	-8.495	-8.495	-8.495	-20.545	-42.625	-63.17	0	-91.32	-6.075
15b	-8.858	-8.858	-8.858	-21.274	-40.95	-62.224	6.028	-93.131	-6.326
15b	-8.277	-8.277	-8.277	-20.587	-42.272	-62.86	3.403	-88.968	-6.326

Table S13. Values of the binding energies (in kJ·mol^{-1}) obtained for the MM-GBSA calculation for (αMan)$_2$ (**6**), βGlc-αMan (**15a**) and βGlc-αMan (**15b**) into the open gate crystal structure of FimH. The docking score corresponding to each written poses given in the first column for comparison.

Compound	docking score	dG Bind	dG Bind Coulomb	dG Bind Covalent	dG Bind Hbond	dG Bind Lipo	dG Bind Solv GB	dG Bind vdW
6	-9.911	-74.892	-55.309	-1.971	-7.511	-16.383	37.241	-30.959
6	-9.128	-70.549	-51.891	3.015	-7.465	-16.918	33.670	-30.961
6	-9.276	-70.410	-53.534	3.162	-7.447	-16.938	35.305	-30.957
6	-9.350	-70.039	-55.046	-3.538	-7.155	-14.473	38.417	-28.244
6	-9.662	-62.924	-55.342	1.712	-6.018	-16.411	41.195	-28.060
6	-9.715	-61.833	-54.909	11.168	-7.484	-16.385	35.225	-29.448
6	-9.891	-57.715	-52.592	3.481	-6.831	-11.897	34.849	-24.724
6	-10.381	-57.269	-57.664	6.834	-6.832	-11.831	36.837	-24.613
15a	-9.561	-72.526	-65.907	4.953	-7.026	-16.522	42.376	-30.399
15a	-9.385	-68.562	-52.098	3.369	-7.281	-17.756	37.052	-31.849
15a	-10.011	-65.128	-50.452	0.362	-7.658	-14.922	37.836	-30.294
15a	-9.886	-64.083	-46.547	4.409	-7.171	-16.031	36.331	-35.075
15a	-7.792	-62.580	-51.413	2.124	-7.539	-11.664	36.560	-30.649
15a	-8.333	-50.782	-53.923	8.660	-8.331	-8.949	37.799	-26.038
15b	-9.340	-78.104	-67.285	1.176	-7.483	-18.111	49.247	-35.649
15b	-9.308	-73.893	-53.374	-0.924	-7.391	-16.475	39.884	-35.613
15b	-8.027	-69.051	-60.856	4.611	-6.526	-15.371	43.137	-34.046
15b	-9.957	-67.367	-60.609	1.242	-7.151	-12.859	39.782	-27.772
15b	-8.263	-63.946	-54.811	5.191	-7.036	-14.056	38.105	-31.340
15b	-9.826	-62.953	-50.106	-0.801	-7.897	-11.166	38.129	-31.112
15b	-8.975	-62.569	-48.445	-0.395	-7.885	-12.044	37.269	-31.069
15b	-9.553	-61.182	-46.916	0.242	-7.876	-11.431	37.011	-32.213

Table S14. Values of the binding energies (in kJ mol^{-1}) obtained for the MM-GBSA calculation for (αMan)$_2$ (**6**), βGlc-αMan (**15a**) and βGlc-αMan (**15b**) into the closed gate crystal structure of FimH. The docking score corresponding to each written poses given in the first column for comparison.

Compound	docking score	dG Bind	dG Bind Coulomb	dG Bind Covalent	dG Bind Hbond	dG Bind Lipo	dG Bind Solv GB	dG Bind vdW
6	-8.231	-68.407	-57.365	-2.980	-7.414	-10.908	42.112	-31.852
6	-9.825	-66.026	-53.273	-0.636	-8.672	-10.913	37.901	-30.433
6	-8.382	-63.734	-51.938	-2.362	-7.632	-11.624	42.152	-32.329
6	-8.216	-63.370	-52.692	0.826	-7.228	-9.907	34.601	-28.969
6	-8.970	-61.021	-53.255	-2.754	-7.633	-9.333	43.410	-31.457
6	-7.520	-59.634	-53.589	5.710	-7.737	-12.628	42.587	-33.979
6	-7.537	-58.512	-54.360	4.030	-6.729	-12.901	43.467	-32.020
15a	-8.552	-60.940	-51.116	-0.961	-7.607	-10.680	41.590	-32.165
15a	-8.544	-56.503	-59.698	2.167	-7.776	-8.346	45.004	-27.853
15a	-8.469	-54.699	-47.726	2.201	-6.452	-10.119	39.536	-32.139
15a	-8.495	-54.360	-61.984	4.620	-8.040	-8.317	47.700	-28.338
15b	-8.858	-70.465	-68.353	0.785	-8.317	-11.658	50.444	-33.366
15b	-8.277	-61.420	-69.895	8.510	-7.360	-10.233	45.115	-27.556

9. References

1. (a) H. Weiss and C. Unverzagt, *Angew. Chem. Int. Ed.,* 2003*,* **42***,* 4261-4263*;* (b) M. Collot and J. Savreux, J. M. Mallet, *Tetrahedron,* 2008*,* **64***,* 1523-1535.
2. (a) M. Kumari, A. Kumar Singh, S. Kumar, K. Achazi, S. Gupta, R. Haag and S. K. Sharma, *Polym. Adv. Technol*., 2014, **25**, 1208-1215; (b) M. Cortes-Clerget, O. Gager, M. Monteil, J. L. Pirat, E. Migianu-Griffoni, J. Deschamp and M. Lecouvey, *Adv. Synth. Catal*., 2016, **358**, 34-40; (c) D. Bélanger, X. Tong, S. Soumaré, Y. L. Dory and Y. Zhao, *Chem. Eur. J.*, 2009, **15**, 4428-4436; (d) P. P. Phadnis and G. Mugesh, *Org. Biomol. Chem*., 2005, **3**, 2476-2481.
3. (a) A. Avenoza, C. Cativiela, F. Corzana, J. M. Peregrina and M. M. Zurbano, *Synthesis*, 1997, 1146-1150; (b) A. Ollivier, M. Goubert, A. Tursun, I. Canet and M. E Sinibaldi, *Arkivoc* (ix), 2010, 108-126.
4. E. D. Goddard-Borger and T. V. Stick, *Org. Lett.,* 2007, **9**, 3797-3800.
5. (a) P. Busca and O. R. Martin, *Tetrahedron Lett.,* 1998, **39**, 8101-8104; (b) V. W.-F. Tai and B. Imperiali, *J. Org. Chem.*, 2001, **66**, 6217-6228.
6. M. Hartmann, A. K. Horst, P. Klemm and T. K. Lindhorst, *Chem. Commun*., 2010, **46**, 330-332.
7. I. Baussanne, J. M. Benito, C. Ortiz Mellet, J. M. García Fernández and J. Defaye, *ChemBioChem*, 2001, **2**, 777-783.
8. (a) N. Firon, I. Ofek, N. Sharon, *Biochem. Biophys. Res. Commun*., 1982, **105**, 1426-1432; (b) N. Firon, S. Ashkenazi, D. Mirelman, I. Oftek, N. Sharon, *Infect. Immun*., 1987, **55**, 472-476.
9. Schrödinger Release 2017-4: Maestro, version 10.5, Schrödinger, LLC, New York, NY, 2017.
10. Schrödinger Release 2017-4: MacroModel, version 11.1, Schrödinger, LLC, New York, NY, 2017.
11. Schrödinger Release 2017-4: LigPrep, Schrödinger, LLC, New York, NY, 2017**.**
12. C. S. Hung, J. Bouckaert, D. Hung, J. Pinkner, C. Widberg, A. DeFusco, C. G. Auguste, R. Strouse, S. Langermann, G. Waksman and S. J. Hultgren, *Mol. Microbiol.*, 2002, **44**, 903-15.
13. J Bouckaert, J. Berglund, M. Schembri, E. De Genst, L. Cools, M. Wuhrer, C.-S. Hung, J. Pinkner, R. Slättegård, A. Zavialov, D. Choudhury, S. Langermann, S. J. Hultgren, L. Wyns, P. Klemm, S. Oscarson, S. D. Knight and H. De Greve, *Mol. Microbiol*., 2005, **55**, 441-455.
14. Schrödinger Release 2017-4: Glide, version 7.0, Schrödinger, LLC, New York, NY, 2017.
15. Schrödinger Release 2017-4: Prime, Schrödinger, LLC, New York, NY, 2017.

8.4 Synthetic procedures for Chapter 5

For the characterization of serine-derived enantiomeric scaffolds, the carbon atoms of the core moiety are numbered as described in **Figure 8.31**. Diastereomers derived from on D-serine are specified by an "a", and their diastereomeric counterparts, based on the L-serine scaffold as "b". Compounds are named according to IUPAC nomenclature.

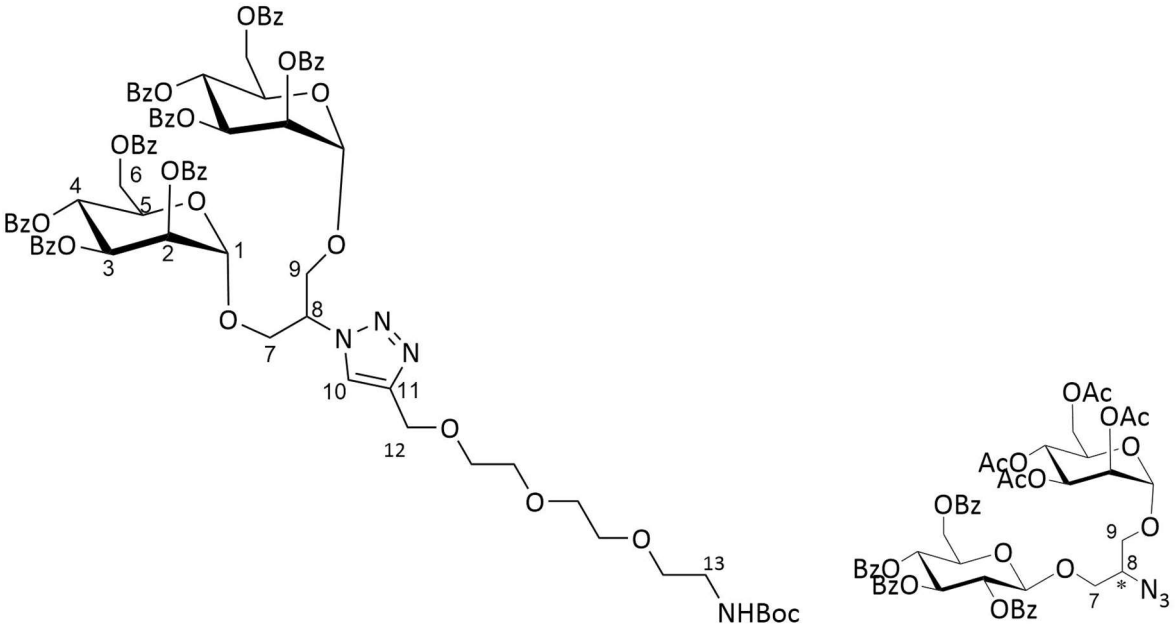

Figure 8.31: Atom numbering for NMR data description of individual substrates.

General procedure for copper(I)-catalyzed azide-alkyne cycloaddition (CuAAC) reaction (general procedure A). The azide moiety and alkyne moiety (2 eq.) were dissolved in *N*,*N*-dimethylformamide (*c* = 0.08 M). Sodium ascorbate (2 eq.) and copper(II) sulphate (1 eq.) were dissolved in water (*N*,*N*-dimethylformamide/water 4/1) and after sonication for cca. 30 min were added to the reaction mixture. The reaction was stirred at room temperature for 12 h then diluted with dichloromethane and 0.1 N ethylenediamine solution in water was added. Aq. phases were extracted with dichloromethane then collected organic phases were dried with magnesium sulfate, filtrated and concentrated. The residue was purified by flash chromatography to afford the expected compound.

General procedure for ester cleavage and subsequent *N*H-Boc cleavage (general procedure B). Ester-protected glycocluster was dissolved in anhydrous methanol (*c* = 0.03 M). Then sodium methoxide (*c* = 5.4 M in methanol, two drops) was added and the mixture was stirred at

room temperature until completion. Then the resulting mixture was neutralized with Amberlite IR120-H^+, diluted with methanol, filtered and concentrated. The residue was taken up into a 1:1 mixture of water and methanol then washed with diethyl ether and the combined aqueous layers were concentrated to dryness. The residue was purified by size exclusion chromatography on Sephadex G10 gel eluted with deionized water. Then the unprotected compound was dissolved in water/trifluoroacetic acid 4/1 and sonicated till the reaction completion. The residue was concentrated till dryness then dissolved in the minimum amount of water then taken to microfiltration and liophylizatation to afford the expected compound.

3-(2-(2-(2-Chloroethoxy)ethoxy)ethoxy)prop-1-yne (2). 60 % sodium hydride in mineral oil (1.80 g, 44 mmol, 1.5 eq.) and 80 % wt. propargyl bromide (9.80 mL, 88 mmol, 3 eq.) were added under inert atmosphere to the solution of alcohol **1** (5.00 g, 29.0 mmol) in anhydrous *N*,*N*-dimethylformamide (*c* = 0.1 M, 30.0 mL) at 0 °C. The reaction was stirred until completion then water was added and aqueous phases were extracted with ethyl acetate. Combined organic phases were dried over magnesium sulfate, filtrated and concentrated. Flash chromatography with ethyl acetate/cyclohexane 1.5/8.5 yielded compound **2** as a yellow oil (3.30 g, 55 %). Analytical and spectroscopy data were found to be in the agreement with the literature.[139]

3-(2-(2-(2-Azidoethoxy)ethoxy)ethoxy)prop-1-yne (3). Sodium azide (3.00 g, 45.1 mmol, 3 eq.) was added under an inert atmosphere to the compound **2** (3.32 g, 15.2 mmol) in anhydrous *N*,*N*-dimethylformamide (*c* = 0.5 M, 30.0 mL). The reaction was stirred at 80 °C until completed and water was poured in. Aqueous phases were extracted with ethyl acetate (3x 50 mL) and the collected organic phases were washed with brine, dried with magnesium sulfate, filtrated and concentrated. Flash chromatography with ethyl acetate/cyclohexane 2/8 yielded compound **3** as a yellow liquid (1.46 g, 45 %). Analytical and spectroscopy data were found to be in the agreement with the literature.[140]

2-(2-(-(Prop-2-yn-1-yloxy)ethoxy)ethoxy)ethanamine (4). To the starting material **3** (1.40 g, 6.0 mmol) in tetrahydrofuran (*c* = 0.5 M, 120 mL), water (12.0 mL) and triphenylphosphine (4.72 g, 18.0 mmol, 3 eq.) were added and the reaction mixture was stirred for 16 h then concentrated. Flash chromatography with dichloromethane/methanol/ammonium solution

80/19/1 yielded compound **4** as yellow oil (1.18 g, 98 %). Analytical and spectroscopy data were found to be in the agreement with the literature.[141]

***N*-*tert*-Butyl-(2-(2-(prop-2-yn-1-yloxy)ethoxy)ethoxy)ethyl) carbamate (5).**
4-Dimethylaminopydridine (146 mg, 1.21 mmol, 0.2 eq.) and di-*tert*-butyl bicarbonate (2.00 g, 9.10 mmol, 1.5 eq.) were added to the compound **4** in anhydrous tetrahydrofuran (*c* = 0.2 M, 30.0 mL) at 0 °C. The reaction mixture was stirred for 3 h at room temperature then concentrated. The residue was dissolved with ethyl acetate and washed with brine, 1 N hydrochloride acid and collected organic phases were dried over magnesium sulfate and then concentrated. Flash chromatography with ethyl acetate/cyclohexane 1/9 to 4/6 yielded compound **5** as a yellow oil (715 mg, 42 %). Analytical and spectroscopy data were found to be in the agreement with the literature.[142]

2-{1-[*N*-*tert*-Butyl-(2-(2-methoxyethoxy)ethyl)carbamoyl]-1*H*-1,2,3-triazol-4-yl}-1,3-di-*O*-(2,3,4,6-tetra-*O*-benzoyl-α-D-mannopyranosyl)-1,3-propanediol (7). General procedure A was applied to the azidodisaccharide residue **6**[104] (210 mg, 171 µmol) and propargylated linker **5** (54.0 mg, 188 µmol, 1.1 eq.) in *N*,*N*-dimethylformamide (*c* = 0.075 M, 2.30 mL). The mixture of sodium ascorbate (67.0 mg, 342 µmol, 2 eq.) in 550 µL water and copper(II) sulfate (42.0 mg, 331 µmol, 1 eq.) after sonicated for cca. 10 min were added to the reaction mixture. The mixture was stirred until completed and then diluted with dichloromethane and 0.1 N ethylenediamine solution was added. Aqueous phases were extracted with dichloromethane then collected organic phases were dried with magnesium sulfate, filtrated and concentrated. Flash chromatography with ethyl acetate/cyclohexane 20/1 to 7/3 yielded compound **7** as an amorphous solid (101 mg, 50 %); R_f = 0.3 (ethyl acetate/cyclohexane 7/3); ^{1}H NMR (500 MHz, $CDCl_3$) δ 8.11-8.08 (m, 4H, 4 H-Ar), 8.02-7.92 (m, 9H, 8 H-Ar, H-10), 7.82-7.79 (m, 4H, 4 H-Ar), 7.61-7.53 (m, 4H, 4 H-Ar), 7.51-7.30 (m, 16H, 16 H-Ar), 7.27-7.25 (m, 2H, 2 H-Ar), 7.25-7.24 (m, 2H, 2 H-Ar), 6.15-6.09 (m, 2H, 2 H-4$_{Man}$), 5.83 (dd, $^3J_{3,4}$ = 10.2 Hz, $^3J_{2,3}$ = 3.3 Hz, 1H, H-3$_{Man}$), 5.73-5.68 (m, 2H, H-2$_{Man}$, H-3$_{Man}$), 5.66 (dd, $^3J_{2,3}$ = 3.2 Hz, $^3J_{1,2}$ = 1.8 Hz, 1H, H-2$_{Man}$), 5.19 (br s, 2H, H-1$_{Man}$, H-8), 5.11 (d, $^3J_{1,2}$ = 1.6 Hz, 1H, H-1$_{Man}$), 4.85-4.77 (m, 2H, H-12 ethylene), 4.77-4.65 (m, 2H, 2 H-6a$_{Man}$), 4.59-4.38 (m, 4H, 2 H-6b$_{Man}$, H-7a, H-9a), 4.37-4.29 (m, 1H, H-5$_{Man}$), 4.23 (dd, ^3J = 10.8 Hz, ^3J = 6.4 Hz, 1H, H-7b or H-9b), 4.16-4.13 (m, 1H, H-7b or H-9b), 4.10-4.06 (m, 1H, H-5$_{Man}$), 3.72 (t, ^3J = 4.8 Hz, 2H, 2 H-ethylene), 3.66-3.58 (m, 2H, 2 H-ethylene), 3.54 (br s, 4H, 4 H-ethylene), 3.47 (t, ^3J = 5.1 Hz, 2H, 2 H-etyhlene),

3.29-3.25 (m, 2H, H-13 ethylene), 1.43 (s, 9H, NH-$CO_2C(C\underline{H}_3)_3$) ppm; ^{13}C NMR (126 MHz, $CDCl_3$) δ 166.1, 166.0, 165.5, 165.4, 165.3, 165.2, (8C, 4 $CH_3\underline{C}$=O, 4 Ph$\underline{C}$=O) 145.4 (C-11), 133.5, 133.2, 133.1, 133.0, 129.9, 129.8, 129.7, 129.1, 128.9, 128.8, 128.6, 128.5, 128.4, 128.3 (20C, 20 C-Ar), 98.3, 97.7 (2C, 2 C-1_{Man}), 70.5, 70.4, 70.2 (4C, 4 C-ethylene), 70.0, 69.9 (4C, 2 C-2_{Man}, 2 C-3_{Man}), 69.8 (C-ethylene), 69.6, 69.4 (2C, 2 C-5_{Man}), 67.2, 66.6 (2C, C-7, C-9), 66.2 (2C, C-4_{Man}), 64.5 (C-12 ethylene), 62.5, 62.3 (2C, 2 C-6_{Man}), 60.0 (C-8), 40.2 (C-13 ethylene), 28.40 (NH-$CO_2C(\underline{C}H_3)_3$) ppm; ESI-HRMS: m/z calcd. for $C_{85}H_{85}N_4O_{25}$: 1561.54832; found 1561.54974.

2-{1-[(2-(2-Methoxyethoxy)ethyl)amino]-1*H*-1,2,3-triazol-4-yl}-1,3-di-*O*-(α-D-mannopyranosyl)-1,3-propanediol (8). General procedure B was applied to starting material **7** (90.0 mg, 576 µmol). Reagents and conditions: sodium methoxide (2-3 drops), anhydrous methanol (*c* = 0.03 M, 2.00 mL). Size exclusion chromatography G10 in water yielded precursor molecule (26.0 mg, 72 %). The residue was dissolved in water/trifluoroacetic acid 4/1 and sonicated for 1 h then concentrated till dryness. The residue was taken to microfiltration and lyophilisation what yielded compound **8** as white foam (100 mg, quantitativ); $[\alpha]_{20}^{D}$= + 400 (*c* 1 , dd water); ^{1}H NMR (600 MHz, D_2O) δ 8.19 (s, 1H, H-10), 5.18-5.14 (m, 1H, H-8), 4.79 (d, $^3J_{1,2}$ = 1.4 Hz, 1H, H-1_{Man}), 4.73 (d, $^3J_{1,2}$ = 1.3 Hz, 1H, H-1_{Man}), 4.68 (s, 2H, H-12 ethyelene), 4.19 (dd, ^2J = 10.8 Hz, ^3J = 8.0 Hz, 1H, H-7a or H-9a), 4.14 (dd, ^2J = 11.1 Hz, ^3J = 4.2 Hz, 1H, H-7a or H-9a), 4.01 (dd, ^2J = 11.0 Hz, ^3J = 7.6 Hz, 1H, H-7b or H-9b), 3.95 (dd, ^2J= 10.8 Hz, ^3J = 3.9 Hz, 1H, H-7b or H-9b), 3.84 (br s, 1H, H-2_{Man}), 3.80-3.75 (m, 2H, H-2_{Man}, H-$6a_{Man}$), 3.74-3.72 (m, 3H, H-$6a_{Man}$, 2 H-ethylene), 3.70-3.61 (m, 11H, 2 H-$6b_{Man}$, 8 H-ethylene, H-3_{Man}), 3.60-3.52 (m, 3H, H-3_{Man}, 2 H-4_{Man}), 3.35-3.32 (m, 1H, H-5_{Man}), 3.21-3.15 (m, 2H, H-13 ethylene), 3.06-3.00 (m, 1H, H-5_{Man}) ppm; ^{13}C NMR (151 MHz, D_2O) δ 144.0 (C-11), 124.9 (C-10), 100.4, 99.6 (2C, 2 C-1_{Man}), 73.1, 73.0 (2C ,2 C-5_{Man}), 70.4 (2C, C-3_{Man}), 69.8 (2C, 2 C-2_{Man}), 69.7, 69.5, 69.5 (2C, 2 C-ethylene), 68.8 (C-ethylene), 66.5 (2C, 2 C-4_{Man}), 66.4 (C-ethylene), 66.3, 66.0 (2C, C-7, C-9), 62.9 (C-12 ethylene), 61.0 (C-8), 60.8, 60.7 (2C, 2 C-6_{Man}), 39.1 (C-13ethylene) ppm; IR (ATR) ν_{max}/cm^{-1} 3354, 2929, 1686, 1050, 646; ESI-HRMS: m/z calcd. for $C_{24}H_{45}N_4O_{15}$ + H^+: 629.28759 $[M+H]^+$; found 629.28773.

(*S*)-2-Azido-1-*O*-(2,3,4,6-tetra-*O*-acetyl-α-D-mannopyranosyl)-3-*O*-(2,3,4,6-tetra-*O*-benzoyl-β-D-glucopyranosyl)-1,3-propanediol (9a). White foam; R_f = 0.3 (ethyl acetate/cyclohexane 4/6); ^{1}H NMR (600 MHz, $CDCl_3$) δ 8.03 (dd, *J* = 7.2 Hz, *J* = 1.1 Hz, 2H, 2 H-Ph_{ortho}), 7.97 (dd, *J* =

8.2 Hz, *J* = 1.0 Hz, 2H, 2 H-Ph$_{ortho}$), 7.90 (dd, *J* = 8.2 Hz, *J* = 1.0 Hz, 2H, 2 H-Ph$_{ortho}$), 7.82 (dd, *J* = 8.2 Hz, *J* = 1.0 Hz, 2H, 2 H-Ph$_{ortho}$), 7.59-7.47 (m, 3H, 3 H-Ar), 7.43-7.27 (m, 9H, 9 H-Ar), 5.91 (dd, $^3J_{2,3}$ = $^3J_{3,4}$ = 9.7 Hz, 1H, H-3$_{Glc}$), 5.71 (dd, $^3J_{3,4}$ = $^3J_{4,5}$ = 9.7 Hz, 1H, H-4$_{Glc}$), 5.54 (dd, $^3J_{2,3}$ = 9.7 Hz, $^3J_{1,2}$ = 7.9 Hz, 1H, H-2$_{Glc}$), 5.31-5.21 (m, 3H, H-2$_{Man}$, H-3$_{Man}$, H-4$_{Man}$), 4.94 (d, $^3J_{1,2}$ = 7.8 Hz, 1H, H-1$_{Glc}$), 4.77 (d, $^3J_{1,2}$ = 1.4 Hz, 1H, H-1$_{Man}$), 4.67 (dd, $^2J_{6a,6b}$ = 12.2 Hz, $^3J_{5,6a}$ = 3.1 Hz, 1H, H-6a$_{Glc}$), 4.51 (dd, $^3J_{6a,6b}$ = 12.2 Hz, $^3J_{5,6b}$ = 4.8 Hz, 1H, H-6b$_{Glc}$), 4.25 (dd, $^2J_{6a,6b}$ = 12.3 Hz, $^3J_{5,6a}$ = 5.2 Hz, 1H, H-6a$_{Man}$), 4.19-4.16 (m, 1H, H-5$_{Glc}$), 4.07-4.01 (m, 2H, H-6b$_{Man}$, H-9a), 4.00-3.92 (m, 1H, H-5$_{Man}$), 3.82-3.66 (m, 3H, H-8, H-7a, H-9b), 3.47 (dd, $^2J_{9a,9b}$ = 10.3 Hz, $^3J_{8,9b}$ = 5.6 Hz, 1H, H-7b), 2.15 (s, 3H, C$\underline{H}_3$C=O), 2.08 (s, 3H, C$\underline{H}_3$C=O), 2.04 (s, 3H, C$\underline{H}_3$C=O), 1.99 (s, 3H, C$\underline{H}_3$C=O) ppm; ^{13}C NMR (151 MHz, $CDCl_3$) δ 170.6, 170.0, 169.8, 169.7, 166.1, 165.8, 165.2, 165.1 (8C, 4 Ph$\underline{C}$=O, 4 $CH_3\underline{C}$=O), 133.5, 133.3, 133.2, 129.9, 129.8, 129.6, 129.2, 128.8, 128.4, 128.3 (20C, 20 C-Ar), 101.4 (C-1$_{Glc}$), 97.9 (C-1$_{Man}$), 72.8 (C-3$_{Glc}$), 72.7 (C-5$_{Glc}$), 72.4 (C-2$_{Glc}$), 71.7 (C-4$_{Glc}$), 69.1 (C-9), 68.9, 68.7, 68.6 (3C, C-3$_{Man}$, C-4$_{Man}$, C-5$_{Man}$), 67.7 (C-7), 65.9 (C-2$_{Man}$), 62.8 (C-6$_{Glc}$), 62.3 (C-6$_{Man}$), 60.2 (C-8), 20.9, 20.7, (4C, $\underline{C}H_3$C=O) ppm.

(*R*)-2-Azido-1-*O*-(2,3,4,6-tetra-*O*-acetyl-α-D-mannopyranosyl)-3-*O*-(2,3,4,6-tetra-*O*-benzoyl-β-D-glucopyranosyl)-1,3-propanediol (9b). White foam; R_f = 0.3 (ethyl acetate/cyclohexane 4/6); ^{1}H NMR (600 MHz, $CDCl_3$) δ 8.03 (dd, *J* = 8.2 Hz, *J* = 1.0 Hz, 2H, 2 H-Ph$_{ortho}$), 7.96 (dd, *J* = 8.2 Hz, *J* = 1.0 Hz, 2H, 2 H-Ph$_{ortho}$), 7.90 (dd, *J* = 8.2 Hz, *J* = 1.0 Hz, 2H, 2 H-Ph$_{ortho}$), 7.82 (dd, *J* = 8.2 Hz, *J* = 1.0 Hz, 2H, 2 H-Ph$_{ortho}$), 7.59-7.47 (m, 3H, 3 H-Ar), 7.46-7.26 (m, 9H, 9 H-Ar), 5.90 (dd, $^3J_{2,3}$ = $^3J_{3,4}$ = 9.7 Hz, 1H, H-3$_{Glc}$), 5.68 (dd, $^3J_{3,4}$ = $^3J_{4,5}$ = 9.7 Hz, 1H, H-4$_{Glc}$), 5.51 (dd, $^3J_{2,3}$ = 9.7 Hz, $^3J_{1,2}$ = 7.9 Hz, 1H, H-2$_{Glc}$), 5.32-5.18 (m, 3H, H-2$_{Man}$, H-3$_{Man}$, H-4$_{Man}$), 4.90 (d, $^3J_{1,2}$ = 7.8 Hz, 1H, H-1$_{Glc}$), 4.75 (d, $^3J_{1,2}$ = 1.4 Hz, 1H, H-1$_{Man}$), 4.66 (dd, $^2J_{6a,6b}$ = 12.2 Hz, $^3J_{5,6a}$ = 3.1 Hz, 1H, H-6a$_{Glc}$), 4.51 (dd, $^2J_{6a,6b}$ = 12.2 Hz, $^3J_{5,6b}$ = 4.8 Hz, 1H, H-6b$_{Glc}$), 4.25 (dd, $^2J_{6a,6b}$ = 12.3 Hz, $^3J_{5,6a}$ = 5.2 Hz, 1H, H-6a$_{Man}$), 4.19-4.17 (m, 1H, H-5$_{Glc}$), 4.03 (dd, $^2J_{6a,6b}$ = 12.3 Hz, $^3J_{5,6b}$ = 2.3 Hz, 1H, H-6b$_{Man}$), 3.97 (dd, $^2J_{7a,7b}$ = 10.5 Hz, $^3J_{7a,8}$ = 4.8 Hz, 1H, H-7a), 3.94-3.88 (m, 1H, H-5$_{Man}$), 3.80-3.76 (m, 1H, H-8), 3.75-3.70 (m, 2H, H-8b, H-9a), 3.58 (dd, $^2J_{9a,9b}$ = 10.2 Hz, $^3J_{8,9b}$ = 3.7 Hz, 1H, H-9b), 2.15 (s, 3H, C$\underline{H}_3$C=O), 2.09 (s, 3H, C$\underline{H}_3$C=O), 2.02 (s, 3H, C$\underline{H}_3$C=O), 1.98 (s, 3H, C$\underline{H}_3$C=O) ppm; ^{13}C NMR (151 MHz, $CDCl_3$) δ 170.7, 169.9, 169.8, 169.7, 166.1, 165.8, 165.2, 165.0 (8C, 4 Ph$\underline{C}$=O, 4 $CH_3\underline{C}$=O), 133.5, 133.3, 133.2, 129.9, 129.8, 129.7, 129.5, 129.2, 128.7, 128.5, 128.4, 128.33 (20C, 20 C-Ar), 101.5 (C-1$_{Glc}$), 97.7 (C-1$_{Man}$), 72.8 (C-3$_{Glc}$), 72.5 (C-3$_{Glc}$), 72.4 (C-4$_{Glc}$), 71.7 (C-2$_{Glc}$), 69.5, 69.2 (3C, C-3$_{Man}$, C-4$_{Man}$, C-5$_{Man}$), 68.9 (C-5$_{Glc}$),

68.5 (C-9), 67.3 (C-7), 65.8 (C-2_{Man}), 62.9 (C-6_{Glc}), 62.3 (C-6_{Man}), 59.7 (C-8), 20.9, 20.8, 20.7, (4C, 4 $\underline{C}H_3C$=O) ppm.

(*S*)-2-{1-[*N*-*tert*-Butyl-(2-(2-methoxyethoxy)ethyl)carbamoyl]-1*H*-1,2,3-triazol-4-yl}-1-*O*-(2,3,4,6-tetra-*O*-acetyl-α-D-mannopyranosyl)-3-*O*-(2,3,4,6-tetra-*O*-benzoyl-β-D-glucopyranosyl)-1,3-propanediol (10a). General procedure A was applied to the azido disaccharide residue **9a** (308 mg, 301 µmol) and propargylated linker **5** (9.0 mg, 331 µmol, 1.1 eq.) in *N*,*N*-dimethylformamide (*c* = 0.08 M, 3.20 mL). The mixture of sodium ascorbate (120 mg, 602 µmol, 2 eq.) in 800 µL water and copper(II) sulfate (8.20 mg, 331 µmol, 1 eq.) was sonicated for cca. 10 min and then added to the reaction mixture. The mixture was stirred until completed then diluted with dichloromethane and 0. 1 N ethylenediamine solution in water was added. Aqueous phases were extracted with dichloromethane then collected organic phases were dried with magnesium sulfate, filtrated and concentrated. Flash chromatography with ethyl acetate/cyclohexane 9/1 yielded compound **10a** as translucent gel (334 mg, 85 %); R_f = 0.3 (ethyl acetate/cyclohexane 9/1); ^{1}H NMR (500 MHz, MeOD) δ 8.09-8.04 (m, 2H, 2 H-Ar), 7.98 (s, 1H, H-10), 7.94-7.88 (m, 4H, 4 H-Ar), 7.81-7.79 (m, 2H, 2 H-Ar), 7.67-7.54 (m, 3H, 3 H-Ar), 7.53-7.38 (m, 7H, 7 H-Ar), 7.37-7.30 (m, 2H, 2 H-Ar), 5.99 (dd, $^3J_{2,3}$ = $^3J_{3,4}$ = 9.7 Hz, 1H, H-3_{Glc}), 5.72 (dd, $^3J_{3,4}$ = $^3J_{4,5}$ = 9.7 Hz, 1H, H-4_{Glc}), 5.46 (dd, $^3J_{2,3}$ = 9.8 Hz, $^3J_{1,2}$ = 7.9 Hz, 1H, H-2_{Glc}), 5.21 (dd, $^3J_{3,4}$ = $^3J_{4,5}$ = 9.9 Hz, 1H, H-4_{Man}), 5.17-5.13 (m, 3H, H-1_{Glc}, H-3_{Man}, H-8), 5.12 (dd, $^3J_{2,3}$ = 3.3 Hz, $^3J_{1,2}$ = 1.7 Hz, 1H, H-2_{Man}), 4.72 (d, $^3J_{1,2}$ = 1.7 Hz, 1H, H-1_{Man}), 4.70-4.54 (m, 2H, H-6_{Glc}), 4.46-4.40 (m, 2H, H-5_{Glc}, H-$6a_{Man}$), 4.38 (br s, 2H, H-12 ethylene), 4.28 (dd, $^2J_{6a,6b}$ = 10.9 Hz, $^3J_{5,6b}$ = 7.6 Hz, 1H, H-$6b_{Man}$), 4.21-4.07 (m, 2H, H-7a, H-9a), 4.02 (dd, $^2J_{7a,7b}$ = 12.3 Hz, $^3J_{7b,8}$ =2.4 Hz, 1H, H-7b), 3.95 (dd, $^2J_{9a,9b}$ = 10.9 Hz, $^3J_{8,9b}$ = 7.0 Hz, 1H, H-9b), 3.72-3.68 (m, 1H, H-5_{Man}), 3.66-3.61 (m, 6H, 6 H-ethylene), 3.60-3.56 (m, 2H, 2 H-ethylene), 3.53 (t, ^3J = 5.6 Hz, 2H, 2 H-ethylene), 3.24 (t, ^3J = 5.6 Hz, 2H, H-13 ethylene), 2.13 (s, 3H, C$\underline{H}_3$C=O), 2.06 (s, 3H, C$\underline{H}_3$C=O), 2.06 (s, 3H, C$\underline{H}_3$C=O), 1.97 (s, 3H, C$\underline{H}_3$C=O), 1.44 (s, 9H, NH-CO_2C(C$\underline{H}_3$)$_3$) ppm; ^{13}C NMR (126 MHz, MeOD) δ 172.3, 171.5, 171.4, 167.5, 167.0, 166.7, 166.6 (8C, 4 $CH_3\underline{C}$=O, 4 Ph$\underline{C}$=O), 145.0 (C-11), 134.8, 134.6, 134.5, 130.9, 130.7, 130.6, 130.3, 130.2, 130.1, 129.8, 129.7, 129.6, 129.5, 125.2 (21C, 20 C-Ar, C-10), 102.2 (C-1_{Glc}), 99.2 (C-1_{Man}), 74.4 (C-3_{Glc}), 73.3 (2C, C-2_{Glc} and C-5_{Glc}), 71.6, 71.5, 71.3, 71.1 (4C, 4 C-ethylene), 70.9 (C-4_{Glc}), 70.6, 70.3, 70.2 (4 C, C-4_{Glc}, C-2_{Man}, C-3_{Man}, C-5_{Man}), 69.4 (C-6_{Man}), 68.1 (C-9), 66.9 (C-4_{Man}), 64.8 (C-10), 63.9

(C-6_{Glc}), 63.3 (C-7), 61.9 (C-8), 41.0 (C-13 etyhelene), 28.8 (NH-$CO_2C(\underline{C}H_3)_3$), 20.7, 20.7, 20.6 (4C, 4 $\underline{C}H_3C$=O) ppm.

(*R*)-2-{1-[*N*-*tert*-Butyl-(2-(2-methoxyethoxy)ethyl)carbamoyl]-1*H*-1,2,3-triazol-4-yl}-1-*O*-(2,3,4,6-tetra-*O*-acetyl-α-D-mannopyranosyl)-3-*O*-(2,3,4,6-tetra-*O*-benzoyl-β-D-glucopyranosyl)-1,3-propanediol (10b). General procedure A was applied to the azido disaccharide residue **9b** (308 mg, 301 µmol) and propargylated linker **5** (9.0 mg, 331 µmol, 1.1 eq.) in *N*,*N*-dimethylformamide (*c* = 0.08 M, 3.20 mL). The mixture of sodium ascorbate (120 mg, 602 µmol, 2 eq.) in 800 µL water and copper(II) sulfate (8.20 mg, 331 µmol, 1 eq.) was sonicated for cca. 10 min then added to the reaction mixture. The mixture was stirred until completed then diluted with dichloromethane and 0.1 N ethylenediamine solution in water was added. Aqueous phases were extracted with dichloromethane then collected organic phases were dried with magnesium sulfate, filtrated and concentrated. Flash chromatography with ethyl acetate/cyclohexane 9/1 yielded compound **10b** as translucent gel (290 mg, 73 %); R_f = 0.3 (ethyl acetate/cyclohexane 9/1); ^{1}H NMR (500 MHz, MeOD) δ 8.09-8.05 (m, 2H, 2 H-Ar), 7.99-7.89 (m, 4H, 4 H-Ar, H-10), 7.81-7.79 (m, 2H, 2 H-Ar), 7.66-7.55 (m, 3H, 3 H-Ar), 7.53-7.44 (m, 5H, 5 H-Ar), 7.43-7.40 (m, 3H, 3 H-Ar), 7.36-7.33 (m, 2H, 2 H-Ar), 6.01 (dd, $^3J_{2,3}$ = $^3J_{3,4}$ = 9.7 Hz, 1H, H-3_{Glc}), 5.74 (dd, $^3J_{3,4}$ = $^3J_{4,5}$ = 9.7 Hz, 1H, H-4_{Glc}), 5.56 (dd, $^3J_{2,3}$ = 9.8 Hz, $^3J_{1,2}$ = 8.0 Hz, 1H, H-2_{Glc}), 5.24-5.19 (m, 4H, H-1_{Glc}, H-2_{Man}, H-4_{Man}, H-8), 5.10 (dd, $^3J_{3,4}$ = 10.1 Hz, $^3J_{2,3}$ = 3.4 Hz, 1H, H-3_{Man}), 4.80 (d, $^3J_{1,2}$ = 1.6 Hz, 1H, H-1_{Man}), 4.71 (dd, $^2J_{6a,6b}$ = 12.2 Hz, $^3J_{5,6a}$ = 3.1 Hz, 1H, H-$6a_{Glc}$), 4.58 (dd, $^2J_{6a,6b}$ = 12.2 Hz, $^3J_{5,6b}$ = 4.6 Hz, 1H, H-$6b_{Glc}$), 4.49-4.39 (m, 4H, H-5_{Glc}, H-$6a_{Man}$, H-12 ethylene), 4.24-4.11 (m, 4H, H-5_{Man}, H-$6b_{Man}$, H-7a, H-9a), 4.01-3.93 (m, 2H, H-7b, H-9b), 3.68, 3.49 (m, 10H, 10 H-ethylene), 3.23 (t, *J* = 5.6 Hz, 1H, H-13 ethylene), 2.14 (s, 3H, $C\underline{H}_3C$=O), 2.09 (s, 3H, $C\underline{H}_3C$=O), 2.05 (s, 3H, $C\underline{H}_3C$=O), 1.97 (s, 3H, $C\underline{H}_3C$=O), 1.45 (s, 9H, NH-$CO_2C(C\underline{H}_3)_3$) ppm; ^{13}C NMR (126 MHz, MeOD) δ 172.4, 171.5, 171.4 (4C, 4 $CH_3\underline{C}$=O), 167.5, 167.0, 166.7, 166.6, 158.6 (5C, NH-$\underline{C}O_2C(CH_3)_3$, 4 Ph$\underline{C}$=O), 145.1 (C-11), 134.8, 134.6, 134.5, 130.9, 130.8, 130.6, 130.4, 130.2, 130.1, 129.8, 129.7, 129.6, 129.5, 125.2 (20C, 20 C-Ar), 125.1 (C-10), 101.9 (C-1_{Glc}), 98.5 (C-1_{Man}), 74.5 (C-3_{Glc}), 73.3, (2C, C-2_{Glc}, C-5_{Glc}), 71.5, 71.3, 71.1 (5 C, 5 C-ethylene), 71.0 (C-4_{Glc}), 70.7 (C-12 ethylene), 70.4, 70.0 (3C, C-2_{Man}, C-3_{Man}, C-5_{Man}), 69.2 (C-6_{Man}), 67.7 (C-7), 66.8 (C-4_{Man}), 63.9, 63.3 (2C, C-6_{Glc}, C-9), 61.44 (C-8), 41.2 (C-13 ethylene), 28.8 (NH-$CO_2C(\underline{C}H_3)_3$), 20.6 (4C, 4 $\underline{C}H_3C$=O) ppm.

(*R*)-2-{1-[(2-(2-Methoxyethoxy)ethyl)amino]-1*H*-1,2,3-triazol-4-yl}-1-*O*-(α-D-mannopyranosyl)-3-*O*-(β-D-glucopyranosyl)-1,3-propanediol (11a). General procedure B was applied to starting material **10a** (334 mg, 254 µmol). Reagents and conditions: sodium methoxide (2-3 drops), anhydrous methanol (*c* = 0.05 M, 5.00 mL). Size exclusion chromatography G10 in water yielded precursor molecule (140 mg, 76 %). The residue was dissolved in water/trifluoroacetic acid 4/1 and sonicated for 1 h then concentrated till dryness. The residue was taken to microfiltration and lyophilisation what yielded compound **11a** as white foam (110 mg, quantitativ); $[\alpha]_{20}^{D}$= + 64 (*c* 1 , dd water); ^{1}H NMR (500 MHz, D_2O) δ 8.17 (s, 1H, H-10), 5.18-5.12 (m, 1H, H-8), 4,70 (d, $^{3}J_{1,2}$ = 1.70 Hz, 1H, H-1_{Man}) 4.66 (s, 2H, H-12 ethylene), 4.35 (d, $^{3}J_{1,2}$ = 7.9 Hz, 1H, H-1_{Glc}), 4.35-4.30 (m, 1H, H-9a), 4.22 (dd, $^{2}J_{9a,9b}$ = 11.6 Hz, $^{3}J_{8,9b}$ = 8.2 Hz, 1H, H-9b), 4.10 (dd, $^{2}J_{7a,7b}$ = 11.0 Hz, $^{3}J_{7a,8}$ = 4.0 Hz, 1H, H-7a), 3.95 (dd, $^{2}J_{7a,7b}$ = 11.0 Hz, $^{3}J_{7b,8}$ = 6.8 Hz, 1H, H-7b), 3.85 (dd, $^{2}J_{6a,6b}$ = 12.4 Hz, $^{3}J_{5,6a}$ = 2.2 Hz, 1H, H-$6a_{Man}$), 3.76 (dd, $^{3}J_{2,3}$ = 3.4 Hz, $^{3}J_{1,2}$ = 1.8 Hz, 1H, H-2_{Man}), 3.75-3.69 (m, 3H, H-$6b_{Man}$, H-6_{Glc}), 3.69-3.64 (m, 9H, H-3_{Glc}, 8 H-ethylene), 3.64-6.61 (m, 2H, 2H-ethylene), 3.54 (dd, $^{3}J_{3,4}$ = $^{3}J_{4,5}$ = 9.8 Hz, 1H, H-4_{Glc}), 3.38 (m, 2H, H-4_{Man}, H-5_{Man}), 3.32-3.26 (m, 1H, H-3_{Man}), 3.21 (m, 1H, H-5_{Glc}), 3.17-3.13 (m, 3H, H-2_{Glc}, H-13 ethylene) ppm; ^{13}C NMR (126 MHz, D_2O) δ 143.8 (C-11), 125.1 (C-10), 102.9 (C-1_{Glc}), 100.2 (C-1_{Man}), 75.9, 75.5 (2C, C-4_{Man}, C-5_{Man}), 73.1 (C-5_{Glc}), 73.0 (C-2_{Glc}), 72.9 (C-3_{Glc}), 70.4 (C-2_{Man}), 69.5 (C-3_{Man}), 69.6, 69.5, (4C, 4 C-ethylene), 68.2 (C-9), 66.2 (3C, C-3_{Glc}, C-7, C-6_{Glc}), 66.3 (C-12 ethylene), 61.2 (C-8), 60.8, 60.7 (3C, C-6_{Man}, C-ethylene), 39.1 (C-13 ethylene) ppm; IR (ATR) ν_{max}/cm^{-1} 3339, 2881, 1675, 1430, 1031, 646; ESI-HRMS: m/z calcd. for $C_{24}H_{45}N_4O_{15}$ + H^+: 629.28759 $[M+H]^+$; found 629.28625.

(*S*)-2-{1-[(2-(2-Methoxyethoxy)ethyl)amino]-1*H*-1,2,3-triazol-4-yl}-1-*O*-(α-D-mannopyranosyl)-3-*O*-(β-D-glucopyranosyl)-1,3-propanediol (11b). General procedure B was applied to starting material **10b** (290 mg, 220 µmol). Reagents and conditions: sodium methoxide (2-3 drops), anhydrous methanol (*c* = 0.05 M, 4.50 mL). Size exclusion chromatography G10 in water yielded precursor molecule (120 mg, 75 %). The residue was dissolved in water/trifluoroacetic acid 4/1 and sonicated for 1 h then concentrated till dryness. The residue was taken to microfiltration and lyophilisation what yielded compound **11b** as white foam (100 mg, quantitativ); $[\alpha]_{20}^{D}$= + 61 (*c* 1 , dd water); ^{1}H NMR (500 MHz, D_2O) δ 8.19 (s, 1H, H-10), 5.19-5.10 (m, 1H, H-8), 4.77 (d, $^{3}J_{1,2}$ = 1.70 Hz, 1H, H-1_{Man}), 4.66 (s, 2H, H-12 ethylene), 4.41 (d, $^{3}J_{1,2}$ = 7.9 Hz, 1H, H-1_{Glc}), 4.37 (dd, $^{2}J_{9a,9b}$ = 10.7 Hz, $^{3}J_{8,9a}$ = 3.8 Hz, 1H, H-9a),

4.15-4.10 (m, 2H, H-7a, H-9b), 3.92 (dd, $^{2}J_{7a,7b}$ = 10.7 Hz, $^{3}J_{7b,8}$ = 3.8 Hz, 1H, H-7b), 3.83-3.80 (m, 2H, H-2_{Man}, H-$6a_{Man}$), 3.72-3.64 (m, 11H, H-$6b_{Man}$, 10 H-ethylene), 3.62-3.65 (m, 2H, H-6_{Glc}), 3.56-3.49 (m, 2H, H-3_{Man}, H-5_{Man}), 3.41 (dd, $^{3}J_{2,3}$ = $^{3}J_{3,4}$ = 9.2 Hz, 1H, H-3_{Glc}), 3.37-3.34 (m, 1H, H-5_{Glc}), 3.28 (dd, $^{3}J_{4,5}$ = 9.8 Hz, $^{3}J_{3,4}$ = 9.0 Hz, 1H, H-4_{Glc}), 3.18-3.14 (m, 3H, H-2_{Glc}, H-13 ethylene), 3.00-2.89 (m, 1H, H-4_{Man}) ppm; ^{13}C NMR (126 MHz, D_2O) δ 143.9 (C-11), 125.0 (C-10), 102.3 (C-1_{Glc}), 99.5 (C-1_{Man}), 76.0 (C-5_{Glc}), 75.6 (C-3_{Glc}), 72.9 (2C, C-2_{Glc}, C-4_{Man}), 70.4 (C-3_{Man}), 69.8 (C-2_{Man}), 69.6, 69.5, 69.0 (4C, 4 C-ethylene), 68.0 (C-9), 66.4 (C-7), 66.3 (C-5_{Man}), 66.1 (C-ethylene), 63.0 (C-12 ethylene), 60.8 (C-8), 60.7 (2C, C-6_{Man}, C-6_{Glc}), 39.1 (C-13 ethylene) ppm; IR (ATR) ν_{max}/cm^{-1} 3332, 2882, 1430, 1674, 1127, 646; ESI-HRMS: m/z calcd. for $C_{24}H_{45}N_4O_{15}$ + H^+: 629.28759 $[M+H]^+$; found 629.28625.

8.4.1 NMR spectra of new molecules for Chapter 5

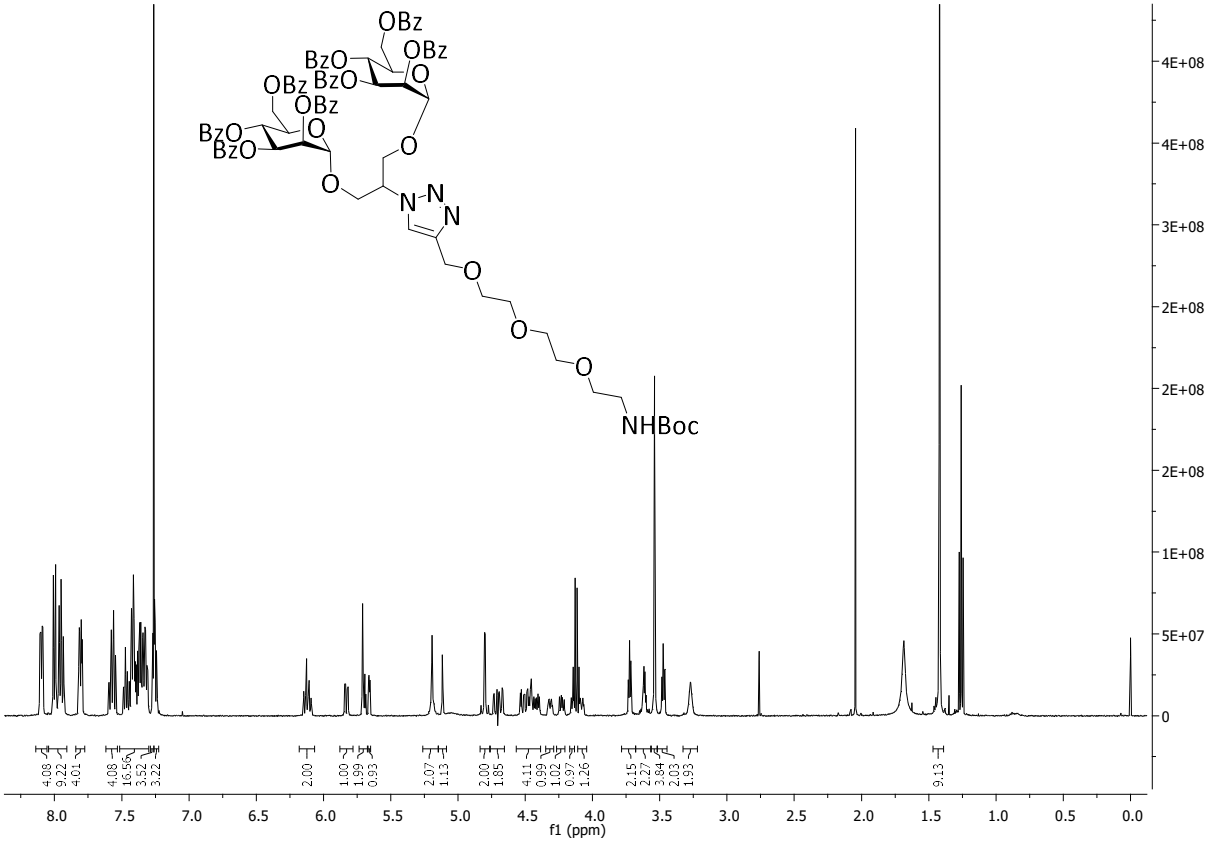

Figure 8.32: ^{1}H NMR (500 MHz, $CDCl_3$) spectrum of compound **7.**

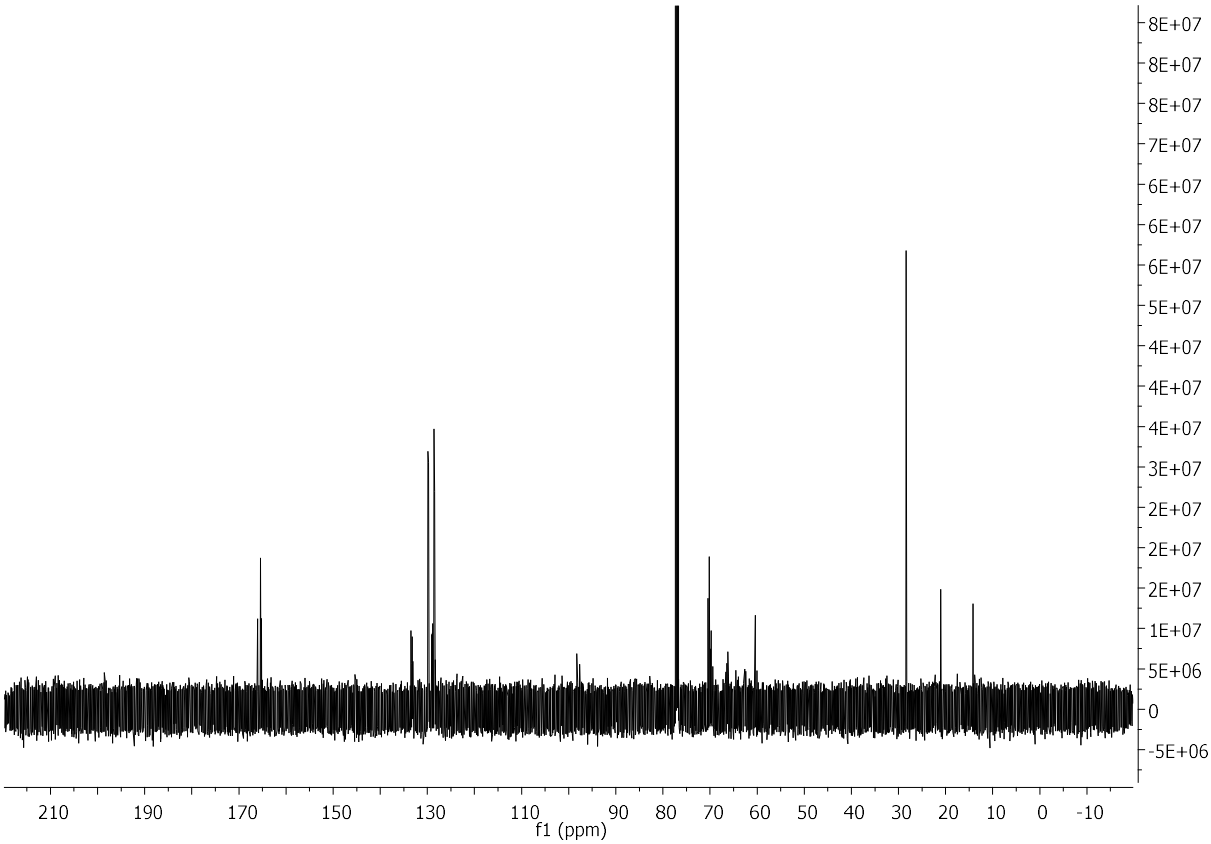

Figure 8.33: ^{13}C NMR (126 MHz, $CDCl_3$) spectrum of compound **7**.

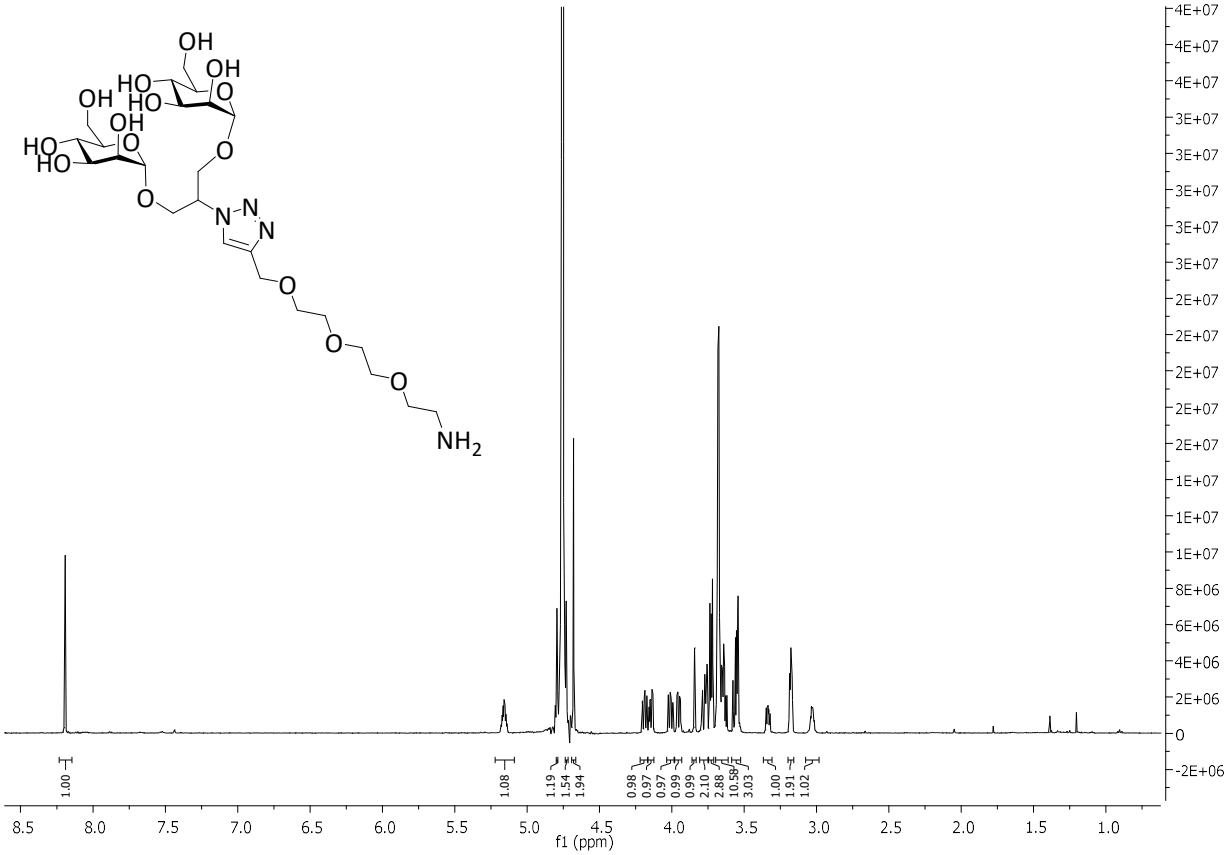

Figure 8.34: ^{1}H NMR (600 MHz, D_2O) spectrum of compound **8.**

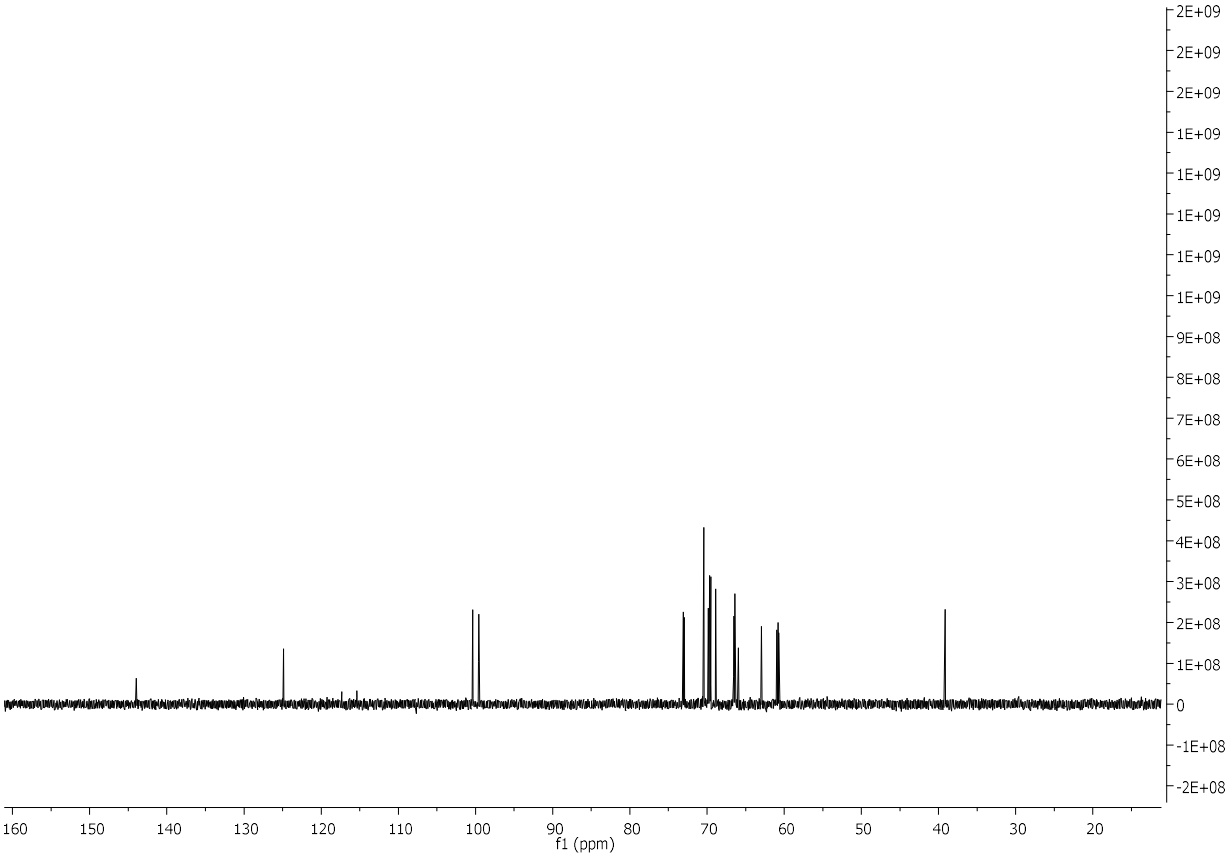

Figure 8.35: ^{13}C NMR (151 MHz, $CDCl_3$) spectrum of compound **8**.

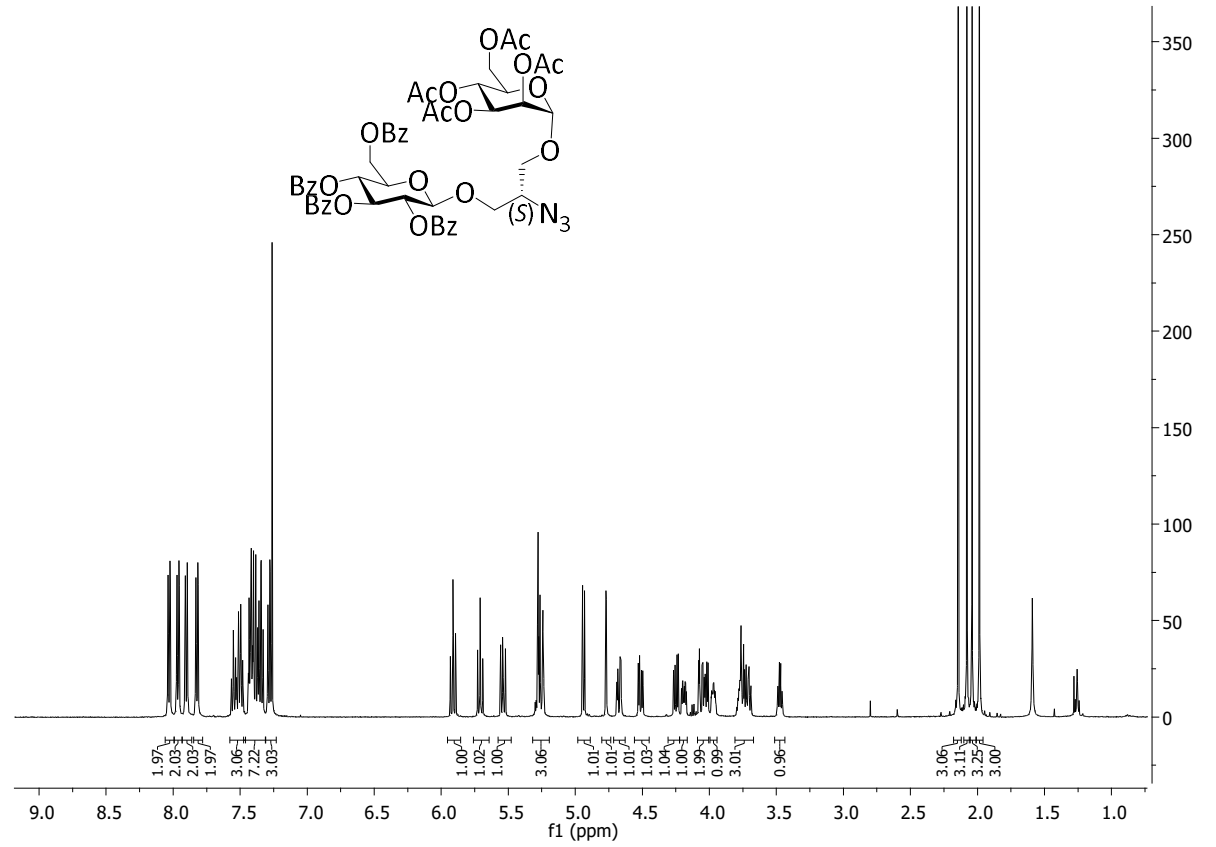

Figure 8.36: ^{1}H NMR (600 MHz, $CDCl_3$) spectrum of compound **9a.**

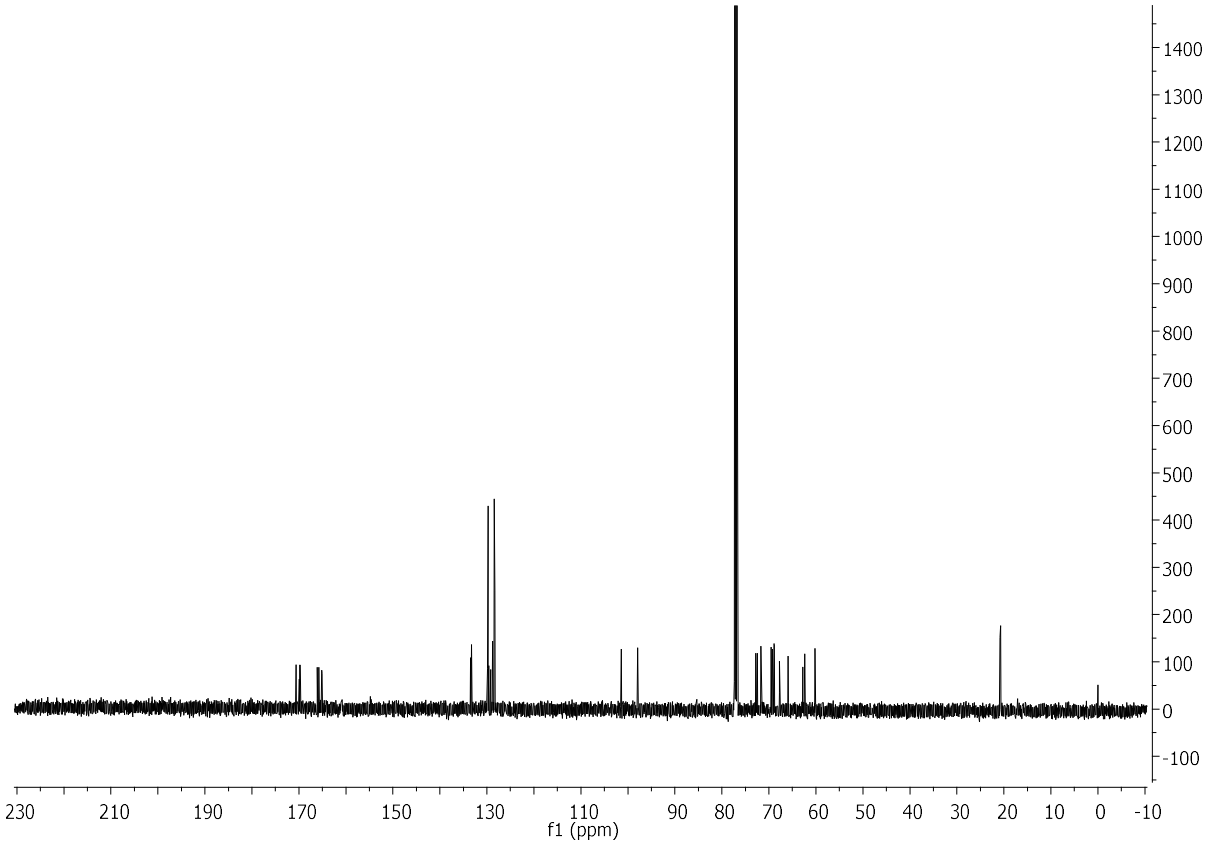

Figure 8.37: ^{13}C NMR (151 MHz, $CDCl_3$) spectrum of compound **9a**.

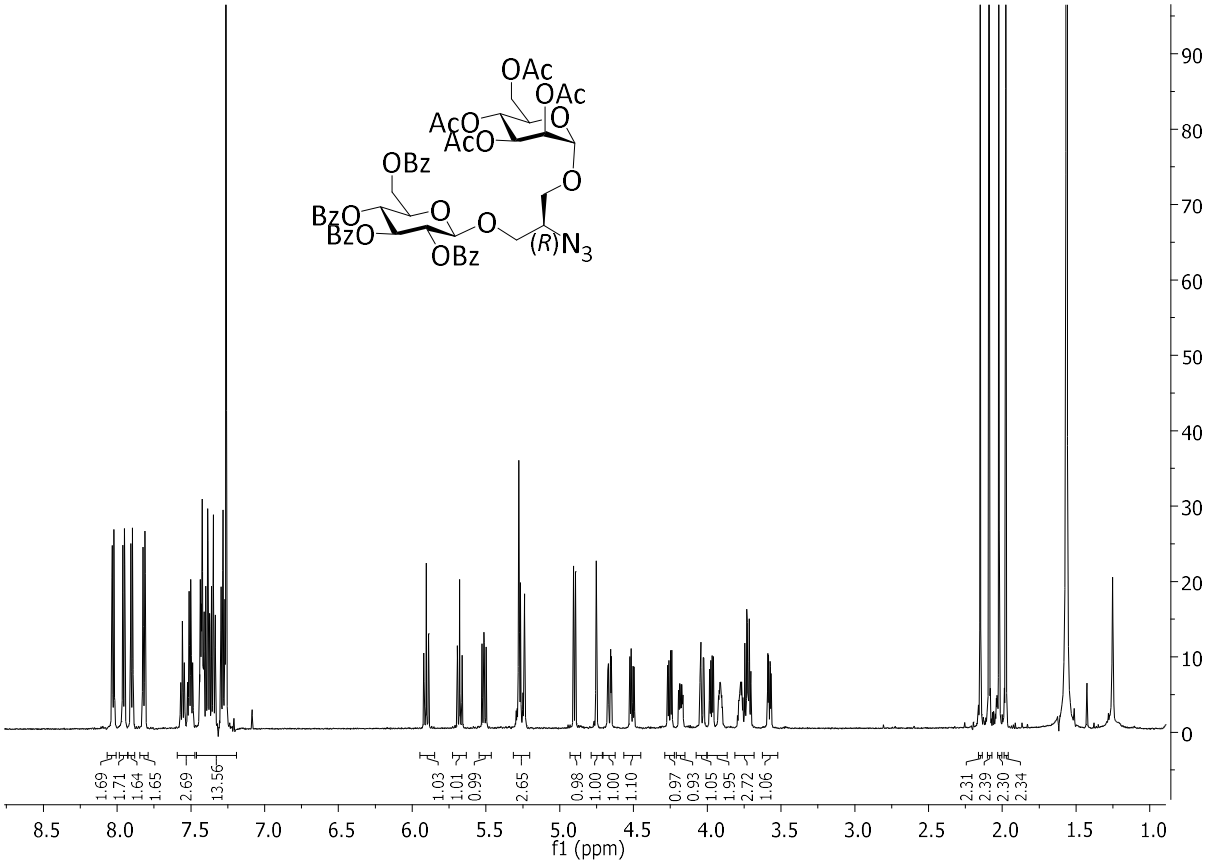

Figure 8.38: ^{1}H NMR (600 MHz, $CDCl_3$) spectrum of compound **9b.**

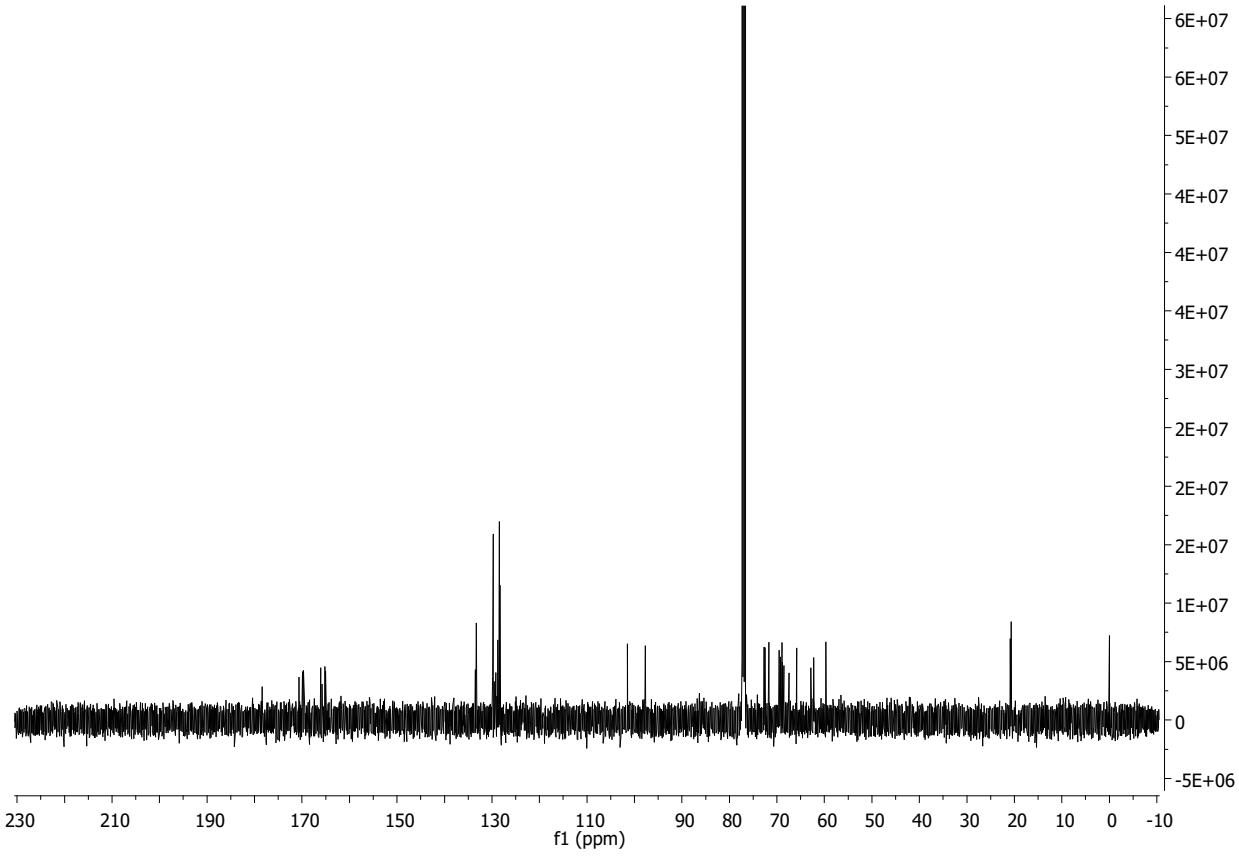

Figure 8.39: ^{13}C NMR (151 MHz, $CDCl_3$) spectrum of compound **9b**.

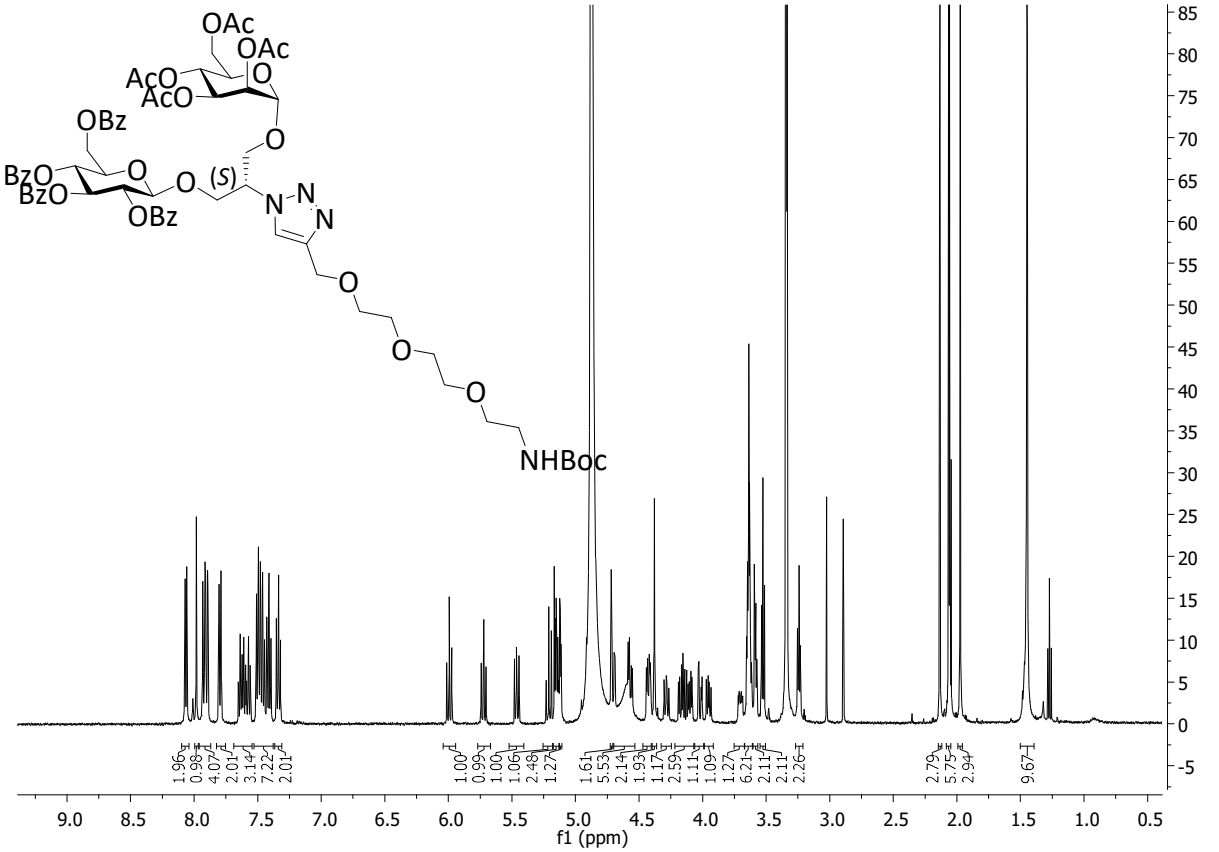

Figure 8.40: ^{1}H NMR (500 MHz, MeOD) spectrum of compound **10a.**

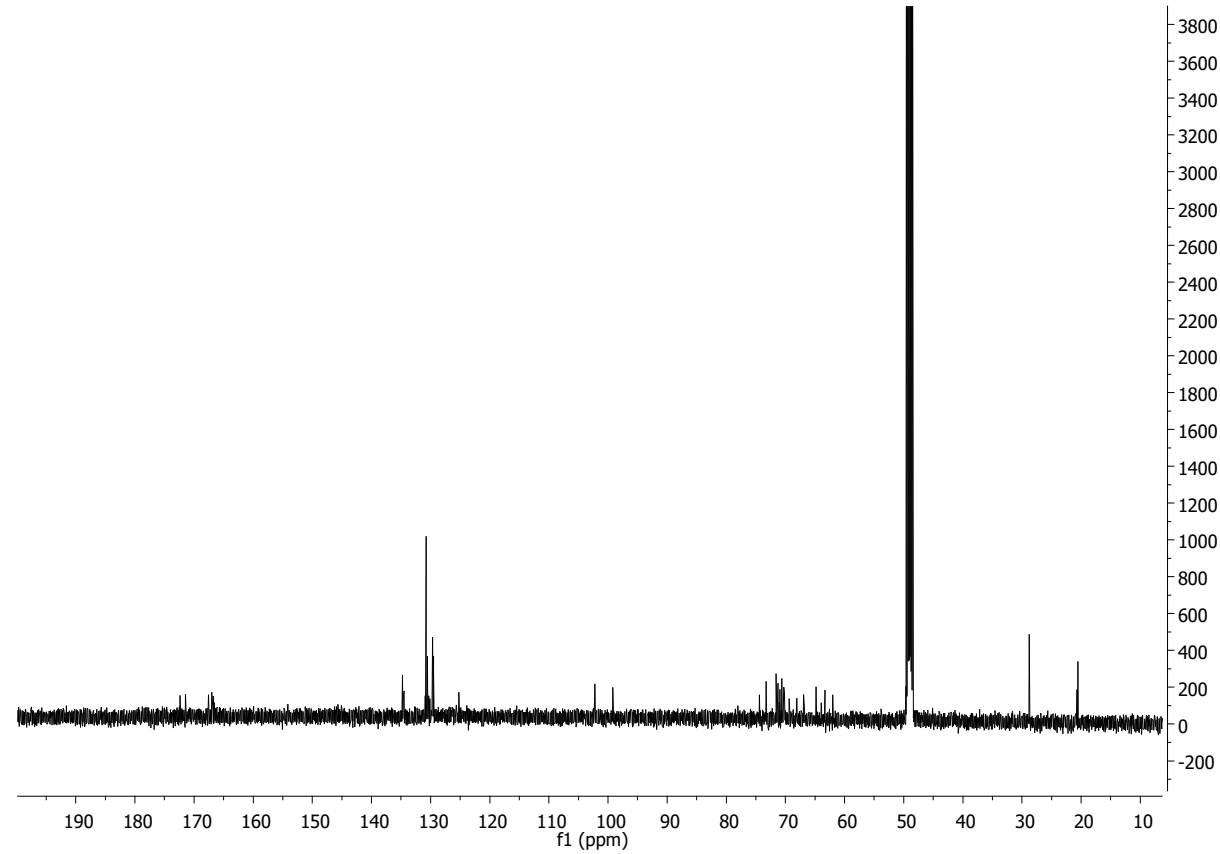

Figure 8.41: ^{13}C NMR (126 MHz, MeOD) spectrum of compound **10a**.

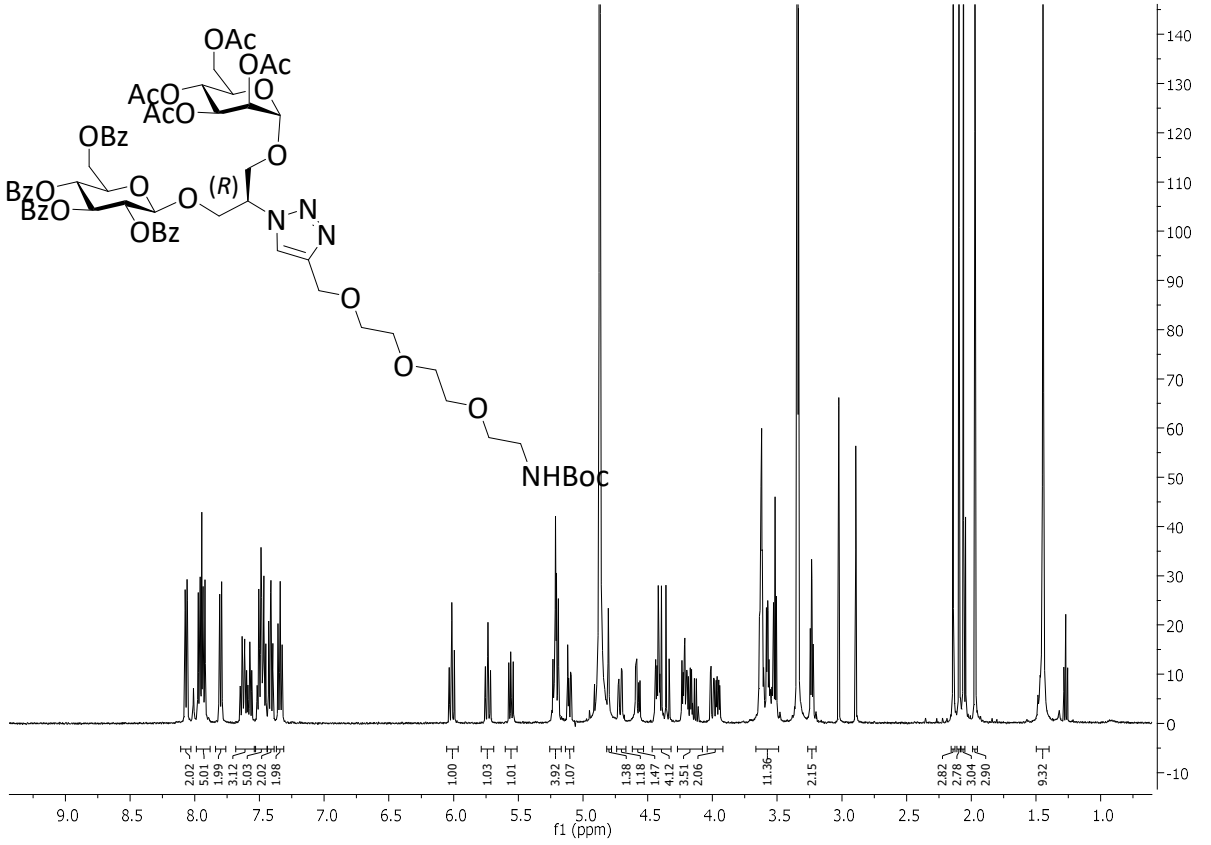

Figure 8.42: ^{1}H NMR (500 MHz, MeOD) spectrum of compound **10b.**

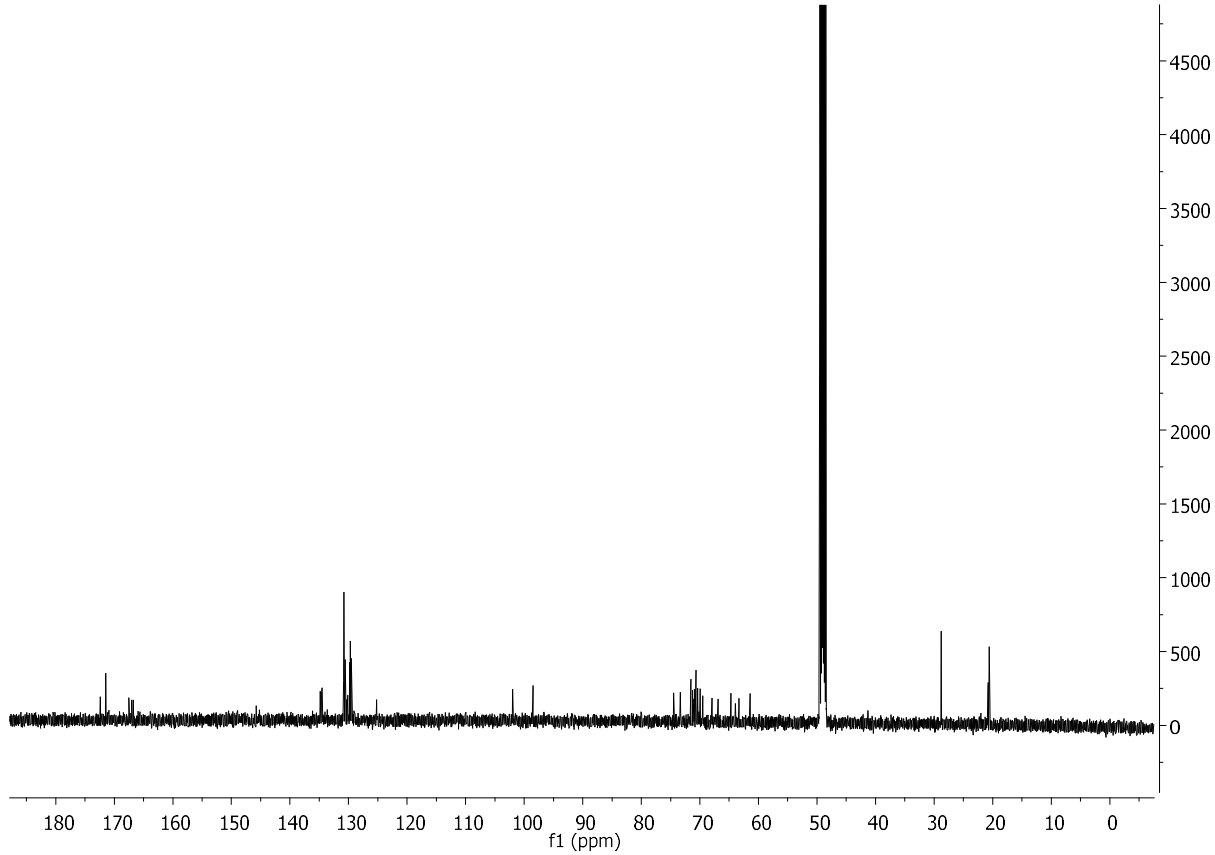

Figure 8.43: ^{13}C NMR (126 MHz, $CDCl_3$) spectrum of compound **10b**.

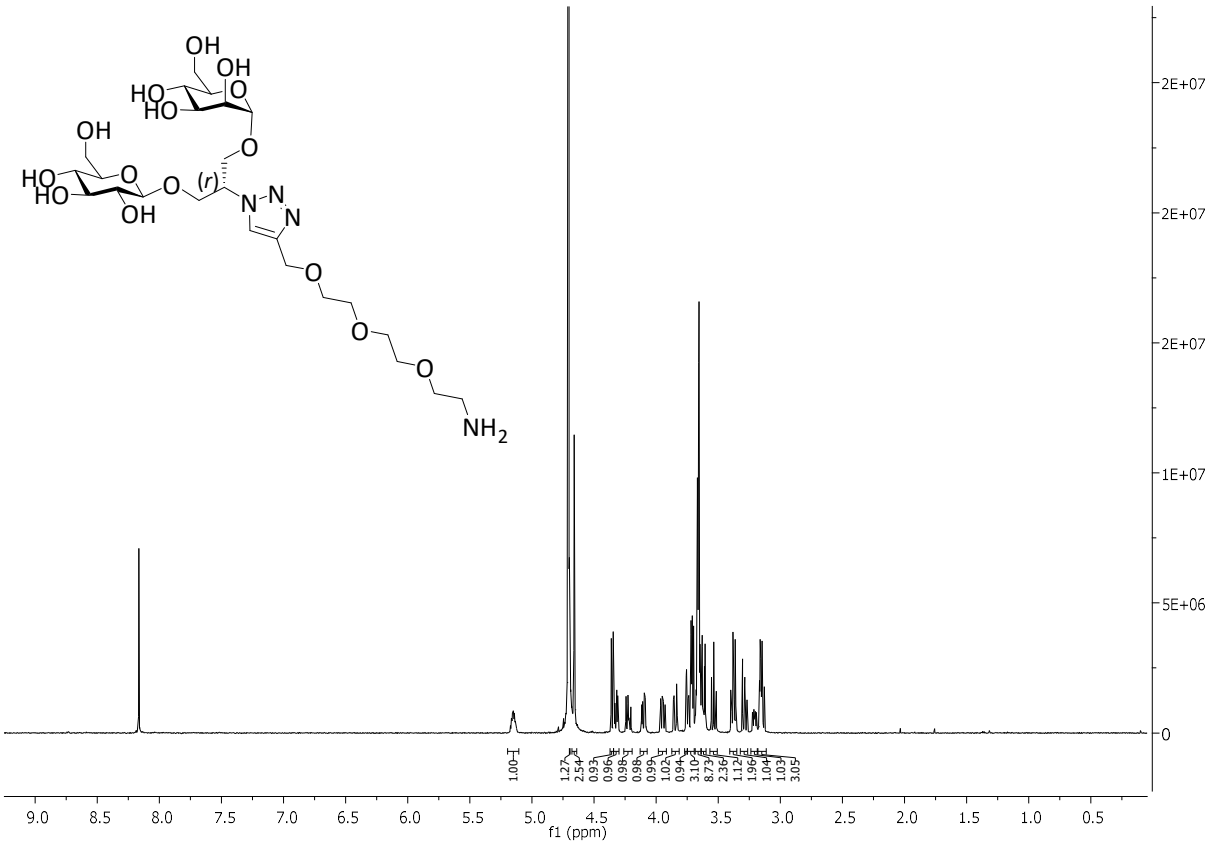

Figure 8.44: ^{1}H NMR (500 MHz, D_2O) spectrum of compound **11a**.

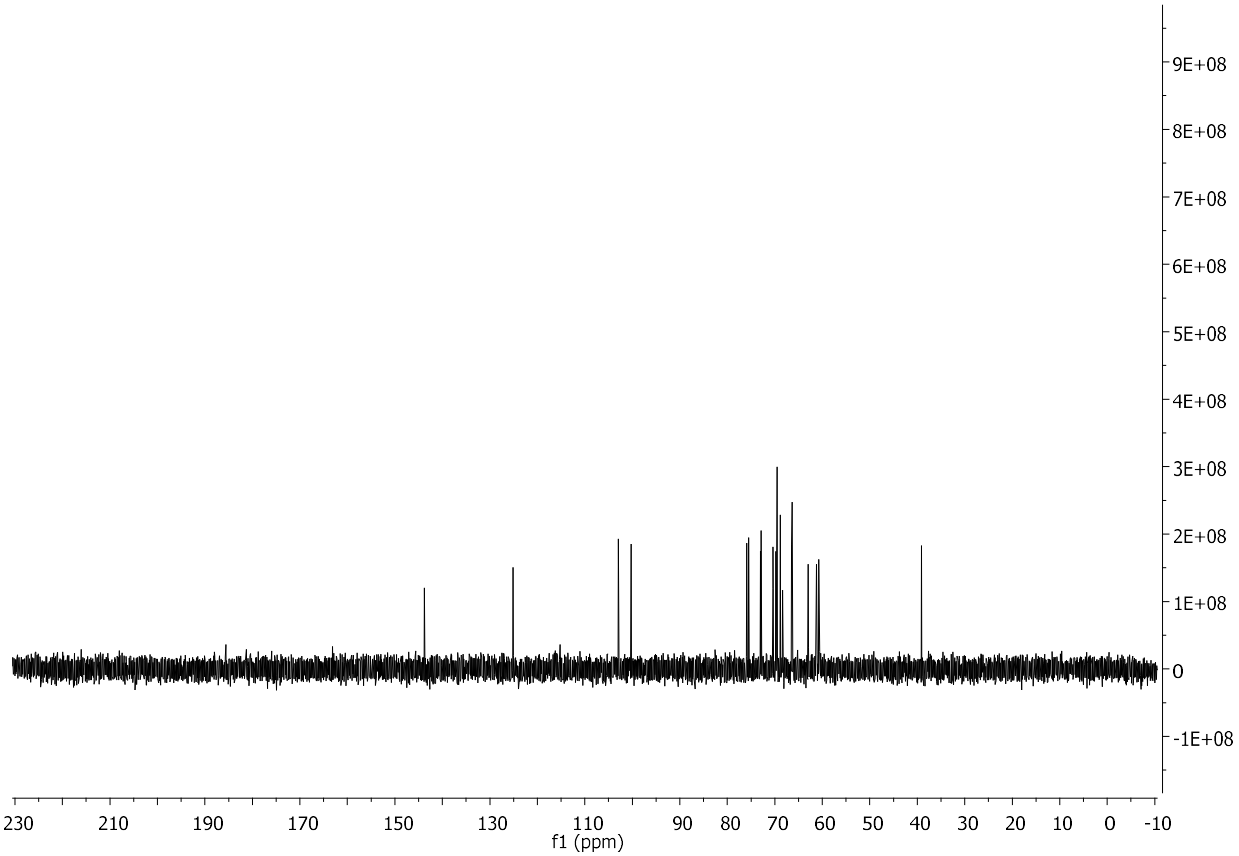

Figure 8.45: ^{13}C NMR (126 MHz, D_2O) spectrum of compound **11a**.

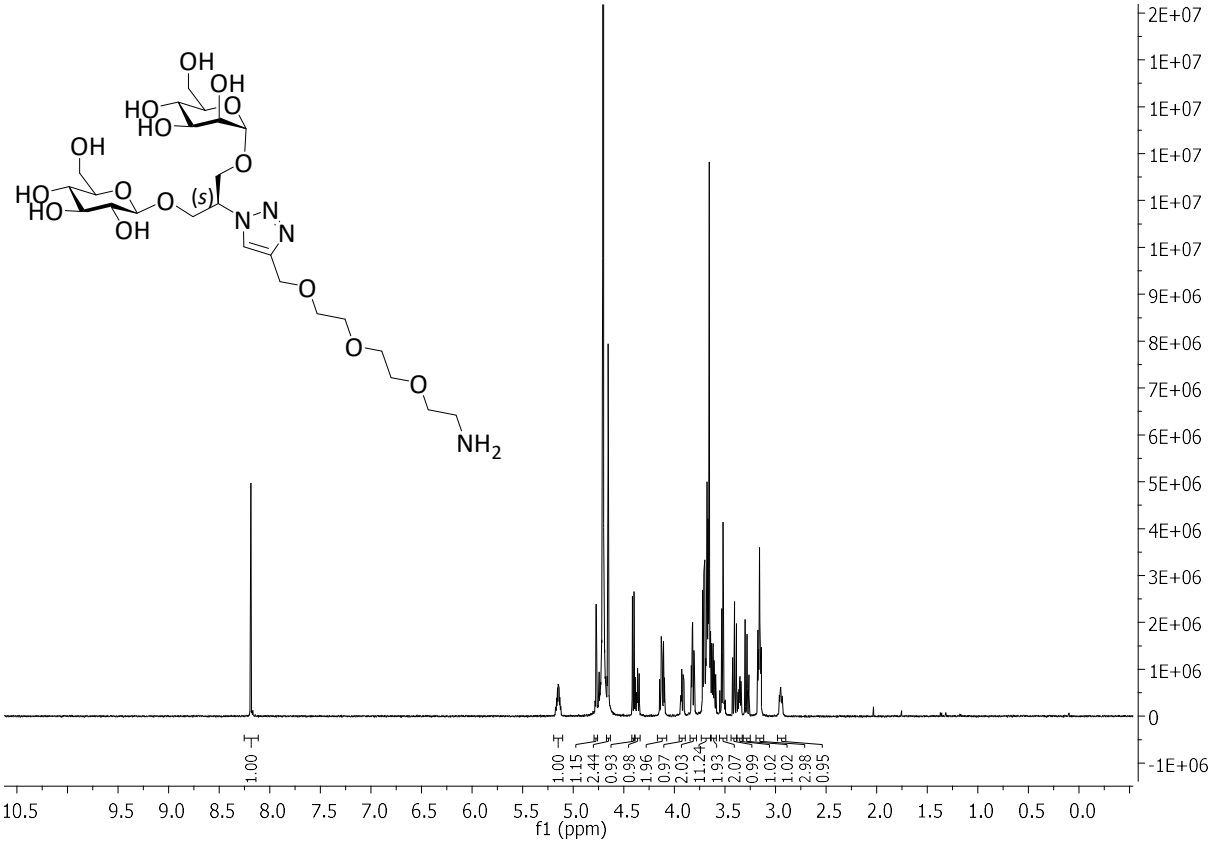

Figure 8.46: ^{1}H NMR (500 MHz, D_2O) spectrum of compound **11b**.

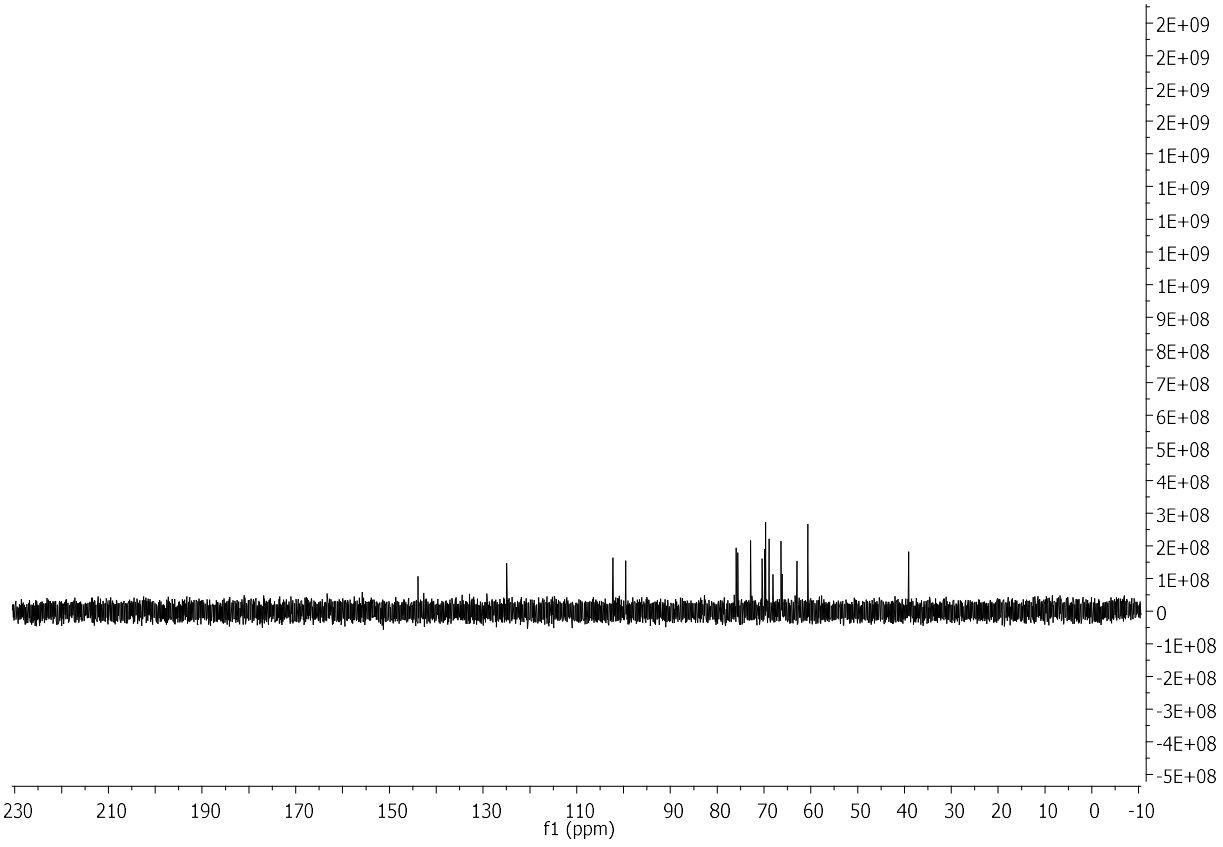

Figure 8.47: ^{13}C NMR (126 MHz, D_2O) spectrum of compound **11b**.

8.5 Synthetic procedures for Chapter 6

For the characterization of serine-derived enantiomeric scaffolds, the carbon atoms of the core moiety are numbered as described in **Figure 8.48**. Compounds derived from D-serine are specified by an "a", and their enantiomeric counterparts, based on L-serine, by a "b". Compounds are named according to IUPAC nomenclature.

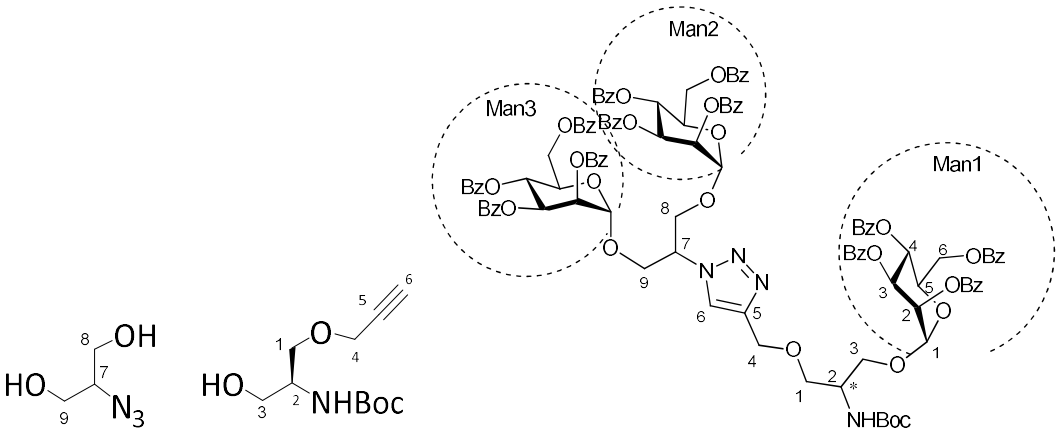

Figure 8.48: Atom numbering for NMR data description of individual substrates.

General procedure for glycosylation (procedure A). To a round bottom flask containing glycosyl acceptor and 3 Å molecular sieves, anhydrous dichloromethane (*c* = 0.1 M) was added. After stirring at room temperature for 15 min, the mixture was cooled to -41 °C (dry ice/acetonitrile) then treated with 2,4,6-collidine (1.2 eq.) and silver trifluoromethanesulfonate (1.2 eq.). Then bromide glycosyl donor (1.2 eq.) was added at an initial temperature of -41 °C. Stirring was continued at -41 °C for three hours and the reaction mixture allowed to warm to room temperature and stirred until completion then diluted with ethyl acetate and filtrated over celite bed. The filtrate is subsequently washed with ice-cold 1 N hydrochloride acid, dried over magnesium sulfate, filtered and concentrated. The crude residue was purified by flash chromatography to afford the expected compound.

General procedure for glycosylation (procedure B). To a round bottom flask with activated 3 Å molecular sieves, trifluoromethanesulfonic anhydride (2 eq.) was added. The mixture was cooled to -70 °C (dry ice/ acetonitrile) and sulfonyl glycosyl donor (2 eq.) in anhydrous dichloromethane (*c* = 0.3 M), 2,6-di-*tert*-butyl pyridine (1.5 eq.) and glycosyl acceptor were added sequentially. The reaction was stirred for 45 min at -60 ˚C and stopped by the addition

of aq. satd. sodium bicarbonate then diluted with dichloromethane and filtrated over celite bed. The filtrate is subsequently washed with brine, dried over magnesium sulfate, filtered and concentrated. The crude residue was purified by flash chromatography to afford the expected compound.

General procedure for propargylation subsequent methyl ester formation (general procedure C). *N*H-Boc-D- or L-serine was added to an ice-cold solution of sodium hydride (2.2 eq.) in anhydrous *N*,*N*-dimethylformamide (*c* = 0.45 M) and the reaction mixture stirred for 30 min. Then propargyl bromide 80 % solution in toluene (1.1 eq.) was added dropwise at 0 °C. The reaction was stirred for 2 h at 0 °C then concentrated. The residue was taken up in water and 1 M hydrochloric acid was added until pH = 2-4 was reached. The aqueous phases were extracted with ethyl acetate and the combined organic layers were dried over magnesium sulfate, filtered and concentrated. The resulting yellow syrup was dissolved in anhydrous *N*,*N*-dimethylformamide (*c* = 0.7 M) and potassium carbonate (1.5 eq.) were added. Afterward, methyl iodide (1.5 eq.) was added dropwise at 0 °C. The mixture was stirred at room temperature until completion then diluted with water and the aqueous phases were extracted with ethyl acetate. The combined organic layers were dried over magnesium sulfate, filtered and concentrated and the residue was purified by flash chromatography to afford the expected compound.

General procedure ester reduction (general procedure D). The starting material was dissolved in anhydrous tetrahydrofuran (*c* = 0.4 M) and 2 M lithium borohydride in tetrahydrofuran (1.5 eq.) was added dropwise at 0 °C. The reaction was stirred for 12 h at room temperature then treated at 0 °C with satd. aq. ammonium chloride. The aqueous phases were extracted with ethyl acetate and the combined organic layers were dried over magnesium sulfate, filtered and concentrated then the residue was purified by flash chromatography to afford the expected compound.

General procedure for copper(I) catalyzed azide-alkyne cycloaddition (CuAAC) reaction (general procedure E). In 32 mL microwave tube azide moiety, alkyne moiety (2 eq.), copper(I) bromide (0.2 eq.) and tris[(1-benzyl-1*H*-1,2,3-triazol-4-yl)methyl]amine (0.05 eq.) were dissolved with anhydrous *N*,*N*-dimethylformamide (*c* = 0.1 M). The reaction was stirred at 60 °C under microwave conditions for 1 hour. The mixture was washed with toluene and

transferred into a flask and concentrated to dryness. Then water and ethyl acetate were poured in and the aqueous phases were extracted with ethyl acetate and the combined organic layers were dried over magnesium sulfate, filtered and concentrated. Then the residue was purified by flash chromatography to afford the expected compound.

General procedure for *N*H-Boc cleavage and subsequent diazotransfer reaction (general procedure F). The starting material was dissolved in anhydrous tetrahydrofuran (*c* = 0.1 M) and 4 M hydrochloric acid in dioxane (5 eq.) was added and the reaction was stirred until completion then concentrated till dryness. The residue was dissolved in a 2:1:1 methanol/dichloromethane/water mixture (*c* = 0.1 M) and potassium carbonate (2 eq.), copper(II) sulfate pentahydrate (0.01 eq.) and imidazole-1-sulfonyl azide hydrochloride (1.6 eq.) were added sequentially. The blue mixture turned brown after stirred for sixteen hours. The reaction mixture was then concentrated to dryness. The residue was diluted with ethyl acetate and water. The aqueous phase was extracted with ethyl acetate and the combined organic phases were washed with brine, dried over magnesium sulfate then concentrated. The residue was purified by flash chromatography to afford the expected compound.

General procedure for ester cleavage (general procedure G). To a solution of the ester protected glycocluster in dry methanol (*c* = 0.03 M), sodium methoxide (*c* = 5.4 M in methanol, two drops) was added and the mixture was stirred at room temperature until completion then neutralized with Amberlite IR120-H^+, diluted with methanol, filtered and concentrated. The residue was taken up into a 1:1 mixture of water and methanol then washed with diethyl ether and the aqueous layer was concentrated to dryness. The residue was purified by size exclusion chromatography on Sephadex G10 gel and eluted with deionized water.

2,3,4,6-Tetra-*O*-benzoyl-α-D-mannopyranosyl bromide (7c). To a round bottom flask with 1,2,3,4,6-penta-*O*-benzoyl-α,β-D-mannopyranoside (3.60 g, 5.13 mmol) in anhydrous dichloromethane (*c* = 0.5 M, 10.2 mL), hydrogen bromide in 33 % (w/w) glacial acetic acid (ca. 5.1 mol/L, 4.50 mL) was added at 0 °C. The mixture was allowed to warm to room temperature then stirred until completion of the reaction, and stopped by adding aq. satd. sodium bicarbonate at 0 ˚C. The aqueous phases were extracted with dichloromethane then the combined organic layers were washed with brine, dried over magnesium sulfate, filtered and concentrated. Flash chromatography with ethyl acetate/cyclohexane 8/92 yielded com-

pound **7c** (2.20 g, 70 %) as a white foam. Analytical and spectroscopic data were found to be in agreement with reported literature.[143]

(2-Methyl-5-*tert*-butylphenyl)-α-D-(2,3,4,6-tetra-*O*-benzoyl)-sulfonyl mannopyranoside (7d). To a round bottom flask with (2-methyl-5-*tert*-butylphenyl)-α-D-(2,3,4,6-tetra-*O*-benzoyl)-thiomannopyranoside (800 mg, 1.10 mmol) in anhydrous dichloromethane (*c* = 0.2 M, 5.30 mL), *meta*-chloroperoxybenzoic acid (363 mg, 1.60 mmol, 1.5 eq.) was added at -20 °C. The mixture was allowed to warm to room temperature then stirred until completion of the reaction and stopped by adding aq. satd. sodium bicarbonate at 0 ˚C. The aqueous phases were extracted with dichloromethane then the combined organic layers were washed with brine, dried over sodium sulfate, filtered and concentrated. Flash chromatography with ethyl acetate/cyclohexane 1.5/8.5 yielded compound **7d** (560 mg, 70 %) as white foam. Analytical and spectroscopic data were found to be in agreement with reported literature.[130, 144]

(*R*)-*N*-*tert*-Butoxycarbonyl-*O*-propargyl-D-serine methyl ester (2a). General procedure C was applied to *N*-Boc-D-serine (2.20 g, 10.7 mmol). Reagents and conditions for the first step: sodium hydride 60 % dispersion in mineral oil (94.0 mg, 23.6 mmol, 2.2 eq.), propargyl bromide (1.30 mL, 11.8 mmol, 1.1 eq.), anhydrous *N*,*N*-dimethylformamide (*c* = 0.45 M, 23.0 mL); Reagents and conditions for second step: potassium carbonate (3.54 g, 25.6 mmol, 1.5 eq.), methyl iodide (1.60 mL, 25.6 mmol, 1.5 eq.), anhydrous *N*,*N*-dimethylformamide (*c* = 0.7 M, 15.4 mL). Flash chromatography with ethyl acetate/cyclohexane 1/9 yielded compound **2a** (1.70 g, 61 %) as a yellow viscous oil; R_f = 0.3 (ethyl acetate/cyclohexane 1/9); $[\alpha]_{20}^{D}$ = - 10.9 (*c* 1, chloroform); ^{1}H NMR (500 MHz, $CDCl_3$) δ 5.37 (br s, 1H, NH), 4.49-4.43 (m, 1H, H-2), 4.15 (d, $^3J_{1,4}$ = 2.4 Hz, 2H, H-4), 3.96 (dd, $^2J_{1a,1b}$ = 9.2 Hz, $^3J_{1a,2}$ = 2.9 Hz, 1H, H-1a), 3.79-3.73 (m, 4H, H-1b, $COOC\underline{H}_3$), 2.45 (t, $^4J_{4,6}$ = 2.4 Hz, 1H, H-6), 1.45 (s, 9H, $NHCO_2C(C\underline{H}_3)_3$) ppm; ^{13}C NMR (126 MHz, $CDCl_3$) δ 170.9 ($\underline{C}OOCH_3$), 155.5 ($NH\underline{C}O_2C(CH_3)_3$), 80.0 ($NHCO_2\underline{C}(CH_3)_3$), 78.8 (C-5), 75.0 (C-6), 69.7 (C-1), 58.5 (C-4), 53.8 (C-2), 52.5 ($COO\underline{C}H_3$), 28.3 ($NHCO_2C(\underline{C}H_3)_3$) ppm.

(*S*)-*N*-*tert*-Butoxycarbonyl-*O*-propargyl-L-serine methyl ester (2b). General procedure C was applied to *N*H-Boc-L-serine (2.20 g, 10.7 mmol). Reagents and conditions for first step: sodium hydride 60 % dispersion in mineral oil (94.0 mg, 23.6 mmol, 2.2 eq.), propargyl

bromide (1.30 mL, 11.8 mmol, 1.1 eq.), anhydrous *N*,*N*-dimethylformamide (*c* = 0.45 M, 23.0 mL); Reagents and conditions for second step: potassium carbonate (3.54 g, 25.6 mmol, 1.5 eq.), methyl iodide (1.60 mL, 25.6 mmol, 1.5 eq.), anhydrous *N*,*N*-dimethylformamide (*c* = 0.7 M, 15.4 mL). Flash chromatography with ethyl acetate/cyclohexane 1/9 yielded compound **2b** (2.10 g, 76 %) as yellow viscous oil. ^{1}H NMR and ^{13}C NMR were found to be in agreement with the reported literature.[145] $[\alpha]_{20}^{D}$ = + 11.5 (*c* 1, chloroform); literature values: $[\alpha]_{20}^{D}$ = + 17.8 (*c* 2.7, chloroform) and $[\alpha]_{21}^{D}$ = + 14.7 (*c* 1.2, chloroform).

(*S*)-2-*N*-(*tert*-Butoxycarbonyl)-1-*O*-(propargyl)-1,3-propanediol (3a). General procedure D was applied to starting material **2a** (1.70 g, 6.61 mmol). Reagents and conditions: 2 M lithium borohydride in tetrahydrofuran (5.0 mL, 1.5 eq.), anhydrous tetrahydrofuran (*c* = 0.4 M, 17.0 mL). Flash chromatography with ethyl acetate/cyclohexane 4/6 yielded compound **3a** (1.0 g, 65 %) as a translucent viscous gel; R_f = 0.3 (ethyl acetate/cyclohexane 3/7); $[\alpha]_{20}^{D}$ = - 29.7 (*c* 1, chloroform); ^{1}H NMR (500 MHz, $CDCl_3$) δ 5.15 (br s, 1H, NH), 4.22-4.10 (m, 2H, H-4), 3.88-3.76 (m, 2H, H-2, H-3a), 3.76-3.59 (m, 3H, H-1, H-3b), 2.47 (t, $^{4}J_{4,6}$ = 2.4 Hz, 1H, H-6), 1.45 (s, 9H, $NHCO_2C(C\underline{H}_3)_3$) ppm; ^{13}C NMR (126 MHz, $CDCl_3$) δ 156.1 ($NH\underline{C}O_2C(CH_3)_3$), 79.8 ($NHCO_2\underline{C}(CH_3)_3$), 79.1 (C-5), 75.0 (C-6), 70.1 (C-1), 63.7 (C-3), 58.6 (C-4), 51.5 (C-2), 28.37 ($NHCO_2C(\underline{C}H_3)_3$) ppm; IR (ATR) ν_{max}/cm^{-1} 3292, 2977, 2119, 1685, 1511, 1366, 1168, 1028, 648; ESI-HRMS: m/z calcd. for $C_{11}H_{18}NO_4$ + Na^+ + H^+ = 252.12008 $[M+Na+H]^+$; found 252.12062.

(*R*)-2-*N*-(*tert*-Butoxycarbonyl)-1-*O*-(propargyl)-1,3-propanediol (3b). General procedure D was applied to starting material **2b** (2.10 g, 8.21 mmol). Reagents and conditions: 2 M lithium borohydride in tetrahydrofuran (6.12 mL, 1.5 eq.), anhydrous tetrahydrofuran (*c* = 0.4 M, 21.0 mL). Flash chromatography with ethyl acetate/cyclohexane 4/6 yielded compound **3b** (1.20 g, 62 %) as a translucent viscous gel; R_f = 0.3 (ethyl acetate/cyclohexane 3/7); $[\alpha]_{20}^{D}$ = + 37.7 (*c* 1, chloroform); ^{1}H NMR (500 MHz, $CDCl_3$) δ ^{1}H NMR (500 MHz, $CDCl_3$) δ 5.13 (br s, 1H, NH), 4.17 (dd, $^{2}J_{4a,4b}$ = 3.4 Hz, $^{2}J_{3,4}$ = 2.4 Hz, 2H, H-4a, H-4b), 3.84-3.78 (m, 2H, H-2, H-1a), 3.74-3.63 (m, 3H, H-1b, H-3), 2.46 (t, $^{4}J_{4,6}$ = 2.4 Hz, 1H, H-6), 2.09 (br s, 1H, OH), 1.45 (s, 9H, $NHCO_2C(C\underline{H}_3)_3$) ppm; ^{13}C NMR (126 MHz, $CDCl_3$) δ 156.1 ($NH\underline{C}O_2C(CH_3)_3$), 79.8 ($NHCO_2\underline{C}(CH_3)_3$), 79.1 (C-5), 75.0 (C-6), 70.2 (C-1), 63.8 (C-3), 58.7 (C-4), 51.53 (C-2), 28.35 ($NHCO_2C(\underline{C}H_3)_3$) ppm; IR (ATR) ν_{max}/cm^{-1} 3293, 2977, 1685, 1511, 1366, 1168, 1028, 648; ESI-HRMS: m/z calcd. for $C_{11}H_{18}NO_4$ + Na^+ + H^+ = 252.12008 $[M+Na+H]^+$; found 252.12062.

(*S*)-2-*N*-(*tert*-Butoxycarbonyl)-1-*O*-{1-[[2-(1,3-di-*O*-(2,3,4,6-tetra-*O*-benzoyl-α-D-mannopyranosyl))-1,3-propanediol]-1*H*-1,2,3-triazol-4-yl]-methyl}-1,3-propanediol (5a).

General procedure E for CuAAC addition was applied to azide moiety **4** (1.0 g, 787 µmol) and alkyne moiety **3a** (360 mg, 1.57 mmol, 2 eq.). Reagents and conditions: copper(I) bromide (21.0 mg, 150 µmol, 0.2 eq.) and tris[(1-benzyl-1*H*-1,2,3-triazol-4-yl)methyl]amine (21.0 mg, 39.0 µmol, 0.05 eq.), anhydrous *N*,*N*-dimethylformamide (*c* = 0.1 M, 7.80 mL), reaction was stirred at T = 60 °C for 1 hour under microwave conditions. Flash chromatography with ethyl acetate/cyclohexane 4.5/5.5 afforded compound **5a** as a white foam (1.10 g, 93 %); R_f = 0.3 (ethyl acetate/cyclohexane 4.5/5.5); $[\alpha]_{20}^{D}$= - 703 (*c* 0.6, chloroform); ^{1}H NMR (500 MHz, $CDCl_3$) δ 8.13-8.06 (m, 4H, 4 H-Ar), 8.04-7.98 (m, 5H, 4 H-Ar, H-6), 7.96-7.92 (m, 4H, 4 H-Ar), 7.83-7.80 (m, 4H, 4 H-Ar), 7.60-7.55 (m, 4H, 4 H-Ar), 7.50-7.44 (m, 2H, 2 H-Ar), 7.44-7.31 (m, 14H, 14 H-Ar), 7.28-7.26 (m, 1H, H-Ar), 7.26-7.23 (m, 3H, 3 H-Ar), 6.17-6.07 (m, 2H, H-4_{Man2}, H-4_{Man3}), 5.82 (dd, $^3J_{3,4}$ = 10.2 Hz, $^3J_{2,3}$ = 3.3 Hz, 1H, H-3_{Man2}), 5.73-5.70 (m, 2H, H-2_{Man3}, H-3_{Man3}), 5.65 (dd, $^3J_{2,3}$ = 3.3 Hz, $^3J_{1,2}$ = 1.8 Hz, 1H, H-2_{Man2}), 5.36-5.30 (m, 1H, NH), 5.24-5.15 (m, 2H, H-1_{Man3}, H-7), 5.10 (d, $^3J_{1,2}$ = 1.6 Hz, 1H, H-1_{Man2}), 4.79 (s, 2H, H-4), 4.77-4.66 (m, 2H, H-$6a_{Man2}$, H-$6a_{Man3}$), 4.56-4.43 (m, 3H, H-$6b_{Man2}$, H-$6b_{Man3}$, H-9a), 4.39 (dd, $^2J_{8a,8b}$ = 10.9 Hz, $^3J_{7,8a}$ = 4.7 Hz, 1H, H-8a), 4.35-4.29 (m, 1H, H-5_{Man2}), 4.23 (dd, $^2J_{8a,8b}$ = 10.9 Hz, $^3J_{7,8b}$ = 7.0 Hz, 1H, H-8b), 4.12-4.07 (m, 2H, H-5_{Man3}, H-9b), 3.84 (s br, 1H, H-2), 3.80-3.73 (m, 2H, H-3a, H-1a), 3.72-3.57 (m, 2H, H-3b, H-1b), 1.38 (s, 9H, $NHCO_2C(C\underline{H}_3)_3$) ppm; ^{13}C NMR (126 MHz, $CDCl_3$) δ 166.1, 165.7, 165.4, 165.3 (8C, 8 PhC=O), 145.5 (C-5), 133.6, 133.5, 133.3, 133.2, 133.1, 129.9, 129.8, 129.7, 129.0, 128.8, 128.6, 128.5, (48C, 48 C-Ar), 128.3 (C-6), 98.3 (C-1_{Man2}), 97.6 (C-1_{Man3}), 79.3 ($NHCO_2\underline{C}(CH_3)_3$), 70.0 (C-1), 69.9 (4C, C-2_{Man2}, C-2_{Man3}, C-3_{Man2}, C-3_{Man3}), 69.6 (C-5_{Man2}), 69.4 (C-5_{Man3}), 67.3 (C-8), 66.6 (C-9), 66.5, 66.2 (2C, C-4_{Man2}, C-4_{Man3}), 64.8 (C-4), 62.6, 62.4 (3C, C-3, C-6_{Man2}, C-6_{Man3}), 60.2 (C-7), 51.5 (C-2), 28.3 ($NHCO_2C(\underline{C}H_3)_3$) ppm; IR (ATR) ν_{max}/cm^{-1} 2970, 1722, 1451, 1260, 1094, 706; ESI-HRMS: m/z calcd. for $C_{82}H_{79}N_4O_{24}$ + H^+ = 1503.50788 $[M+H]^+$; found 1503.50715.

(*R*)-2-*N*-(*tert*-Butoxycarbonyl)-1-*O*-{1-[[2-(1,3-di-*O*-(2,3,4,6-tetra-*O*-benzoyl-α-D-mannopyranosyl))-1,3-propanediol]-1*H*-1,2,3-triazol-4-yl]-methyl}-1,3-propanediol (5b).

General procedure E for CuAAC addition was applied to azide moiety **4** (1.0 g, 787 µmol) and alkyne moiety **3b** (360 mg, 1.57 mmol, 2 eq.). Reagents and conditions: copper(I) bromide (21.0 mg, 150 µmol, 0.2 eq.) and tris[(1-benzyl-1*H*-1,2,3-triazol-4-yl)methyl]amine (21.0 mg,

39.0 µmol, 0.05 eq.), anhydrous *N*,*N*-dimethylformamide (*c* = 0.1 M, 7.80 mL), reaction was stirred at T = 60 °C for 1 hour under microwave conditions. Flash chromatography with ethyl acetate/cyclohexane 4.5/5.5 afforded compound **5b** as a white foam (1.00 g, 85 %); R_f = 0.3 (ethyl acetate/cyclohexane 4.5/5.5); $[a]_{20}^{D}$= - 710 (*c* 1, chloroform); ^{1}H NMR (500 MHz, $CDCl_3$) δ 8.12-8.07 (m, 4H, 4 H-Ar), 8.03-7.92 (m, 9H, 8 H-Ar, H-6), 7.84-7.79 (m, 4H, 4 H-Ar), 7.60-7.54 (m, 4H, 4 H-Ar), 7.51-7.45 (m, 2H, 2 H-Ar), 7.45-7.29 (m, 14H, 14 H-Ar), 7.29-7.27 (m, 2H, 2 H-Ar), 7.26-7.21 (m, 2H, 2 H-Ar), 6.14-6.09 (m, 2H, H-4$_{Man2}$, H-4$_{Man3}$), 5.82 (dd, $^3J_{3,4}$ = 10.2 Hz, $^3J_{2,3}$ = 3.3 Hz, 1H, H-3$_{Man2}$), 5.75-5.67 (m, 2H, H-2$_{Man3}$, H-3$_{Man3}$), 5.67-5.62 (m, 1H, H-2$_{Man2}$), 5.31 (s, 1H, NH), 5.23-5.15 (m, 2H, H-1$_{Man3}$, H-7), 5.10 (d, $^3J_{1,2}$ = 1.7 Hz, 1H, H-1$_{Man2}$), 4.84-4.78 (m, 2H, H-4), 4.78-4.64 (m, 2H, H-6a$_{Man2}$, H-6a$_{Man3}$), 4.56-4.43 (m, 3H, H-6b$_{Man2}$, H-6b$_{Man3}$, H-9a), 4.39 (dd, $^2J_{8a,8b}$ = 10.8 Hz, $^3J_{7,8a}$ =4.7 Hz, 1H, H-8a), 4.35-4.30 (m, 1H, H-5$_{Man2}$), 4.23 (dd, $^2J_{8a,8b}$ = 10.8 Hz, $^3J_{7,8b}$ =7.0 Hz, 1H, H-8b), 4.14-4.04 (m, 2H, H-5$_{Man3}$, H-9b), 3.83 (br s, 1H, H-2), 3.81-3.73 (m, 2H, H-3a, H-1a), 3.71-3.61 (m, 2H, H-3b, H-1b), 3.12 (br s, 1H, -OH), 1.36 (s, 9H, $NHCO_2C(C\underline{H}_3)_3$) ppm; ^{13}C NMR (126 MHz, $CDCl_3$) δ 166.1, 165.7, 165.4, 165.3 (8C, 8 PhC=O), 145.4 (C-5), 133.6, 133.5, 133.3, 133.2, 133.1, 129.9, 129.8, 129.7, 129.0, 128.8, 128.6, 128.5, 128.3, 128.2, 125.3, (48C, 48 C-Ar), 123.4 (C-6), 98.3 (C-1$_{Man2}$), 97.6 (C-1$_{Man3}$), 79.3 ($NHCO_2\underline{C}(CH_3)_3$), 70.1 (C-1), 70.0, 69.9, (4C, C-2$_{Man2}$, C-2$_{Man3}$, C-3$_{Man2}$, C-3$_{Man3}$), 69.6 (C-5$_{Man2}$), 69.5 (C-5$_{Man3}$), 67.3 (C-8), 66.6 (C-9), 66.5 (C-4$_{Man2}$), 66.2 (C-4$_{Man3}$), 64.7 (C-4), 62.6 (C-3), 62.4 (2C, C-6$_{Man2}$, C-6$_{Man3}$), 60.2 (C-7), 51.5 (C-2), 28.3 ($NHCO_2C(\underline{C}H_3)_3$) ppm; IR (ATR) ν_{max}/cm^{-1} 2970, 1722, 1451, 1260, 1094, 706; ESI-HRMS: m/z calcd. for $C_{82}H_{79}N_4O_{24}$ + H^+ = 1503.50788 $[M+H]^+$; found 1503.50703.

(*S*)-2-Azido-1-*O*-{1-[[2-(1,3-di-*O*-(2,3,4,6-tetra-*O*-benzoyl-α-D-mannopyranosyl))-1,3-propanediol]-1*H*-1,2,3-triazol-4-yl]-methyl}-1,3-propanediol (6a). General procedure F was applied to starting material **5a** (750 mg, 500 µmol). Reagents and conditions for first step: 4 M hydrochloric acid in dioxane (10.0 mL, 40 mmol, 80 eq.), anhydrous tetrahydrofuran (*c* = 0.1 M, 5.0 mL). Reaction was completed after 2 h. Reagents and conditions for second step: potassium carbonate (137 mg, 100 µmol, 2 eq.), copper(II) sulfate pentahydrate (2 mg, 5 µmol, 0.01 eq.) and imidazole-1-sulfonyl azide hydrochloride (167 mg, 800 µmol, 1.6 eq.), methanol/dichloromethane/water mixture 2:1:1 (*c* = 0.1 M, 5.0 mL). Flash chromatography with ethyl acetate/cyclohexane 4.5/5.5 afforded compound **6a** as a white foam (443 mg, 63 %); R_f = 0.3 (ethyl acetate/cyclohexane 4/6); $[a]_{20}^{D}$= - 375 (*c* 1, chloroform); ^{1}H NMR

(600 MHz, $CDCl_3$) δ 8.13-8.10 (m, 4H, 4 H-Ar), 8.03-7.98 (m, 5H, 4 H-Ar, H-6), 7.96-7.92 (m, 4H, 4 H-Ar), 7.86-7.78 (m, 4H, 4 H-Ar), 7.65-7.54 (m, 4H, 4 H-Ar), 7.50-7.45 (m, 2H, 2 H-Ar), 7.46-7.39 (m, 6H, 6 H-Ar), 7.39-7.31 (m, 8H, 8 H-Ar), 7.29-7.27 (m, 1H, H-Ar), 7.26-7.23 (m, 3H, 3 H-Ar), 6.13-6.09 (m, 2H, H-4_{Man2}, H-4_{Man3}), 5.82 (dd, $^3J_{3,4}$ = 10.2 Hz, $^3J_{2,3}$ = 3.3 Hz, 1H, H-3_{Man2}), 5.73-5.69 (m, 2H, H-2_{Man3}, H-3_{Man3}), 5.64 (dd, $^3J_{2,3}$ = 3.2 Hz, $^3J_{1,2}$ = 1.8 Hz, 1H, H-2_{Man2}), 5.27-5.19 (m, 1H, H-7), 5.17 (s, 1H, H-1_{Man3}), 5.10 (d, $^3J_{1,2}$ = 1.5 Hz, 1H, H-1_{Man2}), 4.83 (s, 2H, H-4), 4.77-4.65 (m, 2H, H-$6a_{Man2}$, H-$6a_{Man3}$), 4.58-4.45 (m, 3H, H-$6b_{Man2}$, H-$6b_{Man3}$, H-9a), 4.39 (dd, $^2J_{8a,8b}$ = 10.8 Hz, $^3J_{7,8a}$ = 4.6 Hz, 1H), 4.34-4.29 (m, 1H, H-5_{Man2}), 4.23 (dd, $^2J_{8a,8b}$ = 10.9 Hz, $^3J_{7,8b}$ = 7.1 Hz, 1H, H-8b), 4.16-4.04 (m, 2H, H-5_{Man3}, H-9b), 3.89-3.70 (m, 3H, H-1, H-3a), 3.68-6.62 (m, 2H, H-2, H-3b) ppm; ^{13}C NMR (151 MHz, $CDCl_3$) δ 166.1, 165.7, 165.6, 165.4, 165.3 (8C, 8 PhC=O), 145.2 (C-5), 133.6, 133.5, 133.3, 133.2, 133.1, 129.9, 129.8, 129.7, 129.0, 128.8, 128.6, 128.5, 128.4, 128.2, 125.3 (48C, 48 C-Ar), 123.6 (C-6), 98.4 (C-1_{Man2}), 97.6 (C-1_{Man3}), 70.0, 69.9 (4C, C-2_{Man2}, C-2_{Man3}, C-3_{Man2}, C-3_{Man3}), 69.7 (C-1), 69.6 (C-5_{Man2}), 69.4 (C-5_{Man3}), 67.4 (C-8), 66.6 (C-9), 66.5, 66.2 (2C, C-4_{Man2}, C-4_{Man3}), 64.8 (C-4), 62.6, 62.4 (2C, C-6_{Man2}, C-6_{Man3}), 62.2 (C-2), 62.1 (C-3), 60.3 (C-7) ppm; IR (ATR) ν_{max}/cm^{-1} 2955, 2097, 1722, 1259, 1094, 1026, 706; ESI-HRMS: m/z calcd. for $C_{77}H_{69}N_6O_{22}$ + H^+ = 1429.44594 $[M+H]^+$; found 1429.44530.

(*R*)-2-Azido-1-*O*-{1-[[2-(1,3-di-*O*-(2,3,4,6-tetra-*O*-benzoyl-α-D-mannopyranosyl))-1,3-propanediol]-1*H*-1,2,3-triazol-4-yl]-methyl}-1,3-propanediol (6b). General procedure F was applied to starting material **5b** (800 mg, 532 µmol). Reagents and conditions for first step: 4 M hydrochloric acid in dioxane (10.6 mL, 42.5 mmol, 80 eq.), anhydrous tetrahydrofuran (*c* = 0.1 M, 5.30 mL). Reaction was completed after 2 h. Reagents and conditions for second step: potassium carbonate (147 mg, 106 µmol, 2 eq.), copper(II) sulfate pentahydrate (2.0 mg, 5 µmol, 0.01 eq.) and imidazole-1-sulfonyl azide hydrochloride (178 mg, 851 µmol, 1.6 eq.), methanol/dichloromethane/water mixture 2:1:1 (*c* = 0.1 M, 5.3 mL). Flash chromatography with ethyl acetate/cyclohexane 4.5/5.5 afforded compound **6b** as a white foam (556 mg, 73 %); R_f = 0.3 (ethyl acetate/cyclohexane 4/6); $[\alpha]_{20}^{D}$= - 393 (*c* 1, chloroform); ^{1}H NMR (500 MHz, $CDCl_3$) δ 8.15-8.05 (m, 4H, 4 H-Ar), 8.05-7.91 (m, 9H, 8 H-Ar, H-6), 7.88-7.75 (m, 4H, 4 H-Ar), 7.63-7.54 (m, 4H, 4 H-Ar), 7.52-7.46 (m, 2H, 2 H-Ar), 7.45-7.31 (m, 14H, 14 H-Ar), 7.28-7.26 (m, 1H, H-Ar), 7.26-7.24 (m, 3H, 3 H-Ar), 6.14-6.10 (m, 2H, H-4_{Man2}, H-4_{Man3}), 5.82 (dd, $^3J_{3,4}$ = 10.2 Hz, $^3J_{2,3}$ = 3.3 Hz, 1H, H-3_{Man2}), 5.72-5.69 (m, 2H, H-2_{Man3},

H-3$_{Man3}$), 5.64 (dd, $^{3}J_{2,3}$ = 3.2 Hz, $^{3}J_{1,2}$ = 1.7 Hz, 1H, H-2$_{Man2}$) 5.26-5.15 (m, 2H, H-7, H-1$_{Man3}$), 5.10 (d, $^{3}J_{1,2}$ = 1.5 Hz, 1H, H-1$_{Man2}$), 4.86-4.79 (m, 2H, H-4), 4.76-4.65 (m, 2H, H-6a$_{Man2}$, H-6b$_{Man3}$), 4.56-4.45 (m, 3H, H-6b$_{Man2}$, H-6b$_{Man3}$, H-9a), 4.39 (dd, $^{2}J_{8a,8b}$ = 10.9 Hz, $^{3}J_{7,8a}$ = 4.5 Hz, 1H, H-8a), 4.34-4.29 (m, 1H, H-5$_{Man2}$), 4.23 (dd, $^{2}J_{8a,8b}$ = 10.9 Hz, $^{3}J_{7,8b}$ = 7.1 Hz, 1H, H-8b), 4.16-4.01 (m, 2H, H-5$_{Man3}$, H-9b), 3.81-3.70 (m, 3H, H-1, H-3a), 3.70-3.59 (m, 2H, H-2, H-3b), 2.74 (br s, 1H, -OH) ppm; ^{13}C NMR (126 MHz, $CDCl_3$) δ 166.1, 165.7, 165.6, 165.4, 165.3 (8C, 8 PhC=O), 145.2 (C-5), 133.6, 133.5, 133.3, 133.2, 133.1, 129.9, 129.8, 129.7, 129.0, 128.8, 128.6, 128.5, 128.4, 128.2, 125.3 (48C, 48 C-Ar), 123.6 (C-6), 98.4 (C-1$_{Man2}$), 97.6 (C-1$_{Man3}$), 70.0, 69.9, (4C, C-2$_{Man2}$, C-2$_{Man3}$, C-3$_{Man2}$, C-3$_{Man3}$), 69.7 (C-1), 69.6 (2C, C-5$_{Man2}$, C-5$_{Man3}$), 67.4 (C-8), 66.6 (C-9), 66.5, 66.2 (C-4$_{Man2}$, C-4$_{Man3}$), 64.8 (C-4), 62.6, (2C, C-6$_{Man2}$, C-6$_{Man3}$), 62.4 (C-2), 62.2 (C-3), 60.3 (C-7) ppm; IR (ATR) ν_{max}/cm^{-1} 2955, 2097, 1722, 1259, 1094, 1026, 706; ESI-HRMS: m/z calcd. for $C_{77}H_{69}N_6O_{22}$ + H^+ = 1429.44594 $[M+H]^+$; found 1429.44503.

(*R*)-2-Azido-1-*O*-{1-[[2-(1,3-di-*O*-(2,3,4,6-tetra-*O*-benzoyl-α-D-mannopyranosyl))-1,3-propanediol]-1*H*-1,2,3-triazol-4-yl]-methyl}-3-*O*-(2,3,4,6-tetra-*O*-benzoyl-α-D-mannopyranosyl)-1,3-propanediol (9a). General procedure B was applied to acceptor **6a** (100 mg, 70 µmol) and donor **7d** (108 mg, 140 µmol, 2 eq.). Reagents and conditions: trifluoromethanesulfonic anhydride (24.0 µL, 140 µmol, 2 eq.), 2,6-di-*tert*-butylpyridine (22.0 mg, 105 µmol, 1.5 eq.), anhydrous dichloromethane (*c* = 0.3 M, 230 µL), T = -78 °C to -60 °C for 45 min. Flash chromatography with ethyl acetate/cyclohexane 4/6 afforded compound **9a** as α,β-mixture, white foam (20.0 mg, 14 %); R_f = 0.3 (ethyl acetate/cyclohexane 1/1); $[\alpha]_{20}^{D}$= - 71 (*c* 1, chloroform); ESI-HRMS: m/z calcd. for $C_{111}H_{95}N_6O_{31}$ + H^+ = 2007.60363 $[M+H]^+$; found 2007.60374; ^{1}H NMR (500 MHz, $CDCl_3$) δ 8.13-8.07 (m, 6H, 6 H-Ar), 8.05-7.90 (m, 14H, 14 H-Ar), 7.86-7.78 (m, 6H, 6 H-Ar), 7.60-7.52 (m, 7H, 7 H-Ar), 7.49-7.44 (m, 3H, 3 H-Ar), 7.44-7.29 (m, 23H, 23 H-Ar), 7.25-7.21 (m, 2H, 2 H-Ar), 6.16-6.09 (m, 3H, H-4$_{Man1}$, H-4$_{Man3}$, H-4$_{Man2}$), 5.89 (dd, $^{3}J_{3,4}$ = 10.1 Hz, $^{3}J_{2,3}$ = 3.3 Hz, 1H, H-3$_{Man1}$), 5.84 (dd, $^{3}J_{3,4}$ = 10.1 Hz, $^{3}J_{2,3}$ = 3.3 Hz, 1H, H-3$_{Man3}$), 5.75-5.71 (m, 3H, H-2$_{Man1}$, H-2$_{Man2}$, H-3$_{Man2}$), 5.66 (dd, $^{3}J_{2,3}$ = 3.2 Hz, $^{3}J_{1,2}$ =1.8 Hz, 1H, H-2$_{Man3}$), 5.27-5.22 (m, 1H, H-7), 5.20 (br s, 1H, H-1$_{Man2}$), 5.12-5.11 (m, 2H, H-1$_{Man1}$, H-1$_{Man3}$), 4.91-4.85 (m, 2H, H-4), 4.76-4.66 (m, 3H, H-6a$_{Man1}$, H-6a$_{Man2}$, H-6a$_{Man3}$), 4.58-4.39 (m, 6H, H-5$_{Man1}$, H-6b$_{Man1}$, H-6b$_{Man2}$, H-6b$_{Man3}$, H-8a, H-9a), 4.37-4.32 (m, 1H, H-5$_{Man3}$), 4.28-4.19 (m, 1H, H-8b), 4.19-4.15 (m, 2H, H-9b, H-5$_{Man2}$), 4.01 (dd, $^{2}J_{3a,3b}$ =

10.4 Hz, $^{3}J_{3a,2}$ =4.0 Hz, 1H, H-3a), 3.92-3.86 (m, 1H, H-2), 3.85-3.80 (m, 2H, H-1), 3.79-3.64 (m, 1H, H-3b) ppm; ^{13}C NMR (126 MHz, $CDCl_3$) δ 166.1, 166.0, 165.5, 165.4, 165.3, 165.2 (11C, 11 PhC=O), 133.5, 133.4, 133.2, 133.1, 133.0, 129.9, 129.8, 129.7, 129.2, 129.1, 128.9, 128.8, 128.6, 128.5, 128.4, 128.3, (71C, 71 C-Ar), 123.9, (C-6), 98.3 (C-1_{Man3}), 97.9 (C-1_{Man2}), 97.7 (C-1_{Man1}), 70.1, 70.0, 69.9, 69.7 (6 C, C-2_{Man1}, C-2_{Man3}, C-2_{Man2}, C-3_{Man1}, C-3_{Man3}, C-3_{Man2}), 69.7 (C-1), 69.6 (C-5_{Man3}), 69.5 (C-5_{Man1}), 69.12 (C-5_{Man2}), 67.9 (C-3), 67.3 (C-8), 66.6, 66.5, 66.4, 66.3, 66.2 (4C, C-4_{Man1}, C-4_{Man3}, C-4_{Man1}, C-9), 64.9 (C-4), 62.7, 62.6, 62.4 (3C, C-6_{Man1}, C-6_{Man3}, C-6_{Man2}), 60.1 (C-7), 60.0 (C-2) ppm.

Table 8.1: Chemical shifts δ (ppm) for α,β-mixture of **9a**.

	(α) **9a**		(β) **9a**	
Atom	^{1}H-NMR	^{13}C-NMR	^{1}H-NMR	^{13}C-NMR
1_{Man3}	5.12-5.13 (m)	98.3	5.17 (br s)	97.7
2_{Man3}	5.66 (dd)	-	5.71-5.69 (m)	-

Descriptor: - peak was not found

(*R*)-2-*N*-(*tert*-Butoxycarbonyl)-1-*O*-(propargyl)-3-*O*-(3,4,6-tri-*O*-benzoyl-1,2-dioxolanephenyl-β-D-mannopyranosyl)-1,3-propanediol (10a). General procedure A for glycosylation was applied to acceptor **3a** (220 mg, 1.0 mmol) and donor **7c** (763 mg, 1.20 mmol, 1.2 eq.). Reagents and conditions: silver trifluoromethanesulfonate (300 mg, 1.20 mmol, 1.2 eq.), 2,4,6-collidine (154 µL, 1.20 mmol, 1.2 eq.), anhydrous dichloromethane (*c* = 0.1 M, 9.60 mL), T = -41 ˚C to room temperature after three hours. Flash chromatography with ethyl acetate/cyclohexane 3/7 afforded mixture of **10a**$_{exo}$ and **10a**$_{endo}$ as a white foam (668 mg, 86 %); R_f = 0.3 (ethyl acetate/cyclohexane 3/7); $[\alpha]_{20}^{D}$= - 42 (*c* 0.6, chloroform); IR (ATR) ν_{max}/cm^{-1} 2975, 2300, 1719, 1451, 1264, 1091, 1067, 706; ESI-HRMS: m/z calcd. for $C_{45}H_{45}NO_{13}$ + Na^+ = 830.27831 $[M+Na]^+$; found 830.27840. Compound **10a**$_{endo}$: ^{1}H NMR (500 MHz, $CDCl_3$) δ 8.02-7.99 (m, 2H, 2 H-Ar), 7.92-7.88 (m, 4H, 4 H-Ar), 7.69 (dd, *J* = 7.5 Hz, *J* = 1.7 Hz, 2H, 2 H-Ph$_{ortho}$), 7.54-7.46 (m, 3H, 3 H-Ar), 7.41-7.27 (m, 9H, 9 H-Ar), 5.89-5.84 (m, 1H, H-4_{Man}), 5.84 (d, $^{3}J_{1,2}$ = 2.5 Hz, 1H, H-1_{Man}), 5.68 (dd, $^{3}J_{3,4}$ = 9.9 Hz, $^{3}J_{3,2}$ = 3.8 Hz, 1H, H-3_{Man}), 5.08 (t, $^{3}J_{1,2}$ = 3.5 Hz, 1H, H-2_{Man}), 4.82 (br s, 1H, NH), 4.52 (dd, $^{2}J_{6a,6b}$ = 12.0 Hz, $^{3}J_{5,6a}$ = 3.4 Hz, 1H, H-$6a_{Man}$), 4.35 (dd, $^{2}J_{6a,6b}$ = 12.0 Hz, $^{3}J_{5,6b}$ = 4.8 Hz, 1H, H-$6b_{Man}$), 4.16-4.09 (m, 1H, H-5_{Man}), 4.07 (dd, $^{4}J_{1,4}$ = 7.5 Hz, $^{4}J_{4,5}$ = 2.3 Hz, 2H, H-4), 3.93-3.85 (br s, 1H, H-2), 3.61 (dd, $^{2}J_{1a,1b}$ = 9.2 Hz, $^{3}J_{1a,2}$ = 4.0 Hz, 1H, H-1a), 3.57-3.52 (m, 1H, H-3a), 3.49 (dd, $^{3}J_{1a,1b}$ = 9.2 Hz,

$^{3}J_{1b,2}$ = 5.7 Hz, 1H, H-1b), 3.44 (dd, $^{3}J_{3a,3b}$ = 9.4 Hz, $^{3}J_{3b,2}$ = 6.1 Hz, 1H, H-3b), 2.43 (t, ^{4}J = 2.3 Hz, 1H, H-6), 1.39 (s, 9H, $NHCO_2C(C\underline{H}_3)_3$) ppm; ^{13}C NMR (126 MHz, $CDCl_3$) δ 166.0, 165.9, 165.2 (3C, 3 PhC=O), 155.3 ($NH\underline{C}O_2C(CH_3)_3$), 137.9, 133.5, 133.4, 133.0, 130.1, 129.8, 129.7, 129.6, 129.4, 129.0, 128.9, 128.4, 128.3, 128.2, 126.5, 125.3, 122.7 (23C, 23 C-Ar), 122.7 (orthoester C_q), 98.0 (C-1_{Man}), 79.4 (2C, C-5, $NHCO_2\underline{C}(CH_3)_3$), 76.4 (C-$2_{Man}$), 74.8 (C-6), 72.3 (C-$5_{Man}$), 70.8 (C-$3_{Man}$), 68.5 (C-1), 66.5 (C-$4_{Man}$), 63.2 (C-$6_{Man}$), 62.3 (C-3), 58.4 (C-4), 49.4 (C-2), 28.3 ($NHCO_2C(\underline{C}H_3)_3$) ppm.

Table 8.2: Chemical shifts δ (ppm) for compound **10a*endo*** and **10a*exo***.

	10a*endo*		**10a*exo***	
Atom	^{1}H-NMR	^{13}C-NMR	^{1}H-NMR	^{13}C-NMR
1_{Man}	~5.84 (d, $^{3}J_{1,2}$ = 2.5 Hz)	98.0	-	-
2_{Man}	5.08 (t, $^{3}J_{2,3}$ = 3.5 Hz)	76.4	-	-
3_{Man}	5.68 (dd, $^{3}J_{3,4}$ = 9.9 Hz, $^{3}J_{2,3}$ = 3.8 Hz)	70.8	-	-
4_{Man}	5.89-5.84 (m)*	66.5	-	-
5_{Man}	4.14-4.09 (m)	72.3	-	-
$6a_{Man}$	4.52 (dd, $^{2}J_{6a,6b}$ = 12.0 Hz, $^{3}J_{5,6a}$ = 3.4 Hz)	63.2	-	-
$6b_{Man}$	4.35 (dd, $^{2}J_{6a,6b}$ = 12.0 Hz, $^{3}J_{5,6b}$ = 4.8 Hz)			
1a	3.61 (dd, $^{2}J_{1a,1b}$ = 9.2 Hz, $^{3}J_{1a,2}$ = 4.0 Hz)	68.5	3.71 (dd, $^{2}J_{1a,1b}$ = 9.4 Hz, $^{3}J_{1a,2}$ = 3.9 Hz)	-
1b	3.49 (dd, $^{2}J_{1a,1b}$ = 9.0 Hz, $^{3}J_{1a,2}$ = 5.7 Hz)		3.68-3.64 (m)*	
2	3.93-3.85 (m)	49.4	3.83-3.77 (m)	-
3a	3.57-3.52 (m)*	62.3	-	-
3b	3.44 (dd, $^{2}J_{3a,3b}$ = 9.4 Hz, $^{3}J_{2,3a}$ = 6.1 Hz)		-	
4	4.07 (dd, $^{2}J_{4a,4b}$ = 7.5 Hz, $^{4}J_{4,6}$= 2.3 Hz)	58.4	4.16 (dd, $^{2}J_{4a,4b}$ = 5.0 Hz, $^{4}J_{4,6}$ = 2.4 Hz)	58.6
5	-	79.4	-	-
6	2.43 (t, $^{4}J_{4,6}$ = 2.4 Hz)	74.8	2.46 (t, $^{4}J_{4,6}$ = 2.4 Hz)	75.0
*N*HBoc	1.39 (s)	28.3	1.45 (s)	28.3
Ph_{ortho}	7.69 (dd, *J* = 7.5 Hz, *J* = 1.7 Hz)	126.5	-	-
Ph_q	-	122.7	-	-

Descriptors: a) - peak was not found; b) * peak was found in the described region

(*S*)-2-*N*-(*tert*-Butoxycarbonyl)-1-*O*-(propargyl)-3-*O*-(3,4,6-tri-*O*-benzoyl-1,2-dioxolanephenyl-β-D-mannopyranosyl))-1,3-propanediol (10b). General procedure A for glycosylation was applied to acceptor **10b** (230 mg, 1.0 mmol) and donor **7c** (800 mg, 1.21 mmol, 1.2 eq.). Reagents and conditions: silver trifluoromethanesulfonate (310 mg, 1.21 mmol, 1.2 eq.), 2,4,6-collidine (160 µL, 1.21 mmol, 1.2 eq.), anhydrous dichloromethane (*c* = 0.1 M, 10 mL), T = -41 ˚C to room temperature after three hours. Flash chromatography with ethyl acetate/cyclohexane 3/7 afforded mixture of **10b**$_{exo}$ and **10b**$_{endo}$ as white foam (580 mg, 72 %); R_f = 0.3 (ethyl acetate/cyclohexane 3/7); $[\alpha]_{20}^{D}$= - 52 (*c* 1, chloroform); IR (ATR) ν_{max}/cm^{-1} 2975, 2300, 1719, 1451, 1264, 1091, 1067, 706; ESI-HRMS: m/z calcd. For $C_{45}H_{45}NO_{13}$ + Na^+ = 830.27831 $[M+Na]^+$; found 830.27839. Compound **10b**$_{endo}$: ^{1}H NMR (500 MHz, $CDCl_3$) δ 8.02-7.98 (m, 2H, 2 H-Ar), 7.93-7.87 (m, 4H, 4 H-Ar), 7.71-7.66 (m, 2H, 2 H-Ph$_{ortho}$), 7.55-7.46 (m, 3H, 3 H-Ar), 7.39-7.27 (m, 9H, 9 H-Ar), 5.87-5.81 (m, 2H, H-1$_{Man}$, H-4$_{Man}$), 5.68 (dd, $^3J_{3,4}$ = 10.0 Hz, $^3J_{2,3}$ = 4.0 Hz, 1H, H-3$_{Man}$), 5.07 (t, $^3J_{2,3}$ = 3.5 Hz, 1H, H-2$_{Man}$), 4.82 (br s, 1H, NH), 4.52 (dd, $^2J_{6a,6b}$ = 12.0 Hz, $^3J_{5,6a}$ = 3.5 Hz, 1H, H-6a$_{Man}$), 4.36 (dd, $^2J_{6a,6b}$ = 12.0 Hz, $^3J_{5,6b}$ = 4.9 Hz, 1H, H-6b$_{Man}$), 4.15-4.09 (m, 1H, H-5$_{Man}$), 4.07 (t, $^3J_{4,6}$ = 2.6 Hz, 2H, H-4), 3.90 (br s, 1H, H-2), 3.59 (dd, $^2J_{1a,1b}$ = 9.1 Hz, $^3J_{1a,2}$ = 4.1 Hz, 1H, H-1a), 3.56-3.50 (m, 5.8 Hz, 2H, H-1b, H-3a), 3.43 (dd, $^3J_{3a,3b}$ = 9.4 Hz, $^3J_{3b,2}$ = 6.2 Hz, 1H, H-3b), 2.43 (t, $^4J_{4,6}$ = 2.4 Hz, 1H, H-6), 1.40 (s, 9H, $NHCO_2C(C\underline{H}_3)_3$) ppm; ^{13}C NMR (126 MHz, $CDCl_3$) δ 166.0, 165.9, 165.2 (3C, 3 PhC=O), 155.3 ($NH\underline{C}O_2C(CH_3)_3$), 136.1, 133.5, 133.4, 133.0, 129.8, 129.7, 129.6, 129.4, 129.0, 128.9, 128.4, 128.3, 128.2, 126.5, 125.3, 122.6 (23C, 23 C-Ar), 122.7 (orthoester C_q), 98.0 (C-1$_{Man}$), 79.5 ($NHCO_2\underline{C}(CH_3)_3$), 79.5 (C-5), 76.3 (C-2$_{Man}$), 74.8 (C-6), 72.4 (C-5$_{Man}$), 70.8 (C-3$_{Man}$), 68.4 (C-1), 66.5 (C-4$_{Man}$), 63.2 (C-6$_{Man}$), 62.5 (C-3), 58.4 (C-4), 49.3 (C-2), 28.4 ($NHCO_2C(\underline{C}H_3)_3$) ppm.

Table 8.3: Chemical shifts δ (ppm) for compound **10b**$_{exo}$ and **10b**$_{endo}$.

	10b$_{endo}$		**10b**$_{exo}$	
Atom	^{1}H-NMR	^{13}C-NMR	^{1}H-NMR	^{13}C-NMR
1_{Man}	5.87-5.81 (m)*	98.0	-	-
2_{Man}	5.07 (t, $^{3}J_{2,3}$ = 3.5 Hz)	76.3	-	-
3_{Man}	5.68 (dd, $^{3}J_{3,4}$ = 10 Hz, $^{3}J_{2,3}$ = 4 Hz)	70.8	-	-
4_{Man}	5.87-5.81 (m)*	66.5	-	-
5_{Man}	4.15-4.09 (m)	72.4	-	-
$6a_{Man}$	4.52 (dd, $^{2}J_{6a,6b}$ = 12.0 Hz, $^{3}J_{5,6a}$ = 3.5 Hz)	63.2	-	-
$6b_{Man}$	4.36 (dd, $^{2}J_{6a,6b}$ = 12.0 Hz, $^{3}J_{5,6b}$ = 4.9 Hz)		-	
1a	3.59 (dd, $^{2}J_{1a,1b}$ = 9.1 Hz, $^{3}J_{1a,2}$ = 4.1 Hz)	68.4	-	-
1b	3.56-3.50 (m)*		-	
2	3.93-3.85 (m)	49.3	-	-
3a	3.56-3.50 (m)*	62.5	-	-
3b	3.43 (dd, $^{2}J_{3a,3b}$ = 9.4 Hz, $^{3}J_{3b,2}$ = 6.2 Hz)		-	
4	4.07 (t, $^{4}J_{4,6}$ = 2.6 Hz)	58.4	4.17 (dd, $^{2}J_{4a,4b}$ = 3.6 Hz, $^{4}J_{4,6}$ = 2.4 Hz)	-
5	-	79.5	-	-
6	2.43 (t, $^{4}J_{4,6}$ = 2.4 Hz)	74.8	2.46 (t, $^{4}J_{4,6}$ = 2.4 Hz)	-
*N*HBoc	1.40 (s)	28.4	1.45 (s)	28.4
Ph_{ortho}	7.71-7.66 (m)*	126.5	7.71-7.66 (m)*	-
Ph_{q}	-	122.7	-	-

Descriptors: a) - peak was not found; b) * peak was found in the described region.

(*R*)-2-*N*-(*tert*-Butoxycarbonyl)-1-*O*-{1-[[2-(1,3-di-*O*-(2,3,4,6-tetra-*O*-benzoyl-α-D-mannopyranosyl))-1,3-propanediol]-1*H*-1,2,3-triazol-4-yl]}-3-*O*-(3,4,6-tri-*O*-benzoyl-1,2-dioxolanephenyl-β-D-mannopyranosyl)-1,3-propanediol (11a). General procedure E for Cu-AAC addition was applied to azide moiety **4** (482 mg, 378 µmol) and alkyne moiety **10a** (610 mg, 756 µmol, 2 eq.). Reagents and conditions: copper(I) bromide (10.3 mg, 72 µmol, 0.2 eq.) and tris[(1-benzyl-1*H*-1,2,3-triazol-4-yl)methyl]amine (TBTA) (10.0 mg, 19 µmol, 0.05 eq.), anhydrous *N*,*N*-dimethylformamide (*c* = 0.1 M, 3.90 mL), T = 60 ˚C for 1 hour under microwave conditions. Flash chromatography with ethyl acetate/cyclohexane 4/6 afforded mixture of **11a**$_{endo}$ and **11a**$_{exo}$ as a white foam (520 mg, 66 %); R_f = 0.3 (ethyl acetate/cyclohexane 4/6); $[\alpha]_{20}^{D}$= - 47 (*c* 1, chloroform); IR (ATR) ν_{max}/cm^{-1} 2961, 1720, 1451, 1260, 1092, 1067, 1026, 750, 706; ESI-HRMS: m/z calcd. for $C_{116}H_{105}N_4O_{33}$ + H^+ + H^+ = 2081.66556 [M+ 2 H]$^+$; found 2081.66852. Compound **11a**$_{exo}$: ^{1}H NMR (600 MHz, $CDCl_3$) δ 8.11-8.09 (m, 4H, 4 H-Ar), 8.02-7.98 (m, 4H. 4 H-Ar), 7.99-7.91 (m, 7H, 6 H-Ar, H-6), 7.89-7.85

(m, 4H, 4 H-Ar), 7.82-7.80 (m, 4H, 4 H-Ar), 7.68-7.65 (m, 2H, 2 H-Ph), 7.59-7.53 (m, 4H, 4 H-Ar), 7.51-7.47 (m, 1H, H-Ar), 7.46-7.28 (m, 25H, 25 H-Ar), 7.25-7.21 (m, 6H, 6 H-Ar), 6.15-6.09 (m, 2H, H-4_{Man2}, H-4_{Man3}), 5.89 (br s, 1H, H-1_{Man1}), 5.86-5.82 (m, 2H, H-3_{Man2}, H-4_{Man1}), 5.75-5.69 (m, 3H, H-2_{Man2}, H-2_{Man3}, H-3_{Man3}), 5.67-5.66 (m, 1H, H-3_{Man1}), 5.18 (br s, 1H, H-1_{Man3}), 5.15-5.13 (m, 1H, H-7), 5.09 (br s, 2H, H-1_{Man2}, H-2_{Man1}), 4.74-4.70 (m, 3H, H-4, H-$6a_{Man2}$), 4.67 (dd, $^{2}J_{6a,6b}$ = 12.3 Hz, $^{3}J_{5,6a}$ = 2.2 Hz, 1H, H-$6a_{Man3}$), 4.55-4.37 (m, 5H, H-$6a_{Man1}$, H-$6b_{Man2}$, H-$6b_{Man3}$, H-8a, H-9a), 4.35-4.32 (m, 2H, H-5_{Man2}, H-$6b_{Man1}$), 4.23-4.16 (m, 1H, H-8b), 4.14-4.04 (m, 3H, H-5_{Man1}, H-5_{Man3}, H-9b), 3.98 (br s, 1H, H-2), 3.67-3.64 (m, 2H, H-1a, H-3a), 3.58 (dd, $^{2}J_{1a,1b}$ = 9.2 Hz, $^{3}J_{1b,2}$ = 5.9 Hz, 1H, H-1b), 3.53 (dd, $^{2}J_{3a,3b}$ = 9.2 Hz, $^{3}J_{2,3b}$ = 5.6 Hz, 1H, H-3b), 1.29 (s, 9H, $NHCO_2C(C\underline{H}_3)_3$) ppm; ^{13}C NMR (151 MHz, $CDCl_3$) δ 166.1, 166.0, 165.8, 165.6, 165.5, 165.4, 165.3, 165.2, (11C, 11 PhC=O) 155.8 ($NH\underline{C}O_2C(CH_3)_3$), 145.3 (C-5), 137.9, 133.5, 133.4, 133.3, 133.2, 133.1, 132.9, 130.0, 129.8, 129.7, 129.6, 129.3, 129.1, 129.0, 128.9, 128.8, 128.7, 128.6, 128.5, 128.4, 128.3, 128.2, 123.6, (72 C, 71 C-Ar, C-6), 122.9 (orthoester C_q), 98.3 (C-1_{Man2}), 98.0 (C-1_{Man1}), 97.6 (C-1_{Man3}), 79.3 ($NHCO_2\underline{C}(CH_3)_3$), 76.7 (C-$2_{Man1}$), 72.0 (C-$5_{Man1}$), 70.9 (C-$2_{Man2}$), 70.0 (4C, C-$2_{Man3}$, C-$3_{Man1}$, C-$3_{Man3}$, C-$3_{Man2}$), 69.6 (C-$5_{Man2}$), 69.4 (C-$5_{Man3}$), 69.3 (C-1), 67.2 (C-8), 66.6 (C-4_{Man1}), 66.5 (C-9), 66.4 (C-4_{Man2} or C-4_{Man3}), 66.3 (C-4_{Man2} or C-4_{Man3}), 64.6 (C-4), 63.1 (C-6_{Man1}), 62.9 (C-3), 62.6 (C-6_{Man2} or C-6_{Man3}), 62.4 (C-6_{Man2} or C-6_{Man3}), 59.9 (C-7), 49.7 (C-2), 21.5 ($NHCO_2C(\underline{C}H_3)_3$) ppm.

(*S*)-2-*N*-(*tert*-Butoxycarbonyl)-1-*O*-{1-[[2-(1,3-di-*O*-(2,3,4,6-tetra-*O*-benzoyl-α-D-mannopyranosyl))-1,3-propanediol]-1*H*-1,2,3-triazol-4-yl]-methyl}-3-*O*-(3,4,6-tri-*O*-benzoyl-1,2-dioxolanephenyl-β-D-mannopyranosyl)-1,3-propanediol (11b). General procedure E for CuAAC addition was applied to azide moiety **4** (340 mg, 266 µmol) and alkyne moiety **10b** (430 mg, 533 µmol, 2 eq.). Reagents and conditions: copper(I) bromide (7.30 mg, 50 µmol, 0.2 eq.) and tris[(1-benzyl-1*H*-1,2,3-triazol-4-yl)methyl]amine (TBTA) (7.0 mg, 13.0 µmol, 0.05 eq.), anhydrous *N*,*N*-dimethylformamide (*c* = 0.1 M, 2.70 mL), T = 60 ˚C for 1 h under microwave conditions. Flash chromatography with ethyl acetate/cyclohexane 4/6 afforded mixture of **11b**$_{endo}$ and **11b**$_{exo}$ as white foam (368 mg, 65 %); R_f = 0.3 (ethyl acetate/cyclohexane 4/6); $[\alpha]_{20}^{D}$= - 40 (*c* 1, chloroform); IR (ATR) ν_{max}/cm^{-1} 2961, 1721, 1451, 1260, 1093, 1067, 771, 706, 462; ESI-HRMS: m/z calcd. For $C_{116}H_{105}N_4O_{33}$ + H^+ + H^+ = 2081.66748 [M+ 2 H]$^+$; found 2081.66556. Compound **11b**$_{endo}$: ^{1}H NMR (600 MHz, $CDCl_3$) δ 8.11-8.09 (m, 4H, 4 H-Ar), 8.02-7.99 (m, 4H, 4 H-Ar), 7.96-7.90 (m, 7H, 6 H-Ar, H-6), 7.90-7.84

(m, 4H, 4 H-Ar), 7.84-7.79 (m, 4H, 4 H-Ar), 7.68-7.66 (m, 2H, 2 H-Ph), 7.59-7.54 (m, 4H, 4 H-Ar), 7.50-7.38 (m, 12H, 12 H-Ar), 7.37-7.33 (m, 5H, 5 H-Ar), 7.32-7.28 (m, 9H, 9 H-Ar), 7.25-7.22 (m, 6H, 6 H-Ar), 6.15-6.09 (m, 2H, H-4_{Man2}, H-4_{Man3}), 5.87-5.81 (m, 3H, H-1_{Man1}, H-3_{Man2}, H-4_{Man1}), 5.73-5.66 (m, 4H, H-2_{Man2}, H-2_{Man3}, H-3_{Man1}, H-3_{Man3}), 5.18 (d, $^3J_{1,2}$ = 1.1 Hz, 1H, H-1_{Man3}), 5.16-5.12 (m, 1H, H-7), 5.10 (d, $^3J_{1,2}$ = 1.3 Hz, 1H, H-1_{Man2}), 5.09-5.06 (m, 1H, H-2_{Man1}), 4.74-4.71 (m, 3H, H-4, H-$6a_{Man2}$), 4.68 (dd, $^2J_{6a,6b}$ = 12.3 Hz, $^3J_{5,6a}$ = 2.4 Hz, 1H, H-$6a_{Man3}$), 4.53-4.39 (m, 5H, H-$6a_{Man1}$, H-$6b_{Man2}$, H-$6b_{Man3}$, H-8a, H-9a), 4.35-4.32 (m, 2H, H-5_{Man2}, H-$6b_{Man1}$), 4.20 (dd, $^2J_{8a,8b}$ = 10.8 Hz, $^3J_{7,8b}$ =6.6 Hz, 1H, H-8b), 4.13-4.04 (m, 3H, H-5_{Man1}, H-5_{Man3}, H-9b), 3.95 (br s, 1H, H-2), 3.69-3.67 (m, 1H, H-1a), 3.61-3.63 (m, 2H, H-1b, H-3a), 3.57-3.50 (m, 1H, H-3b), 1.22 (s, 9H, $NHCO_2C(C\underline{H}_3)_3$) ppm; ^{13}C NMR (151 MHz, $CDCl_3$) δ 166.1, 166.0, 165.8, 165.5, 165.4, 165.3, 165.1 (11C, 11 PhC=O), 155.8 ($NH\underline{C}O_2C(CH_3)_3$), 145.2 (C-5), 133.5, 133.3, 133.2, 133.1, 132.1, 130.0, 129.8, 129.7, 129.6, 129.3, 129.1, 129.0, 128.8, 128.6, 128.5, 128.4, 128.3, 128.2, 126.6, 125.3, 123.8, (72C, 71 C-Ar, C-6), 122.8 (ortho-ester C_q), 98.3 (C-1_{Man2}), 98.0 (C-1_{Man1}), 97.6 (C-1_{Man3}), 79.2 ($NHCO_2\underline{C}(CH_3)_3$), 76.6 (C-$2_{Man1}$), 72.0 (C-$5_{Man1}$), 70.9 (C-$2_{Man2}$), 70.0 (3C, C-$2_{Man3}$, C-$3_{Man1}$, C-$3_{Man3}$), 69.9 (C-$3_{Man2}$), 69.6 (C-$5_{Man2}$), 69.4 (C-$5_{Man3}$), 69.3 (C-1), 67.3 (C-8), 66.6 (C-4_{Man1}), 66.5 (C-9), 66.4 (C-4_{Man2} or C-4_{Man3}), 66.3 (C-4_{Man2} or C-4_{Man3}), 64.7 (C-4), 63.1 (C-6_{Man1}), 62.6 (2C, C-3, C-6_{Man2}), 62.4 (C-6_{Man3}), 59.9 (C-7), 49.6 (C-2), 28.2 ($NHCO_2C(\underline{C}H_3)_3$) ppm.

(*R*)-2-*N*-(*tert*-Butoxycarbonyl)-1-*O*-{1-[[2-(1,3-di-*O*-(2,3,4,6-tetrahydroxy-α-D-mannopyranosyl))-1,3-propanediol]-1*H*-1,2,3-triazol-4-yl]-methyl}-3-*O*-(3,4,6-tri-*O*-benzoyl-1,2-dioxolanephenyl-β-D-mannopyranosyl)-1,3-propanediol (12a). General procedure G was applied to starting material **11a** (500 mg, 240 µmol). Reagents and conditions: sodium methoxide (4-5 drops), anhydrous methanol (*c* = 0.03 M, 7.40 mL). Size exclusion chromatography G10 in water yielded mixture of **12a**$_{endo}$ and **12a**$_{exo}$ as a white foam (124 mg, 62 %); $[\alpha]_{20}^{D}$= + 126 (*c* 1, dd water); IR (ATR) ν_{max}/cm^{-1} 3341, 2929, 1682, 1050, 1025, 669, 584 ESI-HRMS: m/z calcd. for $C_{39}H_{60}N_4O_{22}$ + Na^+ = 959.35992 $[M+Na]^+$; found 959.35946. Compound **12a**$_{endo}$: ^{1}H NMR (600 MHz, D_2O) δ 8.12 (s, 1H, H-6), 7.60 (dd, *J* = 7.4 Hz, *J* = 2.2 Hz, 2H, H-Ph$_{ortho}$), 7.51-7.41 (m, 3H, 2 H-Ph$_{meta}$, H-Ph$_{para}$), 5.67 (d, $^3J_{1,2}$ = 2.4 Hz, 1H, H-1_{Man1}), 5.18-5.11 (m, 1H, H-7), 4.81 (d, $^3J_{1,2}$ = 1.4 Hz, 1H, H-1_{Man2} or H-1_{Man3}), 4.75 (br s, 1H, H-2_{Man1}), 4.73 (br s, 1H, H-1_{Man2} or H-1_{Man3}), 4.65 (br s, 2H, H-4), 4.21-4.12 (m, 2H, H-8a, H-9a), 4.04-3.98 (m, 3H, H-3_{Man1}, H-8b, H-9b), 3.90-3.85 (m, 2H, H-2, H-2_{Man2} or H-2_{Man3}),

3.81-3.71 (m, 3H, H-2$_{Man2}$ or H-2$_{Man3}$, H-6a$_{Man1}$, H-6a$_{Man3}$), 3.69-6.64 (m, 5H, H-3$_{Man2}$ or H-3$_{Man3}$, H-4$_{Man1}$, H-6b$_{Man1}$, H-6a$_{Man2}$, H-6b$_{Man3}$), 3.61-3.51 (m, 8H, H-1, H-3a, H-3$_{Man2}$ or H-3$_{Man3}$, H-4$_{Man2}$, H-6b$_{Man2}$, H-6b$_{Man3}$), 3.46 (dd, $^{2}J_{3a,3b}$ = 10.1 Hz, $^{3}J_{2,3b}$ = 4.9 Hz, 1H, H-3b), 3.41-3.34 (m, 2H, H-5$_{Man1}$, H-5$_{Man2}$ or H-5$_{Man3}$), 3.07-3.02 (m, 1H, H-5$_{Man2}$ or H-5$_{Man3}$), 1.41 (s, 9H, NHCO$_2$C(C$\underline{H}_3$)$_3$) ppm; ^{13}C NMR (151 MHz, D_2O) δ 157.7 (NH$\underline{C}$O$_2$C(CH$_3$)$_3$), 144.1 (C-5), 130.0, 128.6 (2C, C-Ph$_{para}$, C-Ph$_{meta}$), 126.1 (C-Ph$_{ortho}$), 124.8 (C-6), 122.1 (orthoester C$_q$), 100.3 (C-1$_{Man2}$ or C-1$_{Man3}$), 99.7 (C-1$_{Man1}$), 99.6 (C-1$_{Man2}$ or C-1$_{Man3}$), 81.2 (NHCO$_2\underline{C}$(CH$_3$)$_3$), 79.3 (C-2$_{Man1}$), 75.1 (C-5$_{Man1}$), 73.1, 72.9 (2C, C-5$_{Man2}$, C-5$_{Man3}$), 70.6 (C-3$_{Man1}$), 70.4 (2C, C-3$_{Man2}$, C-3$_{Man3}$), 69.9, 69.8 (2C, C-2$_{Man2}$, C-2$_{Man3}$), 68.9 (C-1), 66.8 (C-4$_{Man1}$), 66.5, 66.4, 66.3, 66.0, (4C, C-4$_{Man2}$, C-4$_{Man3}$, C-8, C-9), 65.9 (C-4), 63.6, 63.2, 61.0, 60.9, 60.7 (4C, C-3, C-6$_{Man1}$, C-6$_{Man2}$, C-6$_{Man3}$, C-7), 49.8 (C-2), 27.7 (NHCO$_2$C($\underline{C}$H$_3$)$_3$) ppm.

Table 8.4: Chemical shifts δ(ppm) for compounds **12a**$_{endo}$ and **12a**$_{exo}$.

	12a$_{endo}$		**12a**$_{exo}$	
Atom	^{1}H-NMR	^{13}C-NMR	^{1}H-NMR	^{13}C-NMR
1$_{Man1}$	5.68 (d, $^{3}J_{1,2}$ = 2.4 Hz)	97.5	-	-
2$_{Man1}$	4.75 (br s)*	79.3	-	-
1$_{Man2,3}$		100.3		100.4
1a	3.58-3.51 (m)*	68.9	-	-
1b	3.58-3.51 (m)*			
2	3.90-3.85 (m)	49.8	-	-
3a	3.61-3.51 (m)*	63.2	-	-
3b	3.46 (dd, $^{2}J_{3a,3b}$ = 10.1 Hz, $^{3}J_{2,3b}$ = 4.9 Hz)		-	
4	4.65 (br s)*	63.3	4.67 (br s)*	63.3
5	-	144.1	-	144.2
6	8.12 (s)	124.8	8.18 (s)	124.8
7	5.15-5.10 (m)*	63.6	5.19-5.15 (m)*	63.6
NHBoc	1.41 (s)	27.7	-	-
Ph$_{ortho}$	7.60 (dd, *J* = 7.5 Hz, *J* = 2.1 Hz)	126.1	-	-
Ph$_{m,}$	7.49-7.43 (m)*	128.6	-	-
Ph$_p$	7.49-7.43 (m)*	130.0	-	-
Ph$_q$		122.1		

Descriptors: a) - peak was not found; b) * peak was found in the described region

(*S*)-2-*N*-(*tert*-Butoxycarbonyl)-1-*O*-{1-[[2-(1,3-di-*O*-(2,3,4,6-tetrahydroxy-α-D-mannopyranosyl))-1,3-propanediol]-1*H*-1,2,3-triazol-4-yl]}-3-*O*-(3,4,6-tri-*O*-benzoyl-1,2-dioxolanephenyl-β-D-mannopyranosyl)-1,3-propanediol (12b). General procedure G was applied to starting material **11b** (170 mg, 240 µmol). Reagents and conditions: sodium methoxide (2-3 drops), anhydrous methanol (*c* = 0.03 M, 2.40 mL). Size exclusion chromatography G10 in water yielded mixture of **12b**$_{endo}$ and **12b**$_{exo}$ as a white foam (42.0 mg, 70 %). $[\alpha]_{20}^{D}$ = + 102 (*c* 0.5, dd water); IR (ATR) ν_{max}/cm^{-1} 3341, 2929, 1687, 1050, 1025, 669, 584; ESI-HRMS: m/z calcd. for $C_{39}H_{60}N_4O_{22}$ + Na^+ = 959.35992 $[M+Na]^+$; found 959.35921. Compound **12b**$_{exo}$: ^{1}H NMR (600 MHz, D_2O) δ 8.18 (s, 1H, H-6), 7.60 (dd, *J* = 7.5 Hz, *J* = 2.1 Hz, 2H, 2 H-Ph$_{ortho}$), 7.49-7.43 (m, 3H, 2 H-Ph$_{meta}$, H-Ph$_{para}$), 5.67 (d, $^3J_{1,2}$ = 2.5 Hz, H-1$_{Man1}$), 5.19-5.15 (m, 1H, H-7), 4.81 (d, $^3J_{1,2}$ = 1.3 Hz, 1H, H-1$_{Man2}$ or H-1$_{Man3}$), 4.79 (br s, 1H, H-2$_{Man1}$), 4.73 (br s, 1H, H-1$_{Man2}$ or H-1$_{Man3}$), 4.67 (br s, 2H, H-4), 4.21-4.12 (m, 2H, H-8a, H-9a), 4.03-3.92 (m, 3H, H-3$_{Man1}$, H-8b, H-9b), 3.90-3.84 (m, 1H, H-2$_{Man2}$ or H-2$_{Man3}$), 3.81-3.71 (m, 4H, H-2, H-2$_{Man2}$ or H-2$_{Man3}$, H-6a$_{Man1}$, H-6a$_{Man2}$ or H-6a$_{Man3}$), 3.70-3.63 (m, 4H, H-3$_{Man2}$ or H-3$_{Man3}$, H-4$_{Man1}$, H-6b$_{Man1}$, H-6a$_{Man2}$ or H-6a$_{Man3}$), 3.61-3.51 (m, 7H, H-1, H-3, H-3$_{Man2}$ or H-3$_{Man3}$, H-4$_{Man2}$, H-4$_{Man3}$, H-6a$_{Man2}$ or H-6a$_{Man3}$, H-6b$_{Man2}$, H-6b$_{Man3}$), 3.41-3.37 (m, 1H, H-5$_{Man1}$), 3.36-3.32 (m, 1H, H-5$_{Man2}$ or H-5$_{Man3}$), 3.10-3.01 (m, 1H, H-5$_{Man2}$ or H-5$_{Man3}$), 1.41 (s, 9H, $NHCO_2C(C\underline{H}_3)_3$) ppm; ^{13}C NMR (151 MHz, D_2O) δ 157.7 ($NH\underline{C}O_2C(CH_3)_3$), 144.2 (C-5), 130.0, 128.6 (2C, C-Ph$_{para}$, C-Ph$_{meta}$), 126.1 (C-Ph$_{ortho}$), 124.7 (C-6), 122.0 (orthoester C$_q$), 100.4 (C-1$_{Man2}$ or C-1$_{Man3}$), 99.6 (C-1$_{Man2}$ or C-1$_{Man3}$), 97.5 (C-1$_{Man1}$), 81.2 ($NHCO_2\underline{C}(CH_3)_3$), 79.2 (C-2$_{Man1}$), 75.2 (C-5$_{Man1}$), 73.1, 72.9 (2C, C-5$_{Man2}$, C-5$_{Man3}$) 70.6 (C-3$_{Man1}$), 70.4 (2C, C-3$_{Man2}$, C-3$_{Man3}$), 69.9, 69.8 (2C, C-2$_{Man2}$, C-2$_{Man3}$), 69.3 (C-1), 66.8 (C-4$_{Man1}$), 66.5, 66.4, 66.3, 66.0 (4C, C-4$_{Man2}$, C-4$_{Man3}$, C-8, C-9), 63.3, (C-4), 61.0, 60.9, 60.8, 60.7, 60.6 (5C, C-6$_{Man1}$, C-6$_{Man2}$, C-6$_{Man3}$, C-7, C-3), 51.7 (C-2), 27.7 ($NHCO_2C(\underline{C}H_3)_3$) ppm.

Table 8.5: Chemical shifts δ (ppm) for compounds **12b**$_{exo}$ and **12b**$_{endo}$.

	12b$_{exo}$		**12b**$_{endo}$	
Atom	^{1}H-NMR	^{13}C-NMR	^{1}H-NMR	^{13}C-NMR
1_{Man1}	5.67 (d, $^{3}J_{1,2}$ = 2.5 Hz)	97.5	-	-
2_{Man1}	4.79 (br s)*	79.2	-	-
$1_{Man2,3}$		100.4		100.3
1a	3.61-3.51 (m)*	69.3	3.58-3.51 (m)*	69.0
1b	3.61-3.51 (m)*		3.58-3.51 (m)*	
2	3.80-3.74 (m)*	51.7	3.90-3.85 (m)*	49.8
3a	3.61-3.51 (m)*	60.7	-	63.2
3b	3.61-3.51 (m)*		3.46 (dd, $^{2}J_{3a,3b}$ = 10.1 Hz, $^{3}J_{2,3b}$ = 4.9 Hz)	
4	4.67 (br s)*	63.3	4.65 (br s)*	63.3
5	-	144.2	-	144.1
6	8.18 (s)	124.7	8.12 (s)	124.8
7	5.19-5.15 (m)*	60.9	5.15-5.10 (m)*	60.9
NHBoc	1.41 (s)	27.7	-	-
Ph_{ortho}	7.60 (dd, *J* = 7.5 Hz, *J* = 2.1 Hz)	126.1	-	-
Ph_{m}	7.49-7.43 (m)*	128.6	-	-
Ph_{p}	7.49-7.43 (m)*	130.0	-	-
Ph_{q}		122.0		

Descriptors: a) - peak was not found; b) * peak was found in the described region.

8.5.1 NMR spectra of new molecules for Chapter 6

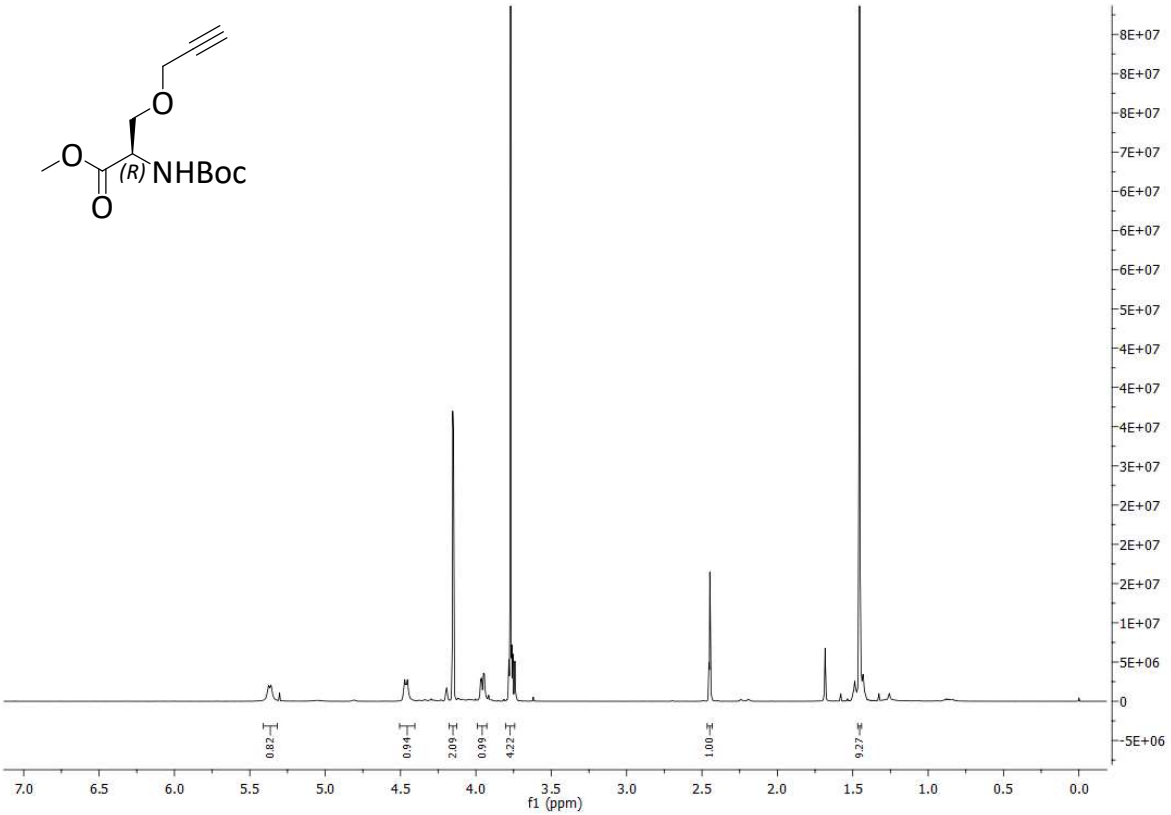

Figure 8.49: ^{1}H NMR (500 MHz, $CDCl_3$) spectrum of compound **2a.**

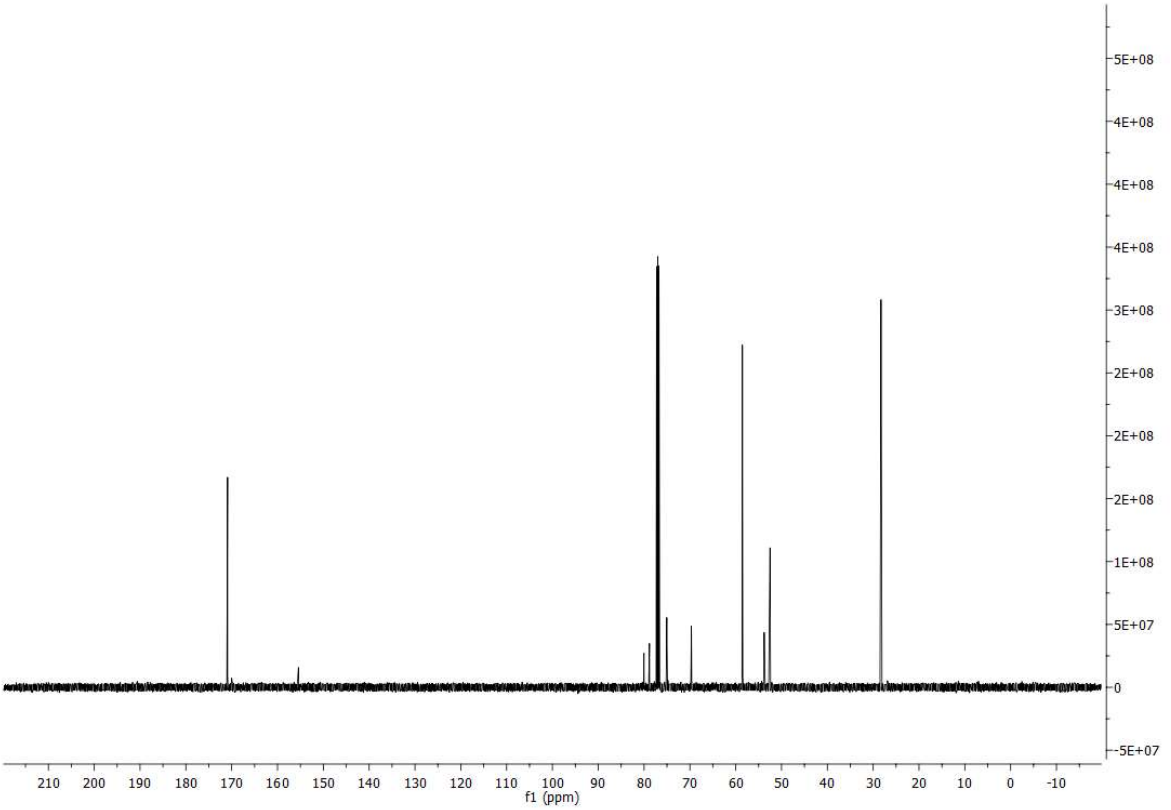

Figure 8.50: ^{13}C NMR (126 MHz, $CDCl_3$) spectrum of compound **2a.**

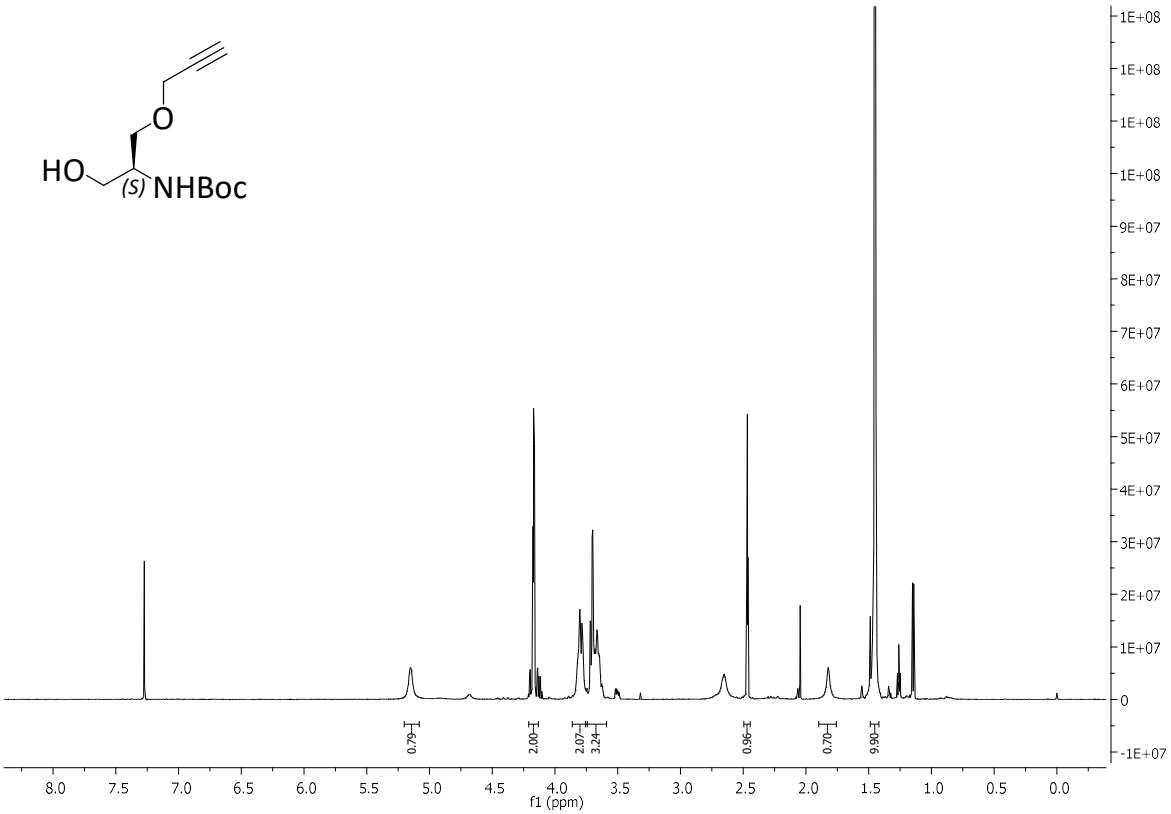

Figure 8.51: ^{1}H NMR (500 MHz, $CDCl_3$) spectrum of compound **3a.**

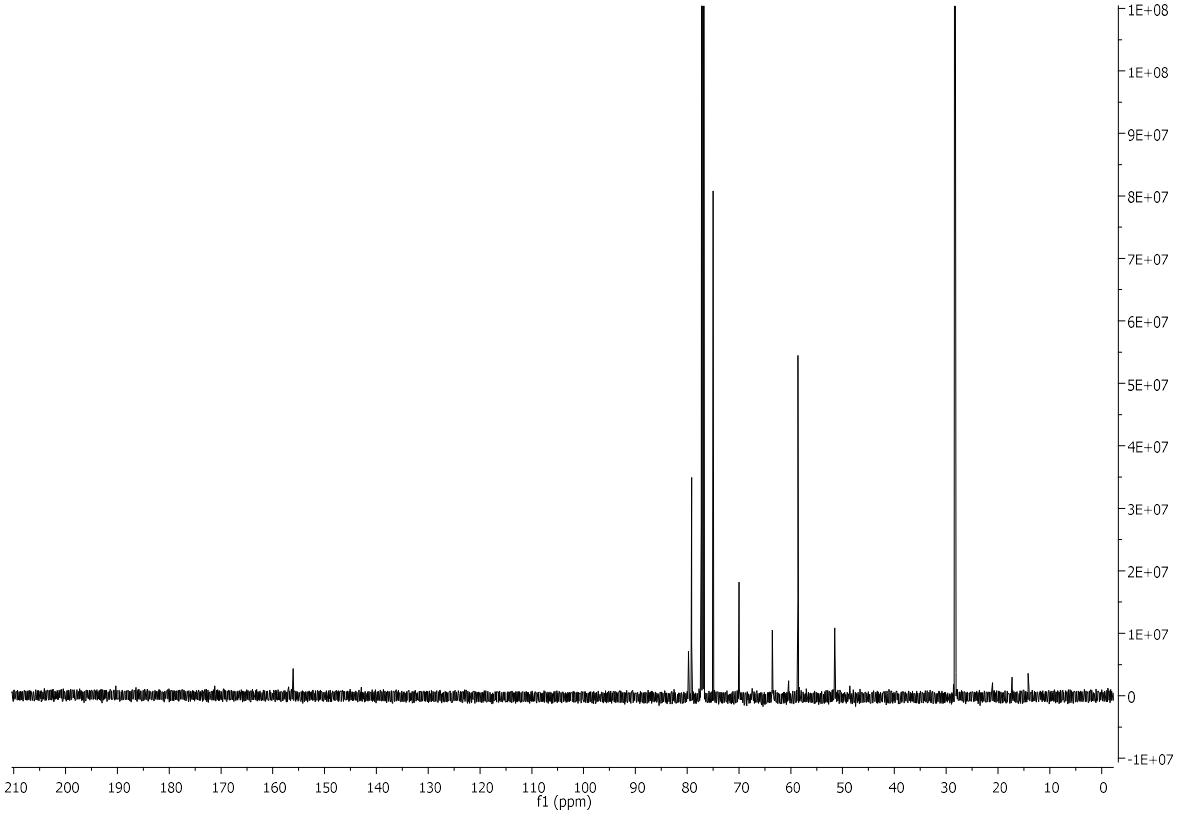

Figure 8.52: ^{13}C NMR (126 MHz, $CDCl_3$) spectrum of compound **3a.**

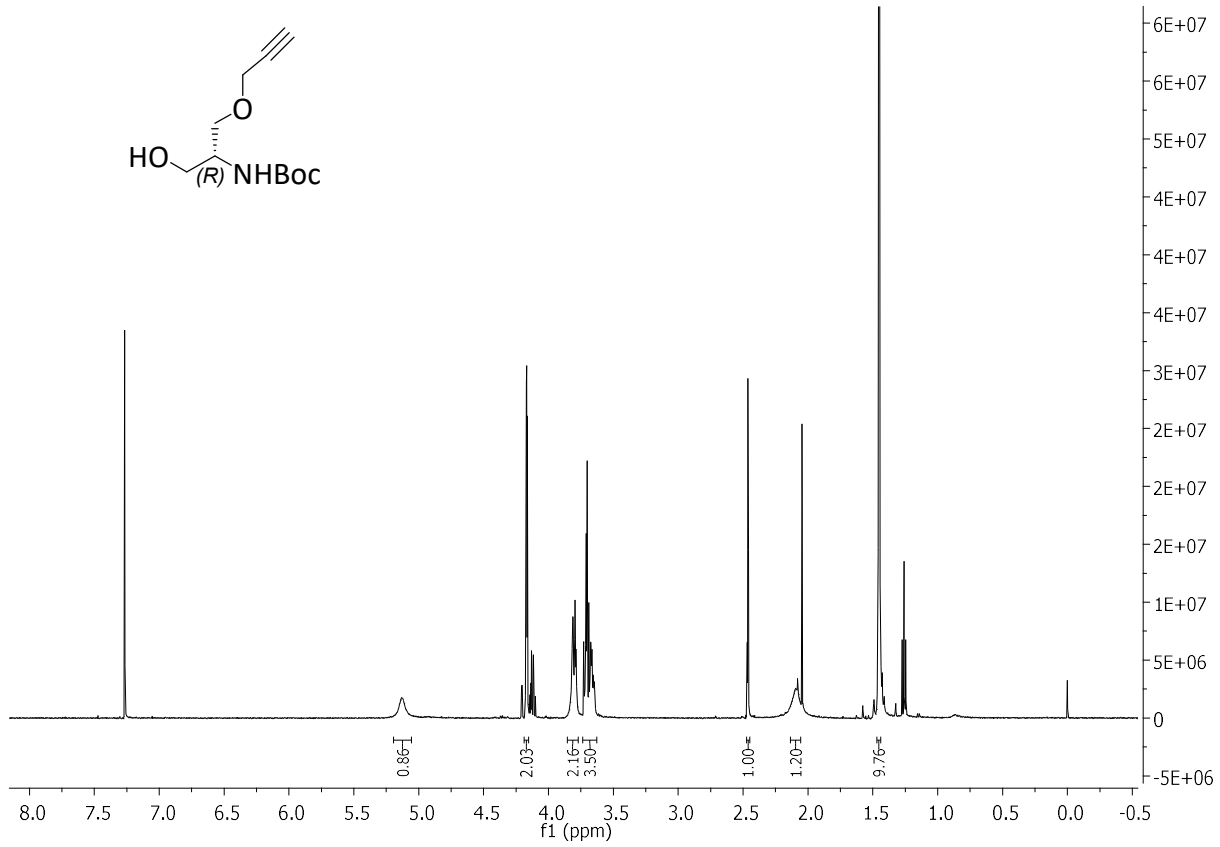

Figure 8.53: ^{1}H NMR (500 MHz, $CDCl_3$) spectrum of compound **3b.**

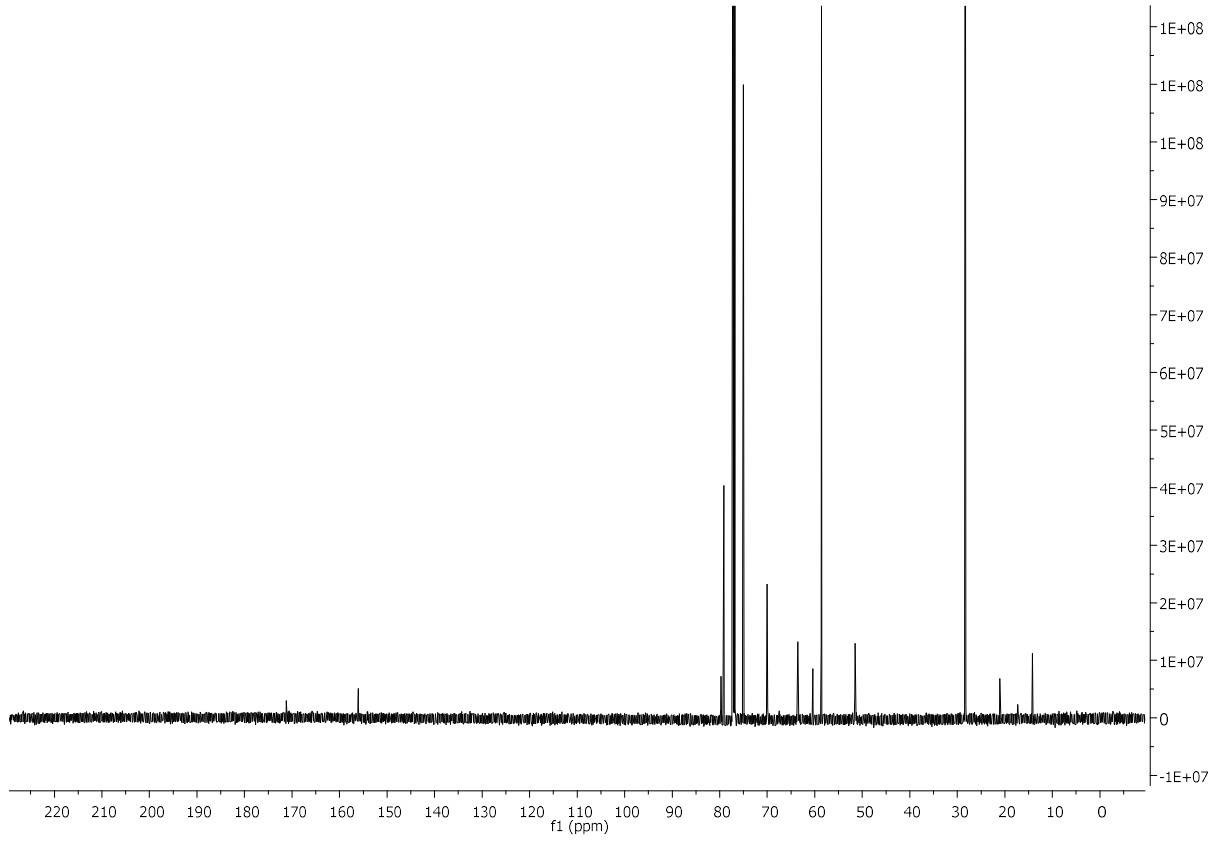

Figure 8.54: ^{13}C NMR (126 MHz, $CDCl_3$) spectrum of compound **3b.**

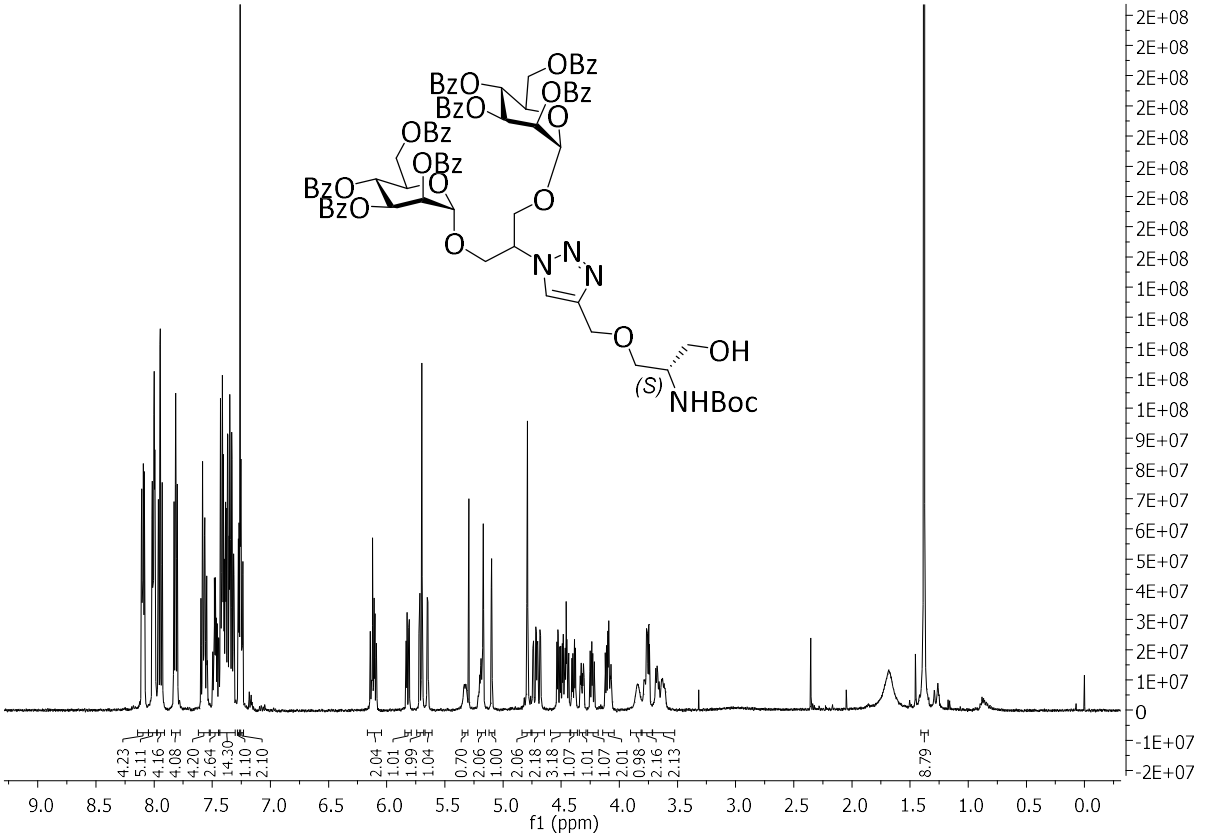

Figure 8.55: ^{1}H NMR (500 MHz, $CDCl_3$) spectrum of compound **5a.**

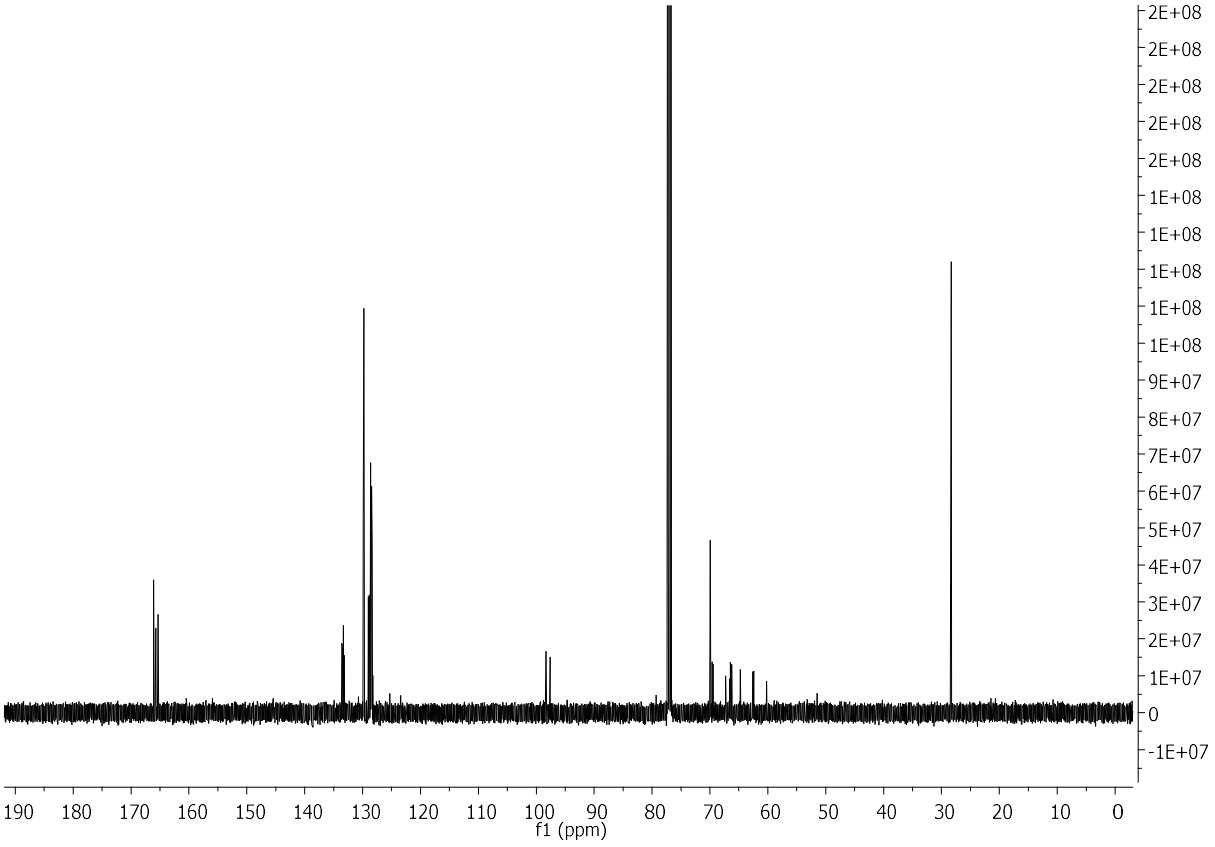

Figure 8.56: ^{13}C NMR (126 MHz, $CDCl_3$) spectrum of compound **5a.**

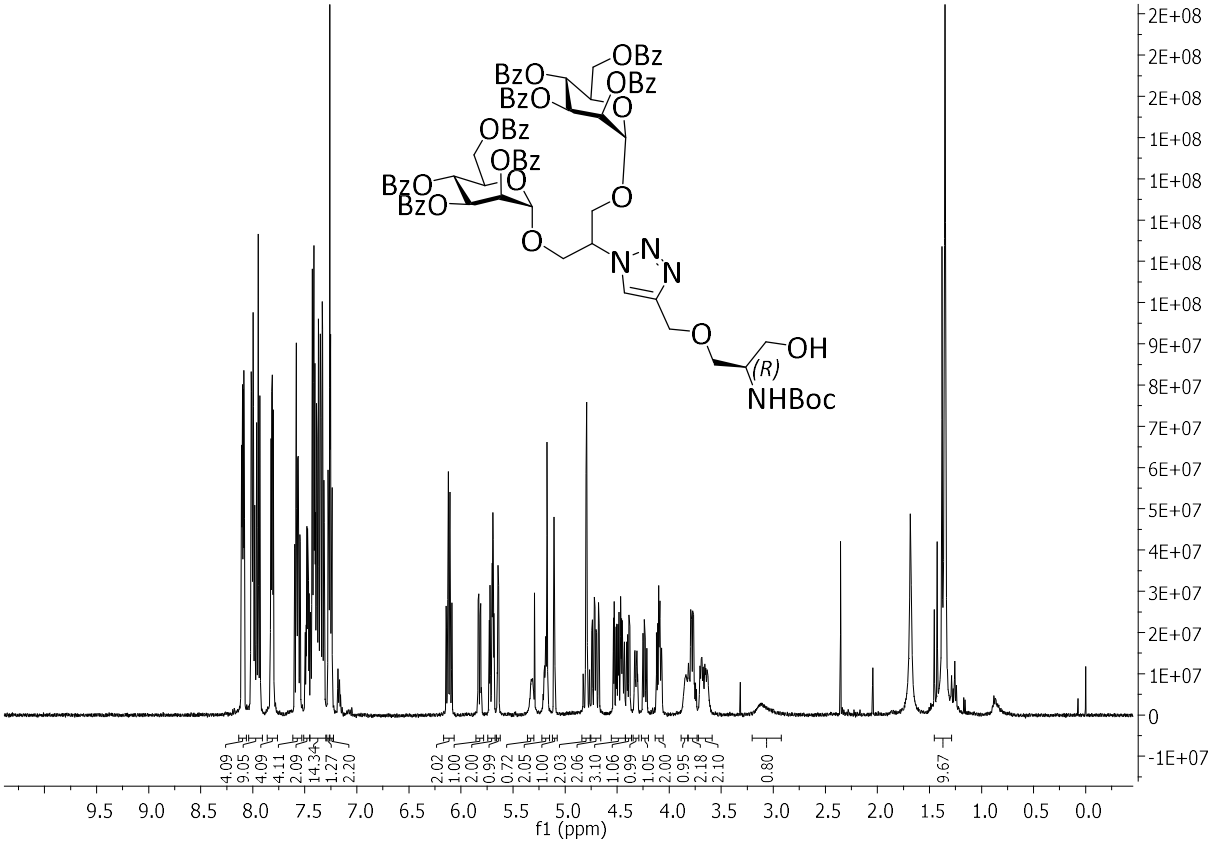

Figure 8.57: ^{1}H NMR (500 MHz, $CDCl_3$) spectrum of compound **5b.**

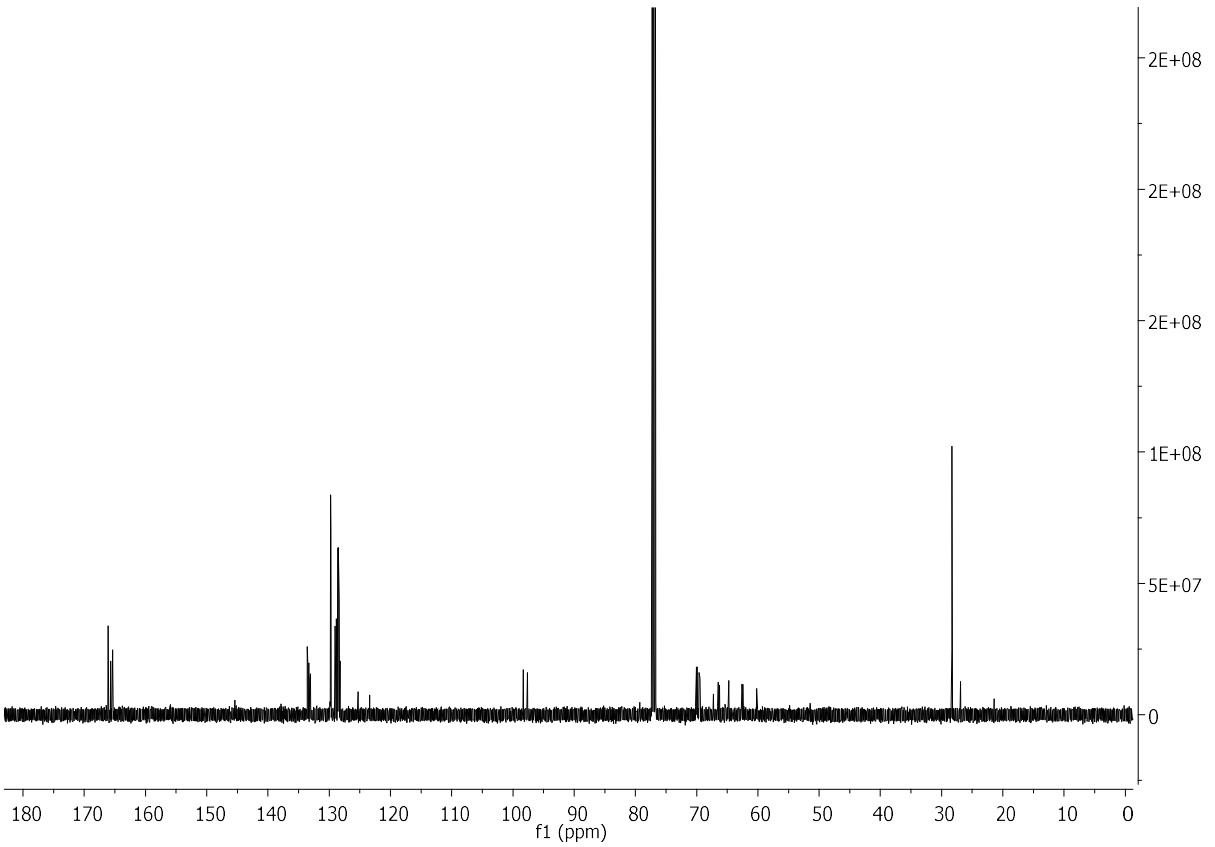

Figure 8.58: ^{13}C NMR (126 MHz, $CDCl_3$) spectrum of compound **5b.**

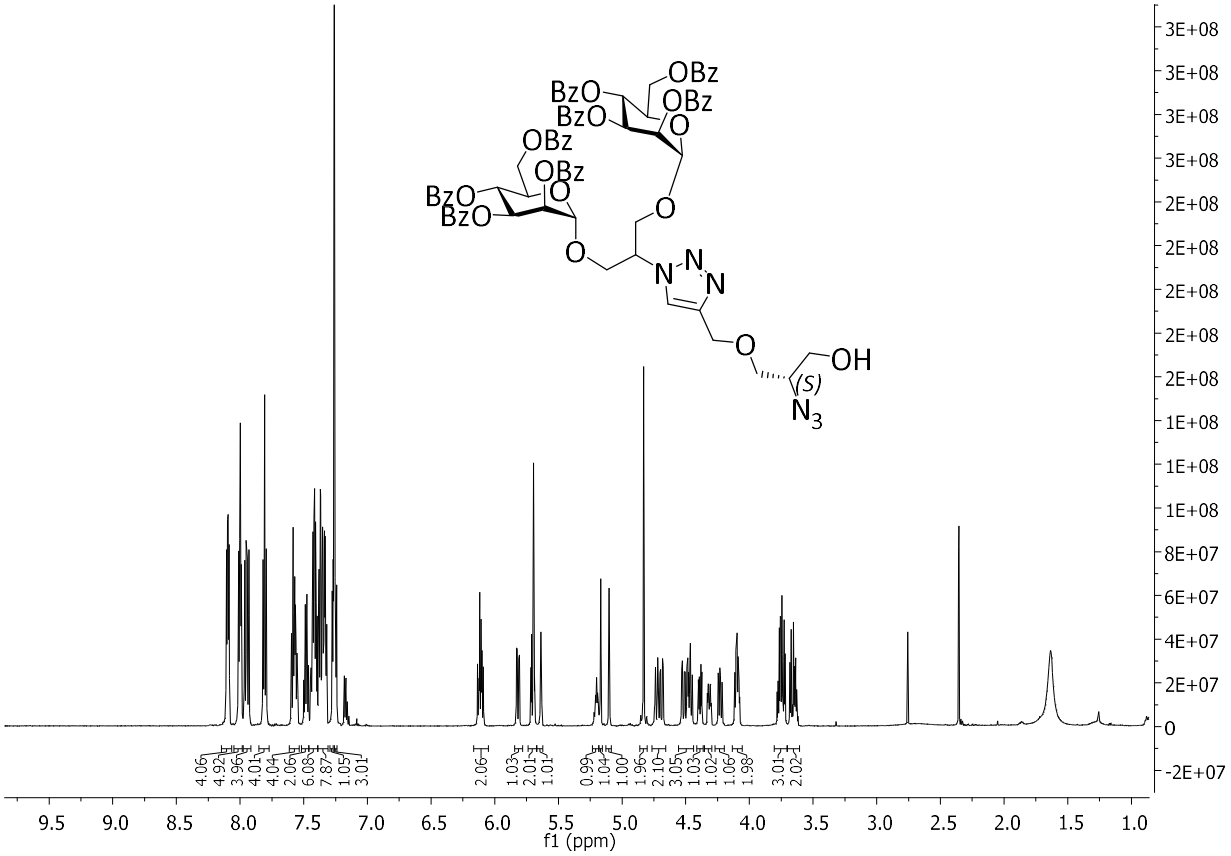

Figure 8.59: ^{1}H NMR (600 MHz, $CDCl_3$) spectrum of compound **6a.**

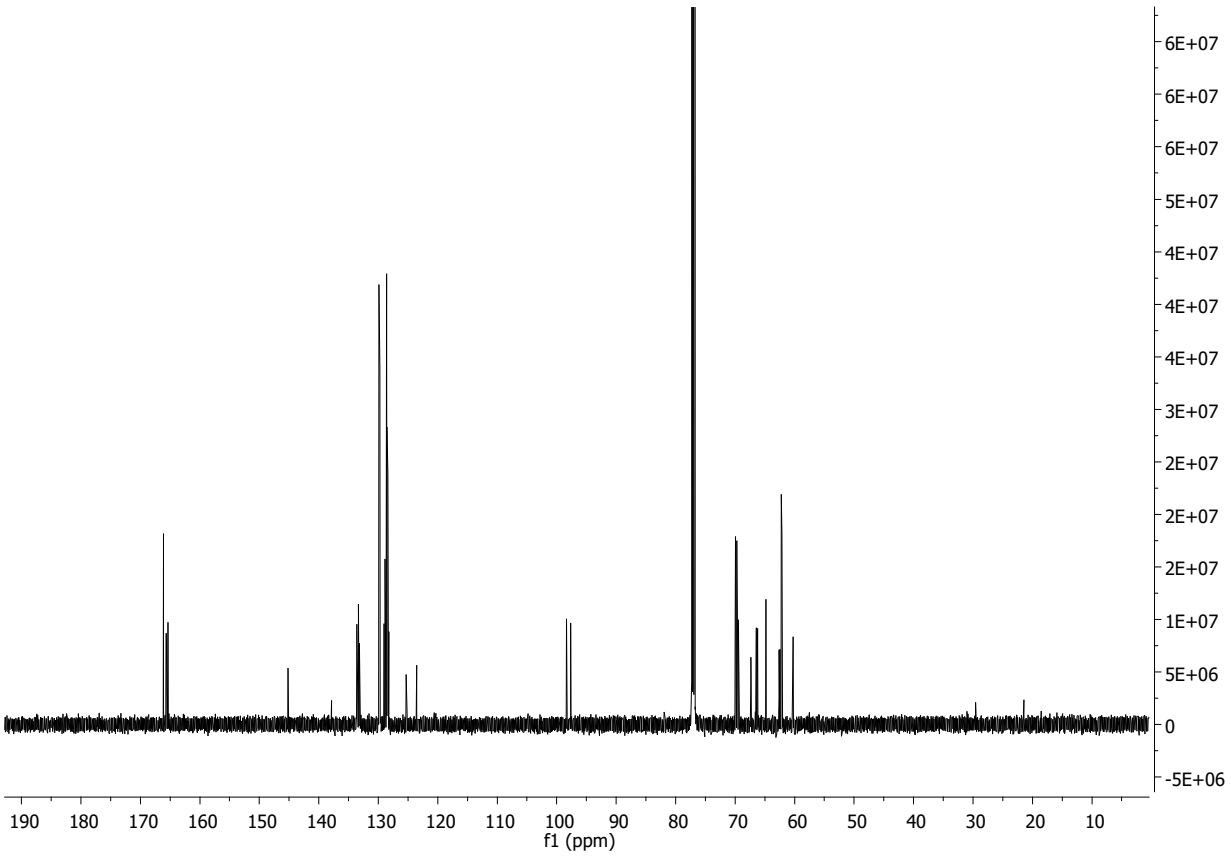

Figure 8.60: ^{13}C NMR (151 MHz, $CDCl_3$) spectrum of compound **6a.**

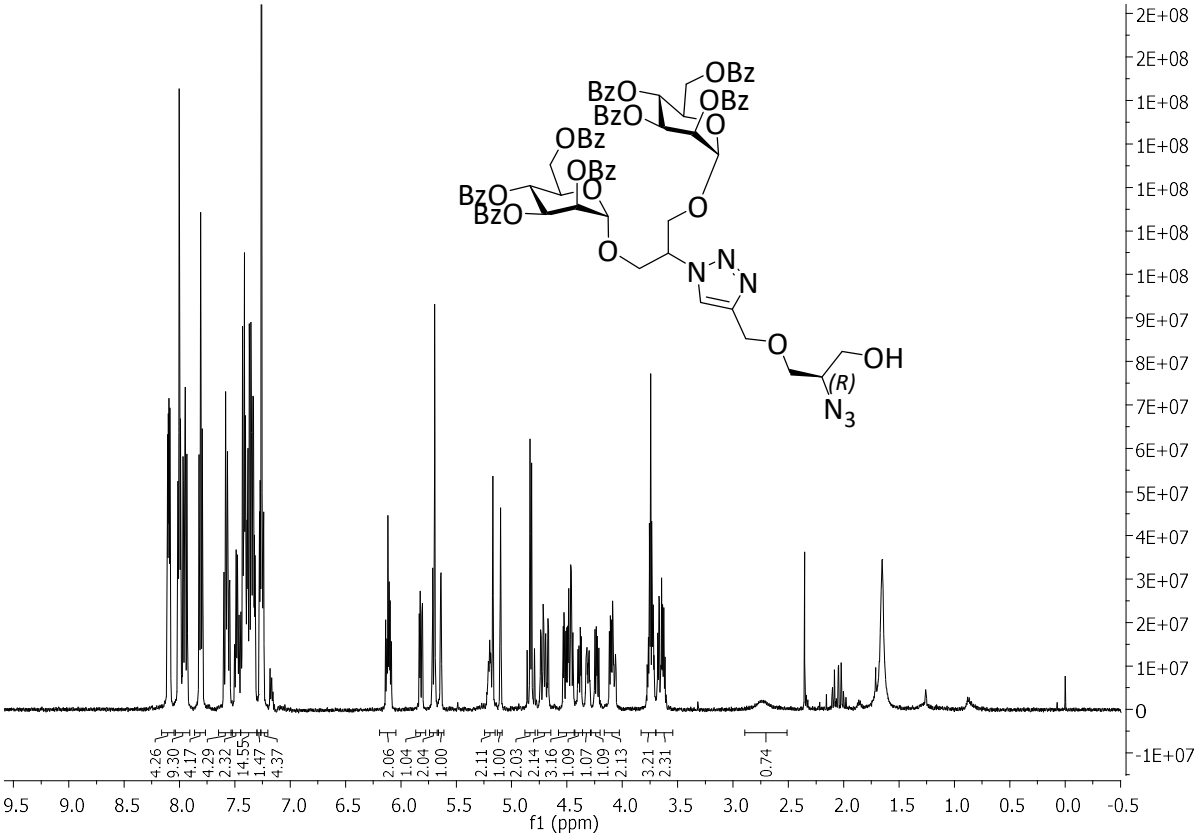

Figure 8.61: ^{1}H NMR (500 MHz, $CDCl_3$) spectrum of compound **6b.**

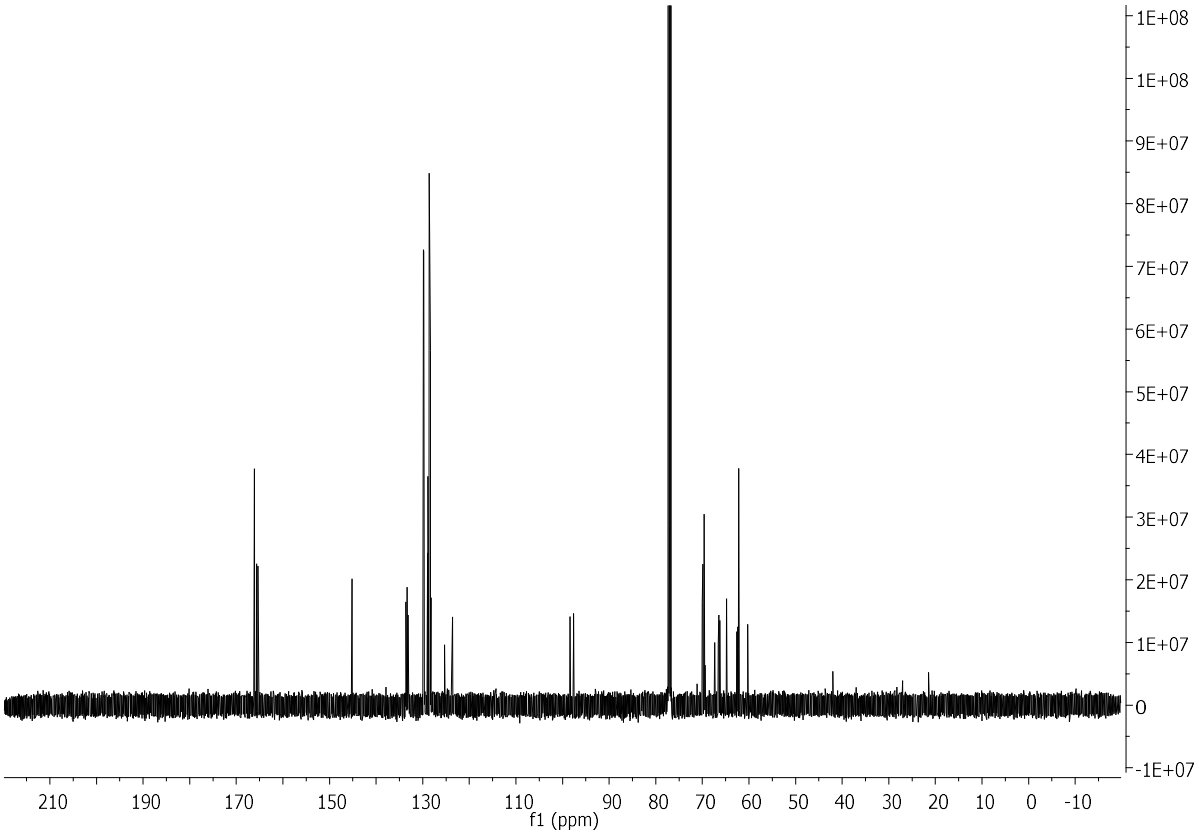

Figure 8.62: ^{13}C NMR (126 MHz, $CDCl_3$) spectrum of compound **6b.**

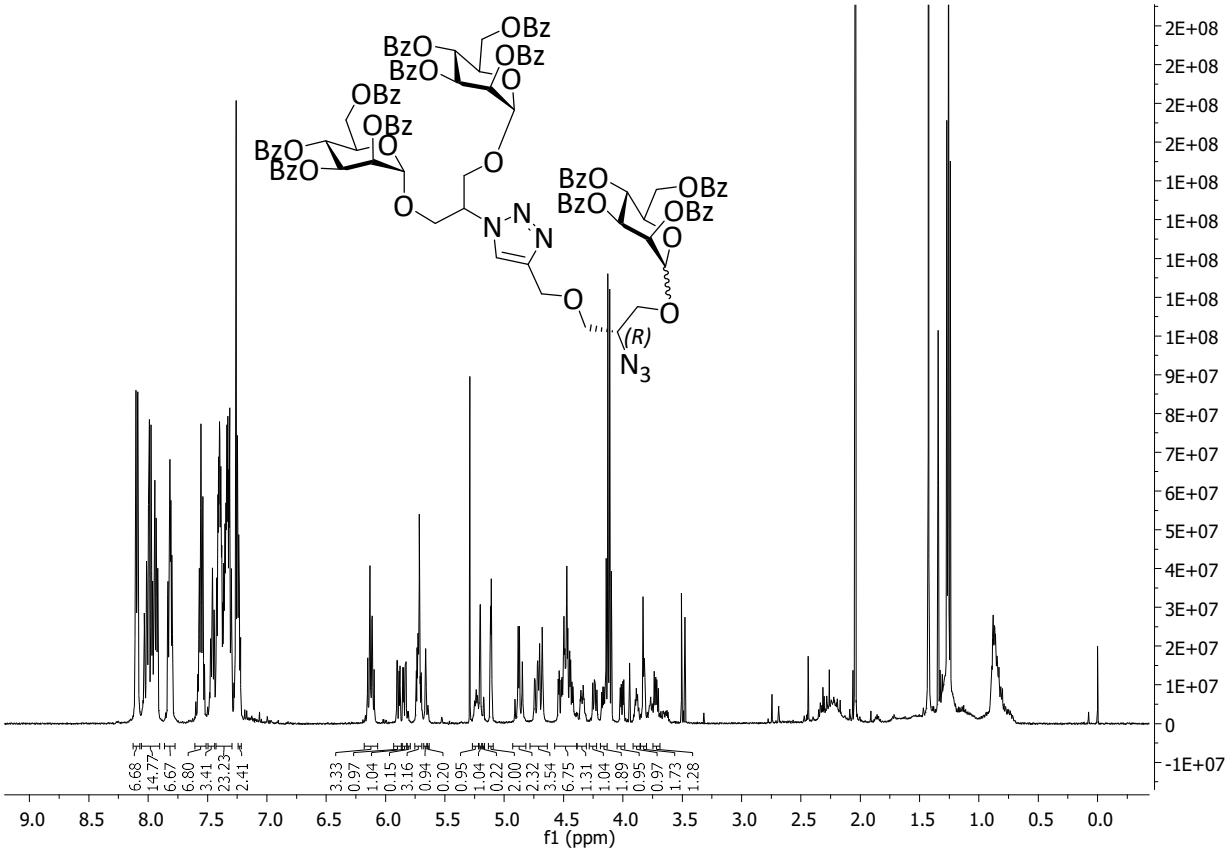

Figure 8.63: ^{1}H NMR (500 MHz, $CDCl_3$) spectrum of compound **9a.**

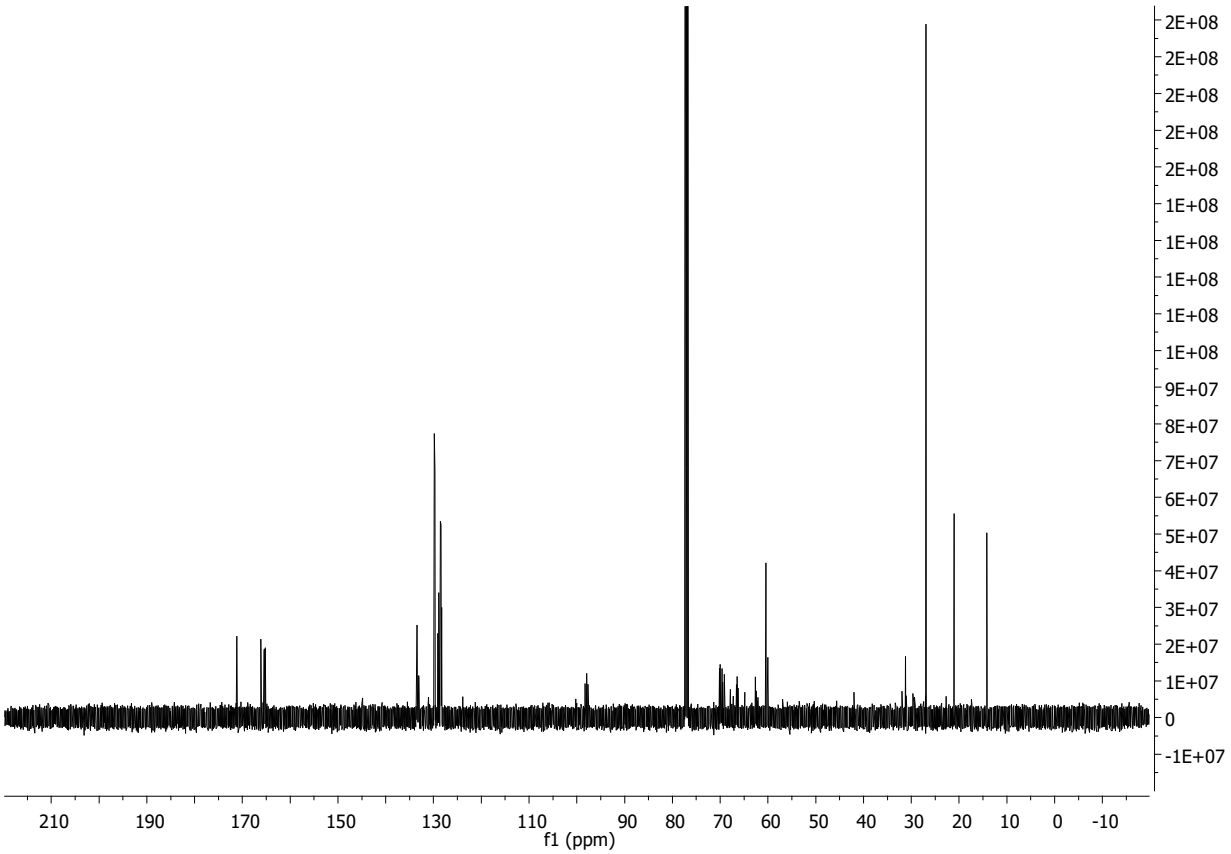

Figure 8.64: ^{13}C NMR (126 MHz, $CDCl_3$) spectrum of compound **9a.**

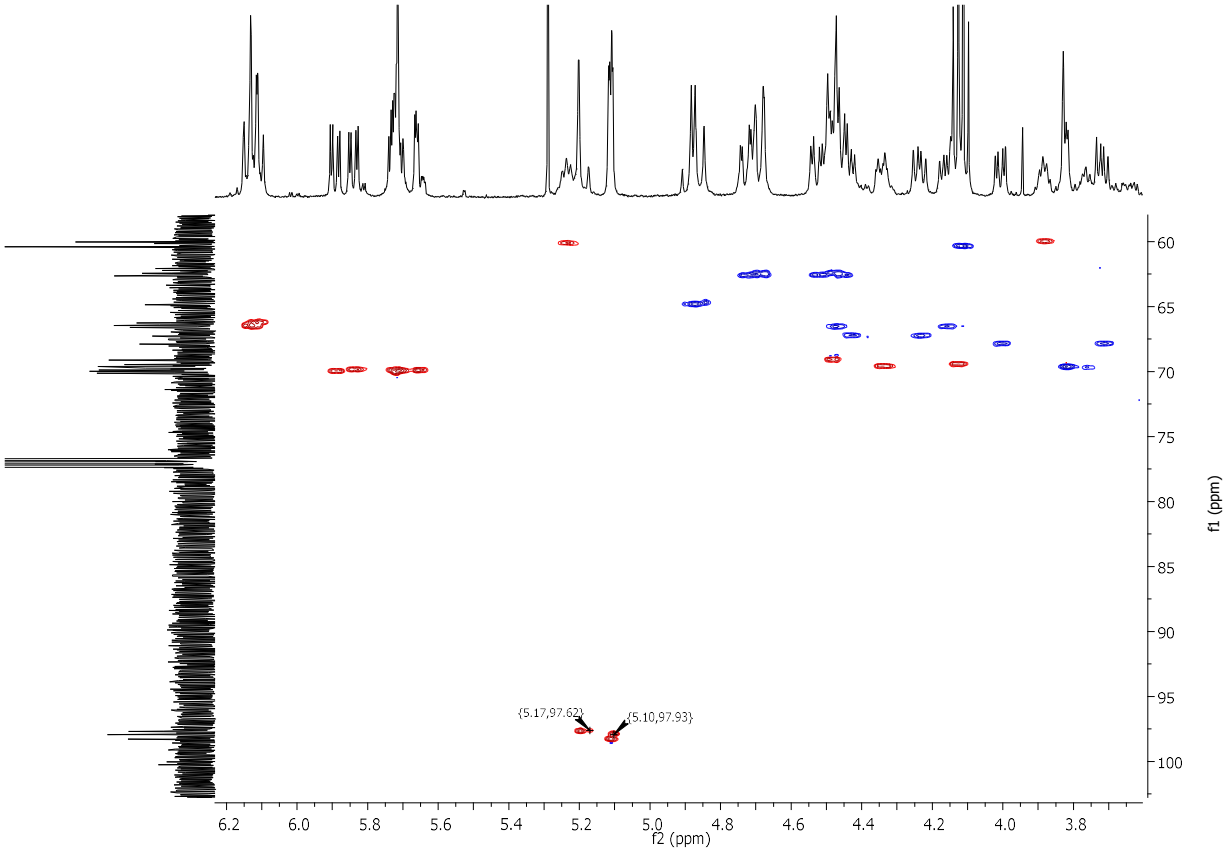

Figure 8.65: HSQC NMR (151 MHz, $CDCl_3$) spectrum pointing on anomers of compound **9a.**

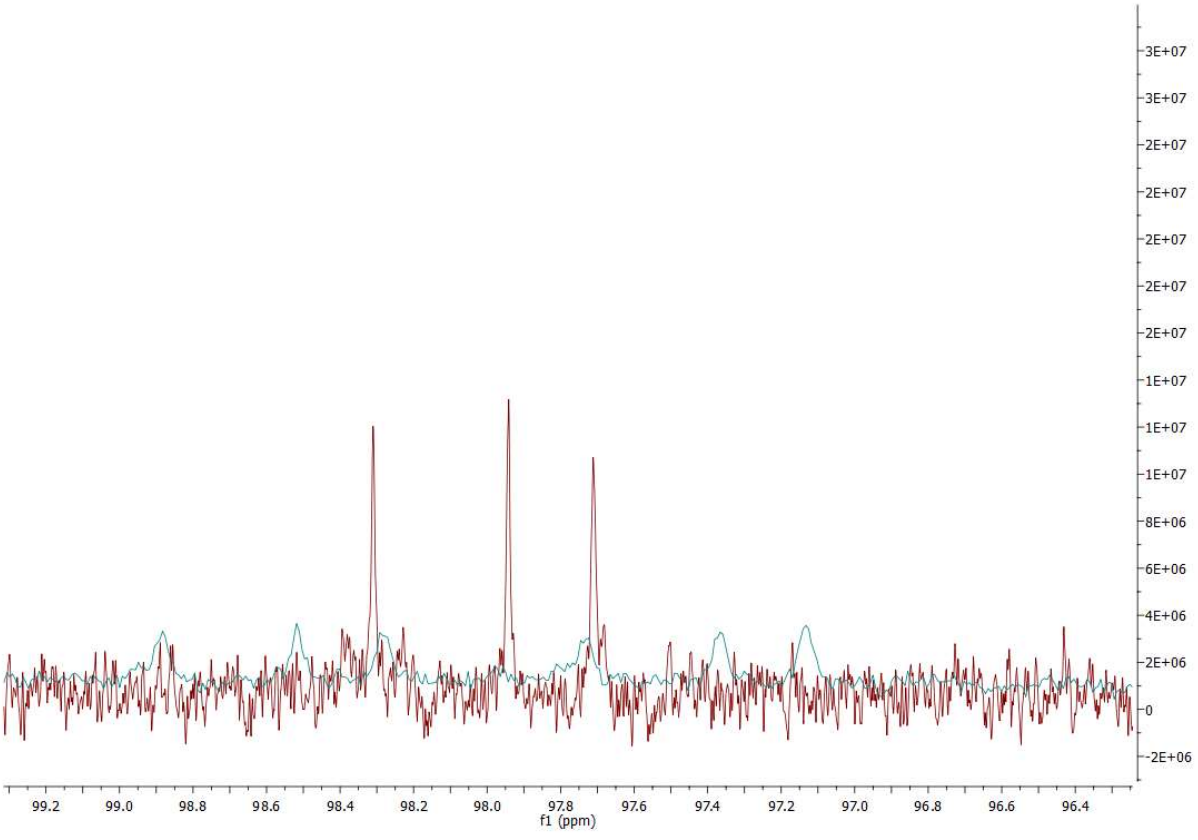

Figure 8.66: ^{13}C gated decoupling NMR (151 MHz, $CDCl_3$) spectrum of **9a** (green) compared with ^{13}C NMR (126 MHz, $CDCl_3$) spectrum of **9a** (red).

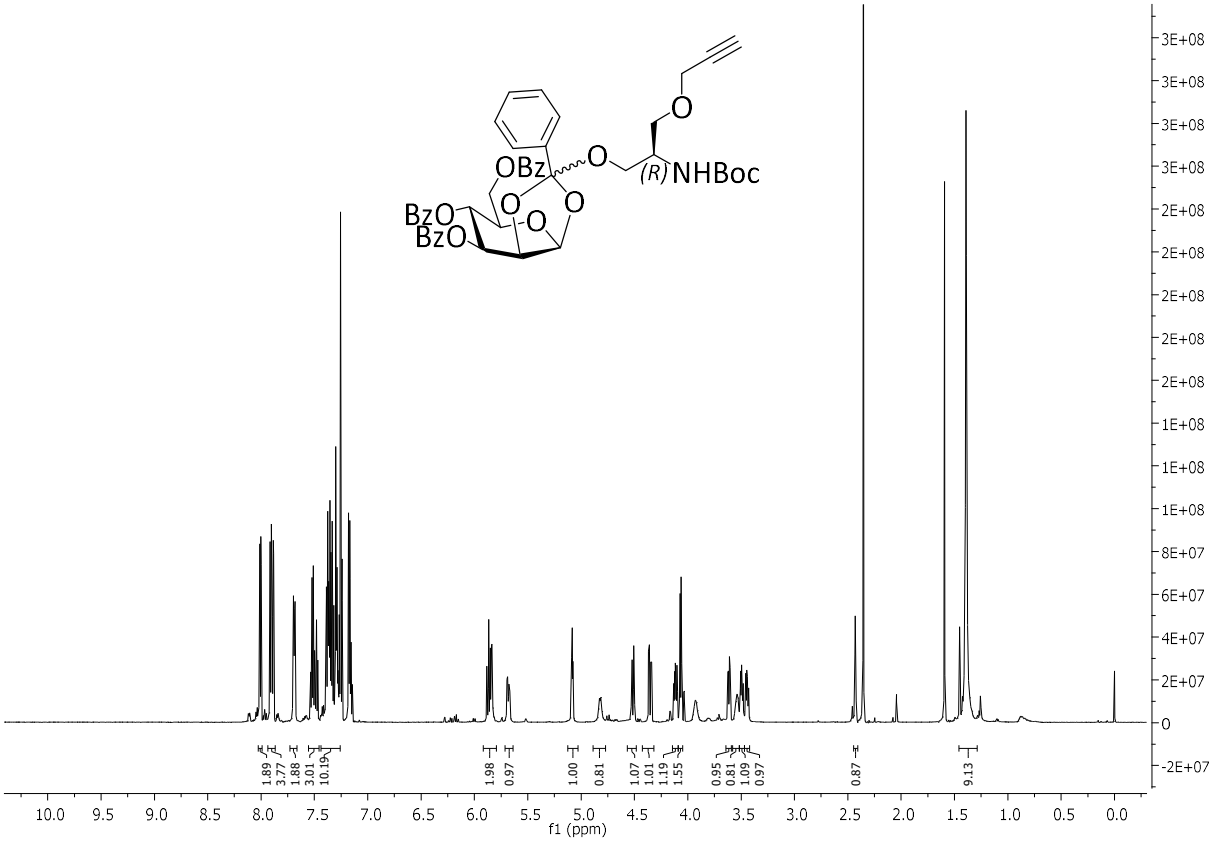

Figure 8.67: ^{1}H NMR (500 MHz, $CDCl_3$) spectrum of compound **10a**.

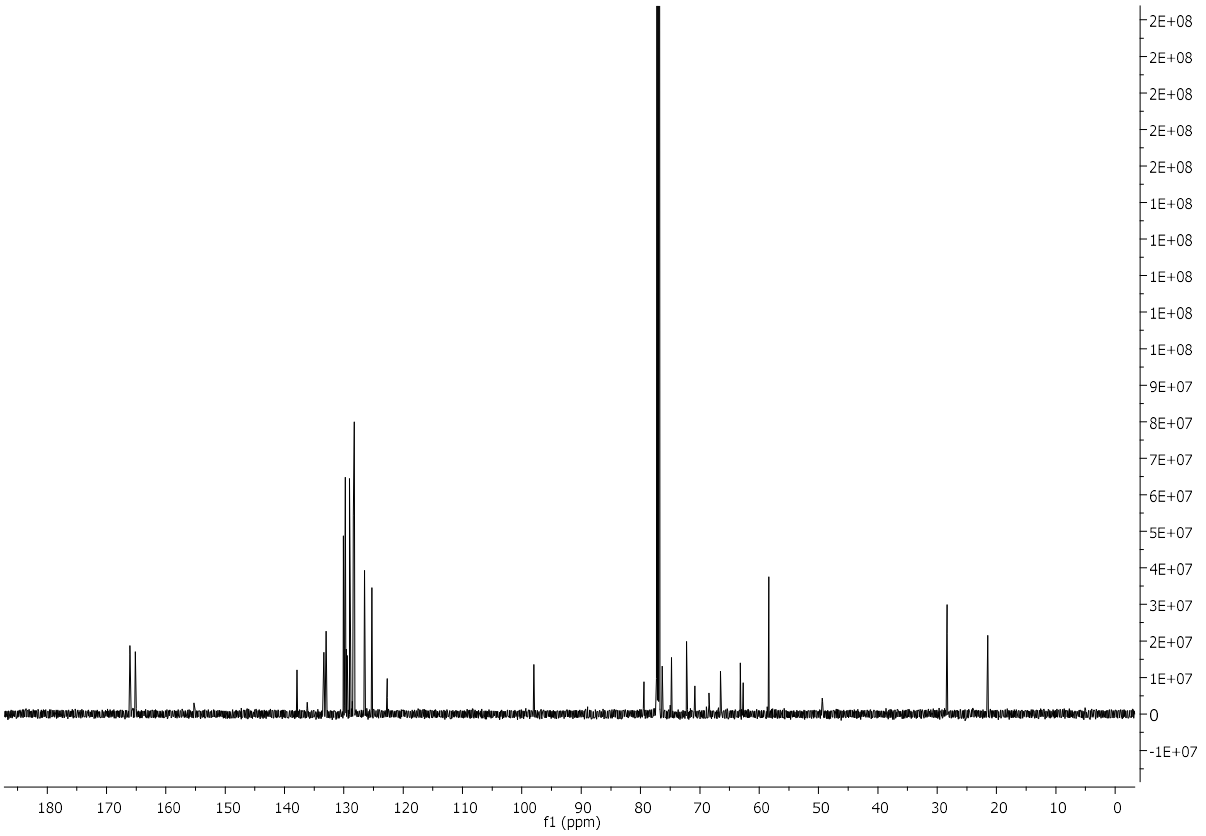

Figure 8.68: ^{13}C NMR (126 MHz, $CDCl_3$) spectrum of compound **10a**.

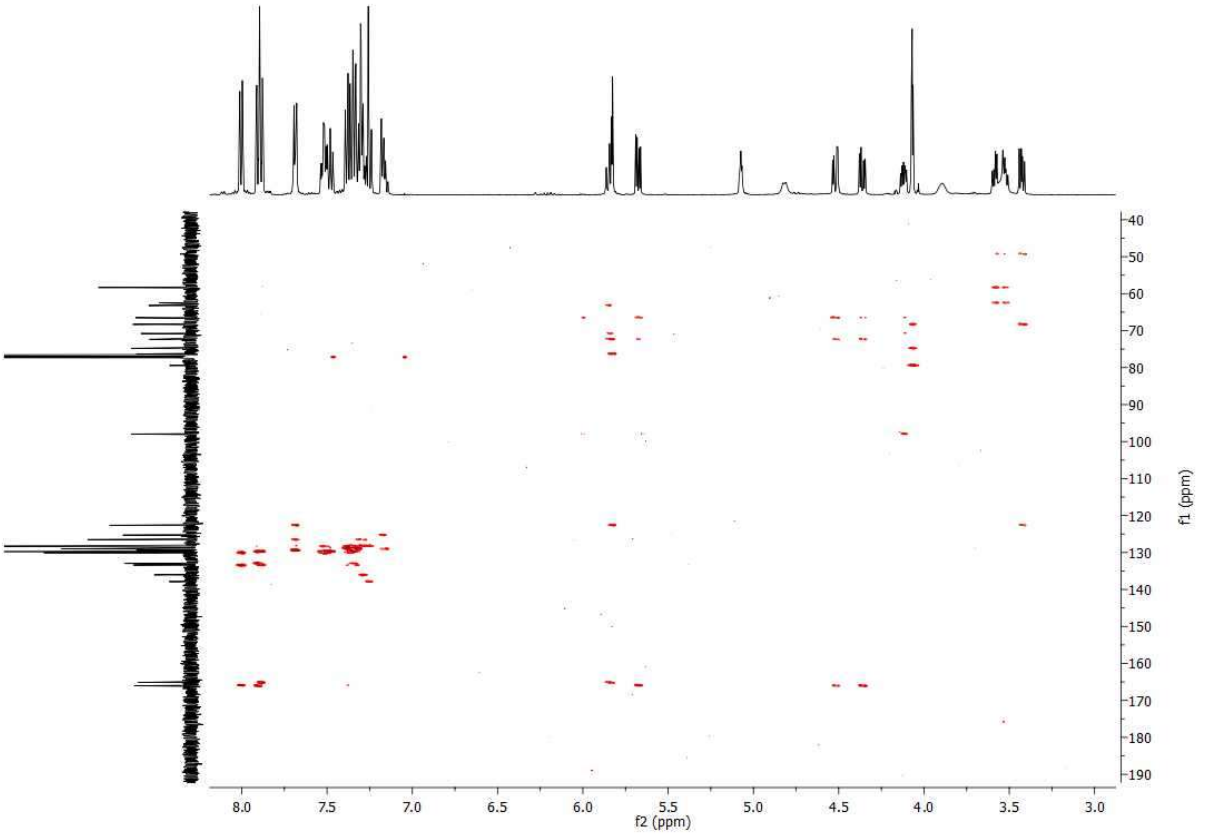

Figure 8.69: HMBC NMR (151 MHz, $CDCl_3$) spectrum of compound **10a**.

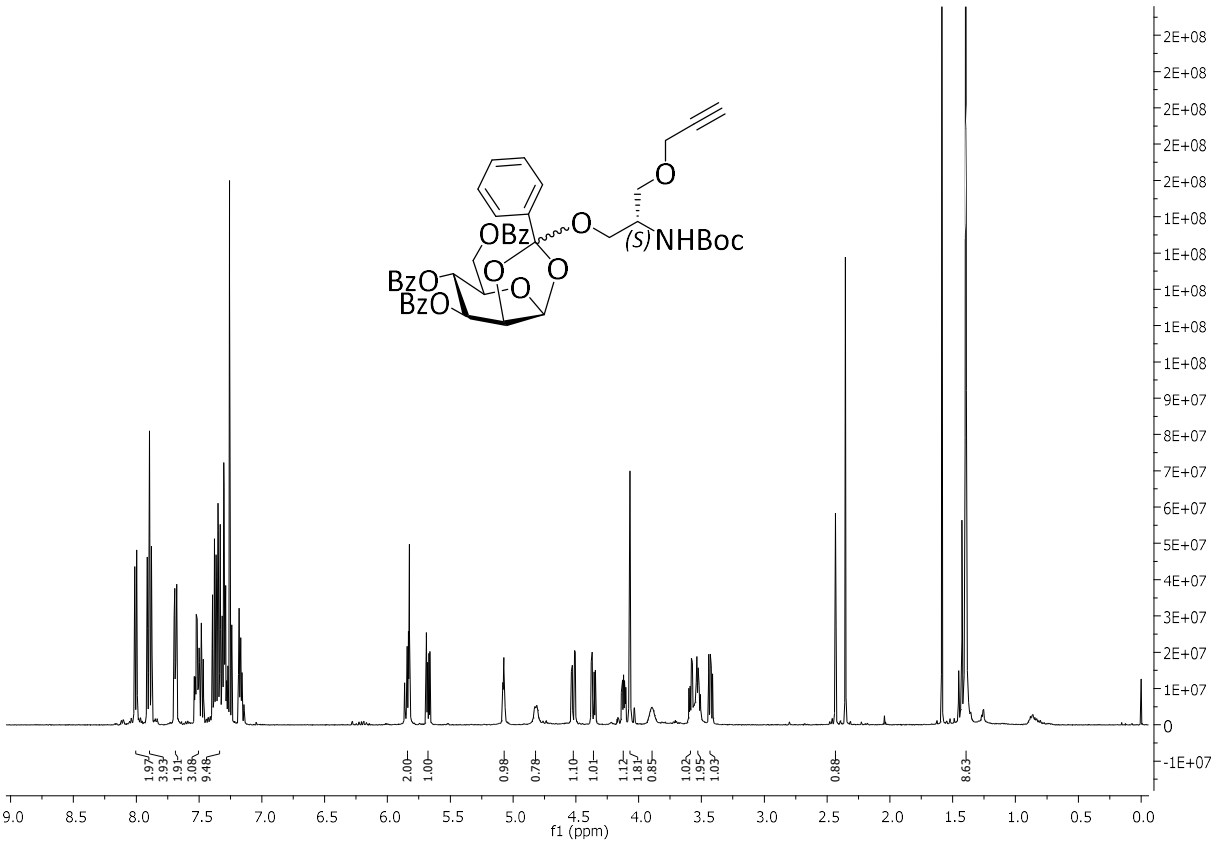

Figure 8.70: ^1H NMR (500 MHz, $CDCl_3$) spectrum of compound **10b**.

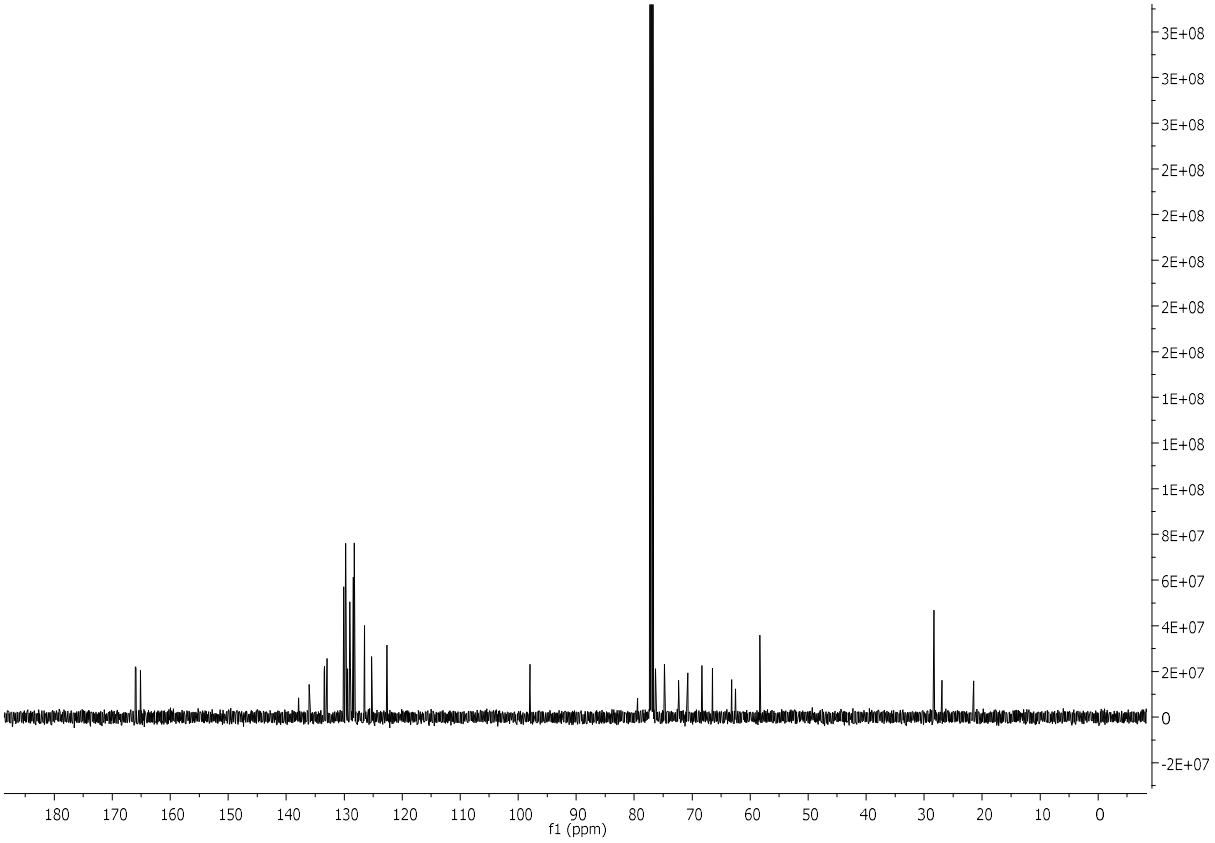

Figure 8.71: ^{13}C NMR (126 MHz, $CDCl_3$) spectrum of compound **10b**.

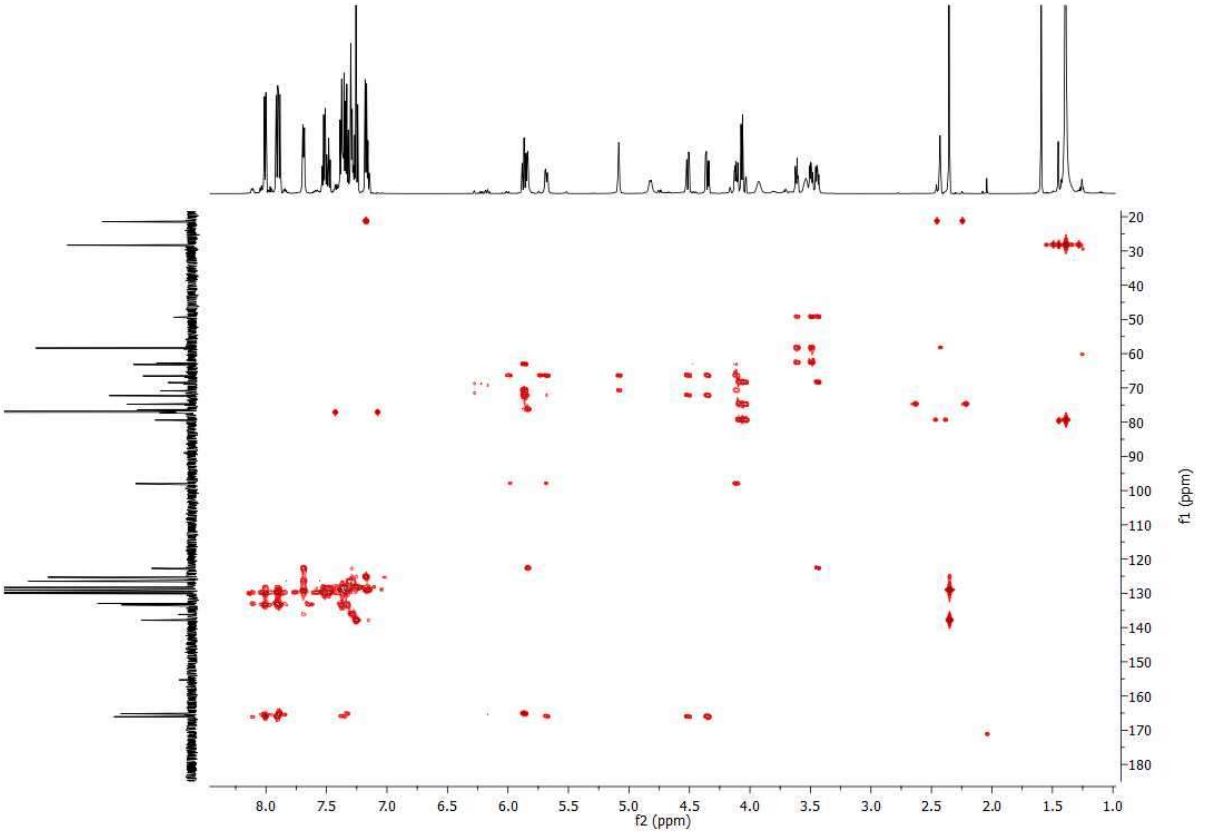

Figure 8.72: HMBC NMR (151 MHz, $CDCl_3$) spectrum of compound **10b**.

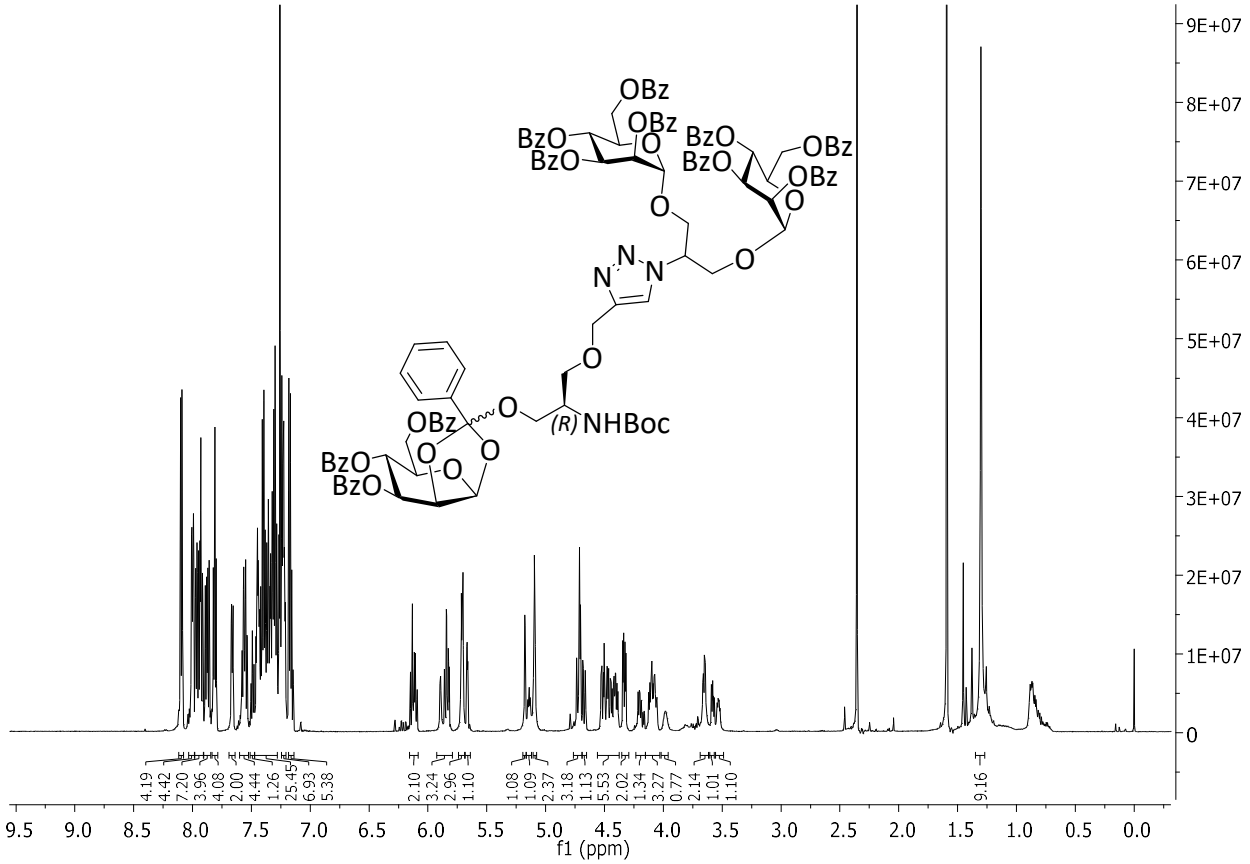

Figure 8.73: ^{1}H NMR (600 MHz, $CDCl_3$) spectrum of compound **11a**.

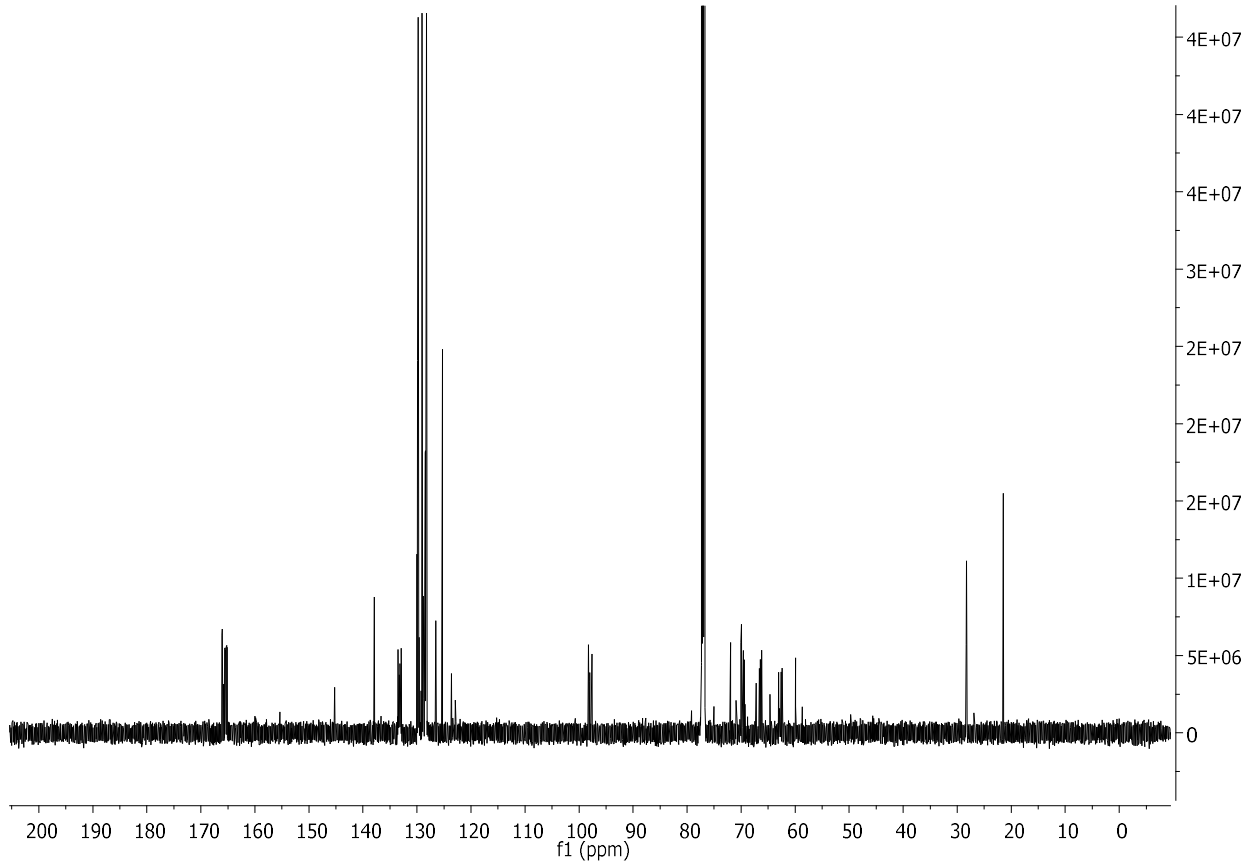

Figure 8.74: ^{13}C NMR (151 MHz, $CDCl_3$) spectrum of compound **11a**.

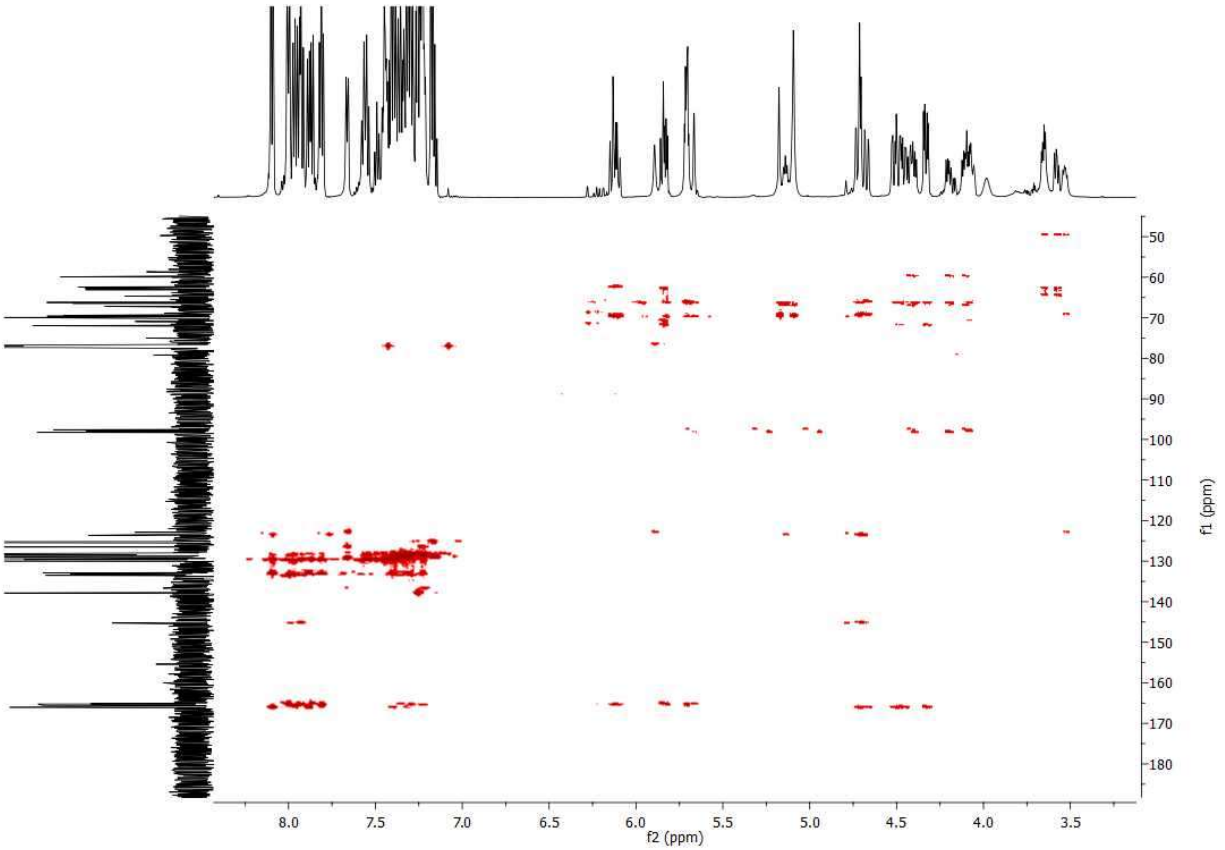

Figure 8.75: HMBC NMR (151 MHz, $CDCl_3$) spectrum of compound **11a**.

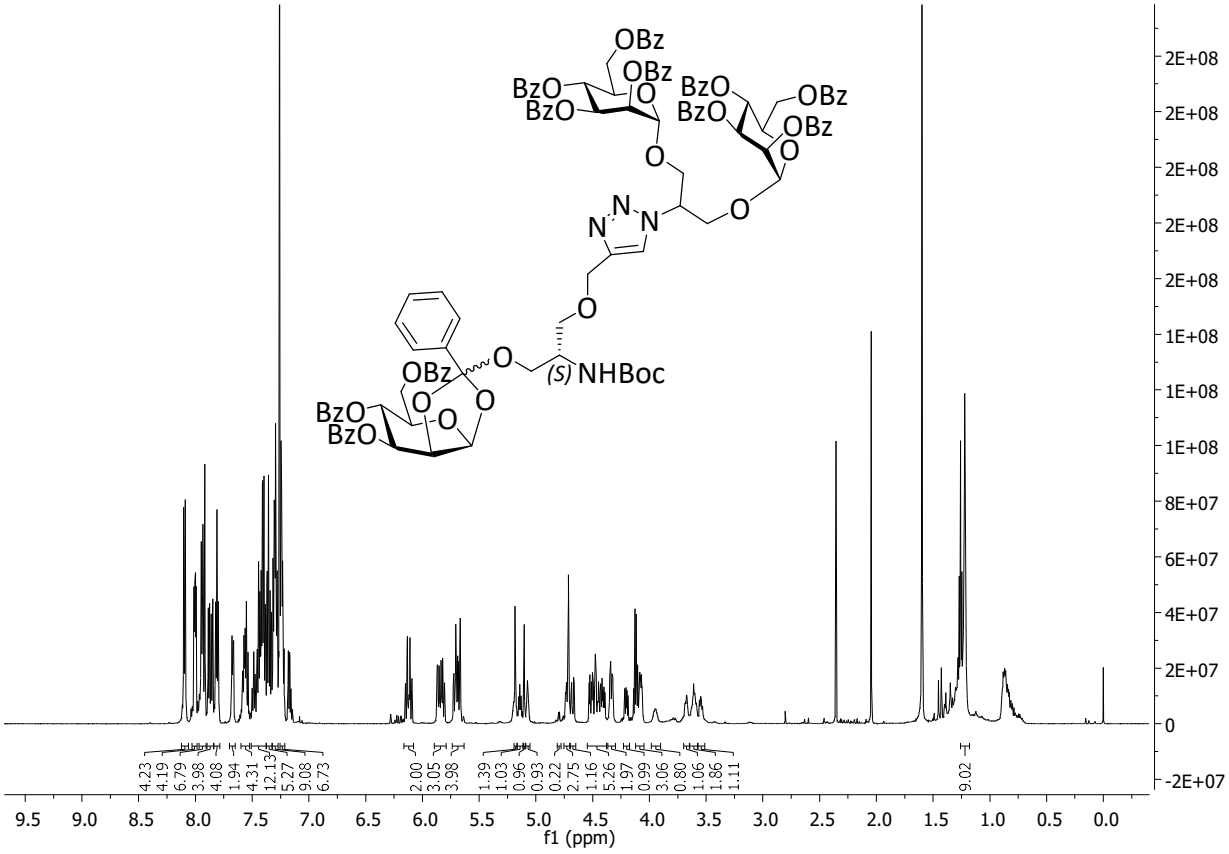

Figure 8.76: ^1H NMR (600 MHz, $CDCl_3$) spectrum of compound **11b**.

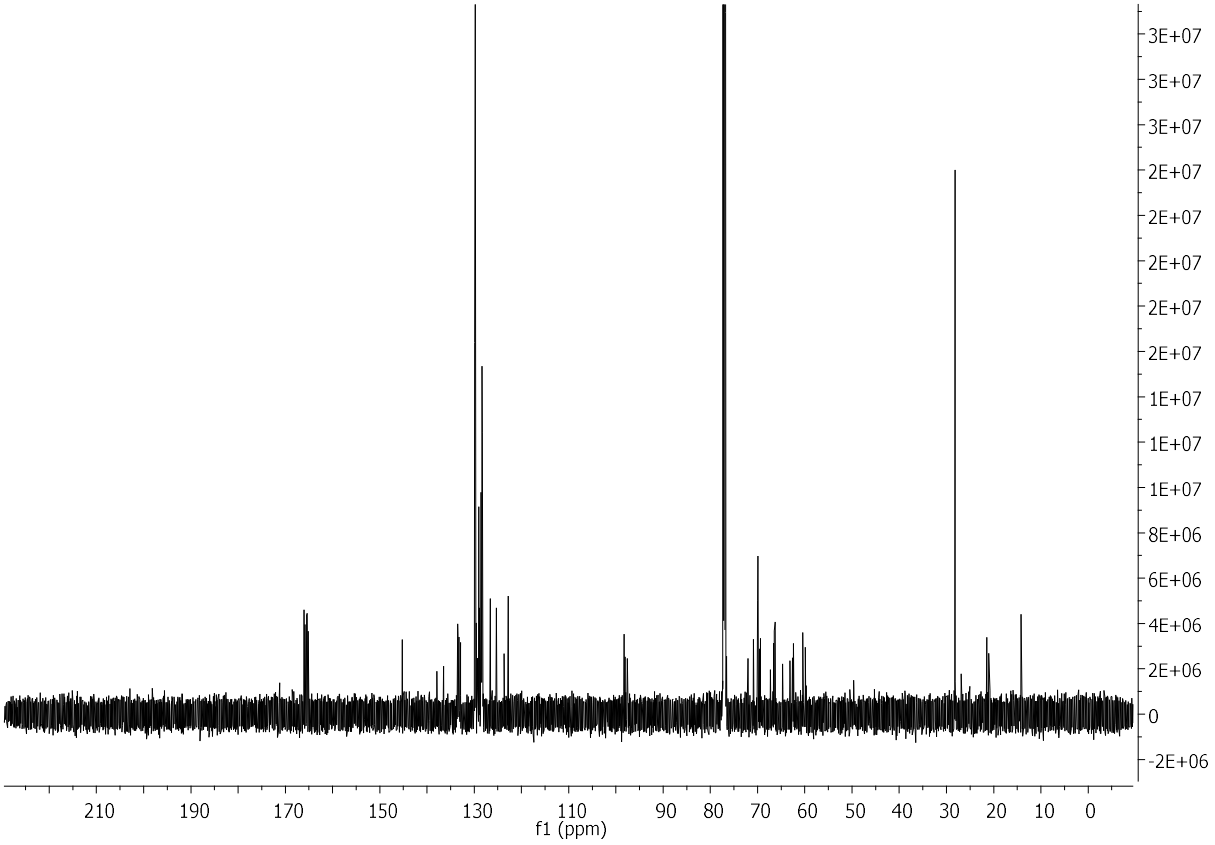

Figure 8.77: ^{13}C NMR (151 MHz, $CDCl_3$) spectrum of compound **11b**.

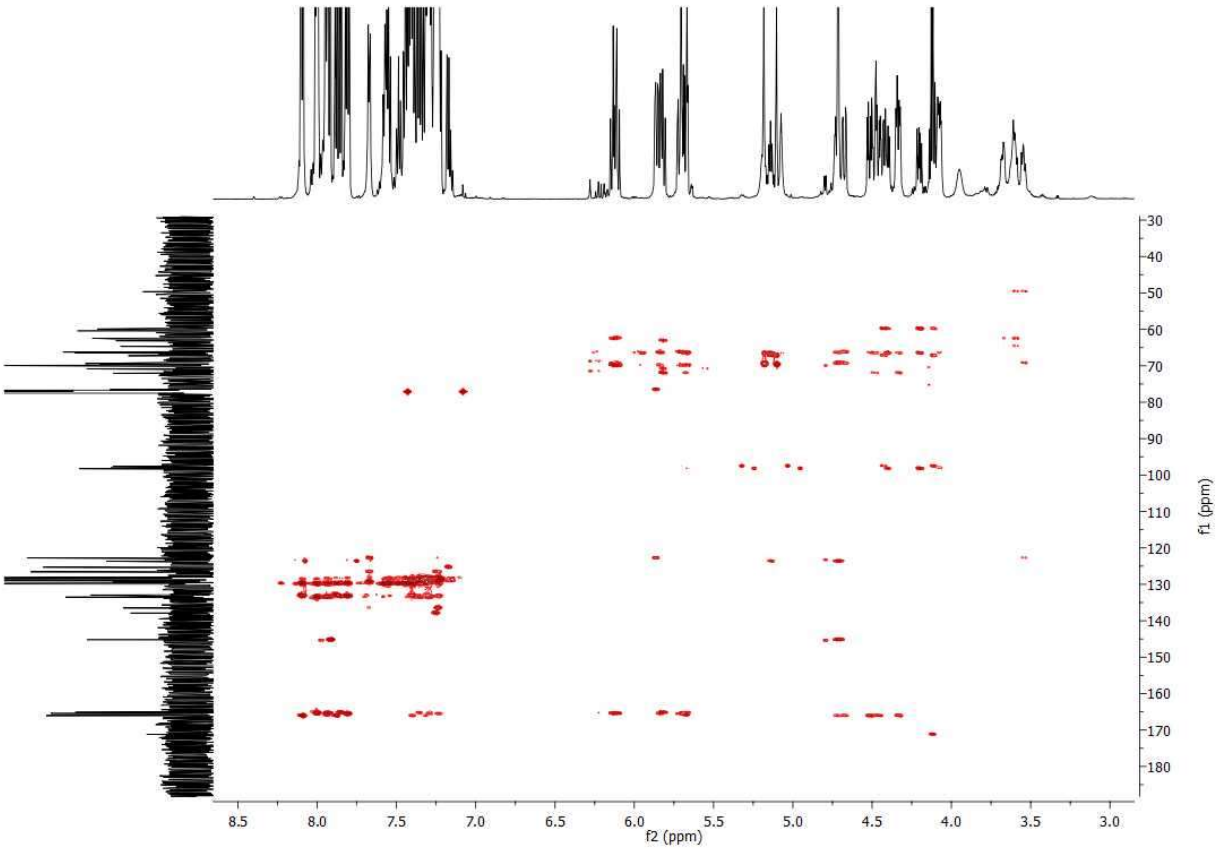

Figure 8.78: HMBC NMR (151 MHz, $CDCl_3$) spectrum of compound **11b**.

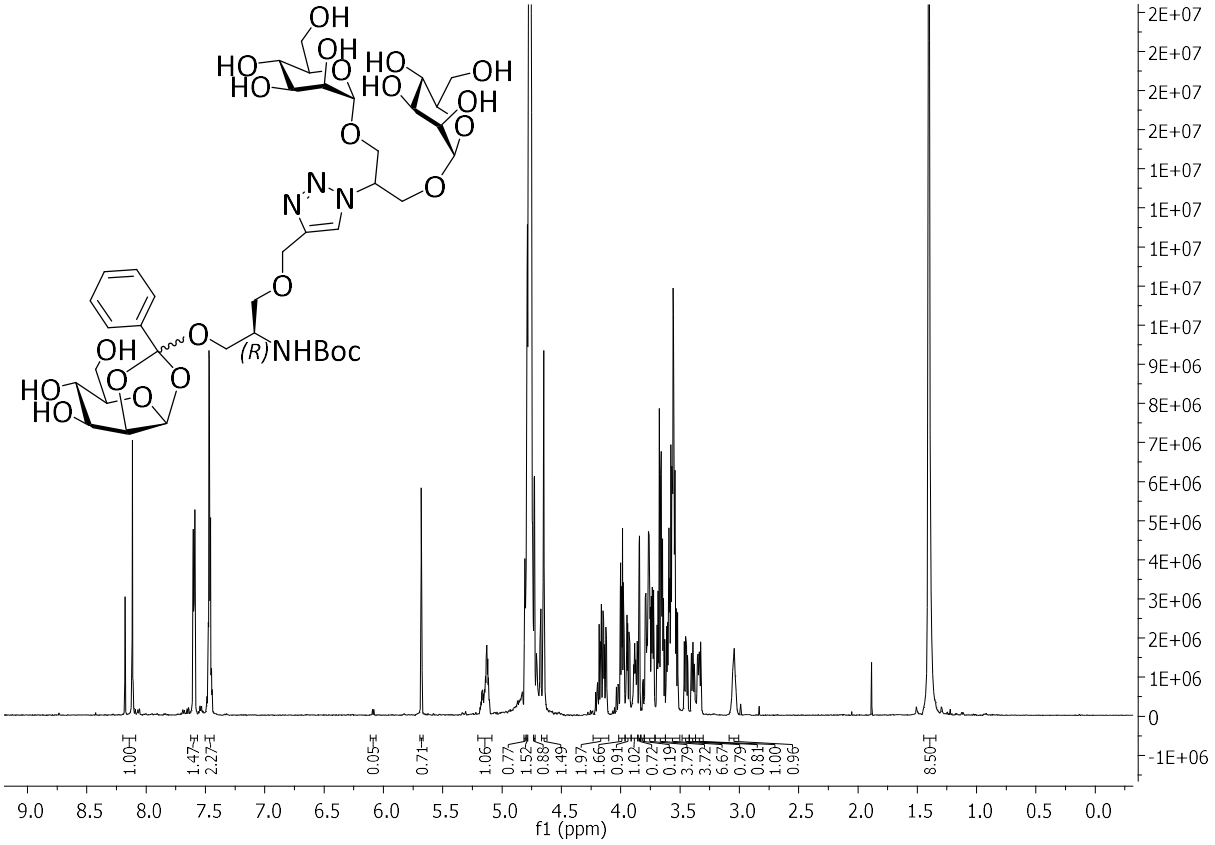

Figure 8.79: ^{1}H NMR (600 MHz, $CDCl_3$) spectrum of compound **12a**.

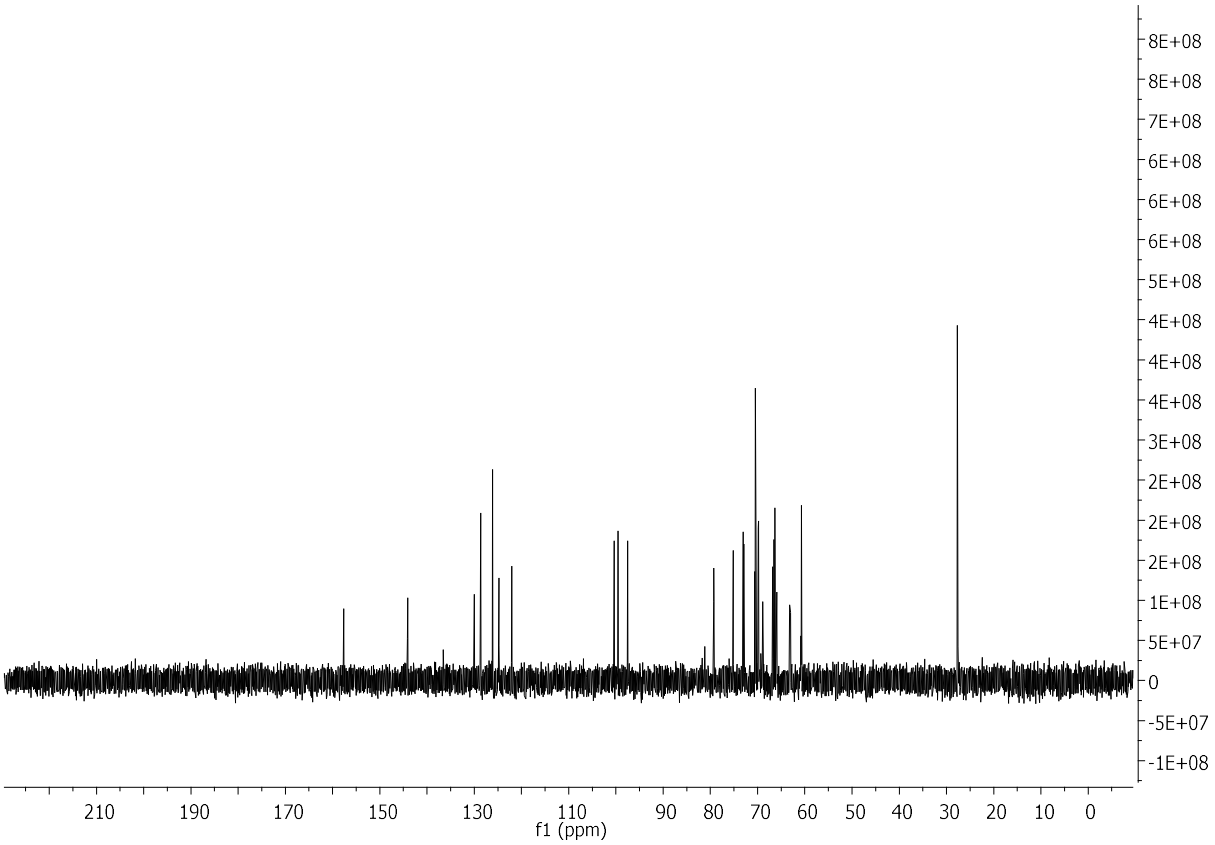

Figure 8.80: ^{13}C NMR (151 MHz, $CDCl_3$) spectrum of compound **12a**.

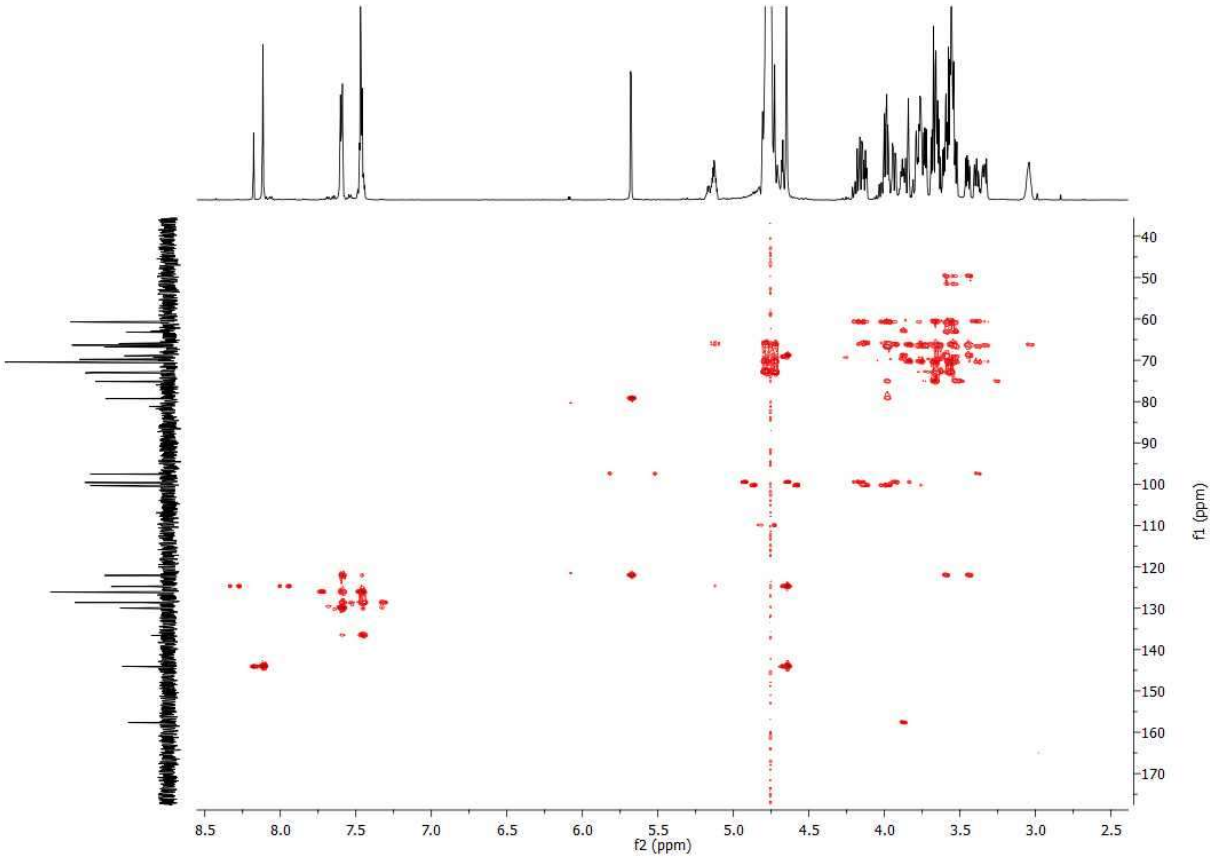

Figure 8.81: HMBC NMR (151 MHz, $CDCl_3$) spectrum of compound **12a**.

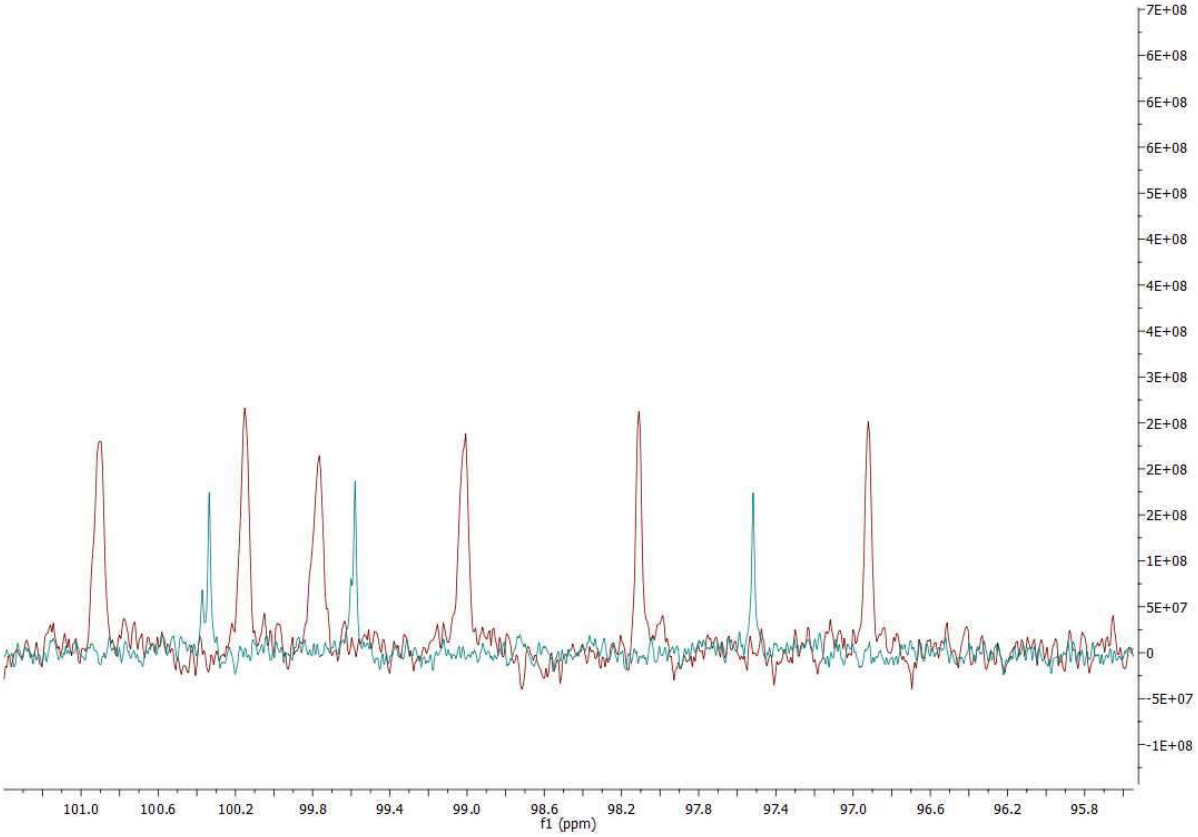

Figure 8.82: ^{13}C gated decoupling NMR (151 MHz, $CDCl_3$) spectrum of **12a** (green) compared with ^{13}C NMR (126 MHz, $CDCl_3$) spectrum of **12a** (red).

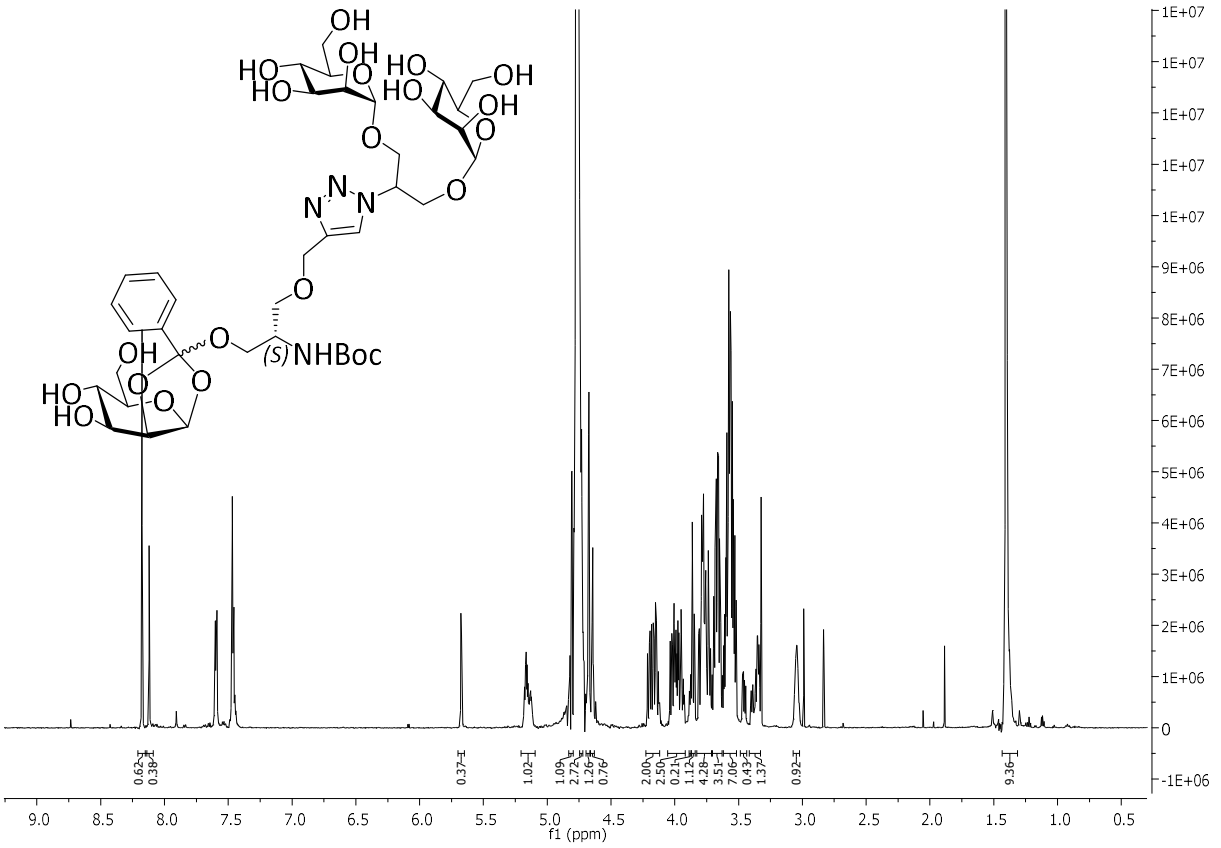

Figure 8.83: ^{1}H NMR (600 MHz, $CDCl_3$) spectrum of compound **12b**.

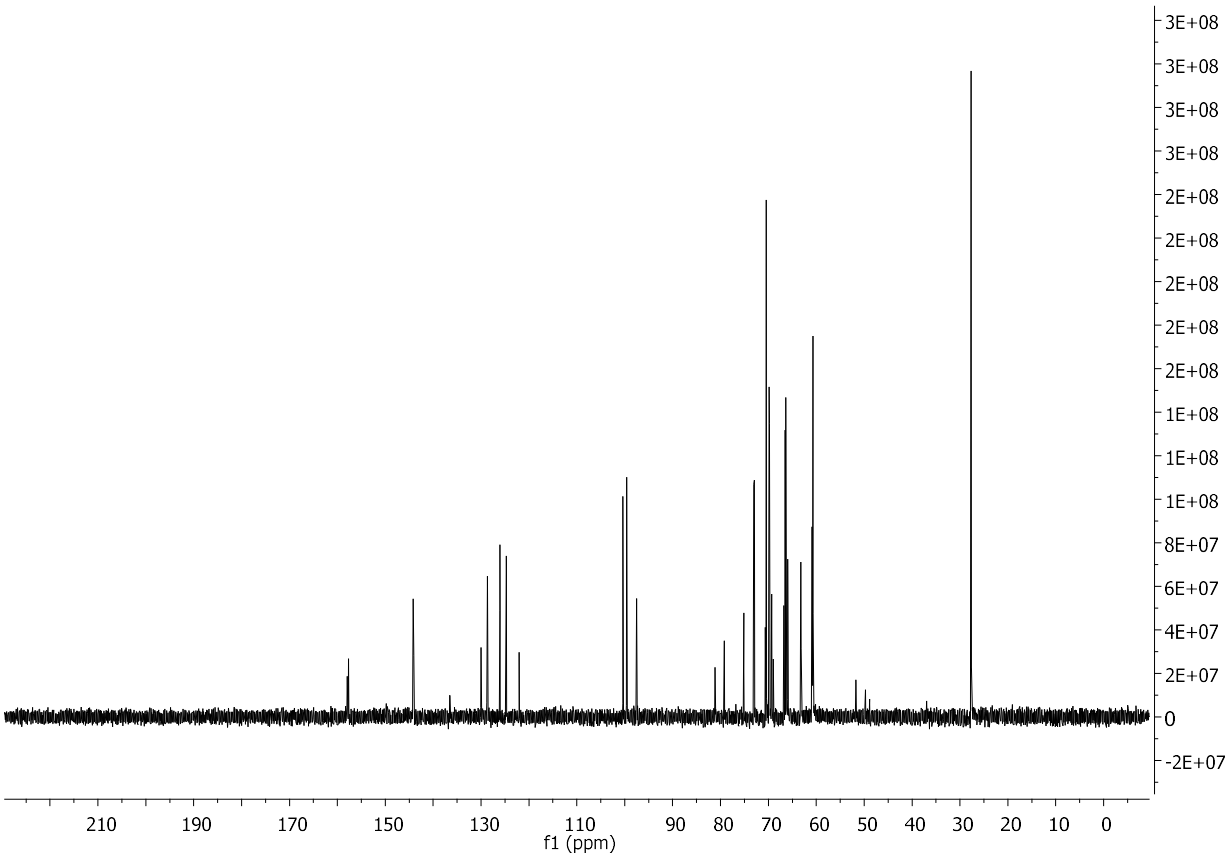

Figure 8.84: ^{13}C NMR (151 MHz, $CDCl_3$) spectrum of compound **12b**.

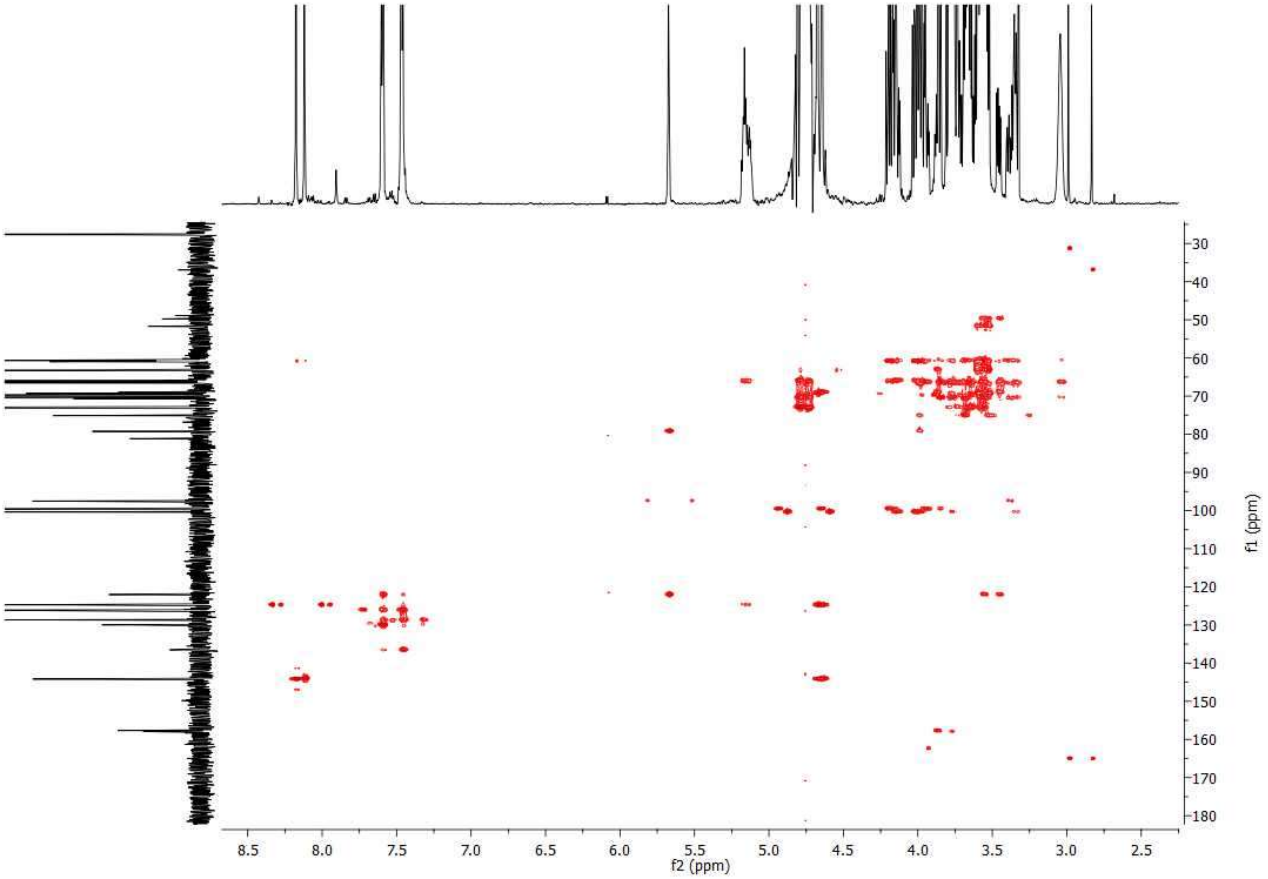

Figure 8.85: HMBC NMR (151 MHz, $CDCl_3$) spectrum of compound **12b**.

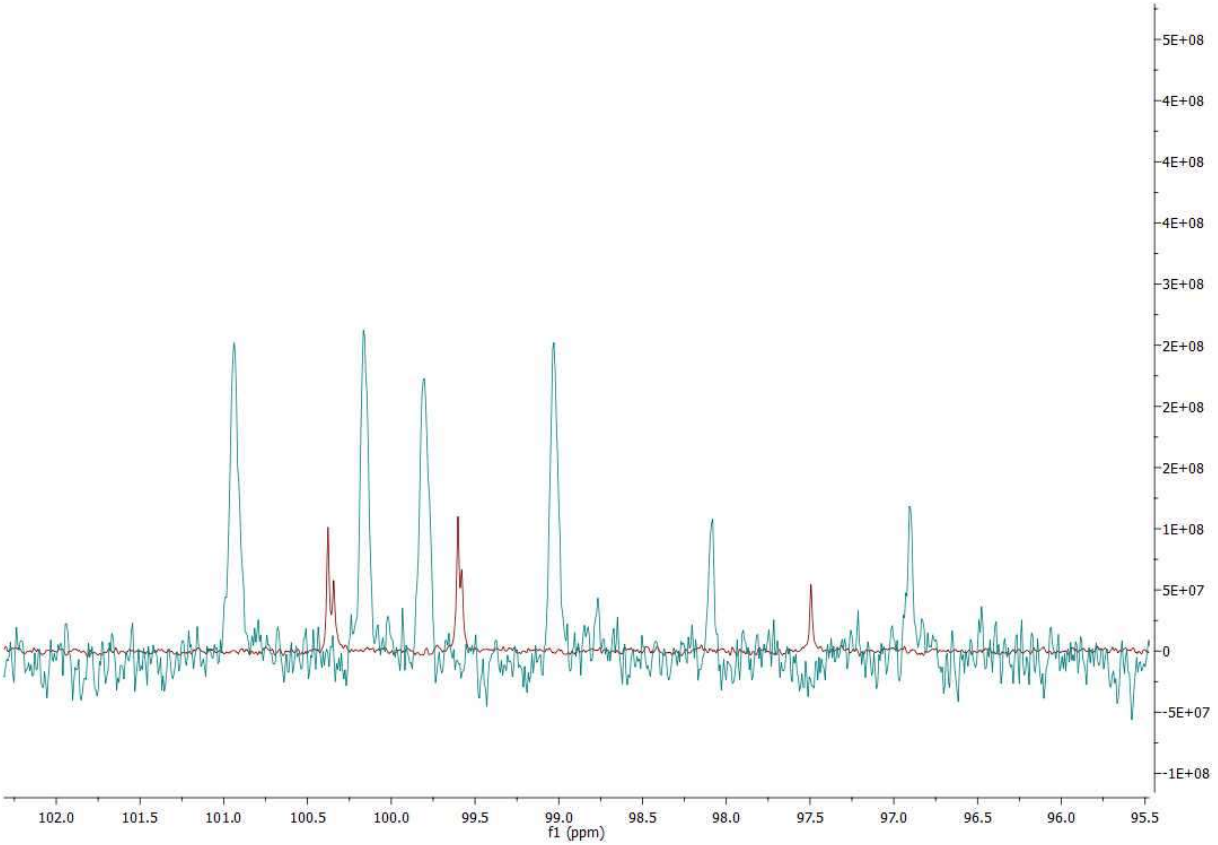

Figure 8.86: ^{13}C gated decoupling NMR (151 MHz, $CDCl_3$) spectrum of **12b** (green) compared to ^{13}C NMR (126 MHz, $CDCl_3$) spectrum of **12b** (red).

8.6 Biological adhesion assays (with reference to chapter 5)

General methods

Buffer solutions and media.

Carbonate buffer: sodium carbonate (10.6 g) and sodium hydrogen carbonate (8.40 g) dissolved in bi-distilled water (1 L), pH = 9.6. PBS buffer: PBS tablets commercially available from Gibco, solution of 2 PBS tablets contain 10 mM sodium phosphate, 2.68 mM potassium chloride and 140 mM sodium chloride in bi-distilled water (1 L), pH = 7.45. PBST buffer (PBS buffer + 0.05 % v/v Tween®20); pH values were adjusted by using 0.1 M aq. hydrochloric acid or 0.1 M aq. sodium hydroxide. LB medium (lysogeny broth medium- sterilized): tryptone (10 g L^{-1}), yeast extract (5 g L^{-1}), sodium chloride (10 g L^{-1}) in bi-distilled water (1 L), pH = 7.0, ampicillin (100 mg L^{-1}) and chloramphenicol (50 mg L^{-1}).

Preparation of bacterial suspension.

To test bacterial adhesion to glycoarrays type 1 fimbriated GFP-PKL1162 *E. coli* bacterial adhesion was investigated. The bacterial *E. coli* strain PKL1162 was cultured from frozen stock in LB media overnight at 37 °C. The bacterial pellet obtained after centrifugation (15 min/ 4000 rpm/ 4 °C), decantated of the media, washed twice with PBS (2 mL) and then suspended in PBS buffer. The bacterial suspension was adjusted to OD_{600} = 0.48 in PBS buffer.

Covalent functionalization on polystyrene surfaces.

The synthesized compounds were tested in triplicates on the same microplate. Serial diluted derivatives **13a**, **13b** and **12** with an initial concentration of *c* = 8 mM were immobilized on the 96- well black microtiter plates (Nunc amino immobilizer surfaces, Polysorp). Immobilization conditions: in carbonate buffer (100 µL per well), pH = 9.6, incubated overnight at 37 °C and 175 rpm. The plates were then washed three times with PBST and remained unreactive surface was blocked with 2-amino-ethanol (*c* = 10 mM) in carbonate buffer (120 µL per well), incubated at 37 °C and 175 rpm for at least two hours. The plates were washed twice with PBST and then once with PBS. Thus prepared glycoarrays can be stored under low temperature (-50 °C) for a longer time period.

Adhesion assays with fimbriated GFP-PKL1162 *E. coli* bacteria under static conditions.

Covalently fabricated glycoclusters on polystyrene surfaces were then used to test bacterial adhesion under static conditions.[96] Thus 50 µL of the bacterial solution in PBS buffer (OD_{600}= 0.48) was added in all wells and incubated for one hour at 37 °C and 100 rpm. The microtiter plates were then washed three times with PBS buffer. Then PBS (120 µL per well) was added in all wells for GFP fluorescence intensity readout at λ_{exc} = 485 nm and λ_{em}= 535 nm. Compounds were tested in three independent experiments. The obtained fluorescence read-out was then used for the calculation of relative bacterial adhesion. In order to calculate valency-corrected values the obtained relative adhesion values of $(\alpha Man)_2$ **12** were divided by the number of clustered mannosyl ligands.

Covalent functionalization on *N*-hydoxysuccinimide glass surfaces.

Commercially available *N*HS glass slides (SuperNHS Microarray Substrate Slides, Arrayit) were fixed in bottom-less microarray hardware 96 wells microplate for glycocluster fabrication. Synthesized derivatives **13a** and **13b** were then fabricated in duplicates on the same glass slide with an initial concentration of *c* = 5 mM and carbonate buffer (100 µL per well). The glass slides were then incubated overnight at ambient temperature and agitation of 250 rpm. So formed glycoarrays are then washed three times with PBST. The glass slides were then soaked in 10 mL solution of 2-amino-ethanol (*c* = 20 mM) and incubated at 37 °C and 175 rpm for three hours to functionalised remained unreactive functional groups. The plates were washed twice with PBST, once with PBS and once with bi-distilled water. Using $N_{2(g)}$ the slides where dried and thus µ-Slide $VI^{0.4}$ (IBIDI) channel slides were stacked on the glass surface providing the 0.4 mm channel hight suitable for the high shear stress range. Thus prepared glass slides were used for the testing of bacterial adhesion under flow conditions.

Adhesion assays with fimbriated GFP-PKL1162 *E. coli* bacteria under flow conditions.

The formed glycoarrays were then used to test bacterial adhesion under flow conditions. In the experimental set up µ-Slide $VI^{0.4}$ (IBIDI) channel slides allowed us to apply flow on three individual wells in the same time period. Bacterial suspension in PBS (OD_{600} = 0.48) was applied under a laminar flow rate of 10 mL/min on the first set of wells to the formed glycoarrays in a time range of 30 min. Then the unbound bacteria were washed with PBS buffer for

10 min under the same flow rate (**Figure 8.96**). Afterward, the channel tubes were changed to the other duplicate set of wells of the same slide. Hence, the same flow conditions were applied. The plate was then fixed in bottomless microarray hardware 96-wells microplate and the channel slides were filled with PBS (120 µL per well) for GFP fluorescence intensity readout at λ_{exc} = 485 nm and λ_{em}= 535 nm. The same experimental set up was used to test bacterial adhesion to the same glycoarrays in three independent experiments. The obtained fluorescence read-out was then used to calculate relative adhesion.

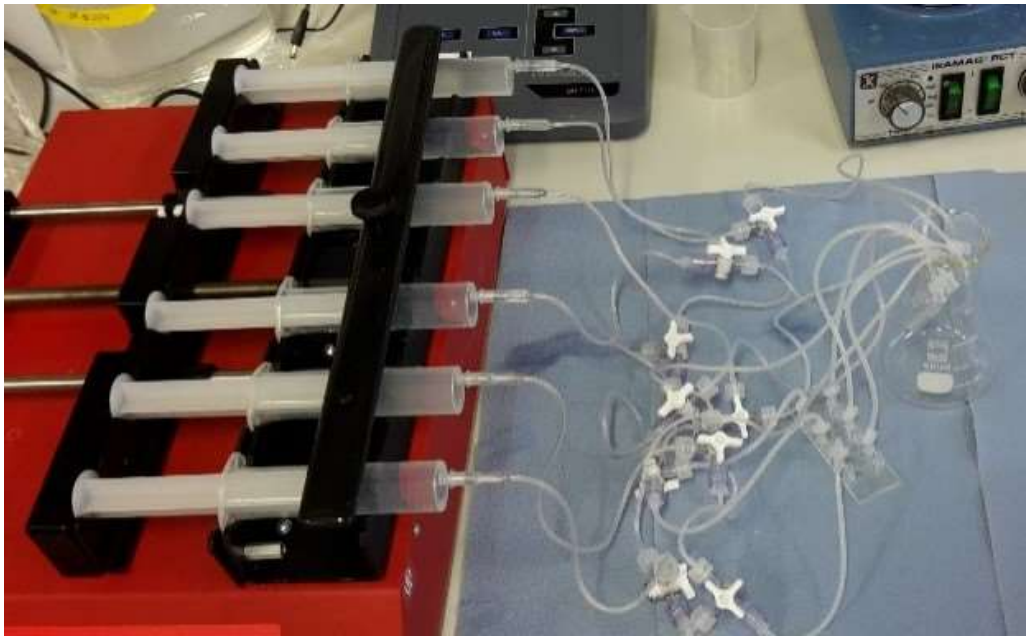

Figure 8.87: Experimental set up to test bacterial adhesion under laminar flow. Three syringes are filled with bacterial suspension and three with PBS buffer. Hence, one set of individual wells could be tested for the adhesion and following the washing step at the time. Then the channel tubes could be used for the second set of individual wells.

Bacterial adhesion under static conditions

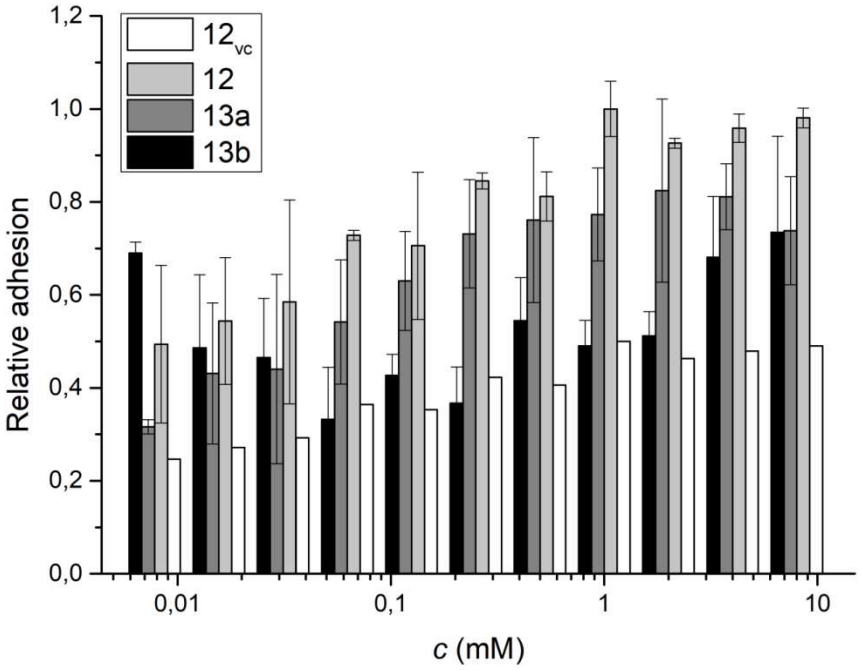

Figure 8.88: Relative adhesion of *E. coli* bacteria to glycoarrays under static conditions at graded concentrations. The relative adhesion values are the mean values from triplicates on the same plate for **13a** and **13b**, and duplicates for **12**. Error bars are given as standard error of the mean.[i]

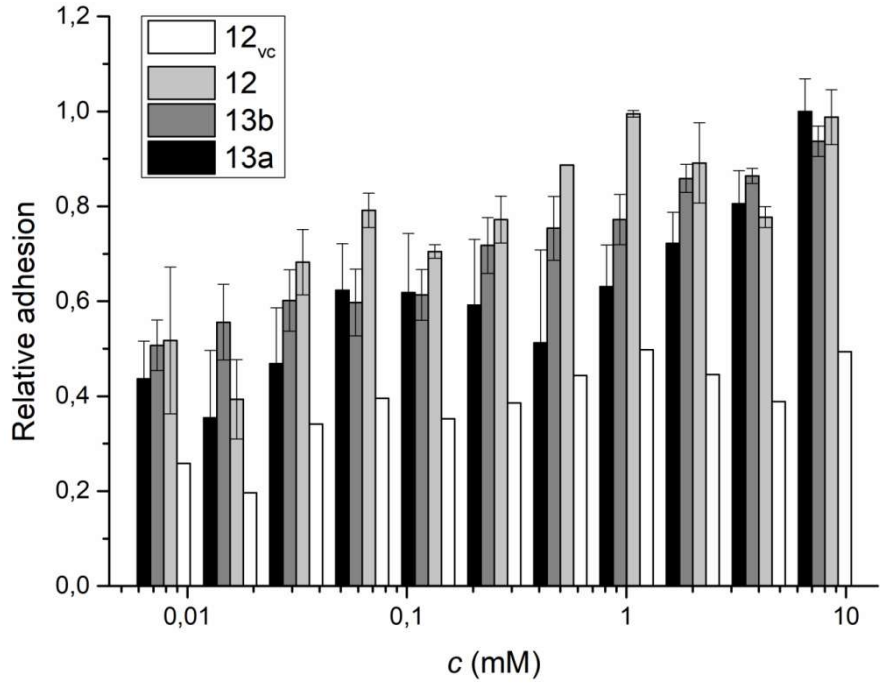

Figure 8.89: Relative adhesion of *E. coli* bacteria to glycoarrays under static conditions at graded concentrations. The relative adhesion values are the mean values from triplicates on the same plate for **13a** and **13b**, and duplicates for **12**. Error bars are given as standard error of the mean.[i]

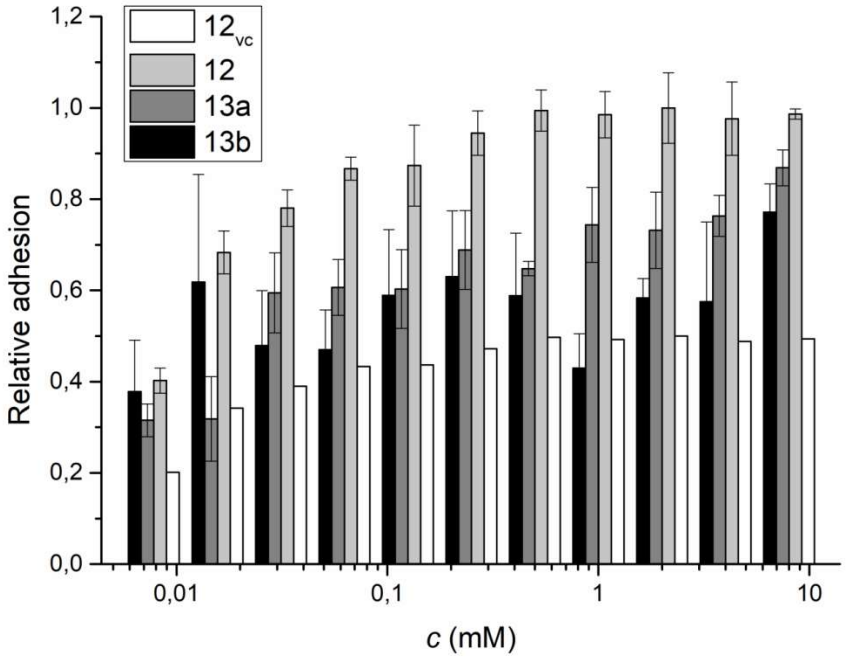

Figure 8.90: Relative adhesion of *E. coli* bacteria to glycoarrays under static conditions at graded concentrations. The relative adhesion values are the mean values from triplicates on the same plate for **13a** and **13b**, and duplicates for **12**. Error bars are given as standard error of the mean.[i]

[i] For the interpretation of the binding assays (cf**. Fig. 8.88**, **8.89** and **8.90**) valency-corrected (vc) adhesion for the divalent cluster mannoside **12** were obtained by dividing the respective adhesion by two. As an alternative to this approach, half concentrations should be applied in the binding assays to obtain valency corrected adhesion to glycoarray **12**.

Bacterial adhesion under flow conditions

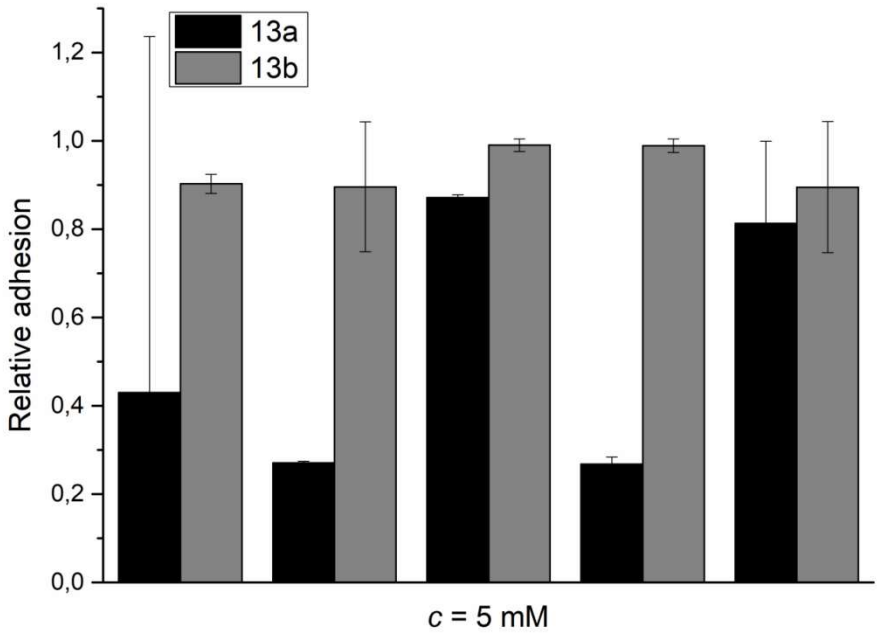

Figure 8.91: Relative adhesion of *E. coli* to glycoarrays under flow conditions. Glycocluster solution of 5 mM in carbonate buffer was used for glycoarray fabrication. Bacterial adhesion was tested in five individually performed experiments. The relative adhesion values are the mean values from duplicates on the same plate. Error bars are given as standard error of the mean.

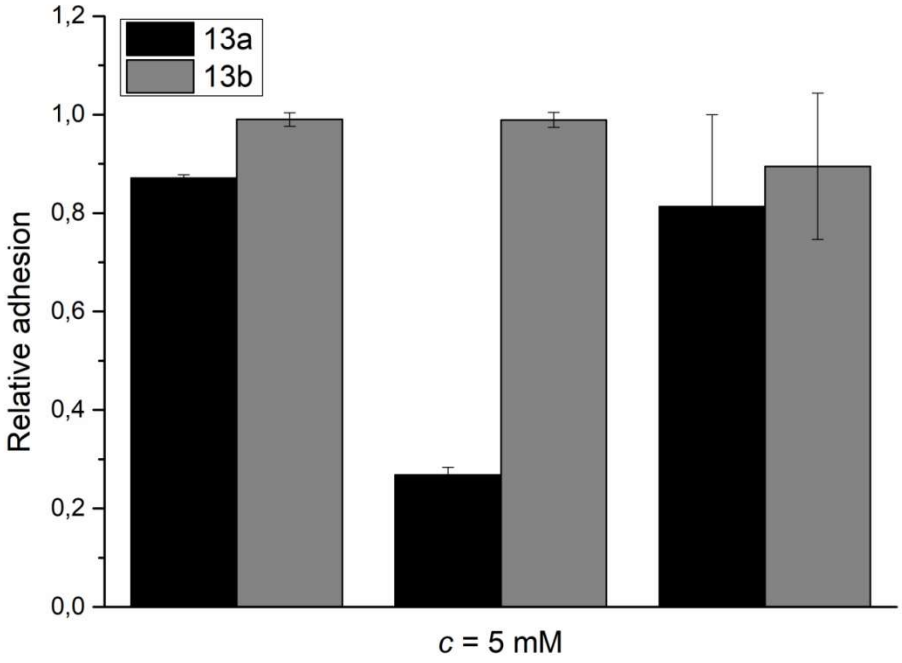

Figure 8.92: Three independently tested assays of *E. coli* bacteria to **13a** and **13b** glycoarrays under flow conditions used for the final determination of the adherence.

9 References

[1] J. D. Watson, F. H. C. Crick, *Nature* **1953**, *171*, 737-738.

[2] K. Landsteiner, H. Raubitschek, *Zbl. Bakt. I. Abt. Orig.* **1907**, *45*, 600-607.

[3] E. Gorter, F. Grendel, *J. Exp. Med.* **1925**, *41*, 439-443.

[4] J. Lombard, *Biol. Direct* **2014**, *9*, 32.

[5] N. Sharon, H. Lis, *Science* **1989**, *246*, 227-234.

[6] A. Varki, M. E. Etzler, R. D. Cummings, J. D. Esko in *Essentials of Glycobiology*, 2nd ed. (Eds.: A. Varki, R. D. Cummings, J. D. Esko, H. H. Freeze, P. Stanley, C. R. Bertozzi, G. W. Hart, M. E. Etzler), Cold Spring Harbor Laboratory Press, Cold Spring Harbor (NY), **2009**.

[7] B. K. Brandley, R. L. Schnaar, *J. Leukoc. Biol.* **1986**, *40*, 97-111.

[8] a) J. B. Sumner, S. F. Howell, *J. Bacteriol.* **1936**, *32*, 227-237; b) N. Sharon, H. Lis, *Science* **1972**, *177*, 949-959.

[9] A. Bandeira, A. Coutinho, C. Martinez, P. Pereira, *Int. Rev. Immunol.* **1988**, *3*, 47-58.

[10] H. H. Xia, N. J. Talley, *Am. J. Gastroenterol* **2001**, *96*, 16-26.

[11] P. C. Pang, P. C. Chiu, C. L. Lee, L. Y. Chang, M. Panico, H. R. Morris, S. M. Haslam, K. H. Khoo, G. F. Clark, W. S. Yeung, A. Dell, *Science* **2011**, *333*, 1761-1764.

[12] a) I. Eggens, B. Fenderson, T. Toyokuni, B. Dean, M. Stroud, S. Hakomori, *J. Biol. Chem.* **1989**, *264*, 9476-9484; b) U. Stelzl, U. Worm, M. Lalowski, C. Haenig, F. H. Brembeck, H. Goehler, M. Stroedicke, M. Zenkner, A. Schoenherr, S. Koeppen, J. Timm, S. Mintzlaff, C. Abraham, N. Bock, S. Kietzmann, A. Goedde, E. Toksoz, A. Droege, S. Krobitsch, B. Korn, W. Birchmeier, H. Lehrach, E. E. Wanker, *Cell* **2005**, *122*, 957-968.

[13] H. Franz, *Adv. Lectin Res.* **1988**, *1*, 10-25.

[14] Y. C. Lee, R. T. Lee, *Acc. Chem. Res.* **1995**, *28*, 321-327.

[15] K. Landsteiner, *J. Pharm. Sci.* **1936**, *52*, 5.

[16] J. M. Rini, *Annu. Rev. Biophys. Biomol. Struct.* **1995**, *24*, 551-577.

[17] a) J. D. Aplin, R. C. Hughes, *Biochim. Biophys. Acta* **1982**, *694*, 375-418; b) N. Sharon, *Immunol. Today* **1984**, *5*, 143-147.

[18] C. A. Williams, M. W. Chase in *Methods in Immunology and Immunochemistry,* Academic Press, New York, **1977**.

[19] a) M. C. Meneghetti, A. J. Hughes, T. R. Rudd, H. B. Nader, A. K. Powell, E. A. Yates, M. A. Lima, *J. R. Soc. Interface* **2015**, *12*, 0589; b) L. Jin, J. P. Abrahams, R. Skinner, M. Petitou, R. N. Pike, R. W. Carrell, *Proc. Natl. Acad. Sci. U. S. A.* **1997**, *94*, 14683-14688.

[20] N. Sharon, *Protein Sci.* **1998**, *7*, 2042-2048.

[21] M. L. Ogilvie, T. K. Gartner, *J. Herpetol.* **1984**, *18*, 285-290.

[22] J. J. Marchalonis, G. M. Edelman, *J. Mol. Biol.* **1968**, *32*, 453-465.

[23] a) J. B. Sumner, *J. Biol. Chem.* **1919**, *37*, 137-142; b) G. M. Edelman, B. A. Cunningham, G. N. Reeke, J. W. Becker, M. J. Waxdal, J. L. Wang, *Proc. Natl. Acad. Sci. U. S. A.* **1972**, *69*, 2580-2584.

[24] J. B. Sumner, S. F. Howell, *J. Bacteriol.* **1936**, *32*, 227-237.

[25] B. Alberts, A. Johnson, J. Lewis, M. Raff, K. Roberts, P. Walter in *Molecular Biology of the Cell*, Garland Science, New York, **2002**.

[26] H. Lis, N. Sharon, *Chem. Rev.* **1998**, *98*, 637-674.

[27] N. Sharon, H. Lis, *Glycobiology* **2004**, *14*, 53-62.

[28] a) J. B. Kaper, J. P. Nataro, H. L. Mobley, *Nat. Rev. Microbiol.* **2004**, *2*, 123-140; b) G. G. Anderson, K. W. Dodson, T. M. Hooton, S. J. Hultgren, *Trends Microbiol.* **2004**, *12*, 424-430; c) V. Sperandio, Y. Nguyen, *Front. Cell. Infect. Microbiol.* **2012**, *2*.
[29] J. D. Schilling, M. A. Mulvey, S. J. Hultgren, *J. Infect. Dis.* **2001**, *183, Suppl 1*, 36-40.
[30] K. D. Hardman, C. F. Ainsworth, *Biochemistry* **1972**, *11*, 4910-4919.
[31] S. D. Knight, J. Bouckaert, *Top. Curr. Chem.* **2009**, *288*, 67-107.
[32] U. Kumlin, S. Olofsson, K. Dimock, N. Arnberg, *Influenza Other Respir Viruses* **2008**, *2*, 147-154.
[33] K. Drickamer, *Curr. Opin. Struct. Biol.* **1999**, *9*, 585-590.
[34] T. K. Lindhorst in *Handbook of Carbohydrate-Modifying Biocatalysts*, 1st ed. (Ed.: P. Grunwald), CRC Press, Singapore, **2016**, pp. 147-215.
[35] G. R. Vasta, *Adv. Exp. Med. Biol.* **2012**, *946*, 21-36.
[36] K. L. Moore, N. L. Stults, S. Diaz, D. F. Smith, R. D. Cummings, A. Varki, R. P. McEver, *J. Cell Biol.* **1992**, *118*, 445-456.
[37] S. Andre, H. Kaltner, J. C. Manning, P. V. Murphy, H. J. Gabius, *Molecules* **2015**, *20*, 1788-1823.
[38] P. Albersheim, A. G. Darvill, M. McNeil, B. S. Valent, J. K. Sharp, E. A. Nothnagel, K. R. Davis, N. Yamazaki, D. J. Gollin, W. S. York, W. F. Dudman, J. E. Darvill, A. Dell in *Structure and Function of Plant Genomes*, (Eds.: O. Ciferri, L. Dure), Springer New York, Boston, **1983**, pp. 293-312.
[39] J. Montreuil in *New Comprehensive Biochemistry, Vol. 29,* (Eds.: J. Montreuil, J. F. G. Vliegenthart, H. Schachter), Elsevier, Amsterdam, **1995**, pp. 1-12.
[40] M. Aronson, O. Medalia, L. Schori, D. Mirelman, N. Sharon, I. Ofek, *J. Infect. Dis.* **1979**, *139*, 329-332.
[41] A. Varki, S. Kornfeld in *Essentials of Glycobiology*, 3rd ed. (Eds.: A. Varki, R.D. Cummings., J.D. Esko et al.), Cold Spring Harbor Laboratory Press, Cold Spring Harbor (NY), **2017**, pp. 321-354.
[42] T. Yamakawa, Y. Nagai, *Trends Biochem. Sci.* **1978**, *3*, 128-131.
[43] T. Wennekes, R. J. B. H. N. van den Berg, R. G. Boot, G. A. van der Marel, H. S. Overkleeft, J. M. F. G. Aerts, *Angew. Chem. Int. Ed. Engl.* **2009**, *48*, 8848-8869.
[44] R. Malhotra, *Biochem. Anal. Biochem.* **2012**, *01*, 2908–2912.
[45] P. Stanley, H. Schachter, N. Taniguchi in *Essentials of Glycobiology*, 2nd ed. (Ed.: A. Varki, R. D. Cummings, J. D. Esko, H. H. Freeze, P. Stanley, C. R. Bertozzi, G. W. Hart, M. E. Etzler), Cold Spring Harbor Laboratory Press, Cold Spring Harbor (NY), **2009**.
[46] I. Brockhausen, H. Schachter, P. Stanley in *Essentials of Glycobiology*, 2nd ed. (Ed.: A. Varki, R. D. Cummings, J. D. Esko, H. H. Freeze, P. Stanley, C. R. Bertozzi, G. W. Hart, M. E. Etzler), Cold Spring Harbor Laboratory Press, Cold Spring Harbor (NY), **2009**.
[47] U. Lindahl, J. Couchman, K. Kimata, and J. D. Esko in *Essentials of Glycobiology*, 3rd ed. (Ed. A. Varki, R. D. Cummings, J. D. Esko et al.), Cold Spring Harbor Laboratory Press, Cold Spring Harbor (NY), **2017**.
[48] C. A. Lingwood, R. Mahfoud in *Microbial Glycobiology*, (Eds.: O. Holst, P. J. Brennan, M. v. Itzstein, A. P. Moran), Academic Press, San Diego, **2010**, pp. 599-621.
[49] G. J. Gerwig, J. F. G. Vliegenthart in *Proteomics in Functional Genomics: Protein Structure Analysis*, (Eds.: P. Jollès, H. Jörnvall), Birkhäuser Basel, Basel, **2000**, pp. 159-186.

[50] a) J. Hofsteenge, D. R. Muller, T. de Beer, A. Loffler, W. J. Richter, J. F. Vliegenthart, *Biochemistry* **1994**, *33*, 13524-13530; b) A. Garcia, L. A. Lenis, C. Jimenez, C. Debitus, E. Quinoa, R. Riguera, *Org. Lett.* **2000**, *2*, 2765-2767.
[51] L. Kjellén, U. Lindahl, *Annu. Rev. Biochem.* **1991**, *60*, 443-475.
[52] K. Meyer, G. L. Hobby, E. Chaffee, M. H. Dawson, *J. Exp. Med.* **1940**, *71*, 137-146.
[53] J. Montreuil, *Adv. Carbohydr. Chem. Biochem.* **1980**, *37*, 157-223.
[54] J. C. Paulson, W. E. Beranek, R. L. Hill, *J. Biol. Chem.* **1977**, *252*, 2356-2362.
[55] J. C. Paulson, J. I. Rearick, R. L. Hill, *J. Biol. Chem.* **1977**, *252*, 2363-2371.
[56] a) J. C. Michalski, G. Strecker, B. Fournet, M. Cantz, J. Spranger, *FEBS Lett.* **1977**, *79*, 101-104; b) G. Strecker, M. C. Peers, J. C. Michalski, T. Hondi-Assah, B. Fournet, G. Spik, J. Montreuil, J. P. Farriaux, P. Maroteaux, P. Durand, *Eur. J. Biochem.* **1977**, *75*, 391-403; c) A. Hofmann, R. Sommer, D. Hauck, J. Stifel, I. Gottker-Schnetmann, A. Titz, *Carbohydr. Res.* **2015**, *412*, 34-42.
[57] a) L. Dorland, H. van Halbeek, J. F. Vleigenthart, H. Lis, N. Sharon, *J. Biol. Chem.* **1981**, *256*, 7708-7711; b) H. Lis, N. Sharon, *J. Biol. Chem.* **1978**, *253*, 3468-3476.
[58] E. Li, S. Kornfeld, *J. Biol. Chem.* **1979**, *254*, 1600-1605.
[59] a) J. Bouckaert, J. Mackenzie, J. L. de Paz, B. Chipwaza, D. Choudhury, A. Zavialov, K. Mannerstedt, J. Anderson, D. Pierard, L. Wyns, P. H. Seeberger, S. Oscarson, H. De Greve, S. D. Knight, *Mol. Microbiol.* **2006**, *61*, 1556-1568; b) B. Xie, G. Zhou, S. Y. Chan, E. Shapiro, X. P. Kong, X. R. Wu, T. T. Sun, C. E. Costello, *J. Biol. Chem.* **2006**, *281*, 14644-14653.
[60] a) J. F. Vliegenthart, *FEBS Lett.* **2006**, *580*, 2945-2950; b) A. Rek, E. Krenn, A. J. Kungl, *Br. J. Pharmacol.* **2009**, *157*, 686-694; c) N. Sharon, *BBA Gen. Subjects* **2006**, *1760*, 527-537; d) S. B. Oppenheimer, M. Alvarez, J. Nnoli, *Acta Histochem.* **2008**, *110*, 6-13; e) C. Bies, C. M. Lehr, J. F. Woodley, *Adv. Drug Deliv. Rev.* **2004**, *56*, 425-435.
[61] a) T. Ogawa, K. Sasajima, *Carbohydr. Res.* **1981**, *93*, 53-66; b) N. Firon, I. Ofek, N. Sharon, *Carbohydr. Res.* **1983**, *120*, 235-249.
[62] R. A. Dwek, *Chem. Rev.* **1996**, *96*, 683-720.
[63] a) L. L. Kiessling, J. E. Gestwicki, L. E. Strong, *Curr. Opin. Chem. Biol.* **2000**, *4*, 696-703; b) M. Mammen, S. K. Choi, G. M. Whitesides, *Angew. Chem. Int. Ed. Engl.* **1998**, *37*, 2754-2794.
[64] G. Ashwell, A. G. Morell, *Adv. Enzymol. Relat. Areas Mol. Biol.* **1974**, 99-128.
[65] R. Haag, *Beilstein J. Org. Chem.* **2015**, *11*, 848-849.
[66] J. J. Lundquist, E. J. Toone, *Chem. Rev.* **2002**, *102*, 555-578.
[67] a) V. Wittmann, R. J. Pieters, *Chem. Soc. Rev.* **2013**, *42*, 4492-4503; b) G. Schwarzenbach, *Helv. Chim. Acta* **1952**, *35*, 2344-2359.
[68] a) C. H. Heldin, *Cell* **1995**, *80*, 213-223; b) J. E. Gestwicki, L. L. Kiessling, *Nature* **2002**, *415*, 81-84; c) L. L. Kiessling, J. E. Gestwicki, L. E. Strong, *Angew. Chem. Int. Ed. Engl.* **2006**, *45*, 2348-2368.
[69] a) T. K. Dam, T. A. Gerken, B. S. Cavada, K. S. Nascimento, T. R. Moura, C. F. Brewer, *J. Biol. Chem.* **2007**, *282*, 28256-28263; b) T. K. Dam, T. A. Gerken, C. F. Brewer, *Biochemistry* **2009**, *48*, 3822-3827.
[70] a) C. Rademacher, J. Guiard, P. I. Kitov, B. Fiege, K. P. Dalton, F. Parra, D. R. Bundle, T. Peters, *Chem. Eur. J.* **2011**, *17*, 7442-7453; b) J. Guiard, B. Fiege, P. I. Kitov, T. Peters, D. R. Bundle, *Chem. Eur. J.* **2011**, *17*, 7438-7441.
[71] P. I. Kitov, J. M. Sadowska, G. Mulvey, G. D. Armstrong, H. Ling, N. S. Pannu, R. J. Read, D. R. Bundle, *Nature* **2000**, *403*, 669.

[72] A. D. Meltzer, D. A. Tirrell, A. A. Jones, P. T. Inglefield, D. M. Hedstrand, D. A. Tomalia, *Macromolecules* **1992**, *25*, 4541-4548.
[73] G. R. Newkome, Z. Yao, G. R. Baker, V. K. Gupta, *J. Org. Chem.* **1985**, *50*, 2003-2004.
[74] M. Ortega-Muñoz, F. Perez-Balderas, J. Morales-Sanfrutos, F. Hernandez-Mateo, J. Isac-García, F. Santoyo-Gonzalez, *Eur. J. Org. Chem.* **2009**, *2009*, 2454-2473.
[75] a) W. B. Turnbull, J. F. Stoddart, *Rev. Mol. Biotechnol.* **2002**, *90*, 231-255; b) D. Appelhans, B. Klajnert-Maculewicz, A. Janaszewska, J. Lazniewska, B. Voit, *Chem. Soc. Rev.* **2015**, *44*, 3968-3996.
[76] J. R. Allen, C. R. Harris, S. J. Danishefsky, *J. Am. Chem. Soc.* **2001**, *123*, 1890-1897.
[77] Mike M. K. Boysen, K. Elsner, O. Sperling, Thisbe K. Lindhorst, *Eur. J. Org. Chem.* **2003**, *22*, 4376-4386.
[78] J. Katajisto, T. Karskela, P. Heinonen, H. Lönnberg, *J. Org. Chem.* **2002**, *67*, 7995-8001.
[79] a) M. Gómez-García, J. M. Benito, D. Rodríguez-Lucena, J.-X. Yu, K. Chmurski, C. Ortiz Mellet, R. Gutiérrez Gallego, A. Maestre, J. Defaye, J. M. García Fernández, *J. Am. Chem. Soc.* **2005**, *127*, 7970-7971; b) M. Gómez-García, J. M. Benito, R. Gutiérrez-Gallego, A. Maestre, C. O. Mellet, J. M. G. Fernández, J. L. J. Blanco, *Org. Biomol. Chem.* **2010**, *8*, 1849-1860; c) M. Gómez-García, J. M. Benito, A. P. Butera, C. O. Mellet, J. M. G. Fernández, J. L. J. Blanco, *J. Org. Chem.* **2012**, *77*, 1273-1288.
[80] J. L. Jiménez Blanco, C. Ortiz Mellet, J. M. García Fernández, *Chem. Soc. Rev.* **2013**, *42*, 4518-4531.
[81] a) C.-H. Liang, S.-K. Wang, C.-W. Lin, C.-C. Wang, C.-H. Wong, C.-Y. Wu, *Angew. Chem. Int. Ed. Eng.* **2011**, *50*, 1608-1612; b) S. G. Gouin, E. Vanquelef, J. M. Fernandez, C. O. Mellet, F. Y. Dupradeau, J. Kovensky, *J. Org. Chem.* **2007**, *72*, 9032-9045; c) G. Despras, L. Möckl, A. Heitmann, I. Stamer, C. Bräuchle, T. K. Lindhorst, *ChemBioChem* **2019**, *20*, 2373-2382.
[82] A. Schierholt, M. Hartmann, T. K. Lindhorst, *Carbohydr. Res.* **2011**, *346*, 1519-1526.
[83] a) O. Srinivas, N. Mitra, A. Surolia, N. Jayaraman, *J. Am. Chem. Soc.* **2002**, *124*, 2124-2125; b) O. Srinivas, N. Mitra, A. Surolia, N. Jayaraman, *Glycobiology* **2005**, *15*, 861-873.
[84] a) V. Chandrasekaran, T. K. Lindhorst, *Chem. Commun.* **2012**, *48*, 7519-7521; b) T. Weber, V. Chandrasekaran, I. Stamer, M. B. Thygesen, A. Terfort, T. K. Lindhorst, *Angew. Chem. Int. Ed. Engl.* **2014**, *53*, 14583-14586.
[85] M. Hartmann, T. K. Lindhorst, *Eur. J. Org. Chem.* **2011**, *2011*, 3583-3609.
[86] J. W. Wehner, M. Hartmann, T. K. Lindhorst, *Carbohydr. Res.* **2013**, *371*, 22-31.
[87] a) R. D. Poretz, I. J. Goldstein, *Biochemistry* **1970**, *9*, 2890-2896; b) I. Baussanne, J. M. Benito, C. Ortiz Mellet, J. M. García Fernández, J. Defaye, *ChemBioChem* **2001**, *2*, 777-783; c) M. Kohn, J. M. Benito, C. Ortiz Mellet, T. K. Lindhorst, J. M. Garcia Fernandez, *ChemBioChem* **2004**, *5*, 771-777.
[88] L. Pasteur, *Mol. Med.* **1995**, *1*, 599-601.
[89] a) A. Schierholt, M. Hartmann, K. Schwekendiek, T. K. Lindhorst, *Eur. J. Org. Chem.* **2010**, *2010*, 3120-3128; b) S. Behren, U. Westerlind, *Molecules* **2019**, *24*, 1004.
[90] J. F. K. a. W. J. L. R. G. Denkewalter, 4410688, US, **1979**
[91] a) D. H. Live, Z.-G. Wang, U. Iserloh, S. J. Danishefsky, *Org. Lett.* **2001**, *3*, 851-854; b) R. Hirschmann, J. Hynes, M. A. Cichy-Knight, R. D. van Rijn, P. A. Sprengeler, P. G. Spoors, W. C. Shakespeare, S. Pietranico-Cole, J. Barbosa, J. Liu, W. Yao, S. Rohrer, A. B. Smith, *J. Med. Chem.* **1998**, *41*, 1382-1391.

[92] E. M. V. Johansson, R. U. Kadam, G. Rispoli, S. A. Crusz, K.-M. Bartels, S. P. Diggle, M. Cámara, P. Williams, K. E. Jaeger, T. Darbre, J. L. Reymond, *MedChemComm* **2011**, *2*, 418-420.
[93] N. Gilboa-Garber, *Methods Enzymol.* **1982**, *83*, 378-385.
[94] S. Wagner, D. Hauck, M. Hoffmann, R. Sommer, I. Joachim, R. Müller, A. Imberty, A. Varrot, A. Titz, *Angew. Chem. Int. Ed. Engl.* **2017**, *56*, 16559-16564.
[95] L. Mydock-McGrane, Z. Cusumano, Z. Han, J. Binkley, M. Kostakioti, T. Hannan, J. S. Pinkner, R. Klein, V. Kalas, J. Crowley, N. P. Rath, S. J. Hultgren, J. W. Janetka, *J. Med. Chem.* **2016**, *59*, 9390-9408.
[96] M. Hartmann, A. K. Horst, P. Klemm, T. K. Lindhorst, *Chem. Commun.* **2010**, *46*, 330-332.
[97] H. D. Flack, *Acta Crystallogr. A.* **2009**, *65*, 371-389.
[98] T. Katsuki, K. B. Sharpless, *J. Am. Chem. Soc.* **1980**, *102*, 5974-5976.
[99] a) J. A. Dale, D. L. Dull, H. S. Mosher, *J. Org. Chem.* **1969**, *34*, 2543-2549; b) J. M. Seco, E. Quiñoá, R. Riguera, *Chem. Rev.* **2004**, *104*, 17-118.
[100] a) Y. Gao, J. M. Klunder, R. M. Hanson, H. Masamune, S. Y. Ko, K. B. Sharpless, *J. Am. Chem. Soc.* **1987**, *109*, 5765-5780; b) D. Tanner, P. Somfai, *Tetrahedron* **1986**, *42*, 5985-5990; c) N. J. Bennett, J. C. Prodger, G. Pattenden, *Tetrahedron* **2007**, *63*, 6216-6231; d) G. Pattenden, G. Rescourio, *Org. Biomol. Chem.* **2008**, *6*, 3428-3438; e) A. Tap, M. Jouanneau, G. Galvani, G. Sorin, M.-I. Lannou, J.-P. Férézou, J. Ardisson, *Org. Biomol. Chem.* **2012**, *10*, 8140-8146; f) F. Russo, F. Wångsell, J. Sävmarker, M. Jacobsson, M. Larhed, *Tetrahedron* **2009**, *65*, 10047-10059.
[101] U. Schmidt, M. Respondek, A. Lieberknecht, J. Werner, P. Fischer, *Synthesis* **1989**, *1989*, 256-261.
[102] S. Hatakeyama, H. Matsumoto, H. Fukuyama, Y. Mukugi, H. Irie, *J. Org. Chem.* **1997**, *62*, 2275-2279.
[103] E. D. Goddard-Borger, R. V. Stick, *Org. Lett.* **2007**, *9*, 3797-3800.
[104] J. Brekalo, G. Despras, T. K. Lindhorst, *Org. Biomol. Chem.* **2019**, *17*, 5929-5942.
[105] D. Sail, P. Kováč, *Carbohydr. Res.* **2012**, *357*, 47-52.
[106] G. H. Veeneman, S. H. van Leeuwen, J. H. van Boom, *Tetrahedron Lett.* **1990**, *31*, 1331-1334.
[107] R. R. Schmidt, W. Kinzy, *Adv. Carbohydr. Chem. Biochem.* **1994**, *50*, 21-123.
[108] S. Hanessian, C. Bacquet, N. Lehong, *Carbohydr. Res.* **1980**, *80*, C17-C22.
[109] a) H. R. Goldschmid, A. S. Perlin, *Can. J. Chem.* **1961**, *39*, 2025-2034; b) J. Banoub, D. R. Bundle, *Can. J. Chem.* **1979**, *57*, 2091-2097; c) A. S. Perlin, *Can. J. Chem.* **1963**, *41*, 399-406.
[110] W. Koenigs, E. Knorr, *Ber. Dtsch. Chem. Ges.* **1901**, *34*, 957-981.
[111] T. K. Lindhorst, *J. Carbohydr. Chem.* **1997**, *16*, 237-243.
[112] a) S. Langermann, R. Möllby, J. E. Burlein, S. R. Palaszynski, C. Gale Auguste, A. DeFusco, R. Strouse, M. A. Schenerman, S. J. Hultgren, J. S. Pinkner, J. Winberg, L. Guldevall, M. Söderhäll, K. Ishikawa, S. Normark, S. Koenig, *J. Infect. Dis.* **2000**, *181*, 774-778; b) C. K. Cusumano, J. S. Pinkner, Z. Han, S. E. Greene, B. A. Ford, J. R. Crowley, J. P. Henderson, J. W. Janetka, S. J. Hultgren, *Sci. Transl. Med.* **2011**, *3*, 109-115; c) R. Sommer, S. Wagner, K. Rox, A. Varrot, D. Hauck, E. C. Wamhoff, J. Schreiber, T. Ryckmans, T. Brunner, C. Rademacher, R. W. Hartmann, M. Brönstrup, A. Imberty, A. Titz, *J. Am. Chem. Soc.* **2018**, *140*, 2537-2545.
[113] I. Ofek, D. L. Hasty, N. Sharon, *FEMS Immunol. Med. Microbiol.* **2003**, *38*, 181-191.

[114] T. Feizi, F. Fazio, W. Chai, C.-H. Wong, *Curr. Opin. Struct. Biol.* **2003**, *13*, 637-645.
[115] a) M. C. Bryan, O. Plettenburg, P. Sears, D. Rabuka, S. Wacowich-Sgarbi, C. H. Wong, *Chem. Biol.* **2002**, *9*, 713-720; b) F. Fazio, M. C. Bryan, O. Blixt, J. C. Paulson, C. H. Wong, *J. Am. Chem. Soc.* **2002**, *124*, 14397-14402.
[116] C. Leteux, M. S. Stoll, R. A. Childs, W. Chai, M. Vorozhaikina, T. Feizi, *J. Immunol. Methods* **1999**, *227*, 109-119.
[117] B. T. Houseman, M. Mrksich, *Chem. Biol.* **2002**, *9*, 443-454.
[118] S. Park, I. Shin, *Angew. Chem. Int. Ed. Engl.* **2002**, *41*, 3180-3182.
[119] a) C. Grabosch, M. Kind, Y. Gies, F. Schweighöfer, A. Terfort, T. K. Lindhorst, *Org. Biomol. Chem.* **2013**, *11*, 4006-4015; b) M. Kleinert, T. Winkler, A. Terfort, T. K. Lindhorst, *Org. Biomol. Chem.* **2008**, *6*, 2118-2132.
[120] a) M. Hartmann, P. Betz, Y. Sun, S. N. Gorb, T. K. Lindhorst, A. Krueger, *Chem. Eur. J.* **2012**, *18*, 6485-6492; b) C. Fessele, S. Wachtler, V. Chandrasekaran, C. Stiller, T. K. Lindhorst, A. Krueger, *Eur. J. Org. Chem.* **2015**, 5519-5525; c) J. M. de la Fuente, A. G. Barrientos, T. C. Rojas, J. Rojo, J. Canada, A. Fernandez, S. Penades, *Angew. Chem. Int. Ed. Engl.* **2001**, *40*, 2257-2261.
[121] a) J. M. Meinders, H. C. van der Mei, H. J. Busscher, *J. Colloid Interface Sci.* **1995**, *176*, 329-341; b) J. Claes, L. Liesenborghs, M. Lox, P. Verhamme, T. Vanassche, M. Peetermans in *Journal of visualized experiments: JoVE*, 2015/07/02 ed., **2015**, p. e52862.
[122] a) W. E. Thomas, E. Trintchina, M. Forero, V. Vogel, E. V. Sokurenko, *Cell* **2002**, *109*, 913-923; b) M. M. Sauer, R. P. Jakob, J. Eras, S. Baday, D. Eriş, G. Navarra, S. Bernèche, B. Ernst, T. Maier, R. Glockshuber, *Nat. Commun.* **2016**, *7*, 10738.
[123] R. R. Isberg, P. Barnes, *Cell* **2002**, *110*, 1-4.
[124] W. E. Thomas, E. Trintchina, M. Forero, V. Vogel, E. V. Sokurenko, *Cell* **2002**, *109*, 913-923.
[125] D. E. Brooks, T. J. Trust, *J. Gen. Microbiol.* **1983**, *129*, 3661-3669.
[126] E. Finger, K. Puri, R. Alon, M. Lawrence, U. Andrian, T. Springer, *Nature* **1996**, *379*, 266-269.
[127] A. P. Fonseca, J. C. Sousa, *Int. J. Antimicrob. Agents* **2007**, *30*, 236-241.
[128] V. Kumar, J. V. Dhabalia, G. G. Nelivigi, M. S. Punia, M. Suryavanshi, *Indian J. Urol.* **2009**, *25*, 461-466.
[129] L. Möckl, C. Fessele, G. Despras, C. Bräuchle, T. K. Lindhorst, *Biochimica et Biophysica Acta (BBA) - General Subjects* **2016**, *1860*, 2031-2036.
[130] a) D. Kahne, S. Walker, Y. Cheng, D. Van Engen, *J. Am. Chem. Soc.* **1989**, *111*, 6881-6882; b) K. C. Nicolaou, H. J. Mitchell, R. M. Rodríguez, K. C. Fylaktakidou, H. Suzuki, S. R. Conley, *Chem. Eur. J.* **2000**, *6*, 3149-3165.
[131] R. R. Schmidt, W. Kinzy, in *Adv. Carbohydr. Chem. Biochem., Vol. 50*, (Ed.: D. Horton), Academic Press, **1994**, pp. 21-123.
[132] a) W. E. Dick, D. Weisleder, J. E. Hodge, *Carbohydr. Res.* **1972**, *23*, 229-242; b) R. H. Dewolfe in *Carboxylic Ortho Acid Derivatives, Vol. 14* (Ed.: R. H. Dewolfe), Elsevier, **1970**, pp. 298-347.
[133] K. Bock, C. Pedersen, *J. Chem. Soc., Perkin Trans. 2* **1974**, 293-297.
[134] W. A. Bubb, *Concept Magn. Reson. A* **2003**, *19A*, 1-19.
[135] J. R. Merritt, E. Naisang, B. Fraser-Reid, *J. Org. Chem.* **1994**, *59*, 4443-4449.
[136] a) M. J. Schweiter, K. B. Sharpless, *Tetrahedron Lett.* **1985**, *26*, 2543-2546; b) R. M. Hanson, K. B. Sharpless, *J. Org. Chem.* **1986**, *51*, 1922-1925.

[137] T. R. Hoye, C. S. Jeffrey, F. Shao, *Nat. Protoc.* **2007**, *2*, 2451-2458.
[138] S. Guillarme, S. Legoupy, N. Bourgougnon, A.-M. Aubertin, F. Huet, *Tetrahedron* **2003**, *59*, 9635-9639.
[139] E. Fernandez-Megia, J. Correa, I. Rodríguez-Meizoso, R. Riguera, *Macromolecules* **2006**, *39*, 2113-2120.
[140] A. Natarajan, W. Du, C.-Y. Xiong, G. L. DeNardo, S. J. DeNardo, J. Gervay-Hague, *Chem. Commun.* **2007**, 695-697.
[141] F. Tran, A. V. Odell, G. E. Ward, N. J. Westwood, *Molecules* **2013**, *18*, 11639-11657.
[142] K. D. Grimes, C. C. Aldrich, *Anal. Biochem.* **2011**, *417*, 264-273.
[143] a) R. K. Ness, H. G. Fletcher, C. S. Hudson, *J. Am. Chem. Soc.* **1950**, *72*, 2200-2205; b) M. Dowlut, D. G. Hall, O. Hindsgaul, *J. Org. Chem.* **2005**, *70*, 9809-9813.
[144] M. Heuckendorff, P. S. Bols, C. B. Barry, T. G. Frihed, C. M. Pedersen, M. Bols, *Chem. Commun.* **2015**, *51*, 13283-13285.
[145] a) Z.-L. Wei, P. A. Petukhov, F. Bizik, J. C. Teixeira, M. Mercola, E. A. Volpe, R. I. Glazer, T. M. Willson, A. P. Kozikowski, *J. Am. Chem. Soc.* **2004**, *126*, 16714-16715; b) K. R. Lutteroth, P. W. R. Harris, T. H. Wright, H. Kaur, K. Sparrow, S.-H. Yang, G. J. S. Cooper, M. A. Brimble, *Org. Biomol. Chem.* **2017**, *15*, 5602-5608.

10 Appendix

10.1 Abbreviations

β- CD	β- cyclodextrin
E. coli	*Escherichia coli*
i- Pr	isopropyl
Asn	asparagine
Arg	arginine
$BacAC_2$	2, 4-diacetamido-2, 4, 6-trideoxy-α-D-glucopyranose
Boc	*tert*-butyloxycarbonyl
BSA	bovine serum albumin
ConA	concanavalin A
CPs	capsular polysaccharides
CRD	carbohydrate recognition domain
Cys	cysteine
CuAAC	copper(I)-catalyzed azide alkyne cycloaddition
DBU	diazabicycloundecene
DET	diethyl tartrate
DMAP	4-dimethyaminopyridine
DMF	dimethylformamide
DTBMP	2, 6-di-*tert*-butyl-4-methylpyridine
EPS	epoxy polysaccharides
ESI-HRMS	electrospray ionization high resolution mass spectroscopy
Fuc	fucose
FucNAc	*N*-acetyl-fucosamine
GAG	glycosaminoglycan

Gal	galactose
GalNAc	*N*-acetylgalctosamine
GBPs	glycan binding proteins
GFP	green fluorescent protein
Glc	glucose
GlcNAc	*N*-acetylglucosamine
GPI	glycosylphosphatidylinositol
GSLs	glycosphingolipids
HMBC	heteronuclear multiple bond coherence
HSQC	heteronuclear single quantum coherence
Hyl	hydroxylysine
Hyp	hydroxyproline
IR	infrared spectroscopy
ITC	isothermal titration calorimetry
LPs	lipopolysaccharides
Man	mannose
MPTPA	α-methoxy-α-(trifluoromethyl)phenylacetic acid
MPTPA-Cl	α-methoxy-α-(trifluoromethyl)phenylacetyl chloride
NMR	nucler magnetic resonance
OEG	oligo(ethylene) glycol
PAMAM	polyamidoamine
PBST	phosphate buffered saline tween
PE	pentaerythritol
PEG	poly(ethylene) glycol
PNA	peanut agglutinin
Pse	pseudo

RIP	relative inhibition potency
SBA	soybean agglutinin
SD	standard deviation
SEM	standard error of the mean
Ser	serine
Sia	sialic acid
SLT	Shiga like toxin
sLeX	sialyl-Lewis X
TBHP	tertiary butyl hydroperoxide
TBTA	tris[(1-benzyl-1H-1, 2, 3-triazol-4-yl)methyl]amine
TfOH	trifluoromethanesulfonic acid
THF	tetrahydrofuran
Thr	threonin
TMSOTf	trimethylsilyl trifluoromethanesulfonate
TRIS	tris(hydroxymethyl)aminomethane
Tyr	tyrosine
UPEC	uropathogenic *Escherichia coli*
UTi	urinary tract infection
Xyl	xylose